

# Biotechnological applications of endophytes in agriculture, environment and industry, 2nd Edition

**Edited by**

Vijay K. Sharma, George Newcombe, Haiyan Li, Daniela Trivella  
and Ravindra Soni

**Published in**

Frontiers in Microbiology  
Frontiers in Bioengineering and Biotechnology



## FRONTIERS EBOOK COPYRIGHT STATEMENT

The copyright in the text of individual articles in this ebook is the property of their respective authors or their respective institutions or funders. The copyright in graphics and images within each article may be subject to copyright of other parties. In both cases this is subject to a license granted to Frontiers.

The compilation of articles constituting this ebook is the property of Frontiers.

Each article within this ebook, and the ebook itself, are published under the most recent version of the Creative Commons CC-BY licence. The version current at the date of publication of this ebook is CC-BY 4.0. If the CC-BY licence is updated, the licence granted by Frontiers is automatically updated to the new version.

When exercising any right under the CC-BY licence, Frontiers must be attributed as the original publisher of the article or ebook, as applicable.

Authors have the responsibility of ensuring that any graphics or other materials which are the property of others may be included in the CC-BY licence, but this should be checked before relying on the CC-BY licence to reproduce those materials. Any copyright notices relating to those materials must be complied with.

Copyright and source acknowledgement notices may not be removed and must be displayed in any copy, derivative work or partial copy which includes the elements in question.

All copyright, and all rights therein, are protected by national and international copyright laws. The above represents a summary only. For further information please read Frontiers' Conditions for Website Use and Copyright Statement, and the applicable CC-BY licence.

ISSN 1664-8714  
ISBN 978-2-8325-4168-5  
DOI 10.3389/978-2-8325-4168-5

## About Frontiers

Frontiers is more than just an open access publisher of scholarly articles: it is a pioneering approach to the world of academia, radically improving the way scholarly research is managed. The grand vision of Frontiers is a world where all people have an equal opportunity to seek, share and generate knowledge. Frontiers provides immediate and permanent online open access to all its publications, but this alone is not enough to realize our grand goals.

## Frontiers journal series

The Frontiers journal series is a multi-tier and interdisciplinary set of open-access, online journals, promising a paradigm shift from the current review, selection and dissemination processes in academic publishing. All Frontiers journals are driven by researchers for researchers; therefore, they constitute a service to the scholarly community. At the same time, the *Frontiers journal series* operates on a revolutionary invention, the tiered publishing system, initially addressing specific communities of scholars, and gradually climbing up to broader public understanding, thus serving the interests of the lay society, too.

## Dedication to quality

Each Frontiers article is a landmark of the highest quality, thanks to genuinely collaborative interactions between authors and review editors, who include some of the world's best academicians. Research must be certified by peers before entering a stream of knowledge that may eventually reach the public - and shape society; therefore, Frontiers only applies the most rigorous and unbiased reviews. Frontiers revolutionizes research publishing by freely delivering the most outstanding research, evaluated with no bias from both the academic and social point of view. By applying the most advanced information technologies, Frontiers is catapulting scholarly publishing into a new generation.

## What are Frontiers Research Topics?

Frontiers Research Topics are very popular trademarks of the *Frontiers journals series*: they are collections of at least ten articles, all centered on a particular subject. With their unique mix of varied contributions from Original Research to Review Articles, Frontiers Research Topics unify the most influential researchers, the latest key findings and historical advances in a hot research area.

Find out more on how to host your own Frontiers Research Topic or contribute to one as an author by contacting the Frontiers editorial office: [frontiersin.org/about/contact](https://frontiersin.org/about/contact)

# Biotechnological applications of endophytes in agriculture, environment and industry, 2nd Edition

## Topic editors

Vijay K. Sharma — Agricultural Research Organization (ARO), Israel  
George Newcombe — University of Idaho, United States  
Haiyan Li — Kunming University of Science and Technology, China  
Daniela Trivella — National Center for Research in Energy and Materials, Brazil  
Ravindra Soni — Department of Agricultural Microbiology, Indira Gandhi Krishi Vishva Vidyalaya, India

## Citation

Sharma, V. K., Newcombe, G., Li, H., Trivella, D., Soni, R., eds. (2023). *Biotechnological applications of endophytes in agriculture, environment and industry, 2nd Edition*. Lausanne: Frontiers Media SA.  
doi: 10.3389/978-2-8325-4168-5

**Publisher's note:** In this 2nd edition, the following article has been added: Zahra ST, Tariq M, Abdullah M, Zafar M, Yasmeen T, Shahid MS, Zaki HEM and Ali A (2023) Probing the potential of salinity-tolerant endophytic bacteria to improve the growth of mungbean [*Vigna radiata* (L.) Wilczek]. *Front. Microbiol.* 14:1149004. doi: 10.3389/fmicb.2023.1149004

## Table of contents

- 05 Editorial: Biotechnological applications of endophytes in agriculture, environment and industry  
Haiyan Li, Vijay K. Sharma, George Newcombe, Daniela Barretto Barbosa Trivella and Ravindra Soni
- 07 *Burkholderia ambifaria* XN08: A plant growth-promoting endophytic bacterium with biocontrol potential against sharp eyespot in wheat  
Chao An, Saijian Ma, Chen Liu, Hao Ding and Wenjiao Xue
- 18 Endophytic *Klebsiella aerogenes* HGG15 stimulates mulberry growth in hydro-fluctuation belt and the potential mechanisms as revealed by microbiome and metabolomics  
Ting Ou, Haiying Gao, Kun Jiang, Jing Yu, Ruolin Zhao, Xiaojiao Liu, Zeyang Zhou, Zhonghuai Xiang and Jie Xie
- 37 Effects of fungal seed endophyte FXZ2 on *Dysphania ambrosioides* Zn/Cd tolerance and accumulation  
Vijay K. Sharma, Shobhika Parmar, Wenting Tang, Haiyan Hu, James F. White Jr. and Haiyan Li
- 50 Bibliometric analysis of artificial intelligence for biotechnology and applied microbiology: Exploring research hotspots and frontiers  
Dongyu Xu, Bing Liu, Jian Wang and Zhichang Zhang
- 63 Effects of antibacterial peptide-producing *Bacillus subtilis*, gallic acid, and cellulase on fermentation quality and bacterial community of whole-plant corn silage  
Zhiheng Zhang, Yuqin Wang, Saiqiao Wang, Lu Zhao, Binglei Zhang, Wanhang Jia, Zhenhan Zhai, Lingping Zhao and Yuanxiao Li
- 79 Endophytes and their potential in biotic stress management and crop production  
Parul Chaudhary, Upasana Agri, Anuj Chaudhary, Ashish Kumar and Govind Kumar
- 101 Enhanced legume growth and adaptation to degraded estuarine soils using *Pseudomonas* sp. nodule endophytes  
Noris J. Flores-Duarte, Sara Caballero-Delgado, Eloisa Pajuelo, Enrique Mateos-Naranjo, Susana Redondo-Gómez, Salvadora Navarro-Torre and Ignacio D. Rodríguez-Llorente
- 118 Drought alleviation efficacy of a galactose rich polysaccharide isolated from endophytic *Mucor* sp. HELF2: A case study on rice plant  
Hiran Kanti Santra and Debdulal Banerjee



- 133 ***Trichoderma asperellum* empowers tomato plants and suppresses *Fusarium oxysporum* through priming responses**  
Amira E. Sehim, Omar A. Hewedy, Khadijah A. Altammar,  
Maryam S. Alhumaidi and Rasha Y. Abd Elghaffar
- 150 **Probing the potential of salinity-tolerant endophytic bacteria to improve the growth of mungbean [*Vigna radiata* (L.) Wilczek]**  
Syeda Tahseen Zahra, Mohsin Tariq, Muhammad Abdullah,  
Marriam Zafar, Tahira Yasmeen, Muhammad Shafiq Shahid,  
Haitham E. M. Zaki and Amanat Ali



## OPEN ACCESS

EDITED AND REVIEWED BY  
William James Hickey,  
University of Wisconsin-Madison, United States

## \*CORRESPONDENCE

Haiyan Li  
✉ lhyxn@163.com  
Vijay K. Sharma  
✉ vjsharma@outlook.in

RECEIVED 29 July 2023  
ACCEPTED 03 August 2023  
PUBLISHED 15 August 2023

## CITATION

Li H, Sharma VK, Newcombe G, Trivella DBB  
and Soni R (2023) Editorial: Biotechnological  
applications of endophytes in agriculture,  
environment and industry.  
*Front. Microbiol.* 14:1269279.  
doi: 10.3389/fmicb.2023.1269279

## COPYRIGHT

© 2023 Li, Sharma, Newcombe, Trivella and  
Soni. This is an open-access article distributed  
under the terms of the [Creative Commons  
Attribution License \(CC BY\)](#). The use,  
distribution or reproduction in other forums is  
permitted, provided the original author(s) and  
the copyright owner(s) are credited and that  
the original publication in this journal is cited, in  
accordance with accepted academic practice.  
No use, distribution or reproduction is  
permitted which does not comply with these  
terms.

# Editorial: Biotechnological applications of endophytes in agriculture, environment and industry

Haiyan Li<sup>1\*</sup>, Vijay K. Sharma<sup>2\*</sup>, George Newcombe<sup>3</sup>,  
Daniela Barretto Barbosa Trivella<sup>4</sup> and Ravindra Soni<sup>5</sup>

<sup>1</sup>Medical School, Kunming University of Science and Technology, Kunming, China, <sup>2</sup>Agricultural Research Organization, The Volcani Center, Rishon LeZion, Israel, <sup>3</sup>Department of Forest, Rangeland and Fire Sciences, University of Idaho, Moscow, ID, United States, <sup>4</sup>Brazilian Biosciences National Laboratory, National Center for Research in Energy and Materials, Campinas, SP, Brazil, <sup>5</sup>Department of Agricultural Microbiology, College of Agriculture, Indira Gandhi Krishi Vishwavidyalaya, Raipur, Chhattisgarh, India

## KEYWORDS

endophytes, agriculture, environment, industry, biotechnological applications

## Editorial on the Research Topic

### Biotechnological applications of endophytes in agriculture, environment and industry

Endophytes are the plant symbionts that live inside the plant tissue without causing any symptoms of disease for a part of their life-cycle. They are an important untapped reservoir of biological resources. They can promote plant growth by improving the physiological and metabolic functions of host plants via nutrient acquisition, nitrogen fixation, phytohormone production, etc., which can be used to promote agricultural yield and food quality. They also have potential applications in enhanced phytoremediation. In addition, endophytes are known to produce various novel antibiotics that can be used in the pharmaceutical, food, and agricultural industries. Functional genomics studies of endophytes provided more information and a better understanding of the network of complex host-endophyte interactions and other associated microbes to harness the biotechnological potential of endophytes more efficiently and sustainably.

The main aim of this Research Topic was to recover the functional role and application of endophytes for agricultural, medicinal, industrial, and environmental purposes. Within this topic, nine articles have been published that complement our knowledge on the occurrence and diversity of endophytes and the role, mechanism, and biotechnological application of endophytes in these fields.

One of the main causes of the global drop in crop productivity is pathogenic microorganisms. Endophytes diminish the injury triggered by pathogens through synthesizing antibiotics, the production of lytic enzymes, secondary metabolites, hormone activation, etc. (Chaudhary et al.). An et al. isolated an endophytic bacterium *Burkholderia ambifaria* XN08 with antagonistic activity against *Rhizoctonia cerealis*, a wheat (*Triticum aestivum* L.) sharp eyespot pathogenic fungus. The colonization of strain XN08 was accompanied by an enhancement of wheat growth and an induction of wheat sharp eyespot resistance by synthesizing a series of plant growth regulators (indole-3-acetic acid, IAA, etc.), producing antifungal compounds (pyrrolnitrin, etc.), and enhancing the

activities of defense enzymes (polyphenol oxidase, peroxidase, and phenylalanine ammonia-lyase). The role of *Trichoderma asperellum* against *Fusarium* wilt disease (FDW) in tomato (*Solanum lycopersicum*) plants was investigated by [Sehim et al.](#) They found that *T. asperellum* exhibited the highest mycelial inhibition rate (53.24%) against *Fusarium oxysporum*. *T. asperellum* enhanced the growth of tomato seeds and controlled the FDW by enhancing the number of leaves, as well as shoot and root length and fresh and dry weights by producing IAA, Phosphate (P) solubilization, and synthesizing bioactive secondary metabolites. Furthermore, *Trichoderma* extract increased shelf-life of tomato fruits by reducing infection by *F. oxysporum* from post-harvest.

Abiotic stress, such as drought and flood stress, heavy metal stress, prevents plants from growing normally and lowers crop output. Endophytes represent safe and effective biological agents that mitigate abiotic stress for plant development. [Ou et al.](#) screened out *Klebsiella aerogenes* HGG15 from 28 endophytic bacteria as having superior plant growth promotion (PGP) traits, including P solubilization, IAA, siderophore, and acetoin production, as well as biosafety for silkworms. Flood tolerance of mulberry (*Morus alba* L.) was increased by inoculated *K. aerogenes* HGG15 by synthesizing a series of abiotic stress response factors and growth promotion stimulators such as glycerolipid, sphingolipid, indole, pyridine, and coumarin. [Santra and Banerjee](#) isolated a Galactose-Rich Heteropolysaccharide (GRH) from endophytic *Mucor* sp. HELF2. Spraying with 50 ppm GRH has alleviated drought stress in rice seedlings (*Oryza sativa* ssp. indica MTU 7093 swarna) by improving relative water content and fresh weight of the tissues, root length, and shoot length, as well as increasing the soluble sugars, prolines, and chlorophyll contents of rice seedlings and elevating the enzymatic antioxidant parameters. The role of seed endophyte FXZ2 on *Dysphania ambrosioides* Zn/Cd tolerance and accumulation was investigated by [Sharma et al.](#) The study suggests that the Zn/Cd tolerance of the host plant was increased by seed endophyte FXZ2 by altering Zn/Cd speciation in rhizospheric soils and exogenous production of phytohormones to promote growth, lowering oxidative damage while enhancing antioxidant properties. In addition, Zn uptake in inoculated plants was decreased, while Cd accumulation was increased in the inoculated plants that were grown in Zn/Cd contaminated soil. Similarly, [Flores-Duarte et al.](#) isolated and selected 4 endophytic rhizobia and non-rhizobia with higher PGP properties and bacterial enzymatic activities from *Medicago* spp., including *Pseudomonas* sp. N4, *Pseudomonas* sp. N8, *Ensifer* sp. N10 and *Ensifer* sp. N12. Inoculation with combinations of *Ensifer* (rhizobia) and *Pseudomonas* increased plant biomass and nodules ameliorating the physiological state of the plants and helping to regulate plant stress mechanisms, while increasing As, Cd, Cu, and Zn accumulation in plant roots, without significant differences in shoot metal accumulation, on nutrient-poor soils and moderately contaminated with metals/loids. Endophytes provide new insights into agricultural production and environmental health.

In the field of livestock feed production such as silage, microbes with antibacterial and other properties have been extensively researched and used. [Zhang et al.](#) assessed the effects of antibacterial peptide-producing *Bacillus subtilis* CP7 on the fermentation quality and bacterial community of different varieties of whole-plant corn

silage. The additive *B. subtilis* CP7 enhanced the quantity of dry matter and crude protein, and improved the structure of the bacterial community following silage.

With the development of technology, artificial intelligence (AI) has been extensively used in the biotechnology and applied microbiology sectors. Deep learning, prediction, support vector machines, object detection, feature representation, synthetic biology, amyloid, human microRNA precursors, systems biology, and single cell RNA-Sequencing were the current hot spots, while microRNA and protein-protein interactions (PPIs) are the future trends in this area ([Xu et al.](#)). Studying PPIs using AI methods provides a better understanding of the complex network of host-endophyte interactions and other associated microbes to harness the biotechnological potential of endophytes more efficiently and sustainably.

In conclusion, endophytes were developed as an eco-friendly microbial agent for overcoming the tasks faced with conventional farming, the environment, and industry. Coupled with the AI, microbiome, and metabolite analyses, the mechanism of the role of endophytes could possibly be studied effectively and deeply, consequently amplifying the application potential of these beneficial microbes.

## Author contributions

HL: Writing—original draft, Writing—review and editing. VS: Writing—review and editing. GN: Writing—review and editing. DT: Writing—review and editing. RS: Writing—review and editing.

## Funding

This work was supported by the Natural Science Foundation of China (42267059) and Yunnan International Joint Laboratory of Research and Development of Crop Safety Production on Heavy Metal Pollution Areas.

## Conflict of interest

The authors declare that the research was conducted in the absence of any commercial or financial relationships that could be construed as a potential conflict of interest.

The author(s) declared that they were an editorial board member of Frontiers, at the time of submission. This had no impact on the peer review process and the final decision.

## Publisher's note

All claims expressed in this article are solely those of the authors and do not necessarily represent those of their affiliated organizations, or those of the publisher, the editors and the reviewers. Any product that may be evaluated in this article, or claim that may be made by its manufacturer, is not guaranteed or endorsed by the publisher.



## OPEN ACCESS

## EDITED BY

Daniela Trivella,  
National Center for Research in Energy  
and Materials, Brazil

## REVIEWED BY

Mohsen Mohamed Elsharkawy,  
Kafrelsheikh University, Egypt  
Vipin Kumar Singh,  
Banaras Hindu University, India  
Sueli Van Der Sand,  
Federal University of Rio Grande do  
Sul, Brazil  
Wei-Liang Kong,  
Nanjing Forestry University, China  
Yanglei Yi,  
Northwest A&F University, China

## \*CORRESPONDENCE

Wenjiao Xue  
x-wenjiao@163.com

## SPECIALTY SECTION

This article was submitted to  
Microbiotechnology,  
a section of the journal  
Frontiers in Microbiology

RECEIVED 29 March 2022

ACCEPTED 04 July 2022

PUBLISHED 28 July 2022

## CITATION

An C, Ma S, Liu C, Ding H and Xue W  
(2022) *Burkholderia ambifaria* XN08: A  
plant growth-promoting endophytic  
bacterium with biocontrol potential  
against sharp eyespot in wheat.  
*Front. Microbiol.* 13:906724.  
doi: 10.3389/fmicb.2022.906724

## COPYRIGHT

© 2022 An, Ma, Liu, Ding and Xue. This  
is an open-access article distributed  
under the terms of the [Creative  
Commons Attribution License \(CC BY\)](#).  
The use, distribution or reproduction  
in other forums is permitted, provided  
the original author(s) and the copyright  
owner(s) are credited and that the  
original publication in this journal is  
cited, in accordance with accepted  
academic practice. No use, distribution  
or reproduction is permitted which  
does not comply with these terms.

# *Burkholderia ambifaria* XN08: A plant growth-promoting endophytic bacterium with biocontrol potential against sharp eyespot in wheat

Chao An, Saijian Ma, Chen Liu, Hao Ding and Wenjiao Xue\*

Research Center for Microbial Metabolites, Shaanxi Institute of Microbiology, Xi'an, China

Plant growth-promoting bacteria (PGPB) have been considered promising biological agents to increase crop yields for years. However, the successful application of PGPB for biocontrol of sharp eyespot in wheat has been limited, partly by the lack of knowledge of the ecological/environmental factors affecting the colonization, prevalence, and activity of beneficial bacteria on the crop. In this study, an endophytic bacterium XN08 with antagonistic activity against *Rhizoctonia cerealis* (wheat sharp eyespot pathogenic fungus), isolated from healthy wheat plants, was identified as *Burkholderia ambifaria* according to the sequence analysis of 16S rRNA. The antibiotic synthesis gene amplification and ultra-performance liquid chromatography-quadrupole time-of-flight mass spectrometry (UPLC-QTOF-MS) analyses were used to characterize the secondary metabolites. The results showed that the known powerful antifungal compound named pyrrolnitrin was produced by the strain XN08. In addition, *B. ambifaria* XN08 also showed the capacity for phosphate solubilization, indole-3-acetic acid (IAA), protease, and siderophore production *in vitro*. In the pot experiments, a derivative strain carrying the green fluorescent protein (GFP) gene was used to observe its colonization in wheat plants. The results showed that GFP-tagged *B. ambifaria* could colonize wheat tissues effectively. This significant colonization was accompanied by an enhancement of wheat plants' growth and an induction of immune resistance for wheat seedlings, which was revealed by the higher activities of polyphenol oxidase (PPO), peroxidase (POD), and phenylalanine ammonia-lyase (PAL). As far as we know, this is the first report describing the colonization traits of *B. ambifaria* in wheat plants. In addition, our results indicated that *B. ambifaria* XN08 might serve as a new effective biocontrol agent against wheat sharp eyespot disease caused by *R. cerealis*.

## KEYWORDS

*Burkholderia ambifaria*, biological control, *Rhizoctonia cerealis*, colonization, antifungal activity

## Introduction

The wheat sharp eyespot, caused predominately by the necrotrophic fungus *Rhizoctonia cerealis*, is one of the most destructive soil-borne fungal diseases in wheat (*Triticum aestivum* L.) and results in yield losses of 10%–40% in the regions of Asia, Oceania, Europe, North America, and Africa (Wang et al., 2018; Zhao et al., 2021). This fungal pathogen can survive in soils or the infected crop residues for a long time, and it reinfects the stems and sheaths of wheat plants in the favorable environmental conditions, blocks the transportation of nutrients, and eventually leads to host death (Su et al., 2020). Traditional agrochemicals, which were still widely used for the effective control of wheat sharp eyespot, had led to an increase in environmental pollution and induced pesticide resistance (Zhang et al., 2017). Therefore, the biological control of wheat sharp eyespot as a green and sustainable agricultural biotechnology has attracted lots of attention (Raymaekers et al., 2020; Xu et al., 2020).

Plant growth-promoting bacteria (PGPB) have been considered promising biological agents for years (Dimkić et al., 2022). They have shown multifunctional plant-promoting ways including the facilitation of nutrient uptake, nitrogen fixation for plant use, the production of plant hormones, direct antagonism against pathogens, and the induction of systemic resistance throughout the plant (Jing et al., 2019). Therefore, many researchers have focused on the exploration of new PGPB with varied beneficial effects in recent years. For example, *Pantoea dispersa*-AA7 and *Enterobacter asburiae*-BY4, which were isolated from sugarcane rhizosphere soils, showed the capacity for nitrogenase and ACC deaminase production (Jing et al., 2019). Saad et al. (2020) isolated 18 strains from the rhizosphere soils of red silk-cotton tree and Chinese banyan and found that *Bacillus thuringiensis* MN419208 exhibited the capacity for plant growth promotion by producing indole-3-acetic acid (IAA) and exopolysaccharides and exerting the capacity of nitrogen fixation, while *Bacillus sonorensis* MN419205, *Bacillus wiedmannii* MN419207, and *Bacillus subtilis* MN419218 showed the antagonistic properties against root rot in *fava beans*. In contrast, a rhizosphere isolated strain of *Pseudomonas* sp. 23S showed antagonistic activity against *Clavibacter michiganensis* subsp. *michiganensis* *in vitro* and reduced the severity of tomato bacterial canker by inducing systemic resistance (Takishita et al., 2018). However, it is inadequate to excavate the wheat association PGPB, especially in screening the biological control agents against sharp eyespot caused by *R. cerealis*.

On the contrary, although many PGPB have shown excellent antagonistic characteristics under laboratory and greenhouse conditions, the successful application of PGPB under field conditions has been limited by its poor colonization capacity (Rilling et al., 2019). In fact, the effective root colonization of PGPB is considered to be a critical factor in achieving successful plant–microbe interaction (Bo et al., 2022).

Compared with the plant rhizobacteria, bacterial endophytes have more opportunities to be in contact with the plant cells, so they could readily exert a direct beneficial effect (Morales-Cedeno et al., 2021).

In our previous study, an endophytic bacterium XN08, which showed great antagonistic activities against varied phytopathogenic fungi including *R. cerealis*, was isolated from healthy wheat plants. The purpose of this study was to evaluate its biocontrol potential against sharp eyespot in wheat. The strain XN08 was identified *via* 16S rRNA analysis, and a known antifungal compound produced by the strain was confirmed by gene amplification and ultra-performance liquid chromatography-quadrupole time-of-flight mass spectrometry (UPLC-QTOF-MS) analyses. To observe its colonization in wheat plants, a derivative strain carrying the green fluorescent protein (*GFP*) gene was constructed. The immune resistance of wheat seedlings was also monitored in this study.

## Materials and methods

### Bacterial strains and growth conditions

The strain XN08 used in this study was obtained from healthy wheat plants in our laboratory. The strain was cultivated in a nutrient broth medium (NB) and maintained at  $-80^{\circ}\text{C}$  in a 20% glycerol solution. GFP-tagged *Burkholderia ambifaria* was cultivated in an NB medium containing 100  $\mu\text{g/ml}$  tetracycline (Tc) for the maintenance of plasmids. *Rhizoctonia cerealis*, which was kindly provided by the Center of Biological Pesticide Research, Northwest Agricultural and Forestry University, was maintained on potato dextrose agar (PDA) slants. *Candida albicans*, which was derived from the Center of Microbiological Detection, Shaanxi Institute of Microbiology, was used as indicator fungi to detect the antifungal activity. The pyrrolnitrin was purchased from ChengDu TongChuangYuan Pharmaceutical Co. Ltd. (Chengdu, China). The Xiaoyan 22 (*T. aestivum* L.) seeds were directly purchased from the market.

### Phylogenetic analysis

The bacterial genomic DNA was isolated and purified using the TaKaRa MiniBEST Bacteria Genomic DNA Extraction Kit (Dalian, China). Genomic DNA was then used as the template for PCR amplification of 16S rRNA gene fragments using the bacterial universal primers (27F-5'-AGAGTTGATCCTGGCTCAG-3' and 1492R-5'-GGTTACCTTGTTCAGACTT-3'). The final amplified reaction volume was 50  $\mu\text{l}$ , containing 5.0  $\mu\text{l}$  of 10 $\times$  Taq buffers, 4.0  $\mu\text{l}$  of 200 mmol/L dNTPs, 2.0  $\mu\text{l}$  of each primer at 10  $\mu\text{M}$ , 0.5  $\mu\text{l}$  of Ex Taq enzyme (TaKaRa, Dalian), 5.0  $\mu\text{l}$  of genomic DNA, and 31.5  $\mu\text{l}$  of sterilized distilled water. PCR amplification was performed



using the Professional Standard 96 Gradient (Biometra, Jena, Germany) with the following cycling parameters: initial denaturation of DNA for 5 min at 95°C, then 30 cycles of denaturation of DNA for 1 min at 94°C, annealing for 1 min at 53°C, extension for 1.5 min at 72°C, and final incubation for 5 min at 72°C (Vasiee et al., 2018). The PCR products were subsequently purified and sequenced using BGI Biotechnology (Shenzhen, China). DNA sequence alignment was performed using BLAST (<https://blast.ncbi.nlm.nih.gov/Blast.cgi>). Finally, phylogenetic trees were constructed using the neighbor-joining (NJ) method implemented in MEGA 5.05 (Arizona State University, Tempe, United States).

## Detection of genes associated with antibiotic biosynthesis using the PCR method

The *Burkholderia* spp. have been reported to produce antimicrobial compounds such as siderophore (required *Cep* gene), pyrrolnitrin (required *Prn* gene), and phenazine acid (required *Pca* gene). We designed three sets of low-degeneracy primers for PCR amplification of these genes. These primers are shown in [Supplementary material 1](#). According to the manufacturer's instructions, the amplification was performed in 50 µl reactions with Taq polymerase (TaKaRa Biotechnology, Dalian, China). The PCR products were detected using gel electrophoresis detection. Finally, the PCR products obtained in this study were sequenced by BGI Biotechnology (Shenzhen, China), and the phylogenetic tree was constructed using the neighbor-joining (NJ) method.

## Evaluation of antifungal activity *in vitro* and *ex vivo*

Antifungal activity of the *Burkholderia* sp. XN08 was evaluated using both the dual plate confrontation assay and the agar diffusion method. The inhibition ratio was calculated as follows (Cui et al., 2019):

$$\text{Inhibition ratio (\%)} = \frac{(\text{Diameter of control fungus} - \text{Diameter of treated fungus})}{(\text{Diameter of control fungus})} \quad (1)$$

The strain XN08, which was pre-cultured on a nutrient agar medium (NA) plate for 24 h, was inoculated into a 500-ml conical flask containing 200 ml of sterile LB broth and then cultured at 230 rpm for 48 h at 37°C. After cultivation, the cells were removed by centrifugation at 8,000 rpm for 10 min at 4°C. The supernatant was added into preheated PDA medium at 55°C. *Rhizoctonia cerealis* was respectively inoculated on the

pure PDA medium plate and PDA medium supplemented with the fermentation broth supernatant of the strain XN08.

Plant leaf tissue was used to determine the antifungal activity of fermentation broth supernatant *ex vivo* as previously described (Fu et al., 2019) with minor modifications. In brief, the top leaves of 14-day-old wheat seedlings with four- to five-leaf stages were used for evaluating the biocontrol efficacy of the fermentation broth supernatant of the strain XN08 against *R. cerealis*. The leaves were wounded at the equator (0.5 mm wide) and inoculated with 5 µl of conidial suspension ( $2 \times 10^5$  spores/ml) of *R. cerealis*. Then, the fermentation broth supernatant of the strain XN08 was sprayed onto the leaf surface. To keep the plant growing, the petioles were wrapped in cotton that contained water to provide nutrients. The leaves were kept in greenhouse system at  $23 \pm 2^\circ\text{C}$  with a relative humidity (RH) of 95% for 6 days. Daily observations were carried out.

## Extraction and identification of antifungal compounds by UPLC-QTOF-MS

The *n*-butanol extracts from the fermentation broth supernatant of XN08 were dissolved with methanol at a concentration of 1 mg/ml, and 50 µl of the solution was added into a 6-mm well in Sabouraud agar medium plates, which were inoculated with *C. albicans* and cultured overnight at 37°C. Then, the plates were incubated at 28°C for 72 h, and the inhibition zones around the wells were observed to determine the antimicrobial activity. The redissolved sample was further purified using reverse-phase high-performance liquid chromatography (Waters 2695, PDA detector 2998) with a C18 column (YMC-Pack Pro C18, 250 × 4.6 mm S-5 µm, 12 nm; YMC CO., LTD, Japan) and eluted with a methanol–water mixture (methanol:water = 8:2) at a flow rate of 1.0 ml/min. The OD at 254 nm was monitored. The MS was operated in negative ion mode and was set to total ion chromatogram mode with the following parameter settings: capillary voltage, 1.0 kV; low collision energy, 6V; source temperature, 100°C; desolvation temperature, 500°C; and desolvation gas flow, 800 L/h. Data acquisition and processing were conducted using Masslynx version 4.1 (Waters, Manchester, United Kingdom).

## Detection of plant growth-promoting traits *in vitro*

### IAA detection

The strain XN08 was propagated overnight in 100 ml of LB medium and then supplemented with 1 ml of L-tryptophan solution with a concentration of 50 µg/ml. After incubation for 42 h, 1 ml aliquot of the supernatant was mixed vigorously with 4 ml of Salkowski's reagent (150 ml of concentrated H<sub>2</sub>SO<sub>4</sub>,



250 ml of distilled H<sub>2</sub>O, and 7.5 ml of 0.5 M FeCl<sub>3</sub>•6H<sub>2</sub>O) and allowed to stand at room temperature for 20 min, and then the color changes were observed (Patten and Glick, 2002).

### Phosphate solubilization detection

A single colony of strain XN08 was spot inoculated onto Pikovskaya's agar plate at 28°C and incubated at 28°C for 48 h. The formation of a halo-zone around the colony was observed (Patten and Glick, 2002).

### Siderophore detection

A single colony of strain XN08 was spot inoculated on CAS medium [medium component (1L): chrome azurol S (CAS), 60.5 mg; hexadecyltrimethyl ammonium bromide (HDTMA), 72.9 mg; piperazine-1, 4-bis (2-ethanesulfonic acid; PIPES), 30.24 g; and 1 mM FeCl<sub>3</sub>•6H<sub>2</sub>O in 10 mM HCl 10 ml agarose (0.9%, w/v)], and then color changes around the colonies were observed visually (Shahid et al., 2012).

### Proteinase detection

A single colony of the strain XN08 was spot inoculated on a modified tryptic soy broth medium and then the zones of proteolysis around the colonies were observed visually (Shahid et al., 2012).

### Pot experiments

Wheat seeds were surface-sterilized in 2.5% sodium hypochlorite for 5 min and in 75% ethanol for 2 min and then soaked in sterile-distilled water for 24 h. The sterilized wheat seeds were put into a sterile 10-ml glass bottle and then cultured for 7 days in the artificial climate box with a temperature of 28°C and 90% RH. The seedlings with consistent growth were selected for the pot experiments. All experiments have been conducted in a 10-ml glass bottle, and each experiment group consisted of four bottles, each of which contains three seedlings.

- **Group 1:** The seedlings were poured with a 2-ml suspension of GFP-tagged *B. ambifaria* (10<sup>7</sup> CFU/ml).
- **Group 2:** The control group consisted of seedlings soaked in 2 ml of sterile water.
- **Group 3:** The seedlings soaked in a 2-ml of sterile water were scratched and inoculated with 500 µl of the suspension of *R. cerealis* containing 1 × 10<sup>8</sup> CFU/ml spores.
- **Group 4:** The seedlings were poured with 2 ml suspension of GFP-tagged *B. ambifaria* (10<sup>7</sup> CFU/mL) and inoculated

with 500 µl of suspension of *R. cerealis* containing 1 × 10<sup>8</sup> CFU/ml spores.

All of the treated seedlings were further cultured in an artificial climate box (RH 90% and temperature 28°C) and then tested for plant growth-promoting and biocontrol properties. Three seedlings were sampled for each treatment at different growth stages. The samples were washed and wiped dry, and then their fresh weight and shoot height were measured.

### Colonization of XN08 in wheat tissues

The seedlings of group 1 were scanned and imaged by CLSM (Laser Scanning Confocal Microscopy; DM6000, Leica Microsystems). The STED beam was generated by a 592-nm depletion beam. All images were detected using hybrid (HyD) detectors controlled by LAS-AX imaging software. All STED images were deconvolved using Huygens software (Scientific Volume Imaging) and analyzed offline using LAS AF Lite (Leica).

### The activities of defense enzymes in wheat

The activity levels of polyphenol oxidase (PPO), peroxidase (POD), and phenylalanine ammonia-lyase (PAL) were determined according to the instructions provided by the manufacturer with the respective enzyme activity assay kits (Nanjing Jiancheng Bioengineering Institute, China). The article numbers of the kits are A136-1-1 (PPO), A084-3-1 (POD), and A137-1-1 (PAL).

## Results

### Identification of the strain XN08

As shown in Figures 1A,B, the strain XN08 exhibited off-white colony morphology and secreted viscoelastic substances on the NA plate. The cells appeared as short rod shapes under the light microscope (Figure 1C). A 1,438 bp region of the 16S rDNA gene was amplified from the genomic DNA of the strain XN08, and the sequence analysis indicated that the strain XN08 shared 99.85% identity with *B. ambifaria* AMMD (Genebank Accessions: CP00040) in the NCBI nr database. The phylogenetic tree was constructed (Figure 1D) using the neighbor-joining method. The result also showed that the strain XN08 had a close relationship with *B.*

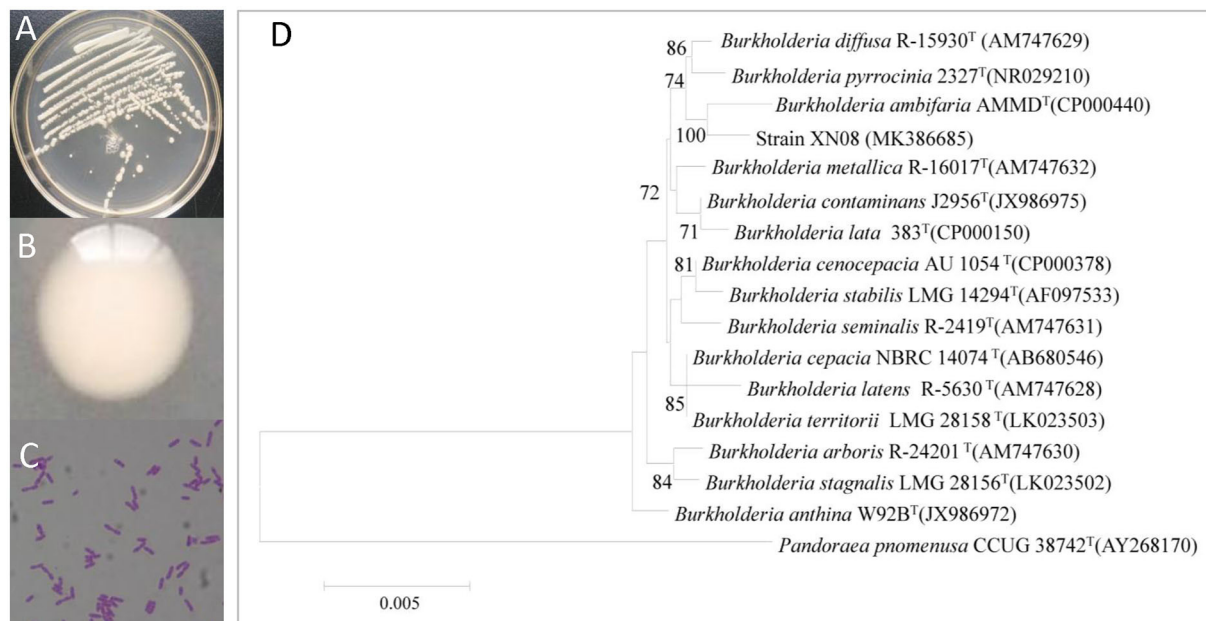


**FIGURE 1** Morphological and molecular identification of the endophytic bacterium XN08. The colonies (A), colony characters (B) of the strain XN08 on LB medium and microscopic characters (C) under a light microscope ( $\times 400$ ), phylogenetic tree of the strain XN08 based on 16S rRNA sequence (D).

*ambifaria* AMMD. Therefore, the strain XN08 was identified as *B. ambifaria*.

## Biocontrol potential of the strain XN08 against *R. cerealis*

Compared with the control group (Figure 2A), *B. ambifaria* XN08 showed dramatically a high antagonistic activity against *R. cerealis* under the co-cultural condition (Figure 2B). In addition, no obvious *R. cerealis* growth was observed on the PDA medium added with the fermentation supernatants of the strain XN08 (Figure 2C). Moreover, the plant leaves sprayed with the supernatant of strain XN08 maintained a healthy green color, and no obvious disease symptoms were observed after inoculation with *R. cerealis* (Figure 2D). Usually, the leaves would become yellow after pathogen infection. The above results demonstrated that the strain XN08 may produce extracellular antifungal compounds.

## Identification of potential antifungal compounds

To predict the potential antifungal substances produced by *B. ambifaria* XN08, PCR was used to detect the biosynthetic

genes of antifungal compounds. Three genes, namely, *Cep*, *R*, *Prn*, and *Pca*, were amplified with predesigned three primers pairs, respectively. A key gene fragment sequence (*Prn* 3, 503 bp) involved in pyrrolnitrin synthesis was successfully amplified (Figures 2E,F). A phylogenetic tree was constructed by sequence alignment using the neighbor-joining method. The sequence had a close relationship with tryptophan halogenase from the *prn* A gene of *B. ambifaria* AMMD (CP009799; Figure 2G). The result indicated that *B. ambifaria* XN08 had the potential to synthesize pyrrolnitrin. An antifungal activity assay was performed to identify the fraction containing the antifungal compound. The *n*-butanol-extracted fraction of *B. ambifaria* XN08 fermentation broth (Figures 2H,I) exhibited obvious antifungal activity against *C. albicans* (Figure 2J). Subsequently, pyrrolnitrin was detected in the *n*-butanol-extracted fraction using the UPLC-QTOF-MS method (Figure 2K).

## In vitro plant growth-promoting traits of the strain XN08

As shown in Figures 2L–O, the strain XN08 exhibited a series of potential plant growth-promoting traits including protease, IAA, and siderophore production. Also, the strain could solubilize phosphate.

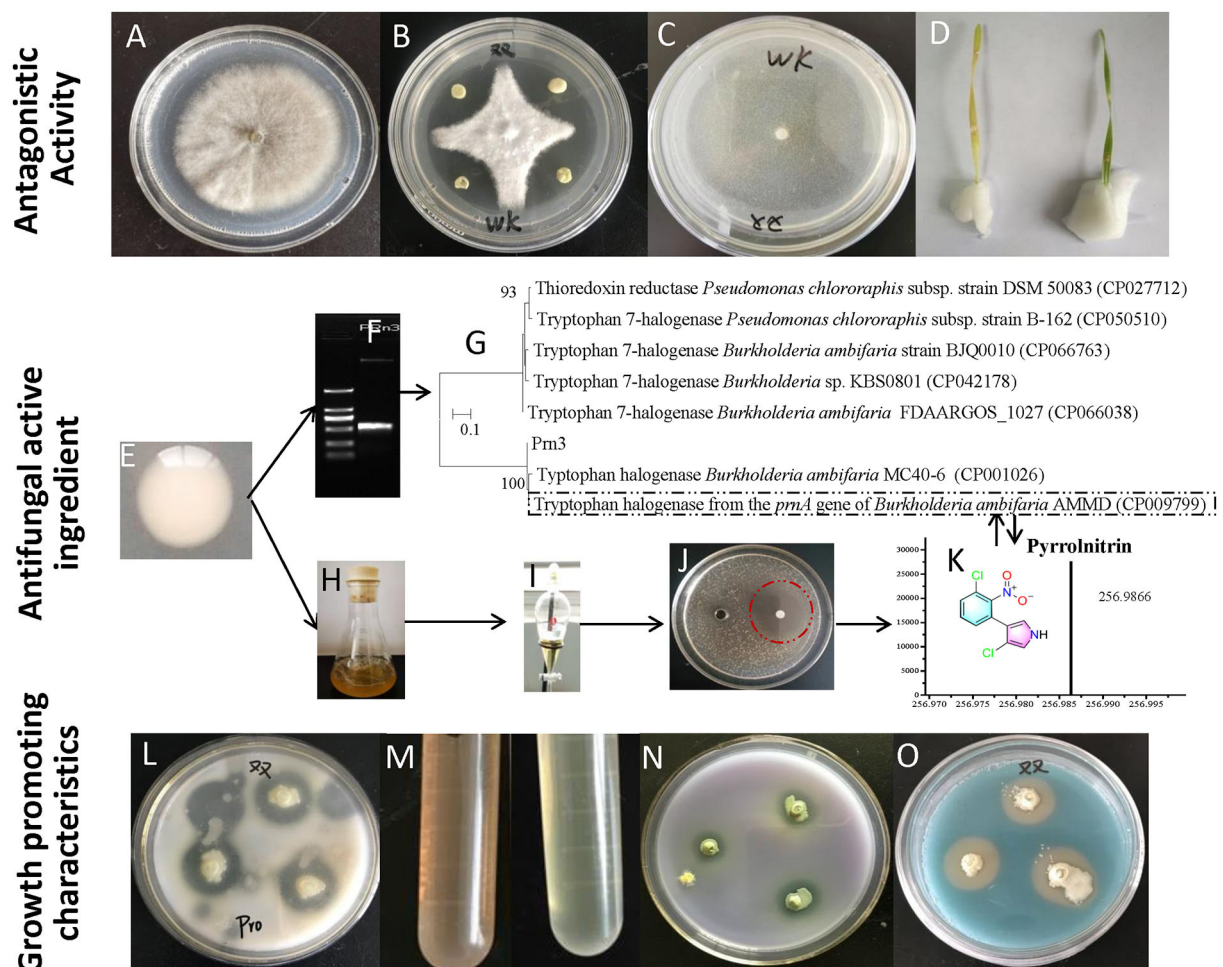


FIGURE 2

Antagonistic activities and plant growth-promoting characteristics of the strain XN08. *R. cerealis* grown on PDA medium (A), *in vitro* antagonism of *B. ambifaria* XN08 against *R. cerealis* (B), *R. cerealis* grown on PDA medium supplemented with the fermentation broth supernatant of *B. ambifaria* XN08 (C), inhibition of the fermentation broth supernatant of the strain XN08 against *R. cerealis* on detached leaves of wheat plants (D), amplification and sequence comparison of the antibiotic synthesis genes (E–G), fermentation of the strain XN08 (H), extraction of antifungal compounds (I), detection of antifungal activities (J), identification of antifungal compounds by UPLC-QTOF-MS method (K), and plant growth-promoting traits of *B. ambifaria* XN08 *in vitro* [(L), proteinase production; (M), IAA production; (N), the capacity of phosphate solubilization; (O), siderophore production].

## Evaluation of plant colonization of GFP-tagged *B. ambifaria*

A derivative strain carrying the *GFP* gene was successfully constructed, and CLSM was used to observe the cells with green fluorescence as shown in Figure 3A. The GFP-tagged *B. ambifaria* showed a slightly weaker antagonistic activity (inhibition ratio of 70.14%) against *R. cerealis* compared with the wild strain XN08 (inhibition ratio of 75.45%; Figures 3B,C). In the pot experiment (Figure 3D), a small number of GFP-tagged *B. ambifaria* cells were found to colonize the root of wheat when the strain was inoculated into the rhizosphere soil of plants for 2 days (Figures 3E,F). At 7 days after inoculation, large numbers of bacterial cells were observed in the root tips (Figures 3G,H).

## Growth-promoting effects of *B. ambifaria* XN08 on wheat in the pot experiments

After 7 days of inoculation, the biological characteristics of the plant changed significantly as shown in Figure 4A. First, shoot height and fresh weight of the seedlings inoculated with both *R. cerealis* and GFP-tagged *B. ambifaria* reached  $15.18 \pm 2.54$  cm and  $0.28 \pm 0.07$  g for each seedling, which were higher than those of the seedlings inoculated with equal volumes of water ( $14.35 \pm 2.78$  cm,  $0.26 \pm 0.06$  g) and the seedlings inoculated with *R. cerealis* ( $6.98 \pm 1.34$  cm and  $0.12 \pm 0.03$  g) (Figures 4B,C). No significant difference was observed between the wheat seedlings with or without *R. cerealis* when inoculated with GFP-tagged *B. ambifaria*.



## Construction of GFP-tagged *B. ambifaria*

## Endophytic colonization of GFP-tagged *B. ambifaria* in the leaves of wheat

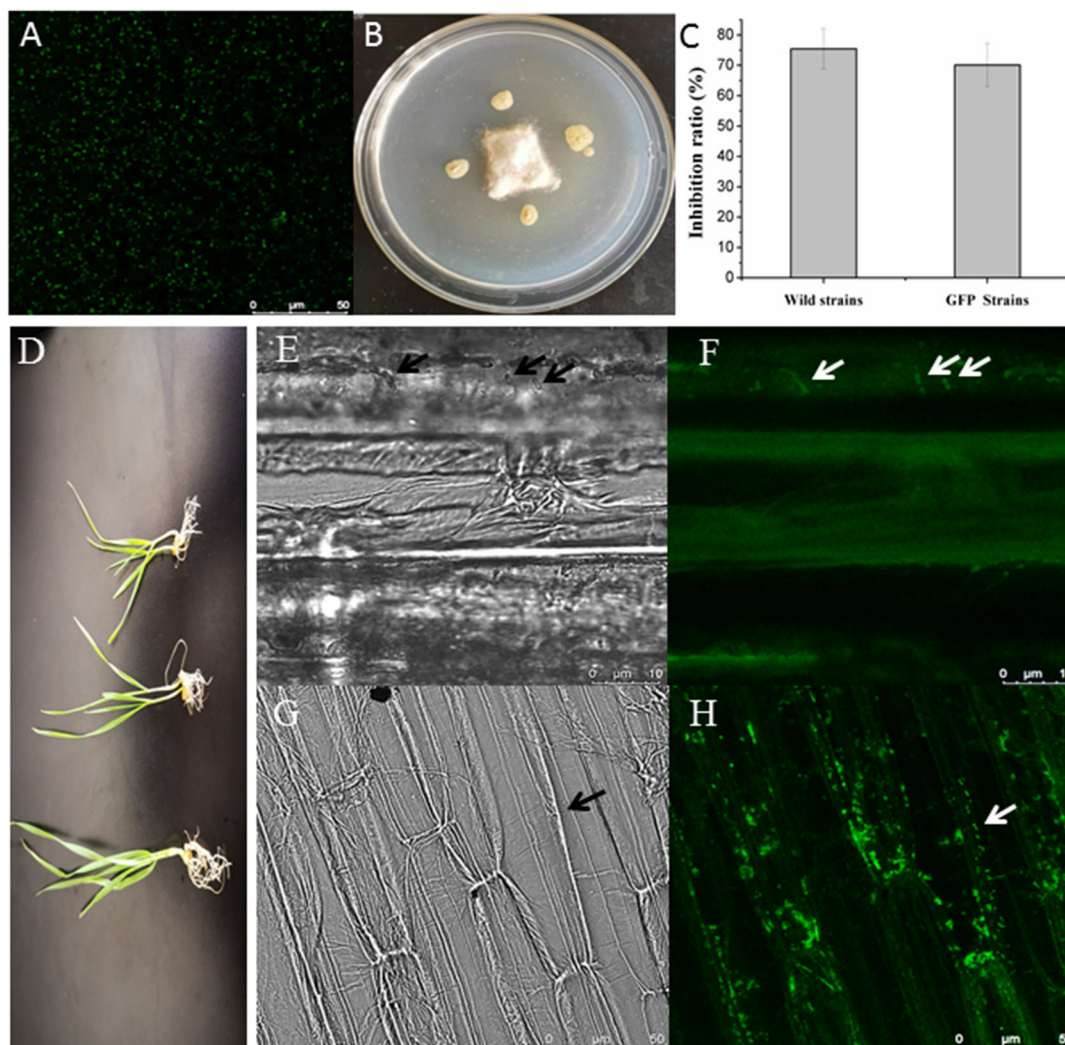


FIGURE 3

Colonization of GFP-tagged *B. ambifaria* in the seedlings of wheat. The observation of GFP-tagged *B. ambifaria* by CLSM (A), antagonistic activities against *R. cerealis* (B,C), the wheat seedlings inoculated GFP-tagged *B. ambifaria* at different growing stages (D), colonization of GFP-tagged *B. ambifaria* XN08 at 2 days after inoculation (photographs under dark (E) and bright (F) fields) and 7 days after inoculation (photographs under dark (G) and bright (H) fields).

In addition, the seedlings inoculated with *R. cerealis* had obvious sharp eyespot symptoms, while those plants inoculated with both *R. cerealis* and GFP-tagged *B. ambifaria* had no obvious symptoms.

The PPO, POD, and PAL enzyme activities of wheat seedlings at different growth stages for different treatment groups were tested. As shown in Figures 4D–F, the activities of PPO, POD, and PAL in the roots of wheat inoculated with both GFP-tagged *B. ambifaria* and *R. cerealis* were higher than those of the other groups and showed peaks at 5, 3, and 3 days after inoculation, respectively.

## Discussion

Wheat hosts a high diversity of endophytic bacteria, including different genera such as *Achromobacter*, *Acinetobacter*, *Arthrobacter*, *Bacillus*, *Burkholderia*, *Chitinophaga*, *Enterobacter*, *Erwinia*, *Flavobacterium*, *Klebsiella*, *Leifsonia*, *Microbispora*, *Micrococcus*, *Micromonospora*, *Mycobacterium*, *Paenibacillus*, *Pantoea*, *Pseudomonas*, *Roseomonas*, *Staphylococcus*, *Streptomyces*, and *Xanthomonas* (Rana et al., 2020). Several studies have exploited wheat-associated PGPB. It was reported that 13 endophytic bacteria isolated from wheat showed multifarious plant beneficial traits

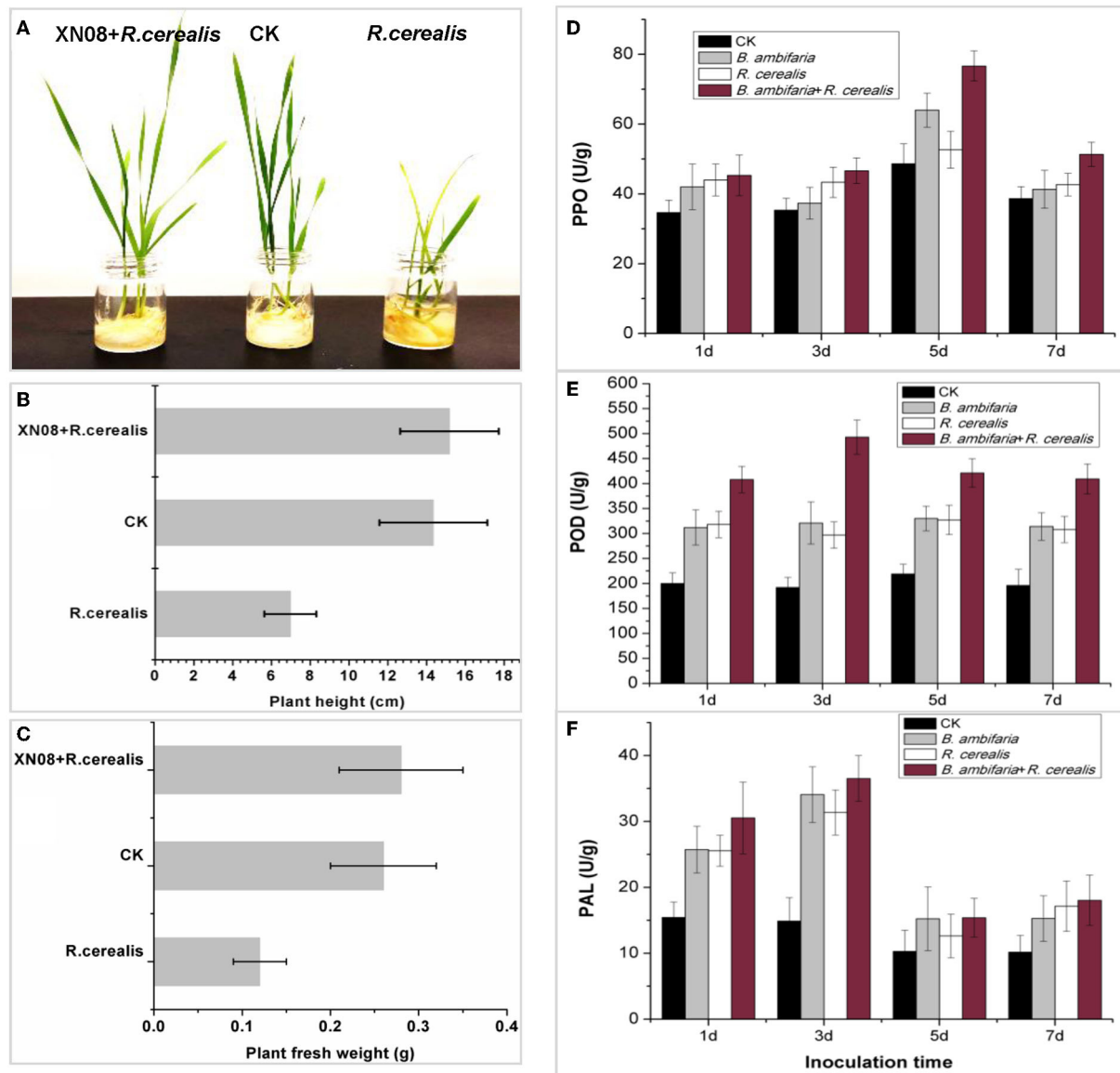


FIGURE 4

Antagonistic activities and plant growth-promoting characteristics of the strain XN08 in the pot experiments. Morphological changes in wheat seedlings (A), plant heights (B), plant fresh weights (C), and the activities of defense enzymes, including PPO (D), POD (E), and PAL (F) under different treatments.

with the capacity of P-solubilization, nitrogenase, and IAA production (Rana et al., 2020). Larran et al. (2016) isolated the endophytes from wheat cultivars and found that the endophytes of *Penicillium* sp., *Bacillus* sp., and *Paecilomyces lilacinus* significantly suppressed the growth of pathogens *in vitro* and have the potential to be developed as new biological agents against the tan spot of wheat. In this study, the endophytic bacterium *B. ambifaria* XN08, which was isolated from healthy wheat plants, showed potential as a novel biological control agent against the wheat sharp eyespot. After all, only *Bacillus* spp. were exploited as biocontrol agents against *R. cerealis* in the previous reports (Ji et al., 2019; Yi et al., 2022).

*Burkholderia* is a genus of gram-negative bacteria with a wide environmental and geographic distribution (Estrada-De los Santos et al., 2001). Over the last years, there was an increasing interest in the genus *Burkholderia* due to its great potential value in plant growth promotion, biocontrol of plant pathogens, and phytoremediation (Bach et al., 2021). It was reported that bacterial endophytes belonging to *Bacillus* and *Burkholderia* genera were the most effective isolates in controlling bacterial and fungal pathogens *in vitro* (Morales-Cedeno et al., 2021). In fact, *Burkholderia* genus has rich antibiotic synthesis genes (Kim et al., 2021), and it has been reported to produce a large number of antifungal substances such as pyrrolnitrin,

siderophores, and phenazines (Mullins et al., 2019), all of which play important roles in controlling fungal diseases in plants. In this study, a known powerful antifungal compound named pyrrolnitrin, production by XN08, was found, proving that the strain is valuable in controlling diseases including the wheat sharp eyespot. In addition, it is quite interesting that pyrrolnitrin production is quorum-sensing regulated, which indicates that efficient environmental colonization is crucial for the effective control of the wheat sharp eyespot disease (Chapalain et al., 2013).

Plant growth promotion and environmental colonization characteristics also determine the great potential of the *Burkholderia* genus as biocontrol agents (Paungfoo-Lonhienne et al., 2016). To observe the bacterial colonization directly and conveniently, a derivative strain carrying *GFP* gene was constructed in this study. The GFP-tagged *B. ambifaria* showed a similar inhibition ratio against *R. cerealis* as the wild-type strain, which indicated that the derivative strain could be used to efficiently observe its colonization in wheat plant tissue. Fluorescent labeling technology was the most intuitive way of representing the colonization of strain and was widely used in studying the plants and microorganisms interaction (Rilling et al., 2019; Sa et al., 2021). A number of potential biocontrol strains, including *Pseudomonas fluorescens*, *Paenibacillus glycanilyticus*, *Burkholderia tropica*, and *Bacillus velezensis*, labeled with a green fluorescent protein have been used to study their colonization capacity in plant tissue (Bernabeu et al., 2015; Kang et al., 2018; Li et al., 2019; Elsayed et al., 2020). However, as far as we know, this is the first time that *B. ambifaria* was labeled with green fluorescent protein to study the colonization characterized in this study.

It was reported that PGPB induced plants defense-related genes expression such as phenylalanine ammonia-lyase (PAL), catalase (CAT), polyphenol oxidase (PPO), peroxidase (POD), and superoxide dismutase (SOD), which might assist the plant to protect from or reduce the impact of pathogen attacks (Jiang et al., 2019; Kamou et al., 2019; Wu et al., 2019; Zhu et al., 2019; Ashajyothi et al., 2020; Singh et al., 2021). Our results showed that the significant colonization of XN08, visually observed with CLSM, was accompanied by the higher activities of PPO, POD, and PAL, which indicated that *B. ambifaria* XN08 was involved in the immune-induced resistance of wheat seedlings. In addition, the results also showed that the endophytic bacterial strain XN08 could significantly improve the growth of wheat inoculated with *R. cerealis*. The fresh weight and shoot height of the seedlings inoculated with both *R. cerealis* and GFP-tagged *B. ambifaria* were similar to those of the control group. Meanwhile, no obvious sharp eyespot symptom was observed for the group seedlings inoculated with both *R. cerealis* and GFP-tagged *B. ambifaria*. It is obvious that XN08 may provide an adequate protection against wheat disease.

On a whole, the results obtained in this study revealed that XN08 had great potential for biological control against

the wheat sharp eyespot. However, it is worth noting that the successful application of XN08 for biocontrol of sharp eyespot in wheat needs knowledge of the ecological/environmental factors affecting the colonization of crops. Therefore, further observation using GFP-tagged *B. ambifaria* under different environmental conditions should be performed.

## Conclusion

Taken together, it was concluded that *B. ambifaria* XN08 was able to efficiently inhibit the growth of *R. cerealis* by producing antifungal compounds and showed the capacity to enhance plant growth by synthesizing a series of plant growth regulators. In addition, this strain exhibited significant colonization in wheat plants, which was accompanied by an enhancement of wheat plants' growth and an induction of immune resistance for wheat seedlings. These data indicated that the strain XN08 might be used as a new biocontrol agent against wheat sharp eyespot.

## Data availability statement

The original contributions presented in the study are included in the article/Supplementary materials, further inquiries can be directed to the corresponding author.

## Author contributions

CA performed the experiments, wrote, and edited the manuscript. WX designed and supervised the project. All experiments were also performed by SM, CL, and HD. All authors contributed to the article and approved the submitted version.

## Funding

This study was simultaneously supported by the National Natural Science Foundation of China (21576160) and the Scientific and Technologic Research Program of Shaanxi Academy of Sciences, China (No. 2018K-09).

## Acknowledgments

The authors thank the National Natural Science Foundation of China for financial support. They also thank Shaanxi Province Academy of Sciences for financial support, authors acknowledge technical support of Dr. Chenlin for the construction of a derivative *Burkholderia ambifaria* strain carrying GFP gene used in this study.



## Conflict of interest

The authors declare that the research was conducted in the absence of any commercial or financial relationships that could be construed as a potential conflict of interest.

## Publisher's note

All claims expressed in this article are solely those of the authors and do not necessarily represent those of their affiliated

organizations, or those of the publisher, the editors and the reviewers. Any product that may be evaluated in this article, or claim that may be made by its manufacturer, is not guaranteed or endorsed by the publisher.

## Supplementary material

The Supplementary Material for this article can be found online at: <https://www.frontiersin.org/articles/10.3389/fmicb.2022.906724/full#supplementary-material>

## References

- Ashajyothi, M., Kumar, A., Sheoran, N., Ganesan, P., Gogoi, R., Subbaiyan, G. K., et al. (2020). Black Pepper (*Piper Nigrum* L.) associated endophytic *Pseudomonas putida* BP25 alters root phenotype and induces defense in rice (*Oryza Sativa* L.) against blast disease incited by *Magnaporthe oryzae*. *Biol. Control*. 143, 104181. doi: 10.1016/j.biocontrol.2019.104181
- Bach, E., Passaglia, L. M. P., Jiao, J. J., and Gross, H. (2021). *Burkholderia* in the genomic era: from taxonomy to the discovery of new antimicrobial secondary metabolites. *Crit. Rev. Microbiol.* 48, 121–160. doi: 10.1080/1040841X.2021.1946009
- Bernabeu, P. R., Pistorio, M., Torres-Tejerizo, G., Estrada-De los Santos, P., Galar, M. L., Boiardi, J. L., et al. (2015). Colonization and plant growth-promotion of tomato by *Burkholderia tropica*. *Sci. Horticulture-amsterdam*. 191, 113–120. doi: 10.1016/j.scienta.2015.05.014
- Bo, T. T., Kong, C. X., Zou, S. X., Mo, M. H., and Liu, Y. J. (2022). *Bacillus nematocida* B16 enhanced the rhizosphere colonization of *Pochonia chlamydosporia* ZK7 and controlled the efficacy of the root-knot nematode *Meloidogyne incognita*. *Microorganisms*. 10, 218. doi: 10.3390/microorganisms10020218
- Chapalain, A., Vial, L., Laprade, N. atacha., Dekimpe, V., Perreault, J., and Déziel, E. (2013). Identification of quorum sensing-controlled genes in *Burkholderia ambifaria*. *MicrobiologyOpen* 2, 226–242. doi: 10.1002/mbo3.67
- Cui, W. Y., He, P. J., Munir, S., He, P. B., Li, X. Y., Li, Y. M., et al. (2019). Efficacy of plant growth promoting bacteria *Bacillus amyloliquefaciens* B9601-Y2 for biocontrol of southern corn leaf blight. *Biol. Control*. 139, 104080. doi: 10.1016/j.biocontrol.2019.104080
- Dimkić, I., Janakiev, T., Petrović, M., Degraffi, G., and Fira, D. (2022). Plant-associated *Bacillus* and *Pseudomonas* antimicrobial activities in plant disease suppression via biological control mechanisms-a review. *Physiol. Mol. Plant. P.* 117, 101754. doi: 10.1016/j.pmp.2021.101754
- Elsayed, T. R., Jacquid, S., Nour, E. H., and Sørensen, S. J., Smalla, K. (2020). Biocontrol of bacterial wilt disease through complex interaction between tomato plant, antagonists, the indigenous rhizosphere microbiota, and *Ralstonia solanacearum*. *Front. Microbiol.* 10, 2835. doi: 10.3389/fmicb.2019.02835
- Estrada-De los Santos, P., Bustillos-Cristales, R., and Caballero-Mellado, J. (2021). *Burkholderia*, a genus rich in plant-associated nitrogen fixers with wide environmental and geographic distribution. *Appl. Environ. Microbiol.* 67, 2790–2798. doi: 10.1128/AEM.67.6.2790-2798.2001
- Fu, M. R., Zhang, X. M., Jin, T., Li, B. Q., Zhang, Z. Q., Tian, S., et al. (2019). Inhibitory of grey mold on green pepper and winter jujube by chlorine dioxide (ClO<sub>2</sub>) fumigation and its mechanisms. *LWT* 100, 335–340. doi: 10.1016/j.lwt.2018.10.092
- Ji, P., Li, W. G., Zheng, Y. X., Wang, Z. H., Huo, Q. X., Hua, C. Y., and Han, C. (2019). Isolation and identification of four novel biocontrol *Bacillus* strains against wheat sharp eyespot and their growth-promoting effect on wheat seedling. *Int. J. Agric. Biol.* 21, 282–288. doi: 10.17957/IJAB/15.0892
- Jiang, C. H., Yao, X. F., Mi, D. D., Li, Z. J., Yang, B. Y., Zheng, Y., et al. (2019). Comparative transcriptome analysis reveals the biocontrol mechanism of *Bacillus velezensis* F21 against *Fusarium Wilt* on Watermelon. *Front. Microbiol.* 10, 652. doi: 10.3389/fmicb.2019.00652
- Jing, L. M., Jeong, J. C., Lee, J. S., Park, J. M., Yang, J. W., Lee, M. H., et al. (2019). Potential of *Pantoea dispersa* as an effective biocontrol agent for black rot in sweet potato. *Sci. Rep.* 9, 16354. doi: 10.1038/s41598-019-52804-3
- Kamou, N. N., Cazorla, F., Kandyas, G., and Lagopodi, A. L. (2019). Induction of defense-related genes in tomato plants after treatments with the biocontrol agents *Pseudomonas chlororaphis* Toza7 and *Clonostachys rosea* Ik726. *Arch. Microbiol.* 202, 257–267. doi: 10.1007/s00203-019-01739-4
- Kang, X. X., Zhang, W. L., Cai, X. C., Zhu, T., Xue, Y. R., and Liu, C. H. (2018). *Bacillus velezensis* CC09: a potential 'vaccine' for controlling wheat diseases. *Mol. Plant. Microbe. Interact.* 31, 623–632. doi: 10.1094/MPMI-09-17-0227-R
- Kim, S., Jo, S., Kim, M. S., and Shin, D. H. (2021). A study of inhibitors of D-glycero-β-d-manno-heptose-1-phosphate adenyltransferase from *Burkholderia pseudomallei* as a potential antibiotic target. *J. Enzyme. Inhib. Med. Chem.* 36, 776–784. doi: 10.1080/14756366.2021.1900166
- Larran, S., Simón, M. R., Moreno, M. V., Santamarina Siurana, M. P., and Perelló, A. (2016). Endophytes from wheat as biocontrol agents against tan spot disease. *Bio. Control*. 92, 17–23. doi: 10.1016/j.biocontrol.2015.09.002
- Li, L. M., Zhang, Z., Pan, S. Y., Li, L., and Li, X. Y. (2019). Characterization and metabolism effect of seed endophytic bacteria associated with peanut grown in South China. *Front. Microbiol.* 10, 2659. doi: 10.3389/fmicb.2019.02659
- Morales-Cedeno, L. R., Orozco-Mosqueda, M. D., Loeza-Lara, P. D., Parra-Cota, F. I., de los Santos-Villalobos, S., and Santoyo, G. (2021). Plant growth-promoting bacterial endophytes as biocontrol agents of pre- and post-harvest diseases: fundamentals, methods of application and future perspectives. *Microbiol. Res.* 242, 126612. doi: 10.1016/j.micres.2020.126612
- Mullins, A. J., Murray, J. A. H., Bull, M. J., Jenner, M., Jones, C., Webster, G., et al. (2019). Genome mining identifies cepacin as a plant-protective metabolite of the biopesticidal bacterium *Burkholderia ambifaria*. *Nat. Microbiol.* 4, 996–1005. doi: 10.1038/s41564-019-0383-z
- Patten, C. L., and Glick, B. R. (2002). Role of *Pseudomonas putida* indoleacetic acid in development of the host plant root system. *Appl. Environ. Microb.* 68, 3795–3801. doi: 10.1128/AEM.68.8.3795-3801.2002
- Paungfoo-Lonhienne, C., Lonhienne, T. G. A., Yeoh, Y. K., Donose, B. C., Webb, R. I., Parsons, J., et al. (2016). Crosstalk between sugarcane and a plant growth promoting *Burkholderia* species. *Sci. Rep.* 6, 37389. doi: 10.1038/srep37389
- Rana, K. L., Kour, D., Kaur, T., Sheikh, T., Yadav, A. M., Kumar, V., et al. (2020). Endophytic microbes from diverse wheat genotypes and their potential biotechnological applications in plant growth promotion and nutrient uptake. *Proc. Natl. Acad. Sci. India* 90, 969–979. doi: 10.1007/s40011-020-01168-0
- Raymaekers, K., Ponet, L., Holtappels, D., Berckmans, B., and Cammue, B. A. (2020). Screening for novel biocontrol agents applicable in plant disease management – a review. *Biol. Control*. 144, 104240. doi: 10.1016/j.biocontrol.2020.104240
- Rilling, J. I., Acuña, J. J., Nannipieri, P., Cassan, F., Maruyama, F., and Jorquera, M. A. (2019). Current opinion and perspectives on the methods for tracking and monitoring plant growth-promoting bacteria. *Soil. Biol. Biochem.* 130, 205–219. doi: 10.1016/j.soilbio.2018.12.012
- Sa, R. B., Zhang, J. L., Sun, J. Z., and Gao, Y. X. (2021). Colonization characteristics of poplar fungal disease biocontrol bacteria n6-34 and the inhibitory

effect on pathogenic fungi by real-time fluorescence quantitative PCR detection. *Curr. Microbiol.* 78, 2916–2925. doi: 10.1007/s00284-021-02529-2

Saad, M. M. G., Kandil, M., and Mohammed, Y. M. M. (2020). Isolation and identification of plant growth-promoting bacteria highly effective in suppressing root rot in fava beans. *Curr. Microbiol.* 77, 2155–2165. doi: 10.1007/s00284-020-02015-1

Shahid, M., Hameed, S., Imran, A., Ali, S., and Elsas, J. D. V. (2012). Root colonization and growth promotion of sunflower (*Helianthus Annuus* L.) by phosphate solubilizing *Enterobacter* sp. Fs-11. *World. J. Microb. Biot.* 28, 2749–2758. doi: 10.1007/s11274-012-1086-2

Singh, P., Singh, R. K., Li, H. B., Guo, D. J., Sharma, A., Lakshmanan, P., et al. (2021). Diazotrophic bacteria *Pantoea dispersa* and *Enterobacter asburiae* promote sugarcane growth by inducing nitrogen uptake and defense-related gene expression. *Front. Microbiol.* 11, 600417. doi: 10.3389/fmicb.2020.600417

Su, Q., Wang, K., and Zhang, Z. Y. (2020). Ecotopic expression of the antimicrobial peptide dmamp1w improves resistance of transgenic wheat to two diseases: sharp eyespot and common root rot. *Int. J. Mol. Sci.* 21, 647. doi: 10.3390/ijms21020647

Takishita, Y., Charron, J. B., and Smith, D. L. (2018). Biocontrol rhizobacterium *Pseudomonas* sp. 23S induces systemic resistance in tomato (*Solanum lycopersicum* L.) against bacterial canker *Clavibacter michiganensis* subsp *michiganensis*. *Front. Microbiol.* 9, 2119. doi: 10.3389/fmicb.2018.02119

Vasiee, A., Behbahani, B. A., Yazdi, F. T., and Mortazavi, S. A. (2018). Diversity and probiotic potential of lactic acid bacteria isolated from Horreh, a traditional Iranian fermented food. *Probiotics. Antimicrob.* 10, 258–268. doi: 10.1007/s12602-017-9282-x

Wang, M., Zhu, X. L., Wang, K., Lu, C. G., Luo, M. Y., Shan, T. L., et al. (2018). Wheat caffeic acid 3-O-methyltransferase Tacomt-3d positively contributes to both resistance to sharp eyespot disease and stem mechanical strength. *Sci. Rep.* 8, 6543. doi: 10.1038/s41598-018-24884-0

Wu, Z. S., Huang, Y. Y., Li, Y., Dong, J. W., Liu, X. C., and Li, C. (2019). Biocontrol of *Rhizoctonia solani* via induction of the defense mechanism and antimicrobial compounds produced by *Bacillus subtilis* SL-44 on Pepper (*Capsicum annuum* L.). *Front. Microbiol.* 10, 2676. doi: 10.3389/fmicb.2019.02676

Xu, Y. L., Li, X. Y., Cong, C., Gong, G. L., Xu, Y. P., Che, J., et al. (2020). Use of resistant *Rhizoctonia cerealis* strains to control wheat sharp eyespot using organically developed pig manure fertilizer. *Sci. Total. Environ.* 726, 138568. doi: 10.1016/j.scitotenv.2020.138568

Yi, Y., Luan, P., Liu, S., Shan, Y., Hou, Z., Zhao, S., Jia, S., and Li, R. (2022). Efficacy of *Bacillus subtilis* XZ18-3 as a biocontrol agent against *Rhizoctonia cerealis* on wheat. *Agriculture* 12, 258. doi: 10.3390/agriculture12020258

Zhang, Z. X., Wang, H. Y., Wang, K. Y., Jiang, L. L., and Wang, D. (2017). Use of lentinan to control sharp eyespot of wheat, and the mechanism involved. *J. Agr. Food. Chem.* 65, 10891–10898. doi: 10.1021/acs.jafc.7b04665

Zhao, X. L., Song, P., Hou, D. Y., Li, Z. L., and Hu, Z. J. (2021). Antifungal activity, identification and isosynthetic potential analysis of fungi against *Rhizoctonia cerealis*. *Ann. Microbiol.* 71, 41. doi: 10.1186/s13213-021-01654-4

Zhu, H. M., Zhao, L. N., Zhang, X. Y., Foku, J. M., Li, J., Hu, W. C., et al. (2019). Efficacy of *Yarrowia lipolytica* in the biocontrol of green mold and blue mold in *Citrus reticulata* and the mechanisms involved. *Biol. Control.* 139, 104096. doi: 10.1016/j.biocontrol.2019.104096



## OPEN ACCESS

## EDITED BY

Vijay K. Sharma,  
Agricultural Research Organization  
(ARO), Israel

## REVIEWED BY

Pooja Suneja,  
Maharshi Dayanand University, India  
Wei Zhang,  
Nanjing Normal University, China  
Ari Fina Bintarti,  
Michigan State University,  
United States

## \*CORRESPONDENCE

Jie Xie  
Healthjie@163.com

## SPECIALTY SECTION

This article was submitted to  
Microbiotechnology,  
a section of the journal  
Frontiers in Microbiology

RECEIVED 26 June 2022

ACCEPTED 29 July 2022

PUBLISHED 12 August 2022

## CITATION

Ou T, Gao H, Jiang K, Yu J, Zhao R,  
Liu X, Zhou Z, Xiang Z and Xie J (2022)  
Endophytic *Klebsiella aerogenes*  
HGG15 stimulates mulberry growth  
in hydro-fluctuation belt  
and the potential mechanisms as  
revealed by microbiome  
and metabolomics.  
*Front. Microbiol.* 13:978550.  
doi: 10.3389/fmicb.2022.978550

## COPYRIGHT

© 2022 Ou, Gao, Jiang, Yu, Zhao, Liu,  
Zhou, Xiang and Xie. This is an  
open-access article distributed under  
the terms of the [Creative Commons  
Attribution License \(CC BY\)](https://creativecommons.org/licenses/by/4.0/). The use,  
distribution or reproduction in other  
forums is permitted, provided the  
original author(s) and the copyright  
owner(s) are credited and that the  
original publication in this journal is  
cited, in accordance with accepted  
academic practice. No use, distribution  
or reproduction is permitted which  
does not comply with these terms.

# Endophytic *Klebsiella aerogenes* HGG15 stimulates mulberry growth in hydro-fluctuation belt and the potential mechanisms as revealed by microbiome and metabolomics

Ting Ou<sup>1</sup>, Haiying Gao<sup>1</sup>, Kun Jiang<sup>1</sup>, Jing Yu<sup>1</sup>, Ruolin Zhao<sup>1</sup>,  
Xiaojiao Liu<sup>1</sup>, Zeyang Zhou<sup>1,2</sup>, Zhonghuai Xiang<sup>1</sup> and Jie Xie<sup>1\*</sup>

<sup>1</sup>State Key Laboratory of Silkworm Genome Biology, Key Laboratory of Sericultural Biology and Genetic Breeding in Ministry of Agriculture, College of Sericulture, Textile and Biomass Science, Southwest University, Chongqing, China, <sup>2</sup>College of Life Science, Chongqing Normal University, Chongqing, China

Growth promotion and stress tolerance induced by endophytes have been observed in various plants, but their effects on mulberry regularly suffering flood in the hydro-fluctuation belt are less understood. In the present study, endophytic *Klebsiella aerogenes* HGG15 was screened out from 28 plant growth promotion (PGP) bacteria as having superior PGP traits *in vitro* and *in planta* as well as biosafety for silkworms. *K. aerogenes* HGG15 could actively colonize into roots of mulberry and subsequently transferred to stems and leaves. The 16S ribosomal RNA (V3–V4 variable regions) amplicon sequencing revealed that exogenous application of *K. aerogenes* HGG15 altered the bacterial community structures of mulberry roots and stems. Moreover, the genus of *Klebsiella* was particularly enriched in inoculated mulberry roots and was positively correlated with mulberry development and soil potassium content. Untargeted metabolic profiles uncovered 201 differentially abundant metabolites (DEMs) between inoculated and control mulberry, with lipids and organo-heterocyclic compounds being particularly abundant DEMs. In addition, a high abundance of abiotic stress response factors and promotion growth stimulators such as glycerolipid, sphingolipid, indole, pyridine, and coumarin were observed in inoculated mulberry. Collectively, the knowledge gained from this study sheds light on potential strategies to enhance mulberry growth in hydro-fluctuation belt, and microbiome and metabolite analyses provide new insights into the growth promotion mechanisms used by plant-associated bacteria.

## KEYWORDS

endophyte, plant growth promotion, flood, microbiome, metabolite

## Introduction

The Three Gorges Reservoir (TGR), the largest reservoir ever built in China, was constructed for the purposes of flood control, hydropower generation, and navigation, where the water level is periodically maintained 145 m above sea level in summer (May–September) but increasing to 175 m in winter (October–April) (Wang et al., 2018; Yin et al., 2020). As a result of this artificial water control, a 30 m water level fluctuation occurs on the banks, called a hydro-fluctuation belt. This annual reverse-seasonal flood maintaining nearly half a year in the TGR has caused serious degradation of the vegetation in the hydro-fluctuation belt, which has led to considerable soil erosion, habitat loss, biodiversity decline, and environmental pollution (Liu and Willison, 2013). Mulberry (*Morus* L.), a woody perennial, is a plant species with potential for revegetating the hydro-fluctuation belt of the TGR due to its strong resistance to flood stress and ability to grow well in this limited-nutrient environment (Huang et al., 2013). However, while initially vigorous, mulberry trees (“Guisangyou 62,” *Morus alba* L.) planted in 2012 at the hydro-fluctuation belt for revegetation were partially dead and their growth status varied considerably, after several years of fluctuating water levels. The well-growing newly planted trees were deeply rooted and had strong trunks and healthy leaves, while poorly-growing newly planted trees had underdeveloped root systems. Moreover, many wild mulberry trees grew exuberantly and had great vitality in the same field, which were planted by local residents and presented prior to the establishment of the TGR, but their genetic background was unclear (Xie et al., 2021). Given that the development of mulberry trees in TGR was often adversely affected by flood stress, there is a need to promote its growth and increase flood tolerance so that it can be used in revegetation efforts.

Exposure of plants to adverse environmental conditions disrupts their metabolism, ultimately leading to reduced fitness and productivity (Montesinos-Navarro et al., 2020). In the course of evolution, plants have evolved an array of protective mechanisms allowing them to adapt and survive in such stressful environments. A crucial step in plant responses is their timely perception of the stress to respond in a rapid and efficient manner. Responses typically involve activation of specific ion channels and kinase cascades and the accumulation of reactive oxygen species and phytohormones, all of which result in appropriate defense reactions and thus increase plant tolerance. Most commonly plants adjust their metabolic pathways to produce a series of anti-stress substances when encountering stress challenges. For instance, the concentrations of secondary metabolites (glycosides, alkaloids, phenolics, terpenoids) are highly accumulated in *Catharanthus roseus* (Saravanan, 2021) and *Elaeis guineensis* (Ibrahim and Jaafar, 2012) when treated with high levels of carbon dioxide. Moreover, maize specifically produced iron-benzoxazinoid complexes to defend against herbivores and further improve their growth (Hu et al., 2018).

Apart from their intrinsic mechanisms, plants also can alleviate the burden of environmental stresses by associating with particular endophytic microbes. Plant endophytes are typically non-pathogenic microbes that colonize in the interior space of plant tissues at some period in their life cycle, including roots, stems, leaves, flowers, fruits, and seeds (Compant et al., 2010; Zhang et al., 2019). They have been shown to play a crucial role in maintaining terrestrial ecosystems since their beneficial functions including defending hosts from biotic stress, alleviating harm from abiotic stress, and supporting host plant nutrition by increasing phosphorus, nitrogen, and iron levels (Bacon and White, 2015). Increased biomass in inoculated plant has been reported as a result of their colonization by a variety of endophytic genera such as *Bacillus* (Xu et al., 2019), *Streptomyces* (Jaemsaeng et al., 2018), *Klebsiella* (Zhang et al., 2017), *Pantoea* (Xie et al., 2017), and *Pseudomonas* (Han et al., 2015). In addition, the improvement of stress resistance in crop plants using endophytic microorganism is cost-effective and ecofriendly for the environment (Olanrewaju et al., 2017; Nascimento et al., 2018). For example, inoculation of endophytic *Bacillus cereus* PE31 could promote the phytoremediation efficiency of *Phytolacca acinosa* in Cadmium contaminated soils (Liu et al., 2022). Moreover, introduction of exogenous endophytes can induce host plants to recruit beneficial taxa. The process alters associated-microbiome composition of host, thus indirectly attributes to plant development as well (Welmillage et al., 2021). The application of endophytic *Rhizobium* sp. RF67 isolated from *Vaccinium angustifolium* resulted in root-associated bacteria variation, which boosted cooperation of plant-growth-promoting endophytes (Yurgel et al., 2022). Moreover, *Piriformospora indica* recruited the member of Firmicutes and decreased Proteobacteria in rice roots, resulting in enhancement of rhizosheath and improvement of drought tolerance (Xu F. Y. et al., 2022). Beneficial interactions between endophyte and plant have gradually become a focus of many studies addressing ecological restoration such as deserts (Jain et al., 2021), saline-alkaline lands (Lu et al., 2021), and oil or heavy metal contaminated lands (Liu et al., 2022). However, the utilization of endophyte and plant to restore ecosystems subjected to repeated flood stress such as the hydro-fluctuation belt of the TGR has not received much attention.

The results of 16S ribosomal amplicon sequencing in our previous study revealed that the complexity of endophytic bacterial interactions in well-growing mulberry trees, including newly planted mulberry and wild mulberry, was higher than it was in poorly-growing mulberry tree. Additionally, well-growing trees were found to have recruited similar endophytic bacteria that enabled them to flourish in hydro-fluctuation belt (Xie et al., 2021). Thus, we hypothesized that endophytic bacteria of well-growing mulberry trees could be a potential resource to promote mulberry growth in such settings. Therefore, objectives of this work were to (i) obtain endosphere-derived bacteria from well-growing mulberry trees and detect their potentials to benefiting the

growth of mulberry *in vitro* and *in planta*; (ii) test plant colonization capability of plant growth promoting bacteria by using of a green fluorescence protein marker; and (iii) further decipher the underlying preliminary mechanisms how bacteria promote mulberry growth by comprehensively interrogating the mulberry associated microbiome and metabolome.

## Materials and methods

### Sample collection and isolation of endophytic bacteria

Samples were collected from well-growing mulberry trees including wild mulberry trees (WM) and newly planted mulberry trees (NM) from the hydro-fluctuation belt in Longjiao Town, Yunyang County, Chongqing Municipality, China (30°49'26" N, 108°52'14" E) in May, 2020. A total of four types of sample were obtained including two compartments (stem and root) of WM and NM. Three biological replicates were performed for each sample. Characteristics of mulberry trees were shown in [Supplementary Table 1](#). These mulberry trees were suffered flood stress lasting for about 6 months. The elevation of this sampling area was approximately at 172 m above sea level and the water level of TGR was about 152 m above sea level at that time. Mulberry stem segments were collected at approximately 25 cm in length where leaves and small side branches had been removed. The sampling depth of root was about 15 cm below soil surface and the length of root segments was about 20 cm. All samples were immediately transported back to the laboratory and stored at 4°C until further processing.

Surface sterilization of the mulberry stem and root was performed according to a previously described procedure ([Xu et al., 2019](#)), and the endophytic bacteria were isolated using the fragmentation technique ([Liotti et al., 2018](#)). Samples were washed with tap water to remove soil and other debris before being cut into pieces with 3.0–5.0 cm in length. The samples were then thoroughly soaked in 75% ethanol and rapidly flame-sterilized. Afterward, samples were peeled to obtain smaller fragments and placed on nutrient agar (NA), Gause's agar (GA), Luria-Bertani agar (LB), and Trypticase Soya agar (TSA) medium at 28°C for 5 days. Isolates with different morphological characteristics were purified and stored with 50% glycerol at –80°C.

### Screening of plant growth promoting bacteria and molecular characterization analysis

The plant growth promotion (PGP) traits of endophytes, including phosphate (P) solubilization, indole-3-acetic acid

(IAA), siderophore, and acetoin production, and antagonistic activity against phytopathogen *Sclerotinia sclerotiorum*, which could seriously infect mulberry flowers and branches, were qualitatively determined by following procedures. Specifically, isolates were inoculated in LB medium and incubated at 30°C with 180 rpm for 16 h, and then 10 µL of each bacterial culture was inoculated on different medium to detect PGP traits, respectively. The ability of isolates to P solubilization was evaluated in Pikovskaya's agar medium containing tricalcium phosphate ([Gaiind, 2016](#)) and the siderophore activity was tested in chrome azurol-s agar medium ([Jasim et al., 2013](#)). The detections of IAA and acetoin activities were conducted in LB medium as described by [Patten and Glick \(1996\)](#) and [Viviji et al. \(2014\)](#), respectively. The antifungal bioactivities were evaluated on PDA medium by the dual culture technique as described by [Xu et al. \(2019\)](#).

Molecular characterization of plant growth promoting bacteria (PGPB) was tested based on 16S rRNA gene sequence. The genomic DNA of PGPB was extracted using a PrepMan Ultra Sample Preparation Reagent kit (Applied Biosystems, Palo Alto, CA, United States) according to the manufacturer's instructions and amplified by PCR using universal 16S rRNA gene primers 27F/1492R ([Ou et al., 2022](#)). Each 25 µL PCR mixture contained 12.5 µL of 2 × Rapid Taq Mater Mix (Vazyme, Nanjing, China), 1 µL of each primer (10 µM), and 10 ng of template DNA. The PCR reaction was carried out using the following conditions: 1 cycle of 95°C for 4 min; followed by 30 cycles of 94°C for 30 s, 55°C for 45 s and 72°C for 1 min; and a final extension at 72°C for 8 min. The PCR amplified products were purified with the DNA Clean & Concentrator™-5 Kit (Zymo Research, United States) and then sequenced by the Sanger method at Sangon Biotechnology Co., Ltd., Shanghai, China. The nucleotide sequences of PGPB were compared using Basic Local Alignment Search Tool (BLAST) method and deposited in NCBI GenBank database. In present study, the isolates with high level of identity (97–100%) were selected as the closest match, and all isolates were classified to the genus level.

### Evaluation of the activity of the bacteria in mulberry

The isolates exhibiting high PGP potentials *in vitro* were selected and their effects on mulberry seedling growth were further evaluated *in planta*. Fresh colony of PGPB was inoculated into LB medium and incubated at 30°C with 180 rpm for 18 h. The cultures were centrifuged at 8000 rpm for 10 min and precipitate was adjusted at  $1 \times 10^7$  CFU/mL using the sterile water ([Ou et al., 2022](#)).

“Guisangyou 62,” a variety of white mulberry, is a potential for phytoremediation since the quick-growth and



ecological-adaptation characterizations (Zhao et al., 2013; Jiang et al., 2019). This mulberry cultivar thus was applied in the present study. Mulberry seeds were surface sterilized with 75% ethanol for 3 min and 10% sodium hypochlorite for 3 min. After five times rinse with sterile distilled water, seeds were placed in a 9-cm-diameter petri dish containing sterilized moistened filter paper and maintained in growth chamber at 25°C with a photoperiod of 12 h at  $200 \mu\text{mol}\cdot\text{m}^{-2}\cdot\text{s}^{-1}$  and 70% humidity. At two-leaf stage, seedlings were transferred to pot which was filled with mixtures of humus and filed soil (4:1; v/v) collected from Southwest University experimental farm (29°49'1" N, 106°24'57" E). The mixed soils were sterilized four times by autoclaving at 121°C for 2 h (Li et al., 2012; Cao et al., 2013). Each pot contained three mulberry seedlings with similar size and height. After 2 weeks, mulberry seedlings with three-leaf were inoculated with PGPBs through irrigating 30 mL of bacterial suspension into soils in each pot, and the mulberry seedlings treated with sterile water were served as control. Each treatment was replicated twenty times. After 30-day inoculation, eight seedlings were randomly selected in each treatment to measure length of root and shoot, fresh and dry weight of root and shoot, and number of root tip.

To assess the effects of PGPBs on mulberry growth under flood stress condition, the remaining mulberry seedlings were completely submerged wherein the water level was 30 cm above soil surface. After 40 days, the degree of cell death of mulberry leaf was determined using Evan's blue staining (Taylor and West, 1980). Finally, nine seedlings were randomly selected and the root fresh weight was calculated, and the total length and fork of roots were analyzed using the GXY-B root analysis system (Hangzhou Lvbo instrument Co., Ltd, Hangzhou, China).

## Bio-safety assessment of plant growth promoting bacteria on silkworms

In order to lay a good foundation for utilization of PGPB to promote mulberry growth in the field, the biosafety was studied through feeding silkworms with PGPBs-infected mulberry leaves. One milliliter of  $1 \times 10^7$  CFU/mL bacterial suspension was sprayed on the surface of each leaf (Xie et al., 2017). The sterile water was used as control. Mulberry leaves dried naturally were applied to feed healthy silkworm larvae (871 × 872 strain) at the 4th instar with two times each day. Afterward, all silkworms were fed with clean mulberry leaves until cocoon formation. Each treatment consisted of three replicates and each replicate contained forty silkworms. The growth status of silkworm was observed every day. The survival rate and rate of cocoon formation of three replicates were determined. Forty silkworms were randomly selected to measure cocoon weight, cocoon shell rate and weight, and pupal weight.

## Identification of HGG15 strain

Based on plant growth promoting activity in mulberry seedlings and bio-safety on silkworm of PGPBs, the HGG15 strain was finally screened out for further study. The morphological characteristics of HGG15 in LB incubated at 37°C for 24 h were recorded and further observed in scanning electron microscope (Hitachi, SU3500, Japan). Gram staining was performed and observed under an optical microscope (Becerra et al., 2016). Series of biochemical tests such as Voges-Proskauer and motility test were conducted using an HK-MID-66 kit (HUANKAI, China) following the protocol provided by the manufacturer. Phylogenetic tree of HGG15 based on 16S rRNA gene sequence was constructed by applying the neighbor-joining method using MEGA version 6.0 with 1,000 replicates of bootstrap values (Tamura et al., 2011).

## Colonization of mulberry by HGG15 strain

To explore colonization characteristics of HGG15 strain in mulberry, the plasmid pGFP4412 containing green fluorescence protein (*gfp*) and kanamycin resistance gene was transformed into the wild type HGG15 strain by electroporation technique. The competent cells were prepared in 10% glycerol and electroporated at 2.5 kv for 5 ms. Transformed colonies that emitted green fluorescence stably under fluorescence microscopy (Leica, DM3000, Germany) were obtained and designated HGG15/*gfp* strain.

The cultivation of mulberry seedlings was shown as described above and roots of mulberry at two-leaf-stage were immersed in  $1 \times 10^7$  CFU/mL bacterial suspension for 4 h and then re-planted into the sterile soil. The sterile distilled water was served as control group. Afterward, seedlings were removed from pots, surface disinfected using 75% ethanol for 1 min, and separated into roots, stems and leaves at different time after inoculation. And then, these tissues of mulberry were cut into small pieces to observe the colonization using fluorescence microscopy. In addition, these tissues were weighed and ground in 1 mL sterile distilled water, and serially diluted and plated on LB plates supplemented with 50  $\mu\text{g}/\text{mL}$  kanamycin to count the number of colony. Three replicates were used for each treatment.

## Detection of mulberry associated bacterial communities after HGG15 inoculation

To explore the potential mechanism of HGG15 strain to promote mulberry growth whether attributed to variation of host-associated microbiome, the rhizosphere soil, root, and stem



of mulberry were collected after 30-day inoculation. A total of nine individual seedlings were randomly selected and three seedlings mixed as one replicate. The rhizosphere soils adhering to the mulberry root approximately 1 mm were obtained using a sterile scalpel. And then, approximately 5 cm roots and stems were collected for each mulberry seedling, and washed with tap water to remove soil and other debris. The root and stem samples were thoroughly soaked in 75% ethanol and rapidly flame-sterilized and stored at  $-80^{\circ}\text{C}$  for further processed.

The DNA of all samples was extracted using FastDNA<sup>®</sup> Spin Kit (MP Bio, Santa Ana, CA, United States) (Xu F. Y. et al., 2022) according to manufacturer's instructions with the moderated modification. Briefly, approximately 0.5 g of stems and roots were homogenized in liquid nitrogen. The prepared stem and root tissues and rhizosphere soil were transferred into Lysing Matrix E Tubes. And then, sodium phosphate buffer and MT buffer were added and supernatants were collected by centrifugation (12,000 rpm, 10 min). Then, 250  $\mu\text{L}$  of PPS was added in tube and centrifuged at 12,000 rpm with 5 min. The upper phase was then collected and transferred to a new tube and 1 mL binding matrix suspension was added. Afterward, 600  $\mu\text{L}$  mixtures were transferred into SPIN<sup>TM</sup> Filter tubes and subsequently centrifuged. Finally, 500  $\mu\text{L}$  SEMW-M was added into SPIN<sup>TM</sup> Filter tubes and centrifuged (12,000 rpm, 2 min), and DNA was eluted using 100  $\mu\text{L}$  DES. The DNA was checked on 1% agarose gel, and DNA concentration and purity were determined with NanoDrop 2000 UV-vis spectrophotometer (Thermo Scientific, Wilmington, NC, United States). The bacterial 16S rRNA gene was amplified with primer pairs 338F (5'-ACTCCTACGGGAGGCAGCA-3') and 806R (5'-GGACTACHVGGGTWTCTAAT-3') (Ou et al., 2019) by an ABI GeneAmp 9700 PCR thermocycler (ABI, CA, United States). Each 20  $\mu\text{L}$  PCR mixture contained 4  $\mu\text{L}$  of 5  $\times$  FastPfu Buffer, 2  $\mu\text{L}$  of 2.5 mM dNTPs, 0.8  $\mu\text{L}$  of each Primer (5  $\mu\text{M}$ ), 0.4  $\mu\text{L}$  of FastPfu Polymerase and 10 ng of template DNA. The PCR reactions were conducted using the following program: 3 min of denaturation at  $95^{\circ}\text{C}$ , 27 cycles of 30 s at  $95^{\circ}\text{C}$ , 30 s for annealing at  $55^{\circ}\text{C}$ , and 45 s for elongation at  $72^{\circ}\text{C}$ , and a final extension at  $72^{\circ}\text{C}$  for 10 min. Sterile water was served as negative control sample to avoid potential microbial contaminants in the DNA extraction and amplification processes. The PCR product was extracted from 2% agarose gel and purified using the AxyPrep DNA Gel Extraction Kit (Axygen Biosciences, Union City, CA, United States) according to manufacturer's instructions. Purified amplicons were pooled in equimolar and paired-end sequenced (2  $\times$  300) on an Illumina MiSeq platform (Illumina, San Diego, CA, United States) by Majorbio Bio-Pharm Technology Co., Ltd. (Shanghai, China). Pairs of reads were spliced into a sequence according to the direct overlap relationship of paired-end reads. At the same time, the quality of reads and splicing effect were controlled and filtered, and correction of the sequence direction was made according to the

end of the box sequence. Finally, the high-quality sequences obtained after filtering were assigned to samples according to barcodes. The raw reads were deposited into the NCBI Sequence Read Archive (SRA) database.

Operational taxonomic units (OTUs) with 97% similarity cutoff (Edgar, 2013) were clustered using UPARSE (version 7.0.1090), and chimeric sequences were identified and removed by VSEARCH (version 1.0.10). The taxonomy of each OTU representative sequence was analyzed using the BLAST algorithm with Silva database (release138<sup>1</sup>) against the bacterial 16S rRNA genes (Pruesse et al., 2007; Quast et al., 2013). Each sample was rarefied to 2000 reads (Beckers et al., 2017). The sequences classified as cyanobacteria and mitochondria were removed from the OTU table. The filtered table was used for further analyses. The  $\alpha$ -diversity including Shannon and Sobs indices was calculated using Mothur software (version 1.30.2) at a 97% identity level (Schloss et al., 2009). The different significances of  $\alpha$ -diversity among samples were compared based one-way analysis of variance (ANOVA). Bacterial community structures were analyzed at different classification levels using R software (version R-3.3.1). The Venn diagram was generated using R script and principal coordinates analysis (PCoA) was conducted based on Bray-Curtis distances at OTU level. The comparison of endophytic bacterial abundance was analyzed using Wilcoxon rank-sum test based on genus level. Moreover, Spearman correlation coefficient of the top 20 abundant bacterial genera and environmental factors including mulberry growth parameters and soil properties was calculated and displayed on the heat map (Zhou et al., 2017).

## Assessments of soil biochemical properties

Approximately 50 g soil samples were collected from each pot containing mulberry for detection of the biochemical properties after 30-day inoculation, and each treatment consisted of three replicates. Specifically, soils were dried at  $105^{\circ}\text{C}$  and filtered by a 2 mm sieve. Afterward, the soil sample was subjected to analyze organic carbon (OC), organic matter (OM), available phosphorus (AP), total potassium (TK), available potassium (AK), and available iron (Fe). Soil properties were analyzed using standard soil test methods as described by the agriculture protocols (Lu, 2000; Zhou et al., 2017). Soil OM, TP, and TK were determined by the dichromate oxidation process, Mo-Sb anti spectrophotometric method, and atomic absorption spectrophotometry, respectively. AP was extracted with  $\text{NH}_4\text{F-HCl}$  solution, and then determined by ultraviolet visible spectrophotometer. AK was extracted with 1 M  $\text{NH}_4\text{OAc}$ , and then determined by flame absorption

<sup>1</sup> <http://www.arb-silva.de>

spectroscopy. Fe was extracted with DTPA-CaCl<sub>2</sub>-TEA, and then determined by atomic absorption spectrophotometry.

## Analysis of mulberry root metabolites

To understand if variations in host metabolism were correlated with HGG15 strain, metabolomics of mulberry root were employed after 30-day inoculation. A total of 18 individual mulberry seedlings were collected in each treatment and three seedlings were randomly mixed as one replicate. Six biological replicates were performed for each treatment. The entire roots were washed with tap water to remove soils and 50 mg of roots were accurately weighed, and then the metabolites were extracted using 400  $\mu$ L of 80% methanol solution containing 2 mg/L L-2-chlorophenylalanine. The mixture was settled at  $-20^{\circ}\text{C}$  and processed by a high-throughput tissue crusher Wonbio-96c (Wonbio Biotechnology, Shanghai, China) at 50 Hz for 6 min, then vortexed for 30 s and ultrasonically treated at 40 Hz for 30 min at  $5^{\circ}\text{C}$ , followed by precipitation for 30 min at  $-20^{\circ}\text{C}$  and centrifugation at 13,000 rpm at  $4^{\circ}\text{C}$  for 15 min. The supernatants were then transferred into vials for subsequent ultra-performance liquid chromatography-tandem mass (UHPLC-MS/MS) spectrometry. A quality-control sample was prepared by mixing 20  $\mu$ L of each sample in order to control the accuracy and stability of the method.

Samples were separated on Thermo UHPLC plat equipped with an Acquity Beh C18 column (2.1 mm  $\times$  100 mm i.d.; 1.7  $\mu$ m; Waters, Milford, DE, United States) by Majorbio Bio-Pharm Technology Co., Ltd. (Shanghai, China). Mobile phase A was 0.1% formic acid in water, and phase B was 0.1% formic acid in acetonitrile: isopropanol (1: 1, v/v). The sample injection volume was 2  $\mu$ L, and the flow rate was set to 0.4 mL/min with a column temperature of  $40^{\circ}\text{C}$ . The gradient condition is as follows: from 0 to 3 min, 5–20% (B); from 3 to 9 min, 20–95% (B); from 9 to 13 min, 95% (B); from 13 to 13.1 min, 95–5% (B), from 13.1 to 16 min, 5% (B) for equilibrating the systems. The mass spectrometric data were collected using a Thermo UHPLC-Q Exactive Mass Spectrometer equipped with an electrospray ionization source operating in either positive or negative ion mode. The optimal parameters were set as follows: scan type: 70–1050 m/z; sheath gas flow rate: 40 psi; aux gas flow rate: 30 psi; aux gas heater temperature:  $400^{\circ}\text{C}$ ; capillary temperature:  $320^{\circ}\text{C}$ ; ion-spray voltage floating,  $-2.8$  kV in negative mode and 3.5 kV in positive mode, respectively; resolution: 17500 ( $\text{MS}^2$ ). Data acquisition was performed with the Data Dependent Acquisition mode.

The raw data were imported into the Progenesis QI 2.3 (Nonlinear Dynamics, Waters, United States) for peak detection and alignment. The preprocessing results generated a data matrix that consisted of the retention time, mass-to-charge ratio values, and peak intensity. The normalized data were used to predict the molecular formula based

on additive ions, molecular ion peaks and fragment ions. Then, peaks were searched in human metabolome database (HMDB)<sup>2</sup> and Metlin database<sup>3</sup> for metabolite identification. Orthogonal partial least squares discriminate analysis (OPLS-DA) and principal components analysis (PCA) analysis were used to determine global metabolic changes. The *P*-values were estimated with paired Student's *T*-test on single dimensional statistical analysis. Variable importance in projection (VIP) of metabolites represented their contributions to the global metabolic changes and the metabolites with VIP > 1 and *P*-value < 0.05 were considered to be differential metabolites. The functions of these metabolites and metabolic pathways were studied using scipyl (Python packages)<sup>4</sup> based on the Kyoto Encyclopedia of Genes and Genomes (KEGG) database. The heatmap of correlation between top 40 metabolites of mulberry root and bacterial genera was generated using the Pearson correlation coefficient.

## Statistical analysis

All data were performed using SPSS Statistics (Version 17.0. Chicago, IL, United States). Differences between treatments in the mulberry seedling and mulberry associated-bacterial diversity were analyzed using Tukey's one-way ANOVA. The statistical significances of silkworm growth and soil properties were analyzed using *T*-test. \*\*\*, \*\*, and \* indicated significant difference at  $P < 0.001$ ,  $P < 0.01$ , and  $P < 0.05$ , respectively.

## Results

### Isolation of endophyte and screening of plant growth promoting bacteria

A total of 343 endophytic bacteria were isolated from mulberry plants. 119 and 88 isolates were obtained from stems and roots of wild mulberry, respectively, while 68 and 68 isolates were obtained from stems and roots of newly planted mulberry, respectively (Supplementary Table 2). Among them, 28 isolates exhibited phenotypes commonly observed bacteria capable of plant growth promotion, including the ability to solubilize P, produce IAA, siderophores, and acetoin, and exhibit antagonism against *Sclerotinia sclerotiorum* as revealed by the presence of an inhibition zone (Table 1), and their near full-length 16S rRNA gene sequences were deposited in the GenBank under accession numbers ON786677-ON786703 and ON090422. A total of 25 and 27 isolates possessed

<sup>2</sup> <http://www.hmdb.ca/>

<sup>3</sup> <https://metlin.scripps.edu/>

<sup>4</sup> <https://docs.scipy.org/doc/scipy/>

P-solubilization and IAA-producing capability, respectively. Moreover, 16 and 25 isolates had the ability to produce siderophores and acetoin, respectively, and fifteen PGPBs had anti-fungal capability *in vitro*. Ultimately, *Enterobacter* sp. HLG5, *Lelliottia* sp. HTJ13, *Pantoea* sp. HLJ21, and *Klebsiella* sp. HGG15 strains were screened as those strains with the highest potential for plant growth promotion based on these traits *in vitro*.

## Effect of plant growth promoting bacteria on mulberry growth and their bio-safety for silkworms

To determine the effect of these four bacteria on mulberry growth, bacterial suspensions were inoculated into mulberry seedlings. Co-cultivation experiments revealed that application of these strains had a large positive impact on mulberry shoot (Figure 1A) and root growth (Figure 1B). The four strains significantly promoted length of mulberry leaf (Figure 1C) and shoot (Figure 1D) ( $P < 0.05$ ) compared with control plants. A corresponding significant increase of fresh weight of mulberry shoots was also observed in endophyte-treated plants (*Enterobacter* sp. HLG5: 81.51%; *Lelliottia* sp. HTJ13: 100.37%; *Klebsiella* sp. HGG15: 158.83%; *Pantoea* sp. HLJ21: 115.89%) (Figure 1E). In addition, mulberry seedlings treated with PGPBs had a higher dry weight of mulberry shoots than controls, increasing by 117.15, 147.82, 184.19, and 122.68% in *Enterobacter* sp. HLG5, *Lelliottia* sp. HTJ13, *Klebsiella* sp. HGG15, and *Pantoea* sp. HLJ21 group, respectively (Figure 1F). All of the bacterial isolates enhanced shoot growth, but differed in their stimulation of the roots of mulberry. The number of root tips of mulberry inoculated with *Enterobacter* sp. HLG5 (64.87%), *Klebsiella* sp. HGG15 (235.21%), and *Pantoea* sp. HLJ21 (165.92%) strains was greatly increased compared to control ( $P < 0.05$ ) (Figure 1G). Moreover, *Klebsiella* sp. HGG15 significantly increased root length (63.28%) (Figure 1H), fresh weight (195.92%) (Figure 1I), and dry weight (348.79%) (Figure 1J).

Additionally, the mulberry roots inoculated with these four strains exhibited greater vigor after 40 days of flood stress (Figure 2A). Specifically, root biomass (30.48 and 71.43%) (Figure 2B), total root length (52.61 and 53.74%) (Figure 2C), and the number of root fork (74.23 and 82.55%) (Figure 2D) were significantly higher in plants treated with *Klebsiella* sp. HGG15 and *Lelliottia* sp. HTJ13 under flood condition, respectively. Moreover, Evan's blue staining to reveal dead tissues indicated leave cell death in mulberry treated with *Klebsiella* sp. HGG15, *Lelliottia* sp. HTJ13, and *Pantoea* sp. HLJ21 were slighter than in control plants or plants treated with *Enterobacter* sp. HLG5 (Figure 2E). Together, these results suggested that both *Klebsiella* sp. HGG15 and *Lelliottia* sp.

HTJ13 had the greatly potential ability to relieve the negative impacts of flood stress on mulberry.

The potential use of PGPBs in the hydro-fluctuation belt of the TGR would require demonstration that they would not interfere with the down-stream uses of mulberry, such as in silk production. The impacts of PGPBs were thus evaluated by feeding them to silkworms. The growth of silkworms fed at the fifth instar and pupal stages presented did not differ from that of control insects (Supplementary Figure 1A). The PGPBs had no negative impacts on whole cocoon weight, pupal weight, cocoon shell weight, and rate of cocoon shell development in silkworms (Supplementary Figures 1B–E). Although the *Enterobacter* sp. HLG5 significantly enhanced whole cocoon weight (16.21%), pupal weight (16.23%), and cocoon shell weight (20.33%) of the survival silkworms (Supplementary Figures 1B–E), the survival rate (53.3%) (Supplementary Figure 1F) and cocoon production rate (65.0%) (Supplementary Figure 1G) of silkworms were significantly decreased in the insects fed *Enterobacter* sp. HLG5, and bodies of the dead silkworms were black and soft. Overall, these results revealed that *Enterobacter* sp. HLG5 strain was harmful to silkworms, while *Lelliottia* sp. HTJ13, *Klebsiella* sp. HGG15, and *Pantoea* sp. HLJ21 all exhibited no toxicity to silkworms.

## Characterization of HGG15 strain

*Klebsiella* sp. HGG15 strain was ultimately selected for further study since it exhibited the plant growth promoting traits *in vitro* and *in planta* as well as posing no bio-safety concerns for silkworms. Colonies of *Klebsiella* sp. HGG15 strain were white on LB medium (Figure 3A). Gram staining and scanning electron microscope results showed it was a short rod and gram-negative bacterium (Figures 3B,C). Meanwhile, the strain produced hydrogen sulfide and nitrate reductase, but was negative for utilization of urea and lactose (Supplementary Table 3). Moreover, phylogenetic analysis based on full length 16S rDNA indicated that it was identical to *Klebsiella aerogenes* (Figure 3D), being consistent with its morphological characteristics, biochemical, and molecule characteristics.

## Colonization and population dynamics of *Klebsiella aerogenes* HGG15/gfp in mulberry

To examine the colonization characteristics of *K. aerogenes* HGG15 in mulberry seedlings, plasmid pGFP4412 containing a *gfp* marker gene was transferred into wild type strain to generate *K. aerogenes* HGG15/gfp strain (Supplementary Figures 2A,B), which exhibited green fluorescence (Supplementary Figure 2C). This strain could be detected in various tissues of mulberry seedling by fluorescence microscopy after inoculation.

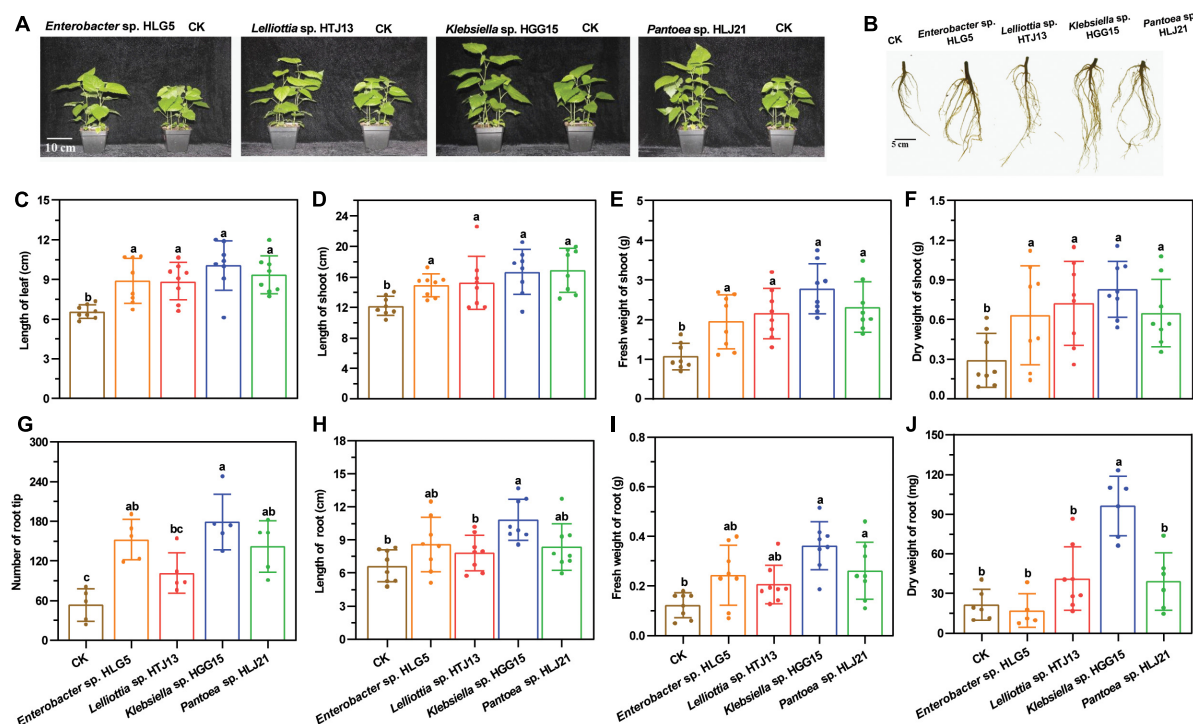


FIGURE 1

The growth promotion ability of potential four PGPBs on mulberry seedlings after 30-day inoculation. (A) The growth status of mulberry applied with the  $1 \times 10^7$  CFU/mL bacterial suspensions. (B) The representative photograph of mulberry root architectures. (C) Length of mulberry leaf. (D) Length of mulberry shoot. (E) Fresh weight of mulberry shoot. (F) Dry weight of mulberry shoot. (G) Number of mulberry root tip. (H) Length of mulberry root. (I) Fresh weight of mulberry root. (J) Dry weight of mulberry root. Values represented the mean  $\pm$  standard deviation of replicates ( $n = 8$ ). Different letters indicated statistical differences using Tukey's one-way ANOVA ( $P < 0.05$ ).

*K. aerogenes* HGG15/gfp first formed bacterial aggregates at the sites of root hair emergence (Figure 4A1) and colonized on the plant lateral roots (Figure 4A2). It subsequently proceeded to enter the plant root epidermis (Figure 4A3) after about 1–2 day post infection (dpi) where many gfp-tagged bacterial cells could be observed in the cortex of stem tissue by 3–5 dpi (Figures 4A4–6). As time progressed, a few colonies could be seen in the petiole and leaf (Figures 4A7–9). As expected, no gfp-labeled cells were ever observed in mulberry seedlings treated with sterile water (Figures 4A8,s,I).

The quantification of *K. aerogenes* HGG15/gfp within plant tissues was performed by selective culturing of plant macerates since the strain had the capability to grow on the LB plates containing 50  $\mu$ g/mL kanamycin (Figure 4B) and exhibited green fluorescence (Figure 4C). The numbers of *K. aerogenes* HGG15/gfp decreased progressively from mulberry roots to the stems and leaves. The localization and distribution of *K. aerogenes* HGG15/gfp within the plants changed with time (Figure 4D). The amount of bacteria in roots gradually decreased after initially multiplying rapidly there. Population size of fresh root tissue was 8.37 and 5.42 lg CFU/g at 3 and 21 dpi, respectively. A similar temporal pattern of colonization of stems and leaves was also seen. Total of 7.65 lg CFU/g in stems

and 7.21 lg CFU/g in leaves were initially seen and dropped to 4.15 lg CFU/g in stems and 3.94 lg CFU/g in leaves by 21 dpi, respectively.

## Mulberry-associated microbiome is influenced by *Klebsiella aerogenes* HGG15

Bacterial community composition of mulberry treated with *K. aerogenes* HGG15 was compared to that of control plants by 16S ribosomal RNA amplicon analysis. Complete data sets were submitted to the NCBI SRA database (Accession Number: SRP367158). All rarefaction curves tended to reach a plateau (Supplementary Figure 3), indicating that the depth of sequencing was sufficient. Changes in  $\alpha$  and  $\beta$  diversity were assessed to detect the effects of *K. aerogenes* HGG15 on mulberry-associated bacterial communities. Alpha diversity assessed by Sob and Shannon indexes was not significantly different between control and *K. aerogenes* HGG15-treated plants, whereas  $\alpha$  diversity strongly varied between different tissues (Supplementary Figure 4A). As expected, the  $\alpha$  diversity was highest in rhizosphere soils and lowest in stems. Moreover,



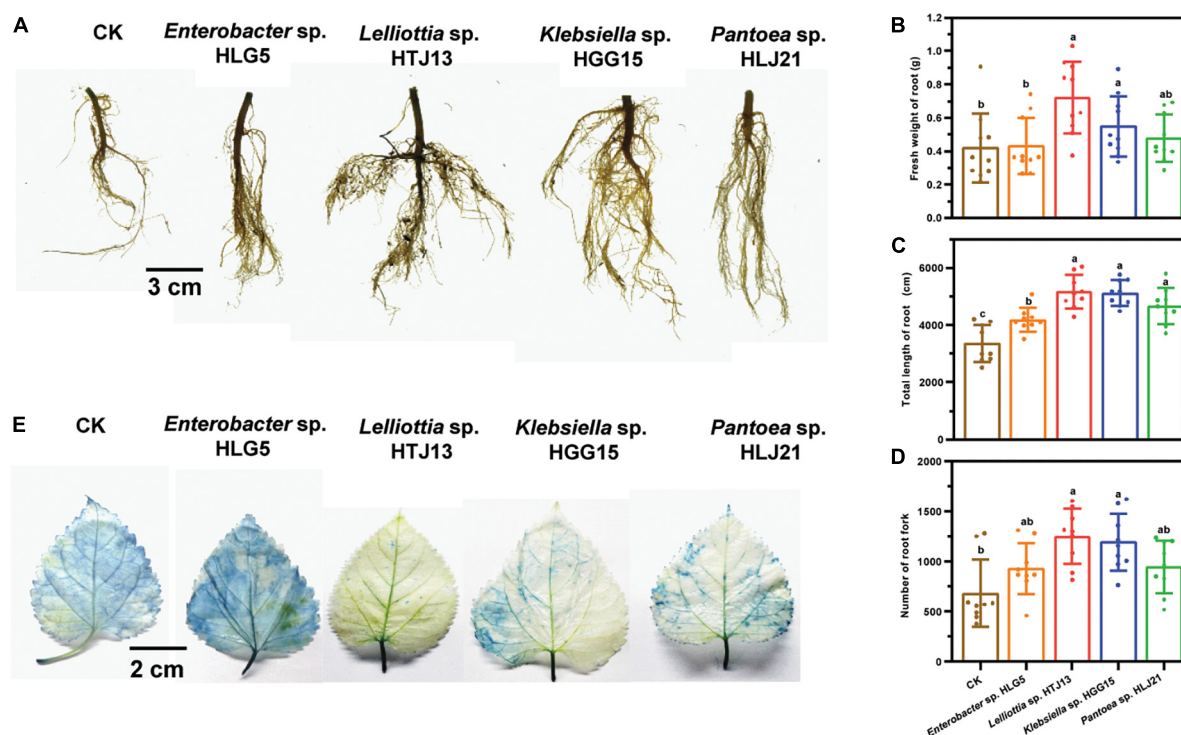


FIGURE 2

Effect of potential four PGPBs on mulberry flood tolerance. (A) Root architecture of mulberry after suffering flood stress. (B) Fresh weight of mulberry root. (C) Total length of mulberry root. (D) Number of mulberry root fork. (E) Representative photograph of the damage of mulberry leaf suffering flood stress by Evan's blue staining. Values represented the mean  $\pm$  standard deviation of replicates ( $n = 9$ ). Different letters indicated statistical differences using Tukey's one-way ANOVA ( $P < 0.05$ ).

the number of shared OTUs and unique OTUs showed a trend of gradual decline from rhizosphere soil to stem (Supplementary Figure 4B). In addition, the results of  $\beta$  diversity analysis as revealed by PCoA showed that bacterial communities mainly formed two separate clusters with the distance between inoculated samples being smaller than between controls (Figure 5A), although the statistical differences of groups were not significant according to PERMANOVA analyses (rhizosphere soil:  $P = 0.2$ ,  $R^2 = 0.3$ ; root:  $P = 0.1$ ,  $R^2 = 0.4$ ; stem:  $P = 0.2$ ,  $R^2 = 0.3$ ). These results indicated that *K. aerogenes* HGG15 strain might impact the bacterial community regardless of whether it was the rhizosphere or endosphere.

To further understand the influence of *K. aerogenes* HGG15 on the shifts of microbial communities, the relative abundance of various bacterial taxa was analyzed. *K. aerogenes* HGG15 altered the composition of bacterial communities in root and stem, however, little differences between the control and inoculation groups were seen in the rhizosphere soil (Figure 5B). At the order level, the relative abundance of Sphingomonadales (HGG15: 29.53%; CK: 17.56%) and Cytophagales (HGG15: 12.15%; CK: 4.75%) were increased in inoculated roots, while the relative abundance of Rhizobiales (HGG15: 17.09%; CK:

34.50%) was decreased (Figure 5B). Moreover, Rhizobiales (HGG15: 42.88%; CK: 11.24%) and Saccharimonadales (HGG15: 15.02%; CK: 0.67%) were more abundant in stems of inoculated plants. In contrast, Pseudomonadales (HGG15: 0.13%; CK: 1.57%), Burkholderiales (HGG15: 4.24%; CK: 27.87%), Propionibacteriales (HGG15: 1.41%; CK: 7.42%), and Corynebacteriales (HGG15: 16.17%; CK: 26.29%) were enriched in stems of control plants. At the genus level, the roots of inoculated plants harbored significantly more *Ohtaekwangia* (HGG15: 11.09%; CK: 3.89%) and *Rhizorhapis* (HGG15: 28.25%; CK: 16.60%) than control plants (Figure 5B). *Rhizobium* (HGG15: 9.88%; CK: 6.52%), *Devosia* (HGG15: 5.52%; CK: 0.67%), *Brevundimonas* (HGG15: 3.72%; CK: 1.12%), *Methylobacterium* (HGG15: 26.70%; CK: 3.60%), and *TM7a* (HGG15: 13.22%; CK: 0.22%) were the predominant genera in the stems of *K. aerogenes* HGG15 inoculated plants, while the relative abundance of *Oxalicibacterium* (HGG15: 0%; CK: 5.39%), *norank\_f\_Oxalobacteraceae* (HGG15: 0%; CK: 10.11%), *Ralstonia* (HGG15: 2.31%; CK: 10.56%), *Aeromicrobium* (HGG15: 1.28%; CK: 6.97%), and *Rhodococcus* (HGG15: 0.51%; CK: 4.04%) were lower than in control plants (Figure 5B). These results revealed that *K. aerogenes* HGG15 substantially shifted endophytic bacterial composition

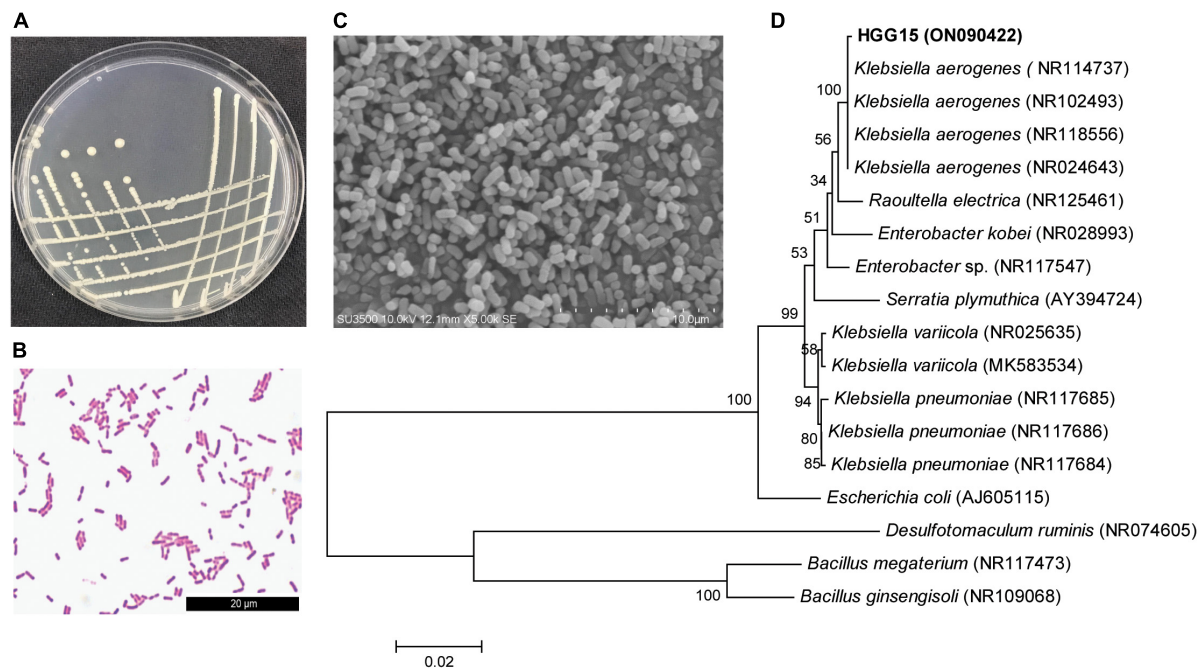


FIGURE 3

Characterization of *Klebsiella* sp. HGG15 strain. (A) Colony feature on LB medium after 24 h. (B) Gram-positive staining. (C) Scanning electron microscopy of bacterial cells. (D) Phylogenetic tree based on 16S rDNA. The tree was constructed by MEGA 6.0 using neighbor-joining analysis of 1,000 bootstrap replications.

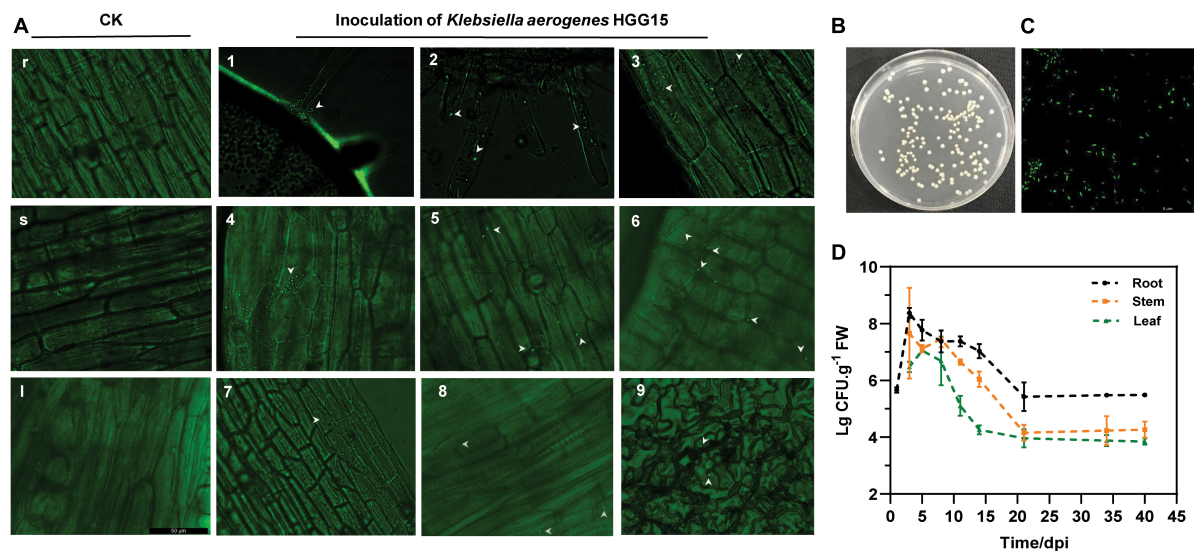


FIGURE 4

Colonization and population dynamics of gfp-tagged *K. aerogenes* HGG15 in mulberry seedlings. (A) Infection and colonization of gfp-tagged *K. aerogenes* HGG15 in mulberry. r, mulberry root of control group in 1 dpi; s, mulberry stem of control group in 3 dpi; l, mulberry petiole of control group in 7 dpi; 1, mulberry root hair of inoculation group in 1 dpi; 2, mulberry lateral root of inoculation group in 1 dpi; 3, mulberry root epidermis of inoculation group in 2 dpi; 4–6, mulberry cortex of inoculation group in 3–5 dpi; 7–8, mulberry petiole of inoculation group in 7 dpi; 9, leaf epidermis of inoculation group in 12 dpi. (B) Cultural feature of gfp-tagged *K. aerogenes* HGG15 re-isolated from mulberry on LB medium containing 50 µg/mL kanamycin. (C) Observation of re-isolated gfp-tagged *K. aerogenes* HGG15 strain under green fluorescence at 488 nm. (D) Population dynamics of gfp-tagged *K. aerogenes* HGG15 in mulberry seedling.



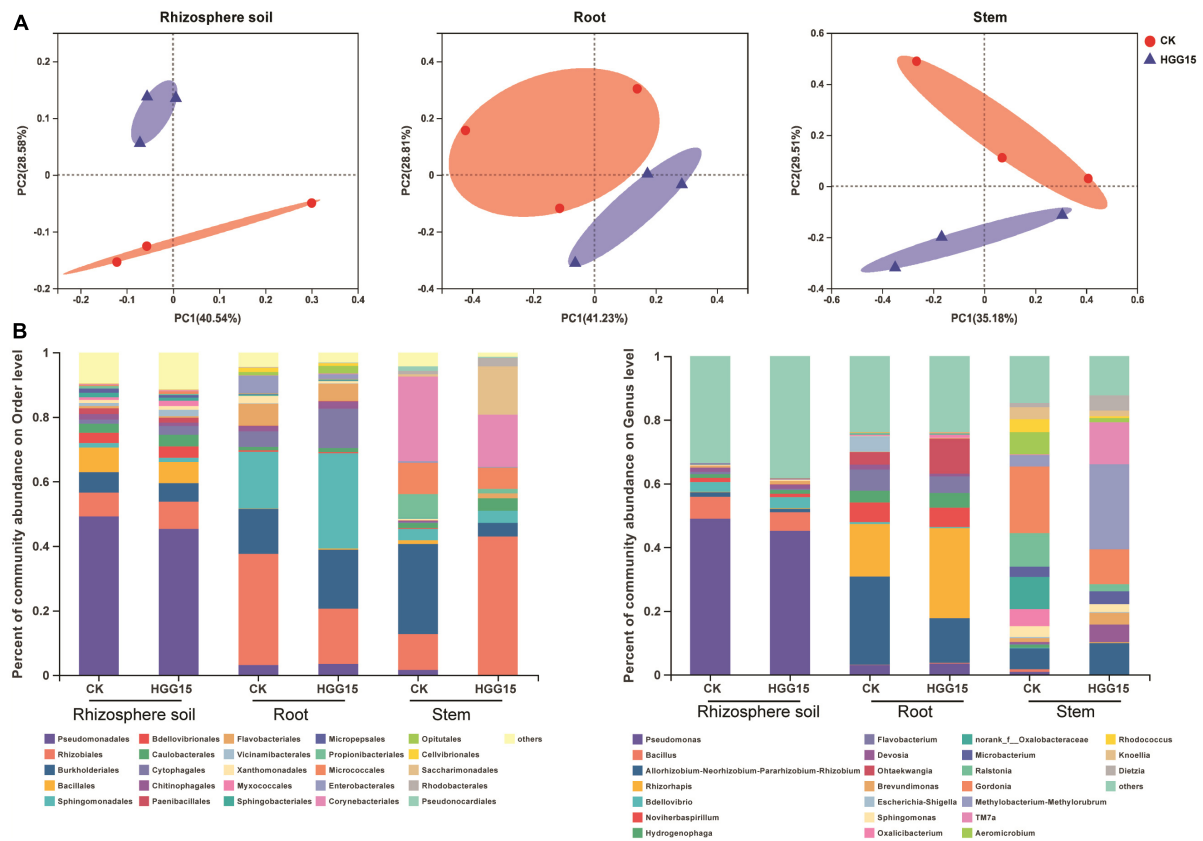


FIGURE 5

Effect of *K. aerogenes* HGG15 strain on mulberry associated bacterial communities. **(A)** Principal coordinate analysis of bacterial communities in the rhizosphere soil, root and stem of mulberry based on Bray–Curtis distances. **(B)** Composition of bacterial communities in the rhizosphere soil, root and stem of mulberry at order (left) and genus (right) level. Taxa with an abundance < 0.01 were included in “others.” Each column represented the mean of three biological replicates.

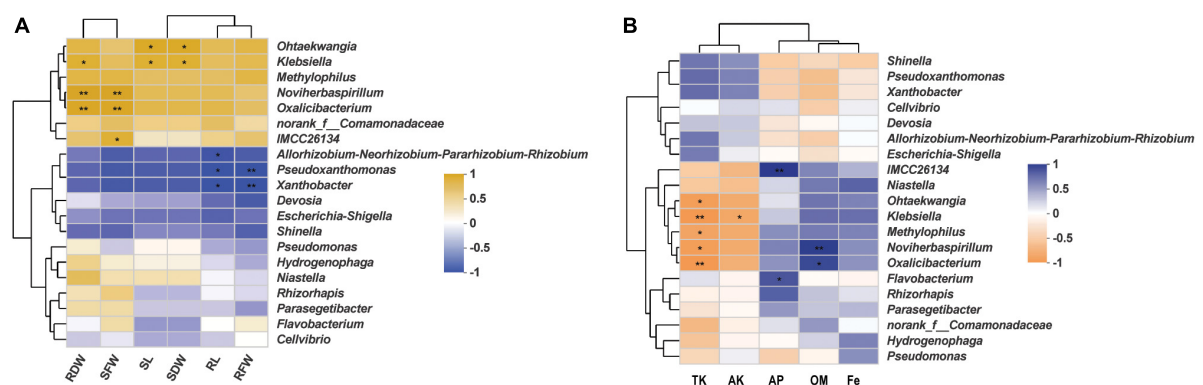


FIGURE 6

The relationship of root bacterial genera and mulberry development and soil properties. **(A)** Heatmap of correlation between mulberry growth parameters and top 20 bacterial genera using the Spearman correlation coefficient. RDW and SDW represented the dry weight of mulberry root and shoot, respectively. RFW and SFW represented the fresh weight of mulberry root and shoot, respectively. SL and RL represented mulberry shoot length and main root length, respectively. **(B)** Heatmap of correlation between soil properties and top 20 bacterial genera using the Spearman correlation coefficient. TK, AK, AP, OM, and Fe represented total potassium, available potassium, available phosphorus, organic matter, and available iron, respectively.

of mulberry seedlings, while it had little effect on bacterial communities in rhizosphere soil.

In order to uncover any significant differences in endophytic communities between *K. aerogenes* HGG15-treated and control plants, the Wilcoxon rank-sum test of bacterial community composition was investigated at the genus level. The relative frequency of *Xanthobacter* and *o\_norank\_c\_Alphaproteobacteria* was significantly lower ( $P < 0.05$ ) in roots of *K. aerogenes* HGG15 treated plants than in controls, while the proportion of *Methyloversatilis* and *MND1* was higher ( $P < 0.05$ ) in treated plants (Supplementary Figure 5A). Notably, the genus of *Klebsiella* was relatively abundant in mulberry roots after inoculating *K. aerogenes* HGG15 ( $P < 0.01$ ), while it was hardly detected in the rhizosphere soil and stem tissues (Supplementary Figure 5B), suggesting *Klebsiella* specifically colonized on mulberry roots. The Spearman correlation of the top 20 bacterial genera in root with mulberry growth indexes (Supplementary Table 4) was further investigated to uncover role of the *Klebsiella* genus. Results revealed that there was a positive relationship between *Klebsiella* and mulberry development, especially in root dry weight, shoot dry weight, and shoot length ( $P < 0.05$ ) (Figure 6A), indicating that *Klebsiella* played a crucial role in promoting mulberry growth. In addition, soil property analysis showed that the content of organic matter was significantly higher in *K. aerogenes* HGG15 group ( $P < 0.01$ ) (Supplementary Figure 6B), and potassium content was lower compared to that in the control group (Supplementary Figures 6C,D) ( $P < 0.01$ ), but the contents of organic carbon, available phosphorus, and iron elements did not show dramatic variation (Supplementary Figures 6A,E,F). Furthermore, a heatmap constructed using the Spearman correlation coefficients was used to determine how the various microbial communities correlated with soil factors, revealing that *Klebsiella* was positively linked to total potassium and available potassium (Figure 6B). Altogether, these results suggested that *K. aerogenes* HGG15 strain significantly affected mulberry endophytic bacterial community, especially in root, and that the abundance of *Klebsiella* genus in root exhibited positive correlations with mulberry development and potassium content of soil, suggesting *Klebsiella* might contribute to mulberry seedling growth.

## *Klebsiella aerogenes* HGG15 affects the mulberry metabolite profile

Since *K. aerogenes* HGG15 colonized on the interior of mulberry roots (Figure 4D) and promoted plant growth, and the genus *Klebsiella* is also a dominant colonizer in mulberry roots (Supplementary Figure 5B), untargeted metabolomics of roots were analyzed to determine if and how this strain affected mulberry metabolites. PCA of metabolites demonstrated that

inoculated and control plants differed in their metabolome regardless of negative mode or positive mode of metabolite analysis (Supplementary Figure 7A). The metabolite profiles of mulberry were then subjected to OPLS-DA, which showed difference between the control and *K. aerogenes* HGG15-treated group in both negative and positive analytic modes (Figure 7A). The score plots of PCA and OPLS-DA exhibited an obvious separation between the control and treatment groups, indicating *K. aerogenes* HGG15 was responsible for the distinction in categories and quantities of metabolites in mulberry. In addition, little variation among the biological replicates of each group was observed (Figure 7A and Supplementary Figure 7A), which illustrated the sufficient reproducibility and reliability of the experiment.

Metabolites with a threshold  $P$ -value  $< 0.05$  and VIP  $> 1$  were considered as differentially accumulated metabolites (DAMs). In total, there were 201 different identifiable metabolites, consisting of 125 and 76 metabolites from the positive and negative ionization modes, where 131 and 70 metabolites were upregulated and downregulated, respectively (Supplementary Figure 7B). According to their molecular structure and function based on the HMDB, the DAMs were classified into eight categories at the superclass level. The most dominant group of DAMs was lipids and lipid-like molecules which contained glycerophospholipids, fatty acyls, glycerolipids, sphingolipids, and prenol lipids. The other DAMs were classified into organoheterocyclic compounds, organic acids and derivatives, organic oxygen compounds, phenylpropanoids and polyketides, nucleosides, nucleotides, and analogues, benzenoids, and organosulfur compounds (Table 2). At the class level, the content of 25 category substances (78.13%, occupying 32 categories), such as glycerolipid, sphingolipid, indole, and pyridine, were significantly upregulated in mulberry after *K. aerogenes* HGG15 treatment (Table 2).

To further understand the DAMs function and the related biological processes they participated in, the top 20 pathways enrichment analysis of the DAMs was conducted using KEGG. The results showed that the ABC transporter, glycerophospholipid metabolism, purine metabolism, arginine biosynthesis, and tryptophan metabolism were significantly enriched (Figure 7B). Most of these pathways are involved in basic biological functions of plants, indicating that primary metabolism in mulberry was significantly affected by *K. aerogenes* HGG15. Furthermore, the VIP values of DEMs were calculated to explore the specifically different metabolites in mulberry. As shown in Figure 7C, the metabolites 2-hydroxy-3-methoxyestrone, PC [18:4(6Z,9Z,12Z,15Z)/0:0], N5-acetyl-N2-gamma-L-glutamyl-L-ornithine, and polyoxyethylene (600) monoricinoleate were significantly decreased in roots after *K. aerogenes* HGG15 treatment. In contrast, some compounds, e.g., octadecanedioic acid, 4-(2-aminophenyl)-2,4-dioxobutanoic acid, pratenol A, flumioxazin, hippurate, 3-methyldioxyindole,

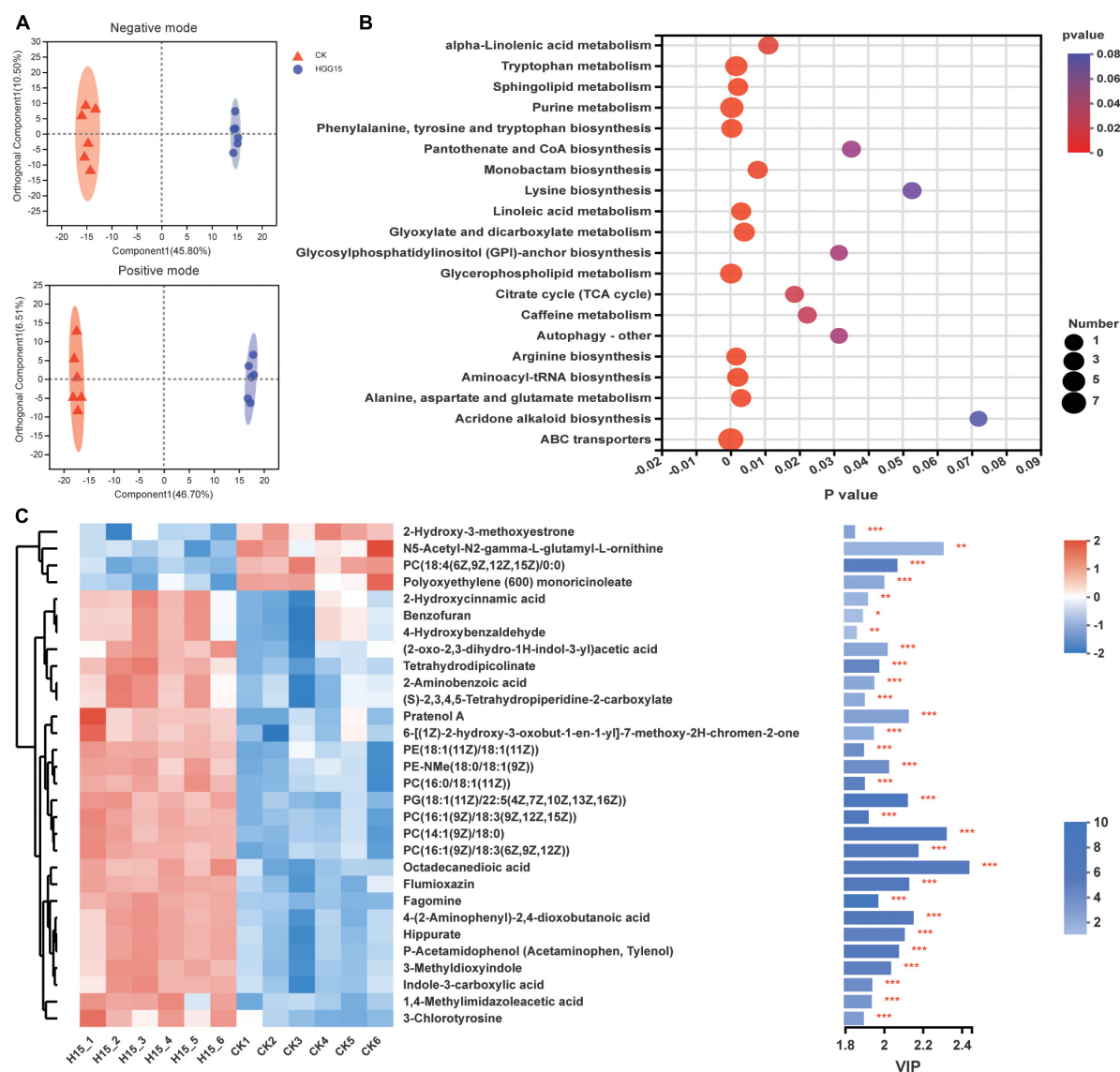


FIGURE 7

Effects of *K. aerogenes* HGG15 strain on metabolites of mulberry root. (A) Orthogonal partial least squares discriminant analysis of mulberry metabolites using positive and negative modes. (B) KEGG pathway enrichment analysis of differentially accumulated metabolites. The x-axis and y-axis represented the *P*-value of enrichment and enrichment pathway, respectively. The size of node represented the amount of metabolite enriched in the pathway. (C) Variable importance in projection scores of top 30 different metabolites between control and inoculated group. Left, heatmap of the differentially accumulated metabolites. The correlation of color and value was shown in the upper right bar. Right, bar chart of differentially accumulated metabolites. The length of bar indicated the contribution degree of this metabolite. The color of bar showed the difference degree of metabolite and the darker color represented the larger value of  $-\log_{10}(P\text{-value})$  as shown in lower right bar.

\*\*\* $P < 0.001$ , \*\* $P < 0.01$ , \* $P < 0.05$ .

tetrahydrodipicolinate, fagomine, 2-aminobenzoic acid, and indole-3-carboxylic acid exhibited strong positive correlations with *K. aerogenes* HGG15 treatment. These results illustrated that the metabolites of mulberry root were strongly influenced by *K. aerogenes* HGG15, likely explaining its large effect on mulberry growth. In addition, a heatmap of correlation was generated to explore the potential relationship between differential bacteria altered by *K. aerogenes* HGG15 and

metabolites of mulberry root. As expected, the metabolites were closely associated with differential bacterial microbiome of mulberry roots (Supplementary Figure 8). In particular, a greatly significant correlation has appeared between DAMs and bacterial taxa such as *o\_norank\_c\_Alphaproteobacteria*, *Klebsiella*, *Methyloversatilis*, *Reyranella*, *Ammoniphilus*, *Conexibacter*, and *Ohtaekwangia*. Thus, differential bacteria altered by *K. aerogenes* HGG15 could further influence

TABLE 1 Characterization of endophytic bacteria for potential plant growth-promoting traits.

| Strains                             | P-solubilization (cm) | IAA (mg/mL) | Siderophores (cm) | Inhibition zone (cm) | Acetoin (μg/mL) |
|-------------------------------------|-----------------------|-------------|-------------------|----------------------|-----------------|
| <i>Enterobacter</i> sp. HLJ6-2      | 0.90                  | 7.15        | —                 | 0.23                 | —               |
| <i>Enterobacter</i> sp. HGJ7-2      | 0.67                  | 19.75       | —                 | —                    | 101.23          |
| <b><i>Enterobacter</i> sp. HLG5</b> | 0.80                  | 2.76        | 0.29              | 0.30                 | 33.87           |
| <i>Atlantibacter</i> sp. HLJ20      | —                     | 6.25        | 0.12              | —                    | 223.44          |
| <i>Atlantibacter</i> sp. HLJ10      | 0.90                  | 2.66        | 0.36              | —                    | 200.35          |
| <i>Pantoea</i> sp. HLJ16-1          | 0.70                  | 6.11        | —                 | 0.31                 | 200.35          |
| <i>Kosakonia</i> sp. HLJ19-2        | 0.60                  | 6.01        | —                 | —                    | 370.67          |
| <i>Leclercia</i> sp. HNG10-2        | 0.27                  | 7.37        | —                 | —                    | 164.74          |
| <b><i>Lelliottia</i> sp. HTJ13</b>  | 0.17                  | 3.53        | 0.24              | 0.13                 | 363.93          |
| <i>Rahnella</i> sp. HNJ30           | 0.13                  | 18.49       | 0.44              | —                    | 254.23          |
| <i>Pantoea</i> sp. HGJ8             | 0.80                  | 13.92       | —                 | —                    | 33.87           |
| <i>Pantoea</i> sp. HGJ11            | —                     | 11.74       | 0.36              | —                    | —               |
| <i>Pantoea</i> sp. HTJ6             | 0.33                  | 5.91        | 0.51              | 0.43                 | 32.91           |
| <b><i>Pantoea</i> sp. HLJ21</b>     | 0.60                  | 10.96       | 0.17              | 1.33                 | 76.21           |
| <i>Pantoea</i> sp. HTJ25            | 0.73                  | 5.86        | 0.40              | —                    | 87.76           |
| <i>Pantoea</i> sp. HNJ8             | 1.03                  | 8.64        | 0.25              | 1.20                 | 165.70          |
| <i>Pantoea</i> sp. HNJ21            | 0.20                  | 6.01        | 0.50              | 0.36                 | 65.63           |
| <i>Pantoea</i> sp. HNJ32            | 0.37                  | 13.05       | —                 | —                    | 32.91           |
| <i>Pantoea</i> sp. HNG24            | 0.93                  | 4.8         | —                 | 0.63                 | 85.84           |
| <i>Klebsiella</i> sp. HNG29         | —                     | 3.39        | 0.20              | 0.30                 | 411.09          |
| <i>Klebsiella</i> sp. HLG11         | 0.67                  | 4.8         | —                 | 0.87                 | 69.48           |
| <i>Klebsiella</i> sp. HLG12         | 0.97                  | 2.51        | —                 | —                    | 19.44           |
| <i>Klebsiella</i> sp. HLG15         | 0.67                  | 5.38        | 0.10              | 0.10                 | 223.44          |
| <i>Klebsiella</i> sp. HLG29         | 0.97                  | 37.56       | 0.23              | —                    | 157.04          |
| <b><i>Klebsiella</i> sp. HGG15</b>  | 0.90                  | 6.69        | 0.38              | 0.40                 | 363.93          |
| <i>Klebsiella</i> sp. HGG18         | 1.10                  | 3.44        | —                 | 0.80                 | 273.48          |
| <i>Klebsiella</i> sp. HGG20         | 1.33                  | —           | —                 | —                    | —               |
| <i>Klebsiella</i> sp. HTG12         | 0.60                  | 3.1         | 0.14              | 0.60                 | 61.78           |
| Total                               | 25                    | 27          | 16                | 15                   | 25              |

The bold isolates were selected as potential PGPBs since their great growth-promoting traits.

mulberry metabolites, where the synergistic linkage of microbiome and metabolites might together contribute to the development of host plant.

## Discussion

Abiotic stresses are the foremost limiting factors for agricultural productivity. Various strategies including transgenic technology and molecular breeding have been considered to assist plant to relieve the stresses of such adverse conditions created by environmental extremes. Such approaches are often time consuming and might meet societal pressures. The modulation of endophytic colonization of plants is gaining wide popularity as an alternate strategy for improving stress tolerance of plants (Glick, 2014; Tiwari et al., 2016), since endophytes could provide sustainable benefits of both improving plant tolerance to biotic or abiotic stresses as well as stimulating plant growth (Bacon and White, 2015; Zhang et al., 2019). Therefore,

the application of endophytes could be a potential method for enhancement of mulberry growth in the hydro-fluctuation belt of the TGR. Bacteria in the genera of *Enterobacter*, *Pantoea*, and *Klebsiella* have been the most extensively studied taxa and have been shown to benefit plant development (Ullah et al., 2019; Xu S. D. et al., 2022). Earlier studies reported that *Enterobacter* sp. E5 increased resistance of banana to *Fusarium* wilt disease (Liu et al., 2019). Zhang et al. (2017) also revealed that the endophyte *Klebsiella* sp. LTGPAF-6F could contribute to both growth promotion and improvement of drought tolerance of wheat in greenhouse studies. In the present study, a total of 28 isolates from mulberry were screened as PGPBs and *Enterobacter* spp., *Pantoea* spp., and *Klebsiella* spp. were the dominant genera with traits, which might play crucial roles in endowing mulberry beneficial traits in hydro-fluctuation belt (Table 1). Among them, four isolates were selected for assessment their PGP traits *in planta* and showed excellent growth stimulating effects to mulberry seedlings regardless of whether they experienced flood stress conditions or not

(Figures 1, 2), and strain *Klebsiella aerogenes* HGG15 was found to be much superior to these other strains.

The plant growth promoting effect of bacteria is correlated with its colonization of host plants. It makes sense that successful colonization is critical for impacts of endophytes and their host plants as has been seen in many studies (Jha and Kumar, 2007; Pavlova et al., 2017; Ullah et al., 2019). In this study, *K. aerogenes* HGG15/gfp initially attached to emerging root hairs and lateral roots, indicating that it likely invades plants through these natural sites. Hallmann and Berg (2006) showed that, like *K. aerogenes* HGG15/gfp, endophytic bacterial population were lower within above-ground tissues, e.g., stem and leaves than in roots. Interestingly, we also found through amplicon sequencing analysis that other *Klebsiella* also preferentially colonized on mulberry roots (Supplementary Figure 5B), which might be the reason why *K. aerogenes* HGG15 greatly influenced root biomass and architecture of mulberry (Figures 1, 2). It has been reported that some *Klebsiella*, such as *K. pneumonia*, are opportunistic pathogens of animals (Li and Huang, 2017; Álvarez-Marín et al., 2021), while major species of *Klebsiella* usually did not cause disease in plants. More importantly, most of *Klebsiella* such as *Klebsiella* sp. D5A (Liu et al., 2016) and *Klebsiella* sp. SBP-8 (Singh et al., 2015) could improve plant utilization of nitrogen, phosphorus, and iron, and contribute to biological control or environmental tolerance. This taxon thus has attracted attentions as a plant growth stimulator in agricultural systems. Notably, the results of our safety evaluation of *K. aerogenes* HGG15 revealed that it had no side effects on the silkworm. These results suggested that the endophytic bacterium *K. aerogenes* HGG15 might be a potential growth promoter for crop plants, but its biosafety will need further evaluation by determining haemolysis, cytotoxicity, antibiotic resistance and genotoxicity.

Inoculation of exogenous bacteria not only influences the microbiome structure of different plant niches (Li et al., 2021), but also can attract certain beneficial bacteria, such as *Rhizobium* (Guo and Chi, 2014), *Methylobacterium* (Alessa et al., 2021), and *Microbacterium* (Vilchez et al., 2018), to promote plant growth and inhibit disease occurrence (Zhuang et al., 2021). We explored the bacterial community in different compartments of mulberry and found that bacterial  $\beta$  diversity in rhizosphere soil, root, and stem of mulberry was influenced by *K. aerogenes* HGG15 (Figure 5A), while there was no obvious effect on  $\alpha$  diversity (Supplementary Figure 4A). The taxonomic composition of endophytic bacteria exhibited differences between the control and inoculated plants, especially those inhabiting in root and stem, but there was little effect of inoculation on rhizosphere soil communities (Figure 5B). *Methylobacterium* was the preponderant bacterial endophyte appearing in *K. aerogenes*-inoculated mulberry. Similar findings were found in soybean (Hara et al., 2019) and pine seeds (Koskimäki et al., 2022), which were dominantly colonized by *Methylobacterium* and exhibited higher biomass of shoots and

TABLE 2 The classification of significantly different metabolites of mulberry root.

| Superclass                              | Class                               | Regulate | Number |
|---|-------------------------------------|----------|--------|
| Lipids and lipid-like molecules         | Glycerophospholipids                | Up/down  | 52     |
|   | Fatty acyls                         | Up/down  | 21     |
|   | Steroids and steroid derivatives    | Up/down  | 4      |
|   | Glycerolipids                       | Up       | 4      |
|   | Sphingolipids                       | Up       | 2      |
|   | Prenol lipids                       | Down     | 1      |
| Organoheterocyclic compounds            | Pyridines and derivatives           | Up       | 4      |
|   | Indoles and derivatives             | Up       | 3      |
|   | Piperidines                         | Up       | 3      |
|   | Tetrahydrofurans                    | Up/down  | 2      |
|   | Benzofurans                         | Up       | 2      |
|   | Imidazopyrimidines                  | Up       | 2      |
|   | Azacyclic compounds                 | Up       | 1      |
|   | Furans                              | Up       | 1      |
|   | Diazines                            | Up       | 1      |
|   | Benzoxazines                        | Up       | 1      |
|   | Benzothiophenes                     | Down     | 1      |
|   | Benzopyrans                         | Up       | 1      |
| Organic acids and derivatives           | Carboxylic acids and derivatives    | Up/down  | 19     |
|   | Keto acids and derivatives          | Down     | 1      |
| Organic oxygen compounds                | Organooxygen compounds              | Up/down  | 11     |
| Phenylpropanoids and polyketides        | Cinnamic acids and derivatives      | Up       | 2      |
|   | Flavonoids                          | Down     | 2      |
|   | Stilbenes                           | Down     | 1      |
|   | Isocoumarins and derivatives        | Up       | 1      |
|   | Coumarins and derivatives           | Up       | 1      |
| Nucleosides, nucleotides, and analogues | Purine nucleotides                  | Up/down  | 2      |
|   | Purine nucleosides                  | Up       | 2      |
| Benzenoids                              | Phenols                             | Up       | 2      |
|   | Benzene and substituted derivatives | Up       | 1      |
| Organosulfur compounds                  | Thioethers                          | Down     | 1      |

roots. This taxon may thus contribute to mulberry growth. Notably, *Ralstonia*, one of the most destructive plant bacterial pathogens (Pan et al., 2013), was markedly decreased in mulberry after inoculation. In addition, compared with control



plants, roots of mulberry treated with *K. aerogenes* HGG15 accumulated significantly less *Xanthobacter* (Supplementary Figure 5A), a potential phytopathogen causing serious disease in cruciferous plants (Mansfield et al., 2012). These results indicated that *K. aerogenes* HGG15 may play a crucial role in antagonizing against pathogens as well as is a good candidate strain as bio-fertilizer, but its antagonistic efficiency should be further studied.

In the process of bacteria-assisted plant growth promotion, some material exchange, energy transformation, and information communication continuously take place among microbes, plant roots, and the soil environments (Sun L. J. et al., 2020; Sun et al., 2022). In our study, the increased content of organic matter and decreased content of potassium in soils of mulberry inoculated with *K. aerogenes* HGG15 were found (Supplementary Figure 6), indicating a feedback effect of this strain on soil processes. This finding is in accordance with previous study that physicochemical properties of soils of *Brassica juncea* were strongly influenced by endophytic bacterial *Serratia marcescens* PRE01 and *Arthrobacter ginsengisoli* PRE05 (Wang et al., 2020). Interestingly, we found that *K. aerogenes* HGG15 strain had a capability to dissolve unavailable potassium *in vitro* (Supplementary Figure 9), suggesting that this strain could transform the unavailable potassium to available form, and thus assisted mulberry trees uptake useful potassium from soil to benefit their growth. Metabolites in plant roots usually exert a variety of functions, such as facilitating primary metabolism and root growth, rhizosphere communication, and plant defense (Doell et al., 2021). Mutualistic interactions of plant with endophyte can facilitate plant growth promotion through the accumulation of beneficial plant metabolites (Kundu et al., 2021), as in the case of fungus *Piriformospora indica* that colonize in Chinese cabbage, which stimulated plant synthesis of metabolites involved in the tryptophan and phenylalanine metabolism as well as  $\gamma$ -aminobutyrate (Hua et al., 2017). Furthermore, *Bacillus amyloliquefaciens* enhanced maize growth by improving nutrient uptake and influencing plant primary metabolism, especially glucose, fructose, alanine and  $\gamma$ -aminobutyric acid metabolism (Vinci et al., 2018). Most differentially abundant compounds found in our study were annotated as lipids and lipid-like molecules (Table 2), especially glycerolipids and sphingolipids, which not only contributed to abiotic and biotic stress resistance but also regulated basically cellular processes (Luttgeharm et al., 2016). It was worth noting that we found the production of indole derivatives affiliated with organoheterocyclic compounds in mulberry was elevated by *K. aerogenes*. These compounds have been shown to enhance lateral root growth (Sun X. et al., 2020). Additionally, the indole-3-carboxylic acid, one of the indole derivatives, is the best known of the auxins, which is involved in camalexin biosynthesis (Wang et al., 2012) and plays an important role in plant pathogen defense (Magnus et al., 1980). *K. aerogenes* HGG15 enhanced the content of indole-3-carboxylic acid

in mulberry roots, suggesting that this strain might induce resistance of host plant to biotic or abiotic stress. Notably, cinnamic acids, isocoumarins, coumarins, and their derivatives, as important phenylpropanoid and polyketide compounds, were significantly upregulated in mulberry after *K. aerogenes* HGG15 inoculation (Table 2). Among them, the downstream substance of cinnamic acid has been described as a potential antioxidant compound in mulberry (Park et al., 2017), which might be beneficial for mulberry development under abiotic stress conditions. Coumarins are known to play a key role in the transport of iron-mobilization in plant and are recognized as plant signals shaping host microbiomes (Stringlis et al., 2018). Moreover, coumarins and their derivatives have been extensively studied for their potential to help plants cope with biotic and abiotic environmental stress (Stringlis et al., 2019). Therefore, the above-mentioned metabolites might be crucial drivers of mulberry growth promotion and its enhanced stress resistance when inoculated with *K. aerogenes* HGG15.

## Conclusion

The growth of mulberry trees is greatly hindered by flood stress and limited-nutrition in the hydro-fluctuation belt of the TGR region. In the current study, *Klebsiella aerogenes* HGG15 was ultimately screened out as having superior plant growth promotion proprieties *in vitro* and strongly stimulated growth and enhanced flood tolerance of mulberry *in planta*. Moreover, it was not harmful to silkworm and could extensively and persistently colonize on mulberry. The inoculation of *K. aerogenes* HGG15 greatly altered the establishment of endophytic bacterial communities in mulberry, especially in roots and stems. In addition, the large change in abundance of abiotic stress response factors and compounds that promote plant growth such as glycerolipid, sphingolipid, indole, pyridine, and coumarin were observed in inoculated mulberry. Taken together, these results of this study help us to understand the interactions between this endophyte and plants and mechanisms driving these interactions, and provide innovative approaches for revegetation in the hydro-fluctuation belt through enhancing microbe-assisted plant growth.

## Data availability statement

The datasets presented in this study can be found in online repositories. The names of the repository/repositories and accession number(s) can be found below: <https://www.ncbi.nlm.nih.gov/genbank/>, SRP367158; ON786677–ON786703; ON090422.

## Author contributions

TO and JX designed the experiments. TO, HG, KJ, JY, and RZ performed the experiments. TO analyzed and wrote the manuscript. JX and XL revised the manuscript. ZZ and ZX conceived the study and contributed resources. All authors contributed to the article and approved the submitted version.

## Funding

This work was supported by JX of the National Natural Science Foundation of China (31870518), Natural Science Foundation of Chongqing (cstc2019jcyj-msxmX0396), and Fundamental Research Funds for the Central Universities (XDJK2019B047).

## Acknowledgments

We are sincerely grateful to Prof. Steven Lindow (University of California, Berkeley, United States) for his critical review and thorough editing of this manuscript. We also thank for agronomist Changyu Qiu (Promotion Station of Sericulture Technology, Guangxi Zhuang Autonomous Region, China) and Chuanshu Huang (Institute of Sericulture Science and

Technology Research, Chongqing, China) for providing mulberry seeds and silkworm eggs, respectively.

## Conflict of interest

The authors declare that the research was conducted in the absence of any commercial or financial relationships that could be construed as a potential conflict of interest.

## Publisher's note

All claims expressed in this article are solely those of the authors and do not necessarily represent those of their affiliated organizations, or those of the publisher, the editors and the reviewers. Any product that may be evaluated in this article, or claim that may be made by its manufacturer, is not guaranteed or endorsed by the publisher.

## Supplementary material

The Supplementary Material for this article can be found online at: <https://www.frontiersin.org/articles/10.3389/fmicb.2022.978550/full#supplementary-material>

## References

- Alessa, O., Ogura, Y., Fujitani, Y., Takami, H., Hayashi, T., Sahin, N., et al. (2021). Comprehensive comparative genomics and phenotyping of *Methylobacterium* species. *Front. Microbiol.* 12:740610. doi: 10.3389/fmicb.2021.740610
- Álvarez-Marin, R., Lepe, J. A., Gasch-Blasi, O., Rodríguez-Martínez, J. M., Calvo-Montes, J., Lara-Contreras, R., et al. (2021). Clinical characteristics and outcome of bacteraemia caused by *Enterobacter cloacae* and *Klebsiella aerogenes*: More similarities than differences. *J. Glob. Antimicrob. Res.* 25, 351–358. doi: 10.1016/j.jgar.2021.04.008
- Bacon, C. W., and White, J. F. (2015). Functions, mechanisms and regulation of endophytic and epiphytic microbial communities of plants. *Symbiosis* 68, 87–98. doi: 10.1007/s13199-015-0350-2
- Becerra, S. C., Roy, D. C., Sanchez, C. J., Christy, R. J., and Burmeister, D. M. (2016). An optimized staining technique for the detection of Gram positive and Gram negative bacteria within tissue. *BMC Res. Notes* 9:216. doi: 10.1186/s13104-016-1902-0
- Beckers, B., De Beeck, M. O., Weyens, N., Boerjan, W., and Vangronsveld, J. (2017). Structural variability and niche differentiation in the rhizosphere and endosphere bacterial microbiome of field-grown poplar trees. *Microbiome* 5, 25–42. doi: 10.1186/s40168-017-0241-2
- Compant, S., Clément, C., and Sessitsch, A. (2010). Plant growth-promoting bacteria in the rhizo- and endosphere of plants: Their role, colonization, mechanisms involved and prospects for utilization. *Soil Biol. Biochem.* 42, 669–678. doi: 10.1016/j.soilbio.2009.11.024
- Cao, X. C., Chen, X. Y., Li, X. Y., Yuan, L., Wu, L. H., and Zhu, Y. H. (2013). Rice uptake of soil adsorbed amino acids under sterilized environment. *Soil. Biol. Biochem.* 62, 13–21. doi: 10.1016/j.soilbio.2013.02.018
- Doell, S., Farahani-Kofoet, R. D., Zrenner, R., Henze, A., and Witzel, K. (2021). Tissue-specific signatures of metabolites and proteins in asparagus roots and exudates. *Hortic. Res.* 8, 86. doi: 10.1038/s41438-021-00510-5
- Edgar, R. C. (2013). UPARSE: Highly accurate OTU sequences from microbial amplicon reads. *Nat. Methods* 10, 996–998. doi: 10.1038/NMETH.2604
- Gaind, S. (2016). Phosphate dissolving fungi: Mechanism and application in alleviation of salt stress in wheat. *Microbiol. Res.* 193, 94–102. doi: 10.1016/j.micres.2016.09.005
- Glick, B. R. (2014). Bacteria with ACC deaminase can promote plant growth and help to feed the world. *Microbiol. Res.* 169, 30–39. doi: 10.1016/j.micres.2013.09.009
- Guo, J. K., and Chi, J. (2014). Effect of Cd-tolerant plant growth-promoting rhizobium on plant growth and Cd uptake by *Lolium multiflorum* Lam. and *Glycine max* (L.) Merr. in Cd-contaminated soil. *Plant Soil* 375, 205–214. doi: 10.1007/s11104-013-1952-1
- Han, Y. L., Wang, R., Yang, Z. R., Zhan, Y. H., Ma, Y., Ping, S. Z., et al. (2015). 1-aminocyclopropane-1-carboxylate deaminase from *Pseudomonas stutzeri* A1501 facilitates the growth of rice in the presence of salt or heavy metals. *J. Microbiol. Biotechnol.* 25, 1119–1128. doi: 10.4014/jmb.1412.12053
- Huang, X. H., Liu, Y., Li, J. X., Xiong, X. Z., Chen, Y., Yin, X. H., et al. (2013). The response of mulberry trees after seedling hardening to summer drought in the hydro-fluctuation belt of Three Gorges Reservoir Areas. *Environ. Sci. Pollut. Res.* 20, 7103–7111. doi: 10.1007/s11356-012-1395-x
- Hallmann, J., and Berg, G. (2006). "Spectrum and population dynamics of bacterial root endophytes," in *Microbial root endophytes*, eds B. J. E. Schulz, C. J. C. Boyle, and T. N. Sieber (Berlin: Springer), 15–31. doi: 10.1007/3-540-33526-9\_2

- Hua, M. D. S., Kumar, R. S., Shyur, L. F., Cheng, Y. B., Tian, Z. H., Oelmüller, R., et al. (2017). Metabolomic compounds identified in *Piriformospora indica*-colonized Chinese cabbage roots delineate symbiotic functions of the interaction. *Sci. Rep.* 7, 9291–9305. doi: 10.1038/s41598-017-08715-2
- Hara, S., Matsuda, M., and Minamisawa, K. (2019). Growth stage-dependent bacterial communities in soybean plant tissues: *Methylobacterium* transiently dominated in the flowering stage of the soybean shoot. *Microbes Environ.* 34, 446–450. doi: 10.1264/jsme2.ME19067
- Hu, L., Mateo, P., Ye, M., Zhang, X., Berset, J. D., Handrick, V., et al. (2018). Plant iron acquisition strategy exploited by an insect herbivore. *Science* 361, 694–697. doi: 10.1126/science.aat4082
- Ibrahim, M. H., and Jaafar, H. Z. E. (2012). Impact of elevated carbon dioxide on primary, secondary metabolites and antioxidant responses of *Eleais guineensis* Jacq. (Oil Palm) seedlings. *Molecules* 17, 5195–5211. doi: 10.3390/molecules17055195
- Jaemsaeng, R., Jantasuriyarat, C., and Thamchaipenet, A. (2018). Molecular interaction of 1-aminocyclopropane-1-carboxylate deaminase (ACC-CD)-producing endophytic *Streptomyces* sp. GMKU 336 towards salt-stress resistance of *Oryza sativa* L. cv. KDML105. *Sci. Rep.* 8, 1950–1965. doi: 10.1038/s41598-018-19799-9
- Jain, R., Bhardwaj, P., Pandey, S. S., and Kumar, S. (2021). *Arnebia euchroma*, a plant species of cold desert in the Himalayas, harbors beneficial cultivable endophytes in roots and leaves. *Front. Microbiol.* 12:696667–696683. doi: 10.3389/fmicb.2021.696667
- Jasim, B., Joseph, A. A., John, C. J., Mathew, J., and Radhakrishnan, E. K. (2013). Isolation and characterization of plant growth promoting endophytic bacteria from the rhizome of *Zingiber officinale*. *3 Biotech* 4, 197–204. doi: 10.1007/s13205-013-0143-3
- Jha, P. N., and Kumar, A. (2007). Endophytic colonization of *Typha australis* by a plant growth-promoting bacterium *Klebsiella oxytoca* strain GR-3. *J. Appl. Microbiol.* 103, 1311–1320. doi: 10.1111/j.1365-2672.2007.03383.x
- Jiang, Y. B., Jiang, S. M., Li, Z. B., Yan, X. P., Qin, Z. X., and Huang, R. Z. (2019). Field scale remediation of Cd and Pb contaminated paddy soil using three mulberry (*Morus alba* L.) cultivars. *Ecol. Eng.* 129, 38–44. doi: 10.1016/j.ecoleng.2019.01.009
- Koskimäki, J. J., Pohjanen, J., Kvist, J., Fester, T., Härtig, C., Podolich, O., et al. (2022). The meristem-associated endosymbiont *Methylobacterium extorquens* DSM13060 reprograms development and stress responses of pine seedlings. *Tree Physiol.* 42, 391–410. doi: 10.1093/treephys/tpab102
- Kundu, A., Mishra, S., Kundu, P., Jogawat, A., and Vadassery, J. (2021). *Piriformospora indica* recruits host-derived putrescine for growth promotion in plants. *Plant. Physiol.* 188, 2289–2307. doi: 10.1093/plphys/kiab536
- Lu, R. K. (2000). *Methods for soil and agriculture chemistry analysis*. Beijing: Chinese Agricultural Science and Technology Press.
- Liu, C. J., Lin, H., Dong, Y. B., and Li, B. (2022). Increase of P and Cd bioavailability in the rhizosphere by endophytes promoted phytoremediation efficiency of *Phytolacca acinosa*. *J. Hazard. Mater.* 431:128546. doi: 10.1016/j.jhazmat.2022.128546
- Lu, Q., Ge, G. T., Sa, D. W., Wang, Z. J., Hou, M. L., and Jia, Y. S. (2021). Effects of salt stress levels on nutritional quality and microorganisms of alfalfa-influenced soil. *PeerJ (San Francisco, CA)* 9:e11729. doi: 10.7717/peerj.11729
- Liu, Y., and Willison, J. H. M. (2013). Prospects for cultivating white mulberry (*Morus alba*) in the drawdown zone of the Three Gorges Reservoir, China. *Environ. Sci. Pollut. Res.* 20, 7142–7151. doi: 10.1007/s11356-013-1896-2
- Liotti, R. G., da Silva Figueiredo, M. I., da Silva, G. F., de Mendonça, E. A. F., and Soares, M. A. (2018). Diversity of cultivable bacterial endophytes in *Paullinia cupana* and their potential for plant growth promotion and phytopathogen control. *Microbiol. Res.* 207, 8–18. doi: 10.1016/j.micres.2017.10.011
- Liu, Y. P., Zhu, A. P., Tan, H. M., Cao, L. X., and Zhang, R. D. (2019). Engineering banana endosphere microbiome to improve *Fusarium wilt* resistance in banana. *Microbiome* 7, 74–89. doi: 10.1186/s40168-019-0690-x
- Li, L. Y., and Huang, H. (2017). Risk factors of mortality in bloodstream infections caused by *Klebsiella pneumoniae*. *Medicine* 96:e7924. doi: 10.1097/MD.0000000000007924
- Li, H., Xiang, D., Wang, C., Li, X. L., and Lou, Y. (2012). Effects of epigeic earthworm (*Eisenia fetida*) and arbuscular mycorrhizal fungus (*Glomus intraradices*) on enzyme activities of a sterilized soil-sand mixture and nutrient uptake by maize. *Biol. Fertil. Soils* 48, 879–887. doi: 10.1007/s00374-012-0679-0
- Liu, W. X., Wang, Q. L., Hou, J. Y., Tu, C., Luo, Y. M., and Christie, P. (2016). Whole genome analysis of halotolerant and alkalotolerant plant growth-promoting rhizobacterium *Klebsiella* sp. D5A. *Sci. Rep.* 6:26710. doi: 10.1038/srep26710
- Li, Q., Xing, Y. N., Fu, X. W., Ji, L., Li, T. Y., Wang, J. N., et al. (2021). Biochemical mechanisms of rhizospheric *Bacillus subtilis*-facilitated phytoextraction by alfalfa under cadmium stress-microbial diversity and metabolomics analyses. *Ecotoxicol. Environ. Saf.* 212:112016. doi: 10.1016/j.ecoenv.2021.112016
- Luttgeham, K. D., Kimberlin, A. N., and Cahoon, E. B. (2016). Plant sphingolipid metabolism and function. *Lipids Plant Algae Dev.* 86, 249–286. doi: 10.1007/978-3-319-25979-6\_11
- Magnus, V., Šoškić, M., Iskrić, S., and Kveder, S. (1980). The separation of indole-3-acetic acid and related compounds in plant extracts by sephadex chromatography. *Anal. Biochem.* 103, 419–425. doi: 10.1016/0003-2697(80)90633-8
- Montesinos-Navarro, A., Pérez-Clemente, R. M., Sánchez-Martín, R., Gómez-Cadenas, A., and Verdú, M. (2020). Phylogenetic analysis of secondary metabolites in a plant community provides evidence for trade-offs between biotic and abiotic stress tolerance. *Evol. Ecol.* 34, 439–451. doi: 10.1007/s10682-020-10044-2
- Mansfield, J., Genin, S., Magori, S., Citovsky, V., Sriariyanum, M., Ronald, P., et al. (2012). Top 10 plant pathogenic bacteria in molecular plant pathology. *Mol. Plant Pathol.* 13, 614–629. doi: 10.1111/j.1364-3703.2012.00804.x
- Nascimento, F. X., Rossi, M. J., and Glick, B. R. (2018). Ethylene and 1-aminocyclopropane-1-carboxylate (ACC) in plant-bacterial interactions. *Front. Plant Sci.* 9:114–131. doi: 10.3389/fpls.2018.00114
- Olanrewaju, O. S., Glick, B. R., and Babalola, O. O. (2017). Mechanisms of action of plant growth promoting bacteria. *World J. Microbiol. Biotechnol.* 33, 197–213. doi: 10.1007/s11274-017-2364-9
- Ou, T., Zhang, M., Huang, Y. Z., Wang, L., Wang, F., Wang, R. L., et al. (2022). Role of rhizospheric *Bacillus megaterium* HGS7 in maintaining mulberry growth under extremely abiotic stress in hydro-fluctuation belt of Three Gorges Reservoir. *Front. Plant Sci.* 13:880125. doi: 10.3389/fpls.2022.880125
- Ou, T., Xu, W. F., Wang, F., Strobel, G., Zhou, Z. Z., Xiang, Z. H., et al. (2019). A microbiome study reveals seasonal variation in endophytic bacteria among different mulberry cultivars. *Comput. Struct. Biotechnol. J.* 17, 1091–1100. doi: 10.1016/j.csbj.2019.07.018
- Pruesse, E., Quast, C., Knittel, K., Fuchs, B. M., Ludwig, W., Peplies, J., et al. (2007). SILVA: A comprehensive online resource for quality checked and aligned ribosomal RNA sequence data compatible with ARB. *Nucleic Acids Res.* 35, 7188–7196. doi: 10.1093/nar/gkm864
- Patten, C. L., and Glick, B. R. (1996). Bacterial biosynthesis of indole-3-acetic acid. *Can. J. Microbiol.* 42, 207–220. doi: 10.1139/m96-032
- Pavlova, A. S., Leontieva, M. R., Smirnova, T. A., Kolomeitseva, G. L., Netrusov, A. I., and Tsavkelova, E. A. (2017). Colonization strategy of the endophytic plant growth-promoting strains of *Pseudomonas fluorescens* and *Klebsiella oxytoca* on the seeds, seedlings and roots of the epiphytic orchid, *Dendrobium nobile* Lindl. *J. Appl. Microbiol.* 123, 217–232. doi: 10.1111/jam.13481
- Pan, Z. C., Xu, J., Prior, P., Xu, J. S., Zhang, H., Chen, K. Y., et al. (2013). Development of a specific molecular tool for the detection of epidemiologically active mulberry causing-disease strains of *Ralstonia solanacearum* phylotype I (historically race 5-biovar 5) in China. *Eur. J. Plant. Pathol.* 137, 377–391. doi: 10.1007/s10658-013-0249-9
- Park, Y. J., Seong, S. H., Kim, M. S., Seo, S. W., Kim, M. R., and Kim, H. S. (2017). High-throughput detection of antioxidants in mulberry fruit using correlations between high-resolution mass and activity profiles of chromatographic fractions. *Plant Methods* 13, 108–124. doi: 10.1186/s13007-017-0258-3
- Quast, C., Pruesse, E., Yilmaz, P., Gerken, J., Schweer, T., Yarza, P., et al. (2013). The SILVA ribosomal RNA gene database project: Improved data processing and web-based tools. *Nucleic Acids Res.* 41, 590–596. doi: 10.1093/nar/gks1219
- Schloss, P. D., Westcott, S. L., Ryabin, T., Hall, J. R., Hartmann, M., Hollister, E. B., et al. (2009). Introducing mothur: Open-source, platform-independent, community-supported software for describing and comparing microbial communities. *Appl. Environ. Microbiol.* 75, 7537–7541. doi: 10.1128/AEM.01541-09
- Singh, R. P., Jha, P., and Jha, P. N. (2015). The plant-growth-promoting bacterium *Klebsiella* sp. SBP-8 confers induced systemic tolerance in wheat (*Triticum aestivum*) under salt stress. *J. Plant Physiol.* 184, 57–67. doi: 10.1016/j.jplph.2015.07.002
- Sun, X. L., Xu, Z. H., Xie, J. Y., Hesselberg-Thomsen, V., Tan, T. M., Zheng, D. Y., et al. (2022). *Bacillus velezensis* stimulates resident rhizosphere *Pseudomonas stutzeri* for plant health through metabolic interactions. *ISME J.* 16, 774–787. doi: 10.1038/s41396-021-01125-3
- Sun, L. J., Cao, X. Y., Tan, C. Y., Deng, Y. Q., Cai, R. Z., et al. (2020). Analysis of the effect of cadmium stress on root exudates of *Sedum plumbizincicola* based on metabolomics. *Ecotoxicol. Environ. Saf.* 205, 111152–111161. doi: 10.1016/j.ecoenv.2020.111152

- Sun, X., Wang, N., Li, P., Jiang, Z. Y., Liu, X. Y., Wang, M. C., et al. (2020). *Endophytic fungus Falciphora oryzae* promotes lateral root growth by producing indole derivatives after sensing plant signals. *Plant Cell Environ.* 43, 358–373. doi: 10.1111/pce.13667
- Stringlis, I., Yu, K., Feussner, K., de Jonge, R., Van Bentum, S., Van Verk, M. C., et al. (2018). MYB72-dependent coumarin exudation shapes root microbiome assembly to promote plant health. *Proc. Natl. Acad. Sci. U.S.A.* 115, E5213–E5222. doi: 10.1073/pnas.1722335115
- Stringlis, I., De Jonge, R., and Pieterse, C. M. J. (2019). The age of coumarins in plant-microbe interactions. *Plant Cell Physiol.* 60, 1405–1419. doi: 10.1093/pcp/pcz076
- Saravanan, S. (2021). Effect of elevated CO<sub>2</sub> on growth and biochemical changes in *Catharanthus roseus*-a valuable medicinal herb. *J. Stress Physiol. Biochem.* 17, 411–422.
- Taylor, J. A., and West, D. W. (1980). The use of Evan's blue stain to test the survival of plant cells after exposure to high salt and high osmotic pressure. *J. Exp. Bot.* 31, 571–576. doi: 10.1093/jxb/31.2.571
- Tamura, K., Peterson, D., Peterson, N., Stecher, G., Nei, M., and Kumar, S. (2011). MEGA5: Molecular evolutionary genetics analysis using maximum likelihood, evolutionary distance, and maximum parsimony methods. *Mol. Biol. Evol.* 28, 2731–2739. doi: 10.1093/molbev/msr121
- Tiwari, S., Lata, C., Chauhan, P. S., and Nautiyal, C. S. (2016). *Pseudomonas putida* attunes morphophysiological, biochemical and molecular responses in *Cicer arietinum* L. during drought stress and recovery. *Plant Physiol. Biochem.* 99, 108–117. doi: 10.1016/j.plaphy.2015.11.001
- Ullah, A., Nisar, M., Ali, H., Hazrat, A., Hayat, K., Keerio, A. A., et al. (2019). Drought tolerance improvement in plants: An endophytic bacterial approach. *App. Environ. Microb.* 103, 7385–7397. doi: 10.1007/s00253-019-10045-4
- Viviji, B., Moons, P., Aertsen, A., and Michiels, C. W. (2014). Acetoin synthesis acquisition favors *Escherichia coli* growth at low pH. *App. Environ. Microb.* 80, 6054–6061. doi: 10.1128/AEM.01711-14
- Vilchez, J. I., Niehaus, K., Dowling, D. N., Gonzalez-Lopez, J., and Manzanera, M. (2018). Protection of pepper plants from drought by *Microbacterium* sp. 3J1 by modulation of the plant's glutamine and  $\alpha$ -ketoglutarate content: A comparative metabolomics approach. *Front. Microbiol.* 9:284–301. doi: 10.3389/fmicb.2018.00284
- Vinci, G., Cozzolino, V., Mazzei, P., Monda, H., Savy, D., Drosos, M., et al. (2018). Effects of *Bacillus amyloliquefaciens* and different phosphorus sources on maize plants as revealed by NMR and GC-MS based metabolomics. *Plant Soil* 429, 437–450. doi: 10.1007/s11104-018-3701-y
- Wang, Y. J., Chen, F. Q., Zhang, M., Chen, S. H., Tan, X. Q., Liu, M., et al. (2018). The effects of the reverse seasonal flooding on soil texture within the hydro-fluctuation belt in the Three Gorges reservoir, China. *J. Soil Sediments* 18, 109–115. doi: 10.1007/s11368-017-1725-1
- Wang, M. Y., Liu, X. T., Chen, Y., Xu, X. J., Yu, B., Zhang, S. Q., et al. (2012). Arabidopsis acetyl-amido synthetase GH3.5 involvement in camalexin biosynthesis through conjugation of indole-3-carboxylic acid and cysteine and upregulation of camalexin biosynthesis genes. *J. Integr. Plant Biol.* 54, 471–485. doi: 10.1111/j.1744-7909.2012.01131.x
- Wang, L., Lin, H., Dong, Y. B., Li, B., and He, Y. H. (2020). Effects of endophytes inoculation on rhizosphere and endosphere microecology of Indian mustard (*Brassica juncea*) grown in vanadium-contaminated soil and its enhancement on phytoremediation. *Chemosphere* 240, 124891–124901. doi: 10.1016/j.chemosphere.2019.124891
- Welmillage, S. U., Zhang, Q., Sreevidya, V. S., Sadowsky, M. J., and Gyaneshwar, P. (2021). Inoculation of *Mimosa pudica* with *Paraburkholderia phymatum* results in changes to the rhizoplane microbial community structure. *Microbes Environ.* 36:ME20153. doi: 10.1264/jsme2.ME20153
- Xu, W. F., Wang, F., Zhang, M., Ou, T., Wang, R. L., Strobel, G., et al. (2019). Diversity of cultivable endophytic bacteria in mulberry and their potential for antimicrobial and plant growth-promoting activities. *Microbiol. Res.* 229, 126328–126339. doi: 10.1016/j.micres.2019.126328
- Xu, F. Y., Liao, H. P., Zhang, Y. J., Yao, M. J., Liu, J. P., Sun, L. Y., et al. (2022). Coordination of root auxin with the fungus *Piriformospora indica* and bacterium *Bacillus cereus* enhances rice rhizosphere formation under soil drying. *ISME J.* 16, 801–811. doi: 10.1038/s41396-021-01133-3
- Xu, S. D., Liu, Y. X., Cernava, T., Wang, H. K., Zhou, Y. Q., Xia, T., et al. (2022). *Fusarium* fruiting body microbiome member *Pantoea agglomerans* inhibits fungal pathogenesis by targeting lipid rafts. *Nat. Microbiol.* 7, 831–843. doi: 10.1038/s41564-022-01131-x
- Xie, J., Xu, W. F., Zhang, M., Qiu, C. Y., Liu, J., Wisniewski, M., et al. (2021). The impact of the endophytic bacterial community on mulberry tree growth in the Three Gorges Reservoir ecosystem, China. *Environ. Microbiol.* 23, 1858–1875. doi: 10.1111/1462-2920.15230
- Xie, J., Shu, P., Strobel, G., Chen, J., Wei, J. H., Xiang, Z. H., et al. (2017). *Pantoea agglomerans* SWG2 colonizes mulberry tissues, promotes disease protection and seedling growth. *Biol. Control* 113, 9–17. doi: 10.1016/j.biocontrol.2017.06.010
- Yin, D. L., Wang, Y. M., Xiang, Y. P., Xu, Q. Q., Xie, Q., Zhang, C., et al. (2020). Production and migration of methylmercury in water-level-fluctuating zone of the Three Gorges Reservoir, China: Dual roles of flooding-tolerant perennial herb. *J. Hazard. Mater.* 381, 120962–120971. doi: 10.1016/j.jhazmat.2019.120962
- Yurgel, S. N., Ajeethan, N., and Smertenko, A. (2022). Response of plant-associated microbiome to plant root colonization by exogenous bacterial endophyte in perennial crops. *Front. Microbiol.* 13:863946. doi: 10.3389/fmicb.2022.8639
- Zhou, Y. J., Li, J. H., Friedman, C. R., and Wang, H. F. (2017). Variation of soil bacterial communities in a chronosequence of rubber tree (*Hevea brasiliensis*) plantations. *Front. Plant Sci.* 8:849–861. doi: 10.3389/fpls.2017.00849
- Zhang, Y., Yu, X. X., Zhang, W. J., Lang, D. Y., Zhang, X. J., Cui, G. C., et al. (2019). Interactions between endophytes and plants: Beneficial effect of endophytes to ameliorate biotic and abiotic stresses in plants. *J. Plant. Biol.* 62, 1–13. doi: 10.1007/s12374-018-0274-5
- Zhang, L., Zhong, J., Liu, H., Xin, K. Y., Chen, C. Q., Li, Q. Q., et al. (2017). Complete genome sequence of the drought resistance-promoting endophyte *Klebsiella* sp. LTGPAP-6F. *J. Biotechnol.* 246, 36–39. doi: 10.1016/j.jbiotec.2017.02.008
- Zhuang, L. B., Li, Y., Wang, Z. S., Yu, Y., Zhang, N., Yang, C., et al. (2021). Synthetic community with six *Pseudomonas* strains screened from garlic rhizosphere microbiome promotes plant growth. *Microb. Biotechnol.* 14, 488–502. doi: 10.1111/1751-7915.13640
- Zhao, S., Shang, X., and Duo, L. (2013). Accumulation and spatial distribution of Cd, Cr, and Pb in mulberry from municipal solid waste compost following application of EDTA and (NH<sub>4</sub>)<sub>2</sub>SO<sub>4</sub>. *Environ. Sci. Pollut. Res.* 20, 967–975. doi: 10.1007/s11356-012-0992-z





## OPEN ACCESS

## EDITED BY

Vineet Kumar,  
National Environmental Engineering  
Research Institute (CSIR), India

## REVIEWED BY

Pankaj Bhatt,  
Purdue University, United States  
Chao He,  
Chinese Academy of Medical Sciences  
& Peking Union Medical College, China  
Mujahid Farid,  
University of Gujrat, Pakistan  
Charu Lata,  
CSIR-National Institute of Science  
Communication and Policy Research,  
India

## \*CORRESPONDENCE

Haiyan Li  
lhyxrn@163.com

†These authors have contributed  
equally to this work

## SPECIALTY SECTION

This article was submitted to  
Microbiotechnology,  
a section of the journal  
Frontiers in Microbiology

RECEIVED 16 July 2022

ACCEPTED 29 August 2022

PUBLISHED 21 September 2022

## CITATION

Sharma VK, Parmar S, Tang W, Hu H,  
White JF Jr and Li H (2022) Effects of  
fungal seed endophyte FXZ2 on  
*Dysphania ambrosioides* Zn/Cd  
tolerance and accumulation.  
*Front. Microbiol.* 13:995830.  
doi: 10.3389/fmicb.2022.995830

## COPYRIGHT

© 2022 Sharma, Parmar, Tang, Hu,  
White and Li. This is an open-access  
article distributed under the terms of  
the [Creative Commons Attribution  
License \(CC BY\)](#). The use, distribution  
or reproduction in other forums is  
permitted, provided the original  
author(s) and the copyright owner(s)  
are credited and that the original  
publication in this journal is cited, in  
accordance with accepted academic  
practice. No use, distribution or  
reproduction is permitted which does  
not comply with these terms.

# Effects of fungal seed endophyte FXZ2 on *Dysphania ambrosioides* Zn/Cd tolerance and accumulation

Vijay K. Sharma<sup>1†</sup>, Shobhika Parmar<sup>1†</sup>, Wenting Tang<sup>1</sup>,  
Haiyan Hu<sup>2</sup>, James F. White Jr.<sup>3</sup> and Haiyan Li<sup>1\*</sup>

<sup>1</sup>Medical School, Kunming University of Science and Technology, Kunming, China, <sup>2</sup>State Key Laboratory of Environmental Geochemistry, Institute of Geochemistry, Chinese Academy of Sciences, Guiyang, China, <sup>3</sup>Department of Plant Biology, Rutgers University, New Brunswick, NJ, United States

Metal-induced oxidative stress in contaminated soils affects plant growth. In the present study, we evaluated the role of seed endophyte FXZ2 on *Dysphania ambrosioides* Zn/Cd tolerance and accumulation. A series of pot experiments were conducted under variable Zn (500, 1,000, and 1,500 mg kg<sup>-1</sup>) and Cd (5, 15, 30, and 60 mg kg<sup>-1</sup>). The results demonstrated that FXZ2-inoculation significantly enhanced the growth of *D. ambrosioides* and improved its chlorophyll and GSH content. In the rhizosphere, FXZ2 inoculation changed the chemical speciation of Zn/Cd and thus affected their uptake and accumulation in host plants. The exchangeable and carbonate-bound fractions (F1 + F2) of Zn decreased in the rhizosphere of FXZ2-inoculated plants (E+) as compared to non-inoculated plants (E-) under Zn stress (500 and 1,000 mg kg<sup>-1</sup>), correspondingly, Zn in the shoots of E+ decreased ( $p < 0.05$ ). However, at Cd stress (30 and 60 mg kg<sup>-1</sup>), the F1 + F2 fractions of Cd in E+ rhizospheric soils increased; subsequently, Cd in the shoots of E+ increased ( $p < 0.05$ ). FXZ2 could exogenously secrete phytohormones IAA, GA, and JA. The study suggests that seed endophyte FXZ2 can increase Zn/Cd tolerance of host plant by altering Zn/Cd speciation in rhizospheric soils, as well as exogenous production of phytohormones to promote growth, lowering oxidative damage while enhancing antioxidant properties. For Zn/Cd accumulation, it has opposite effects: Zn uptake in E+ plants was significantly ( $p < 0.05$ ) decreased, while Cd accumulation in E+ plants was significantly ( $p < 0.05$ ) increased. Thus, FXZ2 has excellent application prospects in Cd phytoextraction and decreasing Zn toxicity in agriculturally important crops.

## KEYWORDS

seed endophytes, *Dysphania ambrosioides*, metal stress, phytoremediation, mechanism, chemical speciation



## Introduction

Plants rely on various metals for normal physiology, but higher or excess metals in the soil not only deteriorate the soil health and change the native microbial community but also adversely affect the physiology and metabolism of plants (Kidd et al., 2012; Chen et al., 2014; Parmar and Singh, 2015; Etesami, 2018). Zinc (Zn) is an essential element for plants, but a higher concentration of Zn in the soil adversely affects plant growth via root growth inhibition, mitotic efficiency, chromosomal aberrations as well as oxidative stress (Jain et al., 2010). Cadmium (Cd) is a non-essential trace element that can cause toxicity even at lower concentrations (Wagner, 1993; Nan et al., 2002; Kuriakose and Prasad, 2008), accumulates readily in the soil and enters the food chain via enrichment in food crops (Wang et al., 2022). The bioavailability, mobility, and toxicity of these metals to plants depend on their chemical forms rather than the total contents (Liu et al., 2007). Therefore, the chemical speciation of metals in the soil may have an important impact on plants (Tüzen, 2003; Ahlf et al., 2009).

It is well known that metal-contaminated soils cause various problems to the surrounding environments, such as plants survival, agricultural production, food safety, and human health; therefore, the remediation of these metal-contaminated soils is of utmost importance (Hussain et al., 2022). Some plants growing in highly metal-contaminated environments evolved to tolerate metal stress; they have potential applications in phytoremediation. Previous studies have demonstrated that plant-associated microbes, i.e., endophytes can increase host plants' metal tolerance properties, enhance their growth, and influence their metal accumulation (Sharma et al., 2019; Rattanapolsan et al., 2021; Ważny et al., 2021; Hussain et al., 2022). It is believed that endophytes induced tolerance and growth improvement of host plants to metal stress by detoxification through chelation and compartmentalization of metal ions, increasing nutrient absorption and root growth, changing the distribution of metal in plant cells, modulating the antioxidative system, and secretion of phytohormones (Bilal et al., 2018; White et al., 2019; Chang et al., 2021; Akhtar et al., 2022).

FXZ2 is a fungal seed endophyte that has been isolated from *Arabidopsis thaliana*, and it has been identified to be *Epicoccum nigrum* (GenBank accession number is ON209455) (Chu et al., 2017). Our previous studies have demonstrated that FXZ2 has high tolerance and adsorption capacity for lead (Pb) and Cd, and it can significantly enhance host plants' growth under Zn/Cd stress. Seed endophytes are attributed to providing beneficial traits such as improving nutrient uptake, reducing susceptibility to drought and temperature stress, and improving the growth of host plants. However, the role of seed endophytes on the plants' metal tolerance and accumulation as well as its mechanisms are still unknown. For the beneficial characteristics that the seed endophyte can be transferred to the

next generation through vertical transmission (Li et al., 2019), therefore, in practice, it has more advantages than the other symbiotic microbes. For example, the seed endophyte RE3-3 *Herbaspirillum frisingense* was successfully transmitted to the next generation seeds of *Phragmites australis* and, consequently, enhanced seedling development and growth under Cd stress (Gao and Shi, 2018).

*Dysphania ambrosioides* (L.) Mosyakin and Clematis is a dominant plant in Pb-Zn mining sites of Huize County, Yunnan Province, China. It has been reported as a Cd-accumulator and a Pb-hyperaccumulator, which showed potential application in phytoremediation of multi-metal-contaminated sites (Wu et al., 2004; Li et al., 2012; Li X. et al., 2016). The present study aimed to investigate the role of fungal seed endophyte FXZ2 on *D. ambrosioides* Zn/Cd tolerance under variable Zn (500, 1,000, and 1,500 mg kg<sup>-1</sup> soil) and Cd (5, 15, 30, and 60 mg kg<sup>-1</sup> soil) stress. Further, the speciation of Zn/Cd in rhizospheric soils of *D. ambrosioides* was tested by Tessier sequential extraction methods. The objective of this study is to elucidate how the seed endophyte FXZ2 altered the metals' chemical speciation in rhizospheric soils and thus affected their absorption, translocation, and accumulation in host plants. The novelty of this work is that it gives important information about the function of seed endophytes in increasing the survival and growth of host plants under metal stress conditions.

## Materials and methods

### Fungal seed endophyte FXZ2

The fungal seed endophyte FXZ2 was previously isolated from the seeds of *Arabidopsis thaliana*, which were collected from the Pb-Zn mining sites of Huize County, Yunnan Province, Southwest China (25°28'17" N, 103°37'34" E) (Chu et al., 2017). FXZ2 was identified to be *Epicoccum nigrum* based on its morphological features and molecular analysis (Chu et al., 2017), and its GenBank database accession number is ON209455<sup>1</sup>. The isolate showed better Pb and Cd tolerance and adsorption capacity, and has been authorized by the Patent Office of the People's Republic of China (ZL 2017 1 0028569. 2). It was submitted to the Chinese General Microbiological Culture Collection Center (CGMCC NO.13573).

### Phytohormone production

To assess for phytohormones jasmonic acid (JA), indole-3-acetic acid (IAA), and gibberellic acid (GA) production, the

<sup>1</sup> <http://www.ncbi.nlm.nih.gov/>

isolate FXZ2 was grown in PDB (potato dextrose broth) at  $28 \pm 2^\circ\text{C}$  for 21 days in a shaker. After that, the culture was filtered and the broth was collected and extracted three times with ethyl acetate, followed by concentration using a vacuum rotary evaporator. Finally, the extract was dissolved in methanol for phytohormone tests according to the manufacturer of plant hormone kits (MLBIO Biotechnology Co., Ltd., Shanghai). A change in the color of the reaction mixture was measured by a spectrophotometer at a wavelength of 450 nm. And the concentrations of IAA, GA, and JA in the extracts were calculated by comparing the OD of the extracts to the standard curve of the IAA, GA, and JA. Three replicates were performed.

## Pot experiments

The mature seeds were collected from naturally growing *D. ambrosioides* and surface sterilized as Li et al. (2012). Subsequently, the seeds were germinated on a plastic tray that contained a fixed soil substrate (perlite: peat moss, 3:7, vol:vol) in a light incubator ( $25 \pm 1/18 \pm 1^\circ\text{C}$ , 16/8 h day/night cycle, 60% relative humidity). Twenty-one days later, the germinated seedlings with equal size were transplanted to the pots (1 seedling/pot), which contained 150 gm of sterilized soil substrate mixed with the overages of  $\text{ZnSO}_4 \cdot 7\text{H}_2\text{O}$  or  $\text{CdCl}_2 \cdot 2.5\text{H}_2\text{O}$  to the final concentration of 0, 500, 1,000, and 1,500 mg Zn  $\text{kg}^{-1}$  and 0, 5, 15, and 30 mg Cd  $\text{kg}^{-1}$ , respectively. The pots were kept in a random configuration and exposed to artificial plant lighting (16/8 h day/night cycle). Every 2–3 days, the plants were irrigated with autoclaved water, and once a week Peter's General Purpose 20-20-20 fertilizer (Grace Sierra Horticultural Products, Milpitas, CA, USA) was given.

For the inoculation, FXZ2 was grown on PDA plates at  $25^\circ\text{C}$  for 7 days. Then, the mycelia were scraped off and suspended in autoclaved distilled water and divided equally into two portions (A and B). Suspension B was autoclaved at  $121^\circ\text{C}$  for 20 min. The pots were randomly divided into two groups (I and II). Further, the plants of group-I were sprayed with suspension A (E+) and group II with autoclaved suspension B (E-) at different time intervals 7, 15, 30, and 45 days of the transplant. The plants were harvested after growing for 60 days, and the fresh leaves were collected from E+ and E- and flash frozen right away with liquid nitrogen, preserved at  $-80^\circ\text{C}$ , and used within 2 weeks for biochemical analysis. Simultaneously, the rhizospheric soil from each pot was collected, air-dried, and kept in poly-bags with proper labels for subsequent analysis.

## Plant growth parameters

### Shoot, root length, and the dry biomass

The harvested plants were washed under tap water and finally rinsed with deionized water. After that, the

plants were divided into shoots (all aboveground parts) and roots (all belowground parts), and the length was measured. Finally, the shoots and roots were oven-dried at  $50\text{--}60^\circ\text{C}$  to constant weight, and then the dry biomass was recorded. The dried plant samples were used for metal content analysis.

### Total chlorophyll content

Ten plants were selected randomly from each group before harvesting, and the total chlorophyll content of the youngest fully developed leaves of each plant was analyzed using a chlorophyll meter (SPAD-502Plus, Konica Minolta, Inc., Tokyo, Japan). And the final chlorophyll content of each group was an average of 10 plants.

### Lipid peroxidation

A chemical assay kit (Nanjing Jiancheng Bioengineering Institute, Nanjing, China) was used to measure the lipid peroxidation extent, which was expressed in nanomoles of malondialdehyde (MDA) formation per gram of tissue. Three replicates were made. To do this, the frozen leaves' tissue was crushed in a chilled phosphate buffer (50 mM, pH 7.2). Then, the homogenate was centrifuged for 10 min at 3,500 rpm and  $4^\circ\text{C}$ . After that, the supernatant was transferred to a new tube and the MDA was measured spectrophotometrically (MAPADA UV-1800 PC).

### Glutathione content

The total glutathione (T-GSH) and oxidized glutathione (GSSG) assay kits were used for GSH analysis (Nanjing Jiancheng Bioengineering Institute, Nanjing, China). To do this, the frozen leaves were homogenized in an extraction buffer (1:4 ratio, wt/vol). Then, the homogenate was centrifuged for 10 min at 3,500 rpm and  $4^\circ\text{C}$ . After that, the supernatant was used for GSH analysis (Rahman et al., 2006).

The absorbance of the assay mixture was measured according to the manufacturer's protocol, and the T-GSH and GSSG content was calculated using the given formulas. The GSH content was expressed in micromoles per gram of fresh leaves, which was the calculated difference of GSSG content from the T-GSH content according to the formula mentioned in the kit.

## Cd/Zn accumulation in the plants

The dried root/shoot samples were homogenized into fine powders, respectively. Then, 0.2 g powders were digested in 5 ml  $\text{HNO}_3$  (65% w/w) at  $110^\circ\text{C}$  for 2 h. After cooling 1 ml  $\text{H}_2\text{O}_2$  (30% w/w) was added and the mixture was heated for 1 h. The digests were then diluted to 50 ml with triple-distilled water (Shen et al., 2013). Finally, the

concentrations of Cd/Zn were estimated by flame atomic absorption spectrometry (Li et al., 2014). The test was performed in triplicate.

## Chemical speciation of Cd/Zn in rhizospheric soils

The chemical speciation of Zn/Cd in rhizospheric soils was tested according to the method of Tessier et al. (1979). The method consists of five steps that give rise to five fractions operationally defined as F1 (exchangeable), F2 (carbonate bound), F3 (Fe-Mn oxides bound), F4 (organic bound), and F5 (residual). Briefly, 1 gm fine powder of the soil was taken into a 50-ml polycarbonate centrifuge tube. First fraction was extracted with 20 ml 1.0 M MgCl<sub>2</sub> (pH 7.0) for 1 h with continuous agitation. The second fraction was extracted with 10 ml 1.0 M sodium acetate (pH adjusted to 5.0 with acetic acid) for 5 h with continuous agitation. The third fraction was extracted with 20 ml 0.04 M NH<sub>2</sub>OH.HCl in 25% sodium acetate (pH 2.0) for 6 h at 96°C in a water bath with occasional agitation. The fourth fraction was extracted with 3 ml 0.02 M HNO<sub>3</sub> and 5 ml 30% H<sub>2</sub>O<sub>2</sub> (pH adjusted to 2.0 with HNO<sub>3</sub>) for 2 h at 96°C in a water bath with occasional agitation; after that, 3 ml 30% H<sub>2</sub>O<sub>2</sub> (pH 2.0 with HNO<sub>3</sub>) was added and extracted for 2 h at 96°C in a water bath with occasional agitation; subsequently, after cooling, 5 ml 3.2 M ammonium acetate in 20% (v/v) HNO<sub>3</sub> was added, and the samples were diluted to 20 ml and agitated continuously for 30 min. The fifth fraction was the residue left from the organic fraction. It was digested with 4 ml HCl-HNO<sub>3</sub> (3:1, v/v) mixture at 80°C for 30 min, then 100°C for 30 min, and finally 120°C for 1 h. After that, cooled and 1 ml HClO<sub>4</sub> was added to continue digestion at 100°C for 20 min, followed by 120°C for 1 h. The concentrations of Zn/Cd were determined by flame atomic absorption spectrometry in different fractions (Li et al., 2014). Triplicates were made. The effect of FXZ2 inoculation (FE) was introduced to evaluate the influence on the chemical speciation of Zn/Cd in the rhizospheric zone. Here,  $FE = (F^{E+} - F^{E-})/F^{E-}$ , where  $F^{E+}$  and  $F^{E-}$  represent the corresponding fractions of metals in the E+ and E- treatments, respectively. The FE data were represented as heatmap drawn using Heatmap function of R version 4.1.1 (2021).

## Statistical analysis

Boxplots were drawn using the ggboxplot function of the ggpubr package (version “0.4.0.999”) in R version 4.1.1 (Core TeamR, 2021) and RStudio 2021.09.0 (R Studio Team, 2021). The difference between E+ and E- was determined using Student's *t*-test significant at the level of <0.05%

performed in RStudio and one-way ANOVA and Duncan test ( $p < 0.05$ ).

## Results and discussion

### The effect of FXZ2 on *Dysphania ambrosioides* growth

No matter at Zn or Cd stress, FXZ2 significantly improved the shoot length of *D. ambrosioides* ( $p < 0.05$ ) (Figures 1, 2). However, it had different effects on the root length and dry biomass of *D. ambrosioides* under Zn stress and Cd stress. At all Zn concentrations, FXZ2 decreased the root length of *D. ambrosioides*, but the difference was only significant ( $p < 0.05$ ) at 1,500 mg kg<sup>-1</sup> Zn stress (Figure 1). Both the dry biomass of shoots and roots of E+ were significantly ( $p < 0.05$ ) higher than those of E- at all Zn concentrations. Contrary to this, at all Cd concentrations, FXZ2 improved the root length of *D. ambrosioides* ( $p > 0.05$ ) except at 30 mg kg<sup>-1</sup> Cd stress ( $p < 0.05$ ) (Figure 2). The dry biomass of E+ shoots was significantly ( $p < 0.05$ ) higher than that of E- shoots. However, the dry biomass of E+ roots was more than that of E- roots at all Cd concentrations, but the difference was only significant ( $p < 0.05$ ) at 15 and 60 mg kg<sup>-1</sup> Cd stress.

Although Zn is an essential element required for plant growth, its high concentration in the soil could affect essential plant metabolic functions and cause retarded growth and senescence (Yadav, 2010). High Cd concentration negatively affects mineral nutrition and carbohydrate metabolism and consequently decreases plant biomass production (John et al., 2009). Increased Cd also alters the activity of antioxidant enzymes, including superoxide dismutase, peroxidase, etc. (Sun et al., 2007). In the present study, it was found that with the increase of Zn/Cd concentration in the soil, both the dry biomass of E+ and E- shoots and roots decreased (Figures 1, 2). But still, the dry biomass of E+ was better than E-. The finding suggests that fungal seed endophyte FXZ2 improved *D. ambrosioides* growth under different Zn/Cd stress. These results are similar to previous studies that microbial inoculation positively affected the plant biomass under Zn and/or Cd stress (He et al., 2013; Bilal et al., 2018; Singh et al., 2018; Zhu et al., 2018; Zhai et al., 2022). In addition, the present study showed that the plant exposure to Cd stress affects the biomass in a dose-dependent manner; similar observations were also reported by other authors (Sun et al., 2007; Kamran et al., 2015; Khan et al., 2015; Shahid et al., 2019; Zhang et al., 2019).

In general, FXZ2 induced enhancement of plant growth indicators such as shoot and root lengths. Their dry weight indicates a plant's ability to tolerate Zn and Cd stress and has shown positive growth (Kamran et al., 2015).

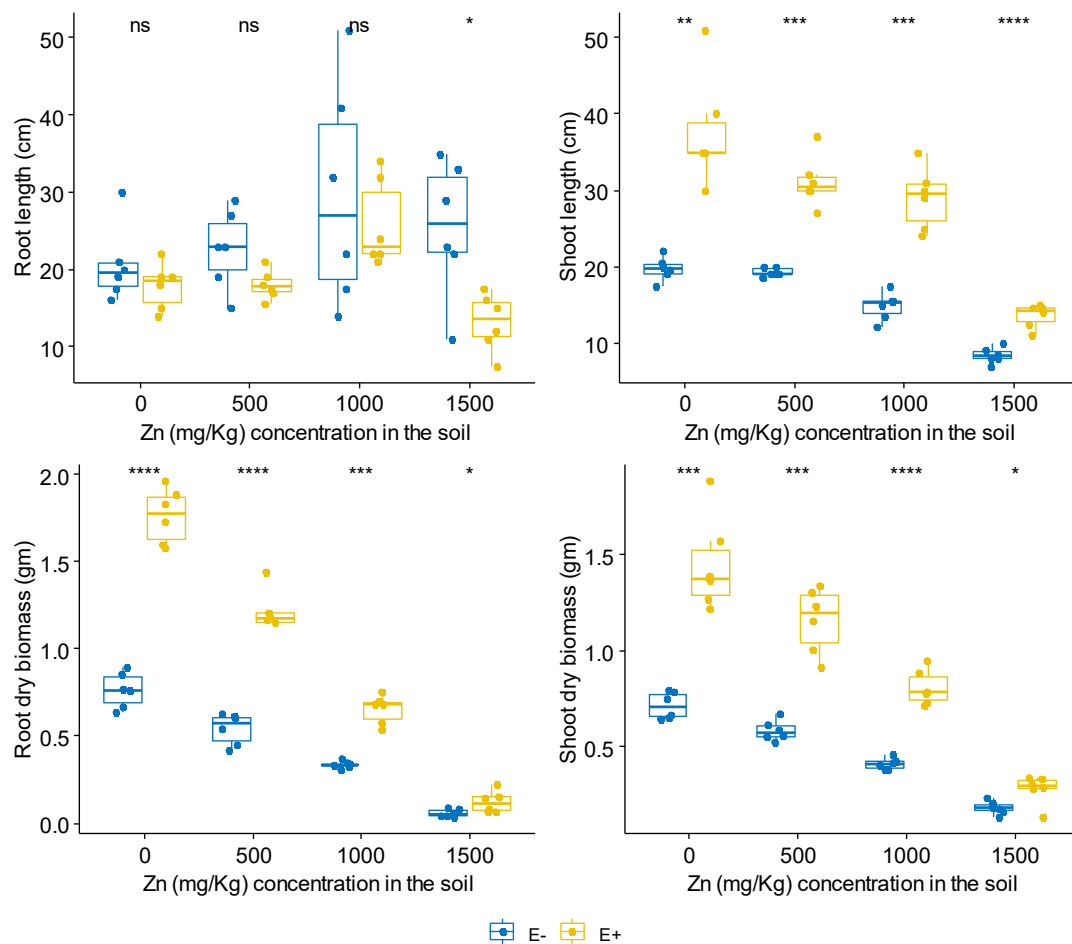


FIGURE 1

The effect of FXZ2 on the growth of *Dysphania ambrosioides* under Zn stress (\* $p < 0.05$ , \*\* $p < 0.005$ , \*\*\* $p < 0.0005$ , \*\*\*\* $p < 0.00005$ , ns  $p > 0.05$  t-test).

Both bacterial and fungal endophytes have been linked to the improved plant growth-related characteristics of the host plants under metal stress (Bilal et al., 2018; Zhu et al., 2018; Shahid et al., 2019; Rattanapolsan et al., 2021; Hussain et al., 2022).

### The effect of FXZ2 on *Dysphania ambrosioides* Zn/Cd accumulation

The uptake and accumulation of Zn/Cd in the shoots and roots of E+ and E- are shown in Table 1. Generally, the Zn concentrations in E+ and E- plants differed from the Zn concentration in the soil (Table 1). At 0 mg kg<sup>-1</sup> Zn stress, the Zn content in the shoots of E+ plants was significantly ( $p < 0.05$ ) high than that of E- plants, however, this was only slightly more ( $p > 0.05$ ) in the roots of E+ plants. Contrary to this, at 500 and 1,000 mg kg<sup>-1</sup> Zn stress, the shoot Zn content in E+ plants was significantly ( $p < 0.05$ ) lower

than that in E- plants, while only slightly more ( $p > 0.05$ ) in E+ plants at 1,500 mg kg<sup>-1</sup> Zn treatment. Similarly, the root Zn content was more ( $p > 0.05$ ) in the E- plants than E+ plants at 500 and 1,000 mg kg<sup>-1</sup> Zn treatment, while less ( $p > 0.05$ ) in E- plants at 0 and 1,500 mg kg<sup>-1</sup> Zn treatments.

The results suggest that the effect of FXZ2 on Zn uptake and accumulation was variable with the Zn content in the soil. Bilal et al. (2018) reported that the consortia endophytic microbes decreased Al and Zn content in the shoots and roots of *Glycine max* L. under 2.5 mM Al and Zn stress. Garg and Singh (2018) found that *Rhizophagus irregularis* combined with silicon amended soil and individually also decreased leaves and roots Zn content under Zn stress (600 and 1,000 mg kg<sup>-1</sup>). While the other studies showed different results; for example, the endophytic bacterium *Sphingomonas* sp. increased Zn uptake in *Sedum alfredii* (Chen et al., 2014). Similarly, dark septate endophyte *Exophiala pisciphila* increased Pb,



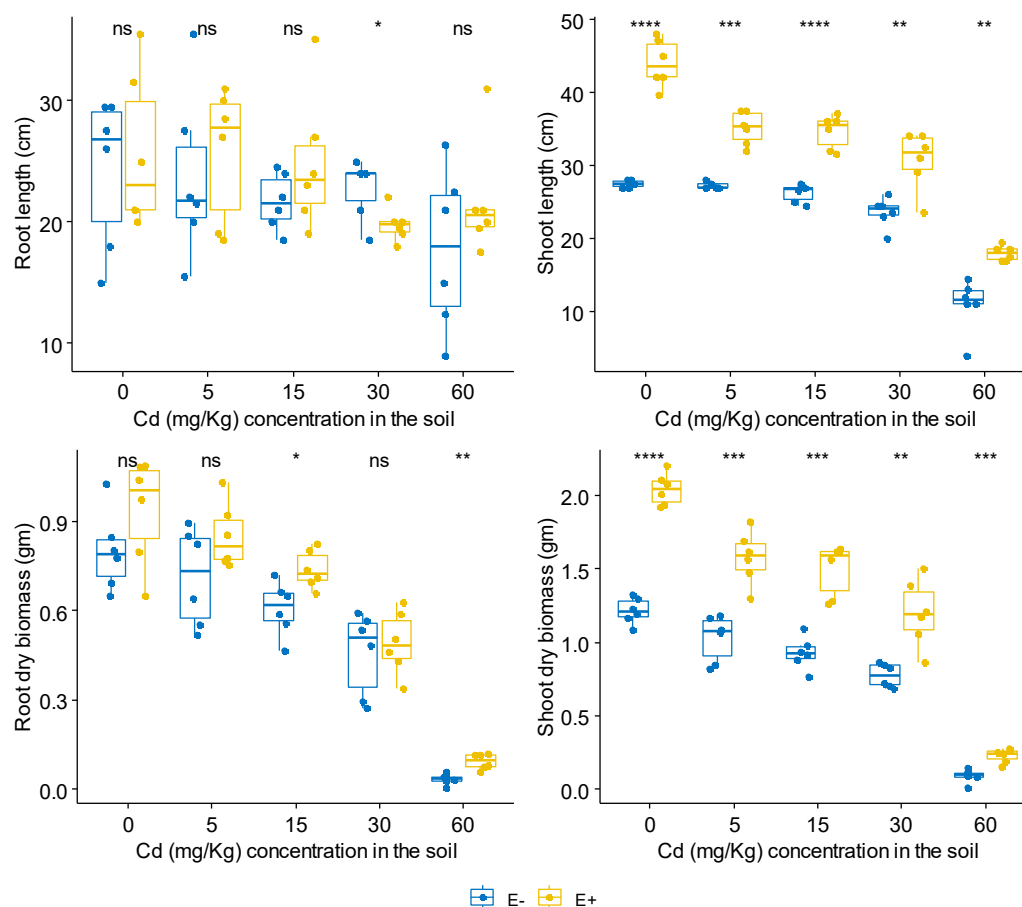


FIGURE 2

The effect of FXZ2 on the growth of *Dysphania ambrosioides* under Cd stress (\* $p < 0.05$ , \*\* $p < 0.005$ , \*\*\* $p < 0.0005$ , \*\*\*\* $p < 0.00005$ , ns  $p > 0.05$  t-test).

Zn, and Cd content in the roots and decreased in the shoots of *Zea mays* L. (Li et al., 2011); rhizobacterium *Enterobacter ludwigii* increased the Zn content in wheat under metal stress (Singh et al., 2018). This indicates that different microbes have different effects on host plant metal accumulation. Therefore, artificial manipulation of these microbes can be exploited to achieve the desired beneficial response.

At 0 mg kg<sup>-1</sup> Cd stress, the Cd content was more ( $p > 0.05$ ) in the shoots and roots of E- than E+ plants. However, the shoot and root Cd contents were higher in E+ plants at all Cd treatments than those in E- plants. The difference was significant ( $p < 0.05$ ) at 60 mg kg<sup>-1</sup> Cd stress, while the difference was non-significant ( $p > 0.05$ ) at 5, 15, and 30 mg kg<sup>-1</sup> Cd (Figures 1, 2 and Table 1). FXZ2-induced Cd content increase in the shoots and roots was consistent with other studies (Ren et al., 2006; Soleimani et al., 2010; Wan et al., 2012; Deng et al., 2013; He et al., 2013). Besides, plant growth-promoting bacteria such as *Rhizobium sultae* and *Pseudomonas* sp. (Chiboub et al., 2019), arbuscular mycorrhizal

fungi (Berthelot et al., 2018; Rafique et al., 2019), and arbuscular mycorrhiza and silicon amended soil in combination as well as alone (Garg and Singh, 2018) were also found to increase Cd accumulation in host plants. However, the finding was opposite to some previous studies that reported relatively lower Cd content in the roots and shoots and roots of the endophyte inoculated plants under Cd stress (Wang et al., 2016; He et al., 2017; Zhan et al., 2017; Shahid et al., 2019). Nevertheless, it is interesting to note that in both cases, growth-promoting endophyte inoculation has potential applications: If the endophyte can increase metal accumulation in host plants, it can be potentially used in phytoextraction. On the other hand, if the endophyte can decrease metal accumulation in host plants, it can be potentially used to reduce the metal content of agriculturally important crops to safe levels of consumption. Generally, metal contents in plant samples depend on the bioavailability of metals in soil (Kim et al., 2015), but this study provides sufficient evidence that endophytes can affect metal accumulation and growth under metal stress (Figures 1, 2 and Table 1).

TABLE 1 Zn/Cd accumulation in the shoots and roots of FXZ2 inoculated plants (E+) and non-inoculated plants (E-).

| The original concentration of Zn/Cd in the soils (mg kg <sup>-1</sup> ) |       | The treatment of FXZ2 | The concentration of Zn/Cd in the plants (mg kg <sup>-1</sup> )* |                    |
|---|-------|-----------------------|--|--------------------|
|   |       |                       | Shoots   | Roots              |
| Zn  | 0     | E-                    | 253.83 ± 4.83a   | 142.03 ± 19.15a    |
|   |       | E+                    | 500.55 ± 69.23b  | 197.67 ± 110.19a   |
|   | 500   | E-                    | 2,113.00 ± 113.86d   | 660.50 ± 65.30ab   |
|   |       | E+                    | 1,850.00 ± 36.72c  | 591.20 ± 17.41ab   |
|   | 1,000 | E-                    | 2,646.33 ± 79.10e  | 1,766.33 ± 453.99c |
|   |       | E+                    | 2,184.67 ± 190.17d   | 1,281.33 ± 90.98bc |
| Cd  | 1,500 | E-                    | 3,180.33 ± 48.79f  | 3,074.33 ± 947.53d |
|   |       | E+                    | 3,370.33 ± 236.05f   | 3,576.33 ± 345.30d |
|   | 0     | E-                    | 0.16 ± 0.08a   | 0.32 ± 0.11a       |
|   |       | E+                    | 0.14 ± 0.02a   | 0.27 ± 0.13a       |
|   | 5     | E-                    | 5.10 ± 0.07ab  | 23.75 ± 1.56ab     |
|   |       | E+                    | 8.39 ± 1.30ab  | 24.91 ± 8.18ab     |
|   | 15    | E-                    | 12.28 ± 0.98abc  | 43.23 ± 6.63ab     |
|   |       | E+                    | 16.97 ± 0.88bc   | 59.50 ± 6.73ab     |
|   | 30    | E-                    | 23.48 ± 0.75cd   | 97.28 ± 24.17bc    |
|   |       | E+                    | 34.48 ± 3.98d  | 167.08 ± 24.79c    |
|   | 60    | E-                    | 91.09 ± 14.61e   | 445.72 ± 125.30d   |
|   |       | E+                    | 120.79 ± 16.51f  | 739.48 ± 38.62e    |

\*The values are Mean ± Std,  $n = 3$ ; The different letters indicate the significant difference ( $p < 0.05$ , one-way ANOVA, Duncan test) between the individual plant part and metal in the different treatments.

## The effect of FXZ2 on Zn/Cd speciation in rhizospheric soils

Zinc and Cd chemical speciation in rhizospheric soils of E+ and E- plants were shown in [Figure 3](#). It was found that under Zn stress (500, 1,000, and 1,500 mg kg<sup>-1</sup> Zn), most of Zn was in F1 (exchangeable fraction). Interestingly, at 500 and 1,000 mg kg<sup>-1</sup> Zn stress, the Zn content of F1 + F2 was relatively less in rhizospheric soils of E+ than E- plants, while it was rather more in E+ plants in the 1,500 mg kg<sup>-1</sup> Zn treatments. This can be correlated to the Zn concentration in the shoots and roots of E+ and E- plants in 500, 1,000, and 1,500 mg kg<sup>-1</sup> Zn treatments. The metal in F4 (organic matter-bound fraction) and F5 (residual fraction) was the least available to plants. Together, these fractions were found relatively more in E+ than E- plants in 500 and 1,000 mg kg<sup>-1</sup> Zn treatments, while it was relatively less in E+ plants in the 1,500 mg kg<sup>-1</sup> Zn treatments. Results differed from previous studies, in which arbuscular mycorrhizal fungi (AMF) and plant growth-promoting rhizobacteria (PGPR) inoculation increased soil Zn mobility by changing Zn to high available fractions from low available fractions ([Boostani et al., 2016](#)).

Under Cd stress, no definite trend was observed in the relative percentage of the different fractions, especially at the low Cd stress (5 and 15 mg kg<sup>-1</sup> Cd), while under high Cd exposure (30 and 60 mg kg<sup>-1</sup> Cd), F1 + F2 were higher

in E+ than E- plants. [Wang et al. \(2016\)](#) also reported a difference in the chemical speciation of Cd in the dark septate endophyte inoculated maize. In another study, endophyte inoculation to *Brassica juncea* increased F1 + F2 fractions of Cd in the rhizosphere compared to the control plants ([Wang et al., 2020](#)). The possible mechanism of the distinct shift in the chemical speciation of an element in rhizospheric soils is by modifying pH through the secreted root exudates ([Long et al., 2013](#)). Endophyte inoculation could affect the subcellular fractions of Cd in the host plant and its chemical forms. For example, AMF colonization increases Cd accumulation in *Medicago sativa* L. by changing Cd into inactive forms, having low toxicity ([Wang et al., 2012](#)). Similar AMF colonization affected Cd uptake and subcellular distribution by changing Cd chemical speciation in rice ([Li H. et al., 2016](#); [Luo et al., 2017](#)). Besides, the observed results of Zn and Cd speciation might affect the anions and pH from ZnSO<sub>4</sub>·7H<sub>2</sub>O and CdCl<sub>2</sub>·2.5H<sub>2</sub>O supplemented to induce Zn and Cd stress, respectively ([Wang et al., 2016](#)).

FXZ2 inoculation affected the chemical speciation in root zone soils of *D. ambrosioides* only to some extent. The effect of FXZ2 inoculation (FE) was variable for the different fractions of Zn and Cd in rhizospheric soils ([Figure 3](#)). The effect was not significant for all fractions of Zn in the different treatments, while in the case of Cd, there were six significant alterations out of a total 25 alterations by FXZ2

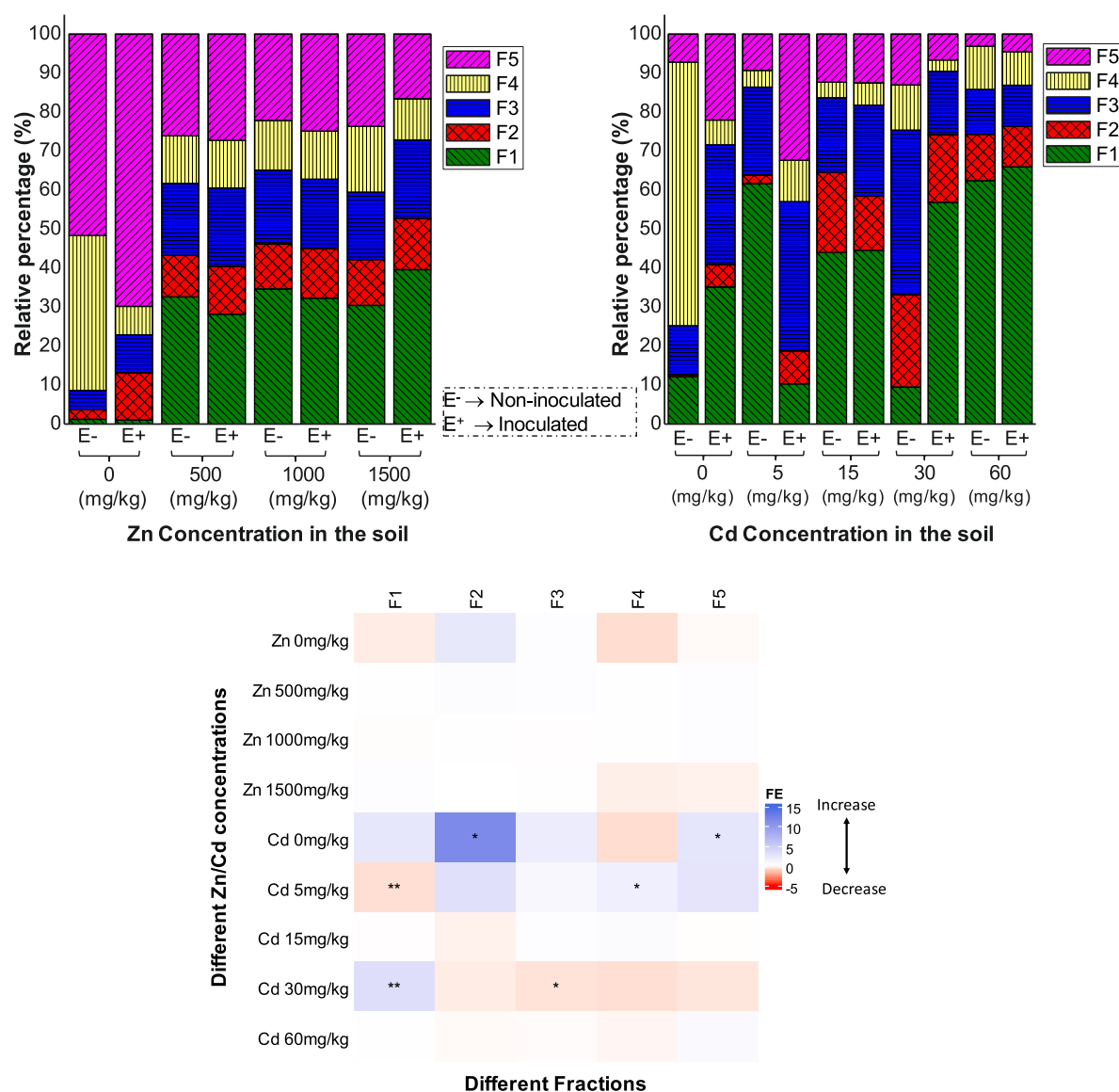


FIGURE 3

The effect of FXZ2 inoculation (FE) on the chemical forms of Zn/Cd in rhizospheric soils of *Dysphania ambrosioides* under Zn/Cd stress. F1: exchangeable fraction; F2: carbonate-bound fraction; F3: Fe-Mn oxides bound; F4: organic bound fraction; F5: residual fraction. The asterisks indicate a significant difference between E<sup>+</sup> and E<sup>-</sup> (\* $p < 0.05$ , \*\* $p < 0.005$ ,  $t$ -test).

inoculation. Chemical speciation in the rhizosphere regulates toxicokinetics, i.e., the uptake and translocation of metals by the plants from the root zone (Uchimiya et al., 2020). The manipulation of the phytomicrobiome can change the rhizosphere by the secretion of root exudates, which can alter the microbial signaling compounds and chemical speciation (Bhatt et al., 2020). It has to be noted that in this study, we evaluated the chemical speciation in the rhizosphere soil only at the time of harvest (60 days). It would be interesting to evaluate how the chemical speciation of metals changes in the rhizosphere when the plant is inoculated with FXZ2 during different time intervals as the plant grows in metal stress

conditions and further how it affects the rhizosphere microbial community.

## The effect of FXZ2 on biochemical factors of *Dysphania ambrosioides*

FXZ2 inoculation had a positive effect on the total chlorophyll content of host plants (Figure 4). With the exception of 1,500 mg kg<sup>-1</sup>, E<sup>+</sup> plants had a relatively higher total chlorophyll content in Zn treatments than E<sup>-</sup> plants. The differences were significant at 0 and 1,500 mg kg<sup>-1</sup> Zn

while non-significant ( $p > 0.05$ ) at 1,000 mg kg<sup>-1</sup> Zn. In Cd treatments, FXZ2 colonization significantly ( $p < 0.05$ ) increased the total chlorophyll content of the host plants except at 30 mg kg<sup>-1</sup> Cd stress ( $p > 0.05$ ). With the increase of Zn and Cd concentration in the soil, the total chlorophyll content was decreased both for E+ and E- plants. The chlorophyll content is a significant indicator of plant growth status (Chen et al., 2010). Exceptionally high Zn in the soil can cause stress in plants, leaf chlorosis, and reduce photosynthesis (Broadley et al., 2007). Moreover, Cd-induced toxicity can adversely affect the plant chlorophyll biosynthesis by preventing  $\delta$ -aminolevulinic acid dehydratase, porphobilinogen deaminase, and protochlorophyllide reductase activity and changing the photosynthetic electron transport at PS-II (Zulfiqar et al., 2021).

Our results supported the finding that the chlorophyll content decreased for the toxicity of Zn or Cd (Zhang et al., 2010; Kamran et al., 2015; Bilal et al., 2018). However, the chlorophyll of E+ plants was relatively higher than that of E- plants. The results agree with Hunt et al. (2005), who recorded that endophyte inoculation to perennial ryegrass increased chlorophyll content. Bilal et al. (2018) also reported that endophytic microbial consortia could significantly enhance the chlorophyll content of the inoculated plants under normal and Al/Zn stress. The low chlorophyll content under the influence of abiotic stress is generally due to the stress-related ROS generation and membrane lipid peroxidation, which further affects the fluidity and selectivity of the membrane (Verma and Mishra, 2005). Furthermore, in plant tissue metal stress results in the generation of ROS, which in the form of hydrogen peroxide and superoxide anion mimic and interrupt normal cellular functions by changing the oxidation/reduction cycle (Khan et al., 2015).

Tripeptide glutathione is one of the crucial plant metabolites having an essential role in the plant defense system as a ROS scavenging molecule. In plants, it occurs mainly in reduced form (GSH), and abundant production in the stress-adapted plant is related to a strongly activated defense system (Gill and Tuteja, 2010). The GSH analysis showed that FXZ2 inoculation affected the GSH content of host plants (Figure 4). In general, the GSH content of E+ plants was higher than E- plants under both Zn and Cd stress. The differences were significant ( $p < 0.05$ ) at 500 and 1,000 mg kg<sup>-1</sup> Zn stress, while under Cd stress, the difference was non-significant ( $p > 0.05$ ). The thiol group of the glutathione is of high-affinity nature, linked to the complexation and detoxification of metals as a chelating compound, and takes part in the antioxidant process (Schat et al., 2002; Yadav, 2010; Cao et al., 2018). Further, it reduces phytotoxicity by forming an inactive glutathione-Cd complex and subcellular compartmentalization (Adamis et al., 2004; Zhang et al., 2019). The higher GSH content in E+ than E- plants suggests the inoculated endophyte induced counteractive mechanisms to check oxidative stress related to metal toxicity. Previous studies

also indicated that inoculation of endophytic microbe can enhance the growth and tolerance of host plants to metal stress through GSH regulation, though the effect on GSH can vary with stress (Khan et al., 2015; He et al., 2017; Zhan et al., 2017).

Metal stress induces oxidative damage in plants, causing lipid peroxidation that disturbs cellular functions and membrane integrity; the injuries can be irreversible (Wan et al., 2012; Khan and Lee, 2013; Khan et al., 2015; Bilal et al., 2018). Malondialdehyde (MDA) is a byproduct of lipid peroxide breakdown. Lower MDA in plant tissue signifies lesser lipid peroxidation. The MDA content of different treatments is presented in Figure 4. It was found that FXZ2 inoculation lowered the MDA content of host plants. The differences were significant ( $p < 0.05$ ) at 500 and 1,500 mg kg<sup>-1</sup> Zn stress and higher Cd stress (30 and 60 mg kg<sup>-1</sup>). The relatively lower MDA in E+ plants suggests that the endophyte FXZ2 had a synergistic role against the oxidative stress due to elevated Zn and Cd. Results from this study are consistent with previous research that endophyte-infected plants had lower MDA contents, for instance, *Achnatherum inebrians* inoculated with endophyte *Neotyphodium gansuense*, and *Solanum nigrum* inoculated with endophyte *Serratia nematodiphila* under Cd stress (Zhang et al., 2010; Wan et al., 2012; Khan et al., 2015), *Glycine max* L. inoculated with endophytic fungus *Paecilomyces formosus* and bacteria *Sphingomonas* sp. under Al/Zn stress (Bilal et al., 2018), and tomato inoculated with two dark septate endophytes *Phialophora mustea* under Zn/Cd stress (Zhu et al., 2018).

## Phytohormone production by FXZ2

Phytohormone indole acetic acid (IAA) is responsible for apical dominance, cell elongation, evolution of vascular tissue, and improvement of plant stress tolerance (Wang et al., 2001; Eyidogan et al., 2012). And gibberellic acid (GA) is primarily responsible for seed germination, stem elongation, flower and trichome initiation, fruit development, and leaf expansion (Yamaguchi, 2008; Liu et al., 2009). Jasmonic acid (JA) has been demonstrated as a significant signaling molecule during plant defense, such as pathogens attack (Qi et al., 2016) and metals stress (Bilal et al., 2017; Per et al., 2018). JA was also reported to alter antioxidant potential, reduce H<sub>2</sub>O<sub>2</sub> and MDA concentrations, and improve photosynthetic pigments concentrations under Pb and Cd stress in different plants (Piotrowska et al., 2009; Ahmad et al., 2017). Some endophytes can exogenously produce phytohormones to mitigate the effects of abiotic stress to host plants (Khan et al., 2012; Bilal et al., 2018; Chang et al., 2021). In the present study, it was found that FXZ2 exogenously secretes IAA ( $3.21 \pm 0.59 \mu\text{M L}^{-1}$ ), GA ( $13.76 \pm 0.20 \text{ pM L}^{-1}$ ), and JA ( $257.70 \pm 43.04 \text{ pM L}^{-1}$ ) in liquid culture. These phytohormones may play some



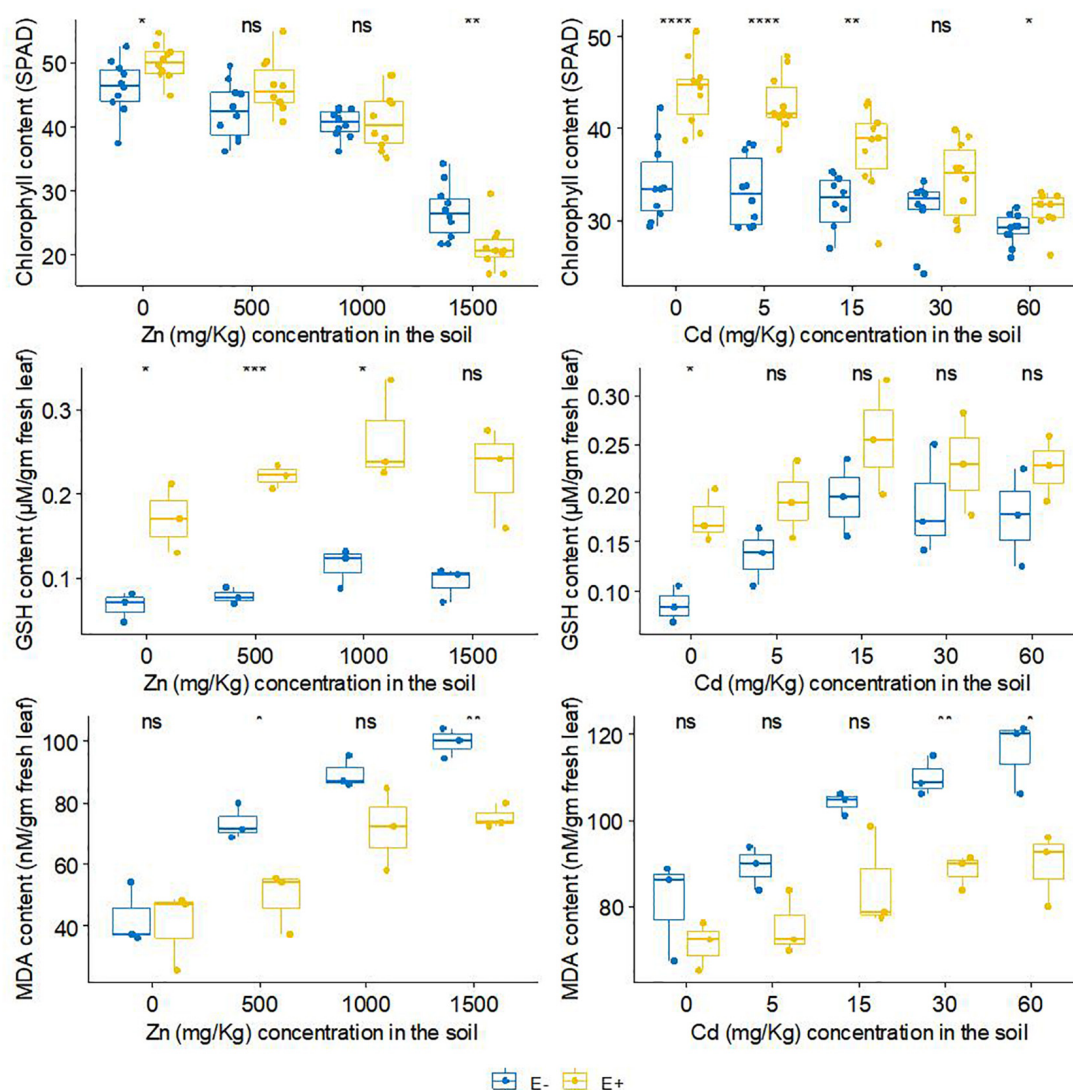


FIGURE 4

The effect of FXZ2 on the Chlorophyll, GSH and MDA content of *Dysphania ambrosioides* under Zn/Cd stress (\* $p < 0.05$ , \*\* $p < 0.005$ , \*\*\* $p < 0.0005$ , \*\*\*\* $p < 0.00005$ , ns  $p > 0.05$   $t$ -test).

roles in plant growth and stress tolerance under Zn/Cd stress. Similarly, some phytohormones producing fungal species, e.g., *Fusarium oxysporum*, *Piriformospora indica*, *Phoma glomerata*, *Penicillium* sp., and *Exophiala pisciphila*, have found to improve host plants' growth and crop productivity (Hasan, 2002; Yuan et al., 2010; Waqas et al., 2012; He et al., 2017). Further, the effect of FXZ2 on the endogenous production of phytohormones and host plants growth under metal stress can be tested on mutant plant cultivars not able to produce phytohormones, e.g., Waito-C (GA deficient mutant rice cultivar) (Khan et al., 2012). This can be a reliable future strategy to know how this endophyte improves the phytohormone content of the host plant and subsequently their growth under metal stress.

## Conclusion

Under variable Zn/Cd stress, seed endophyte FXZ2 significantly improved *D. ambrosioides* growth and its chlorophyll and GSH content. Our results demonstrated that FXZ2 inoculation transformed the Zn/Cd speciation in the rhizosphere of host plants, subsequently affecting their uptake and accumulation. The readily available fractions, i.e., exchangeable and carbonate-bound (F1 + F2) fractions of Zn decreased in E+ as compared to E- plants at 500 and 1,000 mg kg<sup>-1</sup> Zn stress, congruently, Zn in shoots of E+ plants decreased significantly ( $p < 0.05$ ). However, under Cd stress (30 and 60 mg kg<sup>-1</sup>), the effect was different, the Cd concentration in F1 + F2 increased in rhizospheric soils of E+ plants, and

subsequently, Cd accumulation in E+ plants was significantly ( $p < 0.05$ ) increased. Therefore, FXZ2 can have different applications, for example, in agriculturally important crops it can be used to improve Zn tolerance in contaminated soils or in phytoextraction by increasing Cd bioaccumulation at high Cd stress.

Moreover, FXZ2 could exogenously secrete phytohormones IAA, GA, and JA, which could be a key mechanism for promoting host plants' growth under Zn/Cd stress. Further study is required to investigate the role of FXZ2 in the endogenous production of phytohormones in inoculated plants.

## Data availability statement

The original contributions presented in this study are included in the article/supplementary material, further inquiries can be directed to the corresponding author.

## Author contributions

VS: conceptualization, methodology, writing—original draft, investigation, formal analysis, and data curation. SP: conceptualization, methodology, writing—original draft, investigation, formal analysis, and data curation. WT: project investigation and resources and project administration. HH: writing—review and editing and validation. JW: writing—review and editing. HL: conceptualization, supervision, writing—review and editing, validation, resources, funding

acquisition, and project administration. All authors contributed to the article and approved the submitted version.

## Funding

This work was financially supported by the National Natural Science Foundation of China (41867026) and the Natural Science Foundation of Yunnan Province (2019FA019). Funding support was also provided to James White from USDA-NIFA Multistate Project W4147 and the New Jersey Agricultural Experiment Station.

## Conflict of interest

The authors declare that the research was conducted in the absence of any commercial or financial relationships that could be construed as a potential conflict of interest.

## Publisher's note

All claims expressed in this article are solely those of the authors and do not necessarily represent those of their affiliated organizations, or those of the publisher, the editors and the reviewers. Any product that may be evaluated in this article, or claim that may be made by its manufacturer, is not guaranteed or endorsed by the publisher.

## References

- Adamis, P. D., Gomes, D. S., Pinto, M. L. C., Panek, A. D., and Eleutherio, E. C. (2004). The role of glutathione transferases in cadmium stress. *Toxicol. Lett.* 154, 81–88. doi: 10.1016/j.toxlet.2004.07.003
- Ahlf, W., Drost, W., and Heise, S. (2009). Incorporation of metal bioavailability into regulatory frameworks—metal exposure in water and sediment. *J. Soils Sediments* 9, 411–419. doi: 10.1007/s11368-009-0109-6
- Ahmad, P., Alyemeni, M. N., Wijaya, L., Alam, P., Ahanger, M. A., and Alamri, S. A. (2017). Jasmonic acid alleviates negative impacts of cadmium stress by modifying osmolytes and antioxidants in faba bean (*Vicia faba* L.). *Arch. Agron. Soil Sci.* 63, 1889–1899. doi: 10.1080/03650340.2017.1313406
- Akhtar, N., Wani, A. K., Dhanjal, D. S., and Mukherjee, S. (2022). Insights into the beneficial roles of dark septate endophytes in plants under challenging environment: Resilience to biotic and abiotic stresses. *World J. Microbiol. Biotechnol.* 38:79. doi: 10.1007/s11274-022-03264-x
- Berthelot, C., Blaudez, D., Beguiristain, T., Chalot, M., and Leyval, C. (2018). Co-inoculation of *Lolium perenne* with *Funneliformis mosseae* and the dark septate endophyte *Cadophora* sp. in a trace element-polluted soil. *Mycorrhiza* 28, 301–314. doi: 10.1007/s00572-018-0826-z
- Bhatt, P., Verma, A., Verma, S., Anwar, M., Prasher, P., Mudila, H., et al. (2020). Understanding phytomicrobiome: A potential reservoir for better crop management. *Sustainability* 12:5446. doi: 10.3390/su12135446
- Bilal, S., Khan, A. L., Shahzad, R., Asaf, S., Kang, S. M., and Lee, I. J. (2017). Endophytic *Paecilomyces formosus* LHL10 augments *Glycine max* L. adaptation to Ni-contamination through affecting endogenous phytohormones and oxidative stress. *Front. Plant Sci.* 8:870. doi: 10.3389/fpls.2017.00870
- Bilal, S., Shahzad, R., Khan, A. L., Kang, S. M., Imran, Q. M., Al-Harrasi, A., et al. (2018). Endophytic microbial consortia of phytohormones-producing fungus *Paecilomyces formosus* LHL10 and bacteria *Sphingomonas* sp. LK11 to *Glycine max* L. regulates physio-hormonal changes to attenuate aluminum and zinc stresses. *Front. Plant Sci.* 9:1273. doi: 10.3389/fpls.2018.01273
- Boostani, H. R., Chorom, M., Moezzi, A., Karimian, N., Enayatzamir, N., and Zarei, M. (2016). Effect of plant growth-promoting rhizobacteria (PGPR) and arbuscular mycorrhizal fungi (AMF) application on distribution of zinc chemical forms in a calcareous soil with different levels of salinity. *Electro. J. Soil Manag. Sustain. Prod.* 6, 1–24.
- Broadley, M. R., White, P. J., Hammond, J. P., Zelko, I., and Lux, A. (2007). Zinc in plants. *New Phytol.* 173, 677–702. doi: 10.1111/j.1469-8137.2007.01996.x
- Cao, Z. Z., Qin, M. L., Lin, X. Y., Zhu, Z. W., and Chen, M. X. (2018). Sulfur supply reduces cadmium uptake and translocation in rice grains (*Oryza sativa* L.) by enhancing iron plaque formation, cadmium chelation and vacuolar sequestration. *Environ. Pollut.* 238, 76–84. doi: 10.1016/j.envpol.2018.02.083
- Chang, X., Kingsley, K. L., and White, J. F. (2021). Chemical Interactions at the Interface of Plant Root Hair Cells and Intracellular Bacteria. *Microorganisms* 9:1041. doi: 10.3390/microorganisms9051041
- Chen, B., Shen, J., Zhang, X., Pan, F., Yang, X., and Feng, Y. (2014). The endophytic bacterium, *Sphingomonas* SaMR12, improves the potential for zinc phytoremediation by its host, *Sedum alfredii*. *PLoS One* 9:e106826. doi: 10.1371/journal.pone.0106826
- Chen, L., Luo, S., Xiao, X., Guo, H., Chen, J., Wan, Y., et al. (2010). Application of plant growth-promoting endophytes (PGPE) isolated from *Solanum nigrum* L. for phytoextraction of Cd-polluted soils. *Appl. Soil Ecol.* 46, 383–389. doi: 10.1016/j.apsoil.2010.10.003

- Chiboub, M., Jebara, S. H., Abid, G., and Jebara, M. (2019). Co-inoculation Effects of *Rhizobium sulae* and *Pseudomonas* sp. on Growth, Antioxidant Status, and Expression Pattern of Genes Associated with Heavy Metal Tolerance and Accumulation of Cadmium in *Sulla coronaria*. *J. Plant Growth Regul.* 39, 216–228. doi: 10.1007/s00344-019-09976-z
- Chu, L., Li, W., Li, X. Y., Xiong, Z., and Li, H. Y. (2017). Diversity and heavy metal resistance of endophytic fungi from seeds of hyperaccumulators. *Jiangsu. J. Agric. Sci.* 33, 43–49.
- Core TeamR. (2021). R: A Language and Environment for Statistical Computing [computer software]. Vienna: R Foundation for Statistical Computing. Available online at: <https://www.R-project.org/> (accessed August 27, 2022).
- Deng, Z., Zhang, R., Shi, Y., Tan, H., and Cao, L. (2013). Enhancement of phytoremediation of Cd- and Pb-contaminated soils by self-fusion of protoplasts from endophytic fungus *Mucor* sp. CBRF59. *Chemosphere* 91, 41–47. doi: 10.1016/j.chemosphere.2012.11.065
- Etesami, H. (2018). Bacterial mediated alleviation of heavy metal stress and decreased accumulation of metals in plant tissues: Mechanisms and future prospects. *Ecotoxicol. Environ. Safe.* 147, 175–191. doi: 10.1016/j.ecoenv.2017.08.032
- Eyidogan, F., Oz, M. T., Yucel, M., and Oktem, H. A. (2012). “Signal transduction of phytohormones under abiotic stresses,” in *Phytohormones and Abiotic Stress Tolerance in Plants*, eds N. A. Khan, R. Nazar, N. Iqbal, and N. A. Anjum (Berlin: Springer), 1–48. doi: 10.1007/978-3-642-25829-9\_1
- Gao, T., and Shi, X. (2018). Preparation of a synthetic seed for the common reed harboring an endophytic bacterium promoting seedling growth under cadmium stress. *Environ. Sci. a Pollut. Res.* 25, 8871–8879. doi: 10.1007/s11356-018-1200-6
- Garg, N., and Singh, S. (2018). Arbuscular mycorrhiza *Rhizophagus irregularis* and silicon modulate growth, proline biosynthesis and yield in *Cajanus cajan* L. Millsip. (pigeonpea) genotypes under cadmium and zinc stress. *J. Plant Growth Regul.* 37, 46–63. doi: 10.1007/s00344-017-9708-4
- Gill, S. S., and Tuteja, N. (2010). Reactive oxygen species and antioxidant machinery in abiotic stress tolerance in crop plants. *Plant Physiol. Biochem.* 48, 909–930. doi: 10.1016/j.plaphy.2010.08.016
- Hasan, H. A. H. (2002). Gibberellin and auxin-indole production by plant root-fungi and their biosynthesis under salinity-calcium interaction. *Acta Microbiol. et Immunologica Hungarica* 49, 105–118. doi: 10.1556/AMicr.49.20.02.1.11
- He, H., Ye, Z., Yang, D., Yan, J., Xiao, L., Zhong, T., et al. (2013). Characterization of endophytic *Rahnella* sp. JN6 from *Polygonum pubescens* and its potential in promoting growth and Cd, Pb, Zn uptake by *Brassica napus*. *Chemosphere* 90, 1960–1965. doi: 10.1016/j.chemosphere.2012.10.057
- He, Y., Yang, Z., Li, M., Jiang, M., Zhan, F., Zu, Y., et al. (2017). Effects of a dark septate endophyte (DSE) on growth, cadmium content, and physiology in maize under cadmium stress. *Environ. Sci. Pollut. Res.* 24, 18494–18504. doi: 10.1007/s11356-017-9459-6
- Hunt, M. G., Rasmussen, S., Newton, P. C., Parsons, A. J., and Newman, J. A. (2005). Near-term impacts of elevated CO<sub>2</sub>, Nitrogen and fungal endophyte-infection on *Lolium perenne* L. growth, chemical composition and alkaloid production. *Plant Cell Environ.* 28, 1345–1354. doi: 10.1111/j.1365-3040.2005.01367.x
- Hussain, I., Afzal, S., Ashraf, M. A., Rasheed, R., Saleem, M. H., Alatawi, A., et al. (2022). Effect of Metals or Trace Elements on Wheat Growth and Its Remediation in Contaminated Soil. *Journal of Plant Growth Regulation* doi: 10.1007/s00344-022-10700-7
- Jain, R., Srivastava, S., Solomon, S., Shrivastava, A. K., and Chandra, A. (2010). Impact of excess zinc on growth parameters, cell division, nutrient accumulation, photosynthetic pigments and oxidative stress of sugarcane (*Saccharum* spp.). *Acta Physiol. Plantarum* 32, 979–986. doi: 10.1007/s11738-010-0487-9
- John, R., Ahmad, P., Gadgil, K., and Sharma, S. (2009). Cadmium and lead-induced changes in lipid peroxidation, antioxidative enzymes and metal accumulation in *Brassica juncea* L. at three different growth stages. *Arch. Agron. Soil Sci.* 55, 395–405. doi: 10.1080/03650340802552395
- Kamran, M. A., Syed, J. H., Eqani, S. A. M. A. S., Munis, M. F. H., and Chaudhary, H. J. (2015). Effect of plant growth-promoting rhizobacteria inoculation on cadmium (Cd) uptake by *Eruca sativa*. *Environ. Sci. Pollut. Res.* 22, 9275–9283. doi: 10.1007/s11356-015-4074-x
- Khan, A. L., Hamayun, M., Kang, S. M., Kim, Y. H., Jung, H. Y., Lee, J. H., et al. (2012). Endophytic fungal association via gibberellins and indole acetic acid can improve plant growth under abiotic stress: An example of *Paecilomyces formosus* LHL10. *BMC Microbiol.* 12:3. doi: 10.1186/1471-2180-12-3
- Khan, A. L., and Lee, I. J. (2013). Endophytic *Penicillium funiculosum* LHL06 secretes gibberellin that reprograms *Glycine max* L. growth during copper stress. *BMC Plant Biol.* 13:86. doi: 10.1186/1471-2229-13-86
- Khan, A. R., Ullah, I., Khan, A. L., Park, G. S., Waqas, M., Hong, S. J., et al. (2015). Improvement in phytoremediation potential of *Solanum nigrum* under cadmium contamination through endophytic-assisted *Serratia* sp. RSC-14 inoculation. *Environ. Sci. Pollut. Res.* 22, 14032–14042. doi: 10.1007/s11356-015-4647-8
- Kidd, K. A., Muir, D. C., Evans, M. S., Wang, X., Whittle, M., Swanson, H. K., et al. (2012). Biomagnification of mercury through lake trout (*Salvelinus namaycush*) food webs of lakes with different physical, chemical and biological characteristics. *Sci. Total Environ.* 438, 135–143. doi: 10.1016/j.scitotenv.2012.08.057
- Kim, R. Y., Yoon, J. K., Kim, T. S., Yang, J. E., Owens, G., and Kim, K. R. (2015). Bioavailability of heavy metals in soils: Definitions and practical implementation—a critical review. *Environ. Geochem. Health* 37, 1041–1061. doi: 10.1007/s10653-015-9695-y
- Kuriakose, S. V., and Prasad, M. N. V. (2008). Cadmium stress affects seed germination and seedling growth in *Sorghum bicolor* (L.) Moench by changing the activities of hydrolyzing enzymes. *Plant Growth Regul.* 54, 143–156. doi: 10.1007/s10725-007-9237-4
- Li, H., Parmar, S., Sharma, V. K., and White, J. F. (2019). “Seed endophytes and their potential applications,” in *Seed Endophytes*, eds S. Verma and J. White Jr. (Cham: Springer), 35–54. doi: 10.1007/978-3-030-10504-4\_3
- Li, H. Y., Li, D. W., He, C. M., Zhou, Z. P., Mei, T., and Xu, H. M. (2012). Diversity and heavy metal tolerance of endophytic fungi from six dominant plant species in a Pb-Zn mine wasteland in China. *Fungal Ecol.* 5, 309–315. doi: 10.1016/j.funeco.2011.06.002
- Li, T., Liu, M. J., Zhang, X. T., Zhang, H. B., Sha, T., and Zhao, Z. W. (2011). Improved tolerance of maize (*Zea mays* L.) to heavy metals by colonization of a dark septate endophyte (DSE) *Exophiala pisciphila*. *Sci. Total Environ.* 409, 1069–1074. doi: 10.1016/j.scitotenv.2010.12.012
- Li, X., Li, W., Chu, L., White, J. F. Jr., Xiong, Z., and Li, H. (2016). Diversity and heavy metal tolerance of endophytic fungi from *Dysphania ambrosioides*, a hyperaccumulator from Pb-Zn contaminated soils. *J. Plant Interact.* 11, 186–192. doi: 10.1080/17429145.2016.1266043
- Li, H., Luo, N., Zhang, L. J., Zhao, H. M., Li, Y. W., Cai, Q. Y., et al. (2016). Do arbuscular mycorrhizal fungi affect cadmium uptake kinetics, subcellular distribution and chemical forms in rice? *Sci. Total Environ.* 571, 1183–1190. doi: 10.1016/j.scitotenv.2016.07.124
- Li, Y., Wang, H., Wang, H., Yin, F., Yang, X., and Hu, Y. (2014). Heavy metal pollution in vegetables grown in the vicinity of a multi-metal mining area in Gejiu, China: Total concentrations, speciation analysis, and health risk. *Environ. Sci. Pollut. Res.* 21, 12569–12582. doi: 10.1007/s11356-014-3188-x
- Liu, Q., Zhang, Y. C., Wang, C. Y., Luo, Y. C., Huang, Q. J., Chen, S. Y., et al. (2009). Expression analysis of phytohormone-regulated microRNAs in rice, implying their regulation roles in plant hormone signaling. *FEBS Lett.* 583, 723–728. doi: 10.1016/j.febslet.2009.01.020
- Liu, Y., Ma, L., Li, Y., and Zheng, L. (2007). Evolution of heavy metal speciation during the aerobic composting process of sewage sludge. *Chemosphere* 67, 1025–1032. doi: 10.1016/j.chemosphere.2006.10.056
- Long, X. X., Chen, X. M., Wong, J. W. C., Wei, Z. B., and Wu, Q. T. (2013). Feasibility of enhanced phytoextraction of Zn contaminated soil with Zn mobilizing and plant growth-promoting endophytic bacteria. *Trans. Nonferrous Metals Soc. China* 23, 2389–2396. doi: 10.1016/S1003-6326(13)62746-6
- Luo, N., Li, X., Chen, A. Y., Zhang, L. J., Zhao, H. M., Xiang, L., et al. (2017). Does arbuscular mycorrhizal fungus affect cadmium uptake and chemical forms in rice at different growth stages? *Sci. Total Environ.* 599, 1564–1572. doi: 10.1016/j.scitotenv.2017.05.047
- Nan, Z., Li, J., Zhang, J., and Cheng, G. (2002). Cadmium and zinc interactions and their transfer in soil-crop system under actual field conditions. *Sci. Total Environ.* 285, 187–195. doi: 10.1016/S0048-9697(01)00919-6
- Parmar, S., and Singh, V. (2015). Phytoremediation approaches for heavy metal pollution: A review. *J. Plant Sci. Res.* 2:135.
- Per, T. S., Khan, M. I. R., Anjum, N. A., Masood, A., Hussain, S. J., and Khan, N. A. (2018). Jasmonates in plants under abiotic stresses: Crosstalk with other phytohormones matters. *Environ. Exp. Bot.* 145, 104–120. doi: 10.1016/j.envexpbot.2017.11.004
- Piotrowska, A., Bajguz, A., Godlewska-Żyłkiewicz, B., Czerpak, R., and Kamińska, M. (2009). Jasmonic acid as modulator of lead toxicity in aquatic plant *Wolfia arrhiza* (Lemnaceae). *Environ. Exp. Bot.* 66, 507–513. doi: 10.1016/j.envexpbot.2009.03.019
- Qi, P. F., Balcerzak, M., Rocheleau, H., Leung, W., Wei, Y. M., Zheng, Y. L., et al. (2016). Jasmonic acid and abscisic acid play important roles in host-pathogen interaction between *Fusarium graminearum* and wheat during the early stages of



- Fusarium head blight. *Physiol. Mol. Plant Pathol.* 93, 39–48. doi: 10.1016/j.pmp.2015.12.004
- Rafique, M., Ortas, I., Rizwan, M., Sultan, T., Chaudhary, H. J., İşik, M., et al. (2019). Effects of *Rhizophagus clarus* and biochar on growth, photosynthesis, nutrients, and cadmium (Cd) concentration of maize (*Zea mays*) grown in Cd-spiked soil. *Environ. Sci. Pollut. Res.* 26, 20689–20700. doi: 10.1007/s11356-019-05323-7
- Rahman, I., Kode, A., and Biswas, S. K. (2006). Assay for quantitative determination of glutathione and glutathione disulfide levels using enzymatic recycling method. *Nat. Protocols* 1:3159. doi: 10.1038/nprot.2006.378
- Rattanapolsan, L., Nakbanpote, W., and Sangdee, A. (2021). Zinc- and cadmium-tolerant endophytic bacteria from *Murdannia spectabilis* (Kurz) Faden. studied for plant growth-promoting properties, in vitro inoculation, and antagonism. *Arch. Microbiol.* 203, 1131–1148. doi: 10.1007/s00203-020-02108-2
- Ren, A., Gao, Y., Zhang, L., and Xie, F. (2006). Effects of cadmium on growth parameters of glutathione-infected endophyte-free ryegrass. *J. Plant Nutri. Soil Sci.* 169, 857–860. doi: 10.1002/jpln.200520543
- R Studio Team (2021). *RStudio: Integrated Development for R [computer software]*. Boston, MA: RStudio, PBC. Available online at: <http://www.rstudio.com/>
- Schat, H., Llugany, M., Voors, R., Hartley-Whitaker, J., and Bleeker, P. M. (2002). The role of phytochelators in constitutive and adaptive heavy metal tolerances in hyperaccumulator and non-hyperaccumulator metallophytes. *J. Exp. Bot.* 53, 2381–2392. doi: 10.1093/jxb/erf107
- Shahid, M., Javed, M. T., Masood, S., Akram, M. S., Azeem, M., Ali, Q., et al. (2019). *Serratia* sp. CP-13 augments the growth of cadmium (Cd)-stressed *Linum usitatissimum* L. by limited Cd uptake, enhanced nutrient acquisition and antioxidative potential. *J. Appl. Microbiol.* 126, 1708–1721. doi: 10.1111/jam.14252
- Sharma, V. K., Li, X. Y., Wu, G. L., Bai, W. X., Parmar, S., White, J. F. Jr., et al. (2019). Endophytic community of Pb-Zn hyperaccumulator *Arabis alpina* and its role in host plants metal tolerance. *Plant Soil* 437, 397–411. doi: 10.1007/s11104-019-03988-0
- Shen, M., Liu, L., Li, D. W., Zhou, W. N., Zhou, Z. P., Zhang, C. F., et al. (2013). The effect of endophytic *Peyronellaea* from heavy metal-contaminated and uncontaminated sites on maize growth, heavy metal absorption and accumulation. *Fungal Ecol.* 6, 539–545. doi: 10.1016/j.funeco.2013.08.001
- Singh, R. P., Mishra, S., Jha, P., Raghuvanshi, S., and Jha, P. N. (2018). Effect of inoculation of zinc-resistant bacterium *Enterobacter ludwigii* CDP-14 on growth, biochemical parameters and zinc uptake in wheat (*Triticum aestivum* L.) plant. *Ecol. Eng.* 116, 163–173. doi: 10.1016/j.ecoleng.2017.12.033
- Soleimani, M., Hajabbasi, M. A., Afyuni, M., Mirlohi, A., Borggaard, O. K., and Holm, P. E. (2010). Effect of endophytic fungi on cadmium tolerance and bioaccumulation by *Festuca arundinacea* and *Festuca pratensis*. *Int. J. Phytoremediation* 12, 535–549. doi: 10.1080/15226510903353187
- Sun, R. L., Zhou, Q. X., Sun, F. H., and Jin, C. X. (2007). Antioxidative defense and proline/phytochelatin accumulation in a newly discovered Cd-hyperaccumulator, *Solanum nigrum* L. *Environ. Exp. Bot.* 60, 468–476. doi: 10.1016/j.envexpbot.2007.01.004
- Tessier, A., Campbell, P. G., and Bisson, M. (1979). Sequential extraction procedure for the speciation of particulate trace metals. *Anal. Chem.* 51, 844–851. doi: 10.1021/ac50043a017
- Tüzün, M. (2003). Determination of trace metals in the River Yeşilirmak sediments in Tokat, Turkey using sequential extraction procedure. *Microchem. J.* 74, 105–110. doi: 10.1016/S0026-265X(02)00174-1
- Uchimiya, M., Bannon, D., Nakanishi, H., McBride, M. B., Williams, M. A., and Yoshihara, T. (2020). Chemical speciation, plant uptake, and toxicity of heavy metals in agricultural soils. *J. Agric. Food Chem.* 68, 12856–12869. doi: 10.1021/acs.jafc.0c00183
- Verma, S., and Mishra, S. N. (2005). Putrescine alleviation of growth in salt-stressed *Brassica juncea* by inducing antioxidative defense system. *J. Plant Physiol.* 162, 669–677. doi: 10.1016/j.jplph.2004.08.008
- Wagner, G. J. (1993). Accumulation of cadmium in crop plants and its consequences to human health. *Adv. Agron.* 51, 173–212. doi: 10.1016/S0065-2113(08)60593-3
- Wan, Y., Luo, S., Chen, J., Xiao, X., Chen, L., Zeng, G., et al. (2012). Effect of endophyte-infection on growth parameters and Cd-induced phytotoxicity of Cd-hyperaccumulator *Solanum nigrum* L. *Chemosphere* 89, 743–750. doi: 10.1016/j.chemosphere.2012.07.005
- Wang, J. L., Li, T., Liu, G. Y., Smith, J. M., and Zhao, Z. W. (2016). Unraveling the role of dark septate endophyte (DSE) colonizing maize (*Zea mays*) under cadmium stress: Physiological, cytological and genic aspects. *Sci. Rep.* 6:22028. doi: 10.1038/srep22028
- Wang, L., Lin, H., Dong, Y., Li, B., and He, Y. (2020). Effects of endophytes inoculation on rhizosphere and endosphere microecology of Indian mustard (*Brassica juncea*) grown in vanadium-contaminated soil and its enhancement on phytoremediation. *Chemosphere* 240:124891. doi: 10.1016/j.chemosphere.2019.124891
- Wang, S., Dai, H., Wei, S., Skuza, L., and Chen, Y. (2022). Effects of Cd-resistant fungi on uptake and translocation of Cd by soybean seedlings. *Chemosphere* 291:132908. doi: 10.1016/j.chemosphere.2021.132908
- Wang, Y., Huang, J., and Gao, Y. (2012). Arbuscular mycorrhizal colonization alters subcellular distribution and chemical forms of cadmium in *Medicago sativa* L. and resists cadmium toxicity. *PLoS One* 7:e48669. doi: 10.1371/journal.pone.0048669
- Wang, Y., Mopper, S., and Hasenstein, K. H. (2001). Effects of salinity on endogenous ABA, IAA, JA, and SA in *Iris hexagona*. *J. Chem. Ecol.* 27, 327–342. doi: 10.1023/a:1005632506230
- Waqas, M., Khan, A. L., Kamran, M., Hamayun, M., Kang, S. M., Kim, Y. H., et al. (2012). Endophytic fungi produce gibberellins and indoleacetic acid and promotes host-plant growth during stress. *Molecules* 17, 10754–10773. doi: 10.3390/molecules170910754
- Ważny, R., Rozpadek, P., Domka, A., Jędrzejczyk, R. J., Nosek, M., Hubalewska-Mazgaj, M., et al. (2021). The effect of endophytic fungi on growth and nickel accumulation in *Nocca* hyperaccumulators. *Sci. Total Environ.* 768:144666. doi: 10.1016/j.scitotenv.2020.144666
- White, J. F., Kingsley, K. L., Zhang, Q., Verma, R., Obi, N., Dvinskikh, S., et al. (2019). Review: Endophytic microbes and their potential applications in crop management. *Pest. Manag. Sci.* 75, 2558–2565. doi: 10.1002/ps.5527
- Wu, S., Wu, X., Hu, Y., Chen, S., Hu, J., Chen, Y., et al. (2004). Studies on soil pollution around Pb-Zn smelting factory and heavy metals hyperaccumulators. *Ecol. Environ.* 13, 156–157.
- Yadav, S. K. (2010). Heavy metals toxicity in plants: An overview on the role of glutathione and phytochelators in heavy metal stress tolerance of plants. *South African J. Bot.* 76, 167–179. doi: 10.1016/j.sajb.2009.10.007
- Yamaguchi, S. (2008). Gibberellin metabolism and its regulation. *Annu. Rev. Plant Biol.* 59, 225–251. doi: 10.1146/annurev.arplant.59.032607.092804
- Yuan, Z. L., Zhang, C. L., and Lin, F. C. (2010). Role of diverse non-systemic fungal endophytes in plant performance and response to stress: Progress and approaches. *J. Plant Growth Regul.* 29, 116–126. doi: 10.1007/s00344-009-9112-9
- Zhai, Y., Chen, Z., Malik, K., Wei, X., and Li, C. (2022). Effect of Fungal Endophyte *Epichloë bromicola* Infection on Cd Tolerance in Wild Barley (*Hordeum brevisubulatum*). *J. Fungi* 8:366. doi: 10.3390/jof8040366
- Zhan, F., Li, B., Jiang, M., Qin, L., Wang, J., He, Y., et al. (2017). Effects of a root-colonized dark septate endophyte on the glutathione metabolism in maize plants under cadmium stress. *J. Plant Interact.* 12, 421–428. doi: 10.1080/17429145.2017.1385868
- Zhang, X., Fan, X., Li, C., and Nan, Z. (2010). Effects of cadmium stress on seed germination, seedling growth and antioxidative enzymes in *Achnatherum inebrians* plants infected with a Neotyphodium endophyte. *Plant Growth Regul.* 60, 91–97. doi: 10.1007/s10725-009-9422-8
- Zhang, X. F., Hu, Z. H., Yan, T. X., Lu, R. R., Peng, C. L., Li, S. S., et al. (2019). Arbuscular mycorrhizal fungi alleviate Cd phytotoxicity by altering Cd subcellular distribution and chemical forms in *Zea mays*. *Ecotoxicol. Environ. Safe.* 171, 352–360. doi: 10.1016/j.ecoenv.2018.12.097
- Zhu, L., Li, T., Wang, C., Zhang, X., Xu, L., Xu, R., et al. (2018). The effects of dark septate endophyte (DSE) inoculation on tomato seedlings under Zn and Cd stress. *Environ. Sci. Pollut. Res.* 25, 35232–35241. doi: 10.1007/s11356-018-3456-2
- Zulfikar, U., Ayub, A., Hussain, S., Waraich, E. A., El-Esawi, M. A., Ishfaq, M., et al. (2021). Cadmium toxicity in plants: Recent progress on morpho-physiological effects and remediation strategies. *J. Soil Sci. Plant Nutri.* 22, 212–269. doi: 10.1007/s42729-021-00645-3





## OPEN ACCESS

## EDITED BY

Ravindra Soni,  
Indira Gandhi Krishi Vishva Vidyalaya,  
India

## REVIEWED BY

Lata Jain,  
National Institute of Biotic Stress  
Management, India  
Xiao Long,  
Peking Union Medical College Hospital  
(CAMS), China

## \*CORRESPONDENCE

Zhichang Zhang,  
zc Zhang@cmu.edu.cn

## SPECIALTY SECTION

This article was submitted to Bioprocess  
Engineering,  
a section of the journal  
Frontiers in Bioengineering and  
Biotechnology

RECEIVED 19 July 2022

ACCEPTED 23 September 2022

PUBLISHED 07 October 2022

## CITATION

Xu D, Liu B, Wang J and Zhang Z (2022),  
Bibliometric analysis of artificial  
intelligence for biotechnology and  
applied microbiology: Exploring  
research hotspots and frontiers.  
*Front. Bioeng. Biotechnol.* 10:998298.  
doi: 10.3389/fbioe.2022.998298

## COPYRIGHT

© 2022 Xu, Liu, Wang and Zhang. This is  
an open-access article distributed  
under the terms of the [Creative  
Commons Attribution License \(CC BY\)](#).  
The use, distribution or reproduction in  
other forums is permitted, provided the  
original author(s) and the copyright  
owner(s) are credited and that the  
original publication in this journal is  
cited, in accordance with accepted  
academic practice. No use, distribution  
or reproduction is permitted which does  
not comply with these terms.

# Bibliometric analysis of artificial intelligence for biotechnology and applied microbiology: Exploring research hotspots and frontiers

Dongyu Xu<sup>1</sup>, Bing Liu<sup>2</sup>, Jian Wang<sup>3</sup> and Zhichang Zhang<sup>1\*</sup>

<sup>1</sup>Department of Computer, School of Intelligent Medicine, China Medical University, Shenyang, Liaoning, China, <sup>2</sup>Department of Bone Oncology, The People's Hospital of Liaoning Province, Shenyang, Liaoning, China, <sup>3</sup>Department of Pathogenic Biology, School of Basic Medicine, China Medical University, Shenyang, Liaoning, China

**Background:** In the biotechnology and applied microbiology sectors, artificial intelligence (AI) has been extensively used in disease diagnostics, drug research and development, functional genomics, biomarker recognition, and medical imaging diagnostics. In our study, from 2000 to 2021, science publications focusing on AI in biotechnology were reviewed, and quantitative, qualitative, and modeling analyses were performed.

**Methods:** On 6 May 2022, the Web of Science Core Collection (WoSCC) was screened for AI applications in biotechnology and applied microbiology; 3,529 studies were identified between 2000 and 2022, and analyzed. The following information was collected: publication, country or region, references, knowledgebase, institution, keywords, journal name, and research hotspots, and examined using VOSviewer and CiteSpace V bibliometric platforms.

**Results:** We showed that 128 countries published articles related to AI in biotechnology and applied microbiology; the United States had the most publications. In addition, 584 global institutions contributed to publications, with the Chinese Academy of Science publishing the most. Reference clusters from studies were categorized into ten headings: deep learning, prediction, support vector machines (SVM), object detection, feature representation, synthetic biology, amyloid, human microRNA precursors, systems biology, and single cell RNA-Sequencing. Research frontier keywords were represented by microRNA (2012–2020) and protein-protein interactions (PPIs) (2012–2020).

**Abbreviations:** AI, Artificial Intelligence; WoSCC, Web of Science Core Collection; CPI, Compound-Protein Interactions; ACPred-FL, Anti-Cancer Peptide Predictor with Feature Representation Learning; ACPs, Anti-cancer peptides; CRISPR, Clustered Regularly Interspaced Short Palindromic Repeats; SARS-CoV-2, Severe Acute Respiratory Syndrome Coronavirus 2; AD, Alzheimer's Disease; CNN, Convolutional Neural Network; A $\beta$ , amyloid- $\beta$ ; RNN, Recurrent Neural Network; RNA, Ribonucleic Acid; DNN, Deep Neural Networks; DISC, Deep learning Imputation model with semi-supervised learning for Single Cell transcriptomes; PPI, Protein-Protein Interaction; DPPI, Direct physical Protein-Protein Interactions; SVM, Support Vector Machine.

**Conclusion:** We systematically, objectively, and comprehensively analyzed AI-related biotechnology and applied microbiology literature, and additionally, identified current hot spots and future trends in this area. Our review provides researchers with a comprehensive overview of the dynamic evolution of AI in biotechnology and applied microbiology and identifies future key research areas.

#### KEYWORDS

artificial intelligence, biotechnology, bibliometric, deep learning, machine learning, applied microbiology

## Introduction

Since the beginning of the 21st century, the life sciences and biotechnology and applied microbiology sectors have exemplified mankind's technological and revolutionary evolution. In these sectors, among the top 10 scientific breakthroughs published by science journals in recent decades, more than half of research outputs were revolutionarily innovative and breakthrough in nature. Emerging biological sectors include, biomedicine, bio-based chemicals, bioenergy, and genetically modified crop technology (Celikkanat Ozan and Baran, 2013). These areas are cutting-edge, and next-generation biotechnology industries are anticipated to develop rapidly in the future (Lee, 2016). As the front end of these biological industries and value chains, biotechnology and applied microbiology research has adopted a leading position in these industries. Therefore, exploring rapid developments and hot trends in basic biotechnology and applied microbiology research is pivotal in guiding biotechnology current achievements and developing new, downstream bio-industry markets.

AI represents advanced computer technology, and is a highly complex system integrating mathematics, statistics, probability, logic, ethics, and other disciplines. It primarily includes deep learning, machine learning, convolution and recurrent neural networks (CNN and RNN, respectively), full revolutionary networks (FCNs), and other specific methods. AI is extensively used in different industries, in particular biotechnology and the life sciences. In recent years, several major research developments have been achieved, including the AI-mediated prediction of protein structure, which was breakthrough of the year in 2021 (Baek et al., 2021). By exploiting complex simulation algorithms, AI has revolutionized disease diagnostics, drug research and development, functional genomics, biomarker recognition, and medical imaging diagnostics, and critically, has provided a vital reference point for disease diagnostic, prediction, and treatment strategies (Dlamini et al., 2020).

To facilitate AI research and progress in biotechnology and applied microbiology, bibliometric analyses and reviews are used to equip scientists with in-depth understandings of the application, its ongoing evolution, and future prospects. From

a database search spanning 1 January 2000 to 31 December 2021, we used bibliometric methods to analyze scientific papers on AI applications in biotechnology and applied microbiology, including papers published in different jurisdictions and by institutions. We examined journals where AI biotechnological research studies were published, investigated the “top 10 cited studies”, and enumerated how many times popular studies were cited. We clustered the reference network of cited studies, and investigated the subject knowledge base. Research hotspots were identified using burst keywords, which provided invaluable indicators for future research. Our research remit was to provide researchers with a macro understanding and micro analysis of the AI biotechnological field. When compared with traditional systematic reviews, we provided an intuitive, timely, and logical framework to track biotechnological developments and explore specific knowledge areas.

## Methods

On 6 January 2022, we used the Web of Science Core Collection (WoSCC) to download data (2000–2021), which were independently verified by DX and ZZ. The following search terms were used: (“deep learning” OR “machine learning” OR “convolutional neural network\*” OR CNN\* OR RNN OR “Recurrent neural network\*” OR “Fully Convolutional Network\*” OR FCN\*). The Web of Science category was “Biotechnology Applied Microbiology”, and documents were gathered. From studies, the following basic information was gathered: authors, abstract, title, institution, journal, keywords, country/region, and references. Studies indexed in the database were included, whereas the following were excluded: 1) book chapters, data papers, meeting abstracts and proceedings papers, repeated articles, and editorials, and 2) unpublished studies with limited data for analysis. In total, 79 duplicates were excluded. A study overview (search process and analyses) is provided (Figure 1).

We described publication traits, including country, institute, journals, and keywords. The H-index is an important indicator and was used to reflect the value of scientific research (Eyre-Walker and Stoletzki, 2013). The

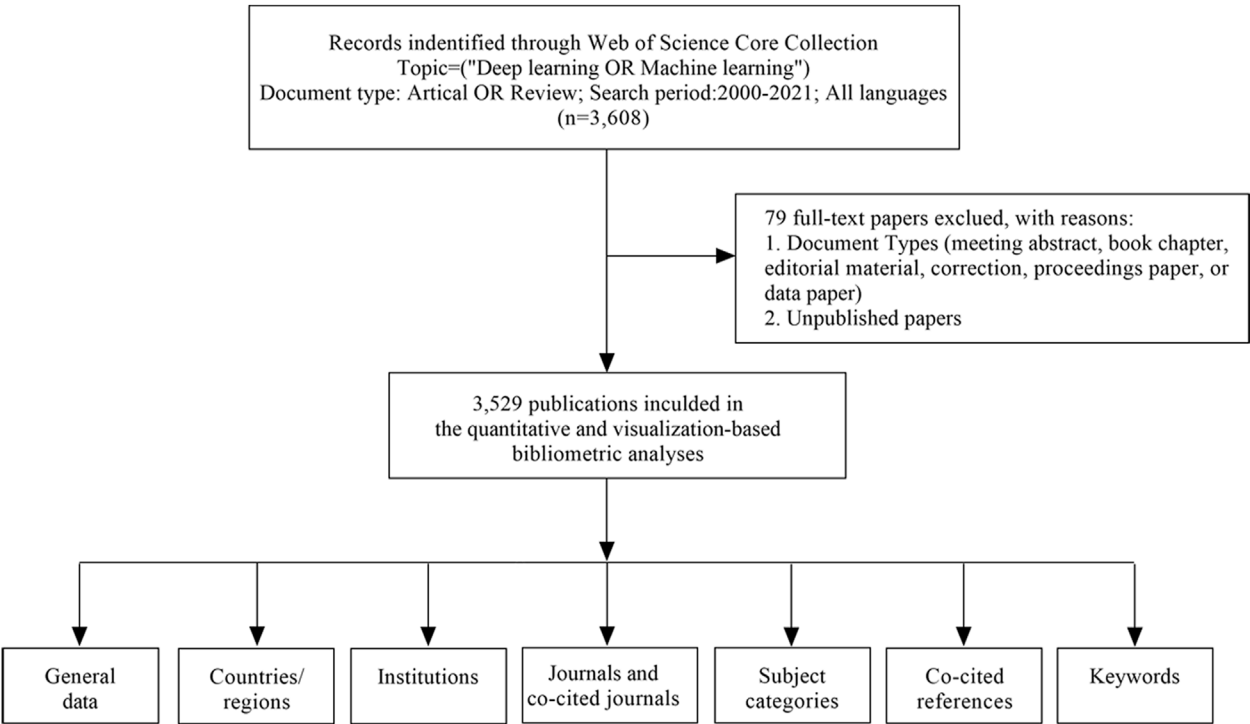


**FIGURE 1**  
A frame flow diagram. The diagram showed details selection criteria for ABAM publications from WoSCC database and the steps of bibliometric analysis.

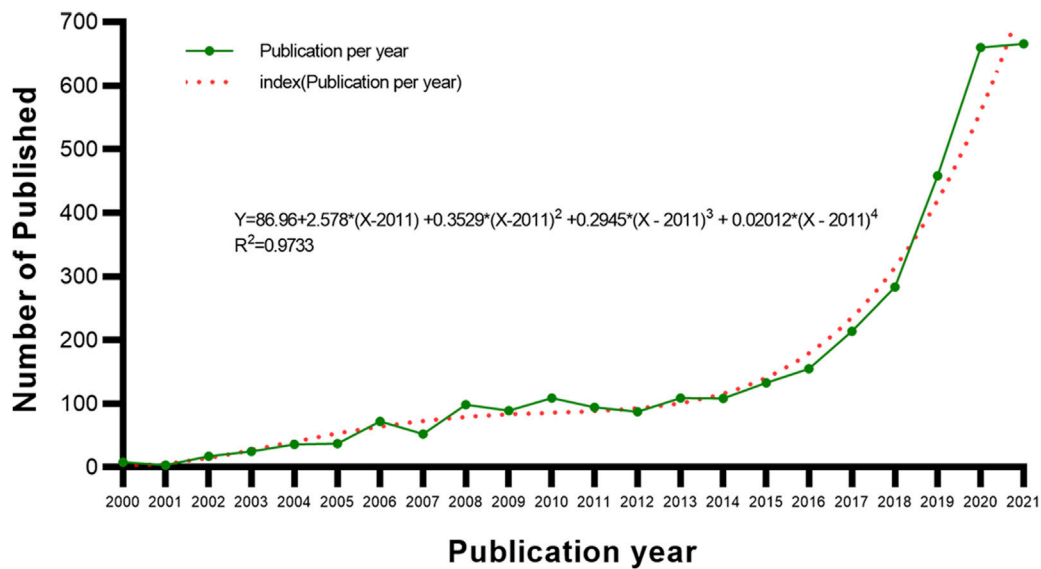
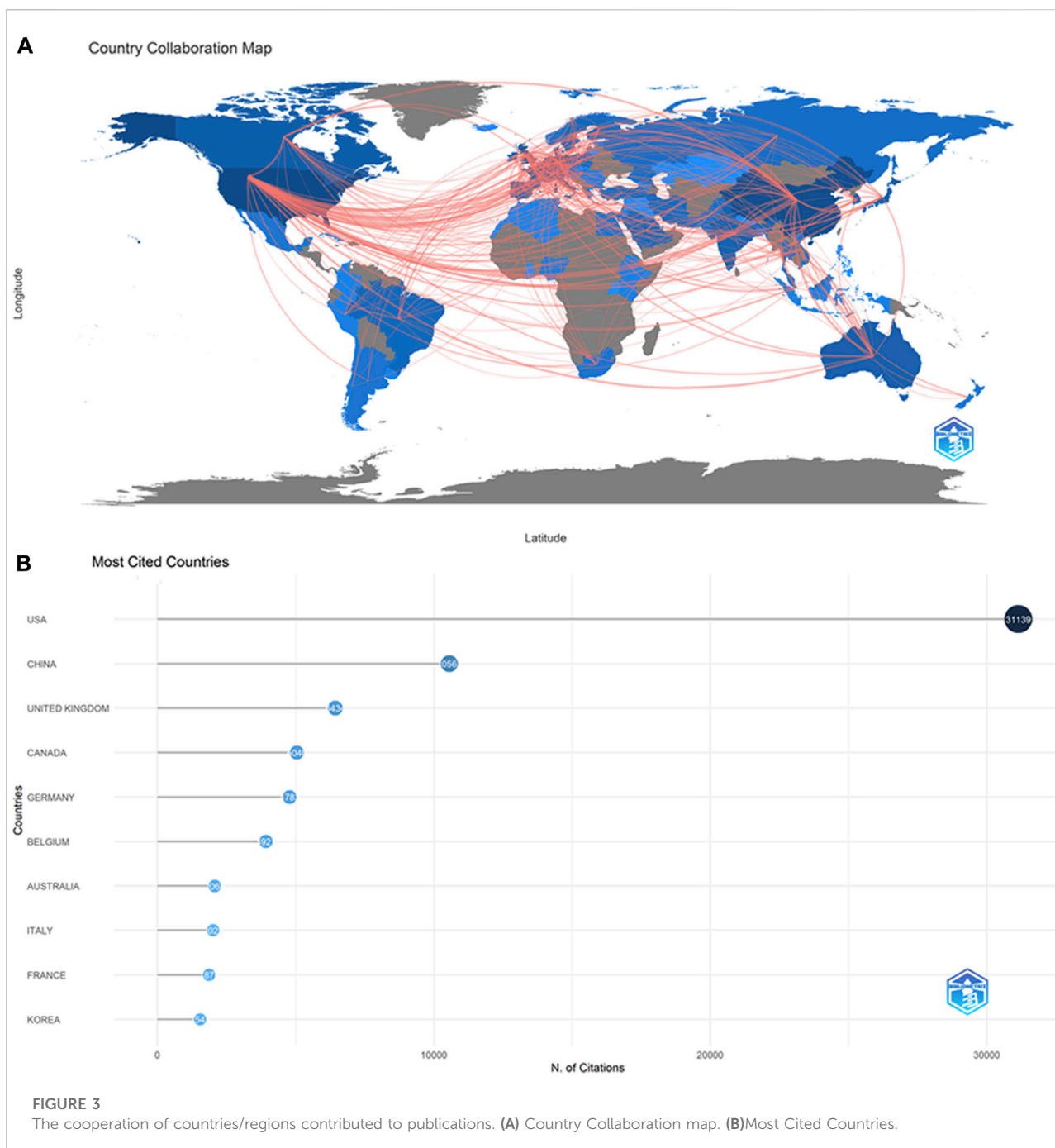


**FIGURE 2**  
Trends in the number of publications on ABAM from 2000 to 2021.



Literature Metrology websites; <http://bibliometric.com/>, VOSviewer (Leiden University, Leiden, Netherlands), and CiteSpace V (Drexel University, Philadelphia, PA, United States) were used to visualize collaborative networks in institutes/countries/keywords/journals and co-occurrence analyses. In CiteSpace, we conducted reference co-citation analyses, constructed knowledge maps, and identified burst keywords to generate new recurrent keywords (Chen, 2006).

## Results

### Article distribution by publication year

The literature retrieval showed that the research on AI in this topic began in 2000. From 2000 to 2021, 3,529 papers were published, and AI with Biotechnology and Applied Microbiology (ABAM) related publication trends identified (Figure 2). Studies



TABLE 1 Top 10 countries/regions and relevant institutions.

| Rank | Countries/regions | Count | Total citations | H-index | Institutions                   | Count | H-index |
|------|-------------------|-------|-----------------|---------|--------------------------------|-------|---------|
| 1    | United States     | 1308  | 31139           | 91      | CHINESE ACAD SCI               | 85    | 26      |
| 2    | China             | 826   | 10561           | 61      | STANFORD UNIV                  | 52    | 32      |
| 3    | Germany           | 258   | 4783            | 44      | SHANGHAI JIAO TONG UNIV        | 46    | 17      |
| 4    | United Kingdom    | 223   | 6434            | 49      | UNIV CAMBRIDGE                 | 37    | 16      |
| 5    | Canada            | 158   | 5040            | 37      | CARNEGIE MELLON UNIV           | 36    | 16      |
| 6    | Australia         | 128   | 2068            | 27      | TSINGHUA UNIV                  | 32    | 18      |
| 7    | Italy             | 121   | 2022            | 28      | UNIV ELECT SCI & TECHNOL CHINA | 31    | 16      |
| 8    | Japan             | 121   | 1327            | 30      | HARVARD UNIV                   | 31    | 30      |
| 9    | South Korea       | 120   | 1547            | 25      | TIANJIN UNIV                   | 30    | 17      |
| 10   | France            | 99    | 1875            | 29      | UNIV WASHINGTON                | 30    | 17      |

TABLE 2 Top 10 cited references on artificial intelligence for biotechnology and applied microbiology.

| Rank | Source titles        | Title of reference  | Count | Interpretation of findings  |
|------|----------------------|---|-------|---|
| 1    | NATURE               | Deep learning.  | 203   | This paper studied the back propagation algorithm of deep learning  |
| 2    | J MACH LEARN RES     | Dropout: a simple way to prevent neural networks from overfitting.                      | 176   | This study improved neural network performance in supervised learning tasks   |
| 3    | NAT BIOTECHNOL       | Predicting the sequence specificities of DNA-and RNA-binding proteins by deep learning. | 151   | This study used deep learning techniques to identify sequence specificities in DNA and RNA binding proteins   |
| 4    | INT C LEARNING R     | Adam: A method for stochastic optimization.   | 132   | In this paper, a stochastic gradient descent optimization algorithm, based on the first derivative, was proposed for the first time. It was used for large data, sparse data processing, and super parameter easy adjustment. |
| 5    | J MACH LEARN RES     | Scikit-learn: Machine learning, in python.  | 126   | This article introduced scikit learning, a python module that integrated different contemporary machine learning algorithms   |
| 6    | NAT METHODS          | Predicting effects of noncoding variants with deep learning-based sequence model.       | 118   | Based on deep learning, this study developed an algorithmic framework to identify functional effects from noncoding mutations   |
| 7    | ACM T INTEL SYST TEC | LIBSVM: A library for support vector machines.  | 91    | This study helped users apply support vector machine (SVM) to their applications.   |
| 8    | COMMUN ACM           | ImageNet classification with deep convolutional neural networks.                        | 90    | In this study, a large-scale deep CNN was used to classify 1.2 million high-resolution images   |
| 9    | NATURE               | An integrated encyclopedia of DNA elements in the human genome.                         | 81    | This study systematically mapped chromatin structure, transcription, transcription factor association, and histone modification regions.  |
| 10   | SIGKDD EXPLORATIONS  | The WEKA data mining software: an update.   | 79    | The widely used, open source machine learning software Weka was introduced in this paper and allowed researchers access the latest technologies in machine learning.  |

in this area are increasing year on year, and suggest the establishment of an important research trend.

Institutes, countries, and regions

We observed that 128 countries/regions published ABAM studies: collaborations between countries (Figure 3) and the top 10 countries (Table 1) are outlined. The United States published the most studies (1308), then China (826), Germany (258), and the United Kingdom (223). Some countries, such as United States, China, Germany, and United Kingdom, showed high centrality (marked by dark

blue), indicating that these countries likely played an important role in research of this topic and made great contributions.

We identified 584 institutes which contributed to ABAM publications; the top 10 are outlined (Table 1). Institutional collaborations are shown (Figure 4). The Chinese Academy of Sciences recorded the most publications (85), followed by the universities of Stanford (52), Shanghai Jiao Tong (46), and Cambridge (37).

Figure 4 emphasizes the close and complex cooperative relationship between different organizations. The VOSviewer platform can be used to analyze the centrality of organizations. The purple circle represents centrality, and the

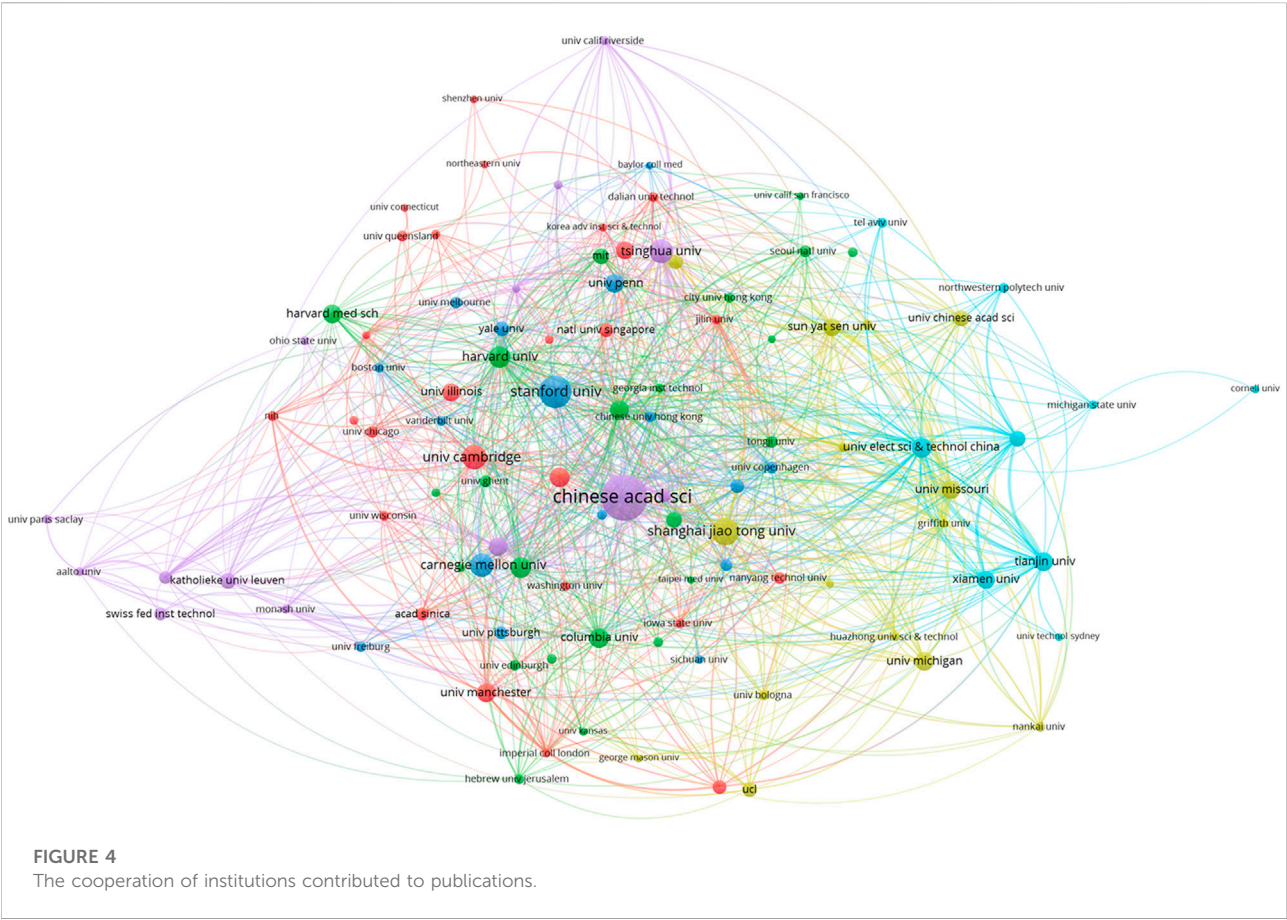


TABLE 3 Highly link strength of the top 20 occurrence keywords.

| Rank | Keyword                      | Occurrence | Total link strength | Rank | Keyword                     | Occurrence | Total link strength |
|------|------------------------------|------------|---------------------|------|-----------------------------|------------|---------------------|
| 1    | Machine learning             | 782        | 420                 | 11   | Prediction                  | 44         | 52                  |
| 2    | Deep learning                | 318        | 183                 | 12   | Biomarkers                  | 39         | 49                  |
| 3    | Classification               | 82         | 95                  | 13   | Algorithms                  | 36         | 40                  |
| 4    | Convolutional neural network | 72         | 51                  | 14   | Bioinformatics              | 33         | 51                  |
| 5    | Artificial intelligence      | 60         | 61                  | 15   | Cancer                      | 30         | 44                  |
| 6    | Random forest                | 57         | 58                  | 16   | Genomics                    | 28         | 39                  |
| 7    | Support vector machine       | 56         | 41                  | 17   | Clustering                  | 25         | 20                  |
| 8    | Feature selection            | 52         | 62                  | 18   | Data mining                 | 25         | 29                  |
| 9    | Gene expression              | 50         | 61                  | 19   | Rna-seq                     | 21         | 28                  |
| 10   | Neural networks              | 46         | 41                  | 20   | Natural language processing | 19         | 16                  |

area of the circle is proportional to the centrality. The Chinese Academy of Sciences and Stanford University are the most prominent organizations, showing that they conducted more research in this area.

### Journals

In any research field, referential relationships between academic journals often reflect knowledge exchange, where



A dual-map overlay of journals (Figure 6) was used to show citing and cited journals on the left and right, respectively, while citation relationships were reflected by colored paths—these analyses showed that studies published in Genetics/Molecular/

## References

We generated a co-citation reference network to measure the scientific relevance of related studies (Figure 7). Cluster setting parameters: top N% = 0.5 and # years per slice = 1. The Modularity Q score = 0.7135, which was > 0.5 and showed the network was reasonably separated into loosely coupled clusters. Weighted mean silhouette score = 0.9229, which was > 0.5, therefore cluster homogeneity was acceptable.





(Manavalan et al., 2019), cluster #5 “synthetic biology” (Wu et al., 2016), cluster #6 “amyloid” (Charoenkwan et al., 2021), cluster #7 “human microRNA precursors” (Wang et al., 2011), cluster #8 “systems biology” (Zou et al., 2015b), and cluster #9 “scRNA-Seq (single cell RNA-Sequencing)” (Arisdakessian et al., 2019).



Occurrences Burst History

### Top 14 Keywords with the Strongest Citation Bursts

| Keywords                        | Year | Strength | Begin | End  | 2000 - 2021 |
|---------------------------------|------|----------|-------|------|-------------|
| microarray                      | 2000 | 4.78     | 2003  | 2017 |             |
| algorithm                       | 2000 | 15       | 2006  | 2014 |             |
| computational molecular biology | 2000 | 8.84     | 2006  | 2011 |             |
| gene expression                 | 2000 | 8.36     | 2006  | 2017 |             |
| sequence analysis               | 2000 | 5.13     | 2006  | 2014 |             |
| markov chain                    | 2000 | 3.76     | 2006  | 2011 |             |
| statistics                      | 2000 | 5.35     | 2009  | 2017 |             |
| combinatorial optimization      | 2000 | 3.46     | 2009  | 2014 |             |
| gene network                    | 2000 | 3.17     | 2009  | 2011 |             |
| data mining                     | 2000 | 5.18     | 2012  | 2017 |             |
| prediction                      | 2000 | 3.49     | 2012  | 2017 |             |
| microRNA                        | 2000 | 3.27     | 2012  | 2020 |             |
| random forest                   | 2000 | 3.22     | 2012  | 2017 |             |
| protein-protein interaction     | 2000 | 3.19     | 2012  | 2020 |             |

FIGURE 8

The keywords with the strongest citation bursts of publications on ABAM from 2000 to 2021.

## Keywords

Analysis of keywords can provide a summary of the topics of each study and explore the hotspots and directions in this research area.

Keywords extracted from ABAM studies were processed, and the top 20 are given in Table 3. Temporal hotspot trend shifts, on the basis of the top 14 keywords with the strongest citation bursts, were analyzed and included the following. The burst keywords in 2006–2011 were computational molecular biology (2006–2011), Markov chain (2006–2011), and gene network (2009–2011). The burst keywords in 2006–2014 were algorithm (2006–2014), sequence analysis (2006–2014), and combinatorial optimization (2009–2014). The burst keywords in 2003–2017 were microarray (2003–2017), gene expression (2006–2017), statistics (2009–2017), data mining (2012–2017), prediction (2012–2017), and random forest (2012–2017). The current research hotspots are microRNA (2012–2020) and protein–protein interaction (2012–2020) (Figure 8).

## Discussion

### General data

In this study, 3,529 ABAM papers, confirming to search terms and inclusion/exclusion criteria, were published

between 2000 and 2021. The United States published most studies (1308, 26.6%), with China second (826, 16.8%). China had five of the top 10 institutions, with four in the United States, and one in the United Kingdom. The journal in which most publications were published was Bioinformatics, which majorly contributed to ABAM research. Additionally, the top 10 cited studies were examined: the top study was cited 203 times and was published by LeCun et al. in NATURE (LeCun et al., 2015). The second rated study was cited 176 times and published by Srivastava et al. in J MACH LEARN RES (Srivastava et al., 2014).

### Knowledge base

From previous studies, the application of deep learning related technologies to microbiology and biotechnology has been significant and generated many research achievements. As indicated (Figure 6), when we clustered co-cited references, key clustering nodes identified knowledge bases in this research field: #0 “deep learning”, #1 “prediction”, #2 “SVM”, #3 “object detection”, #4 “feature representation”, #5 “synthetic biology”, #6 “amyloid”, #7 “human microRNA precursors”, #8 “systems biology”, and

#9 “scRNA-Seq”. Herein, we describe the knowledge bases according to different clusters.

In #0 “deep learning”, a DeepBind software tool, based on deep learning, was developed by Alipanahi et al. (2015), and identified DNA and RNA binding protein sequence specificity. The tool was used to develop regulatory process models in biological systems and identify pathogenic variants. In other work, Beck et al. (2020) generated a deep learning-based, pre-trained, drug-target interaction model, Molecule Transformer-Drug Target Interaction, which identified commercially available drugs targeting SARS-CoV-2 proteins.

In #1 “prediction”, Tsubaki et al. (2019) studied end-to-end representation learning of compounds and proteins, and developed a Compound-Protein Interactions (CPI) prediction strategy for virtual screening in drug discovery by combining protein convolution neural networks (CNN) and compound graph neural networks. In other work, Almagro Armenteros et al. (2017) developed a prediction algorithm based on deep neural networks which relied only on sequence information for protein subcellular localization.

In #2 “SVM”, Ozer et al. (2020) showed that SVM provided solutions for high-throughput data analyses and contextualization; the approach rapidly determined timelines for invasive cancer diagnostics and treatment, and provided solutions for biomedical, bioengineering, and clinical applications. In other work, a SVM technology model constructed by Zhang et al. (2018) used joint information from multiple bone turnover markers, which improved diagnostic efficiency for osteoporosis, almost in perfect agreement with the dual-energy X-ray absorptiometry.

In #3 “object detection”, the approach by Zhang et al. (2020), exploited a deep object detection technique and was used to study contacts between protein secondary structure elements, and predict tertiary structural protein topology. Einhäuser et al. (2017) developed a foveal object detector to detect eye movement, which significantly reduced metabolic costs and computational complexity, and provided insights on visual system evolution with eye movement.

In #4 “feature representation”, an effective feature representation learning model ACPred-FL was developed by Wei et al. (2018), and used to rapidly and accurately identify new Anti-cancer peptides (ACPs) in many candidate proteins and peptides. The learning method developed by Peng et al. (2020) was based on feature representation learning and deep neural network (DTI-CNN), and was used to predict drug-target interactions and reduce time and experimental costs. In other research, from deep representation learning features with 107 dimensions, Lv et al. (2020) devised a sub-Golgi protein localization identification method, which exploited one feature type to accurately predict sub-Golgi protein localization.

#5 “synthetic biology” is a logical extension of recombinant technology or genetic engineering fields (Katz et al., 2018). Using

integrated synthetic biology, Nguyen et al. (2021) developed a wearable face-mask, with a lyophilized CRISPR sensor, to non-invasively detect SARS-CoV-2 at room temperature within 90 min. Cubillos-Ruiz et al. (2021) proposed that synthetic biology could be used to program living cells with therapeutic functions; their cell-based therapeutic design is currently undergoing rapid development in medicine, and may provide effective treatment solutions for human diseases.

In #6 “amyloid”, Charoenkwan et al. (2021) generated the first scorecard-based predictor for the accurate analysis, prediction, characterization, and identification of amyloid, on a large scale, to generate functional information for therapeutic intervention strategies. Cerebral amyloid- $\beta$  (A $\beta$ ) is an Alzheimer’s disease (AD) trait. Machine learning methods were used to identify cognitive performance and demographic variables for noninvasive testing of A $\beta$  deposition, which can detect the effect of anti-amyloid drugs in the non-dementia population (Ko et al., 2019).

In #7 “human microRNA precursors”, Zheng et al. (2020) used CNN and RNN approaches to automatically extract complex RNA sequence features to efficiently detect and predict human pre-microRNAs. Kamenetzky et al. (2016) identified a novel pre-microRNA in the *Echinococcus multilocularis* genome using a machine learning approach, which could help control and prevent the global zoonotic infectious disease alveolar echinococcosis.

In #8 “systems biology”, Reel et al. (2021) integrated different machine learning prediction algorithms to analyze different omics data to identify new biomarkers for systems biology. In their research, Weiskittel et al. (2021) outlined how systems biology algorithms layer machine learning and biological components could provide system-level analyses of single-cell omics data to clarify complex biological mechanisms. The powerful combination of systems biology, single cell omics, and machine learning could promote further, beneficial biomedical research.

In #9 “scRNA-Seq”, in an unbiased manner in single cells, scRNA-Seq assesses functions in individual cells and cell-to-cell variability (Lin et al., 2020). Based on deep neural networks, Arisdakessian et al. (2019) formulated an interpolation algorithm Deepimpute based on DNN. Dropout layers and loss function were used to learn data patterns and to deal with gaps in scRNA-Seq data. He et al. (2020) developed DISC, a deep learning imputation model with semi-supervised learning for single cell transcriptomes. DISC can deduce gene expression and structures obscured by dropouts, enhanced gene and cell structures, recovered poor gene expression, and improved cell identification. Using machine learning methods (deep learning) combined with scRNA-Seq datasets, issues such as reducing dimensions, missing values, denoizing sc data, and explaining zero expansion, can be solved. Machine learning methods can be exploited to comprehensively process scRNA-Seq data, improve follow-up analyses in stem cells, identify cell subsets, and support regenerative medicine and cell therapy strategies (Yan et al., 2021).

## Research frontiers and hotspots

Typically, keywords are used to concentrate on contemporary research concepts, while burst keywords represent research frontiers and emerging trends. CiteSpace was used to capture burst keywords, from which two research frontiers were identified: microRNA (2012–2020) and Protein-Protein Interaction (PPIs) (2012–2020). Importantly, we hypothesize these keywords exemplify future research frontiers.

MicroRNAs are noncoding single stranded RNAs that regulate development and gene transcription. Predicting and identifying connections between miRNAs and disease using AI-related methods is highly significant for unraveling pathogenic, preventative, prognostic, and pathological mechanisms implicated in diseases.

Zou et al. (2015a) predicted correlations between microRNAs and disease using two approaches: KATZ combined social network analysis and machine learning, while CATAPULT was a supervised machine learning method. Both were applied to 242 known associations between microRNAs and disease, and used 3-fold cross validation and leave-one-out cross-validation to evaluate method performance.

Wen et al. (2018) used the deep learning-based approach DeepMir Tar and extracted 750 features from a relatively large data set at different levels to predict human miRNA target sites. DeepMir Tar provided a new way to reveal miRNA biological function, as well as gene therapy and drug discovery for human diseases.

In large-scale RNA sequencing studies, Liu et al. developed a computational model called MirTarget which predicted genome-wide miRNA targets. Machine learning methods were used to train miRNA targeting feature data with miRNA binding and target down-regulation features, thus MirTarget showed better performances when compared with other algorithms (Liu and Wang, 2019).

Zheng et al. (2020) used CNN and RNN models to predict human pre-miRNAs; sequences were combined with predicted pre-miRNA secondary structures as input features to avoid feature extraction and selection processes by hand. Models were easily trained for handling training datasets; they demonstrated low generalization errors and were satisfactory for test datasets (Zheng et al., 2020).

Protein-protein interactions are very important in such cell life activities as transcriptional regulation, signal transduction, and drug signal transduction. Study of PPIs has become a research hotspot in bioinformatics. However, it is time-consuming and costly to identify PPIs using experimental methods (Chen et al., 2019).

People are more inclined to use artificial intelligence methods, like machine-learning, to automatically identify PPIs, which helps understanding of the molecular roots of disease on one hand, and provides new ideas for drug research and development on the other

hand. Also, this effectively reduces experimental costs (Yu et al., 2021).

Based on a deep learning algorithm, Sun et al. (2017) designed a stacked autoencoder and investigated sequence-based PPIs predictions; the prediction accuracy of different external datasets was 87.99%–99.21%. These high-throughput methods increased our understanding of protein roles, disease etiology, and therapy design.

Hashemifar et al. (2018) developed a Direct Physical Protein-Protein Interactions (DPPI) deep learning framework, which modeled and predicted PPIs from sequence information. By adopting a deep, Siamese-like CNN which used high-quality experimental PPI data, evolutionary information from a predicted protein pair, and combined these data with random projection and data enhancement, PPIs were successfully predicted (Hashemifar et al., 2018).

Zeng et al. (2019) formulated DeepPPISP, a novel end-to-end deep learning framework. To examine local contextual features, authors used a sliding window to acquire neighbor features from target amino acids. To analyze global sequence features, a text CNN extracted features from protein sequences. To predict PPI sites, local contextual and global sequence characteristics were combined (Zeng et al., 2019).

Sequence-based deep learning technologies have been successfully used to predict PPIs. However, Yang et al. (2020) indicted these methods only focus on sequence information and ignore structural information in PPI networks. Such information, including degree, location, and adjacent nodes in graphs, are vital for PPI predictions. These authors generated a graph-based deep learning method for predicting PPIs, and demonstrated an accuracy of 99.15%, which improved on existing sequence-based methods (Yang et al., 2020).

In their method based on deep learning, Liu-Wei et al. (2021) developed deepviral, which predicted PPIs between humans and viruses. The method processed protein sequences and phenotypic characteristics to reveal infectious disease mechanisms and elucidate potential treatment methods (Liu-Wei et al., 2021).

## Conclusion

We generated an objective, systematic, and comprehensive bibliometric analysis of scientific studies associated with deep learning, machine learning, CNN, RNN, and FCNs in ABAM. Moreover, we identified the research basis, future trends, and current hotspots in this field. Identified knowledge bases were: deep learning, prediction, SVMs, object detection, feature representation, synthetic biology, amyloid, human microRNA precursors, systems biology, and scRNA-Seq. Furthermore, microRNAs and PPIs were identified as future research frontiers and trends.

We identified some study limitations; publications over an extended period (2000–2021) were gathered, therefore, some

studies were incomplete and may have introduced publication bias into our research, potentially affecting analysis outcomes.

## Author contributions

DX and ZZ conceived and designed the study; ZZ and DX wrote and integrated sections; BL and JW retrieved references. All authors read and approved the final manuscript.

## Funding

Grants, supporting this study, were funded to Dongyu Xu (2021-AFCEC-529) from the Association of Fundamental Computing Education in Chinese Universities (AFCEC).

## References

- Alipanahi, B., Delong, A., Weirauch, M. T., and Frey, B. J. (2015). Predicting the sequence specificities of DNA- and RNA-binding proteins by deep learning. *Nat. Biotechnol.* 33, 831–838. doi:10.1038/nbt.3300
- Almagro Armenteros, J. J., Sønderby, C. K., Sønderby, S. K., Nielsen, H., Winther, O., and Hancock, J. (2017). DeepLoc: Prediction of protein subcellular localization using deep learning. *Bioinformatics* 33, 4049–4395. doi:10.1093/bioinformatics/btx548
- Arisdakessian, C., Poirion, O., Yunits, B., Zhu, X., and Garmire, L. X. (2019). DeepImpute: An accurate, fast, and scalable deep neural network method to impute single-cell RNA-seq data. *Genome Biol.* 20, 211. doi:10.1186/s13059-019-1837-6
- Baek, M., Dimaio, F., Anishchenko, I., Dauparas, J., Ovchinnikov, S., Lee, G. R., et al. (2021). Accurate prediction of protein structures and interactions using a three-track neural network. *Science* 373, 871–876. doi:10.1126/science.abj8754
- Beck, B. R., Shin, B., Choi, Y., Park, S., and Kang, K. (2020). Predicting commercially available antiviral drugs that may act on the novel coronavirus (SARS-CoV-2) through a drug-target interaction deep learning model. *Comput. Struct. Biotechnol. J.* 18, 784–790. doi:10.1016/j.csbj.2020.03.025
- Celikkanat Ozan, D., and Baran, Y. (2013). Comparative development of knowledge-based bioeconomy in the European Union and Turkey. *Crit. Rev. Biotechnol.* 34, 269–280. doi:10.3109/07388551.2013.792771
- Chang, C.-C., and Lin, C.-J. (2011). Libsvm: A library for support vector machines. *ACM Trans. Intelligent Syst. Technol.* 2, 1–27. doi:10.1145/1961189.1961199
- Charoenkwan, P., Kanthawong, S., Nantasenamat, C., Hasan, M. M., and Shoombuatong, W. (2021). iAMY-SCM: Improved prediction and analysis of amyloid proteins using a scoring card method with propensity scores of dipeptides. *Genomics* 113, 689–698. doi:10.1016/j.ygeno.2020.09.065
- Chen, C. (2006). CiteSpace II: Detecting and visualizing emerging trends and transient patterns in scientific literature. *J. Am. Soc. Inf. Sci. Technol.* 57, 359–377. doi:10.1002/asi.20317
- Chen, C., Zhang, Q., Ma, Q., and Yu, B. (2019). LightGBM-PPI: Predicting protein-protein interactions through LightGBM with multi-information fusion. *Chemom. Intelligent Laboratory Syst.* 191, 54–64. doi:10.1016/j.chemolab.2019.06.003
- Cubillos-Ruiz, A., Guo, T., Sokolovska, A., Miller, P. F., Collins, J. J., Lu, T. K., et al. (2021). Engineering living therapeutics with synthetic biology. *Nat. Rev. Drug Discov.* 20, 941–960. doi:10.1038/s41573-021-00285-3
- Dlamini, Z., Francies, F. Z., Hull, R., and Marima, R. (2020). Artificial intelligence (AI) and big data in cancer and precision oncology. *Comput. Struct. Biotechnol. J.* 18, 2300–2311. doi:10.1016/j.csbj.2020.08.019
- Einhäuser, W., Akbas, E., and Eckstein, M. P. (2017). Object detection through search with a foveated visual system. *PLoS Comput. Biol.* 13, e1005743. doi:10.1371/journal.pcbi.1005743
- Eyre-Walker, A., and Stoletzki, N. (2013). The assessment of science: The relative merits of post-publication review, the impact factor, and the number of citations. *PLoS Biol.* 11, e1001675. doi:10.1371/journal.pbio.1001675
- Furey, T. S., Cristianini, N., Duffy, N., Bednarski, D. W., Schummer, M., and Haussler, D. (2000). Support vector machine classification and validation of cancer tissue samples using microarray expression data. *Bioinformatics* 16, 906–914. doi:10.1093/bioinformatics/16.10.906
- Hall, M., Frank, E., Holmes, G., Pfahringer, B., Reutemann, P., and Witten, I. H. (2009). The WEKA data mining software. *SIGKDD Explor. Newsl.* 11, 10–18. doi:10.1145/1656274.1656278
- Hashemifar, S., Neyshabur, B., Khan, A. A., and Xu, J. (2018). Predicting protein-protein interactions through sequence-based deep learning. *Bioinformatics* 34, i802–i810. doi:10.1093/bioinformatics/bty573
- He, Y., Yuan, H., Wu, C., and Xie, Z. (2020). Disc: A highly scalable and accurate inference of gene expression and structure for single-cell transcriptomes using semi-supervised deep learning. *Genome Biol.* 21, 170. doi:10.1186/s13059-020-02083-3
- Hung, J., Goodman, A., Ravel, D., Lopes, S. C. P., Rangel, G. W., Nery, O. A., et al. (2020). Keras R-CNN: Library for cell detection in biological images using deep neural networks. *BMC Bioinforma.* 21, 300. doi:10.1186/s12859-020-03635-x
- Kamenetzky, L., Stegmayer, G., Maldonado, L., Macchiaroli, N., Yones, C., and Milone, D. H. (2016). MicroRNA discovery in the human parasite *Echinococcus multilocularis* from genome-wide data. *Genomics* 107, 274–280. doi:10.1016/j.ygeno.2016.04.002
- Katz, L., Chen, Y. Y., Gonzalez, R., Peterson, T. C., Zhao, H., and Baltz, R. H. (2018). Synthetic biology advances and applications in the biotechnology industry: A perspective. *J. Industrial Microbiol. Biotechnol.* 45, 449–461. doi:10.1007/s10295-018-2056-y
- Kingma, D. P., and Ba, J. (2014). Adam: A method for stochastic optimization. *arXiv preprint arXiv:1412.6980*.
- Ko, H., Ihm, J.-J., and Kim, H.-G. (2019). Cognitive profiling related to cerebral amyloid beta burden using machine learning approaches. *Front. Aging Neurosci.* 11, 95. doi:10.3389/fnagi.2019.00095
- Kourou, K., Exarchos, T. P., Exarchos, K. P., Karamouzis, M. V., and Fotiadis, D. I. (2015). Machine learning applications in cancer prognosis and prediction. *Comput. Struct. Biotechnol. J.* 13, 8–17. doi:10.1016/j.csbj.2014.11.005
- Krizhevsky, A., Sutskever, I., and Hinton, G. E. (2017). ImageNet classification with deep convolutional neural networks. *Commun. ACM* 60, 84–90. doi:10.1145/3065386
- Lecun, Y., Bengio, Y., and Hinton, G. (2015). Deep learning. *Nature* 521, 436–444. doi:10.1038/nature14539
- Lee, D.-H. (2016). Bio-based economies in Asia: Economic analysis of development of bio-based industry in China, India, Japan, Korea, Malaysia and Taiwan. *Int. J. Hydrogen Energy* 41, 4333–4346. doi:10.1016/j.ijhydene.2015.10.048

## Conflict of interest

The authors declare that the research was conducted in the absence of any commercial or financial relationships that could be construed as a potential conflict of interest.

## Publisher's note

All claims expressed in this article are solely those of the authors and do not necessarily represent those of their affiliated organizations, or those of the publisher, the editors and the reviewers. Any product that may be evaluated in this article, or claim that may be made by its manufacturer, is not guaranteed or endorsed by the publisher.



- Lin, E., Mukherjee, S., and Kannan, S. (2020). A deep adversarial variational autoencoder model for dimensionality reduction in single-cell RNA sequencing analysis. *BMC Bioinforma.* 21, 64. doi:10.1186/s12859-020-3401-5
- Liu, W., and Wang, X. (2019). Prediction of functional microRNA targets by integrative modeling of microRNA binding and target expression data. *Genome Biol.* 20, 18. doi:10.1186/s13059-019-1629-z
- Liu-Wei, W., Kafkas, S., Chen, J., Dimonaco, N. J., Tegnér, J., Hoehndorf, R., et al. (2021). DeepViral: Prediction of novel virus–host interactions from protein sequences and infectious disease phenotypes. *Bioinformatics* 37, 2722–2729. doi:10.1093/bioinformatics/btab147
- Lv, Z., Wang, P., Zou, Q., Jiang, Q., and Xu, J. (2020). Identification of sub-Golgi protein localization by use of deep representation learning features. *Bioinformatics* 36, 5600–5609. doi:10.1093/bioinformatics/btaa1074
- Manavalan, B., Basith, S., Shin, T. H., Wei, L., Lee, G., and Hancock, J. (2019). mAHTPred: a sequence-based meta-predictor for improving the prediction of anti-hypertensive peptides using effective feature representation. *Bioinformatics* 35, 2757–2765. doi:10.1093/bioinformatics/bty1047
- Nguyen, P. Q., Soenksen, L. R., Donghia, N. M., Angenent-Mari, N. M., De Puig, H., Huang, A., et al. (2021). Wearable materials with embedded synthetic biology sensors for biomolecule detection. *Nat. Biotechnol.* 39, 1366–1374. doi:10.1038/s41587-021-00950-3
- Ozer, M. E., Sarica, P. O., and Arga, K. Y. (2020). New machine learning applications to accelerate personalized medicine in breast cancer: Rise of the support vector machines. *OMICS A J. Integr. Biol.* 24, 241–246. doi:10.1089/omi.2020.0001
- Pedregosa, F., Varoquaux, G., Gramfort, A., Michel, V., Thirion, B., Grisel, O., et al. (2011). Scikit-learn: Machine learning in Python. *J. Mach. Learn. Res.* 12, 2825–2830.
- Peng, J., Li, J., and Shang, X. (2020). A learning-based method for drug-target interaction prediction based on feature representation learning and deep neural network. *BMC Bioinforma.* 21, 394. doi:10.1186/s12859-020-03677-1
- Reel, P. S., Reel, S., Pearson, E., Trucco, E., and Jefferson, E. (2021). Using machine learning approaches for multi-omics data analysis: A review. *Biotechnol. Adv.* 49, 107739. doi:10.1016/j.biotechadv.2021.107739
- Srivastava, N., Hinton, G., Krizhevsky, A., Sutskever, I., and Salakhutdinov, R. (2014). Dropout: A simple way to prevent neural networks from overfitting. *J. Mach. Learn. Res.* 15, 1929–1958.
- Sun, T., Zhou, B., Lai, L., and Pei, J. (2017). Sequence-based prediction of protein protein interaction using a deep-learning algorithm. *BMC Bioinforma.* 18, 277. doi:10.1186/s12859-017-1700-2
- The ENCODE Project Consortium (2012). An integrated encyclopedia of DNA elements in the human genome. *Nature* 489, 57–74.
- Tsubaki, M., Tomii, K., Sese, J., and Wren, J. (2019). Compound–protein interaction prediction with end-to-end learning of neural networks for graphs and sequences. *Bioinformatics* 35, 309–318. doi:10.1093/bioinformatics/bty535
- Wang, Y., Chen, X., Jiang, W., Li, L., Li, W., Yang, L., et al. (2011). Predicting human microRNA precursors based on an optimized feature subset generated by GA-SVM. *Genomics* 98, 73–78. doi:10.1016/j.ygeno.2011.04.011
- Wei, L., Zhou, C., Chen, H., Song, J., Su, R., and Hancock, J. (2018). ACPred-FL: A sequence-based predictor using effective feature representation to improve the prediction of anti-cancer peptides. *Bioinformatics* 34, 4007–4016. doi:10.1093/bioinformatics/bty451
- Weiskittel, T. M., Correia, C., Yu, G. T., Ung, C. Y., Kaufmann, S. H., Billadeau, D. D., et al. (2021). The trifecta of single-cell, systems-biology, and machine-learning approaches. *Genes* 12, 1098. doi:10.3390/genes12071098
- Wen, M., Cong, P., Zhang, Z., Lu, H., Li, T., and Kelso, J. (2018). DeepMirTar: A deep-learning approach for predicting human miRNA targets. *Bioinformatics* 34, 3781–3787. doi:10.1093/bioinformatics/bty424
- Wu, G., Yan, Q., Jones, J. A., Tang, Y. J., Fong, S. S., and Koffas, M. a. G. (2016). Metabolic burden: Cornerstones in synthetic biology and metabolic engineering applications. *Trends Biotechnol.* 34, 652–664. doi:10.1016/j.tibtech.2016.02.010
- Yan, R., Fan, C., Yin, Z., Wang, T., and Chen, X. (2021). Potential applications of deep learning in single-cell RNA sequencing analysis for cell therapy and regenerative medicine. *Stem Cells* 39, 511–521. doi:10.1002/stem.3336
- Yang, F., Fan, K., Song, D., and Lin, H. (2020). Graph-based prediction of Protein-protein interactions with attributed signed graph embedding. *BMC Bioinforma.* 21, 323. doi:10.1186/s12859-020-03646-8
- Yu, B., Chen, C., Wang, X., Yu, Z., Ma, A., and Liu, B. (2021). Prediction of protein–protein interactions based on elastic net and deep forest. *Expert Syst. Appl.* 176, 114876. doi:10.1016/j.eswa.2021.114876
- Zeng, M., Zhang, F., Wu, F.-X., Li, Y., Wang, J., Li, M., et al. (2019). Protein–protein interaction site prediction through combining local and global features with deep neural networks. *Bioinformatics* 36, 1114–1120. doi:10.1093/bioinformatics/btz699
- Zhang, Q., Zhu, J., Ju, F., Kong, L., Sun, S., Zheng, W.-M., et al. (2020). Issec: Inferring contacts among protein secondary structure elements using deep object detection. *BMC Bioinforma.* 21, 503. doi:10.1186/s12859-020-03793-y
- Zhang, T., Liu, P., Zhang, Y., Wang, W., Lu, Y., Xi, M., et al. (2018). Combining information from multiple bone turnover markers as diagnostic indices for osteoporosis using support vector machines. *Biomarkers* 24, 120–126. doi:10.1080/1354750x.2018.1539767
- Zheng, X., Fu, X., Wang, K., and Wang, M. (2020). Deep neural networks for human microRNA precursor detection. *BMC Bioinforma.* 21, 17. doi:10.1186/s12859-020-3339-7
- Zhou, J., and Troyanskaya, O. G. (2015). Predicting effects of noncoding variants with deep learning-based sequence model. *Nat. Methods* 12, 931–934. doi:10.1038/nmeth.3547
- Zou, Q., Li, J., Hong, Q., Lin, Z., Wu, Y., Shi, H., et al. (2015a). Prediction of MicroRNA-disease associations based on social network analysis methods. *BioMed Res. Int.* 2015, 1–9. doi:10.1155/2015/810514
- Zou, Q., Li, J., Song, L., Zeng, X., and Wang, G. (2015b). Similarity computation strategies in the microRNA-disease network: A survey. *Briefings Funct. Genomics.*



## OPEN ACCESS

## EDITED BY

Haiyan Li,  
Kunming University of Science and  
Technology, China

## REVIEWED BY

Zongfu Hu,  
Inner Mongolia Minzu University, China  
Ping Li,  
Guizhou University,  
China

## \*CORRESPONDENCE

Yuqin Wang  
wangyq6836@163.com

<sup>†</sup>These authors have contributed equally to  
this work

## SPECIALTY SECTION

This article was submitted to  
Microbiotechnology,  
a section of the journal  
Frontiers in Microbiology

RECEIVED 25 August 2022

ACCEPTED 16 September 2022

PUBLISHED 17 October 2022

## CITATION

Zhang Z, Wang Y, Wang S, Zhao L, Zhang B,  
Jia W, Zhai Z, Zhao L and Li Y (2022) Effects  
of antibacterial peptide-producing *Bacillus  
subtilis*, gallic acid, and cellulase on  
fermentation quality and bacterial  
community of whole-plant corn silage.  
*Front. Microbiol.* 13:1028001.  
doi: 10.3389/fmicb.2022.1028001

## COPYRIGHT

© 2022 Zhang, Wang, Wang, Zhao, Zhang,  
Jia, Zhai, Zhao and Li. This is an open-  
access article distributed under the terms  
of the [Creative Commons Attribution  
License \(CC BY\)](https://creativecommons.org/licenses/by/4.0/). The use, distribution or  
reproduction in other forums is permitted,  
provided the original author(s) and the  
copyright owner(s) are credited and that  
the original publication in this journal is  
cited, in accordance with accepted  
academic practice. No use, distribution or  
reproduction is permitted which does not  
comply with these terms.

# Effects of antibacterial peptide-producing *Bacillus subtilis*, gallic acid, and cellulase on fermentation quality and bacterial community of whole-plant corn silage

Zhiheng Zhang<sup>†</sup>, Yuqin Wang<sup>\*†</sup>, Saiqiao Wang, Lu Zhao,  
Binglei Zhang, Wanhong Jia, Zhenhan Zhai,  
Lingping Zhao and Yuanxiao Li

College of Animal Science and Technology, Henan University of Science and Technology, Luoyang, China

In the current study, we assessed the effects of antibacterial peptide-producing *Bacillus subtilis* (BS), gallic acid (GA) and cellulase (CL) on the fermentation quality and bacterial community of various varieties of whole-plant corn silage. Three different varieties of whole-plant corn (Yuqing386, Enxian298, and Nonghe35) were treated with 0.02% BS (fresh material basis), 0.2% GA (fresh material basis) and 0.02% CL (fresh material basis), after which 45 days of anaerobic fermentation were conducted. With the exception of its low dry matter content, the results showed that Yuqing386's crude protein, water-soluble carbohydrate, and lactic acid contents were significantly higher than those of the other two corn varieties. However, its acid detergent fiber and cellulose contents were significantly lower than those of the other two corn varieties. Among the three corn variety silages, Yuqing386 had the highest relative abundance of *Lactobacillus* at the genus level and the biggest relative abundance of *Firmicutes* at the phylum level. In addition, the three additives markedly enhanced the quantity of dry matter and crude protein as compared to the control group. The application of GA considerably decreased the level of neutral detergent fiber while significantly increasing the content of lactic acid and water-soluble carbohydrates. Even though all additives enhanced the structure of the bacterial community following silage, the GA group experienced the greatest enhancement. On a phylum and genus level, the GA group contains the highest relative abundance of *Firmicutes* and *Lactobacillus*, respectively. Overall, of the three corn varieties, Yuqing386 provides the best silage qualities. GA has the biggest impact among the additions employed in this experiment to enhance the nutritional preservation and fermentation quality of whole-plant corn silage.

## KEYWORDS

whole-plant corn silage, *Bacillus subtilis*, gallic acid, cellulases, fermentation quality, bacterial community

## Introduction

The moist forages can be effectively preserved using silage. Silage is produced by the fermentation of lactic acid bacteria (LAB) in anaerobic conditions, which can increase feed palatability, extend storage period, and reduce nutrient loss (Ni et al., 2017). Lactic acid bacteria have the ability to transform water-soluble carbohydrates (WSC) into organic acids, primarily lactic acid, during the ensiling process, lowering the pH, and preventing the growth of harmful microorganisms (Li and Nishino, 2011). Silage has always been a significant source of roughage for ruminant diets.

The manufacture of silage has made extensive use of crop feeds, including whole-plant corn, alfalfa, natural forages and others (Dunière et al., 2013). Additionally, whole-plant corn (WPC), which has a high biological yield and a bounty of water-soluble carbohydrates, has grown to be the most extensively utilized silage material globally (McDonald et al., 1991). WPC silage quality is influenced by a range of factors, including as variety, harvest stage, additives, and so on (Nazli et al., 2018; Wang et al., 2019a). Variety is a key component among them. According to Ferraretto et al. (2015) research, feeding dairy cows various types of corn silage had an impact on their consumption of dry matter, milk production, and starch digestibility. Varying types of WPC silage have different nutritional values and economic advantages, according to research by Nazli et al. (2018). To manage the quality of WPC silage, it is crucial to choose high-quality corn varieties.

The competition between undesirable microorganisms and lactic acid bacteria during the ensiling process, which may be significantly increased by employing additives, is what determines the quality of WPC silage (Wang et al., 2019a). Numerous silage additives have been researched and used in the production of silage for many years in order to further enhance the nutritional value and fermentation quality of silage (Muck et al., 2018). Based on their biochemical characteristics, silage additives can be classified as inoculants, chemicals, or enzymes (Sun et al., 2010). These additives are crucial for enhancing the microbial community of silages, nutritional value, and fermentation properties. Previous investigations have demonstrated that some metabolites of *Bacillus subtilis* (BS) can have antibacterial properties, and it can produce lactic acid by reducing pyruvate in anaerobic environment (Gandra et al., 2017; Lanna-Filho et al., 2017). In addition, BS and its metabolites can significantly increase the amount of lactic acid bacteria and aerobic stability in corn silages when used as a silage additive (Bonaldi et al., 2021). The natural organic acid gallic acid (GA), also known as 3,4,5-trihydroxybenzoic acid, has three phenolic hydroxyl groups and one carboxyl group (Badhani et al., 2015). According to reports, GA has broad-spectrum antibacterial activities, which might mean that it can disintegrate the structural integrity of bacteria or prevent the development of bacterial biofilms (Kang et al., 2008; Díaz-Gómez et al., 2013). Additionally, GA can prevent protein hydrolysis during the ensiling process,

which is an advantage of its polyhydroxy structure, which enhances protein binding (Jayanegara et al., 2019). He et al. (2020) reported that adding gallic acid to high-moisture mulberry leaves and stylo silage can improve the fermentation quality and protein preservation. Wang et al. (2021) also found that adding gallic acid to whole plant soybean silage was an effective strategy to protect feed nutrition and improve silage quality. As a consequence, GA could be the potential silage additive. Cellulase (CL) are currently the most popular enzyme in silage. In silage, CL primarily breaks down plant cell walls, releases a significant quantity of soluble sugar, and supplies a enough substrate for lactic acid bacteria fermentation (Muck et al., 2018). The combined addition of CL and galactosidase to alfalfa silage has been shown to dramatically lower the amount of ammonia nitrogen while increasing the amount of lactic acid and the relative abundance of lactic acid bacteria (Hu et al., 2021).

Few studies, to our knowledge, have looked into the impact of antibacterial peptide-producing BS and GA, on WPC silage. As a result, three varieties of corn, Yuqing386 (YQ), Enxiai298 (EXA), and Nonghe35 (NH) were ensiled in the current study with three different types of silage additives (BS, GA, and CL), and their chemical compositions, fermentation traits, and bacterial communities were evaluated after 45 days of fermentation. The purpose was to evaluate the application effect of antibacterial peptide-producing BS and GA in WPC silage, at the same time, high-quality corn varieties were selected. We intend to offer a theoretical foundation and statistical backing for the actual use of WPC silage.

## Materials and methods

### Raw materials and silage preparation

At the experimental teaching base of the College of Animal Science and Technology, Henan University of Science and Technology (Monsoon climate of medium latitudes: 34°35'N, 112°24'E, elevation 140 m, annual mean temperature 12.2–24.6°C, and average annual precipitation 528–800 mm), three varieties of corn, YQ, EXA, and NH, were planted on June 28, 2020 and harvested on October 7, 2020. Within an hour, a forage cutter (zengguang9zp-0.4, Zengguang group Co. Ltd., Yongkang, China) chopped the collected WPC into pieces measuring 1–2 cm. Following that, the chopped WPC were immediately ensiled with: (1) No additive (CK); (2) 0.02% *Bacillus subtilis* CP7 (BS) of fresh material (FM; Zhangye Aolin Beier Biological Technology Co. Ltd., China); (3) 0.2% Gallic acid (GA) of FM (Shanghai Yuanye Biological Technology Co. Ltd., China); and (4) 0.02% Cellulase (CL) of FM (Shanghai Yuanye Biological Technology Co. Ltd., China). After fully mixed, put the sample into a unidirectional exhaust fermentation bag (23 cm × 30 cm; Chenguang Shiye Co. Ltd., Wenzhou, China) in the amount of 500 g per bag. A total of 36 bags (3 varieties of raw material × 4 treatments × 3 replicates) were made and stored at room temperature and avoid light. After

45 days of ensiling, the chemical composition, fermentation characteristics, and bacterial community diversity were assessed.

## Chemical composition and fermentation characteristics analysis

After 45 days of ensiling, the silages and fresh materials were dried in a 65°C oven for 48 h, and then ground into powder with a knife mill (Zhejiang Yili Industry and Trade Co. Ltd., Zhejiang, China) through a 1 mm screen for subsequent layer analysis. The dry matter (DM) content of silages was measured by drying at 105°C in an electric blast drying oven for 4 h. The total nitrogen (TN) content was determined by Kjeldahl method (Krishnamoorthy et al., 1982; K1301, Chensheng Instrument Co. Ltd., Shanghai, China), and then the crude protein (CP) was equal to the TN × 6.25. Ether extract (EE), acid detergent lignin (ADL) and Ash shall be detected according to the procedures described by (AOAC, 2000). The contents of neutral detergent fiber (NDF) and acid detergent fiber (ADF) were determined with the ANKOM 2000i fiber analyzer (ANKOM 2000i, Anborui Science and Technology Co. Ltd., Beijing, China) according to the method of Van Soest et al. (1991). The contents of water-soluble carbohydrates (WSC) was determined by anthrone method (Murphy, 1958). The hemicellulose (HC) content was calculated by subtracting ADF from NDF, cellulose (CEL) content was the difference between ADF and ADL, and the holocellulose (HoC) content was the sum of HC and CEL (Ren et al., 2015). In addition, the biological degradation potential (BDP) was calculated by reference to Agneessens et al. (2015) using HoC divided by ADL.

Meanwhile, to determine the fermentation characteristics of silage, 20 g of each sample was weighed, added 180 ml distilled water, shake well, and then placed it in a refrigerator at 4°C for 24 h. After extraction, the filtrate was filtered through 4 layers of cheese cloth followed by 2 layers of filter paper. One aliquot of the filtrate was used to determine the pH of the filtrate immediately with a glass electrode pH meter (FE28, METTLER TOLEDO, Shanghai, China), and another aliquot was frozen at −20°C for the determination of organic acids and ammonia nitrogen (NH<sub>3</sub>-H). The content of NH<sub>3</sub>-N was determined by phenol hypochlorite colorimetry (Broderick and Kang, 1980). The content of lactic acid (LA) was determined by p-hydroxybiphenyl colorimetry method as the process described by Barnett (1951). Prior to examining the butyric acid (BA) and acetic acid (AA) concentrations, the filtrate was centrifuged at 10,000 rpm/min for 10 min, and the supernatant was detected by gas chromatography (GC-6800, Beifen Tianpu, Beijing, China). The analytical column was a quartz glass filled column (Φ 6 mm × 2 m), with a column temperature of 150°C and inlet temperature of 220°C; the injection volume was 1 µl; the FID detector temperature was 280°C; the carrier gas was high-purity N<sub>2</sub> with a flow rate of 30 ml/min and a pressure of 200 kPa; the gas was H<sub>2</sub> with a flow rate of 30 ml/min; the auxiliary gas was air with a flow rate of 300 ml/min. Finally, the flieg score (FS) was computed using equation given by Wang et al. (2017).

## 16S rDNA sequencing analysis

### DNA extraction and PCR amplification

By using Power Soil DNA Isolation Kit (MO BIO Laboratories), total bacterial DNA was isolated from samples in line with the guidelines provided by the manufacturer. The ratios of 260 nm/280 nm and 260 nm/230 nm were used to evaluate the quality and amount of DNA. Following that, DNA was kept at −80°C until further processing. The common primer pair (Forward primer, 5'-ACTCCTACGGGAGGCAGCA-3'; Reverse primer, 5'-GGACTACHVGGGTWTCTAAT-3') together with adapter sequences and barcode sequences were used to amplify the V3-V4 region of the bacterial 16S rRNA gene. 50 µl of a total volume were used for the PCR amplification, including 10 µM of each primer, 10 µl of buffer, 10 µl of high GC enhancer, 1 µl of dNTP, 0.2 µl of Q5 High-Fidelity DNA Polymerase, and 60 ng/µl of genomic DNA. Following a preliminary denaturation at 95°C for 5 min, there were 15 cycles of 95°C for 1 min, 50°C for 1 min, and 72°C for 1 min, with a final extension at 72°C for 7 min. Through the use of VAHTSTM DNA Clean Beads, the PCR products from the first step were purified. After then, a second round of PCR was carried out in a 40 µl reaction that comprised 10 µM of each primer, 20 µl of 2 × Phusion HF MM, 8 µl of ddH<sub>2</sub>O, and 10 µl PCR products from the previous round. Following a preliminary denaturation at 98°C for 30 s, there were 10 cycles of 98°C for 10 s, 65°C for 30 s, and 72°C for 30 s, with a final extension at 72°C for 5 min. Finally, Quant-iT™ dsDNA HS Reagent was used to quantify each PCR products and pool them all together. The purified, pooled sample was subjected to high-throughput sequencing analysis of bacterial rRNA genes on the Illumina Miseq 2500 platform (2 × 250 paired ends) at Beijing Tsingke Biotechnology Co, LTD in Beijing, China.

### Bioinformatic analysis of sequencing data

Firstly, Trimmomatic (version 0.33) was used to filter the quality of the raw reads, then FLASH (version 1.2.11) was used to splice double-ended reads and remove chimeras (UCHIME, version 8.1). Finally, high-quality sequences were obtained for subsequent analysis. Operational taxonomic units (OTUs) were clustered using USEARCH (version 10.0) with a 97% sequence similarity. By default, 0.005% of the number of sequences was used as the threshold to filter OTUs. The α-diversity was calculated by using QIIME2.<sup>1</sup> R was also used to analyzed and display cluster heat maps, relative abundances of various microorganisms, and principal component analysis (PCA).

### Statistical analysis

The fermentation characteristics and chemical composition data of silages were analyzed by two-way ANOVA in SPSS

<sup>1</sup> <https://qiime2.org/> (Accessed September 9, 2022).



software. The significant difference was then indicated at the level of  $p < 0.05$  using Duncan's multiple range tests to assess differences between treatments.

## Results

### Characteristics of fresh whole-plant corn of three different varieties before ensiling

The chemical compositions of the three different varieties of corn pre ensiling are shown in [Table 1](#). The contents of several important indicators such as DM, CP, WSC, and NDF in YQ were 31.38% / FM, 8.02% / DM, 11.03% / DM, and 56.27% / DM, respectively. The contents of these components in EXA were DM (33.81% / FM), CP (8.57% / DM), WSC (9.86% / DM), and NDF (55.33% / DM). In NH, the contents of DM, CP, WSC, and NDF were 35.37% / FM, 7.85% / DM, 9.13% / DM, and 54.86% / DM, respectively.

### Effects of varieties and additives on the chemical composition of whole-plant corn silage

The effects of varieties and additives on the chemical components of WPC silage such as DM, CP, EE, Ash, and WSC are presented in [Table 2](#). When the variety was the main effect, EXA and NH had significantly larger DM contents than YQ ( $p < 0.05$ ), the CP content in each treatment group showed that YQ and EXA were significantly higher than those of NH ( $p < 0.05$ ). Only in CL treatment group, EE content showed that YQ was significantly less than EXA ( $p < 0.05$ ). Ash content showed that there were significant differences among the three cultivars in GA treatment group ( $p < 0.05$ ), and  $YQ > NH > EXA$ . WSC content in CK group YQ was

significantly higher than EXA ( $p < 0.05$ ), and there were significant differences in GA and CL groups ( $p < 0.05$ ), and the expression was  $YQ > EXA > NH$ . When the additive was the main effect, in YQ and NH, the content of DM in each additive group was significantly higher than that in the CK group ( $p < 0.05$ ). In YQ and EXA, the content of CP in each additive was significantly higher than those in the CK group ( $p < 0.05$ ). In NH, the content of CP in GA and CL groups were significantly higher than BS and CK groups ( $p < 0.05$ ); EE only in YQ, CL groups were significantly lower than BS and CK groups ( $p < 0.05$ ); WSC in YQ, the GA and CL groups were significantly higher than the CK group ( $p < 0.05$ ); and the BS group was significantly lower than the CK group ( $p < 0.05$ ). In EXA and NH, the content of WSC in GA group was significantly higher than the CL group ( $p < 0.05$ ), BS and CK groups were significantly lower than the CL group ( $p < 0.05$ ). And the interaction effect of varieties and additives had a significant effect on CP of WPC silage ( $p < 0.05$ ), had a highly significant effect on WSC ( $p < 0.01$ ) but not significant effect on DM, EE and Ash ( $p > 0.05$ ).

### Effects of varieties and additives on lignocellulosic composition of whole-plant corn silage

The effects of varieties and additives on the lignocellulosic components of WPC silage such as NDF, ADF, ADL, CEL, HC, and HoC are demonstrated in [Table 3](#). When variety was the main effect, the content of NDF and HoC did not differ significantly between varieties ( $p > 0.05$ ); the content of ADF and CL were not significantly different among the varieties in the CK group ( $p > 0.05$ ), in the other treatment groups, YQ and EXA were significantly lower than NH ( $p < 0.05$ ); The ADL content of YQ and EXA was significantly higher than that of NH only in the GA group ( $p < 0.05$ ); the HC content of YQ and EXA was significantly higher than that of NH only in the BS group ( $p < 0.05$ ). When the additive was the main effect, the NDF content in YQ only showed that the GA group was significantly lower than the other treatment groups ( $p < 0.05$ ). The ADF content in YQ showed that the CL group was significantly lower than the BS and CK groups ( $p < 0.05$ ), and in EXA, the CL and GA groups were significantly lower than the BS and CK groups ( $p < 0.05$ ). ADL in YQ, the CL group was significantly lower than the BS group ( $p < 0.05$ ), and in NH, the additives groups were significantly lower than the CK group ( $p < 0.05$ ). Only in EXA, the CEL content of the GA and CL groups was significantly lower than that of the CK group ( $p < 0.05$ ); the HoC content only in YQ, the GA and CL groups were significantly lower than the CK group ( $p < 0.05$ ). HC content in different treatments groups showed no significant difference ( $p > 0.05$ ). The interaction between varieties and additives only had a significant effect on CEL content ( $p < 0.05$ ).

**TABLE 1** Chemical composition of fresh whole-plant corn of three different varieties before ensiling ( $\pm$ SD,  $n=3$ ).

| Items                             | Corn varieties   |                  |                  |
|-----------------------------------|------------------|------------------|------------------|
|                                   | YQ               | EXA              | NH               |
| Dry matter / % FM                 | 31.38 $\pm$ 3.37 | 33.81 $\pm$ 4.11 | 35.37 $\pm$ 3.94 |
| Crude protein / % DM              | 8.02 $\pm$ 0.59  | 8.57 $\pm$ 0.30  | 7.85 $\pm$ 0.26  |
| Ether extract / % DM              | 3.78 $\pm$ 0.66  | 3.82 $\pm$ 0.35  | 3.69 $\pm$ 0.28  |
| Ash / % DM                        | 4.90 $\pm$ 0.61  | 5.03 $\pm$ 0.76  | 4.60 $\pm$ 0.56  |
| Acid detergent fiber / % DM       | 19.62 $\pm$ 1.46 | 21.39 $\pm$ 2.45 | 23.98 $\pm$ 2.04 |
| Neutral detergent fiber / % DM    | 56.27 $\pm$ 2.08 | 55.33 $\pm$ 2.26 | 54.86 $\pm$ 3.59 |
| Water soluble carbohydrate / % DM | 11.03 $\pm$ 1.72 | 9.86 $\pm$ 1.32  | 9.13 $\pm$ 1.85  |

FM, fresh matter; DM, dry matter; YQ, corn variety Yuqing 386; EXA, corn variety Enxai 298; NH, corn variety Nonghe35.

TABLE 2 Effects of varieties and additives on the chemical compositions of whole-plant corn silage ( $\pm$ SD,  $n=3$ ).

| Items                             | Treatments | Varieties             |                        |                        | Significance |    |              |
|-----------------------------------|------------|-----------------------|------------------------|------------------------|--------------|----|--------------|
|                                   |            | YQ                    | EXA                    | NH                     | V            | T  | V $\times$ T |
| <sup>2</sup> Dry matter / % FM    | CK         | $27.59 \pm 0.06^{Aa}$ | $31.93 \pm 0.16^{Ca}$  | $30.84 \pm 0.10^{Ba}$  | **           | ** | NS           |
|                                   | BS         | $29.82 \pm 0.24^{Ab}$ | $32.47 \pm 0.44^{Ba}$  | $32.33 \pm 0.26^{Bab}$ |              |    |              |
|                                   | GA         | $30.31 \pm 0.38^{Ab}$ | $33.58 \pm 0.17^{Ba}$  | $33.87 \pm 0.46^{Bb}$  |              |    |              |
|                                   | CL         | $31.09 \pm 0.30^{Ab}$ | $32.27 \pm 0.29^{ABa}$ | $33.42 \pm 0.19^{Bb}$  |              |    |              |
| Crude protein / %                 | CK         | $8.11 \pm 0.18^{Ba}$  | $8.39 \pm 0.10^{Ba}$   | $7.00 \pm 0.14^{Aa}$   | **           | ** | *            |
| DM                                | BS         | $9.90 \pm 0.20^{Cb}$  | $8.96 \pm 0.02^{Bb}$   | $7.07 \pm 0.14^{Aa}$   |              |    |              |
|                                   | GA         | $9.81 \pm 0.12^{Bb}$  | $9.53 \pm 0.06^{Bc}$   | $8.77 \pm 0.13^{Ab}$   |              |    |              |
|                                   | CL         | $9.72 \pm 0.24^{Bb}$  | $9.68 \pm 0.13^{Bc}$   | $8.16 \pm 0.09^{Ab}$   |              |    |              |
|                                   | CK         | $3.85 \pm 0.11^{Ab}$  | $3.39 \pm 0.08^{Aa}$   | $3.72 \pm 0.15^{Aa}$   | NS           | NS | NS           |
| Ether extract / % DM              | BS         | $3.72 \pm 0.10^{Ab}$  | $3.29 \pm 0.06^{Aa}$   | $3.40 \pm 0.11^{Aa}$   |              |    |              |
|                                   | GA         | $3.39 \pm 0.07^{Aab}$ | $3.31 \pm 0.05^{Aa}$   | $3.65 \pm 0.17^{Aa}$   |              |    |              |
|                                   | CL         | $3.04 \pm 0.01^{Aa}$  | $3.55 \pm 0.10^{Ba}$   | $3.40 \pm 0.07^{ABa}$  |              |    |              |
|                                   | CK         | $5.16 \pm 0.09^{Aa}$  | $6.29 \pm 1.22^{Aa}$   | $4.52 \pm 0.04^{Aa}$   | NS           | NS | NS           |
| Ash / % DM                        | BS         | $4.85 \pm 0.09^{Aa}$  | $5.11 \pm 0.27^{Aa}$   | $5.08 \pm 0.06^{Aa}$   |              |    |              |
|                                   | GA         | $5.33 \pm 0.12^{Ca}$  | $3.57 \pm 0.07^{Aa}$   | $4.52 \pm 0.10^{Ba}$   |              |    |              |
|                                   | CL         | $4.97 \pm 0.16^{Aa}$  | $4.45 \pm 0.17^{Aa}$   | $4.85 \pm 0.10^{Aa}$   |              |    |              |
|                                   | CK         | $4.51 \pm 0.08^{Bb}$  | $4.11 \pm 0.24^{Aa}$   | $4.28 \pm 0.16^{ABa}$  | **           | ** | **           |
| Water soluble carbohydrate / % DM | BS         | $4.07 \pm 0.23^{Aa}$  | $4.11 \pm 0.18^{Aa}$   | $4.21 \pm 0.10^{Aa}$   |              |    |              |
|                                   | GA         | $6.48 \pm 0.04^{Cc}$  | $6.04 \pm 0.04^{Bc}$   | $5.18 \pm 0.27^{Ac}$   |              |    |              |
|                                   | CL         | $6.55 \pm 0.03^{Cc}$  | $5.52 \pm 0.17^{Bb}$   | $4.85 \pm 0.08^{Ab}$   |              |    |              |
|                                   | CK         |                       |                        |                        |              |    |              |

<sup>1</sup>Capital letters indicate significant differences between varieties under the same treatment ( $p < 0.05$ ). Lowercase letters indicate significant differences among different treatments of the same variety ( $p < 0.05$ ).

<sup>2</sup>FM, fresh matter; DM, dry matter; YQ, corn variety Yuqing 386; EXA, corn variety Enxai 298; NH, corn variety Nonghe35; CK, no additives; BS, 0.02% *Bacillus subtilis* CP7 of FM; GA, 0.2% gallic acid of FM; CL, 0.02% cellulase of FM; V, corn varieties effect; T, treatments effect; V  $\times$  T, the interaction effect of treatments and corn varieties. \* $p < 0.05$ ; \*\* $p < 0.01$ ; NS, no significant effect.

## Effects of varieties and additives on fermentation quality of whole-plant corn silage

The effects of varieties and additives on the fermentation quality of WPC silage such as pH, LA, AA, PA, BA, and  $\text{NH}_3\text{-N}$  / TN were displayed in Table 4. When variety was the main effect, the pH value only in the CL group showed that EXA and NH were significantly lower than YQ ( $p < 0.05$ ); the LA content of the three corn varieties in the CK and CL groups showed significant difference ( $p < 0.05$ ), and  $\text{YQ} > \text{NH} > \text{EXA}$ , in the BS group, YQ and NH were significantly higher than EXA ( $p < 0.05$ ). There was no significant difference in AA content among different varieties in each treatment group ( $p > 0.05$ ); BA content in CK group and GA group showed that YQ was significantly higher than the other two varieties ( $p < 0.05$ ), and in CL group showed that YQ was significantly higher than NH ( $p < 0.05$ ).  $\text{NH}_3\text{-N}$  / TN in both GA and CK groups showed that YQ was significantly higher than EXA and NH ( $p < 0.05$ ), and in BS group the performance of YQ was significantly higher than that of EXA ( $p < 0.05$ ). When the additive was the main effect, the pH value of the GA group was significantly lower than that of the BS group only in EXA ( $p < 0.05$ ). The LA content in YQ showed that the BS group was significantly higher than the GA and CL groups ( $p < 0.05$ ), and the CK group was

significantly lower than the GA and CL groups ( $p < 0.05$ ), in EXA, all treatments showed significant differences ( $p < 0.05$ ), and GA group  $>$  BS group  $>$  CL group  $>$  CK group, in NH, BS. and GA groups were significantly higher than CL and CK groups ( $p < 0.05$ ). There was no significant difference in the contents of AA and BA among different treatment groups in each variety ( $p > 0.05$ );  $\text{NH}_3\text{-N}$  / TN in YQ showed that CL group was significantly lower than BS and CK groups ( $p < 0.05$ ), and GA group was significantly lower than the CK group ( $p < 0.05$ ), in EXA, the GA group was significantly lower than the BS and CK groups ( $p < 0.05$ ), and in NH, the GA, and CL groups were significantly lower than the BS and CK group ( $p < 0.05$ ). The interaction of varieties and additives only had a very significant effect on LA content ( $p < 0.01$ ). PA was not detected in all groups in this experiment.

## Effects of varieties and additives on BDP and FS of whole-plant corn silage

The effects of varieties and additives on BDP and FS of WPC silage are presented in Figure 1. When variety was the main effect, BDP showed significant differences among the three varieties in the GA group ( $p < 0.05$ ), and  $\text{NH} > \text{EXA} > \text{YQ}$ , in the CL group, showed NH and EXA were significantly

TABLE 3 Effects of varieties and additives on lignocellulosic compositions of whole-plant corn silage ( $\pm$ SD,  $n=3$ ).

| Items                                       | Treatments | Varieties              |                        |                       | Significance |    |              |
|---|------------|------------------------|------------------------|-----------------------|--------------|----|--------------|
|   |            | YQ                     | EXA                    | NH                    | V            | T  | V $\times$ T |
| <sup>2</sup> Neutral detergent fiber / % DM | CK         | $51.93 \pm 1.22^{Ab}$  | $50.07 \pm 2.46^{Aa}$  | $49.40 \pm 2.16^{Aa}$ | NS           | NS | NS           |
|   | BS         | $50.31 \pm 0.33^{Aab}$ | $48.45 \pm 1.33^{Aa}$  | $49.21 \pm 0.47^{Aa}$ |              |    |              |
|   | GA         | $45.47 \pm 0.97^{Aa}$  | $47.84 \pm 1.55^{Aa}$  | $49.37 \pm 0.63^{Aa}$ |              |    |              |
|   | CL         | $46.83 \pm 0.72^{Aab}$ | $46.63 \pm 1.47^{Aa}$  | $48.30 \pm 0.20^{Aa}$ |              |    |              |
| Acid detergent fiber / % DM                 | CK         | $18.83 \pm 0.52^{Ab}$  | $20.74 \pm 1.09^{Ab}$  | $21.64 \pm 0.65^{Aa}$ | **           | ** | NS           |
|   | BS         | $18.50 \pm 0.80^{Ab}$  | $18.01 \pm 0.60^{Aab}$ | $22.09 \pm 0.17^{Ba}$ |              |    |              |
|   | GA         | $17.27 \pm 0.38^{Aab}$ | $14.08 \pm 0.64^{Aa}$  | $22.55 \pm 0.84^{Ba}$ |              |    |              |
|   | CL         | $15.28 \pm 0.33^{Aa}$  | $14.42 \pm 0.29^{Aa}$  | $20.16 \pm 0.57^{Ba}$ |              |    |              |
| Acid detergent lignin / % DM                | CK         | $2.99 \pm 0.22^{Ab}$   | $3.16 \pm 0.22^{Aa}$   | $3.68 \pm 0.14^{Ab}$  | *            | ** | NS           |
|   | BS         | $3.64 \pm 0.02^{Ab}$   | $3.05 \pm 0.27^{Aa}$   | $2.68 \pm 0.14^{Aa}$  |              |    |              |
|   | GA         | $3.34 \pm 0.05^{Bab}$  | $2.70 \pm 0.16^{ABa}$  | $2.31 \pm 0.07^{Aa}$  |              |    |              |
|   | CL         | $2.82 \pm 0.10^{Aa}$   | $2.38 \pm 0.16^{Aa}$   | $2.08 \pm 0.14^{Aa}$  |              |    |              |
| Cellulose / % DM                            | CK         | $15.84 \pm 0.57^{Aa}$  | $17.58 \pm 0.89^{Ab}$  | $17.96 \pm 0.56^{Aa}$ | **           | ** | *            |
|   | BS         | $14.87 \pm 0.80^{Aa}$  | $14.97 \pm 0.44^{Aab}$ | $19.41 \pm 0.18^{Ba}$ |              |    |              |
|   | GA         | $13.93 \pm 0.40^{Aa}$  | $11.38 \pm 0.60^{Aa}$  | $20.25 \pm 0.78^{Ba}$ |              |    |              |
|   | CL         | $12.45 \pm 0.41^{Aa}$  | $12.04 \pm 0.41^{Aa}$  | $18.08 \pm 0.69^{Ba}$ |              |    |              |
| Hemicellulose / % DM                        | CK         | $33.10 \pm 1.48^{Aa}$  | $29.32 \pm 3.29^{Aa}$  | $27.76 \pm 2.29^{Aa}$ | NS           | NS | NS           |
|   | BS         | $31.81 \pm 0.49^{Ba}$  | $30.43 \pm 0.98^{ABa}$ | $27.12 \pm 0.63^{Aa}$ |              |    |              |
|   | GA         | $28.20 \pm 0.70^{Aa}$  | $33.76 \pm 1.38^{Aa}$  | $26.82 \pm 1.46^{Aa}$ |              |    |              |
|   | CL         | $31.56 \pm 0.46^{Aa}$  | $32.21 \pm 1.71^{Aa}$  | $28.14 \pm 0.59^{Aa}$ |              |    |              |
| Holocellulose / % DM                        | CK         | $48.94 \pm 1.02^{Ab}$  | $46.91 \pm 2.67^{Aa}$  | $45.72 \pm 2.27^{Aa}$ | NS           | NS | NS           |
|   | BS         | $46.67 \pm 0.34^{Aab}$ | $45.4 \pm 1.34^{Aa}$   | $46.53 \pm 0.58^{Aa}$ |              |    |              |
|   | GA         | $42.13 \pm 0.96^{Aa}$  | $45.14 \pm 1.39^{Aa}$  | $47.06 \pm 0.70^{Aa}$ |              |    |              |
|   | CL         | $44.01 \pm 0.76^{Aa}$  | $44.25 \pm 1.31^{Aa}$  | $46.22 \pm 0.30^{Aa}$ |              |    |              |

<sup>1</sup>Capital letters indicate significant differences between varieties under the same treatment ( $p < 0.05$ ). Lowercase letters indicate significant differences among different treatments of the same variety ( $p < 0.05$ ).

<sup>2</sup>FM, fresh matter; DM, dry matter; YQ, corn variety Yuqing 386; EXA, corn variety Enxai 298; NH, corn variety Nonghe35; CK, no additives; BS, 0.02% *Bacillus subtilis* CP7 of FM; GA, 0.2% gallic acid of FM; CL, 0.02% cellulase of FM; V, corn varieties effect; T, treatments effect; V  $\times$  T, the interaction effect of treatments and corn varieties. \* $p < 0.05$ ; \*\* $p < 0.01$ ; NS, no significant effect.

higher than YQ ( $p < 0.05$ ). The FS of YQ in both CK and GA groups was significantly lower than that of EXA and NH ( $p < 0.05$ ). When additive was the main effect, BDP in YQ, CL and CK groups were significantly higher than BS and GA groups ( $p < 0.05$ ), and in NH, GA, and CL groups were significantly higher than CK groups ( $p < 0.05$ ). FS in YQ, each additive group was significantly higher than CK group ( $p < 0.05$ ); in EXA, GA group was significantly higher than the other groups ( $p < 0.05$ ); in NH, GA, and CL group was significantly higher than the CK group ( $p < 0.05$ ).

## Diversity of the bacterial community in whole-plant corn silage with different treatments

The  $\alpha$ -diversity of bacterial communities in fresh materials and WPC silage was displayed in Table 5 of this study. The reads in each group ranged from 77,928 to 48,656, with the highest reads in the YQ-CL group (77,928) and the lowest in

the YQ-FM group (48,656), with an average of 67,172. Shannon and Simpson showed that it was significantly lower than that of fresh corn material after silage ( $p < 0.05$ ); Shannon showed the highest NH-FM and the lowest YQ-GA in all groups; Simpson showed the highest EXA-FM and the lowest YQ-GA. Among the three corn varieties, OTUs, ACE, Chao1, Shannon, and Simpson of YQ were significantly lower than the other two varieties ( $p < 0.05$ ). The interaction of varieties and additives had very significant effect on OTUs, ACE, Chao1 and Simpson ( $p < 0.01$ ). The Coverage of each group in this experiment was above 99%, indicating that the sequencing results represented the real situation of the microorganisms in the samples. The results of  $\beta$ -diversity analysis of fresh raw materials and WPC silage are shown in Figure 2, it could be seen from the principal component analysis (PCA) that PCo 1 and PCo 2 were 61.90 and 11.55%, respectively. At the same time, the bacterial communities of the fresh raw materials of the three corn varieties were separated from each other, and the bacterial communities of the fresh raw materials and WPC silage were also significantly separated.

TABLE 4 Effects of varieties and additives on fermentation quality of whole-plant corn silage ( $\pm$ SD,  $n=3$ ).

| Items                                     | Treatments | Varieties             |                       |                       | Significance |    |              |
|---|------------|-----------------------|-----------------------|-----------------------|--------------|----|--------------|
|   |            | YQ                    | EXA                   | NH                    | V            | T  | V $\times$ T |
| <sup>2</sup> pH                           | CK         | $3.88 \pm 0.01^{Aa}$  | $3.91 \pm 0.02^{Ab}$  | $3.92 \pm 0.01^{Aa}$  | NS           | NS | NS           |
|   | BS         | $3.90 \pm 0.00^{Aa}$  | $3.96 \pm 0.01^{Ab}$  | $3.91 \pm 0.02^{Aa}$  |              |    |              |
|   | GA         | $3.87 \pm 0.02^{Aa}$  | $3.87 \pm 0.01^{Aa}$  | $3.93 \pm 0.01^{Aa}$  |              |    |              |
|   | CL         | $3.90 \pm 0.00^{Aa}$  | $3.93 \pm 0.00^{Bab}$ | $3.93 \pm 0.01^{Ba}$  |              |    |              |
| Lactic acid / (mg, g <sup>-1</sup> DM)    | CK         | $67.08 \pm 0.28^{Ca}$ | $47.82 \pm 0.41^{Aa}$ | $64.30 \pm 0.46^{Bb}$ | **           | ** | **           |
|   | BS         | $73.43 \pm 0.63^{Bc}$ | $60.66 \pm 0.08^{Ac}$ | $73.44 \pm 0.43^{Bc}$ |              |    |              |
|   | GA         | $69.65 \pm 0.26^{Ab}$ | $71.8 \pm 0.70^{Ad}$  | $72.35 \pm 0.59^{Ac}$ |              |    |              |
|   | CL         | $69.68 \pm 0.41^{Cb}$ | $58.06 \pm 0.41^{Ab}$ | $61.01 \pm 0.50^{Ba}$ |              |    |              |
| Acetic acid / (mg, g <sup>-1</sup> DM)    | CK         | $7.49 \pm 0.36^{Aa}$  | $6.08 \pm 0.26^{Aa}$  | $7.43 \pm 0.32^{Aa}$  | NS           | NS | NS           |
|   | BS         | $6.83 \pm 0.57^{Aa}$  | $6.50 \pm 0.14^{Aa}$  | $7.49 \pm 0.39^{Aa}$  |              |    |              |
|   | GA         | $5.95 \pm 0.14^{Aa}$  | $6.14 \pm 0.16^{Aa}$  | $7.08 \pm 0.36^{Aa}$  |              |    |              |
|   | CL         | $5.80 \pm 0.33^{Aa}$  | $6.46 \pm 0.56^{Aa}$  | $6.72 \pm 0.11^{Aa}$  |              |    |              |
| Propionic acid / (mg, g <sup>-1</sup> DM) | CK         | ND                    | ND                    | ND                    | —            | —  | —            |
|   | BS         | ND                    | ND                    | ND                    |              |    |              |
|   | GA         | ND                    | ND                    | ND                    |              |    |              |
|   | CL         | ND                    | ND                    | ND                    |              |    |              |
| Butyric acid / (mg, g <sup>-1</sup> DM)   | CK         | $0.20 \pm 0.01^{Ba}$  | $0.04 \pm 0.01^{Aa}$  | $0.06 \pm 0.01^{Aa}$  | **           | NS | NS           |
|   | BS         | $0.07 \pm 0.02^{Aa}$  | ND                    | $0.05 \pm 0.01^{Aa}$  |              |    |              |
|   | GA         | $0.17 \pm 0.01^{Ba}$  | $0.03 \pm 0.00^{Aa}$  | $0.05 \pm 0.01^{Aa}$  |              |    |              |
|   | CL         | $0.17 \pm 0.04^{Ba}$  | ND                    | $0.05 \pm 0.00^{Aa}$  |              |    |              |
| NH <sub>3</sub> -N / TN / %               | CK         | $5.03 \pm 0.23^{Bc}$  | $3.33 \pm 0.17^{Abc}$ | $3.82 \pm 0.05^{Ab}$  | **           | NS | NS           |
|   | BS         | $4.75 \pm 0.12^{Bbc}$ | $3.70 \pm 0.15^{Ac}$  | $4.01 \pm 0.19^{ABb}$ |              |    |              |
|   | GA         | $3.66 \pm 0.22^{Bab}$ | $2.31 \pm 0.08^{Aa}$  | $2.59 \pm 0.19^{Aa}$  |              |    |              |
|   | CL         | $3.21 \pm 0.28^{Aa}$  | $2.73 \pm 0.20^{Ab}$  | $2.82 \pm 0.11^{Aa}$  |              |    |              |

<sup>1</sup>Capital letters indicate significant differences between varieties under the same treatment ( $p < 0.05$ ). Lowercase letters indicate significant differences among different treatments of the same variety ( $p < 0.05$ ).

<sup>2</sup>FM, fresh matter; DM, dry matter; YQ, corn variety Yuqing 386; EXA, corn variety Enxian 298; NH, corn variety Nonghe35; CK, no additives; BS, 0.02% *Bacillus subtilis* CP7 of FM; GA, 0.2% gallic acid of FM; CL, 0.02% cellulase of FM; V, corn varieties effect; T, treatments effect; V  $\times$  T, the interaction effect of treatments and corn varieties. \* $p < 0.05$ ; \*\* $p < 0.01$ ; NS, no significant effect.

## Bacterial relative abundance of whole-plant corn silage with different treatments

The relative abundance of bacterial communities for fresh raw material and WPC silage with different treatments at the phylum is presented in Figure 3 (Circos map). As seen by the Circos map, *Proteobacteria*, *Bacteroidetes*, *Cyanobacteria*, *Firmicutes*, and *Actinobacteria* were the top five phyla bacteria attached to the 3 fresh corn raw materials. The relative abundances of the top five phyla that attached to YQ-FM were *Proteobacteria* (76.08%), *Bacteroidetes* (18.35%), *Cyanobacteria* (2.68%), *Firmicutes* (1.73%) and *Actinobacteria* (0.66%), respectively; The relative abundances of the top five phyla that attached to EXA-FM were *Proteobacteria* (64.88%), *Bacteroidetes* (14.09%), *Cyanobacteria* (8.10%), *Actinobacteria* (5.27%), and *Firmicutes* (4.44%), respectively. The relative abundances of the top five phyla that attached to NH-FM were *Proteobacteria* (45.69%), *Cyanobacteria* (21.15%), *Bacteroidetes* (11.69%), *Actinobacteria* (8.29%), and *Firmicutes* (6.40%), respectively. After fermentation, the dominant phylum

in each treatment group was *Firmicutes*. In YQ, the GA group had the highest relative abundance of *Firmicutes*, and the BS group had the lowest relative abundance of *Firmicutes*, at 91.47 and 79.10%, respectively. In EXA, the relative abundance of *Firmicutes* was the maximum in the CK group and the minimum in the GA group, 73.86 and 68.60%, respectively. In NH, the relative abundance of *Firmicutes* was the highest in the GA group and the lowest in the CL group, 66.80 and 59.02%, respectively. The relative abundance of *Firmicutes* in the three varieties WPC silage was YQ > EXA > NH. After fermentation, each treatment group's relative abundance of *Proteobacteria* declined noticeably, and the relative abundance of *Bacteroidetes* likewise trended lower. In YQ, the BS group had the largest relative abundance of *proteobacteria*, that was 18.40%, while the GA group had the lowest relative abundance, which was 6.38%; In EXA, the relative abundance of *Proteobacteria* was the highest in the CL group and the lowest in the CK group, 23.71 and 20.74%, respectively; In NH, the relative abundance of *Proteobacteria* in the CL group was the highest, and the GA group was the lowest, 31.57 and 23.62%, respectively; And the relative abundance of *Proteobacteria* in the three varieties



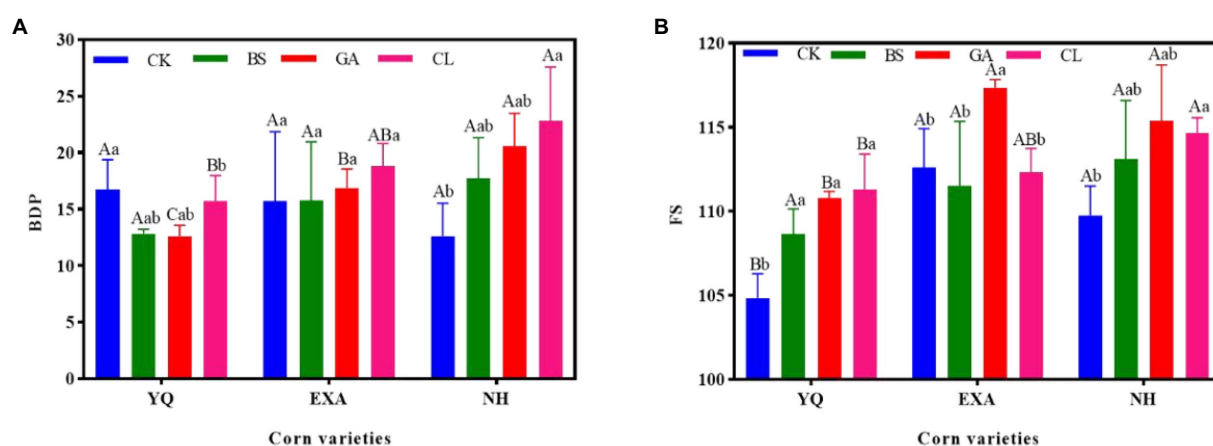


FIGURE 1

Effects of Varieties and Additives on (A) BDP and (B) FS of Whole-plant corn silage. BDP, biological degradation potential; FS, flieg score; YQ, corn variety Yuqing 386; EXA, corn variety Enxai 298; NH, corn variety Nonghe35; CK, no additives; BS, 0.02% *Bacillus subtilis* CP7 of FM; GA, 0.2% gallic acid of FM; CL, 0.02% cellulase of FM; capital letters indicate significant differences between varieties under the same treatment ( $p < 0.05$ ). Lowercase letters indicate significant differences among different treatments of the same variety ( $p < 0.05$ ).

WPC silage was  $NH > EXA > YQ$ . The relative abundance of *Bacteroidetes* was reduced to less than 1% in YQ by the application of several additives; In EXA and NH, the effects of each additive were reversed, increasing the relative abundance of *Bacteroidetes* bacteria to more than 1%; while the relative abundance of *Bacteroidetes* bacteria in the three species of WPC silage was ranked  $NH > YQ > EXA$ .

The bacterial community at the genus level was assessed to further show the impact of varieties and additives on the bacterial community in WPC silage (Figures 4, 5). The accumulation columnar map (Figure 4) illustrated the diversity and abundance of bacterial community at various genus levels. *Enterobacteriaceae* (36.62%), *Sphingobacterium* (8.61%), and *Chryseobacterium* (7.16%) were the top three dominant genera attached to YQ-FM; *Enterobacteriaceae* (11.57%), *Serratia* (8.87%), and *Acinetobacter* (7.76%) were the top three dominant genera that attached to EXA-FM; and the top three dominant genera attached to NH-FM were *Chloroplast* (18.49%), *Rosenbergiella* (6.07%), and *Mitochondria* (5.63%). After fermentation, *Lactobacillus* emerged as the dominant genus in each treatment group. In YQ and NH, the relative abundance of *Lactobacillus* was both the highest in the GA group, at 87.56 and 62.18%, respectively, and the lowest both in the BS group, at 73.84 and 49.29%, respectively; in EXA, the relative abundance of *Lactobacillus* was the highest in CK group, and the GA group was the lowest, at 71.01 and 65.68%, respectively. The relative abundance of *Lactobacillus* in the silage of the three corn varieties was ranked  $YQ > EXA > NH$ . The relative abundance of *Enterobacteriaceae* decreased significantly in YQ and EXA, remained basically unchanged in NH, and only increased slightly in NH-CL group. In all groups, the relative abundance of *Enterobacteriaceae* was the lowest in YQ-GA group and the highest in NH-CL group, which were 0.92 and 6.62%, respectively. After the silage was completed, *Klebsiella* increased in all groups except the YQ-BS group. The relative abundance of

*Sphingobacterium* showed a downward trend after fermentation. Except for the four groups of YQ-CK, NH-BS, NH-GA, and NH-CL, the relative abundance of *Sphingobacterium* in the other groups was at the level of 1%. In addition, corn raw materials were grouped into one category, and WPC silage of three varieties were grouped into one category, respectively. The bacteria of the first three genera of relative abundance (*Lactobacillus*, *Klebsiella*, and *Enterobacteriaceae*) were grouped into one class, and the other different genera were grouped into another class.

## Discussion

### Chemical compositions, lignocellulosic compositions, and fermentation quality of whole-plant corn silage with different treatments

DM content reflects the nutritional value and fermentation quality of whole-plant corn silage, and further determines the economic benefits of silage (Kennington et al., 2005). Khan et al. (2015) reported that corn silage feeding dairy cow with dry matter content in the range 30–35% had a positive effect on improving their milk production. In this experiment, after silage, the content of DM in YQ and NH used different additives were significantly higher than those in the CK group. At the same time, except for the YQ-CK and YQ-BS groups with lower DM content, the DM content of the other treatment groups were within the range 30–35%, this might be a good phenomenon for the dairy cow breeding industry. Guo et al. (2013) showed that higher moisture content of silage raw material can lead to *Clostridium*-based fermentation, which produces butyric acid and results in poor silage quality and huge economic losses. The lower DM content of YQ-CK and YQ-BS in this experiment may be because the

TABLE 5 Alpha diversity of bacterial communities in whole-plant corn silage with different treatments.

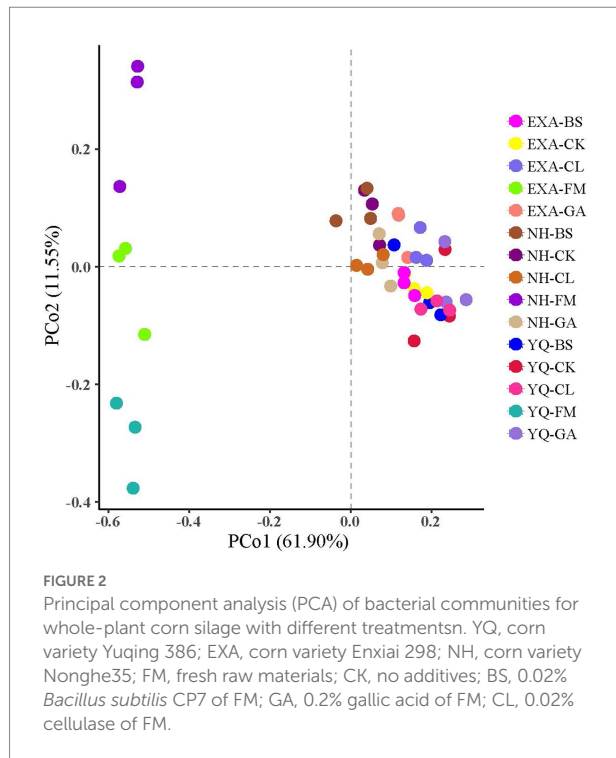
| Items             | Treatments | Varieties                                |                               |                              | Significance |    |       |
|-------------------|------------|--|-------------------------------|------------------------------|--------------|----|-------|
|                   |            | YQ                                       | EXA                           | NH                           | V            | T  | V × T |
| <sup>2</sup> OTUs | FM         | <sup>1</sup> 268.67 ± 4.04 <sup>Ab</sup> | 454.00 ± 4.64 <sup>Bb</sup>   | 496.33 ± 1.37 <sup>Cc</sup>  | **           | ** | **    |
|                   | CK         | 236.67 ± 20.27 <sup>Aa</sup>             | 394.33 ± 2.31 <sup>Ba</sup>   | 480.00 ± 1.70 <sup>Bbc</sup> |              |    |       |
|                   | BS         | 327.33 ± 5.72 <sup>Ab</sup>              | 440.33 ± 14.03 <sup>Bab</sup> | 469.00 ± 8.18 <sup>Bb</sup>  |              |    |       |
|                   | GA         | 322.33 ± 1.81 <sup>Ab</sup>              | 468.00 ± 3.68 <sup>Cb</sup>   | 416.33 ± 1.29 <sup>Ba</sup>  |              |    |       |
|                   | CL         | 322.00 ± 6.69 <sup>Ab</sup>              | 445.67 ± 2.78 <sup>Cb</sup>   | 395.00 ± 1.70 <sup>Ba</sup>  |              |    |       |
| ACE               | FM         | 294.41 ± 4.68 <sup>Aa</sup>              | 464.35 ± 3.77 <sup>Bb</sup>   | 500.27 ± 1.30 <sup>Cb</sup>  | **           | *  | **    |
|                   | CK         | 300.44 ± 21.05 <sup>Aa</sup>             | 430.19 ± 2.48 <sup>Ba</sup>   | 490.51 ± 2.09 <sup>Bb</sup>  |              |    |       |
|                   | BS         | 383.49 ± 2.51 <sup>Ab</sup>              | 467.46 ± 9.16 <sup>Bb</sup>   | 480.98 ± 5.46 <sup>Bb</sup>  |              |    |       |
|                   | GA         | 384.60 ± 9.41 <sup>Ab</sup>              | 481.46 ± 1.39 <sup>Bb</sup>   | 445.00 ± 1.78 <sup>Ba</sup>  |              |    |       |
|                   | CL         | 380.45 ± 2.55 <sup>Ab</sup>              | 459.76 ± 2.55 <sup>Cab</sup>  | 428.99 ± 2.77 <sup>Ba</sup>  |              |    |       |
| Chao1             | FM         | 306.19 ± 7.82 <sup>Ab</sup>              | 468.49 ± 2.89 <sup>Bab</sup>  | 502.18 ± 1.22 <sup>Bb</sup>  | **           | NS | **    |
|                   | CK         | 300.08 ± 24.22 <sup>Aa</sup>             | 438.87 ± 4.38 <sup>Ba</sup>   | 496.65 ± 3.28 <sup>Bb</sup>  |              |    |       |
|                   | BS         | 382.80 ± 3.05 <sup>Ab</sup>              | 477.53 ± 6.78 <sup>Bb</sup>   | 487.42 ± 5.55 <sup>Bb</sup>  |              |    |       |
|                   | GA         | 392.30 ± 9.73 <sup>Ab</sup>              | 484.96 ± 1.07 <sup>Bb</sup>   | 447.86 ± 1.73 <sup>Ba</sup>  |              |    |       |
|                   | CL         | 377.00 ± 3.23 <sup>Ab</sup>              | 467.66 ± 3.92 <sup>Cab</sup>  | 434.18 ± 4.22 <sup>Ba</sup>  |              |    |       |
| Shannon           | FM         | 4.33 ± 0.21 <sup>Ab</sup>                | 6.15 ± 0.12 <sup>Bc</sup>     | 6.30 ± 0.28 <sup>Bb</sup>    | **           | ** | NS    |
|                   | CK         | 1.57 ± 0.09 <sup>Aa</sup>                | 2.27 ± 0.06 <sup>Ba</sup>     | 3.57 ± 0.08 <sup>Ca</sup>    |              |    |       |
|                   | BS         | 2.06 ± 0.17 <sup>Aa</sup>                | 2.51 ± 0.07 <sup>Bab</sup>    | 4.05 ± 0.06 <sup>Ba</sup>    |              |    |       |
|                   | GA         | 1.23 ± 0.08 <sup>Aa</sup>                | 2.85 ± 0.07 <sup>Bb</sup>     | 3.24 ± 0.05 <sup>Ba</sup>    |              |    |       |
|                   | CL         | 1.62 ± 0.12 <sup>Aa</sup>                | 2.46 ± 0.05 <sup>Bab</sup>    | 3.49 ± 0.02 <sup>Ca</sup>    |              |    |       |
| Simpson           | FM         | 0.87 ± 0.02 <sup>Ac</sup>                | 0.96 ± 0.00 <sup>Ac</sup>     | 0.93 ± 0.02 <sup>Ac</sup>    | **           | ** | **    |
|                   | CK         | 0.35 ± 0.03 <sup>Ab</sup>                | 0.49 ± 0.01 <sup>Ba</sup>     | 0.71 ± 0.01 <sup>Cab</sup>   |              |    |       |
|                   | BS         | 0.48 ± 0.04 <sup>Ab</sup>                | 0.53 ± 0.01 <sup>Ab</sup>     | 0.75 ± 0.01 <sup>Bb</sup>    |              |    |       |
|                   | GA         | 0.24 ± 0.02 <sup>Aa</sup>                | 0.56 ± 0.01 <sup>Bb</sup>     | 0.65 ± 0.00 <sup>Ca</sup>    |              |    |       |
|                   | CL         | 0.34 ± 0.03 <sup>Ab</sup>                | 0.53 ± 0.01 <sup>Bab</sup>    | 0.74 ± 0.00 <sup>Cb</sup>    |              |    |       |
| Coverage          | FM         | 0.9990                                   | 0.9996                        | 0.9998                       | —            | —  | —     |
|                   | CK         | 0.9989                                   | 0.9992                        | 0.9995                       |              |    |       |
|                   | BS         | 0.9987                                   | 0.9993                        | 0.9996                       |              |    |       |
|                   | GA         | 0.9986                                   | 0.9995                        | 0.9993                       |              |    |       |
|                   | CL         | 0.9991                                   | 0.9994                        | 0.9993                       |              |    |       |
| Reads             | FM         | 48,656                                   | 65,471                        | 51,324                       | —            | —  | —     |
|                   | CK         | 68,503                                   | 76,053                        | 67,463                       |              |    |       |
|                   | BS         | 62,553                                   | 73,266                        | 67,362                       |              |    |       |
|                   | GA         | 65,463                                   | 65,044                        | 74,515                       |              |    |       |
|                   | CL         | 77,928                                   | 69,011                        | 74,961                       |              |    |       |

<sup>1</sup>Capital letters indicate significant differences between varieties under the same treatment ( $p < 0.05$ ). Lowercase letters indicate significant differences among different treatments of the same variety ( $p < 0.05$ ).

<sup>2</sup>FM, fresh matter; DM, dry matter; YQ, corn variety Yuqing 386; EXA, corn variety Enxai 298; NH, corn variety Nonghe35; CK, no additives; BS, 0.02% *Bacillus subtilis* CP7 of FM; GA, 0.2% gallic acid of FM; CL, 0.02% cellulase of FM; V, corn varieties effect; T, treatments effect; V × T, the interaction effect of treatments and corn varieties. \* $p < 0.05$ ; \*\* $p < 0.01$ ; NS, no significant effect.

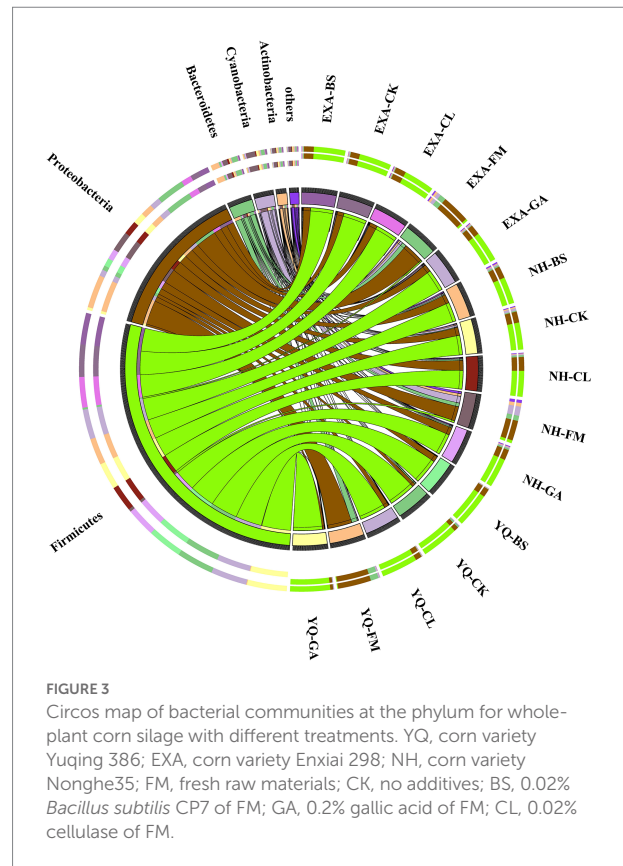
moisture content of YQ raw material is higher, which leads to the growth of undesired microorganisms and consumes more DM. CP is an important indicator reflecting the nutritional value of silage. WSC is an important microbial fermentation substrate in the silage process. It is generally believed that the content of WSC > 5% DM can meet the needs of microorganisms in the fermentation process, thereby ensuring the fermentation quality (Ni et al., 2017). The WSC content of each type of corn raw materials used in this investigation complied with the aforementioned standards.

After silage, in YQ and EXA, the content of CP in BS group was significantly higher than that in CK group, and in YQ, the content of WSC in BS group was significantly lower than that in CK group. Bai et al. (2020) found that the CP content of alfalfa silage increased significantly compared with the CK group after adding *Bacillus subtilis* producing antimicrobial peptide, while the WSC was lower than the CK group, which agreed with the findings of this investigation. This may be the antibacterial peptide produced by the additive can efficiently thwart undesirable bacteria'



physiological activities and promote the activities of LAB, thus consuming a great number of WSC and better protecting CP from degradation, so that the content of CP is relatively increased and the content of WSC is significantly reduced. In this experiment, the content of CP in GA and CL group was significantly higher than that in CK group, and the content of WSC was significantly higher than that in BS group and CK group. Previous studies have shown that gallic acid has anti-fungal, anti-viral, anti-inflammatory and anti-oxidant effects (Choubey et al., 2018; Kahkeshani et al., 2019). This might be the cause of the greater CP and WSC contents in the GA group compared to the CK group. Cellulase can improve the degradation rate of fiber in plant cell wall and produce more WSC as fermentation substrate, this can accelerated the fermentation process by promoting the physiological activities of lactic acid bacteria, protect proteins from degradation by undesired microorganisms, which further improves the content of CP and WSC (Cai et al., 2019). In addition, there were some differences in the contents of DM, CP, EE, ash and WSC of WPC silage of different varieties. The DM contents of EXA and NH were higher, and the CP and WSC contents of YQ and EXA were higher. The research of Cherney et al. showed that there will be differences in the content of chemical components of whole-plant corn silage of different varieties, which is consistent with the results of this study (Cherney et al., 2004). This might be because there were some differences in the growth period of different corn varieties, so the accumulation law of chemical components was also different, resulting in different content of chemical components after silage.

Lignocellulosic components mainly include NDF, ADF, ADL, Cl, HC, and HoC, which are related to the palatability and



biodegradability of silage. In this study, the NDF and ADF contents of all varieties of WPC decreased after silage, this was consistent with the research results in whole-plant corn silage with lactic acid bacteria and organic acid by Jiang et al. (2020). Such results indicate that silage process can be used as biochemical pretreatment to promote the degradation of lignocellulose components, so as to realize further utilization (Aichinger et al., 2015; Zhao et al., 2018). The NDF content in YQ, ADF content in EXA and ADL content in NH all showed the same rule that was compared with CK group, the content of this index was significantly reduced after adding gallic acid. In addition, the CEL and HoC contents of GA group were significantly lower than those of CK group in all corn varieties in this experiment. This might be because the use of gallic acid played its acidic role, which could rapidly reduce the pH of silage, thus promoting the acid hydrolysis reaction of NDF, ADF, and ADL. The ADF and ADL contents of CL group were significantly lower than those of CK group in corn variety YQ, CEL, and HoC contents of CL group were significantly lower than those of CK group in all corn varieties. It is explained that the used of cellulase causes an enzymatic reaction in the silage process, which decomposes the cellulose structural carbohydrates in the plant cell wall, resulting in a decrease in the contents of NDF, ADF, HoC, and so on (Desta et al., 2016). BDP is an index to measure the degradability of silage (Agneessens et al., 2015), which is derived from HoC and ADL. In this experiment, in corn varieties EXA and NH, the BDP of each additive group was higher than that of CK group, indicated that several additives used in this

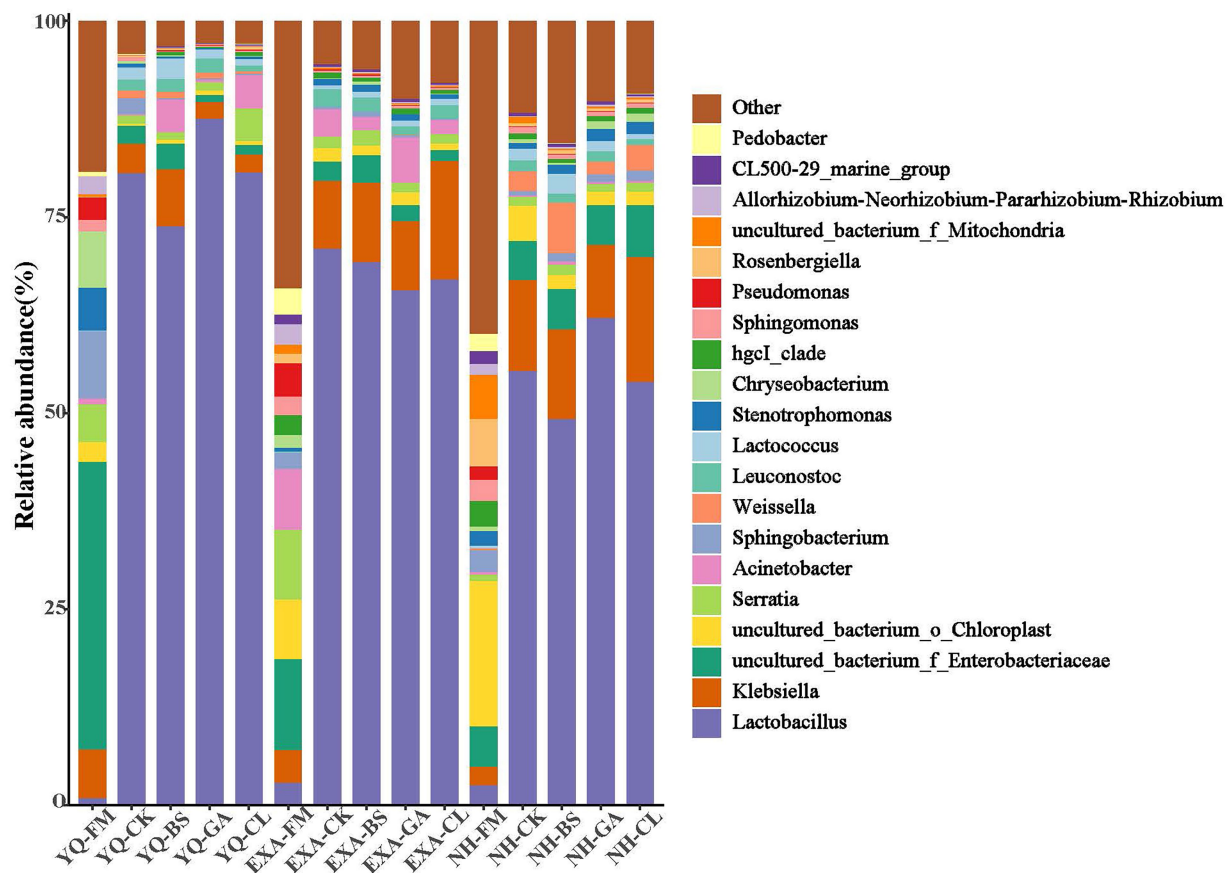


FIGURE 4

Relative abundance of bacterial communities at the genus levels for whole-plant corn silage with different treatments. YQ, corn variety Yuqing 386; EXA, corn variety Enxai 298; NH, corn variety Nonghe35; FM, fresh raw materials; CK, no additives; BS, 0.02% *Bacillus subtilis* CP7 of FM; GA, 0.2% gallic acid of FM; CL, 0.02% cellulase of FM.

experiment were helpful to improve the biodegradability of silage. In addition, in this experiment, ADF, ADL, HC, and CL were different among different varieties WPC silage. [Benefield et al. \(2006\)](#) and [Borreani et al. \(2018\)](#) found that the composition of CP, EE, and other chemical components varied significantly and NDF, ADF, and other lignocellulosic components between different varieties of whole-plant corn silage. This is similar to the results of this experiment. It may be that different corn varieties have different genetic backgrounds, which leads to this difference.

pH, lactic acid, and  $\text{NH}_3\text{-N}$  / TN are the main indexes to measure the fermentation quality of silage. It is generally believed that high-quality silage has pH < 4.2, lactic acid content of 4–6%,  $\text{NH}_3\text{-N}$  / TN < 10% ([Wang et al., 1999](#); [Shao et al., 2005](#); [Yuan et al., 2012](#)). In this research, the pH values of all treatment were between 3.8–4.0, indicated that the WPC is easy to be prepared into high-quality silage. [Lara et al. \(2016\)](#) found that the addition of *Bacillus subtilis* will reduce the LA content in corn silage. In this experiment, the LA content of BS group in YQ and NH was considerably larger than that of CK group and CL group. *Bacillus subtilis* can create LA by pyruvate reduction under anaerobic circumstances, according to Cruz Ramos [Hugo et al. \(2000\)](#),

which might account for the elevated LA level in the BS group in our test. It also might be that the addition of antimicrobial peptide-producing BS promoted the proliferation of homofermentative lactic acid bacteria in WPC silage, resulting in more LA ([Bai et al., 2020](#)). Among all corn varieties, LA content in GA group was significantly increased than that in CK group, aside from the acidity of GA, it should be owed to its anti-bacterial property benefiting the dominance establishment of lactic acid bacteria and reduced negative nutrient competition ([He et al., 2020](#)). In YQ and EXA, compared with CK group, LA content in CL group was significantly increased. [Zhao et al. \(2021\)](#) found that cellulase can increase LA content in silage, in the study of the interaction between cellulase and lactic acid bacteria on the mixed silage of soybean residue and corn straw. Which is consistent with the results of our experiment, it is explained that the structural carbohydrates in the WPC were degraded to a great extent, so that the soluble sugars are released, providing additional fermentation substrates for the fermentation of lactic acid bacteria, thus producing more LA ([Stokes, 1992](#)). Furthermore, the presence of PA was not detected at all in this test, and the content of BA was extremely low, which is similar to



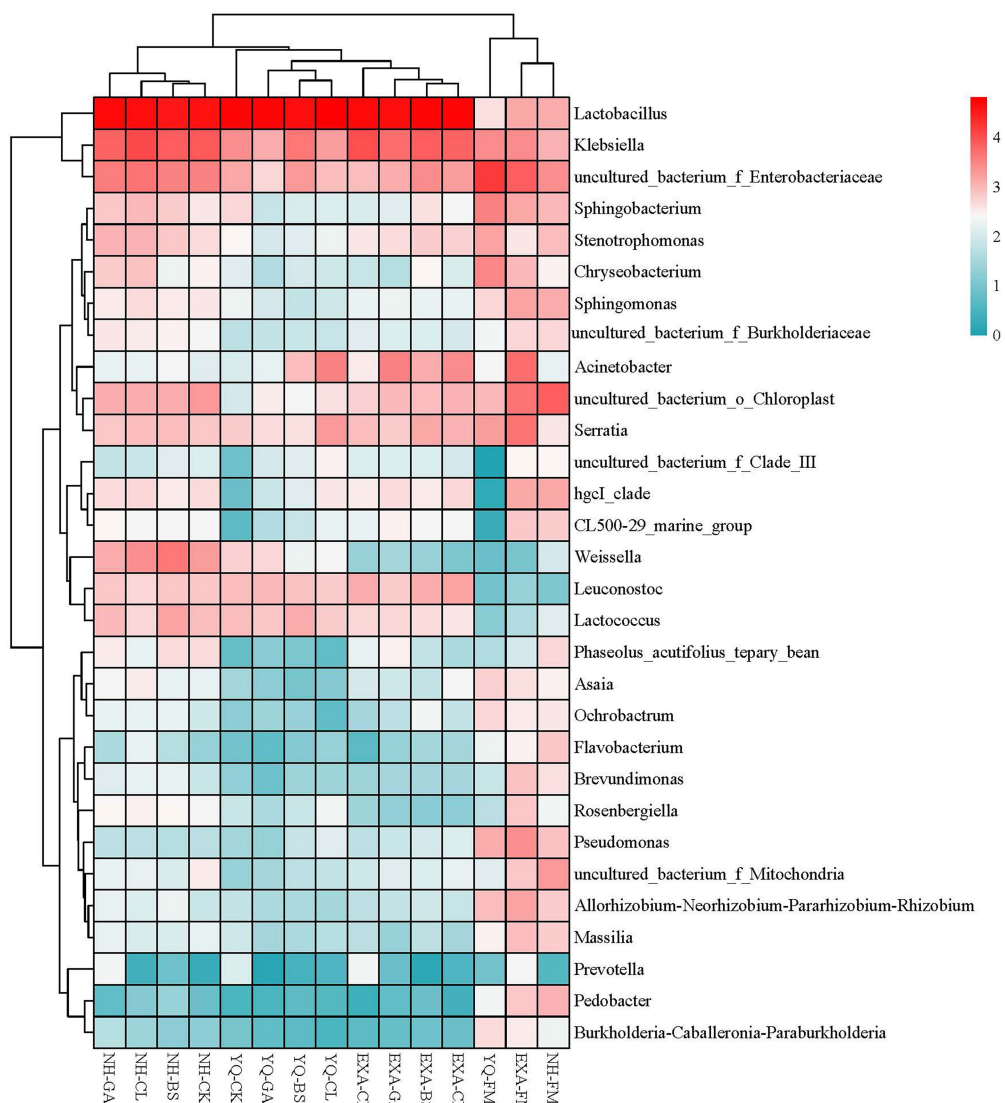


FIGURE 5

Community heat map of bacterial genera for whole-plant corn silage with different treatments. YQ, corn variety Yuqing 386; EXA, corn variety Enxai 298; NH, corn variety Nonghe35; FM, fresh raw materials; CK, no additives; BS, 0.02% *Bacillus subtilis* CP7 of FM; GA, 0.2% gallic acid of FM; CL, 0.02% cellulase of FM.

the study of Wang et al. (2019b) in alfalfa and stylo silage mixed with *Moringa oleifera* leaves. This indicates that the WPC silage had better quality in this experiment. It is reported that heterofermentative lactic acid bacteria can produce acetic acid and propionic acid during silage (Xu et al., 2021). We speculated that the fact that propionic acid was not detected in this experiment might be due to the absence of heterofermentative lactic acid bacteria activity during silage in this experiment. In principle, protein degradation will not be avoided during silage. This converts total nitrogen (TN) to non-protein nitrogen (NPN) including small peptides, amino acid free nitrogen, and  $\text{NH}_3\text{-N}$  (He et al., 2020). In addition, ammonia nitrogen is a more accurate indicator of protein hydrolysis, reflecting the deamination of amino acids or peptides (Li et al., 2018). In

present study,  $\text{NH}_3\text{-N}$  / TN of GA group and CL group were significantly lower than that of BS group and CK group among all varieties. Wang et al. (2021) showed that gallic acid can reduce the content of  $\text{NH}_3\text{-N}$  in whole plant soybean silage, which is consistent with the results of our test. The deamination of peptides or amino acids in silage may be restricted by the GA addition, resulting in less  $\text{NH}_3\text{-N}$  being produced and greater nutrient protection in WPC silage. FS is calculated by DM and pH, and it is a comprehensive reflection of DM content and pH value (Wang et al., 2017). In this test, FS of each group is greater than 100, which belongs to excellent level. This also shows that WPC is a high-quality raw material for silage production. In all groups, the FS of EXA-GA group was the highest, which also benefited from its higher DM and lower pH. In addition, some

fermentation indexes, such as pH, LA, and  $\text{NH}_3\text{-N}$  / TN, were significantly different among corn varieties. Darby and Lauer (2002) showed that the fermentation quality of whole-plant corn silage would not be different due to different corn varieties. This was different from the results of this experiment, which may be because the corn varieties he selected have the same growth period and similar genetic background, resulting in no difference in the fermentation quality of WPC silage.

## Bacterial community diversity of whole-plant corn silage with different treatments

Silage process is a complex microbial symbiosis system, in which many microorganisms participate. Therefore, its structural composition and diversity affect the fermentation quality and nutrients (Zhou et al., 2016). Bacterial alpha diversity is mainly used to reflect species richness, evenness and sequencing depth (Caporaso et al., 2012), which is represented in diversity (Shannon and Simpson indexes), richness (Chao1 index), and OTUs. In this study, in YQ and EXA, the ACE, and Chao1 index of each additive group were higher than those of CK group, and GA group was the highest. In YQ and NH, Shannon and Simpson index of GA group and CL group were lower than CK group, and both of them were the lowest in GA group. This indicates that GA group has high species richness and low biodiversity. According to records, the greater the abundance of dominant bacteria, the lower the diversity of microbial community, and vice versa (Ogunade et al., 2018). This may be due to the fact that the antibacterial and acidic properties of gallic acid inhibit the activities of non acid tolerant microorganisms, thereby increasing the relative abundance of acid tolerant microorganisms (Xu et al., 2019). In addition, among the three varieties, the ACE, Chao1, Shannon and Simpson index are the lowest in YQ, which indicates that YQ silage has lower species richness and diversity. This may be caused by the difference of microbial composition carried by different varieties of corn silage materials, or the difference of microbial community structure caused by different nutritional composition of different corn silage materials.

The results of principal component analysis can be used to distinguish the bacterial communities of different treatment groups. Fresh WPC materials of three varieties (YQ-FM, EXA-FM, and NH-FM) gathered in the second and third quadrants, and all WPC silage gathered in the first and fourth quadrants. The raw materials of the three corn varieties were clearly separated. Therefore, it can be explained that there are differences in bacterial communities among the three different varieties of WPC raw materials. There were also differences in bacterial communities between WPC silage and corn raw materials. This is due to the anaerobic conditions of silage. Under anaerobic conditions, a large number of microbial life activities attached to fresh corn raw materials were inhibited and gradually replaced by facultative anaerobic and acid resistant lactic acid bacteria (Ni et al., 2017).

## Bacterial relative abundance of whole-plant corn silage with different treatments

Silage is formed by microorganisms community under extremely complex environment, and bacteria play an important role in the whole fermentation process (Li et al., 2019; Yang et al., 2019). In this study, before silage, *Proteobacteria* was the dominant phylum of fresh raw materials of three varieties of corn, followed by *Bacteroidetes* and *cyanobacteria*. After silage, *Firmicutes* evolved into a new dominant phylum in all treatment groups. However, the relative abundance of *Proteobacteria* decreased significantly and became the second dominant phylum, such results are also reflected in the research of Keshri et al. (2018). Previous studies have shown that *Firmicutes* can produce acid and secrete a variety of enzymes in anaerobic environment, and anaerobic and low pH environment help to promote the growth and reproduction of *Firmicutes* (Wang et al., 2018; Ali et al., 2020). In this experiment, after silage, among corn varieties YQ and NH, the relative abundance of *Firmicutes* was the highest in GA group, and the relative abundance of *Proteobacteria* was the lowest in GA group. This may be because the addition of GA rapidly reduces the pH of WPC silage, which provides strong conditions for the growth and reproduction of *Firmicutes*, and promotes the relative abundance of *Firmicutes* in GA group to increase significantly and the relative abundance of *Proteobacteria* to decrease significantly. *Firmicutes* can decompose macromolecules like cellulose and starch (Romero et al., 2017). Therefore, it is inferred that the changes of lignocellulosic composition in this study may also be related to *Firmicutes*. Furthermore, among the three corn varieties, the relative abundance of *Firmicutes* is the highest in YQ, which might be related to the higher WSC content of YQ, which also indicates that corn variety YQ might have higher potential to make silage.

Further, we studied the changes at genus level of bacterial community in WPC silage. Before silage, the dominant bacteria of different varieties of WPC silage raw materials were different. But mainly *Enterobacteriaceae*, *Chloroplast*, *Sphingobacterium*, *Serratia*, *Chryseobacterium*, *Acinetobacter*, *Rosenbergiella*, and *Mitochondria*. However, the relative abundance of *Lactobacillus*, which plays a major role in the silage process, was very low. After silage, the dominant genus in all groups was *Lactobacillus*, followed by *Klebsiella*, *Enterobacteriaceae*, *Acinetobacter*, and *Serratia*, and different groups have different relative abundances. As is known to all, *Lactobacillus* plays a key role in increasing LA and reducing pH, and high-level *Lactobacillus* has also become a symbol of high-quality silage (Mu et al., 2020). In this study, we observed that the addition of GA to corn varieties YQ and NH increased the relative abundance of *Lactobacillus*. This may be because the acidity of GA rapidly lowered the pH of silage or because its antibacterial properties prevented the growth of undesirable microorganisms and created an ideal environment for the *Lactobacillus* to flourish. However, this phenomenon is not shown in the variety EXA, so it is inferred that this may be caused by the amplification of the differences in the genetic

background of different corn varieties. *Klebsiella* is a facultative anaerobic bacterium, which is a genus of *Enterobacteriaceae* under *Proteobacteria*. It can produce carbon dioxide and cause a variety of diseases (Podschn and Ullmann, 1998; Wang et al., 2022). In this experiment, *Klebsiella* is the second dominant genus in silage, and previous studies have had similar results (Ogunade et al., 2018). Compared with that before fermentation, the relative abundance of *Klebsiella* only decreased in YQ silage, and the use of BS and GA seemed to promote the growth of *Klebsiella*, which was obviously undesirable. However, it is worth noting that in YQ silage and NH silage, the addition of GA inhibited the growth of *Klebsiella* compared with CK group. Hu et al. (2018) reported that adding mixed organic acid salts to WPC silage can reduce the relative abundance of *Klebsiella*, which might be an effective means to improve this phenomenon. Because *Enterobacteria* can compete with LAB to produce acetic acid during fermentation, resulting in the loss of nutrients, it is undesired in silage (Muck, 2010). Although there was a noticeable decline in relative abundance of *Enterobacteria* in the current research compared to that before silage, the relative abundance of *Enterobacteraceae* was still rather high in silage. Fortunately, in YQ silage and EXA silage, the addition of GA and CL has a certain effect on reducing the relative abundance of *Enterobacteria*. Although *Acinetobacter* requires oxygen, it can rely on acetate to survive in an anaerobic environment (Fuhs and Chen, 1975). Previous studies have reported that the increase of the relative abundance of *Acinetobacter* was associated with the increase of acetic acid content (Ogunade et al., 2017). However, this correlation is not reflected in this study, and the specific reasons need to be further studied. *Serratia* usually produces 2,3-butanediol (McDonald et al., 1991), but no 2,3-butanediol was detected in this study. This is irrelevant, because even if *Serratia* exists, it becomes next to nothing after the fermentation process. Remarkably, the addition of GA seems to have a certain inhibitory effect on the survival of *Serratia*, although this effect is very weak. This was might decided by the antibacterial properties of GA. There was another interesting phenomenon, Parvin et al. (2010) found that *Serratia* can be detected in ryegrass silage, but not in raw materials before silage, which is quite different from the results of this test. It may be attributed to the difference of silage materials or geographical location. After all, forage species, geographical location, maturity, the type of fertilizer used and the competition of epiphytic microbial communities are all factors that affect the spatial structure of microbial communities in silage (McGarvey et al., 2013). It can be seen from the community heat map of bacterial genera (Figure 5) that the grouped clusters were mainly grouped into four categories. The fresh corn raw materials were grouped into one class, and the WPC silage of each variety after silage were grouped into three other classes. This was not only consistent with the previous results of this experiment, but also confirmed that corn varieties had an important impact on WPC silage. Additionally, we noticed that among the three fresh corn raw materials, NH and EXA were classified as one class, YQ was classified as another one class and carried less *Lactobacillus*.

However, the relative abundance of *Lactobacillus* in YQ after silage was the highest among the three varieties, suggesting that YQ might had high potential for producing high-quality WPC silage. Overall, we screened out the best corn variety among the three test varieties. Moreover, several additives were helpful to improve the quality of WPC silage, but the most significant effect was GA. This indicated the potential of GA as a new silage additive.

## Conclusion

It is concluded that, after silage, YQ has higher CP, WSC, LA contents and lower NDF, ADF contents; its *Firmicutes* and *Lactobacillus* has the highest relative abundance on the phylum and genus levels, respectively. The three additives increased the contents of DM, CP and LA to a certain extent, reduced the value of NDF, ADF and  $\text{NH}_3\text{-N/TN}$ , and the value of BDP was relatively higher than that of the CK group; In addition, the used of additives also improved the bacterial community structure, in which the relative abundance of *Firmicutes* on the phylum level and *Lactobacillus* on the genus level were the highest in GA group. The above results showed that YQ quality was the best among the three corn varieties, and GA has the most significant effect on the quality improvement of WPC silage among the three silage additives, which can be recommended to be used in actual operation.

## Data availability statement

The data presented in the study are deposited in the NCBI repository (<https://www.ncbi.nlm.nih.gov/>), accession number PRJNA882789; The original contributions presented in the study are included in the article/Supplementary material, further inquiries can be directed to the corresponding author.

## Author contributions

ZZhan, YW, LiZ, and YL designed the experiment. ZZhan wrote the original draft. YW contributed to the review of the paper and the acquisition of the funding. ZZhan, BZ, and ZZhai conducted experiments. SW, LuZ, and WJ contributed to the experiment methods and material consult. ZZhan and ZZhai performed data analysis and result visualization. All authors contributed to the article and approved the submitted version.

## Funding

This research was financially supported by the China Agriculture Research System (CARS-38) and the National “13th five-years plan” Key Research and Development Project sub topic of China (2018YFD0502001).

## Conflict of interest

The authors declare that the research was conducted in the absence of any commercial or financial relationships that could be construed as a potential conflict of interest.

## Publisher's note

All claims expressed in this article are solely those of the authors and do not necessarily represent those of their affiliated

organizations, or those of the publisher, the editors and the reviewers. Any product that may be evaluated in this article, or claim that may be made by its manufacturer, is not guaranteed or endorsed by the publisher.

## Supplementary material

The Supplementary material for this article can be found online at: <https://www.frontiersin.org/articles/10.3389/fmicb.2022.1028001/full#supplementary-material>

## References

- Agneessens, L., Viaene, J., Nest, T. V., Vandecasteele, B., and De Neve, S. (2015). Effect of ensiled vegetable crop residue amendments on soil carbon and nitrogen dynamics. *Sci. Hortic.* 192, 311–319. doi: 10.1016/j.scienta.2015.06.034
- Aichinger, P., Kuprian, M., Probst, M., Insam, H., and Ebner, C. (2015). Demand-driven energy supply from stored biowaste for biomethanisation. *Bioresour. Technol.* 194, 389–393. doi: 10.1016/j.biortech.2015.06.147
- Ali, N., Wang, S., Zhao, J., Dong, Z., Li, J., Nazar, M., et al. (2020). Microbial diversity and fermentation profile of red clover silage inoculated with reconstituted indigenous and exogenous epiphytic microbiota. *Bioresour. Technol.* 314:123606. doi: 10.1016/j.biortech.2020.123606
- AOAC (2000). *Official methods of analysis*, 17th Edn. Arlington, VA: Association of Official Analytical Chemists.
- Badhani, B., Sharma, N., and Kakkar, R. (2015). Gallic acid: a versatile antioxidant with promising therapeutic and industrial applications. *RSC Adv.* 5, 27540–27557. doi: 10.1039/C5RA01911G
- Bai, J., Xu, D., Xie, D., Wang, M., Li, Z., and Guo, X. (2020). Effects of antibacterial peptide-producing *Bacillus subtilis* and *Lactobacillus buchneri* on fermentation, aerobic stability, and microbial community of alfalfa silage. *Bioresour. Technol.* 315:123881. doi: 10.1016/j.biortech.2020.123881
- Barnett, A. J. G. (1951). The colorimetric determination of lactic acid in silage. *Biochem. J.* 49, 527–529. doi: 10.1042/bj0490527
- Benefeld, B. C., Liñeiro, M., Ipharraguerre, I. R., and Clark, J. H. (2006). Nutrient dense corn grain and corn silage for dairy cows. *J. Dairy Sci.* 89, 1571–1579. doi: 10.3168/jds.S0022-0302(06)72224-X
- Bonaldi, D. S., Carvalho, B. F., Ávila, C. L. d. S., and Silva, C. F. (2021). Effects of *Bacillus subtilis* and its metabolites on corn silage quality. *Lett. Appl. Microbiol.* 73, 46–53. doi: 10.1111/lam.13474
- Borreani, G., Tabacco, E., Schmidt, R. J., Holmes, B. J., and Muck, R. E. (2018). Silage review: factors affecting dry matter and quality losses in silages. *J. Dairy Sci.* 101, 3952–3979. doi: 10.3168/jds.2017-13837
- Broderick, G. A., and Kang, J. H. (1980). Automated simultaneous determination of ammonia and Total amino acids in ruminal fluid and in vitro Media. *J. Dairy Sci.* 63, 64–75. doi: 10.3168/jds.S0022-0302(80)82888-8
- Cai, Y., Du, Z., Yamasaki, S., Ngulube, D., Tinga, B., Macome, F., et al. (2019). Community of natural lactic acid bacteria and silage fermentation of corn Stover and sugarcane tops in Africa. *Asian-Austral. J. Anim. Sci.* 33, 1252–1264. doi: 10.5713/ajas.19.0348
- Caporaso, J. G., Lauber, C. L., Walters, W. A., Berg-Lyons, D., Huntley, J., Fierer, N., et al. (2012). Ultra-high-throughput microbial community analysis on the Illumina HiSeq and MiSeq platforms. *ISME J.* 6, 1621–1624. doi: 10.1038/ismej.2012.8
- Cherney, D. J. R., Cherney, J. H., and Cox, W. J. (2004). Fermentation characteristics of corn forage ensiled in mini-silos. *J. Dairy Sci.* 87, 4238–4246. doi: 10.3168/jds.S0022-0302(04)73569-9
- Choubey, S., Goyal, S., Varughese, R. L., Kumar, V., Sharma, K. A., and Beniwal, V. (2018). Probing Gallic acid for its broad Spectrum applications. *Mini-Rev. Med. Chem.* 18, 1283–1293. doi: 10.2174/1389557518666180330114010
- Darby, H. M., and Lauer, J. G. (2002). Harvest date and hybrid influence on corn forage yield, quality, and preservation. *Agron. J.* 94, 559–566. doi: 10.2134/agronj2002.5590
- Desta, S. T., Yuan, X., Li, J., and Shao, T. (2016). Ensiling characteristics, structural and nonstructural carbohydrate composition and enzymatic digestibility of Napier grass ensiled with additives. *Bioresour. Technol.* 221, 447–454. doi: 10.1016/j.biortech.2016.09.068
- Díaz-Gómez, R., López-Solís, R., Obreque-Slier, E., and Toledo-Araya, H. (2013). Comparative antibacterial effect of gallic acid and catechin against *Helicobacter pylori*. *LWT-Food Sci. Technol.* 54, 331–335. doi: 10.1016/j.lwt.2013.07.012
- Dunière, L., Sindou, J., Chaucheyras-Durand, F., Chevallier, I., and Thévenot-Sergentet, D. (2013). Silage processing and strategies to prevent persistence of undesirable microorganisms. *Anim. Feed Sci. Technol.* 182, 1–15. doi: 10.1016/j.anifeeds.2013.04.006
- Ferraretto, L. F., Fonseca, A. C., Sniffen, C. J., Formigoni, A., and Shaver, R. D. (2015). Effect of corn silage hybrids differing in starch and neutral detergent fiber digestibility on lactation performance and total-tract nutrient digestibility by dairy cows. *J. Dairy Sci.* 98, 395–405. doi: 10.3168/jds.2014-8232
- Fuhs, G. W., and Chen, M. (1975). Microbiological basis of phosphate removal in the activated sludge process for the treatment of wastewater. *Microb. Ecol.* 2, 119–138. doi: 10.1007/BF02010434
- Gandra, J. R., Oliveira, E. R., Gandra, E. R. d. S., Takiya, C. S., Goes, R. H. T. B. d., Oliveira, K. M. P., et al. (2017). Inoculation of *Lactobacillus buchneri* alone or with *Bacillus subtilis* and total losses, aerobic stability, and microbiological quality of sunflower silage. *J. Appl. Anim. Res.* 45, 609–614. doi: 10.1080/09712119.2016.1249874
- Guo, X. S., Undersander, D. J., and Combs, D. K. (2013). Effect of *Lactobacillus* inoculants and forage dry matter on the fermentation and aerobic stability of ensiled mixed-crop tall fescue and meadow fescue. *J. Dairy Sci.* 96, 1735–1744. doi: 10.3168/jds.2045-5786
- He, L., Chen, N., Lv, H., Wang, C., Zhou, W., Chen, X., et al. (2020). Gallic acid influencing fermentation quality, nitrogen distribution and bacterial community of high-moisture mulberry leaves and stylo silage. *Bioresour. Technol.* 295:122255. doi: 10.1016/j.biortech.2019.122255
- Hu, Z., Chang, J., Yu, J., Li, S., and Niu, H. (2018). Diversity of bacterial community during ensiling and subsequent exposure to air in whole-plant maize silage. *Asian-Austral. J. Anim. Sci.* 31, 1464–1473. doi: 10.5713/ajas.17.0860
- Hu, Z., Ma, D., Niu, H., Chang, J., Yu, J., Tong, Q., et al. (2021). Enzyme additives influence bacterial communities of *Medicago sativa* silage as determined by Illumina sequencing. *AMB Express* 11:5. doi: 10.1186/s13568-020-01158-5
- Hugo, C. R., Tamara, H., Marco, M., Hafed, N., Elena, P.-S., Oliver, D., et al. (2000). Fermentative metabolism of *Bacillus subtilis*: physiology and regulation of gene expression. *J. Bacteriol.* 182, 3072–3080. doi: 10.1128/JB.182.11.3072-3080.2000
- Jayanegara, A., Sujarnoko, T. U. P., Ridla, M., Kondo, M., and Kreuzer, M. (2019). Silage quality as influenced by concentration and type of tannins present in the material ensiled: a meta-analysis. *J. Anim. Physiol. Anim. Nutr.* 103, 456–465. doi: 10.1111/jpn.13050
- Jiang, F., Cheng, H., Liu, D., Wei, C., An, W., Wang, Y., et al. (2020). Treatment of whole-plant corn silage with lactic acid bacteria and organic acid enhances quality by elevating acid content, reducing pH, and inhibiting undesirable microorganisms. *Front. Microbiol.* 11:593088. doi: 10.3389/fmicb.2020.593088
- Kahkeshani, N., Farzaei, F., Fotouhi, M., Alavi, S., Bahrami, R., Naseri, R., et al. (2019). Pharmacological effects of gallic acid in health and disease: a mechanistic review. *Iran. J. Basic Med. Sci.* 22, 225–237. doi: 10.22038/ijbms.2019.32806.7897
- Kang, M.-S., Oh, J.-S., Kang, I.-C., Hong, S.-J., and Choi, C.-H. (2008). Inhibitory effect of methyl gallate and gallic acid on oral bacteria. *J. Microbiol.* 46, 744–750. doi: 10.1007/s12275-008-0235-7
- Kennington, L. R., Hunt, C. W., Szasz, J. I., Grove, A. V., and Kezar, W. (2005). Effect of cutting height and genetics on composition, intake, and digestibility of corn silage by beef heifers 1. *J. Anim. Sci.* 83, 1445–1454. doi: 10.2527/2005.8361445x
- Keshri, J., Chen, Y., Pinto, R., Kroupitski, Y., Weinberg, Z. G., and Sela Saldinger, S. (2018). Microbiome dynamics during ensiling of corn with and without *Lactobacillus*



- plantarum inoculant. *Appl. Microbiol. Biotechnol.* 102, 4025–4037. doi: 10.1007/s00253-018-8903-y
- Khan, N. A., Yu, P., Ali, M., Cone, J. W., and Hendriks, W. H. (2015). Nutritive value of maize silage in relation to dairy cow performance and milk quality. *J. Sci. Food Agric.* 95, 238–252. doi: 10.1002/jsfa.6703
- Krishnamoorthy, U., Muscato, T. V., Sniffen, C. J., and Van Soest, P. J. (1982). Nitrogen fractions in selected feedstuffs. *J. Dairy Sci.* 65, 217–225. doi: 10.3168/jds.S0022-0302(82)82180-2
- Lanna-Filho, R., Souza, R. M., and Alves, E. (2017). Induced resistance in tomato plants promoted by two endophytic bacilli against bacterial speck. *Trop. Plant Pathol.* 42, 96–108. doi: 10.1007/s40858-017-0141-9
- Lara, E. C., Basso, F. C., de Assis, F. B., Souza, F. A., Berchielli, T. T., and Reis, R. A. (2016). Changes in the nutritive value and aerobic stability of corn silages inoculated with *Bacillus subtilis* alone or combined with *Lactobacillus plantarum*. *Anim. Prod. Sci.* 56, 1867–1874. doi: 10.1071/AN14686
- Li, Y., and Nishino, N. (2011). Bacterial and fungal communities of wilted Italian ryegrass silage inoculated with and without *Lactobacillus rhamnosus* or *Lactobacillus buchneri*. *Lett. Appl. Microbiol.* 52, 314–321. doi: 10.1111/j.1472-765X.2010.03000.x
- Li, X., Tian, J., Zhang, Q., Jiang, Y., Wu, Z., and Yu, Z. (2018). Effects of mixing red clover with alfalfa at different ratios on dynamics of proteolysis and protease activities during ensiling. *J. Dairy Sci.* 101, 8954–8964. doi: 10.3168/jds.2018-14763
- Li, P., Zhang, Y., Gou, W., Cheng, Q., Bai, S., and Cai, Y. (2019). Silage fermentation and bacterial community of bur clover, annual ryegrass and their mixtures prepared with microbial inoculant and chemical additive. *Anim. Feed Sci. Technol.* 247, 285–293. doi: 10.1016/j.anifeeds.2018.11.009
- McDonald, P., Henderson, A. R., and Heron, S. (1991). *The biochemistry of silage*. Aberswyth: Chalcombe Publications.
- McGarvey, J. A., Franco, R. B., Palumbo, J. D., Hnasko, R., Stanker, L., and Mitloehner, F. M. (2013). Bacterial population dynamics during the ensiling of *Medicago sativa* (alfalfa) and subsequent exposure to air. *J. Appl. Microbiol.* 114, 1661–1670. doi: 10.1111/jam.12179
- Mu, L., Xie, Z., Hu, L., Chen, G., and Zhang, Z. (2020). Cellulase interacts with *Lactobacillus plantarum* to affect chemical composition, bacterial communities, and aerobic stability in mixed silage of high-moisture amaranth and rice straw. *Bioresour. Technol.* 315:123772. doi: 10.1016/j.biortech.2020.123772
- Muck, R. E. (2010). Silage microbiology and its control through additives. *Rev. Bras. Zootec.* 39, 183–191. doi: 10.1590/s1516-35982010001300021
- Muck, R. E., Nadeau, E. M. G., McAllister, T. A., Contreras-Govea, F. E., Santos, M. C., and Kung, L. (2018). Silage review: recent advances and future uses of silage additives. *J. Dairy Sci.* 101, 3980–4000. doi: 10.3168/jds.2017-13839
- Murphy, R. P. (1958). A method for the extraction of plant samples and the determination of total soluble carbohydrates. *J. Sci. Food Agric.* 9, 714–717. doi: 10.1002/jsfa.2740091104
- Nazli, M. H., Halim, R. A., Abdullah, A. M., Hussin, G., and Samsudin, A. A. (2018). Potential of four corn varieties at different harvest stages for silage production in Malaysia. *Asian-Austral. J. Anim. Sci.* 32, 224–232. doi: 10.5713/ajas.18.0175
- Ni, K., Wang, F., Zhu, B., Yang, J., Zhou, G., Pan, Y., et al. (2017). Effects of lactic acid bacteria and molasses additives on the microbial community and fermentation quality of soybean silage. *Bioresour. Technol.* 238, 706–715. doi: 10.1016/j.biortech.2017.04.055
- Ogunade, I. M., Jiang, Y., Kim, D. H., Cervantes, A. A. P., Arriola, K. G., Vyas, D., et al. (2017). Fate of *Escherichia coli* O157: H7 and bacterial diversity in corn silage contaminated with the pathogen and treated with chemical or microbial additives. *J. Dairy Sci.* 100, 1780–1794. doi: 10.3168/jds.2016-11745
- Ogunade, I. M., Jiang, Y., Pech Cervantes, A. A., Kim, D. H., Oliveira, A. S., Vyas, D., et al. (2018). Bacterial diversity and composition of alfalfa silage as analyzed by Illumina MiSeq sequencing: effects of *Escherichia coli* O157: H7 and silage additives. *J. Dairy Sci.* 101, 2048–2059. doi: 10.3168/jds.2017-12876
- Parvin, S., Wang, C., Li, Y., and Nishino, N. (2010). Effects of inoculation with lactic acid bacteria on the bacterial communities of Italian ryegrass, whole crop maize, Guinea grass and Rhodes grass silages. *Anim. Feed Sci. Technol.* 160, 160–166. doi: 10.1016/j.anifeeds.2010.07.010
- Podschun, R., and Ullmann, U. (1998). *Klebsiella* spp. as nosocomial pathogens: epidemiology, taxonomy, typing methods, and pathogenicity factors. *Clin. Microbiol. Rev.* 11, 589–603. doi: 10.1128/CMR.11.4.589
- Ren, H., Xu, N., Li, J., Li, Z., Zhao, T., Pei, F., et al. (2015). Effects of different mixed ratio of maize straw and cabbage wastes on silage quality. *J. Biobased Mater. Bioenergy* 9, 88–94. doi: 10.1166/jbmb.2015.1494
- Romero, J. J., Zhao, Y., Balseca-Paredes, M. A., Tiezzi, F., Gutierrez-Rodriguez, E., and Castillo, M. S. (2017). Laboratory silo type and inoculation effects on nutritional composition, fermentation, and bacterial and fungal communities of oat silage. *J. Dairy Sci.* 100, 1812–1828. doi: 10.3168/jds.2016-11642
- Shao, T., Zhang, Z. X., Shimojo, M., Wang, T., and Masuda, Y. (2005). Comparison of fermentation characteristics of Italian ryegrass (*Lolium multiflorum* Lam.) and Guinea grass (*Panicum maximum* Jacq.) during the early stage of ensiling. *Asian-Austral. J. Anim. Sci.* 18, 1727–1734. doi: 10.5713/ajas.2005.1727
- Stokes, M. R. (1992). Effects of an enzyme mixture, an inoculant, and their interaction on silage fermentation and dairy production I. *J. Dairy Sci.* 75, 764–773. doi: 10.3168/jds.S0022-0302(92)77814-X
- Sun, P., Wang, J. Q., and Zhang, H. T. (2010). Effects of *Bacillus subtilis* natto on performance and immune function of preweaning calves. *J. Dairy Sci.* 93, 5851–5855. doi: 10.3168/jds.2010-3263
- Van Soest, P. J., Robertson, J. B., and Lewis, B. A. (1991). Methods for dietary fiber, neutral detergent fiber, and nonstarch polysaccharides in relation to animal nutrition. *J. Dairy Sci.* 74, 3583–3597. doi: 10.3168/jds.S0022-0302(91)78551-2
- Wang, J., Chen, L., Yuan, X., Guo, G., Li, J., Bai, Y., et al. (2017). Effects of molasses on the fermentation characteristics of mixed silage prepared with rice straw, local vegetable by-products and alfalfa in Southeast China. *J. Integr. Agric.* 16, 664–670. doi: 10.1016/S2095-3119(16)61473-9
- Wang, C., He, L., Xing, Y., Zhou, W., Yang, F., Chen, X., et al. (2019a). Effects of mixing *Neolamarckia cadamba* leaves on fermentation quality, microbial community of high moisture alfalfa and stylo silage. *Microb. Biotechnol.* 12, 869–878. doi: 10.1111/1751-7915.13429
- Wang, C., He, L., Xing, Y., Zhou, W., Yang, F., Chen, X., et al. (2019b). Fermentation quality and microbial community of alfalfa and stylo silage mixed with *Moringa oleifera* leaves. *Bioresour. Technol.* 284, 240–247. doi: 10.1016/j.biortech.2019.03.129
- Wang, Y., McAllister, T. A., Xu, Z. J., Gruber, M. Y., Skadhauge, B., Jende-Strid, B., et al. (1999). Effects of proanthocyanidins, dehulling and removal of pericarp on digestion of barley grain by ruminal micro-organisms. *J. Sci. Food Agric.* 79, 929–938. doi: 10.1002/(SICI)1097-0010(19990501)79:6<929::AID-JSFA249>3.0.CO;2-W
- Wang, Q., Wang, R., Wang, C., Dong, W., Zhang, Z., Zhao, L., et al. (2022). Effects of cellulase and *Lactobacillus plantarum* on fermentation quality, chemical composition, and microbial community of Mixed Silage of whole-plant corn and Peanut vines. *Appl. Biochem. Biotechnol.* 194, 2465–2480. doi: 10.1007/s12010-022-03821-y
- Wang, Y., Wang, C., Zhou, W., Yang, F., Chen, X., and Zhang, Q. (2018). Effects of wilting and *Lactobacillus plantarum* addition on the fermentation quality and microbial community of *Moringa oleifera* leaf silage. *Front. Microbiol.* 9:1817. doi: 10.3389/fmicb.2018.01817
- Wang, C., Zheng, M., Wu, S., Zou, X., Chen, X., Ge, L., et al. (2021). Effects of Gallic acid on fermentation parameters, protein fraction, and bacterial community of Whole Plant Soybean Silage. *Front. Microbiol.* 12:662966. doi: 10.3389/fmicb.2021.662966
- Xu, D., Ding, W., Ke, W., Li, F., Zhang, P., and Guo, X. (2019). Modulation of metabolome and bacterial community in Whole Crop Corn Silage by inoculating Homofermentative *Lactobacillus plantarum* and Heterofermentative *Lactobacillus buchneri*. *Front. Microbiol.* 9:3299. doi: 10.3389/fmicb.2018.03299
- Xu, D., Wang, N., Rinne, M., Ke, W., Weinberg, Z. G., Da, M., et al. (2021). The bacterial community and metabolome dynamics and their interactions modulate fermentation process of whole crop corn silage prepared with or without inoculants. *Microb. Biotechnol.* 14, 561–576. doi: 10.1111/1751-7915.13623
- Yang, L., Yuan, X., Li, J., Dong, Z., and Shao, T. (2019). Dynamics of microbial community and fermentation quality during ensiling of sterile and nonsterile alfalfa with or without *Lactobacillus plantarum* inoculant. *Bioresour. Technol.* 275, 280–287. doi: 10.1016/j.biortech.2018.12.067
- Yuan, X., Yu, C., Shimojo, M., and Shao, T. (2012). Improvement of fermentation and nutritive quality of straw-grass silage by inclusion of wet Hullless-barley distillers' grains in Tibet. *Asian-Austral. J. Anim. Sci.* 25, 479–485. doi: 10.5713/ajas.2011.11435
- Zhao, J., Dong, Z., Li, J., Chen, L., Bai, Y., Jia, Y., et al. (2018). Ensiling as pretreatment of rice straw: the effect of hemicellulase and *Lactobacillus plantarum* on hemicellulose degradation and cellulose conversion. *Bioresour. Technol.* 266, 158–165. doi: 10.1016/j.biortech.2018.06.058
- Zhao, C., Wang, L., Ma, G., Jiang, X., Yang, J., Lv, J., et al. (2021). Cellulase interacts with lactic acid bacteria to affect fermentation quality, microbial community, and ruminal degradability in mixed silage of soybean residue and corn Stover. *Animals* 11:334. doi: 10.3390/ani11020334
- Zhou, Y., Drouin, P., and Lafrenière, C. (2016). Effect of temperature (5–25°C) on epiphytic lactic acid bacteria populations and fermentation of whole-plant corn silage. *J. Appl. Microbiol.* 121, 657–671. doi: 10.1111/jam.13198



## OPEN ACCESS

## EDITED BY

Ravindra Soni,  
Indira Gandhi Krishi Vishwavidyalaya,  
India

## REVIEWED BY

Harim Verma,  
Government of Uttar Pradesh, India  
Deep Chandra Suyal,  
Eternal University, India  
Siddhartha Singh,  
Central Agricultural University, India

## \*CORRESPONDENCE

Anuj Chaudhary  
anujchaudharysvp@gmail.com

## SPECIALTY SECTION

This article was submitted to  
Microbiotechnology,  
a section of the journal  
Frontiers in Microbiology

RECEIVED 30 April 2022

ACCEPTED 12 September 2022

PUBLISHED 17 October 2022

## CITATION

Chaudhary P, Agri U, Chaudhary A,  
Kumar A and Kumar G (2022)  
Endophytes and their potential  
in biotic stress management and crop  
production.  
*Front. Microbiol.* 13:933017.  
doi: 10.3389/fmicb.2022.933017

## COPYRIGHT

© 2022 Chaudhary, Agri, Chaudhary,  
Kumar and Kumar. This is an  
open-access article distributed under  
the terms of the [Creative Commons  
Attribution License \(CC BY\)](#). The use,  
distribution or reproduction in other  
forums is permitted, provided the  
original author(s) and the copyright  
owner(s) are credited and that the  
original publication in this journal is  
cited, in accordance with accepted  
academic practice. No use, distribution  
or reproduction is permitted which  
does not comply with these terms.

# Endophytes and their potential in biotic stress management and crop production

Parul Chaudhary<sup>1</sup>, Upasana Agri<sup>1</sup>, Anuj Chaudhary<sup>2\*</sup>,  
Ashish Kumar<sup>1</sup> and Govind Kumar<sup>3</sup>

<sup>1</sup>Govind Ballabh Pant University of Agriculture and Technology, Pantnagar, Uttarakhand, India,

<sup>2</sup>Shobhit University, Gangoh, Uttar Pradesh, India, <sup>3</sup>Indian Council of Agricultural Research (ICAR)-Central Institute for Subtropical Horticulture, Lucknow, India

Biotic stress is caused by harmful microbes that prevent plants from growing normally and also having numerous negative effects on agriculture crops globally. Many biotic factors such as bacteria, fungi, virus, weeds, insects, and nematodes are the major constraints of stress that tends to increase the reactive oxygen species that affect the physiological and molecular functioning of plants and also led to the decrease in crop productivity. Bacterial and fungal endophytes are the solution to overcome the tasks faced with conventional farming, and these are environment friendly microbial commodities that colonize in plant tissues without causing any damage. Endophytes play an important role in host fitness, uptake of nutrients, synthesis of phytohormone and diminish the injury triggered by pathogens via antibiosis, production of lytic enzymes, secondary metabolites, and hormone activation. They are also reported to help plants in coping with biotic stress, improving crops and soil health, respectively. Therefore, usage of endophytes as biofertilizers and biocontrol agent have developed an eco-friendly substitute to destructive chemicals for plant development and also in mitigation of biotic stress. Thus, this review highlighted the potential role of endophytes as biofertilizers, biocontrol agent, and in mitigation of biotic stress for maintenance of plant development and soil health for sustainable agriculture.

## KEYWORDS

biotic stress, endophytes, plant growth, sustainable agriculture, biocontrol

## Introduction

Agricultural strengthening is an important factor to the food safety for the rising world population. The recovery of soil fertility and crop health by the usage of chemical fertilizers not only affects the soil health by decreasing the water holding capacity, depleting soil fertility, and diminishing soil nutrient and microflora but also poses a

threat to human health and ecosystem. By considering all these problems, researchers are attentive for the substitution of chemical fertilizers with microbial-based fertilizers (Granada et al., 2018). Application of endophytes as biofertilizers can be a better approach to improve soil microbial status that stimulates the natural soil microbiota, therefore influencing nutrient accessibility and decomposition of organic matter (Fasusi et al., 2021). Endophytes are microbes that live within the host plant and have the capability to colonize plant roots without causing harm to the plants. They increase plant growth, act as biocontrol agent and protect the host from pest naturally, and endure tolerance against numerous biotic/abiotic stresses. Endophytes capable of producing several growth hormones such as IAA, ACC deaminase, increased in uptake of K ions in plant tissues, and decreased ethylene level are an alternate mechanism to alleviate stress conditions in various plants (Fan et al., 2020; Agri et al., 2022). They are also able to improve the uptake of nutrients such as nitrogen, magnesium, zinc, sulfur, and phosphorus from soil and provide to the host plant for better growth and survival (Agri et al., 2021).

Both bacterial and fungal endophytes hold tremendous potential for being used as biocontrol agent. Endophytes show antagonistic activity against disease-causing phytopathogens and diminish the damage attributed to phytopathogens. They produce several bioactive antimicrobial and antiviral metabolites along with producing various antioxidants to suppress pathogens (Gouda et al., 2016). Moreover, diverse range of fungal species especially entomopathogenic fungi have been known to exert long-term preventive measure for insect population (Litwin et al., 2020). Different bacteria such as *Bacillus*, *Pseudomonas*, *Pedobacter*, and *Acidobacterium* involved in mineral solubilization, metabolite production, and N<sub>2</sub> fixation. Several fungal strains including *Beauveria bassiana*, *B. metarhizium*, *M. robertsii*, *Chaetomium globosum*, and *Acremonium* spp. are successful in plant protection (Grabka et al., 2022). With a wide host range, endophytic fungus becomes advantageous as compared to other biocontrol agents. Notably, *Trichoderma viride* isolated from *Spilanthes paniculata* showed broad range activity against *Colletotrichum capsici*, *Fusarium solani*, and *Pythium aphanidermatum* (Qi et al., 2019).

Crop plants undergo various environmental stresses during their growth period that ultimately results in reduced crop productivity. Genetic and physical growth alteration due to several environmental cues restricts the full plant development in their growth period. One such biotic stress occurs by the recurrent attack on plants by phytopathogens such as bacteria, virus, fungi, and herbivores, which ultimately reduce plant vigor and death of host plant in extreme conditions (Pandey et al., 2017). In agricultural field, biotic stress especially caused by bacteria and fungal phytopathogens is the major cause of pre- and post-harvest losses. Plant being sessile in nature responds to stress conditions accordingly through various stimulatory mechanisms. They have evolved unique

physiological, biological, and molecular adaptation strategies to adjust the adverse conditions and promote plant growth. However, the extent of stress and climatic extremity makes them unable to cope up with the challenges raised by the environment (Chitnis et al., 2020). The generalized defense system in plants is unable to fully relieve the pressure and meet the demands of multistress tolerance to thrive and survive. So far, genetic engineering and other chemical and physical methods have been used to get stress tolerant cultivars. But they do not provide stress tolerance capacity for a very long time, and also, they are not ecofriendly. Thus, harnessing the potential of beneficial endophytes present in the nature for disease management could be an alternative strategy for improving plant resistance and resilience in crop varieties (Zheng et al., 2021). This will not only reduce chemical inputs but mitigate environmental stress without causing adverse effects. Useful endophytic microbes residing in the plant tissues are promising measure to remediate stressful conditions in a natural way.

## Endophytes

Plants are associated with a wide range of microbial community having positive, negative, or neutral kind of response in their host plant. Majority of the research is focused on the known epiphytic beneficial microbes colonizing the rhizosphere zones. However, plant growth-promoting endophytes are the subset of rhizosphere microbiome that is important determinants of plant microecosystems (Khali et al., 2018; Chaudhary et al., 2021a). The potential of endophytes as a bioinoculant is thus far to be sightseen to the complete potential due to few shortcomings. Such endosymbiont groups of microbes are diverse and harbored in almost every other plant species found in nature (Nair and Padmavathy, 2014). They mutually reside and proliferate within the plant tissues such as stems, roots, seeds, fruit, buds, and leaves deprived of producing any damage to the host plants (Specian et al., 2012). A small change in the diversity of plant endophytic communities can have significant impact over plant growth regulation and environmental adaptation (Vandenkoornhuyse et al., 2015). Gradual co-evolution in plant endophytic associations has eventually led to a positive response toward each other existence and influence vital activities in their host plant (Wang and Dai, 2011).

Endophytes are potent microbial resource needed to be explored for their application in agriculture sector. Most of the beneficial growth-promoting species belongs to the facultative group of endophytes that live in soil freely but colonizes crop plants under suitable conditions (Gaiero et al., 2013). Almost every other plant species hosts various bacterial, fungal, or actinomycete endophytes that may regulate plant and soil health. Various plant growth parameters are regulated by the colonization of endophytes and based on the microenvironment

and the host's metabolic capacity; they biosynthesize various compounds emanating growth-promoting activities similar to rhizospheric microbes (Chaudhary et al., 2021b, 2022). They maintain stable symbiosis through secreting various bioactive compounds contributing to colonization and plant growth (Gouda et al., 2016). The attributes associated with endophytes include the production of extracellular enzymes (Khan et al., 2014), bioremediation, synthesis of secondary metabolites against phytopathogens (Mousa and Raizada, 2013), and induced systemic resistance (Constantin et al., 2019). But mainly, endophytic bacterial and fungal strains confer propound impacts on the overall health and maintenance of crop plants under different environmental conditions via nitrogen fixation, phosphate solubilization, siderophore, and phytohormones production and by conferring tolerance to various stresses. Additionally, N-fixing endophytes *Novosphingobium sediminicola*, *Ochrobactrum intermedium* (from sugarcane) and *Bradyrhizobium*, *Kosakonia*, and *Paraburkholderia* (from rice) carry nitrogen fixation genes (Muangthong et al., 2015; Okamoto et al., 2021).

Both climatic and edaphic factors equally contribute to the nature and action of endophytes toward plants (Kandel et al., 2017a). Under different condition, they also enhance the levels of plant growth-promoting hormones (cytokines, gibberellins, and auxin) and facilitate nutrient cycling whenever required (Egamberdieva et al., 2017; Chaudhary and Sharma, 2019). Few are known to produce polyamines, including putrescine, cadaverine, spermidine, and spermine, which involved in lateral root development and stress adaptations (Couee et al., 2004). Numerous growth-promoting bacterial and fungal endophytes have been reported till date. Microbial symbionts are suitable to maximize crop productivity, but more research is required to understand the significance in plant growth (Chaudhary et al., 2021c). However, complete understanding of the mechanisms and the genetic regulation utilized by endophytes in plant growth regulation is an important aspect to be studied for their application under field conditions.

## Diversity and distribution of endophytic microbes for maintenance of soil health and plant productivity

### Microbial root endophytes

Roots are the main habitat and colonization route for the bacterial and fungal endophytes. The main entry points for bacterial colonization are root hairs, root cracks, or wounds formed by microbial or nematode activities. The other major sites for root colonization include intercellular spaces in cortex and epidermis (Compant et al., 2005). Endophytes

such as *Pseudomonas putida* and *P. fluorescens* colonized the olive through root hairs (Mercado-Blanco and Prieto, 2012). An axenically phytopromotional fungal root endophyte *Piriformospora indica* begins root colonization in the cortex region by a biotrophic growth phase and continues with cell death-dependent phase. Inoculation of *P. indica* promotes plant growth, early flowering, higher seed yield, and adaptation to stresses in various host plants such as *Phaseolus vulgaris*, *Triticum aestivum*, and *Cicer arietinum* (Varma et al., 2012; Ansari et al., 2014).

Rhizospheric microorganisms are enriched with nutrients and influence plant growth through soil nutrient recycling and nutrient uptake (Kukreti et al., 2020; Kumari et al., 2020). Overall root endosphere is metagenomically diverse and most often dominated by beneficial *Proteobacteria* (50%), *Actinobacteria*, *Firmicutes*, and *Bacteroidetes* (10%) (Liu et al., 2017). In association with roots, such microbe produces several compounds that influence plant development. Plant hormones such as gibberellins, cytokinins, and indole acetic acid (IAA) highly facilitate plant growth. In addition, few are known to promote plant mycorrhization. For instance, ACC deaminase (1-aminocyclopropane-1-carboxylic acid) containing *Arthrobacter protophormiae* enhanced nodulation in *Pisum sativum* (Barnawal et al., 2014). The other best-known fungal root colonizers are known as dark septate endophytes (DSE). The *Phialocephala fortinii* s.l. *Acephala applanata* species complex (PAC) species of *Ascomycetes* are the DSE fungi in forestry systems. In the study, dual inoculation of PAC positively increases plant biomass in spruce (Reininger and Sieber, 2013).

Endophytes living under extreme conditions such as Antarctica are also known to boost crop productivity. Under stressed condition, where mycorrhizae are generally low in abundance, different fungal endophytes potentially act as the prime root mutualistic symbionts (Mandyam et al., 2010). In terms of increasing nutrient acquisition of nutrients such as phosphorus from the roots and increasing the host fitness, both root-associated endophytes and mycorrhizal fungi provide benefits in a very similar manner. However, furthestmost fungal endophytes do not endure an obligate biotrophic life phase and live at smallest part of their life cycle separated from the plant (Park and Eom, 2007). The only two known vascular plant, i.e., *Colobanthus quitensis* and *Deschampsia Antarctica* from such extreme condition harbors *Penicillium* species. *Penicillium* (root endophyte) helps in growth of vascular plants in Antarctic region via enhancing nitrogen acquisition and nutrient uptake by significantly increasing yield. The mechanism involved in nitrogen acquisition is attributed to the litter protein breakdown and amino acid mineralization (Oses-Pedraza et al., 2020). In total, two fungal strains isolated from Antarctic plants rhizosphere, i.e., *Penicillium brevicompactum* and *P. chrysogenum* isolated from plants rhizosphere, i.e., *Colobanthus quitensis* and *Deschampsia Antarctica* increased



the final yield by 42% in lettuce and 68% in tomato plants in comparison with control (Molina-Montenegro et al., 2020). Several genera of beneficial root endophytes have been reported from medicinal plants such as *Pseudomonas*, *Xanthomonas*, *Bacillus*, *Inquilinus*, and *Pedobacter*. They have been associated with stimulation of growth activities such as production of secondary metabolites, solubilizing phosphate, and upregulating the expression of certain stress regulating genes under stress conditions (Rat et al., 2021).

Horizontal transmission colonization of the root endosphere *via* the rhizosphere. Types of endophytes: Passive endophytes – They penetrate through cracks present at root emergence area, root tips, or those created by pathogens; facultative endophytes – They live exterior to the host in certain phase of their life cycle and are frequently allied with plants from its adjoining soil; obligate endophytes – they depend plant metabolism for their survival; endofungal bacteria – Bacterial symbionts of fungi occur inside fungal spores and hyphae.

## Endophytic community in aerial tissues (phyllosphere)

Not all endophytes enter *via* root zones and move through the xylem vessels, they harbor diverse communities that enter the aerial tissues *via* above-ground surfaces too. Different entry routes chosen by many plant-promoting endophytes are stem (laimosphere), fruits (carposphere), leaves (Phyllosphere), seeds (spermasphere), and flowers (anthosphere) (Lindow and Brandl, 2003). Endophytes that live within the leaf tissues and stems are well documented. Phyllosphere microbes are an important component of microbial communities that live asymptomatically within leaves and also known for plant health maintenance (Ritpitakphong et al., 2016). Besides being the largest microbial habitat on Earth, the functional roles of phyllosphere residents are still less understood over the rhizosphere microbiome. It is estimated that their abundance in nature may exceed  $10^{62}$  cells globally. *Proteobacteria*, *Actinobacteria*, and *Bacteroidetes* were the most abundant phyla associated with *A. thaliana*, *Populus*, and *Salix* (Redford et al., 2010; Firrincieli et al., 2020). The most abundant genus of phyllosphere region is *Pseudomonas* in tomato plants (Dong et al., 2019). Leaf endophytes including bacteria and fungi are the subset of phyllosphere endophytes. Leaf endophytes most of the times comprise five phyla, *Proteobacteria* (90%), *Actinobacteria* (2.5%), *Plancomycetes* (1.4%), *Verrucomicrobia*, and *Acidobacteria* (1.1 and 0.5%) (Romero et al., 2014). They live inside the leaf and maintain symbiotic relationship with the host plants.

It is evident to suggest that endophytes enter leaves and stems through openings such as stomata and hydathodes through dispersion with the help of rain, soil, or pollinators (Frank et al., 2017). For instance, *Gluconobacter diazotrophicus*

enters through stomata in sugarcane plants (James et al., 2001). After reaching this site, endophyte strains multiply and form a thin layer of biofilm. Apart from this, some may enter to the inner tissues and start residing as endophytes where further microbes could colonize themselves into xylem. They further colonize and multiply in different organs including anthosphere, phylloplane, carposphere, and caulosphere (Meyer and Leveau, 2012). Numerous growth-promoting foliar endophytes have been identified through high-throughput screening procedures. Despite this, the gaps still hinder their field application and practical exploitation in agriculture. Not only bacterial species but also fungal strains equally promote plant growth through nutrient recycling, i.e., carbon and nitrogen, provide resistance to pathogens and assist in leaf litter decomposition (Arnold et al., 2007). Various fungal species such as *Penicillium aurantiogriseum*, *Fusarium incarnatum*, *Trichoderma harzianum*, and *Fusarium proliferatum* have been reported from wheat plant (Ripa et al., 2019). Seed-borne endophytic microbes are not fully explored and are of great interest. They potentially produce phytohormones, enzymes, and antimicrobial compounds and improve plant development. The main property of seed endophytes is their vertical transmission. Such microbes are naturally useful in that they signify not only a termination for the community assemblage in the seed, but also an early idea for community gathering in the new seedling (Shahzad et al., 2018). Seed-borne endophytes (bacterial and fungal) benefit seeds by facilitating the germination of seeds in soil.

They are of great interest because they pass their characters to next generation through vertical transmission. This provides important traits in plant growth which are determined by both microbe and plant genomes. Also, seed consists of a limited range of microbial species and has progressed *via* co-selection with the host plant species (Vujanovic et al., 2019). Additionally, this could probably result in reducing the phytopathogenic asset in demand to the sustenance of plant development (Cope-Selby et al., 2017). In addition, they have the ability form endospores and maintain plant growth by phytase activity, regulating cell motility, modulating endogenous phytohormones such as cytokinins that break seed dormancy, enhancing soil structure, and degrading xenobiotics. For instance, fungal endophytes *Epichloe* are stated to support their host plants in growth promotion. Similarly, fungi *Penicillium chrysogenum*, *Trichoderma*, and *Phoma* sp. isolated from *Opuntia* spp. are known to be involved in seed germination (Delgado-Sánchez et al., 2013). In a study, *Paraburkholderia phytofirmans* PsJN actively colonized different seeds of maize, soy, and pepper. Also, wheat seeds colonized with *Paraburkholderia phytofirmans* PsJN showed significant alteration in spike onset compared with non-treated plants under pot and field experiments (Mitter et al., 2017). There are different pathways adapted by seed-borne endophytes. Few enter *via* xylem tissues, through stigma and

exogenous pathway where seeds are dirtied from the exterior source. The floral parts of the plant tissue have not been studied extensively for the growth-promoting endophytes. An endophytic fungus, *Lasiodiplodia* sp. ME4-2 isolated from floral parts of *Viscum coloratum* which involved in production of important metabolites regulating plants growth such as indole-3 carboxylic acid and secondary metabolites such as 2-phenylethanol (Qian et al., 2014).

## Endophytic plant growth-promoting mechanisms

Endophytes being potential agent impart beneficial effects on their host plant are well-acknowledged inoculants to encourage the plant growth directly/indirectly. Plant growth occurs directly (endophyte–pathogen interaction) through regulating the attainment of vital nutrients such as phosphorous and nitrogen, modulating level of hormones. Indirectly through enhanced plant defense, endophytes could help in biocontrol of phytopathogens by production of antibiotics, regulating defense mechanism by induced systemic resistance, declining the quantity of iron accessible to pathogen, and pathogen inhibition through volatile compounds (Figure 1). Here are the few direct mechanisms involved in plant development.

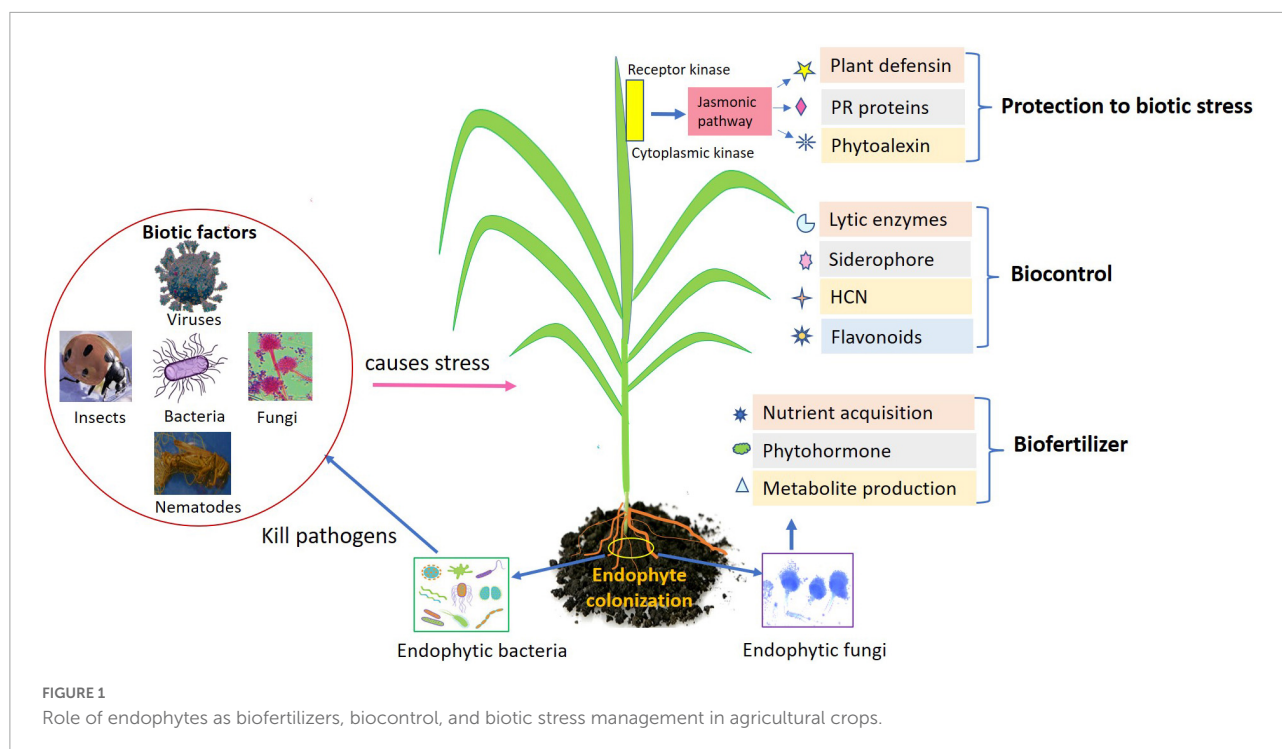
## Production of phytohormones

Numerous endophytes are identified to produce plant growth hormones (Supplementary Table 1). Hormones stimulate plant growth through regulating structural and morphological changes in response to gravity or light stimuli. They secrete gibberellic acid, cytokinin, auxins such as indole acetic acid, and ethylene. They do not only increase the overall root biomass through enhancing root surface area and root length but are known to act as signal molecules between endomicrobes and plants (Spaepen et al., 2007). In addition, they have been well known to enhance root length and root surface area, control the rate of vegetative growth, and increase the rate at which root and xylem develop. Other indole-related compounds such as indole-3-lactic acid (ILA) and indole acetamide (IAM) also found in different endophytic strains such as *Azospirillum brasilense* which is formed as an intermediate during the auxin biosynthetic pathways. For instance, the root endophyte *Piriformospora indica* produced auxin through utilizing IAA biosynthetic pathway (Xu et al., 2018). The IAA production by endophytes is considered an important factor in plant growth regulation. Khan et al. (2014) reported that *Sphingomonas* sp. (endophyte) isolated from the foliar region of *Tephrosia apollinea* improved

growth activity in tomato plants through indole acetic acid ( $11.23 \mu\text{M mL}^{-1}$ ). In another study, *Micrococcus yunnanensis* RWL-2, *Pantoea dispersa* RWL-3, *Micrococcus luteus* RWL-3, and *Staphylococcus epidermidis* RWL-7 were analyzed using GC-MS and found to produce IAA ( $11.50\text{--}38.80 \mu\text{g mL}^{-1}$ ). When inoculated in rice plants, they significantly increased main growth-promoting attributes in rice plants, i.e., dry biomass, shoot and root length, chlorophyll, and protein contents (Shahzad et al., 2017). Endophytic fungi (*Falciphora oryzae*) helped in lateral root growth while reduced the primary root height (Sun et al., 2020). Also, IAA activity in endophytes also reported to increase nitrogenase activity in rice through showing transcriptional changes in nitrogen-fixing root nodules (Defez et al., 2016). Fungi are also able to produce gibberellins, auxins, and cytokinins important as chemical signaling. Endophytic fungus (*Porostereum spadiceum*) produces gibberellins and rescue growth of soybean under normal and salt affected by promoting seed germination and increasing chlorophyll content (Hamayun et al., 2017). Several endophytic fungi including *A. flavus*, *Paecilomyces formosus*, *P. glomerata*, *Penicillium corylophilum*, *Rhizopus stolonifer*, and *Pochonia chlamydosporia* (Khan et al., 2012). Almost all the gibberellic acid producing fungal endophytes belong to *Ascomycetes* group; however, *P. spadiceum* belonging to the Basidiomycota is the first endophyte to produce gibberellic acid and involved in phytostimulation (Waqas et al., 2012). Cytokinins are important group of plant hormones that are involved in apical dominance, chloroplast maturation, cell proliferation and differentiation, seed germination, prevention of senescence, and plant–pathogen signaling mechanisms. Bacterial endophytes *Pseudomonas*, *Sphingomonas*, *Stenotrophomonas*, and *Arthrobacter* sp. isolated from humic-treated cucumber plants produced several cytokinins (cis-zeatin cytokinin, riboside type zeatin, isopentenyladenine, and isopentenyladenosine) greater than  $30 \text{ pmol/ml}$  (De Hita et al., 2020).

## Endophytic diazotrophic bacteria as biofertilizer

Endophytes being successful colonizers of different plants act potentially as biological nitrogen fixers and act as an alternative nitrogen source for crop production. They face less competition over other rhizospheric microbes and directly fix atmospheric  $\text{N}_2$  make it accessible to plants. Moreover, the partial pressure of oxygen inside the plant tissue is suitable in comparison with the outer surface for efficient nitrogen fixation as low partial pressure supports the proper functioning of  $\text{O}_2$ -sensitive nitrogenase enzyme (Cocking, 2003). Nitrogen is a vital macronutrient that the plants require because it promotes



shoot growth and aid in reproduction and main constituent of chlorophyll. Dinitrogen is an inaccessible form of nitrogen present in air and converted by diazotrophs into soluble, non-toxic form ammonia *via* biological process of nitrogen fixation. The ammonia-oxidizing bacteria and the nitrifying bacteria then transform this ammonia into nitrite and nitrate, respectively. Denitrifying occurs in the deeper soil horizons, converting the unused nitrate to atmospheric nitrogen, which ultimately escapes to the atmosphere as dinitrogen gas. This is the usual nitrogen cycle pathway (Mahanty et al., 2017). Several nitrogen-fixing bacteria have been reported such as *Azospirillum brasilense*, *Acetobacter diazotrophicus*, *Klebsiella oxytoca*, *Rhizobium* sp., and *Burkholderia cepacia* (Kong and Hong, 2020). In addition, various non-leguminous plants such as wheat, sorghum, maize, and rice harbor free-living nitrogen-fixing bacteria. For instance, *Gluconacetobacter diazotrophicus*, *Herbaspirillum rubrisubalbicans*, and *Burkholderia silvantisantica* can fix nitrogen in the intercellular spaces of sugarcane stems (Lery et al., 2011). Endophytes isolated from rice such as *Bradyrhizobium* sp. and *Paraburkholderia* sp., showed acetylene reduction properties and high sugar content contributing to high nitrogen-fixing ability. High content of sugar in different crops such as sweet potato, pineapple, and sugar has known to assist endophytic N-fixing activity among non-leguminous plants (Okamoto et al., 2021). *Acetobacter diazotrophicus* and *Azoarcus* isolated from sugarcane and kallar grass potentially fixed atmospheric nitrogen up to  $150 \text{ kg N ha}^{-1} \text{ year}^{-1}$  (Gupta et al., 2012).

## Phosphate solubilization

Phosphate solubilization is an important mechanism involved in solubilizing the insoluble phosphate into soluble form like orthophosphate. Plant requires a major amount of phosphorus for enhanced productivity in the range of  $30 \mu\text{mol l}^{-1}$ , but limited amount is available to plants which make this nutrient a limiting factor in soil. Endophytes have the capability to solubilize unsolvable phosphates or have the ability to liberate organic phosphates though production of acids such as malic, gluconic, and citric acids. Endophytic bacteria that have been reported to mobilize phosphorus through mineralization and solubilization include *Pseudomonas* spp., *Bacillus megaterium*, *Azotobacter*, *Paenibacillus*, *Thiobacillus*, and *Serratia* (Jahan et al., 2013; Kang et al., 2014).

*Pseudomonas fluorescens* strains isolated from *Miscanthus giganteus* showed great variation in phosphate solubilization capacity with highest solubilization recorded about  $1,312 \text{ mg L}^{-1}$ . Furthermore, when inoculated with the potential strains, high weight of shoot and root was observed in pea plants as compared to control (Otieno et al., 2015). The major endophytic fungi belong to genera *Curvularia*, *Piriformospora*, *Penicillium*, and *Aspergillus* and *Trichoderma*. Symbiotic association of mycorrhizal fungi with plants has been recognized to surge the passage of phosphorus in plants. It is evident from a study that apart from mycorrhizal associations, endophytic bacteria equally contribute to the P solubilization. Poplar samples when inoculated with P solubilizing *Rahnella* and *Burkholderia* sp.

strains showed a root architecture with greater root volume under tomography-based root imaging (Varga et al., 2020). Endophytic fungi *Penicillium* and *Aspergillus* isolated from roots of *Taxus wallichiana* solubilized P and produced phosphatase and phytase enzymes (Adhikari and Pandey, 2019). Kang et al. (2014) observed that *Bacillus megaterium* regulates the content of amino acids and carbohydrates to promote the growth of mustard plant.

## Siderophore biosynthesis

Siderophores are low molecular weight composites produced by several microorganisms including endophytes to scavenge iron and make it available to plants. Endophytes are known to synthesize hydroxamate, carboxylate, and phenolate type of siderophore to converse plant protection against phytopathogens. It also assists plant growth and yield by providing iron to plants under iron deficient conditions (Rajkumar et al., 2010). It also facilitates better nutrient mobilization in comparison with rhizospheric counterparts. They are better adapted to the activities of internal tissues of the plants, in terms of originating from the internal microbiome (Verma et al., 2021). Large numbers of bacterial endophytes are there to contain property of iron chelation such as *Azotobacter*, *Bacillus*, *Enterobacter*, *Arthrobacter*, *Nocardia*, and *Streptomyces* (Bokhari et al., 2019).

Biofortification of *Enterococcus hirae* and *Arthrobacter sulfonivorans* in wheat grains not only efficiently makes bioavailability of iron and zinc micronutrients but it also significantly increases plant growth up to 20% in comparison with control (Singh et al., 2018). Bacterial siderophore (catechol and hydroxamate type) isolated from *Arabidopsis thaliana*, *F. rubra* and *Agrostis capillaris*, growing on the heavy metals contaminated area significantly improved growth rate in *Festuca rubra* and *Brassica napus* (Grobelač and Hiller, 2017).

## Role of endophytes as biocontrol agents

Many researchers have previously reported the use of bacterial and fungal endophytes for disease management in plants. *Serendipita indica* conferred resistance against *Fusarium* and *Rhizoctonia solani* and demonstrated antioxidant capacity *in vitro* (del Barrio-Duque et al., 2019). In another study, production of Bacillomycin D protein by *Bacillus amyloliquefaciens* helped in showing antagonistic activity against fungus *Fusarium graminearum* (Gu et al., 2017). Seed application of *B. bassiana* 11-98 efficiently colonized tomato and cotton seedling and protect plants against *Rhizoctonia solani* and *Pythium myriotylum*. Possible mechanisms were coiling of hyphae, induction of resistance, and production

of lytic enzymes, thus protecting the older plants from root rot. However, biocontrol practices through endophytes may be achieved through direct inhibition of pathogens or indirectly by establishing the plant's systemic resistance (Santoyo et al., 2016). The other involved mechanisms include competition for niche and resources, production of cell wall degrading enzymes, initiation of induced systemic resistance (ISR), and quenching the quorum sensing of pathogens (Rajesh and Rai, 2014). Apart from this, several antibiotic compounds and lytic enzymes produced by endophytes reduce disease severity in many plants. For instance, many fungal genera *Fusarium*, *Trichoderma*, and *Botryosphaeria* secrete enzymes such as cellulose, 1,3- glucanases, amylase, and glutaminase which can aid in reducing phytopathogens through inhibiting the cell wall (Ait-Lahsen et al., 2001). Biological control also depends upon many factors such as host specificity, physical structure of soil, inoculum used, and the prevalent environmental conditions. The ability to colonize the plant tissue makes them a better biological control agent than others in having better biological compatibility when applied to plants (Rabiey et al., 2019). Under genomic studies, endophytes were also found to contain several notable genes pertaining to pathogenesis regulation which were previously not found in rhizospheric bioinoculants (Brewer et al., 2016). Also, endophytes are more protected from external factors such as radiations, temperature, and pressure when compared to epiphytes (Andreote et al., 2014). However, a deeper understanding on their mechanism and mode of action is still required to better exploit endophytes as biocontrol agents. Here are the few mechanisms employed by endophytes in controlling diseases in plants.

## Production of secondary metabolites with antifungal and antibacterial properties

Most of the endophytes are known to produce secondary metabolites exhibiting good antibacterial and antifungal activities preventing the growth of harmful microorganisms. Various metabolites such as alkaloids, phenols, flavonoids, peptides, steroids, and terpenoids are isolated from both bacterial and fungal endophytic strains (Supplementary Table 2). Alkaloids possess firm potential in inhibiting the proliferation of microbes. Fungal endophytes such as *Clavicipitaceae* sp. isolated from grass family showed production of alkaloids, which are harmful for aphids (Panaccione et al., 2014). Alkaloids are identified as to contaminate precise hosts and causes slight damage to non-target organisms. Altersetin alkaloid isolated from *Alternaria* spp. displayed a strong antibacterial effect on pathogenic bacteria (Hellwig et al., 2002; Akutse et al., 2013). GS-MS analysis showed production of thermostable metabolites such as d-norandrostane and



longifolenaldehyde by *A. alternata* AE1 isolated from neem leaves. Both the compounds have bactericidal and antioxidant properties and showed zone of inhibition against numerous gram-positive and gram-negative bacteria (Chatterjee et al., 2019). Gond et al. (2015) evaluated the effect of antifungal proteins such as iturin A, bacillomycin, and fengycin isolated from *Bacillus* spp. in controlling fungal pathogen *Fusarium moniliforme*. Antifungal protein designated as Efe-AfpA isolated from *Epichloe festucae* showed disease resistance against pathogen *Sclerotinia homoeocarpa* causing dollar spot disease (Tian et al., 2017). Apart from this, many endophytes are widely reported being associated with antibiotic activity. Lipopeptides produced by several endophytes may show antimicrobial and surfactant activities and well known for their antibiotic activity. *Bacillus amyloliquefaciens* strain produces lipopeptides having biocontrol activity toward *Erysiphe cichoracearum* (fungal pathogen). The fengycin, iturin, and surfactin produced by *Bacillus* sp. helped in inhibiting the growth of fungal pathogen. Also, pellicle biofilm formation affected the colonization ability of pathogens (Jiao et al., 2021).

## Bio control strategies through quorum quenching

Quorum sensing (QS) is a signaling mechanism that controls growth and metabolism in single-cell microorganisms such as bacteria. Density-dependent cell-to-cell communication controls most of the traits which are helpful in endophytes as well a key controller of virulence in pathogens (Frederix and Downie, 2011). The factors responsible for virulence such as biofilm formation, toxin production, antibiotic resistance, exopolysaccharides (EPS), and degradative exoenzymes secretions are highly regulated by quorum sensing signaling. This mechanism takes place via small diffusible signaling molecules called autoinducers (Seitz and Blokesch, 2013). For instance, many pathogenic bacteria such as *Pseudomonas* and *Ralstonia* primarily use acylated homoserine lactones (AHLs) to communicate while producing virulence (Mansfield et al., 2012). They cause great damage to crops. Therefore, antiquorum sensing approach could be harnessed to trigger the phenotype of pathogen to block infection (Chen et al., 2013). Quenching process is regulated by interfering with virulence-associated activities such as modification of signals, catalysis of degrading enzymes such as AHL-lactonase, and inhibition of signal synthesis (Dong et al., 2002). Lactonase enzyme works through removing the lactone ring from the acyl moiety of AHLs and ultimately inactivates AHLs (Murugayah and Gerth, 2019). Endophytic bacteria and fungi provide plethora of bioactive molecules, which can act as an inhibiting agents including QS quenching enzymes such as lactonase, acylase, and QS inhibitor molecules (LaSarre and Federle, 2013). Such agents can provide promising approach to control phytopathogens

and suppress virulence expression in them. They assist in degrading quorum-sensing signals from pathogenic microbes and disrupt intercellular communication (Rutherford and Bassler, 2012). Endophytes with quorum quenching activity attenuate virulence factors rather than killing the microbes or limit the cell growth. This property effectively reduces the selective pressure associated with bactericidal agents (Chen et al., 2013). QS and *in-silico* analysis showed antiquorum sensing and antibiofilm potential of *Alternaria alternata* isolated from *Carica papaya* against pathogen *Pseudomonas aeruginosa*. Significant decrease in cyanin, alginate, and rhamnolipid production was observed. Protease activity such as LasA protease activity and Las B protease activity responsible for virulence was correlated with decrease in biofilm formation (Mishra et al., 2020).

Endophytes such as *B. firmus* and *Enterobacter asburiae* PT39 showed effective degrading capability of AHL by preventing violacein production (80%) in biosensor strain. Still, cell-free lysate when applied to *P. aeruginosa* PAO1 and PAO1-JP2 biofilm caused decrease in biofilm formation (Rajesh and Rai, 2014). In a study, AHL-degrading bacteria *Pseudomonas nitroreducens* potentially degraded diverse variety of AHL including *N*-(3-oxododecanoyl)-L-homoserine lactone (OdDHL) in *D. Zea* EC1. It fully degraded OdDHL (0.2 mmol/L) in 48 h. Furthermore, the application of this strain as a biocontrol agent might considerably reduce soft rot disease produced by *D. zeae* EC1 to suppress tissue maceration in numerous host plants (Zhang et al., 2021). These observations demonstrate that QQ strains have huge potential to reduce the disease harshness due to QS-modified pathogenic bacteria. Antivirulence activity can also be achieved by an engineered endophytic bacterium through introducing quorum-quenching gene. For instance, to control *Burkholderia glumae* which causes grain rots of rice, an *N*-acyl-homoserine lactonase (*aiiA*) gene from *Bacillus thuringiensis* was inoculated into *Burkholderia* sp. KJ006 to repress *N*-acyl-homoserine lactone (Cho et al., 2007). Thus, quorum-quenching microbes provide great potential as biocontrol agents. There are several advantages of introducing quorum-quenching microbes into plants. Being compatible in nature endophytes occupies most of the cellular space without leaving space for later-invading phytopathogens (Kung and Almeida, 2014).

## General plant defense responses against biotic stress

Plants are attacked by various pathogens, parasites, and herbivores, all of which cause biotic stress. Various pests belonging to Lepidoptera, Hemiptera, Orthoptera, and Diptera are well known for damage crop plants. Pests destroy more than 40% of the world's crops every year (FAO, 2021). Also,

the fungal parasites are hidden robbers that inhibit the plants growth either by killing the host cell through secretion of toxin or biotrophic fungi that feed on living host cell. Host plants become a source of nutrients for such harmful parasites. In some biotrophic fungi, haustoria plays a major role in absorbing nutrients from host tissues (Szabo and Bushnell, 2001). Plant viruses also cause leaf chlorosis, spotted wilt, stunted growth in several important plants such as tomato, cucumber, potato, and sugarcane (Roossinck et al., 2015). In addition, nematodes feed on different plant parts (seeds, roots, flowers, leaves, and stems) and cause wounds on the plants. Quick reproduction ability in mites and insects also makes them vectors of other pathogens such as virus and bacteria (Maafi et al., 2013; Adam et al., 2014).

Plants have evolved a plethora of defense mechanisms to combat broad-spectrum pests and pathogens (Rejeb et al., 2014). The defense mechanism could be performed, with toxic metabolites deposited, and it could be inducible. Upon pathogen attack, the innate immune system gets activated that prevents the pathogen entry and terminate their growth. It is a primary defense that contains physical barriers such as waxy cuticles, rigid cell wall, and trichomes to avoid phytopathogens. Cuticle not only restricts the entry of liquid and gas fluxes but also protects plants against pathogens, xenobiotics, and irradiation (Serrano et al., 2014). Trichomes can also have negative or positive effects depending on the target pests through their impact on the behavior of herbivore natural enemies. For instance, the presence of leaf trichomes positively inhabited predatory mite *Typhlodromus pyri* on grapes. On the other hand, European ridge mite favored grape varieties with low trichomes (Loughner et al., 2008). Plants can also produce a variety of secondary metabolites to protect themselves from herbivores and harmful microorganisms. Numerous metabolites, such as amines, peptides, alkaloids, cyanogenic glucosides, phenolics, polyacetylenes, non-protein amino acids, and quinines, contribute significantly to disease reduction in plants. Different concentrations and compositions of such compounds work synergistically for defense mechanism (Wink, 2018).

Few defense mechanisms are consecutive (production of phytoanticipins) that are preformed and induced (phytoalexin production) that are activated after pathogen attack. Phytoalexins are low molecular weight compounds that possess antimicrobial. There are wide varieties of phenolic compounds, which assist in phenotypic plasticity and act as inhibitors, pesticides and contain anti herbivory roles (Kant et al., 2015). As rapidly the host plant is infested by pathogen, it displays accretion of phenolics and causes increase in host metabolism. Mainly, hydroquinones, caffeic acid, gallic acids, hydroxycinnamates, and 5-hydroxynaphthoquinones are effective allelochemicals (Cheng and Cheng, 2015). Caffeic acid (200 µg/ml) in tobacco root exudates defends tobacco plants from infection by *Ralstonia solanacearum*. It resulted in

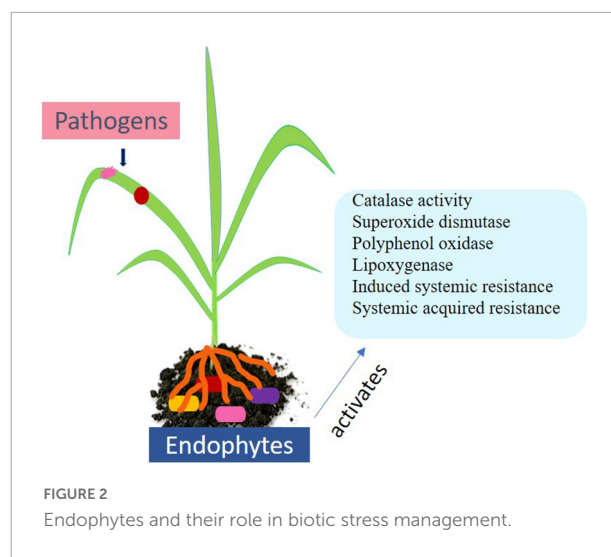


FIGURE 2  
Endophytes and their role in biotic stress management.

thinning of cell membrane and created irregular cavities in cells. Moreover, expression of *IecM* and *epsE* genes associated with inhibition of biofilm formation was also observed and exhibited important prospect in plant defense (Li et al., 2021). In plants, complex network of antioxidative defense system to counter harmful reactive oxygen species (ROS) comprised free radicals such as  $\text{OH}\cdot$ ,  $\text{O}^{\cdot-}$ , and non-radicals such as  $\text{H}_2\text{O}_2$  and  $^1\text{O}_2$  which are formed under unfavorable circumstances (Huang et al., 2019). ROS scavenging mechanism includes enzymatic components such as catalase, guaiacol peroxidase, superoxide dismutase, dehydroascorbate reductase, and glutathione reductase. Non-enzymatic antioxidants such as reduced glutathione, ascorbic acid, carotenoids, and flavonoids help in scavenging oxidative stress (Das and Roy Choudhury, 2014).

Additionally, plant hormones such as salicylic acid, ethylene, and jasmonic acid play central role in biotic stress signaling. Plants also possess an innate immunity system to recognize microbe-associated patterns (PAMP) such as lipopolysaccharides, peptidoglycan, and bacterial flagellin. Such immunity is called PAMP triggered immunity. Herbivores are recognized through herbivore-associated molecular patterns (HAMPs) (Zhang and Zhou, 2010). Other immune response includes transcription methods in the host nucleus and recognizing Avr proteins that are avirulent in nature. Effector triggered immunity arouses hypersensitive responses (HRs) and causes programmed cell death (PCD) in diseased and nearby cells (Howden and Huitema, 2012). A long-lasting and broad-spectrum pathogen resistance against secondary infection known as systemic acquired resistance (SAR) is conserved among diverse plants (Figure 2). Diverse group of molecules including salicylic acid is increased in tissues that occur systematically after localized exposure to a pathogen or after treatment with synthetic or natural compounds (War et al., 2011).

## Endophytes as parasites: Hyperparasitism

It is a biocontrol strategy in which the parasitic host is plant pathogen. In fungi, hyperparasitism is frequently observed, but it is rarely seen in bacteria. Instead of using chemicals, it is frequently used to protect plants against pathogens. *Trichoderma* species, a well-known necrotrophic mycoparasite that targets host mycelium, is the most prevalent hyperparasite (Steyaert et al., 2003; Qualhato et al., 2013). Fungal parasite *Trichoderma harzianum* has a potential ability to parasitize *Epichloe typhina*, an agent that causes choke disease in grasses (Węgrzyn and Górzyska, 2019). It showed the capability of parasitizing the already-grown mycelium of *E. typhina*. Predatory bacterium such as *Bdellovibrio bacteriovorus* has the uncommon property to use the bacterial cytoplasm as nutrients (Harini et al., 2013). Several pathogenic microbes are predated by *Xanthomonas vesicatoria* including *Erwinia carotovora*, *Pseudomonas syringae*, and *E. herbicola* (McNeely et al., 2017). *Trichoderma* spp. has been found to parasitize *Rhizoctonia solani* hyphae, thus inhibiting the disease production (Harman et al., 2004). This property can be used to treat plant diseases such as damping off in soybean seedlings and root rot in sugar beet.

## Competition for space, infection, and nutrients

Pathogen adapts to nutrient-rich niches such as the rhizosphere, phyllosphere, phloem, and xylem. Pathogens choose different routes into the plant based on their survival needs. Few enter through stomata such as *Pseudomonas syringae*, while others use nectarthodes such as *Erwinia amylovora*, which causes potato fire blight disease (Melotto et al., 2008; Gudesblat et al., 2009). Furthermore, some pathogens have a distinct acquisition strategy and rely entirely on the host plant for nutrition (Fatima and Senthil-Kumar, 2015). Biotrophic pathogens consume nutrients from host tissues. Such pathogens invading plant tissues are competitively prevented by non-pathogenic endophytes already residing in the tissue. Endophytes being ubiquitously present can act through colonization and can resist the pathogen attack through competing for resources which could be available to pathogens through niche overlap. This could be understood from the study by Blumenstein et al. (2015) showing elm (*Ulmus* spp.) endophytes exhibiting extensive niche overlap against Dutch elm disease pathogen. Carbon utilizing profiles of asymptomatic endophytes showed high competition with respect to the utilization of sugar alcohols, monosaccharides, and tri- and tetra-saccharide. In another study, *Lecanicillium* reduced the available nutrients on the leaves

while also inducing plant responses during root colonization (Litwin et al., 2020).

## Lytic enzymes as plant disease antagonist

Extracellular enzymes that exhibit biocontrol activity are being increasingly explored as potential antimicrobials to target pathogenic microbes. Numerous endophytes have been reported to produce different lytic enzymes such as chitinase, cellulase, proteases, hemicellulases, and amylase, which aid the hydrolysis of polymers (Dutta et al., 2014; Bodhankar et al., 2017). Lytic enzymes play vital role in the colonization of endophytes in the host cells through formation of polysaccharide and protein biofilms (Limoli et al., 2015). However, it also helps in controlling plant pathogens through cell wall degradation process (Cao et al., 2009). Specifically, fungal cell wall mostly comprises of polysaccharides that provide structural stiffness to the cell wall in phytopathogens. Therefore, the interference in the glycosidic bonds through enzymatic lysis can deteriorate the cell wall and thereby cause cell death. For instance, extracellular enzyme chitinase isolated from *P. aeruginosa* suppressed phytopathogen *Xanthomonas campestris*, which causes black rot disease in cruciferous vegetables (Mishra and Arora, 2012).

Lytic enzymes chitinases,  $\beta$  1-3 glucanases, and proteases secreted from *Trichoderma harzianum*, and *Trichoderma viride* significantly reduced the incidence of collar rot disease by *Aspergillus niger* (Gajera and Vakharia, 2012). It assists in the breakdown of glycosidic bond. Similarly,  $\beta$ -1, 3-glucanases synthesized from *Trichoderma harzianum* showed antagonistic activity through hydrolyzing O-glycosidic linkage of  $\beta$ -glucan chains in cell wall of parasitic fungi *Sclerotinia sclerotiorum*. It is a serious disease that causes white mold in *Phaseolus vulgaris* (Vázquez-Garcidueñas et al., 1998). However, individual applications of lytic enzymes producers are ineffective, whereas application with another mechanism works well.

## Induced resistance in plants

It is an indirect mechanism through which endophytes inhibit pathogens. Endophytes behold the property to decrease disease susceptibility upon pathogen attack by triggering induced resistance in their host plant (Card et al., 2016). Resistance patterns primarily ISR mediated by phytohormones such as ethylene or jasmonic acid and systemic acquired resistance (SAR) linked with the salicylic acid regulation is the known signaling pathways (Figure 2). Root colonization by endophytes and expression of pathogenesis-related genes is often correlated with the elicitation of induced systemic

resistance against infection. For instance, root endophyte *Fusarium solani* has been shown to reduce infection in tomato through activating pathogenesis-related genes such as PR5 and PR7 (Kavroulakis et al., 2007). The endophyte *Bacillus pumilus* along with synthetic benzothiadiazole triggered ISR in contrast to bacterial spot disease in pepper occurred due to *Xanthomonas axonopodis* (Yi et al., 2013). *Fusarium oxysporum* strain Fo47 via endophytic-mediated resistance (EMR) was found to suppress various wilt diseases in tomato, flax, watermelon, and pepper (Larkin and Fravel, 1999; Trouvelot et al., 2002). *Epichloe* spp. showed the ability to potentiate expression of salicylic acid defense mechanism against *Blumeria graminis* (Kou et al., 2021). Expression of pathogenesis-related PR1 protein and callose deposition by *Bacillus cereus* induced ISR against *Botrytis cinerea* and simultaneously activated the SA- and JA/ET (Nie et al., 2017).

## Modulation of biotic stress controlling mechanisms by endophytes

Microbial endophytes are well identified for their potential role in plant growth-promoting activities. However, their multidimensional interaction with broad range of host plants makes them potential candidate in stress tolerance mechanism (Tamosiune et al., 2017). Endophytic microbes are reported to have numerous beneficial effects in comparison with other PGPRs in colonizing the internal tissues and remain protected from the harsh environment and less nutritional requirement (Pandey et al., 2019). Endophytes commonly reside in plant tissues and benefit their host plant by eliciting defense response toward pathogen outbreak and protect them from different environmental stress (Nanda et al., 2019). Microbial endophytes being inhabitants of plant tissues are known to exhibit unique host's gene expression, physiological and metabolic response essential in conferring resistance against pests, herbivores, and phytopathogens. Pathogens cause various harmful diseases in plants and interfere with growth mechanisms of plants. It reduces photosynthetic rate, results in stunted growth, and damages plant tissues (Pérez-Bueno et al., 2019). Endophytes produce numerous compounds that help plants to interfere with pathogen by recognizing pathogen related structures. Several metabolites such as volatiles and antibiotics and hormones effectively control the expression genes related to stress response and improve plant growth through induced resistance (Lu et al., 2021).

Some studies reported the similarity of bioactive compounds by endophytic microbes to those formed by host plants (Puri et al., 2006). Different antioxidant enzymes such as peroxidase (POD), polyphenol oxidase, phenylalanine ammonia lyase (PAL), lipoxygenase, and chitinase alleviate biotic stress. Peroxidase enzymes are involved in the wide

range of progressions with hypersensitive response, cross-linking of phenolics, lignifications, phytoalexin production, and suberization (Prasannath, 2017). Lipoxygenase belongs to non-heme iron containing deoxygenase that participates in stress response through lipid oxidation and acts as signal molecule to communicate with plants, pathogens, and allied endophytes as reported by Veronico et al. (2006). Different endophytes are known to produce peroxidase enzyme, which play important part in the conversion of  $H_2O_2$  into  $H_2O$  as reported by Caverzan et al. (2012). Endophytes boost plant immunity by ISR, SAR, pathogenesis-related proteins and via production of numerous phytohormones to overcome the pathogen stress (Romera et al., 2019; Oukala et al., 2021). Several microbes produce surfactin, mycosubtilin, and lipopeptides, which activated the plant innate immune response. It was observed that surfactin production suppresses the *Fusarium* invasion during seed germination (Eid et al., 2021). Suppression of virulence genes such as vir A and vir G and expression of defense-related genes such as PR1, STS, and ANTS induced resistance toward *N. parvum* and *B. cinerea* as reported by Haidar et al. (2016).

## Remodeling and reinforcement of cell wall to cause physical barriers against pathogens

Bacterial and fungal endophytes change chemical and physical characteristic to confer resistance against phytopathogens and herbivory (Supplementary Table 3). High deposition levels of callose in guard cells protect plants from herbivory that cause extensive tissue damage. Callose is  $\beta$ -(1,3)-D-glucan which protects plant tissues from pathogen attack. It is usually deposition among the cell wall and plasma membrane at site of pathogen invasion, at the plasmodesmata and on other plant tissue to slow down pathogen attack (Wang et al., 2021). For instance, endophytic bacteria *B. amyloliquefaciens* and *P. fluorescens* increase callose deposition in guard cells and immunize the *W. somnifera* plant leaves against *A. alternata* (Mishra et al., 2018). Callose deposition and increased lamina density provides resistance to the host plants. It protects plants from different herbivores precisely from leaf wounding ants and aphids (Khare et al., 2018). Upregulation of genes related to cellulose and lignin deposition and hardening of host cell wall were enhanced through inoculation of foliar endophytic fungus *Colletotrichum tropicale* isolated from *T. cocoa*. High cellulose and lignin deposition protects cocoa tree from black pod disease caused due to *Phytophthora* spp. (Mejía et al., 2014). In most cases, fungal endophytes limit insect growth rate, reducing insect survival and oviposition. Consortium of chitinase producing endophytes *Chitiniphilus* sp. MTN22 and *Streptomyces* sp. MTN14 showed uniform lignifications and callose deposition in *B. moneri* protecting against *Meloidogyne*



*incognita* nematode. Callose deposition in leaves was found preferentially in the interveinal region of host leaves (Gupta et al., 2017). Succession of structural variations is observed in *Arabidopsis thaliana* seedlings through callose deposition when inoculated with *Gluconacetobacter diazotrophicus* and protected the plant from *Ralstonia solanacearum* infection (Rodriguez et al., 2019).

Protection efficacy of *B. phytofirmans* PsJN against *Botrytis cinera* was correlated with the callose deposition and H<sub>2</sub>O<sub>2</sub> production. Further primer expression of PR genes (PR1, PR2, PR5, and JAZ) and modulation in leaf carbohydrate metabolites and sugar levels after pathogen attack were reported from the study (Miotto-Vilanova et al., 2016). Rapid creation of papillae upon pathogen attack especially against fungal pathogens acts as physical fence to limit pathogen entry into the host tissues. Resistance to fungal pathogen is often correlated with the rapid formation of cell wall appositions called papillae, which forms specifically upon interaction between plant and endophytes in response to pathogen attack (Collins et al., 2003). Furthermore, to papillae, phenolic conjugates associated with papillae contribute directly in antifungal activity that forms cross-linking to form a toughened wall that cannot be simply degraded by pathogens and their associated enzymes (Zeyen et al., 2002). These are some successful cell wall-associated defense response mediated through endophytes that can stop invasive pathogens at an initial phase, before the creation of disease in plants.

## Stimulation of bioactive metabolites

Secondary metabolites involved in defense response toward pests, herbivores, and pathogens. Different plant microbes specially endosymbionts secrete various metabolites and regulate defense mechanisms and having antimicrobial properties. Plant secondary metabolites such as steroids, alkaloids, phenolics, flavonoids, and terpenoids function in innate immunity and defense response signaling (Isah, 2019). *Phomopsis* sp. (fungal endophyte) produce VOCs comprised of butanol, acetone, sabinene, 1-butanol, and phenethyl alcohol, which inhibit the *Ascomycetes* and *Deuteromycetes* growth (Singh et al., 2011). VOCs such as caryophyllene, 2-methoxy-4-vinylphenol, and 3,4-dimethoxystyrol having antifungal actions released from *Sarocladium brachiariae* endophytic fungi found to be effective against *Fusarium oxysporum* (Yang et al., 2021). Colonization of asexual *Epichloe festucae* in agricultural forage grasses provided protection against herbivorous insects (Hennessy et al., 2016).

Alkaloid production from Clavicipitaceae and Ascomycota decreases herbivore feeding and virus transmission. Oxidative burst and phytoalexin production improved resistance against *Botrytis cinera* by grapevine cells and leaf-associated bacteria

*Pseudomonas fluorescens* (Verhagen et al., 2011). Phytoalexins are low molecular compound containing antimicrobial, antifungal, and antiviral activities, which involved in electron transport and phosphorylation, causes rapid and complete termination of respiration in *B. cinerea* conidia (Pezet and Pont, 1990). Endophytic bacteria (*P. migulae* 8R6) showed ACC deminase activity, which limits the phytoplasma-induced damages in periwinkle through regulating the stress-related hormone such as ethylene. It improved resistance toward infection of phytoplasma and reduced the quantity of symptomatic plants up to 93% (Gamalero et al., 2017). Analysis of free amino acid in diseased leaves showed significant impact of *P. citrinum* and *A. terreus* to disease resistance and promotion of sunflower growth (Waqas et al., 2015). Change in the amino acids delays and changes the progression of pathogenic microbes. Surfactin especially surfactin A and other lipopeptides purified from *Bacillus subtilis*, *Fusarium oxysporum*, *F. moniliforme*, and *F. solani* were known to play major role in antifungal activity (Sarwar et al., 2018).

## Priming of the plant defense system

Endophytes can protect plants against pathogen attack via the host by triggering induced resistance via several molecular events. Upon pathogen attack, the interaction between plant endophytic associations leads to an alteration in second messenger such as Ca<sup>2+</sup> in the cytosol (Vadassery and Oelmüller, 2009). It acts as signaling molecule in sensing microbe-associated molecular patterns (MAMPs) and initiates induction of complex immune response. After activation of certain signals, bacterial and fungal endophytes that are attached to cell surface receptors activate kinases (cell surface receptor). When kinases are stimulated, they phosphorylated and send signals to ethylene/jasmonic acid or salicylic acid against phytopathogens which triggers ET/JA transduction pathways (Conn et al., 2008; Ryan et al., 2008). Endophytic colonization with the host plants downregulates the expression of genes associated with biotic stress defense response.

Usually, different phytohormones such as jasmonic acid, ethylene, and salicylic acid triggers induced resistance. JA and ET pathways are known to encourage resistance toward necrotrophic pathogens, but the SA pathway activates resistance toward the biotrophic and hemibiotrophic pathogen (Ding et al., 2011). ISR is normally triggered upon endophytic colonization of roots and immunes the plant body for future attack from pathogens. Several compounds such as flavonoids, polyphenols, phytoalexins, and signal transduction pathways were activated by jasmonate/SA or ethylene (Leon-Reyes et al., 2009; Lebeis et al., 2015). The first report indicating the induced systemic resistance by *Pseudomonas fluorescens* 89B-61 elicited resistance against cucumber anthracnose (Wei et al., 1991).

Increased synthesis of phenolic metabolites is often correlated with induced systemic resistance. Contact among *B. distachyon* and *Microdochium bolleyi* (endophytic fungus) isolated from wheat roots induced ISR against pathogen attack of *Fusarium culmorum*. Endophytic fungi upregulated expression of certain genes such as *chitinase 1*, *BdLOX3*, and *TaBH1* induced ISR in wheat (Matušinsky et al., 2022).

Some endophytes can also regulate stress management through SAR mediated by salicylic acid (Pieterse et al., 2014). SA is often associated with building up of pathogenesis-related (PR) proteins and chitinase. *Paenibacillus* strain (PB2) used to control *Mycosphaerella graminicola* induced pathogenesis-related proteins (PR1), which is considered as a marker of SAR (Samain et al., 2019). *Bacillus subtilis* activated a durable defense response in *Arabidopsis thaliana* against *P. syringae* pv. tomato DC3000 facilitated through salicylic acid/ethylene and NPR1 protein (Rudrappa et al., 2010). *Bacillus subtilis* and *Pseudomonas fluorescens*-mediated systemic alleviated the biotic stress in *Solanum lycopersicum* against *Sclerotium rolfsii* (Cappellari et al., 2019). *B. aryabhattai* showed induction of defense-related genes protein (PR1) and phytoalexin-deficient 3 in *A. thaliana*. PR1 gene expression was higher in treated plants (Portieles et al., 2021). Endophytes shows the upregulation of different genes and unique signaling pathway according to dissimilar colonization tactics as reported by Morelli et al. (2020).

There are reports indicating the distinction of endophytic mediated resistance from ISR and SAR as jasmonate, salicylic acid, and ethylene are not involved (Pieterse et al., 2014). Root endophytes *Fusarium oxysporum* strains Fo 47 and CS-20 have the ability to induce endophytic mediated resistance in tomato and cucumber and protect them against vascular and root pathogens such as *Verticillium dahliae* and *Pythium ultimum* (Benhamou et al., 2002). Endophytic mediated resistance in case of *Fusarium* species differs from ISR and SAR in terms of no association of resistance with jasmonic acid and ethylene. Also, tomato plant established a tri-partite interaction with endophytic *Fusarium oxysporum* and other organisms residing in the host plants. Grasses often establish tripartite association among endophytic fungi, arbuscular Mycorrhizal fungi, and *Leymus chinensis* (Liu et al., 2020).

## Defense-related enzymes

Defense mechanisms through endophytes are mediated through the activation of multiple defense compounds and enzymes at the site of pathogen attack. Various enzymes such as PAL, POD, and superoxide dismutase (SOD) are important antioxidant enzymes, which help in defense oxidative stress and lipid peroxidation during pathogen invasion (Birben et al., 2012). Other defense enzymes such as ammonia lyase, chitinase, and  $\beta$ -1-3 glucanase are associated with resistance induction in plants. Several endophytic strains confirmed the production of

chitinase enzyme. Some of them are *Colletotrichum sublineolum*, *Streptomyces hygroscopicus*, and *Bacillus cereus*, which are known to inhibit the growth of phytopathogenic fungi such as *Rhizoctonia solani*, *Fusarium oxysporum*, *Aspergillus niger*, and *B. cinerea* (Wang et al., 2001; Brzezinska and Jankiewicz, 2012). ROS that are harmful for plants are neutralized enzymes such as superoxide dismutases, catalases, peroxidase, glutathione-S-transferases, and alkyl hydroperoxide reductases. Consortium of *Polyporus vinctus*, *Trichoderma reesei*, and *Sphingobacterium tabacisoli* accumulated defense enzymes such as PAL, POD, and polyphenol oxidase. It triggered systemic resistance contrary to *Fusarium* wilt of banana and showed first line of defense (Savani et al., 2020). Various enzymes are known to mitigate oxidative stress. *Bacillus subtilis* (EPC5) isolated from coconut root samples showed biocontrol activity against *Ganoderma lucidum*, which is the causal agent of basal stem rot on coconut palm through higher induction of phenols, peroxidase, polyphenol oxidase, and phenylalanine lyase (Rajendran et al., 2015).

Evaluation of potential *Streptomyces* spp. viz. *S. diastaticus*, *S. olivochromogenes*, *S. collinus*, and *S. griseus* triggered systemic resistance and significantly increased total phenolics, flavonoids, superoxide dismutase, ascorbate peroxidase, and guaiacol peroxidase which ultimately induced resistance against *Sclerotium rolfsii* in chickpea (Singh and Gaur, 2017). Endophytic fungi (*Fusarium sambucinum*) isolated from mangrove forest efficiently produced defense enzymes such as laccase (41.5 U L<sup>-1</sup>), manganese peroxidase (23.6 U L<sup>-1</sup>), endo-xylanase, and biosurfactant (Martinho et al., 2019). These enzymes promote the hydrolysis of lignin and decrease the degree of polymerization exposing the microfibrils to other enzymatic attack. Lipoxygenase genes detected in fungal endophyte *Paraconiothyrium variabile* isolated from conifer *Cephalotaxus harringtonia* showed inhibitory effect on *Fusarium oxysporum*, which causes vascular wilt in conifers. Lipoxygenase genes *pvlox1* and *pvlox2* unregulated the stress response and acted as stress marker and signaling compound when exposed to invading phytopathogens (Bärenstrauch et al., 2020). It is observed that stress factors affect growth of plants and productivity. In the present situation, thorough and efficient research on the response of endophytes on different essential crops is comparatively inadequate under field conditions. Indeed, understanding the association between crop and beneficial microbes can lead to better agricultural performs that augment plant fitness and improved the yield.

## Molecular mechanism of host–endophyte interaction

It is less understood how the endophyte and host interact. To effectively manipulate the mutualistic link between the two, it is crucial to identify, isolate, and characterize the genes involved in such beneficial interactions. A novel approach for

closely examining endophytism and revealing the characteristics required to harbor plants as a habitat has been made available through endophyte genome analysis (Kaul et al., 2016). It has revealed genes important for endophytic lifestyle that are found frequently in endophyte genome such as those involved in N fixation, mineral acquisition, and stress tolerance related (Martinez-Garcia et al., 2015). Exudates such as organic acids, proteins, and amino acids are released by plants from their roots, acting as communications signals between host plant and bacterial endophytes (Kawasaki et al., 2016). Endophytic bacterial colonization is a multistage process that includes chemotactic movement toward roots, attachment to root surfaces, entry inside the root, and movement (Kandel et al., 2017b). There are various genes such as *fliC3*, *MgIB*, *pilX*, *FliI*, *Aer*, and *CheZ*, which involved in chemotaxis and motility (Samanta et al., 2016; Liu et al., 2018). *Gilmaniella* sp. inoculation in *Atractylodes lancea* upregulated the genes and proteins such as terpene skeleton biosynthesis as well as farnesene synthase related to primary metabolism (carbohydrate metabolism, carbon fixation) which improve plant growth (Yuan et al., 2019). Additionally, they noticed an increase in genes related to signaling such as those related to ethylene response factors, heat stress, trielix, and basic loop helices. Sesquiterpenoid, phytoalexins such as gossypol and heliocides can protect cotton plants from herbivores infections (Yang et al., 2013). The overexpression of oryzalexin's genes (*OsTPS19*) and monoterpene S-limonene serve protective metabolite against *Magnaporthe oryzae* and provide resistance to plants toward infection (Chen et al., 2018). Wheat plants have improved resistance to *Fusarium* head blight due to the presence of *Fhb7* gene in endophytic *Epichloe* fungus, which encodes glutathione-S-transferase involved in trichothecenes detoxification (Wang et al., 2020). Dinkins et al. (2017) observed that *Epichloe coenophiala* altered the expression of several WRKY transcription factors linked to the increased resistance in *Lolium arundinaceum*. Endophytic fungus increased the expression of iron transporters and genes involved in fatty acid production to encourage the *Noccaea* plant development (Ważny et al., 2021).

## Omics approach to study endophytes and host plants interaction

Multomics, which includes genomes, transcriptomics, proteomics, and metabolomics, are becoming increasingly important in plant-microbe interaction (Kaul et al., 2016). The potential value of endophytes can be investigated using modern high-throughput genomic technology. An in-depth examination of endophytes in terms of sequencing and biological evolution has greatly increased interest in endophyte

research (Selosse et al., 2022). Endophyte genome-wide analysis directly reflects endophyte colonization preferences and genetic characteristics on various hosts. This makes it much easier to find the related genes involved in host growth, development, insertion elements, metabolism, and surface attachment (Subudhi et al., 2018). *Pantoea ananatis*, an endophytic bacterium with enormous biological potential, contains genes for hydrolase and fusylic acid resistance protein (Wu et al., 2020).

Proteomic analysis using mass spectrometry identified differentially expressed proteins (DEPs) related to the endophytic *Gluconacetobacter* and sugarcane interaction which involved in signaling and cellular recognition (Lery et al., 2011). Using multiomics analysis, researchers discovered that liposaccharide and adhesins are potential molecular determinants underlying the divergent phenotypic behavior of closely related species during plant-host colonization (Monteiro et al., 2012). RNA sequencing and microarray enables the identification of differentially expressed genes, which involved in upregulation of nutrient acquisition and chemotaxis (*nifH*, *sbpA*, and *trpB*) in wheat roots colonized by *Azospirillum brasilense* (Camilios-Neto et al., 2014). Proteomics and transcriptomics were used to decode the effect of endophytes on the host *Atractylodes lancea* as reported by Yuan et al. (2019). Metabolomic analysis is a popular technique for quantifying metabolites. It can be used to complement transcriptomic and proteomic data, allowing for a well understanding of host phenotypical structures and elucidating plant-microbe interaction and mechanism (Chen et al., 2022). During various stages of plant development, endophytes synthesize a variety of secondary metabolites and mediate an increase in metabolites biosynthesis in particular species and organs (Zhai et al., 2017). The DEGs and metabolites of anthracnose-resistant cultivars of *Camellia oleifera* indicate the critical function of flavonoid biosynthesis in the defense toward anthracnose using transcriptome and metabolomics (Yang et al., 2022). Barley metabolo-transcriptome profiling revealed the activation of the HvCERK1 gene, which confers resistance to *Fusarium graminearum* as reported by Karre et al. (2017).

Microarray-based gene expression analysis revealed single inoculation of endophytic *Bacillus megaterium* isolated from black pepper root encouraged growth elevation in *A. thaliana* Col O seeds by upregulation of biotic stress related genes such as *MYB4*, *MYB7*, *WRR4*, *ATOSM34*, and *ATHCHIB*. Also, the bacterial colonization inside the host tissues triggered ethylene-responsive genes such as *ERF71* and *RAP2*. Other genes such as *BAP1*, *BTK4*, *MKK9*, and *AIB1* were found associated with jasmonic acid and salicylic acid transduction pathways (Vibhuti et al., 2017). In another study, rice seed primed with *Pseudomonas putida* BP25 endogenously colonized rice and altered root growth and defensive response against *Magnaporthe oryzae*. Defense-related phenols, peroxidase, and both volatile and nonvolatile metabolites were found in

primed plants. Also, pathogenesis-related genes associated with systemic acquired resistance, i.e., *OsPRI-1* and *OsPR3* were downregulated by endophytic colonization. Growth-related genes playing important role in intermodal elongation such as *OsAcO4* and *OsACS6* were observed regulating plant growth and protecting it against blast disease (Ashajyothi et al., 2020).

Although endophytic microorganisms possess great potential in the agricultural field still, there are certain challenges involved with the field application of endophytes that are restricting their wide use. When introduced into a crop plant, many factors prevail which must be evaluated for their wide application from lab to field. First, many fungal endophytes produce toxic secondary metabolites such as mycotoxins which cause infection in their host plants upon colonization and reach up to fruits and seeds. There is still a need to study upon their colonization and viability of the desired inoculants (Chitnis et al., 2020). It is important to focus on their unpredictable behavior and inadequate colonization of the target site in field trial. Instead of proper establishment of the biological strain, single-strain endophyte inoculants under application do not show desired plant growth activity. Well-formulated consortia could be more promising and help in plant growth promotion through circumventing some of the critical limitations such as crop specificity of microbes. In addition, it is necessary to raise awareness among the farmers about the product's efficacy of endophytes in comparison with harmful chemical fertilizers. Main attention for the introduction of endophytes is the better understanding of plant-microbe interactions under different sets of conditions that will help in reducing bulk production of inoculum doses (Fadiji and Babalola, 2020). Modifying the root exudation chemistry of plants to choose a more beneficial microbiome is one of the most effective strategies. The use of advance biotechnological tools to investigate both the community and functionalities of endophytic microorganisms could be helpful (White et al., 2019). Understanding the genetics and engineering of their complex interactions through next generation sequencing could be helpful in revealing their taxonomic and functional diversity. However, multiple field trails, sampling at different times and locations under different environmental factors, are an important factor to improve their performance under field conditions. Also, future studies can focus on the development of endophytic nanoparticle which could provide a new aspect of metabolism regulation under extreme condition.

## Conclusion

At present, increasing the productivity of crops is important without any disturbance to the soil fertility, to fulfil food needs and provide a healthy environment for our future generations. But due to the incidence of diverse kind of pest and pathogen in crops, it leads to the decrease in yield of crop plants resulting

substantial crop losses every year. To diminish the loss of crop yield and to control the diseases, different effective methods should be used. Endophytes are eco-friendly, non-toxic, easily applicable, and cost-effective in nature, so farmers use them as a substitute to fertilizers for sustainable agriculture. More research needs consideration on the biochemical, molecular, and genetic mechanisms of endophytes decisive for stress resistance in different crops. Omics approach can help unravel the functions of complex plant microbiome, providing information about competent microbes in terms of stress tolerance and plant productivity. Endophytes and their metabolites must be explored to the multiomics level as potentially fruitful research in the biological control of plant diseases.

## Author contributions

PC and AC performed conceptualization and wrote the manuscript. UA wrote the manuscript. AK and GK helped in editing the manuscript. All authors contributed to the article and approved the submitted version.

## Acknowledgments

The authors acknowledge the Microbiology Department, Govind Ballabh Pant University of Agriculture and Technology.

## Conflict of interest

The authors declare that the research was conducted in the absence of any commercial or financial relationships that could be construed as a potential conflict of interest.

## Publisher's note

All claims expressed in this article are solely those of the authors and do not necessarily represent those of their affiliated organizations, or those of the publisher, the editors and the reviewers. Any product that may be evaluated in this article, or claim that may be made by its manufacturer, is not guaranteed or endorsed by the publisher.

## Supplementary material

The Supplementary Material for this article can be found online at: <https://www.frontiersin.org/articles/10.3389/fmicb.2022.933017/full#supplementary-material>



## References

- Abdelshafy Mohamad, O. A., Ma, J. B., Liu, Y. H., Zhang, D., Hua, S., Bhute, S., et al. (2020). Beneficial endophytic bacterial populations associated with medicinal plant *Thymus vulgaris* alleviate salt stress and confer resistance to *Fusarium oxysporum*. *Front. Plant Sci.* 11:47. doi: 10.3389/fpls.2020.00047
- Adam, M., Westphal, A., Hallmann, J., and Heuer, H. (2014). Specific microbial attachment to root knot nematodes in suppressive soil. *Appl. Environ. Microbiol.* 80, 2679–2686. doi: 10.1128/AEM.03905-13
- Adhikari, P., and Pandey, A. (2019). Phosphate solubilization potential of endophytic fungi isolated from *Taxus wallichiana* Zucc. roots. *Rhizosphere* 9, 2–9. doi: 10.1016/j.rhisph.2018.11.002
- Agri, U., Chaudhary, P., and Sharma, A. (2021). In vitro compatibility evaluation of agrisable nanochitosan on beneficial plant growth-promoting rhizobacteria and maize plant. *Natl. Acad. Sci. Lett.* 44, 555–559. doi: 10.1007/s40009-021-01047-w
- Agri, U., Chaudhary, P., Sharma, A., and Kukreti, B. (2022). Physiological response of maize plants and its rhizospheric microbiome under the influence of potential bioinoculants and nanochitosan. *Plant Soil* 474, 451–468. doi: 10.1007/s11104-022-05351-2
- Ait-Lahsen, H., Soler, A., Rey, M., de la Cruz, J., Monte, E., and Llobell, A. (2001). An antifungal exo- $\alpha$ -1, 3-glucanase (AGN13. 1) from the biocontrol fungus *Trichoderma harzianum*. *Appl. Environ. Microbiol.* 67, 5833–5839. doi: 10.1128/AEM.67.12.5833-5839.2001
- Akutse, K., Maniania, N., Fiaboe, K., Van Den Berg, J., and Ekesi, S. (2013). Endophytic colonization of *Vicia faba* and *Phaseolus vulgaris* (Fabaceae) by fungal pathogens and their effects on the life-history parameters of *Liriomyza huidobrensis* (Diptera: Agromyzidae). *Fungal Ecol.* 6, 293–301. doi: 10.1016/j.funeco.2013.01.003
- Andreote, F. D., Gumiore, T., and Durrer, A. (2014). Exploring interactions of plant microbiomes. *Sci. Agric.* 71, 528–539. doi: 10.1590/0103-9016-2014-0195
- Ansari, M. W., Gill, S. S., and Tuteja, N. (2014). Piriformospora indica a powerful tool for crop improvement. *Proc. Indian Natl. Sci. Acad.* 80, 317–324. doi: 10.16943/ptinsa/2014/v80i2/55109
- Arnold, A. E., Henk, D. A., Eells, R. L., Lutzoni, F., and Vilgalys, R. (2007). Diversity and phylogenetic affinities of foliar fungal endophytes in loblolly pine inferred by culturing and environmental PCR. *Mycologia* 99, 185–206. doi: 10.1080/15572536.2007.11832578
- Ashajyothi, M., Kumar, A., Sheoran, N., Ganesan, P., Gogoi, R., Subbaiyan, G. K., et al. (2020). Black pepper (*Piper nigrum* L.) associated endophytic *Pseudomonas putida* BP25 alters root phenotype and induces defense in rice (*Oryza sativa* L.) against blast disease incited by *Magnaporthe oryzae*. *Biol. Control.* 143:104181. doi: 10.1016/j.biocontrol.2019.104181
- Bärenstrauch, M., Mann, S., Jacquemin, C., Bibi, S., Sylla, O. K., Baudouin, E., et al. (2020). Molecular crosstalk between the endophyte *Paraconiophyrium variabile* and the phytopathogen *Fusarium oxysporum*—Modulation of lipoxigenase activity and beauvericin production during the interaction. *Fungal Genet. Biol.* 139:103383. doi: 10.1016/j.fgb.2020.103383
- Barnawal, D., Bharti, N., Maji, D., Chantotiya, C. S., and Kalra, A. (2014). ACC deaminase-containing *Arthrobacter protophormiae* induces NaCl stress tolerance through reduced ACC oxidase activity and ethylene production resulting in improved nodulation and mycorrhization in *Pisum sativum*. *J. Plant Physiol.* 171, 884–894. doi: 10.1016/j.jplph.2014.03.007
- Benhamou, N., Garand, C., and Goulet, A. (2002). Ability of nonpathogenic *Fusarium oxysporum* strain Fo47 to induce resistance against *Pythium ultimum* infection in cucumber. *Appl. Environ. Microbiol.* 68, 4044–4060. doi: 10.1128/AEM.68.8.4044-4060.2002
- Birben, E., Sahiner, U. M., Sackesen, C., Erzurum, S., and Kalayci, O. (2012). Oxidative stress and antioxidant defense. *World Allergy Organ. J.* 5, 9–19. doi: 10.1097/WOX.0b013e3182439613
- Blanco, Y., Blanch, M., Piñón, D., Legaz, M., and Vicente, C. (2005). Antagonism of *Gluconacetobacter diazotrophicus* (a sugarcane endosymbiont) against *Xanthomonas albilineans* (pathogen) studied in alginate-immobilized sugarcane stalk tissues. *J. Biosci. Bioeng.* 99, 366–371. doi: 10.1099/00221287-131-9-2449
- Blumenstein, K., Albrechtsen, B. R., Martín, J. A., Hultberg, M., Sieber, T. N., Helander, M., et al. (2015). Nutritional niche overlap potentiates the use of endophytes in biocontrol of a tree disease. *BioControl* 60, 655–667. doi: 10.1007/s10526-015-9668-1
- Bodhankar, S., Grover, M., Hemanth, S., Reddy, G., Rasul, S., Yadav, S. K., et al. (2017). Maize seed endophytic bacteria: Dominance of antagonistic, lytic enzyme-producing *Bacillus* spp. *3Biotech* 7, 1–13. doi: 10.1007/s13205-017-0860-0
- Bokhari, A., Essack, M., Lafi, F. F., Andres-Barrao, C., Jalal, R., Alamoudi, S., et al. (2019). Bioprospecting desert plant *Bacillus* endophytic strains for their potential to enhance plant stress tolerance. *Sci. Rep.* 9, 1–13. doi: 10.1038/s41598-019-54685-y
- Brewer, T., Handley, K., Carini, P., Gibert, J., and Fierer, N. (2016). Genome reduction in an abundant and ubiquitous soil bacterial lineage. *Nat. Microbiol.* 2:16198. doi: 10.1038/nmicrobiol.2016.198
- Brzezinska, M. S., and Jankiewicz, U. (2012). Production of antifungal chitinase by *Aspergillus niger* LOCK 62 and its potential role in the biological control. *Curr. Microbiol.* 65, 666–672. doi: 10.1007/s00284-012-0208-2
- Cai, X. Q., Lin, N., Chen, W., and Hu, F. P. (2010). Control effects on litchi downy blight disease by endophytic bacterial strain Tb2 and its pathogenesis-related proteins. *Acta Hort.* 863, 631–636.
- Camilios-Neto, D., Bonato, P., Wassem, R., Tadra-Sfeir, M. Z., Brusamarello-Santos, L. C., Valdameri, G., et al. (2014). Dual RNA-seq transcriptional analysis of wheat roots colonized by *Azospirillum brasilense* reveals up-regulation of nutrient acquisition and cell cycle genes. *BMC Genomics* 15:378. doi: 10.1186/1471-2164-15-378
- Cao, R., Liu, X., Gao, K., Mendgen, K., Kang, Z., Gao, J., et al. (2009). Mycoparasitism of endophytic fungi isolated from reed on soilborne phytopathogenic fungi and production of cell wall-degrading enzymes in vitro. *Curr. Microbiol.* 59, 584–592. doi: 10.1007/s00284-009-9477-9
- Cappellari, L. D. R., Santoro, M. V., Schmidt, A., Gershenzon, J., and Banchio, E. (2019). Improving phenolic total content and monoterpene in *Mentha x piperita* by using salicylic acid or methyl jasmonate combined with Rhizobacteria inoculation. *Int. J. Mol. Sci.* 21:50. doi: 10.3389/fmol.2022.851002
- Card, S., Johnson, L., Teasdale, S., and Caradus, J. (2016). Deciphering endophyte behaviour: The link between endophyte biology and efficacious biological control agents. *FEMS Microbiol. Ecol.* 92:fiw114. doi: 10.1093/femsec/fiw114
- Caverzan, A., Passaia, G., Rosa, S. B., Ribeiro, C. W., Lazzarotto, F., and Margis-Pinheiro, M. (2012). Plant responses to stresses: Role of ascorbate peroxidase in the antioxidant protection. *Genet. Mol. Biol.* 35, 1011–1019. doi: 10.1590/s1415-47572012000600016
- Chatterjee, S., Ghosh, R., and Mandal, N. C. (2019). Production of bioactive compounds with bactericidal and antioxidant potential by endophytic fungus *Alternaria alternata* AE1 isolated from *Azadirachta indica* A. Juss. *PLoS One* 14:e0214744. doi: 10.1371/journal.pone.0214744
- Chaudhary, A., Chaudhary, P., Upadhyay, A., Kumar, A., and Singh, A. (2021a). Effect of gypsum on plant growth promoting rhizobacteria. *Environ. Ecol.* 39, 1248–1256. doi: 10.1007/s11356-019-05327-3
- Chaudhary, A., Parveen, H., Chaudhary, P., Khatoon, H., and Bhatt, P. (2021b). “Rhizospheric microbes and their mechanism,” in *Microbial technology for sustainable environment*, eds P. Bhatt, S. Gangola, D. Udayanga, and G. Kumar (Singapore: Springer), 79–93. doi: 10.1007/978-981-16-3840-4\_6
- Chaudhary, P., and Sharma, A. (2019). Response of nanogypsum on the performance of plant growth promotory bacteria recovered from nanocompound infested agriculture field. *Environ. Ecol.* 37, 363–372.
- Chaudhary, P., Chaudhary, A., Bhatt, P., Kumar, G., Khatoon, H., Rani, A., et al. (2022). Assessment of soil health indicators under the influence of nanocompounds and *Bacillus* spp. in *Field Condition*. *Front. Environ. Sci.* 9:769871. doi: 10.3389/fenvs.2021.769871
- Chaudhary, P., Khati, P., Chaudhary, A., Gangola, S., Kumar, R., and Sharma, A. (2021c). Bioinoculation using indigenous *Bacillus* spp. improves growth and yield of *Zea mays* under the influence of nanozeolite. *3Biotech* 11:11. doi: 10.1007/s13205-020-02561-2
- Chen, F., Gao, Y., Chen, X., Yu, Z., and Li, X. (2013). Quorum quenching enzymes and their application in degrading signal molecules to block quorum sensing-dependent infection. *Int. J. Mol. Sci.* 14, 17477–17500. doi: 10.3390/ijms140917477
- Chen, L., Shi, H., Heng, J., Wang, D., and Bian, K. (2019). Antimicrobial, plant growth-promoting and genomic properties of the peanut endophyte *Bacillus velezensis* LDO2. *Microbiol. Res.* 218, 41–48. doi: 10.1016/j.micres.2018.10.002
- Chen, M., Yang, L., Li, Q., Shen, Y., Shao, A., Lin, S., et al. (2011). Volatile metabolites analysis and molecular identification of endophytic fungi bn12 from *Cinnamomum camphora* chvar. borneol. *China J. Chin. Mater. Med.* 36, 3217–3221.
- Chen, X., Chen, H., Yuan, J. S., Köllner, T. G., Chen, Y., and Guo, Y. (2018). The rice terpene synthase gene OsTPS19 functions as an (S)-limonene synthase

in planta, and its overexpression leads to enhanced resistance to the blast fungus *Magnaporthe oryzae*. *Plant Biotechnol. J.* 16, 1778–1787. doi: 10.1111/pbi.12914

Chen, X.-L., Sun, M.-C., Chong, S.-L., Si, J.-P., and Wu, L.-S. (2022). Transcriptomic and metabolomic approaches deepen our knowledge of plant–endophyte interactions. *Front. Plant Sci.* 12:700200. doi: 10.3389/fpls.2021.700200

Cheng, F., and Cheng, Z. (2015). Research progress on the use of plant allelopathy in agriculture and the physiological and ecological mechanisms of allelopathy. *Front. Plant Sci.* 6:1020. doi: 10.3389/fpls.2015.01020

Chithra, S., Jasim, B., Sachidanandan, P., Jyothis, M., and Radhakrishnan, E. K. (2014). Piperine production by endophytic fungus *Colletotrichum gloeosporioides* isolated from *Piper nigrum*. *Phytomedicine* 21, 534–540. doi: 10.1016/j.phymed.2013.10.020

Chitnis, V. R., Suryanarayanan, T. S., Nataraja, K. N., Prasad, S. R., Oelmüller, R., and Shaanker, R. U. (2020). Fungal endophyte-mediated crop improvement: The way ahead. *Front. Plant Sci.* 11:561007. doi: 10.3389/fpls.2020.561007

Cho, H. S., Park, S. Y., Ryu, C. M., Kim, J. F., Kim, J. G., and Park, S. H. (2007). Interference of quorum sensing and virulence of the rice pathogen *Burkholderia glumae* by an engineered endophytic bacterium. *FEMS Microbiol. Ecol.* 60, 14–23. doi: 10.1111/j.1574-6941.2007.00280.x

Cocking, E. C. (2003). Endophytic colonization of plant roots by nitrogen-fixing bacteria. *Plant Soil* 252, 169–175. doi: 10.1023/A:1024106605806

Collins, N. C., Thordal-Christensen, H., Lipka, V., Bau, S., Kombrink, E., Qiu, J. L., et al. (2003). SNARE-protein-mediated disease resistance at the plant cell wall. *Nature* 425, 973–977. doi: 10.1038/nature02076

Compant, S., Reiter, B., Sessitsch, A., Nowak, J., Clément, C., and Ait Barka, E. (2005). Endophytic colonization of *Vitis vinifera* L. by plant growth-promoting bacterium *Burkholderia* sp. strain PsN. *Appl. Environ. Microbiol.* 71, 1685–1693.

Conn, V. M., Walker, A. R., and Franco, C. M. M. (2008). Endophytic actinobacteria induce defense pathways in *Arabidopsis thaliana*. *Mol. Plant Microbe Interact.* 21, 208–218. doi: 10.1094/MPMI-21-2-0208

Constantin, M. E., De Lamo, F. J., Vlieger, B. V., Rep, M., and Takken, F. L. (2019). Endophyte-mediated resistance in tomato to *Fusarium oxysporum* is independent of ET, JA, and SA. *Front. Plant Sci.* 10:979. doi: 10.3389/fpls.2019.00979

Cope-Selby, N., Cookson, A., Squance, M., Donnison, I., Flavell, R., and Farrar, K. (2017). Endophytic bacteria in *Miscanthus* seed: Implications for germination, vertical inheritance of endophytes, plant evolution and breeding. *GCB Bioen.* 9, 57–77. doi: 10.1111/gcbb.12364

Couee, I., Hummel, I., Sulmon, C., Gouesbet, G., and El Amrani, A. (2004). Involvement of polyamines in root development. *Plant Cell Tissue Organ. Cult.* 76, 1–10. doi: 10.1023/A:1025895731017

Das, K., and Roy Choudhury, A. (2014). Reactive oxygen species (ROS) and response of antioxidants as ROS-scavengers during environmental stress in plants. *Front. Environ. Sci.* 2:53. doi: 10.3389/fenvs.2014.00053

De Hita, D., Fuentes, M., Zamarreño, A. M., Ruiz, Y., and Garcia-Mina, J. M. (2020). Culturable bacterial endophytes from sedimentary humic acid-treated plants. *Front. Plant Sci.* 11:837. doi: 10.3389/fpls.2020.00837

Defez, R., Esposito, R., Angelini, A., and Bianco, C. (2016). Overproduction of indole-3-acetic acid in free-living rhizobia induces transcriptional changes resembling those occurring inside nodule bacteroids. *Mol. Plant Microbe Interact.* 29, 484–495. doi: 10.1094/MPMI-01-16-0010-R

del Barrio-Duque, A., Ley, J., Samad, A., Antonielli, L., Sessitsch, A., and Compant, S. (2019). Beneficial endophytic bacteria-*Serendipita indica* interaction for crop enhancement and resistance to phytopathogens. *Front. Microbiol.* 10:2888. doi: 10.3389/fmicb.2019.02888

Delgado-Sánchez, P., Jiménez-Bremont, J. F., Guerrero-González, Mde, L., and Flores, J. (2013). Effect of fungi and light on seed germination of three *Opuntia* species from semiarid lands of central Mexico. *J. Plant Res.* 126, 643–649. doi: 10.1007/s10265-013-0558-2

Deng, X., Song, X., Halifu, S., Yu, W., and Song, R. (2020). Effects of dark septate endophytes strain A024 on damping-off biocontrol, plant growth, and the rhizosphere soil environment of *Pinus sylvestris* var. *mongolica* annual seedlings. *Plants* 9:913. doi: 10.3390/plants9070913

Ding, L., Xu, H., Yi, H., Yang, L., Kong, Z., Zhang, L., et al. (2011). Resistance to hemi-biotrophic *F. graminearum* infection is associated with coordinated and ordered expression of diverse defense signaling pathways. *PLoS One* 6:e19008.

Dinkins, R. D., Nagabhyru, P., Graham, M. A., Boykin, D., and Schardl, C. L. (2017). Transcriptome response of *Lolium arundinaceum* to its fungal endophyte *Epichloë coenophiala*. *New Phytol.* 213, 324–337. doi: 10.1111/nph.14103

Dong, C.-J., Wang, L.-L., Li, Q., and Shang, Q.-M. (2019). Bacterial communities in the rhizosphere, phyllosphere and endosphere of tomato plants. *PLoS One* 14:e0223847. doi: 10.1371/journal.pone.0223847

Dong, Y. H., Gusti, A. R., Zhang, Q., Xu, J. L., and Zhang, L. H. (2002). Identification of quorum-quenching N-acyl homoserine lactonases from *Bacillus* species. *Appl. Environ. Microbiol.* 68, 1754–1759. doi: 10.1128/AEM.68.4.1754-1759.2002

Dubey, A., Saiyam, D., Kumar, A., Hashem, A., Abd\_Allah, E. F., and Khan, M. L. (2021). Bacterial root endophytes: Characterization of their competence and plant growth promotion in soybean (*Glycine max* (L.) Merr.) under drought stress. *Int. J. Environ. Res. Public Health* 18:931. doi: 10.3390/ijerph18030931

Dutta, D., Puzari, K. C., Gogoi, R., and Dutta, P. (2014). Endophytes: Exploitation as a tool in plant protection. *Brazil. Arch. Biol. Technol.* 57, 621–629. doi: 10.1590/S1516-8913201402043

Egamberdieva, D., Wirth, S. J., Shurigin, V. V., Hashem, A., and Abd\_Allah, E. F. (2017). Endophytic bacteria improve plant growth, symbiotic performance of chickpea (*Cicer arietinum* L.) and induce suppression of root rot caused by *Fusarium solani* under salt stress. *Front. Microbiol.* 8:1887. doi: 10.3389/fmicb.2017.01887

Eid, A. M., Fouda, A., Abdel-Rahman, M. A., Salem, S. S., Elsaied, A., Oelmüller, R., et al. (2021). Harnessing bacterial endophytes for promotion of plant growth and biotechnological applications: An overview. *Plants* 10:935. doi: 10.3390/plants10050935

Fadiji, A. E., and Babalola, O. O. (2020). Elucidating mechanisms of endophytes used in plant protection and other bioactivities with multifunctional prospects. *Front. Bioeng. Biotechnol.* 8:467. doi: 10.3389/fbioe.2020.00467

Fan, D., Subramanian, S., and Smith, D. L. (2020). Plant endophytes promote growth and alleviate salt stress in *Arabidopsis thaliana*. *Sci. Rep.* 10, 1–18. doi: 10.1038/s41598-020-69713-5

FAO (2021). *Climate change fans spread of pests and threatens plants and crops, new FAO study*. Rome: FAO.

Fasusi, O. A., Cruz, C., and Babalola, O. O. (2021). Agricultural sustainability: Microbial biofertilizers in rhizosphere management. *Agriculture* 11:163. doi: 10.3390/agriculture11020163

Fatima, U., and Senthil-Kumar, M. (2015). Plant and pathogen nutrient acquisition strategies. *Front. Plant Sci.* 6:750. doi: 10.3389/fpls.2015.00750

Firricioli, A., Khorasani, M., Frank, A. C., and Doty, S. L. (2020). Influences of climate on phyllosphere endophytic bacterial communities of wild poplar. *Front. Plant Sci.* 11:203. doi: 10.3389/fpls.2020.00203

Fouda, A., Eid, A. M., Elsaied, A., El-Beley, E. F., Barghoth, M. G., Azab, E., et al. (2021). Plant growth-promoting endophytic bacterial community inhabiting the leaves of *Pulicaria incisa* (Lam.) DC inherent to arid regions. *Plants* 10:76. doi: 10.3390/plants10010076

Frank, A. C., Saldierna Guzmán, J. P., and Shay, J. E. (2017). Transmission of bacterial endophytes. *Microorganisms* 5:70. doi: 10.3390/microorganisms5040070

Frederix, M., and Downie, J. A. (2011). Quorum sensing: Regulating the regulators. *Adv. Microb. Physiol.* 58, 23–80. doi: 10.1111/1574-6976.12004

Gaiero, J. R., McCall, C. A., Thompson, K. A., Day, N. J., Best, A. S., and Dunfield, K. E. (2013). Inside the root microbiome: Bacterial root endophytes and plant growth promotion. *Am. J. Bot.* 100, 1738–1750. doi: 10.3732/ajb.1200572

Gajera, H. P., and Vakharia, D. N. (2012). Production of lytic enzymes by *Trichoderma* isolates during in vitro antagonism with *Aspergillus niger*, the causal agent of collar rot of peanut. *Braz. J. Microbiol.* 43, 43–52. doi: 10.1590/S1517-83822012000100005

Gamalerio, E., Marzachi, C., Galetto, L., Veratti, F., Massa, N., and Bona, E. (2017). An 1-aminocyclopropane-1-carboxylate (ACC) deaminase-expressing endophyte increases plant resistance to flavescence dorée phytoplasma infection. *Plant Biosyst.* 151, 331–340. doi: 10.1080/11263504.2016.1174172

Gond, S. K., Bergen, M. S., Torres, M. S., and White, J. F. Jr. (2015). Endophytic *Bacillus* spp. produce antifungal lipopeptides and induce host defence gene expression in maize. *Microbiol. Res.* 172, 79–87. doi: 10.1016/j.micres.2014.11.004

Gos, F. M., Savi, D. C., Shaaban, K. A., Thorson, J. S., Aluizio, R., Possiede, Y. M., et al. (2017). Antibacterial activity of endophytic actinomycetes isolated from the medicinal plant *Vochysia divergens* (Pantanal, Brazil). *Front. Microbiol.* 8:1642. doi: 10.3389/fmicb.2017.01642

Gouda, S., Das, G., Sen, S. K., Shin, H. S., and Patra, J. K. (2016). Endophytes: A treasure house of bioactive compounds of medicinal importance. *Front. Microbiol.* 7:1538. doi: 10.3389/fmicb.2016.01538

Grabka, R., d'Entremont, T. W., Adams, S. J., Walker, A. K., Tanney, J. B., Abbasi, P. A., et al. (2022). Fungal endophytes and their role in agricultural plant protection against pests and pathogens. *Plants* 11:384. doi: 10.3390/plants11030384

- Granada, C. E., Passaglia, L. M., De Souza, E. M., and Sperotto, R. A. (2018). Is phosphate solubilization the forgotten child of plant growth-promoting rhizobacteria? *Front. Microbiol.* 9:2054. doi: 10.3389/fmicb.2018.0205
- Grobelak, A., and Hiller, J. (2017). Bacterial siderophores promote plant growth: Screening of catechol and hydroxamate siderophores. *Int. J. Phytoremed.* 19, 825–833. doi: 10.1080/15226514
- Gu, Q., Yang, Y., Yuan, Q., Shi, G., Wu, L., Lou, Z., et al. (2017). Bacillomycin D produced by *Bacillus amyloliquefaciens* is involved in the antagonistic interaction with the plant-pathogenic fungus *Fusarium graminearum*. *Appl. Environ. Microbiol.* 83, e1075–e1017. doi: 10.1128/AEM.01075-17
- Gudesblat, G. E., Torres, P. S., and Vojno, A. A. (2009). Stomata and pathogens: Warfare at the gates. *Plant Sig. Behav.* 4, 1114–1116. doi: 10.4161/psb.4.12.10062
- Gupta, G., Panwar, J., Akhtar, M. S., and Jha, P. N. (2012). “Endophytic nitrogen-fixing bacteria as biofertilizer,” in *Sustainable agriculture reviews*, ed. E. Lichtfouse (Dordrecht: Springer), 183–221. doi: 10.1007/978-94-007-5449-2\_8
- Gupta, R., Singh, A., Srivastava, M., Singh, V., Gupta, M. M., and Pandey, R. (2017). Microbial modulation of bacoside A biosynthetic pathway and systemic defense mechanism in *Bacopa monnieri* under *Meloidogyne incognita* stress. *Sci. Rep.* 7, 1–11. doi: 10.1038/srep41867
- Haidar, R., Deschamps, A., Roudet, J., Calvo-Garrido, C., Bruez, E., Rey, P., et al. (2016). Multi-organ screening of efficient bacterial control agents against two major pathogens of grapevine. *Biol. Control.* 92, 55–65. doi: 10.1016/j.biocontrol.2015.09.003
- Hamayun, M., Hussain, A., Khan, S. A., Kim, H. Y., Khan, A. L., Waqas, M., et al. (2017). *Gibberellins* producing endophytic fungus *Porostereum spadiceum* AGH786 rescues growth of salt affected soybean. *Front. Microbiol.* 8:686. doi: 10.3389/fmicb.2017.00686
- Harini, K., Ajila, V., and Hegde, S. (2013). *Bdellovibrio bacteriovorus*: A future antimicrobial agent? *J. Indian Soc. Periodontol.* 17:823. doi: 10.4103/0972-124X.124534
- Harman, G. E., Howell, C. R., Viterbo, A., Chet, I., and Lorito, M. (2004). Trichoderma species—opportunistic, avirulent plant symbionts. *Nat. Rev. Microbiol.* 2, 43–56. doi: 10.1038/nrmicro797
- Harsonowati, W., Marian, M., Surono, and Narisawa, K. (2020). The effectiveness of a dark septate endophytic fungus, *Cladophialophora chaetospora* SK51, to mitigate strawberry fusarium wilt disease and with growth promotion activities. *Front. Microbiol.* 11:585. doi: 10.3389/fmicb.2020.00585
- Hassan, S. E. D. (2017). Plant growth-promoting activities for bacterial and fungal endophytes isolated from medicinal plant of *Teucrium polium* L. *J. Adv. Res.* 8, 687–695. doi: 10.1016/j.jare.2017.09.001
- Hazarika, S. N., Saikia, K., Borah, A., and Thakur, D. (2021). Prospecting endophytic bacteria endowed with plant growth promoting potential isolated from *Camellia sinensis*. *Front. Microbiol.* 12:738058. doi: 10.3389/fmicb.2021.738058
- Hellwig, V., Grothe, T., Mayer-Bartschmid, A. N. K. E., Endermann, R., Geschke, F. U., Henkel, T., et al. (2002). Altersetin, a new antibiotic from cultures of endophytic *Alternaria* spp. Taxonomy, fermentation, isolation, structure elucidation and biological activities. *J. Antibiot.* 55, 881–892. doi: 10.1002/chin.200312204
- Hennessy, L. M., Popay, A. J., Finch, S. C., Clearwater, M. J., and Cave, V. M. (2016). Temperature and plant genotype alter alkaloid concentrations in ryegrass infected with an *Epichloë* endophyte and this affects an insect herbivore. *Front. Plant Sci.* 7:1097. doi: 10.3389/fpls.2016.01097
- Howden, A. J. M., and Huitema, E. (2012). Effector-triggered post-translational modifications and their role in suppression of plant immunity. *Front. Plant Sci.* 3:160. doi: 10.3389/fpls.2022.879366
- Huang, H., Ullah, F., Zhou, D. X., Yi, M., and Zhao, Y. (2019). Mechanisms of ROS regulation of plant development and stress responses. *Front. Plant Sci.* 10:800. doi: 10.3389/fpls.2019.00800
- Isah, T. (2019). Stress and defense responses in plant secondary metabolites production. *Biol. Res.* 52:39. doi: 10.1186/s40659-019-0246-3
- Ismail, M. A., Amin, M. A., Eid, A. M., Hassan, S. E. D., Mahgoub, H. A., Lashin, I., et al. (2021). Comparative Study between exogenously applied plant growth hormones versus metabolites of microbial endophytes as plant growth-promoting for *Phaseolus vulgaris* L. *Cells* 10:1059. doi: 10.3390/cells10051059
- Jahan, M., Mahallati, M. N., Amiri, M. B., and Ehyayi, H. R. (2013). Radiation absorption and use efficiency of sesame as affected by biofertilizers inoculation in a low input cropping system. *Ind. Crops Prod.* 43, 606–611. doi: 10.1016/j.indcrop.2012.08.012
- James, E. K., Olivares, F. L., de Oliveira, A. L. M., and dos Reis, F. B. (2001). Further observations on the interaction between sugar cane and *Gluconacetobacter diazotrophicus* under laboratory and greenhouse conditions. *J. Exp. Bot.* 52, 747–760. doi: 10.1093/jexbot/52.357.747
- Ji, S. H., Gururani, M. A., and Chun, S. C. (2014). Isolation and characterization of plant growth promoting endophytic diazotrophic bacteria from Korean rice cultivars. *Microbiol. Res.* 169, 83–98. doi: 10.1016/j.micres.2013.06.003
- Jiao, R., Cai, Y., He, P., Munir, S., Li, X., Wu, Y., et al. (2021). *Bacillus amyloliquefaciens* YN201732 produces lipopeptides with promising biocontrol activity against fungal pathogen *Erysiphe cichoracearum*. *Front. Cell. Infect. Microbiol.* 11:598999. doi: 10.3389/fcimb.2021.598999
- Khare, E., Mishra, J., and Arora, N. K. (2018). Multifaceted interactions between endophytes and plant: Developments and prospects. *Front. Microbiol.* 9:2732. doi: 10.3389/fmicb.2018.02732
- Kandel, S. L., Firrincieli, A., Joubert, P. M., Okubara, P. A., Leston, N. D., and McGeorge, K. M. (2017a). An in vitro study of bio-control and plant growth promotion potential of salicaceae endophytes. *Front. Microbiol.* 8:386. doi: 10.3389/FMICB.2017.00386/BIBTEX
- Kandel, S. L., Joubert, P. M., and Doty, S. L. (2017b). Bacterial endophyte colonization and distribution within plants. *Microorganisms* 5:77. doi: 10.3390/microorganisms5040077
- Kang, S. M., Radhakrishnan, R., You, Y. H., Joo, G. J., Lee, I. J., Lee, K. E., et al. (2014). Phosphate solubilizing *Bacillus megaterium* mj1212 regulates endogenous plant carbohydrates and amino acids contents to promote mustard plant growth. *Indian J. Microbiol.* 54, 427–433. doi: 10.1007/s12088-014-0476-6
- Kant, M. R., Jonckheere, W., Knegt, B., Lemos, F., Liu, J., Schimmel, B. C. J., et al. (2015). Mechanisms and ecological consequences of plant defence induction and suppression in herbivore communities. *Ann. Bot.* 115, 1015–1051. doi: 10.1093/aob/mcv054
- Karre, S., Kumar, A., Dhokane, D., and Kushalappa, A. C. (2017). Metabolite-transcriptome profiling of barley reveals induction of chitin elicitor receptor kinase gene (HvCERK1) conferring resistance against *Fusarium graminearum*. *Plant Mol. Biol.* 93, 247–267. doi: 10.1007/s11103-016-0559-3
- Kaul, S., Sharma, T., and Dhar, M. K. (2016). “Omics” tools for better understanding the plant–endophyte interactions. *Front. Plant Sci.* 7:955. doi: 10.3389/fpls.2016.00955
- Kavroulakis, N., Ntougias, S., Zervakis, G. I., Ehaliotis, C., Haralampidis, K., and Papadopoulou, K. K. (2007). Role of ethylene in the protection of tomato plants against soil-borne fungal pathogens conferred by an endophytic *Fusarium solani* strain. *J. Exp. Bot.* 58, 3853–3864. doi: 10.1093/jxb/erm230
- Kawasaki, A., Donn, S., Ryan, P. R., Mathesius, U., Devilla, R., and Jones, A. (2016). Microbiome and exudates of the root and rhizosphere of *Brachypodium distachyon*, a model for wheat. *PLoS One* 11:e0164533. doi: 10.1371/JOURNAL.PONE.0164533
- Khalil, A. M. A., Hassan, S. E. D., Alsharif, S. M., Eid, A. M., Eweis, E. E. D., Azab, E., et al. (2021). Isolation and characterization of fungal endophytes isolated from medicinal plant *Ephedra pachyclada* as plant growth-promoting. *Biomolecules* 11:140. doi: 10.3390/biom11020140
- Khan, A. L., Hamayun, M., Kang, S. M., Kim, Y. H., Jung, H. Y., Lee, J. H., et al. (2012). Endophytic fungal association via gibberellins and indole acetic acid can improve plant growth under abiotic stress: An example of *Paecilomyces formosus* LHL10. *BMC Microbiol.* 12:3. doi: 10.1186/1471-2180-12-3
- Khan, A. L., Waqas, M., Kang, S. M., Al-Harrasi, A., Hussain, J., Al-Rawahi, A., et al. (2014). Bacterial endophyte *Sphingomonas* sp. LK11 produces gibberellins and IAA and promotes tomato plant growth. *J. Microbiol.* 52, 689–695. doi: 10.1007/s12275-014-4002-7
- Khati, P., Parul, Bhatt, P., Nisha, Kumar, R., and Sharma, A. (2018). Effect of nanozeolite and plant growth promoting rhizobacteria on maize. *3Biotech* 8:141. doi: 10.1007/s13205-018-1142-1
- Kong, P., and Hong, C. (2020). Endophytic *Burkholderia* sp. SSG as a potential biofertilizer promoting boxwood growth. *PeerJ* 8:e9547. doi: 10.7717/peerj.9547
- Kou, M. Z., Bastías, D. A., Christensen, M. J., Zhong, R., Nan, Z. B., and Zhang, X. X. (2021). The plant salicylic acid signalling pathway regulates the infection of a biotrophic pathogen in grasses associated with an *Epichloë* endophyte. *J. Fungi* 7:633. doi: 10.3390/jof7080633
- Kukreti, B., Sharma, A., Chaudhary, P., Agri, U., and Maithani, D. (2020). Influence of nanosilicon dioxide along with bioinoculants on *Zea mays* and its rhizospheric soil. *3Biotech* 10:345. doi: 10.1007/s13205-020-02329-8
- Kumari, S., Sharma, A., Chaudhary, P., and Khati, P. (2020). Management of plant vigor and soil health using two agrisafe nanocompounds and plant growth promotory rhizobacteria in Fenugreek. *3Biotech* 10, 1–11. doi: 10.1007/s13205-020-02448-2



- Kung, S. H., and Almeida, R. P. P. (2014). Biological and genetic factors regulating natural competence in a bacterial plant pathogen. *Microbiology* 160, 37–46. doi: 10.1099/mic.0.070581-0
- Lang, M., Zhou, J., Chen, T., Chen, Z., Malik, K., and Li, C. (2021). Influence of interactions between nitrogen, phosphorus supply and epichloëbrassicola on growth of wild barley (*Hordeum brevisubulatum*). *J. Fungi* 7:615. doi: 10.3390/jof7080615
- Larkin, R. P., and Fravel, D. R. (1999). Mechanisms of action and dose-response relationships governing biological control of Fusarium wilt of tomato by nonpathogenic Fusarium spp. *Phytopathology* 89, 1152–1161. doi: 10.1094/PHYTO.1999.89.12.1152
- LaSarre, B., and Federle, M. J. (2013). Exploiting quorum sensing to confuse bacterial pathogens. *Microbiol. Mol. Biol. Rev.* 77, 73–111. doi: 10.1128/MMBR.00046-12
- Lebeis, S. L., Paredes, S. H., Lundberg, D. S., Breakfield, N., Gehring, J., McDonald, M., et al. (2015). Salicylic acid modulates colonization of the root microbiome by specific bacterial taxa. *Science* 349, 860–864. doi: 10.1126/science.aaa8764
- Leon-Reyes, A., Spoel, S. H., De Lange, E. S., Abe, H., Kobayashi, M., Tsuda, S., et al. (2009). Ethylene modulates the role of NONEXPRESSOR OF PATHOGENESIS-RELATED GENES1 in cross talk between salicylate and jasmonate signaling. *Plant Physiol.* 149, 1797–1809. doi: 10.1104/pp.108.133926
- Lery, L. M. S., Hemery, A. S., Nogueira, E. M., von Krüger, W. M. A., and Bisch, P. M. (2011). Quantitative proteomic analysis of the interaction between the endophytic plant-growth-promoting bacterium *Gluconacetobacter diazotrophicus* and sugarcane. *Mol. Plant Microbe Interact.* 24, 562–576. doi: 10.1094/MPMI-08-10-0178
- Li, S., Pi, J., Zhu, H., Yang, L., Zhang, X., and Ding, W. (2021). Caffeic acid in tobacco root exudate defends tobacco plants from infection by *Ralstonia solanacearum*. *Front. Plant Sci.* 12:690586. doi: 10.3389/fpls.2021.690586
- Li, X. H., Han, X. H., Qin, L. L., He, J. L., Cao, Z. X., Gu, Y. C., et al. (2019). Isochromanes from *Aspergillus fumigatus*, an endophytic fungus from *Cordyceps sinensis*. *Nat. Product Res.* 33, 1870–1875. doi: 10.1080/14786419.2018.1478824
- Limoli, D. H., Jones, C. J., and Wozniak, D. J. (2015). Bacterial extracellular polysaccharides in biofilm formation and function. *Microbiol. Spectrum* 3, 3–3. doi: 10.1128/microbiolspec.MB-0011-2014
- Lindow, S. E., and Brandl, M. T. (2003). Microbiology of the phyllosphere MINIREVIEW microbiology of the phyllosphere. *Appl. Environ. Microbiol.* 69, 1875–1883. doi: 10.1128/AEM.69.4.1875
- Lingqi, Z., Su, G., Hua, S., and Rongcheng, W. (1999). Isolation, determination and aroma product characterization of fungus producing irone. *Jun Wu Xi Tong Mycosyst.* 18, 49–54.
- Litwin, A., Nowak, M., and Róžalska, S. (2020). Entomopathogenic fungi: Unconventional applications. *Rev Environ Sci Biotechnol.* 19, 23–42. doi: 10.1007/s11157-020-09525-1
- Liu, H., Carvalhais, L. C., Crawford, M., Singh, E., Dennis, P. G., Pieterse, C. M., et al. (2017). Inner plant values: Diversity, colonization and benefits from endophytic bacteria. *Front. Microbiol.* 8:2552. doi: 10.3389/fmicb.2017.02552
- Liu, H., Wu, M., Liu, J., Qu, Y., Gao, Y., and Ren, A. (2020). Tripartite interactions between endophytic fungi, arbuscular mycorrhizal fungi, and *Leymus chinensis*. *Microb. Ecol.* 79, 98–109. doi: 10.1007/s00248-019-01394-8
- Liu, W., Sun, Y., Shen, R., Dang, X., Liu, X., and Sui, F. (2018). A chemotaxis-like pathway of *Azorhizobium caulinodans* controls flagella-driven motility, which regulates biofilm formation, exopolysaccharide biosynthesis, and competitive nodulation. *Mol. Plant Microbe Interact.* 31, 737–749. doi: 10.1094/MPMI-12-17-0290-R
- Loughner, R., Goldman, K., Loeb, G., and Nyrop, J. (2008). Influence of leaf trichomes on predatory mite (*Typhlodromus pyri*) abundance in grape varieties. *Exp. Appl. Acarol.* 45, 111–122. doi: 10.1007/s10493-008-9183-5
- Lu, H., Wei, T., Lou, H., Shu, X., and Chen, Q. (2021). A critical review on communication mechanism within plant-endophytic fungi interactions to cope with biotic and abiotic stresses. *J. Fungi* 7:719. doi: 10.3390/jof7090719
- Maafi, Z. T., Taheri, Z. M., and Subbotin, S. A. (2013). First report of the giant stem nematode. *Ditylenchus gigas*, from broad bean in Iran. *Plant Dis.* 97, 1005–1005. doi: 10.1094/PDIS-01-13-0069-PDN
- Macedo-Raygoza, G. M., Valdez-Salas, B., Prado, F. M., Prieto, K. R., Yamaguchi, L. F., Kato, M. J., et al. (2019). *Enterobacter cloacae*, an endophyte that establishes a nutrient-transfer symbiosis with banana plants and protects against the black sigatoka pathogen. *Front. Microbiol.* 10:804. doi: 10.3389/fmicb.2019.00804
- Madhaiyan, M., Peng, N., Te, N. S., Hsin, C. I., Lin, C., Lin, F., et al. (2013). Improvement of plant growth and seed yield in *Jatropha curcas* by a novel nitrogen-fixing root associated *Enterobacter* species. *Biotechnol. Biofuels* 6, 1–13. doi: 10.1186/1754-6834-6-140
- Maela, M. P., van der Walt, H., and Serepa-Dlamini, M. H. (2022). The antibacterial and anticancer activities and bioactive constituents' identification of *Alectra sessiliflora* bacterial endophytes. *Front. Microbiol.* 13:870821. doi: 10.3389/fmicb.2022.870821
- Mahanty, T., Bhattacharjee, S., Goswami, M., Bhattacharyya, P., Das, B., Ghosh, A., et al. (2017). Biofertilizers: A potential approach for sustainable agriculture development. *Environ. Sci. Pollut. Res.* 24, 3315–3335.
- Mandym, K., Loughin, T., and Jumpponen, A. (2010). Isolation and morphological and metabolic characterization of common endophytes in annually burned tallgrass prairie. *Mycologia* 102, 813–821.
- Manganyi, M. C., Regnier, T., Tchatchouang, C. D. K., Bezuidenhout, C. C., and Ateba, C. N. (2019). Antibacterial activity of endophytic fungi isolated from *Sceletium tortuosum* L. (Kougoed). *Ann. Microbiol.* 69, 659–663. doi: 10.1007/s13213-019-1444-5
- Mansfield, J., Genin, S., Magori, S., Citovsky, V., Sriariyanum, M., Ronald, P., et al. (2012). Top 10 plant pathogenic bacteria in molecular plant pathology. *Mol. Plant Pathol.* 13, 614–629. doi: 10.1111/j.1364-3703.2012.00804.x
- Martinez-Garcia, P. M., Ruano-Rosa, D., Schilero, E., Prieto, P., Ramos, C., and Rodríguez-Palenzuela, P. (2015). Complete genome sequence of *Pseudomonas fluorescens* strain P1CF7, an indigenous root endophyte from olive (*Olea europaea* L.) and effective biocontrol agent against *Verticillium dahlia*. *Stand. Genomic Sci.* 10:10. doi: 10.1186/1944-3277-10-10
- Martinho, V., dos Santos Lima, L. M., Barros, C. A., Ferrari, V. B., Passarini, M. R. Z., Santos, L. A., et al. (2019). Enzymatic potential and biosurfactant production by endophytic fungi from mangrove forest in Southeastern Brazil. *AMB Express* 9, 1–8. doi: 10.1186/s13568-019-0850-1
- Matušínský, P., Sedláková, B., and Běla, D. (2022). Compatible interaction of *Brachypodium distachyon* and endophytic fungus *Microdochium bolleyi*. *PLoS One* 17:e0265357. doi: 10.1371/journal.pone.0265357
- McNeely, D., Chanyi, R. M., Dooley, J. S., Moore, J. E., and Koval, S. F. (2017). Biocontrol of *Burkholderia cepacia* complex bacteria and bacterial phytopathogens by *Bdellovibrio bacteriovorus*. *Can. J. Microbiol.* 63, 350–358. doi: 10.1139/cjm-2016-0612
- Mejía, L. C., Herre, E. A., Sparks, J. P., Winter, K., García, M. N., Van Bael, S. A., et al. (2014). Pervasive effects of a dominant foliar endophytic fungus on host genetic and phenotypic expression in a tropical tree. *Front. Microbiol.* 5:479. doi: 10.3389/fmicb.2014.00479
- Melotto, M., Underwood, W., and He, S. Y. (2008). Role of stomata in plant innate immunity and foliar bacterial diseases. *Annu. Rev. Phytopathol.* 46, 101–122. doi: 10.1146/annurev.phyto.121107.104959
- Mercado-Blanco, J., and Prieto, P. (2012). Bacterial endophytes and root hairs. *Plant Soil* 361, 301–306.
- Metwally, A. M., Kadry, H. A., Atef, A., Mohammad, A. E. I., Ma, G., Cutler, S. J., et al. (2014). Nigrospora a new isochromene derivative from the endophytic fungus *Nigrospora sphaerica*. *Phytochem. Lett.* 7, 1–5. doi: 10.1016/j.phytol.2013.09.001
- Meyer, K. M., and Leveau, J. H. (2012). Microbiology of the phyllosphere: A playground for testing ecological concepts. *Oecologia* 168, 621–629. doi: 10.1007/s00442-011-2138-2
- Miotto-Vilanova, L., Jacquard, C., Courteaux, B., Wortham, L., Michel, J., Clément, C., et al. (2016). *Burkholderia phytofirmans* PsJN confers grapevine resistance against *Botrytis cinerea* via a direct antimicrobial effect combined with a better resource mobilization. *Front. Plant Sci.* 7:1236. doi: 10.3389/fpls.2016.01236
- Mishra, A., Singh, S. P., Mahfooz, S., Singh, S. P., Bhattacharya, A., Mishra, N., et al. (2018). Endophyte-mediated modulation of defense-responsive genes and systemic resistance in *Withania somnifera* (L.) Dunal under Alternaria alternata stress. *Appl. Environ. Microbiol.* 84, e2845–e2817. doi: 10.1128/AEM.02845-17
- Mishra, R., Kushveer, J. S., Khan, M. I. K., Pagal, S., Meena, C. K., Murali, A., et al. (2020). 2,4-Di-tert-butylphenol isolated from an endophytic fungus, *Daldinia eschscholtzii*, reduces virulence and quorum sensing in *Pseudomonas aeruginosa*. *Front. Microbiol.* 11:1668. doi: 10.3389/fmicb.2020.01668
- Mishra, S., and Arora, N. K. (2012). Evaluation of rhizospheric *Pseudomonas* and *Bacillus* as biocontrol tool for *Xanthomonas campestris* pv *campestris*. *World J. Microbiol. Biotechnol.* 28, 693–702. doi: 10.1007/s11274-011-0865-5
- Mitter, B., Pfaffenbichler, N., Flavell, R., Compant, S., Antonielli, L., Petric, A., et al. (2017). A new approach to modify plant microbiomes and traits by introducing beneficial bacteria at flowering into progeny seeds. *Front. Microbiol.* 8:11. doi: 10.3389/fmicb.2017.00011
- Mohamad, O. A., Li, L., Ma, J. B., Hatab, S., Xu, L., Guo, J. W., et al. (2018). Evaluation of the antimicrobial activity of endophytic bacterial populations from



Chinese traditional medicinal plant licorice and characterization of the bioactive secondary metabolites produced by *Bacillus atrophaeus* against *Verticillium dahliae*. *Front. Microbiol.* 9:924. doi: 10.3389/fmicb.2018.00924

Molina-Montenegro, M. A., Acuña-Rodríguez, I. S., Torres-Díaz, C., Gundel, P. E., and Dreyer, I. (2020). Antarctic root endophytes improve physiological performance and yield in crops under salt stress by enhanced energy production and Na<sup>+</sup> sequestration. *Sci. Rep.* 10, 1–10. doi: 10.1038/s41598-020-62544-4

Monteiro, R. A., Balsanelli, E., Tuleski, T., Faoro, H., Cruz, M. L., and Wassem, R. (2012). Genomic comparison of the endophyte *Herbaspirillum seropedicae* SmR1 and the phytopathogen *Herbaspirillum rubrisubalbicans* M1 by suppressive subtractive hybridization and partial genome sequencing. *FEMS Microbiol. Ecol.* 80, 441–451. doi: 10.1111/j.1574-6941.2012.01309.x

Morelli, M., Bahar, O., Papadopoulou, K. K., Hopkins, D. L., and Obradović, A. (2020). Role of endophytes in plant health and defense against pathogens. *Front. Plant Sci.* 11:1312. doi: 10.3389/fpls.2020.01312

Mousa, W. K., and Raizada, M. N. (2013). The diversity of anti-microbial secondary metabolites produced by fungal endophytes: An interdisciplinary perspective. *Front. Microbiol.* 4:65. doi: 10.3389/fmicb.2013.00065

Muangthong, A., Youpensuk, S., and Rerkasem, B. (2015). Isolation and characterisation of endophytic nitrogen fixing bacteria in sugarcane. *Trop. Life Sci. Res.* 26:41.

Murugayah, S. A., and Gerth, M. L. (2019). Engineering quorum quenching enzymes: Progress and perspectives. *Biochem Soc. Trans.* 47, 793–800. doi: 10.1042/BST20180165

Nair, D. N., and Padmavathy, S. (2014). Impact of endophytic microorganisms on plants, environment and humans. *Sci. World J.* 2014:250693. doi: 10.1155/2014/250693

Nanda, S., Mohanty, B., and Joshi, R. K. (2019). *Endophyte-mediated host stress tolerance as a means for crop improvement. Endophytes and secondary metabolites*. Cham: Springer, 677–701. doi: 10.1007/978-3-319-76900-4\_28-1

Nie, P., Li, X., Wang, S., Guo, J., Zhao, H., and Niu, D. (2017). induced systemic resistance against *Botrytis cinerea* by *Bacillus cereus* AR156 through a JA/ET- and NPR1-dependent signaling pathway and activates PAMP-triggered immunity in *Arabidopsis*. *Front. Plant Sci.* 8:238. doi: 10.3389/fpls.2017.00238

Nischitha, R., Vasanthkumari, M. M., Kumaraswamy, B. E., and Shivanna, M. B. (2020). Antimicrobial and antioxidant activities and chemical profiling of *Curvularia tsudae* endophytic in *Cynodon dactylon* (L.) Pers. 3 *Biotech* 10, 1–12. doi: 10.1007/s13205-020-02250-0

Nxumalo, C. I., Ngidi, L. S., Shandu, J. S. E., and Maliehe, T. S. (2020). Isolation of endophytic bacteria from the leaves of *Anredera cordifolia* CIX1 for metabolites and their biological activities. *BMC Complement. Med. Ther.* 20:300. doi: 10.1186/s12906-020-03095-z

Okamoto, T., Shinjo, R., Nishihara, A., Uesaka, K., Tanaka, A., Sugiura, D., et al. (2021). Genotypic variation of endophytic nitrogen-fixing activity and bacterial flora in rice stem based on sugar content. *Front. Plant Sci.* 12:719259. doi: 10.3389/fpls.2021.719259

Oses-Pedraza, R., Torres-Díaz, C., Lavín, P., Retamales-Molina, P., Atala, C., Gallardo-Cerda, J., et al. (2020). Root endophytic *Penicillium* promotes growth of Antarctic vascular plants by enhancing nitrogen mineralization. *Extremophiles* 24, 721–732. doi: 10.1007/s00792-020-01189-7

Otieno, N., Lally, R. D., Kiwanuka, S., Lloyd, A., Ryan, D., Germaine, K. J., et al. (2015). Plant growth promotion induced by phosphate solubilizing endophytic *Pseudomonas* isolates. *Front. Microbiol.* 6:745. doi: 10.3389/fmicb.2015.00745

Oukala, N., Aissat, K., and Pastor, V. (2021). Bacterial endophytes: The hidden actor in plant immune responses against biotic stress. *Plants* 10:1012. doi: 10.3390/plants10051012

Panaccione, D. G., Beaulieu, W. T., and Cook, D. (2014). Bioactive alkaloids in vertically transmitted fungal endophytes. *Funct. Ecol.* 28, 299–314. doi: 10.1111/1365-2435.12076

Pandey, P. K., Samanta, R., and Yadav, R. N. S. (2019). Inside the plant: Addressing bacterial endophytes in biotic stress alleviation. *Arch. Microbiol.* 201, 415–429. doi: 10.1007/s00203-019-01642-y

Pandey, P., Irulappan, V., Bagavathiannan, M. V., and Senthil-Kumar, M. (2017). Impact of Combined abiotic and biotic stresses on plant growth and avenues for crop improvement by exploiting physio-morphological traits. *Front. Plant Sci.* 8:537. doi: 10.3389/fpls.2017.00537

Pansanit, A., and Pripdeevech, P. (2018). Antibacterial secondary metabolites from an endophytic fungus, *Arthrinium* sp. MFLUCC16-1053 isolated from *Zingiber cassumunar*. *Mycology* 9, 264–272. doi: 10.1080/21501203.2018.1481154

Park, S. H., and Eom, A. H. (2007). Effects of mycorrhizal and endophytic fungi on plant community: A microcosm study. *Mycobiology* 35, 186–190. doi: 10.4489/MYCO.2007.35.4.186

Pérez-Bueno, M. L., Pineda, M., and Barón, M. (2019). Phenotyping plant responses to biotic stress by chlorophyll fluorescence imaging. *Front. Plant Sci.* 10:1135. doi: 10.3389/fpls.2019.01135

Pezet, R., and Pont, V. (1990). Ultrastructural observations of pterostilbene fungitoxicity in dormant conidia of *Botrytis cinerea* Pers. *J. Phytopathol.* 129, 19–30. doi: 10.1111/j.1439-0434.1990.tb04286.x

Pieterse, C. M. J., Zamioudis, C., Berendsen, R. L., Weller, D. M., Van Wees, S. C. M., and Bakker, P. A. (2014). Induced systemic resistance by beneficial microbes. *Annu. Rev. Phytopathol.* 52, 347–375. doi: 10.1146/annurev-phyto-082712-102340

Pingping, S., Jianchao, C., Xiaohui, J., and Wenhui, W. (2017). Isolation and characterization of *Bacillus amyloliquefaciens* L-1 for biocontrol of pear ring rot. *Hortic. Plant J.* 3, 183–189.

Portieles, R., Xu, H., Yue, Q., Zhao, L., Zhang, D., Du, L., et al. (2021). Heat-killed endophytic bacterium induces robust plant defense responses against important pathogens. *Sci. Rep.* 11, 1–14. doi: 10.1038/s41598-021-91837-5

Prasannath, K. (2017). Plant defense-related enzymes against pathogens: A review. *AGRIEAST* 11, 38–48. doi: 10.4038/agriest.v11i1.33

Puri, S. C., Nazir, A., Chawla, R., Arora, R., Riyaz-ul-Hasan, S., Amna, T., et al. (2006). The endophytic fungus *Trametes hirsuta* as a novel alternative source of podophyllotoxin and related aryl tetralin lignans. *J. Biotechnol.* 122, 494–510. doi: 10.1016/j.jbiotec.2005.10.015

Qi, D., Zou, L., Zhou, D., Chen, Y., Gao, Z., Feng, R., et al. (2019). Taxonomy and broad-spectrum antifungal activity of *Streptomyces* sp. SCA3-4 isolated from rhizosphere soil of *Opuntia stricta*. *Front. Microbiol.* 10:1390. doi: 10.3389/fmicb.2019.01390

Qian, C. D., Fu, Y. H., Jiang, F. S., Xu, Z. H., Cheng, D. Q., Ding, B., et al. (2014). *Lasiodiplodia* sp. ME4-2, an endophytic fungus from the floral parts of *Viscum coloratum*, produces indole-3-carboxylic acid and other aromatic metabolites. *BMC Microbiol.* 14:297. doi: 10.1186/s12866-014-0297-0

Qualhato, T. F., Lopes, F. A. C., Steindorff, A. S., Brandao, R. S., Jesuino, R. S. A., and Ulhoa, C. J. (2013). Mycoparasitism studies of *Trichoderma* species against three phytopathogenic fungi: Evaluation of antagonism and hydrolytic enzyme production. *Biotechnol. Lett.* 35, 1461–1468. doi: 10.1007/s10529-013-1225-3

Rabiey, M., Hailey, L. E., Roy, S. R., Grenz, K., Al-Zadaji, M. A., Barrett, G. A., et al. (2019). Endophytes vs tree pathogens and pests: Can they be used as biological control agents to improve tree health? *Eur. J. Plant Pathol.* 155, 711–729. doi: 10.1007/s10658-019-01814-y

Rajendran, L., Akila, R., Karthikeyan, G., Raguchander, T., and Samiyappan, R. (2015). Defense related enzyme induction in coconut by endophytic bacteria (EPC 5). *Acta Phytopathol. Entomol. Hung.* 50, 29–43. doi: 10.1556/038.50.2015.14

Rajesh, P. S., and Rai, R. V. (2014). Quorum quenching activity in cell-free lysate of endophytic bacteria isolated from *Pterocarpus santalinus* Linn., and its effect on quorum sensing regulated biofilm in *Pseudomonas aeruginosa* PAO1. *Microbiol. Res.* 169, 561–569. doi: 10.1016/j.micres.2013.10.005

Rajkumar, M., Ae, N., Prasad, M. N. V., and Freitas, H. (2010). Potential of siderophore-producing bacteria for improving heavy metal phytoextraction. *Trends Biotechnol.* 28, 142–149. doi: 10.1016/j.tibtech.2009.12.002

Rashid, M. H. O., Khan, A., Hossain, M. T., and Chung, Y. R. (2017). Induction of systemic resistance against aphids by endophytic *Bacillus velezensis* YC7010 via expressing PHYTOALEXIN DEFICIENT4 in *Arabidopsis*. *Front. Plant Sci.* 8:211. doi: 10.3389/fpls.2017.00211

Rat, A., Naranjo, H. D., Krigas, N., Grigoriadou, K., Maloupa, E., Alonso, A. V., et al. (2021). Endophytic bacteria from the roots of the medicinal plant *Alkanna tinctoria* Tausch (Boraginaceae): Exploration of plant growth promoting properties and potential role in the production of plant secondary metabolites. *Front. Microbiol.* 12:113. doi: 10.1016/j.micres.2018.04.006

Redford, A. J., Bowers, R. M., Knight, R., Linhart, Y., and Fierer, N. (2010). The ecology of the phyllosphere: Geographic and phylogenetic variability in the distribution of bacteria on tree leaves. *Environ. Microbiol.* 12, 2885–2893. doi: 10.1111/j.1462-2920.2010.02258.x

Reininger, V., and Sieber, T. N. (2013). Mitigation of antagonistic effects on plant growth due to root co-colonization by dark septate endophytes and ectomycorrhiza. *Environ. Microbiol. Rep.* 5, 892–898. doi: 10.1111/1758-2229.12091

Rejeb, I. B., Pastor, V., and Mauch-Mani, B. (2014). Plant responses to simultaneous biotic and abiotic stress: Molecular mechanisms. *Plants* 3, 458–475. doi: 10.3390/plants3040458

- Ripa, F. A., Cao, W. D., Tong, S., and Sun, J. G. (2019). Assessment of plant growth promoting and abiotic stress tolerance properties of wheat endophytic fungi. *BioMed Res. Int.* 2019:6105865. doi: 10.1155/2019/6105865
- Ritpitakphong, U., Falquet, L., Vimolstut, A., Berger, A., Métraux, J.-P., and L'Haridon, F. (2016). The microbiome of the leaf surface of *Arabidopsis* protects against a fungal pathogen. *New Phytol.* 210, 1033–1043. doi: 10.1111/nph.13808
- Rodriguez, M. V., Tano, J., Ansaldi, N., Carrau, A., Srebot, M. S., Ferreira, V., et al. (2019). Anatomical and biochemical changes induced by gluconacetobacter diazotrophicus stand up for *Arabidopsis thaliana* seedlings from *Ralstonia solanacearum* infection. *Front. Plant Sci.* 10:1618. doi: 10.3389/fpls.2019.01618
- Romera, F. J., García, M. J., Lucena, C., Martínez-Medina, A., Aparicio, M. A., Ramos, J., et al. (2019). Induced systemic resistance (ISR) and Fe deficiency responses in dicot plants. *Front. Plant Sci.* 10:287. doi: 10.3389/fpls.2019.00287
- Romero, F. M., Marina, M., and Pieckenstain, F. L. (2014). The communities of tomato (*Solanum lycopersicum* L.) leaf endophytic bacteria, analyzed by 16S-ribosomal RNA gene pyrosequencing. *FEMS Microbiol. Lett.* 351, 187–194. doi: 10.1111/1574-6968.12377
- Romero-Arguelles, R., Romo-Sánchez, C. I., Morán-Santibáñez, K., Tamez-Guerra, P., Quintanilla-Licea, R., Orozco-Flores, A. A., et al. (2022). In vitro antitumor activity of endophytic and rhizosphere gram-positive bacteria from *Ibervillea sonorae* (S. Watson) greene against L5178Y-R lymphoma cells. *Int. J. Environ. Res. Public Health* 19:894. doi: 10.3390/ijerph19020894
- Roossinck, M. J., Martin, D. P., and Roumagnac, P. (2015). Plant virus metagenomics: Advances in virus discovery. *Phytopathology* 105, 716–727. doi: 10.1094/PHYTO-12-14-0356-RVW
- Rudrappa, T., Biedrzycki, M. L., Kunjeti, S. G., Donofrio, N. M., Czymbek, K. J., Paul, W. P., et al. (2010). The rhizobacterial elicitor acetoin induces systemic resistance in *Arabidopsis thaliana*. *Commun. Integr. Biol.* 3, 130–138. doi: 10.4161/cib.3.2.10584
- Rutherford, S. T., and Bassler, B. L. (2012). Bacterial quorum sensing: Its role in virulence and possibilities for its control. *Cold Spring Harb. Perspect. Med.* 2:a012427. doi: 10.1101/cshperspect.a012427
- Ryan, R. P., Germaine, K., Franks, A., Ryan, D. J., and Dowling, D. N. (2008). Bacterial endophytes: Recent developments and applications. *FEMS Microbiol. Lett.* 278, 1–9. doi: 10.1111/j.1574-6968.2007.00918.x
- Saber, W. I. A., Ghoneem, K. M., Rashad, Y. M., and Al-Askar, A. A. (2017). *Trichoderma harzianum* WKY1: An indole acetic acid producer for growth improvement and anthracnose disease control in sorghum. *Biocontrol Sci. Technol.* 27, 654–676.
- Samain, E., Aussenac, T., and Selim, S. (2019). The effect of plant genotype, growth stage, and *Mycosphaerella graminicola* strains on the efficiency and durability of wheat-induced resistance by *Paenibacillus* sp. Strain B2. *Front. Plant Sci.* 10:587. doi: 10.3389/fpls.2019.00587
- Samanta, D., Widom, J., Borbat, P. P., Freed, J. H., and Crane, B. R. (2016). Bacterial energy sensor aer modulates the activity of the chemotaxis kinase CheA based on the redox state of the flavin cofactor. *J. Biol. Chem.* 291, 25809–25814. doi: 10.1074/JBC.C116.757492
- Santoyo, G., Moreno-Hagelsieb, G., Del Carmen Orozco-Mosqueda, M., and Glick, B. R. (2016). Plant growth-promoting bacterial endophytes. *Microbiol. Res.* 183, 92–99. doi: 10.1016/j.micres.2015.11.008
- Sarwar, A., Hassan, M. N., Imran, M., Iqbal, M., Majeed, S., Brader, G., et al. (2018). Biocontrol activity of surfactin A purified from *Bacillus* NH-100 and NH-217 against rice bakanae disease. *Microbiol. Res.* 209, 1–13. doi: 10.1016/j.micres.2018.01.006
- Savani, A. K., Bhattacharyya, A., and Baruah, A. (2020). Endophyte mediated activation of defense enzymes in banana plants pre-immunized with covert endophytes. *Indian Phytopathol.* 73, 433–441. doi: 10.1007/s42360-020-00245-8
- Sdiri, Y., Lopes, T., Rodrigues, N., Silva, K., Rodrigues, I., Pereira, J. A., et al. (2022). Biocontrol Ability and production of volatile organic compounds as a potential mechanism of action of olive endophytes against *Colletotrichum acutatum*. *Microorganisms* 10:571. doi: 10.3390/microorganisms10030571
- Seitz, P., and Blokesch, M. (2013). Cues and regulatory pathways involved in natural competence and transformation in pathogenic and environmental Gram-negative bacteria. *FEMS Microbiol. Rev.* 37, 336–363. doi: 10.1111/j.1574-6976.2012.00353.x
- Selosse, M. A., Petrolini, R., Mujica, M. I., Laurent, L., Perez-Lamarque, B., and Figura, T. (2022). The waiting room hypothesis revisited by orchids: Were orchid mycorrhizal fungi recruited among root endophytes? *Ann. Bot.* 129, 259–270. doi: 10.1093/aob/mcab134
- Serrano, M., Coluccia, F., Torres, M., L'Haridon, F., and Métraux, J. P. (2014). The cuticle and plant defense to pathogens. *Front. Plant Sci.* 5:274. doi: 10.3389/fpls.2014.00274
- Shahzad, R., Khan, A. L., Bilal, S., Asaf, S., and Lee, I. J. (2018). What is there in seeds? Vertically transmitted endophytic resources for sustainable improvement in plant growth. *Front. Plant Sci.* 9:24. doi: 10.3389/fpls.2018.00024
- Shahzad, R., Waqas, M., Khan, A. L., Al-Hosni, K., Kang, S. M., Seo, C. W., et al. (2017). Indoleacetic acid production and plant growth promoting potential of bacterial endophytes isolated from rice (*Oryza sativa* L.) seeds. *Acta Biol. Hung.* 68, 175–186. doi: 10.1556/018.68.2017.2.5
- Singh, D., Geat, N., Rajawat, M. V. S., Prasanna, R., Kar, A., Singh, A. M., et al. (2018). Prospecting endophytes from different Fe or Zn accumulating wheat genotypes for their influence as inoculants on plant growth, yield, and micronutrient content. *Ann. Microbiol.* 68, 815–833. doi: 10.1007/s13213-018-1388-1
- Singh, S. K., Strobel, G. A., Knighton, B., Geary, B., Sears, J., and Ezra, D. (2011). An endophytic *Phomopsis* sp. possessing bioactivity and fuel potential with its volatile organic compounds. *Microb. Ecol.* 61, 729–739. doi: 10.1007/s00248-011-9818-7
- Singh, S. P., and Gaur, R. (2017). Endophytic *Streptomyces* spp. underscore induction of defense regulatory genes and confers resistance against *Sclerotium rolfsii* in chickpea. *Biol. Control.* 104, 44–56. doi: 10.1016/j.biocontrol.2016.10.011
- Song, Y., Chen, D., Lu, K., Sun, Z., and Zeng, R. (2015). Enhanced tomato disease resistance primed by arbuscular mycorrhizal fungus. *Front. Plant Sci.* 6:786. doi: 10.3389/fpls.2015.00786
- Spaepen, S., Vanderleyden, J., and Remans, R. (2007). Indole-3-acetic acid in microbial and microorganism-plant signaling. *FEMS Microbiol. Rev.* 31, 425–448. doi: 10.1111/j.1574-6976.2007.00072.x
- Specian, V., Sarragiotto, M. H., Pamphile, J. A., and Clemente, E. (2012). Chemical characterization of bioactive compounds from the endophytic fungus *Diaporthe helianthi* isolated from *Luehea divaricata*. *Braz. J. Microbiol.* 43, 1174–1182. doi: 10.1590/S1517-838220120003000045
- Steyaert, J. M., Ridgway, H. J., Elad, Y., and Stewart, A. (2003). Genetic basis of mycoparasitism: A mechanism of biological control by species of *Trichoderma*. *N. Z. J. Crop Hortic. Sci.* 31, 281–291. doi: 10.1080/01140671.2003.9514263
- Subudhi, E., Sahoo, D. R. K., Dey, S., Das, A., and Sahoo, K. (2018). *Unraveling plant-endophyte interactions: An omics insight*. Cham: Springer Nature, 249–267. doi: 10.1007/978-3-319-76900-4\_2-1
- Su, Z., Mao, L. J., Li, N., Feng, X. X., Yuan, Z. L., Wang, L. W., et al. (2013). Evidence for biotrophic lifestyle and biocontrol potential of dark septate endophyte *Harpophora oryzae* to rice blast disease. *PLoS One* 8:e61332. doi: 10.1371/journal.pone.0061332
- Sun, X., Wang, N., Li, P., Jiang, Z., Liu, X., Wang, M., et al. (2020). Endophytic fungus *Falciphora oryzae* promotes lateral root growth by producing indole derivatives after sensing plant signals. *Plant Cell Environ.* 43, 358–373. doi: 10.1111/pce.13667
- Surono, and Narisawa, K. (2018). The inhibitory role of dark septate endophytic fungus *Phialocephala fortinii* against *Fusarium* disease on the *Asparagus officinalis* growth in organic source conditions. *Biol. Control* 120, 159–167.
- Szabo, L. J., and Bushnell, W. R. (2001). Hidden robbers: The role of fungal haustoria in parasitism of plants. *Proc. Natl. Acad. Sci.* 98, 7654–7655. doi: 10.1073/pnas.151262398
- Taghavi, S., Garafola, C., Monchy, S., Newman, L., Hoffman, A., Weyens, N., et al. (2009). Genome survey and characterization of endophytic bacteria exhibiting a beneficial effect on growth and development of poplar trees. *Appl. Environ. Microbiol.* 75, 748–757. doi: 10.1128/AEM.02239-08
- Tamosiune, I., Baniulis, D., and Stanys, V. (2017). “Role of endophytic bacteria in stress tolerance of agricultural plants: Diversity of microorganisms and molecular mechanisms,” in *Probiotics in agroecosys*, eds V. Kumar, M. Kumar, S. Sharma, and R. Prasad (Singapore: Springer), 1–29. doi: 10.1007/978-981-10-4059-7\_1
- Tian, Z., Wang, R., Ambrose, K. V., Clarke, B. B., and Belanger, F. C. (2017). The *Epichloë festucae* antifungal protein has activity against the plant pathogen *Sclerotinia homoeocarpa*, the causal agent of dollar spot disease. *Sci Rep.* 7:5643. doi: 10.1038/s41598-017-06068-4
- Tiwari, R., Kalra, A., Darokar, M. P., Chandra, M., Aggarwal, N., Singh, A. K., et al. (2010). Endophytic bacteria from *Ocimum sanctum* and their yield enhancing capabilities. *Curr. Microbiol.* 60, 167–171. doi: 10.1007/s00284-009-9520-x
- Trouvelot, S., Olivain, C., Recorbet, G., Migheli, Q., and Alabouvette, C. (2002). Recovery of *Fusarium oxysporum* Fo47 mutants affected in their biocontrol activity after transposition of the *Fot1* element. *Phytopathology* 92, 936–945. doi: 10.1094/PHYTO.2002.92.9.936
- Ulrich, K., Kube, M., Becker, R., Schneek, V., and Ulrich, A. (2021). Genomic analysis of the endophytic *Stenotrophomonas* strain 169 reveals features related to plant-growth promotion and stress tolerance. *Front. Microbiol.* 12:1542. doi: 10.3389/fmicb.2021.687463

- Vadassery, J., and Oelmüller, R. (2009). Calcium signaling in pathogenic and beneficial plant microbe interactions: What can we learn from the interaction between *Piriformospora indica* and *Arabidopsis thaliana*. *Plant Sig. Behav.* 4, 1024–1027. doi: 10.4161/psb.4.11.9800
- Vandenkooornhuysen, P., Quaiser, A., Duhamel, M., Le Van, A., and Dufresne, A. (2015). The importance of the microbiome of the plant holobiont. *New Phytol.* 206, 1196–1206. doi: 10.1111/nph.13312
- Varga, T., Hixson, K. K., Ahkami, A. H., Sher, A. W., Barnes, M. E., Chu, R. K., et al. (2020). Endophyte-promoted phosphorus solubilization in *Populus*. *Front. Plant Sci.* 11:567918. doi: 10.3389/fpls.2020.567918
- Varma, A., Bakshi, M., Lou, B., Hartmann, A., and Oelmueller, R. (2012). *Piriformospora indica*: A novel plant growth-promoting mycorrhizal fungus. *Agric. Res.* 1, 117–131. doi: 10.1007/s40003-012-0019-5
- Vázquez-Garcidueñas, S., Leal-Morales, C. A., and Herrera-Estrella, A. (1998). Analysis of the  $\beta$ -1, 3-glucanolytic system of the biocontrol agent *Trichoderma harzianum*. *Appl. Environ. Microbiol.* 64, 1442–1446. doi: 10.1128/AEM.64.4.1442-1446.1998
- Verhagen, B., Trotel-Aziz, P., Jeandet, P., Baillieu, F., and Aziz, A. (2011). Improved resistance against *Botrytis cinerea* by grapevine-associated bacteria that induce a prime oxidative burst and phytoalexin production. *Phytopathology* 101, 768–777. doi: 10.1094/PHYTO-09-10-0242
- Verma, S. K., Sahu, P. K., Kumar, K., Pal, G., Gond, S. K., Kharwar, R. N., et al. (2021). Endophyte roles in nutrient acquisition, root system architecture development and oxidative stress tolerance. *J. Appl. Microbiol.* 131, 2161–2177. doi: 10.1111/jam.15111
- Veronico, P., Giannino, D., Melillo, M. T., Leone, A., Reyes, A., Kennedy, M. W., et al. (2006). A novel lipoxygenase in pea roots. Its function in wounding and biotic stress. *Plant Physiol.* 141, 1045–1055. doi: 10.1104/pp.106.081679
- Vibhuti, M., Kumar, A., Sheoran, N., Nadakkakath, A. V., and Eapen, S. J. (2017). Molecular basis of endophytic *Bacillus megaterium*-induced growth promotion in *Arabidopsis thaliana*: Revelation by microarray-based gene expression analysis. *J. Plant Growth Reg.* 36, 118–130. doi: 10.1007/s00344-016-9624-z
- Vujanovic, V., Islam, M. N., and Daida, P. (2019). Transgenerational role of seed microbiome—an endosymbiotic fungal composition as a prerequisite to stress resilience and adaptive phenotypes in Triticum. *Sci. Rep.* 9, 1–13. doi: 10.1038/s41598-019-54328-2
- Wang, H., Sun, S., Ge, W., Zhao, L., Hou, B., and Wang, K. (2020). Horizontal gene transfer of Fhb7 from fungus underlies *Fusarium* head blight resistance in wheat. *Science* 368:eaba5435. doi: 10.1126/science.aba5435
- Wang, S. Y., Moyne, A. L., Thottappilly, G., Wu, S. J., Locy, R. D., and Singh, N. K. (2001). Purification and characterization of a *Bacillus cereus* exochitinase. *Enzyme Microb. Technol.* 28, 492–498. doi: 10.1016/s0141-0229(00)00362-8
- Wang, Y., and Dai, C. C. (2011). Endophytes: A potential resource for biosynthesis, biotransformation, and biodegradation. *Ann. Microbiol.* 61, 207–215. doi: 10.1007/s13213-010-0120-6
- Wang, Y., Li, X., Fan, B., Zhu, C., and Chen, Z. (2021). Regulation and function of defense-related callose deposition in plants. *Int. J. Mol. Sci.* 22:2393. doi: 10.3390/ijms22052393
- Waqas, M., Khan, A. L., Hamayun, M., Shahzad, R., Kim, Y. H., Choi, K. S., et al. (2015). Endophytic infection alleviates biotic stress in sunflower through regulation of defence hormones, antioxidants and functional amino acids. *Eur. J. Plant Pathol.* 141, 803–824. doi: 10.1007/s10658-014-0581-8
- Waqas, M., Khan, A. L., Kamran, M., Hamayun, M., Kang, S. M., Kim, Y. H., et al. (2012). Endophytic fungi produce gibberellins and indoleacetic acid and promotes host-plant growth during stress. *Molecules* 17, 10754–10773. doi: 10.3390/molecules170910754
- War, A. R., Paulraj, M. G., War, M. Y., and Ignacimuthu, S. (2011). Role of salicylic acid in induction of plant defense system in chickpea (*Cicer arietinum* L.). *Plant Sig. Behav.* 6, 1787–1792. doi: 10.4161/psb.6.11.17685
- Ważny, R., Rozpačdek, P., Domka, A., Jędrzejczyk, R. J., Nosek, M., and Hubalewska-Mazgaj, M. (2021). The effect of endophytic fungi on growth and nickel accumulation in *Noccaea hyperaccumulators*. *Sci. Total Environ.* 768:144666. doi: 10.1016/j.scitotenv.2020.144666
- Węgrzyn, E., and Górzynska, K. (2019). Influence of the fungal hyperparasite *Trichoderma harzianum* on the growth of *Epichloë typhina*, an agent of choke disease in grasses. *J. Plant Dis. Protect.* 126, 39–45.
- Wei, G., Kloepper, J. W., and Tuzun, S. (1991). Induction of systemic resistance of cucumber to *Colletotrichum orbiculare* by select strains of plant growth-promoting rhizobacteria. *Phytopathology* 81, 1508–1512.
- White, J. F., Kingsley, K. I., Kowalski, K. P., Irizarry, I., Micci, A., and Soares, M. A. (2017). Disease protection and allelopathic interactions of seed-transmitted endophytic pseudomonads of invasive reed grass (*Phragmites australis*). *Plant Soil* 422, 195–208.
- White, J. F., Kingsley, K. L., Zhang, Q., Verma, R., Obi, N., Dvinskikh, S., et al. (2019). Endophytic microbes and their potential applications in crop management. *Pest Manag. Sci.* 75, 2558–2565.
- Wink, M. (2018). Plant secondary metabolites modulate insect behavior—steps toward addiction? *Front. Physiol.* 9:364. doi: 10.3389/fphys.2018.00364
- Wu, L., Li, X., Ma, L., Blom, J., Wu, H., Gu, Q., et al. (2020). The “pseudo-pathogenic” effect of plant growth-promoting Bacilli on starchy plant storage organs is due to their  $\alpha$ -amylase activity which is stimulating endogenous opportunistic pathogens. *Appl. Microbiol. Biotechnol.* 104, 2701–2714. doi: 10.1007/s00253-020-10367-8
- Xia, C., Zhang, X. X., Christensen, M. J., Nan, Z. B., and Li, C. J. (2015). *Epichloë* endophyte affects the ability of powdery mildew (*Blumeria graminis*) to colonise drunken horse grass (*Achnatherum inebrians*). *Fungal Ecol.* 16, 26–33.
- Xu, L., Wu, C., Oelmüller, R., and Zhang, W. (2018). Role of phytohormones in piriformospora indica-induced growth promotion and stress tolerance in plants: More questions than answers. *Front. Microbiol.* 9:1646. doi: 10.3389/fmicb.2018.01646
- Yang, C. Q., Wu, X. M., Ruan, J. X., Hu, W. L., Mao, Y. B., and Chen, X. Y. (2013). Isolation and characterization of terpene synthases in cotton (*Gossypium hirsutum*). *Phytochem* 96, 46–56. doi: 10.1016/j.phytochem.2013.09.009
- Yang, C., Wu, P., Yao, X., Sheng, Y., Zhang, C., Lin, P., et al. (2022). Integrated transcriptome and metabolome analysis reveals key metabolites involved in *Camellia oleifera* defense against anthracnose. *Int. J. Mol. Sci.* 23:536. doi: 10.3390/ijms23010536
- Yang, Y., Chen, Y., Cai, J., Liu, X., and Huang, G. (2021). Antifungal activity of volatile compounds generated by endophytic fungi *Sarocladium brachiariae* HND5 against *Fusarium oxysporum* f. sp. cubense. *PLoS One* 16:e0260747. doi: 10.1371/journal.pone.0260747
- Yi, H. S., Yang, J. W., and Ryu, C. M. (2013). ISR meets SAR outside: Additive action of the endophyte *Bacillus pumilus* INR7 and the chemical inducer, benzothiadiazole, on induced resistance against bacterial spot in field-grown pepper. *Front. Plant Sci.* 4:122. doi: 10.3389/fpls.2013.00122
- You, J. M., Xiong, K., Mu, S., Guo, J., Guo, X. L., Duan, Y. Y., et al. (2018). Identification of endophytic bacteria Bzj1 and research on biological control of root rot of *Atractylodes Macrocephala*. *Zhongguo Zhong Yao Za Zhi* 3, 478–483. doi: 10.19540/j.cnki.cjcm.20180105.008
- Yuan, J., Zhang, W., Sun, K., Tang, M.-J., Chen, P.-X., Li, X., et al. (2019). Comparative transcriptomics and proteomics of *Atractylodes lancea* in response to endophytic fungus *Gilmaniella* sp. AL12 reveals regulation in plant metabolism. *Front. Microbiol.* 10:1208. doi: 10.3389/fmicb.2019.01208
- Zeyen, R. J., Carver, T. L. W., and Lyngkjær, M. F. (2002). “Epidermal cell papillae,” in *The powdery mildews: A comprehensive treatise*, eds R. R. Belanger, W. R. Buschnell, A. J. Dik, and T. L. W. Carver (St. Paul, MN: APS Press), 107–125.
- Zhai, X., Jia, M., Chen, L., Zheng, C. J., Rahman, K., and Han, T. (2017). The regulatory mechanism of fungal elicitor-induced secondary metabolite biosynthesis in medicinal plants. *Crit. Rev. Microbiol.* 43, 238–261. doi: 10.1080/1040841X.2016.1201041
- Zhang, J., and Zhou, J. M. (2010). Plant immunity triggered by microbial molecular signatures. *Mol. Plant* 3, 783–793. doi: 10.1093/mp/ssp035
- Zhang, W., Fan, X., Li, J., Ye, T., Mishra, S., Zhang, L., et al. (2021). Exploration of the quorum-quenching mechanism in *Pseudomonas nitroreducens* W-7 and its potential to attenuate the virulence of *Dickeya zeae* EC1. *Front. Microbiol.* 12:694161. doi: 10.3389/fmicb.2021.694161
- Zheng, R., Li, S., Zhang, X., and Zhao, C. (2021). Biological activities of some new secondary metabolites isolated from endophytic fungi: A review study. *Int. J. Mol. Sci.* 22:959. doi: 10.3390/ijms22020959





## OPEN ACCESS

## EDITED BY

George Newcombe,  
University of Idaho,  
United States

## REVIEWED BY

Parul Chaudhary,  
G. B. Pant University of Agriculture and  
Technology, India  
Julia W. Neilson,  
University of Arizona,  
United States

## \*CORRESPONDENCE

Ignacio D. Rodríguez-Llorente  
irodri@us.es

<sup>†</sup>These authors have contributed equally to  
this work and share last authorship

## SPECIALTY SECTION

This article was submitted to  
Microbiotechnology,  
a section of the journal  
Frontiers in Microbiology

RECEIVED 28 July 2022

ACCEPTED 06 October 2022

PUBLISHED 20 October 2022

## CITATION

Flores-Duarte NJ, Caballero-Delgado S,  
Pajuelo E, Mateos-Naranjo E,  
Redondo-Gómez S, Navarro-Torre S and  
Rodríguez-Llorente ID (2022) Enhanced  
legume growth and adaptation to degraded  
estuarine soils using *Pseudomonas* sp.  
nodule endophytes.  
*Front. Microbiol.* 13:1005458.  
doi: 10.3389/fmicb.2022.1005458

## COPYRIGHT

© 2022 Flores-Duarte, Caballero-Delgado,  
Pajuelo, Mateos-Naranjo, Redondo-  
Gómez, Navarro-Torre and Rodríguez-  
Llorente. This is an open-access article  
distributed under the terms of the [Creative  
Commons Attribution License \(CC BY\)](#). The  
use, distribution or reproduction in other  
forums is permitted, provided the original  
author(s) and the copyright owner(s) are  
credited and that the original publication in  
this journal is cited, in accordance with  
accepted academic practice. No use,  
distribution or reproduction is permitted  
which does not comply with these terms.

# Enhanced legume growth and adaptation to degraded estuarine soils using *Pseudomonas* sp. nodule endophytes

Noris J. Flores-Duarte<sup>1</sup>, Sara Caballero-Delgado<sup>1</sup>,  
Eloisa Pajuelo<sup>1</sup>, Enrique Mateos-Naranjo<sup>2</sup>,  
Susana Redondo-Gómez<sup>2</sup>, Salvadora Navarro-Torre<sup>1†</sup>  
and Ignacio D. Rodríguez-Llorente<sup>1\*†</sup>

<sup>1</sup>Department of Microbiology and Parasitology, Faculty of Pharmacy, University of Sevilla, Sevilla, Spain, <sup>2</sup>Department of Plant Biology and Ecology, Faculty of Biology, University of Sevilla, Sevilla, Spain

The joint estuary of Tinto and Odiel rivers (SW Spain) is one of the most degraded and polluted areas in the world and its recovery is mandatory. Legumes and their associated bacteria are recommended sustainable tools to fight against soils degradation and loss of fertility due to their known positive impacts on soils. The aim of this work was to isolate and characterize plant growth promoting nodule endophytes (PGPNE) from inside nodules of *Medicago* spp. naturally growing in the estuary of the Tinto and Odiel Rivers and evaluate their ability to promote legume adaptation in degraded soils. The best rhizobia and non-rhizobia among 33 endophytes were selected based on their plant growth promoting properties and bacterial enzymatic activities. These strains, identified as *Pseudomonas* sp. N4, *Pseudomonas* sp. N8, *Ensifer* sp. N10 and *Ensifer* sp. N12, were used for *in vitro* studies using *Medicago sativa* plants. The effects of individual or combined inoculation on seed germination, plant growth and nodulation were studied, both on plates and pots containing nutrient-poor soils and moderately contaminated with metals/loids from the estuary. In general, inoculation with combinations of rhizobia and *Pseudomonas* increased plant biomass (up to 1.5-fold) and nodules number (up to 2-fold) compared to single inoculation with rhizobia, ameliorating the physiological state of the plants and helping to regulate plant stress mechanisms. The greatest benefits were observed in plants inoculated with the consortium containing the four strains. In addition, combined inoculation with *Ensifer* and *Pseudomonas* increased As and metals accumulation in plant roots, without significant differences in shoot metal accumulation. These results suggest that PGPNE are useful biotools to promote legume growth and phytostabilization potential in nutrient-poor and/or metals contaminated estuarine soils.

## KEYWORDS

contaminated estuarine soils, enhanced nodulation, nodule endophytes, plant growth-promoting bacteria, phytostabilization



## Introduction

Industrial and mining activity releases toxic metal/loids into the environment, such as As, Cd, Cu, and Pb, all of them very harmful to human health and most living beings (FAO and ITPS, 2015). In turn this has caused the degradation of soils, either by the modification of pH or by originating a decrease in the number of arable lands causing a problem at social, economic, and environmental levels (Singh et al., 2010; Chen et al., 2013). Heavy metals are dangerous because they are not degradable either chemically or biologically, being able to remain in the environment for hundreds or thousands of years (Herrera Marcano, 2011). These metals have also been repressing the enzymatic activity of the soils, causing a decrease in the growth and respiration of the populations of microorganisms, thus altering the diversity present in the rhizosphere (Abdu et al., 2017; Aponte et al., 2020). Marshes of river estuaries are particularly sensitive to heavy metals contamination by metals deposition. A good example is the combined estuary of Tinto and Odiel rivers (Huelva, SW Spain), known as one of the most contaminated regions in the world (Hudson-Edwards et al., 1999). Levels of toxic metal/loids as high as 125 ppm of As, 890 ppm of Cu, 275 ppm of Pb or 1,500 ppm of Zn in the Odiel river marshes, and 2 to 3-fold these levels in the Tinto River marshes, have been reported in the last decade (Mesa et al., 2015a; Navarro-Torre et al., 2017). These levels exceed those allowed by regional and national legislation in natural parks, agricultural and industrial soils (Junta de Andalucía and Consejería de Medio Ambiente, 1999).

One solution to this great environmental problem is the implantation of pioneering crops able to regenerate the soil and improve its yield, respecting the environment. This kind of strategies should include the use of leguminous plants (belonging to the *Fabaceae* family), due to their great benefits. First, legumes are an important product in the food industry both for human and animal consumption worldwide, since they are very rich in protein, fiber, vitamins, and minerals and also has a low cost, being highly consumed in underdeveloped countries (Ferreira et al., 2021). Second, legumes play a very important role in agriculture as cover crops, since they improve soil fertility increasing crops yield, help the constant movement of soil nutrients and release matter into the soil (Stagnari et al., 2017; Ferreira et al., 2021). Third, legumes are good candidates to adapt to degraded soils affected by biotic and abiotic factors, particularly these plants play an important role in the regeneration of soils degraded by heavy metals due to their ability to accumulate metals in the roots without affecting plant growth (Mesa et al., 2015b; Flores-Duarte et al., 2022a).

Legumes are capable of fixing atmospheric nitrogen through symbiosis with many genera of soil nitrogen-fixing bacteria, called rhizobia, which penetrate the roots through the root hairs, forming nodules in which nitrogen fixation takes place (Poole et al., 2018). But nodules are not only occupied by rhizobia, within the legume nodules there are another great variety of bacteria called non-rhizobial nodule-associated bacteria (NAB; Rajendran

et al., 2012), non-rhizobial endophytes (NRE; De Meyer et al., 2015), or just nodule endophytes (Velázquez et al., 2013). These bacteria do not induce nodule formation but can colonize nodules accompanying rhizobia forming a beneficial association and enhancing nodulation and plant growth. Within this group, bacteria of the genera, *Acinetobacter*, *Agrobacterium*, *Bacillus*, *Burkholderia*, *Pseudomonas* and *Variovorax*, among others, have been found (Shiraishi et al., 2010; Martínez-Hidalgo and Hirsch, 2017; Bessadok et al., 2020). These nodule endophytes usually behave as plant growth promoting bacteria (PGPB).

Soil health and fertility are directly influenced by beneficial plant-microbe relationships that determine soil biodiversity (Vishwakarma et al., 2020). Plant-PGPB interactions have shown to provide benefits in plant growth and development by facilitating the acquisition of nutrients (Fasusi et al., 2021) and producing phytohormones related with plant and root length growth, and the formation of root hairs and lateral roots, such as cytokinin, gibberellins, abscisic acid, and IAA (Raza et al., 2019). Through atmospheric nitrogen fixation (Roy et al., 2020), phosphate mobilization/solubilization (Etesami et al., 2021) and siderophores production (Lurthy et al., 2020; Kang et al., 2021) bacteria provide N, P, Fe, and Zn to plants. PGPB also play a determinant role in plant adaptation and tolerance to biotic and abiotic stress (Chaudhary et al., 2022). For example, bacteria with ACC-deaminase activity are able to break the ethylene precursor ACC, altering plant stress perception (Penrose and Glick, 2003; Chandwani and Amaresan, 2022).

Microorganisms have an important role in pollutant detoxification and heavy metal plant stress resistance (Caracciolo and Terenzi, 2021). Soil microorganisms have developed different resistance mechanisms, such as metal biosorption, bioaccumulation, modification of metal chemical state (methylation) or production of chelating compounds, particularly siderophores and biosurfactants, that cause a lowering in metal availability for plants (Verma and Kuila, 2019), then diminishing plant metal content (Caracciolo and Terenzi, 2021). PGPB are directly involved in metal detoxification through the production of secondary metabolites, such as siderophores, ACC or IAA (Caracciolo and Terenzi, 2021). Particularly in legumes, nitrogen-fixing bacteria and endophytes inside nodules have probed to reduce metal translocation to aerial parts and increase plant nitrogen content and growth in metal contaminated soils (Navarro-Torre et al., 2020; Flores-Duarte et al., 2022b).

In a recent work, a consortium of PGPB, including *Pseudomonas*, *Chryseobacterium* and *Priestia* genera, showed their ability to promote *Medicago sativa* growth and adaptation in poor-nutrient soils (Flores-Duarte et al., 2022b). These bacteria were isolated from the rhizosphere of different legumes growing in estuarine soils with low levels of minerals and organic matter. It is well accepted that endophytes maintain a much closer relationship with the plant and have lower competition with soil microorganisms than rhizospheric bacteria (Adeleke and Babalola, 2021; Dwibedi et al., 2022). The present work is aimed to determine whether a consortium of endophytes isolated from

TABLE 1 Physicochemical properties and micronutrients concentrations of soil from high marshes of the Odiel River.

| Physicochemical properties                       |               |             |                      |              |                                     |              |                |              |
|--|---------------|-------------|----------------------|--------------|-------------------------------------|--------------|----------------|--------------|
| Location   | Texture (%) * |             | Organic material (%) |              | Conductivity (μS·cm <sup>-1</sup> ) |              | pH             |              |
| High marsh                                       | 72/13/15      |             | 0.9 ± 0.01           |              | 13.1 ± 0.3                          |              | 6.8 ± 0.2      |              |
| Metal/lloid concentration (mg·kg <sup>-1</sup> ) |               |             |                      |              |                                     |              |                |              |
| Location   | As            | Cd          | Cu                   | Zn           | Mg                                  | Na           | Fe             | P            |
| High marsh                                       | 27.9 ± 2.2    | 0.38 ± 0.01 | 316.7 ± 3.20         | 345.0 ± 7.10 | 0.789 ± 0.01                        | 0.369 ± 0.01 | 9345.56 ± 9.35 | 0.056 ± 0.01 |

Values are mean  $\pm$  S.D. ( $n = 3$ ). \*Texture (sand/silt/clay percentage).

nodules could enhance legume growth in degraded soils more efficiently than rhizosphere bacteria, introducing soil metal contamination as additional stress.

The objectives that arise in this work are the following: (i) isolation and characterization of rhizobia and endophytes from nodules of *Medicago* spp. naturally growing in the Odiel river estuary (Huelva, Spain); (ii) selection of rhizobia and nodule endophytes based on their properties, enzymatic activities and ability to tolerate metal/lloids; (iii) determine the ability of the selected bacteria to promote *M. sativa* growth, nodulation and metal accumulation in Odiel marshes soils under greenhouse conditions.

## Materials and methods

### Collection of samples and soil characterization

Nodulated wild plants of *Medicago* spp. were collected from high marshes of the Odiel river estuary (Huelva, Spain; 37°150'N, 6°580'W; SW Spain) in February 2020. Soil samples (15–20 cm deep) were collected using a shovel, gloves and plastic bags. The samples were immediately transported to the laboratory and stored at 4°C. Three homogeneous soil samples were deposited in sterile bottles for chemical soil analysis, as described by Mateos-Naranjo et al. (2015). The soil texture (percentage of sand, silt, and clay) was determined using the Bouyoucos hydrometer method (Bouyoucos, 1936). Electrical conductivity was measured with a Crison-522 conductivity meter (Spain) and pH and redox potential with a Crison pH/mVp-506 portable meter (Spain). The concentration of nutrients in the soil was measured by inductively coupled plasma-optical emission spectroscopy (ICP-OES; ARLFisons3410, Thermo Scientific, Waltham, MA, United States). The amount of organic matter was determined by the method of Walkley and Black (1934). Results are presented in Table 1.

### Isolation of endophytic bacteria from nodules of *Medicago* spp.

Nodules were excised from roots with a scalpel, washed with water and placed on tubes. Samples were immersed in 70%

(v/v) ethanol for 1 min with manual agitation to disinfect the surface. Then, they were washed again with sterile water and immersed in 3% (v/v) sodium hypochlorite for 15 min under continuous agitation and finally washed four times with sterile distilled water. Disinfected nodules were deposited in a mortar with 1 ml of sterile 0.9% (w/v) saline solution and grinded. Portions of 100  $\mu\text{l}$  of the resulting mix were to spread and extended with a spatula in Petri dishes with TY medium (tryptone-yeast extract agar) and TSA (tryptone soya agar, Intrin Biotechnology, Korea). Plates were incubated for 72 h at 28°C. Controls of nodule surface disinfection and solution sterility were performed. Bacteria were separated based on the different colony morphology and cell morphology was observed by Gram stain using an Olympus CX41 microscope with the 100x objective.

### Determination of plant growth promoting properties and enzymatic activities

The ACC deaminase activity was assessed as described by Penrose and Glick (2003) and adapted by Mesa et al. (2015a). Activity was measured by monitoring  $\alpha$ -ketobutyric acid at 540 nm in a spectrophotometer (Lambda25; PerkinElmer, Waltham, MA, United States), and the amount of  $\alpha$ -ketobutyric acid was determined using a standard curve with known concentrations. ACC deaminase activity was expressed in  $\mu\text{moles}$  of  $\alpha$ -ketobutyrate per mg of protein per hour. To verify nitrogen fixation, strains were plated in nitrogen free broth (NFB; Döbereiner, 1995) for 5 days at 28°C. Indole-3-acetic acid (IAA) production was determined using a colorimetric technique by incubating 3 ml of a liquid culture of TY or TSB supplemented with L-tryptophan (0.1 mg/ml) and incubated at 28°C for 72 h at 200 rpm. Cultures were then centrifuged for 5 min at 13,000 rpm and supernatants transferred to glass tubes. The appearance of a pink color after adding 4 ml of Salkowski's reagent (Gordon and Weber, 1951) indicated that the test was positive. The amount of IAA was calculated by measuring the absorbance at 535 nm in a spectrophotometer (Lambda 25; Perkin Elmer, Waltham, MA, USA). Phosphate solubilization was carried out on plates with NBRIP medium (phosphate growth medium from the National Institute of Botanical Research) as

described by Nautiyal (1999). The appearance of a transparent halo after 7 days of incubation at 28°C indicated that the bacteria had the capacity to solubilize phosphates. 100 µl of bacterial culture medium was added to each well. The formation of biofilms will be prolonged by checking the adhesion capacity of the bacteria in microplates with 96 wells in TY or liquid TSB at 28°C, incubating for 4 days, after incubation each well was stained with 200 µl of 0.01% crystal violet as described by del Castillo et al. (2012). Siderophores production was determined by the appearance of an orange halo around the well containing 100 µl of bacterial culture in CAS medium (Chromeazurool S), after incubation for 7 days at 28°C (Schwyn and Neilands, 1987). Enzymatic activities were determined on plates incubated at 28°C for 7 days. Pectinase and cellulase activities were examined as described by Elbeltagy et al. (2000). For pectinase activity, strains were plated on ammonium mineral agar (AMA). Plates were revealed with 2% CTAB and positive bacteria showed a halo around. For cellulase activity, strains were plated on solid M9 minimal medium supplemented with yeast extract (0.2%) and carboxymethylcellulose (1%). Plates were developed by covering the plate with 1 mg/ml Congo Red solution for 15 min and decolorizing with 1 M NaCl for 15 min. The appearance of a clear halo indicated positive result. Chitinase activity was performed as described by Mesa et al. (2015a). Amylase activity was performed on starch agar plates (Scharlab, Barcelona, Spain) and revealed with 10 ml lugol. The formation of a transparent halo indicated positive result. Lipase and protease activities were observed by the presence of halos around the bacteria after incubation in casein agar and Tween 80 mediums, respectively, as described by Prescott (2002). And finally, the DNase activity was determined by cultures on DNA agar plates revealed with 1 M HCl.

For PGP properties and enzyme activities, positive and negative controls from BIO-181 group collection were used (Supplementary Table 1).

## Tolerance to metals/loids

The isolated bacteria were plated in TY and TSA medium with increasing concentrations of As, Cd, Cu and Zn, from 1 M NaAsO<sub>2</sub>, 1 M CdCl<sub>2</sub>, 1 M CuSO<sub>4</sub>, 1 M ZnSO<sub>4</sub> stock solutions. Plates were incubated for 24–48 h at 28°C and tolerance expressed as the maximum tolerable concentration (MTC), that is the maximum concentration that allows visible bacterial growth.

## Analysis of diversity and identification of isolates

The diversity of the isolated endophytes was analyzed by performing a Box-PCR. Bacterial genomic DNA was isolated using a G-spin™ Genomic DNA Extraction Kit for Bacteria

(Intron Biotechnology, Gyeonggi-do, Korea) with the instructions determined by the manufacturer. Box-PCR was performed using 1 µl of DNA and Box A1R primer (5'-CTACGGCAAG GCGACGCTGACG-3') using the Maxime™ PCR PreMix kit (i-Taq™; Intron Biotechnology, Gyeonggi-do, Korea) and following the PCR conditions: initial denaturation at 94°C for 2 min, 30 cycles of denaturation at 94°C for 20 s, annealing at 52°C for 20 s, extension at 72°C for 1 min, and final extension at 72°C for 5 min. Electrophoresis was performed in a 1.5% (w/v) agarose gel and a voltage of 70 V for 2 h. Representative bacteria of each different Box-PCR profile were identified by 16S rRNA gene amplification using 16F27 and 16R1488 primers (Navarro-Torre et al., 2016) and the Maxime™ PCR PreMix kit (i-Taq™; Intron Biotechnology, Gyeonggi-do, Korea) following the next PCR conditions: initial denaturation at 94°C for 2 min, 30 cycles of denaturation at 94°C for 20 s, annealing at 58°C for 10 s, extension at 72°C for 50 s, and final extension at 72°C for 5 min. Electrophoresis was performed in a 1% (w/v) agarose gel and a voltage of 120 V for 30 min. PCR products were purified with the enzyme ExoSAP IT (Affymetrix, Santa Clara, CA, USA), following the manufacturer instructions, and sequenced by the StabVida company (Caparica, Portugal). Then, 16S rRNA gene sequences were compared with those deposited in the EzBioCloud database (Yoon et al., 2017) using the Ez-Taxon e service ([www.ezbiocloud.net/eztaxon](http://www.ezbiocloud.net/eztaxon); accessed July 2022). Finally, 16S rRNA gene sequences were deposited in the NCBI GenBank.

## Inoculant design

Selected bacteria were grown together on TY plates to test growth compatibility as described in Navarro-Torre et al. (2016). The inoculants were prepared by cultivating selected strains separately in TSB or TY at 28°C for 24 h and 200 rpm. Afterwards, cultures containing 10<sup>8</sup> cells mL<sup>-1</sup> were transferred to sterile Falcon tubes to be centrifuged at 8000 rpm for 10 min, washing twice with sterile 0.9% (w/v) saline solution, to remove traces of the culture medium (Navarro-Torre et al., 2016). At the end of the washes the cultures were resuspended in a sterile liquid nitrogen deficient buffered nodulation medium (BNM; Ehrhardt et al., 1992), or sterile water for experiments under greenhouse conditions. For co-inoculation and consortium inoculation designs, bacteria were mixed after resuspension. Inoculation conditions were defined as follow: C-: non inoculation; N4: inoculation with *Pseudomonas* sp. N4; N8: inoculation with *Pseudomonas* sp. N8; N10: inoculation with *Ensifer* sp. N10; N12: inoculation with *Ensifer* sp. N12; N4 + N10: co-inoculation with *Pseudomonas* sp. N4 and *Ensifer* sp. N10; N8 + N10: co-inoculation with *Pseudomonas* sp. N8 and *Ensifer* sp. N10; N4 + N12: co-inoculation with *Pseudomonas* sp. N4 and *Ensifer* sp. N12; N8 + N12: co-inoculation with *Pseudomonas* sp. N8 and *Ensifer* sp. N12; CSN: inoculation with *Pseudomonas* sp. N4, *Pseudomonas* sp., N8 *Ensifer* sp. N10 and *Ensifer* sp. N12.

## Labelling of *Pseudomonas* with fluorescence and microscopy

*Pseudomonas* strains (*Pseudomonas* sp. N4 and *Pseudomonas* sp. N8) were marked with the fluorescent protein mCherry by triparental matting, mixing the donor *Escherichia coli* DH5 $\alpha$  containing the plasmid pMP7604 (Lagendijk et al., 2010), the helper strain *E. coli* containing pRK600 (Finan et al., 1986) and *Pseudomonas* strains spontaneously resistant to rifampicin (100  $\mu$ g/ml) as recipients. 100  $\mu$ l aliquots of TSB overnight cultures were plated on TSA containing rifampicin (100  $\mu$ g/ml) and tetracycline (10  $\mu$ g/ml). Fluorescent *Pseudomonas* resistant to both antibiotics thus containing the plasmid were selected. *M. sativa* plants were co-inoculated with the rhizobia (*Ensifer* sp. N10 or *Ensifer* sp. N12) and labelled *Pseudomonas* in square plates (12  $\times$  12 cm), 20 seedlings per condition, as described below. After 28 days, roots and nodules were cut with a sterile scalpel and 0.5 mm cuts observed (Mesa et al., 2015b). Fluorescent bacteria in plant tissues were visualized using a laser scanning spectral confocal optical microscope (Zeiss LSM 7 DUO, Zeiss, Jena, Germany) with an objective Plan-Apochromat 20X/0.8 M27, filters of 572–727, and a laser of 561 nm (5.3%). Images were processed with ZEN2011 software (Zeiss, Jena, Germany).

## *Medicago sativa* seeds germination and nodulation on plates

Alfalfa (*M. sativa*) seeds were surface disinfected following the protocol described by Navarro-Torre et al. (2019) by immersing them for 10 min in 70% (v/v) ethanol, followed by 30 min in sodium hypochlorite at 3% (v/v) under gentle agitation, washing 6 times with sterile distilled water. The next step was to immerse 50 seeds in each inoculant for 1 h and for the non-inoculated control (C-) seeds were immersed for 1 h in 0.9% (w/v) NaCl. Seeds were transferred to plates containing 0.9% (w/v) water-agar (5 repetitions per condition and 10 seeds per plate) or water-agar plates containing a mixture of 7.5  $\mu$ M As, Cd, Cu, and Zn, prepared from the stock solutions described above (paragraph 2.4), and finally incubated in the dark at 28°C. Germination was observed every 24 h for 7 days in absence of metals and for 21 days in presence of metals.

For *in vitro* nodulation experiment, pre-germinated seeds were transferred to square plates (12  $\times$  12 cm) with nitrogen-free BNM-agar medium (Ehrhardt et al., 1992), supplemented with sodium arsenite at a concentration of 30  $\mu$ M. or in absence of arsenite.  $\text{NH}_4\text{NO}_3$  was added to all plates at a concentration of 1 mM. 10 seeds were deposited in each plate and 5 replicates per treatment were performed. The seeds were inoculated or co-inoculated under the conditions described above using the selected bacteria, and non-inoculated seeds were used as controls. The plates were placed in a vertical position, incubated at 22°C with a cycle of 8 h of darkness and 16 h of light (120–130  $\mu$ E m

$^{-2}\cdot\text{s}^{-1}$ ) in a growth chamber (AGP-700-HR ESP; Radiber, Barcelona, Spain). Plants were harvested after 21 days and nodules from each condition were counted.

## Experiments under greenhouse conditions

Soil was collected from the upper marshes of the Odiel River and sterilized in an autoclave at 121°C and 1 atm of overpressure for 30 min. This sterilization was repeated twice. To confirm soil sterilization, 3 samples of 1 g of soil were washed by shaking in 10 ml of sterile water. After decanting for 10 min, three samples of 100  $\mu$ l of supernatant per tube were plated on TSA and no growth was observed on plates incubated 48 h at 28°C. Plastic pots (11 cm squared pots with 12 cm height) were filled with 1 kg of the previously sterilized soil (3:1, three parts of the soil from the marshes and one part of sterile perlite) and 2 pre-germinated seeds were placed per pot, 8 pots per condition. The experiment lasted 60 days and plants were irrigated with sterile water once a week (50 ml) and weekly inoculated with their respective inoculum (50 ml of cultures). The greenhouse had controlled light and temperature conditions; natural light was supplemented with fluorescent/incandescent lamps to get a photoperiod of 16 h light: 8 h dark; and the temperature was adjusted to 25°C during the day and 15°C during the night. At the end, the length of roots and shoots were measured, the number of nodules and leaves were counted, the diameters of the leaves were determined, and the nitrogen content in the plant was evaluated using an InfrAlyzer 300 (Technicon, Tarrytown, NY, United States), as described by Carrasco et al. (2005). Finally, samples were placed in an oven at 80°C for 48 h to determine the dry weight of both shoots and roots separately.

## Determination of photosynthetic parameters and total chlorophyll content

For the determination of gas exchange, leaves were randomly selected from *M. sativa* plants and measured with an infrared gas analyzer (IRGA) LI-6400 (LI-COR Biosciences, Lincoln, NE, USA) equipped with a Li-6,400-02B leaf light chamber. Measurements were made between 9 am and 2 pm under a photosynthetic photon flux density of 1,500  $\mu\text{mol m}^{-2} \text{s}^{-1}$ , a vapor pressure deficit of 2–3 kPa, at a temperature of approximately 25°C and an environment of  $\text{CO}_2$  concentration of 400  $\mu\text{mol}\cdot\text{mol}^{-1}$  air. Gas exchange stabilization (120 s) was equilibrated, and measurements were recorded to determine the net photosynthetic rate ( $A_N$ ). In addition, a fluorometric analysis was performed to study the energy use efficiency of photosystem II (PSII). The maximum quantum efficiency of PSII photochemistry (Fv/Fm) and the quantum efficiency of PSII ( $\Phi_{\text{PSII}}$ ) were determined using a



saturation pulse method described in Genty et al. (1989). Selected leaves were light- and dark-adapted for 30 min, followed by a saturated actinic light pulse of  $10,000 \mu\text{mol m}^{-2} \text{s}^{-1}$  for 0.8 s at noon ( $1700 \mu\text{mol photons m}^{-2} \text{s}^{-1}$ ) using a FMS-2 modulated fluorimeter (Hansatech Instruments Ltd., Pentney, United Kingdom). Details are described in Schreiber et al. (1986). With the recorded data, the electron transport rate (ETR) was calculated as described in Krall and Edwards (1992). Finally, the total content of chlorophyll described by Hiscox and Israelstam (1979) was determined. 50 mg of randomly selected leaves were ground using a mortar containing 100% acetone: 0.9% saline solution (4.1; v/v). The resulting extract was resuspended in acetone and measured at 652 nm using a spectrophotometer (Lambda 25; PerkinElmer, Waltham, MA, United States) and the total chlorophyll content was determined using the formula described by Arnon (1949). Samples were run in duplicate.

## Antioxidant enzyme analysis

Guaiacol peroxidase (GPX), catalase (CAT), superoxide dismutase (SOD) and ascorbate peroxidase (APX) enzymatic activity were measured with leaves and roots randomly collected from each of the treatments at the end of the experiment. Immediately after the collection, the samples were deposited in nitrogen liquid and stored at  $-80^{\circ}\text{C}$  until homogenized. 48 h after storage, 500 mg of plant material were homogenized in extraction buffer (50 mM sodium phosphate buffer at pH 7.6) and centrifuged at  $4^{\circ}\text{C}$  and 9,000 rpm for 20 min, and the plant extract was stored at  $-80^{\circ}\text{C}$ . Total protein concentration was measured in the plant extract following the Bradford method (Bradford, 1976) using a BSA standard curve. In guaiacol peroxidase activity (GPX), guaiacol oxidation was measured at 470 nm. Catalase (CAT) was determined by measuring the disappearance of  $\text{H}_2\text{O}_2$  at 240 nm. Superoxide dismutase (SOD) activity was assayed using autoxidation of pyrogallol at 325 nm. Finally, for ascorbate peroxidase (APX), the oxidation of L-ascorbate was measured at 290 nm. For the determination of the autoxidation of substrates, control tests were carried out without the presence of the enzyme extract. Enzymatic activities were expressed as units per  $\mu\text{g}$  of protein and were measured in triplicate.

## Statistical analysis

Statistical analyzes were determined using Statistical version 12.0 software (Statsoft Inc., Tulsa, OK, United States). The normality of the results was verified using the Kolmogorov Smirnov test. The results of each treatment were compared using one-way ANOVA, and Fisher test was performed to determine statistical differences.

## Results

### Isolation and characterization of endophytic bacteria from nodules

#### Soil characterization

Bacteria were isolated from nodules of *Medicago* spp. that grows naturally in the high marshes of the Odiel River. The soil was composed of 72% sand, 0.9% organic matter, had low electrical conductivity and nutrients content, as well as moderate amounts of As, Cd, Cu and Zn. The soil characteristics are presented in Table 1.

#### Isolation of endophytes

A total of 33 endophytic bacteria were isolated from *Medicago* spp. nodules (13 strains grew in TY and 20 in TSA). They were identified based on colony morphology (color and shape of the colonies), cellular morphology (cocci, bacilli, coccobacilli) and type of cell wall by Gram staining (Gram positive or Gram negative). Other aspects such as grouping, if any (clusters, chains), or the presence of spores (central or terminal) were also observed. 85% of the strains were Gram negative bacilli and 15% were Gram positive bacilli, and only one of them presented spores (Supplementary Table 2). Subsequently, a Box-PCR of the 33 strains was performed in order to study the collection genotypically (Supplementary Figure 1). Several of the isolates showed identical band profiles, so the study was reduced to 24 strains for which the 16S rRNA genes were partially sequenced. The sequences showed similarity with *Achromobacter*, *Bacillus*, *Enterobacter*, *Ensifer*, *Lelliottia*, *Priestia* and *Pseudomonas* genera, being *Pseudomonas* and *Lelliottia* the most represented (Table 2).

### Characterization of PGP properties, enzymatic activities and metals tolerance

PGP properties of the endophytes were determined, showing all of them four to five out of six analyzed properties, while two strains presented the six properties (Table 3; Supplementary Table 3). All the bacteria were able to produce siderophores and most of them (30) solubilized phosphate (Supplementary Table 3). N4 strain showed the highest production of siderophores according to the diameter of the halo in CAS medium (Table 3; Supplementary Table 3) and N15, N20, N30 and N31 were the best phosphate solubilizers (Supplementary Table 3). A high number of strains were able to grow in N free medium (30 isolates) and/or produced auxins (27 isolates). N8 strain produced the highest concentration of IAA, close to  $18 \text{ mg L}^{-1}$  (Table 3; Supplementary Table 3). 20 strains formed biofilm and 11 isolates showed ACC deaminase activity, presenting N8 strain the highest activity, close to  $10 \mu\text{mol } \alpha\text{-ketobutyrate mg protein}^{-1} \text{ h}^{-1}$  (Table 3; Supplementary Table 3).

The presence of enzymatic activities in the endophytes was studied (Supplementary Table 4). Cellulase and protease activities were the most abundant, since they were found in 22 and 17 strains, respectively (Supplementary Table 3). A low number of

TABLE 2 Identification of cultivable entophytic bacteria isolated from nodules of *Medicago* spp. using the EzBiocloud database.

| Strain     | Sequence size (bp) | Related species                    | % ID         | Accession number |
|------------|--------------------|------------------------------------|--------------|------------------|
| N1         | 461                | <i>Achromobacter piechaudii</i>    | 99.57        | OP060607         |
| N2         | 602                | <i>Lelliottia jeotgali</i>         | 96.75        | OP060608         |
| N3         | 343                | <i>Lelliottia jeotgali</i>         | 95.27        | OP060609         |
| <b>N4</b>  | <b>1,154</b>       | <b><i>Pseudomonas mucoides</i></b> | <b>97.47</b> | <b>OP060610</b>  |
| N5         | 722                | <i>Lelliottia jeotgali</i>         | 98.53        | OP060611         |
| N6         | 1,218              | <i>Achromobacter spanius</i>       | 99.01        | OP060612         |
| N7         | 1,147              | <i>Lelliottia jeotgali</i>         | 98.27        | OP060613         |
| <b>N8</b>  | <b>1,127</b>       | <b><i>Pseudomonas mucoides</i></b> | <b>99.13</b> | <b>OP060614</b>  |
| N9         | 694                | <i>Lelliottia jeotgali</i>         | 99.54        | OP060615         |
| <b>N10</b> | <b>1,111</b>       | <b><i>Ensifer meliloti</i></b>     | <b>98.83</b> | <b>OP060616</b>  |
| N11        | 1,126              | <i>Pseudomonas mucoides</i>        | 98.84        | OP060617         |
| <b>N12</b> | <b>863</b>         | <b><i>Ensifer meliloti</i></b>     | <b>99.88</b> | <b>OP060618</b>  |
| N13        | 1,051              | <i>Lelliottia amnigena</i>         | 97.71        | OP060619         |
| N14        | 865                | <i>Priestia megaterium</i>         | 99.65        | OP060620         |
| N15        | 1,310              | <i>Pseudomonas lactis</i>          | 97.10        | OP060621         |
| N16        | 1,035              | <i>Pseudomonas lactis</i>          | 99.13        | OP060622         |
| N18        | 1,374              | <i>Bacillus velezensis</i>         | 96.44        | OP060623         |
| N20        | 1,328              | <i>Pantoea vagans</i>              | 95.41        | OP060624         |
| N21        | 678                | <i>Pseudomonas lactis</i>          | 99.26        | OP060625         |
| N23        | 949                | <i>Enterobacter huaxiensis</i>     | 96.63        | OP060626         |
| N25        | 1,257              | <i>Bacillus proteolyticus</i>      | 95.83        | OP060627         |
| N30        | 1,314              | <i>Pseudomonas capeferrum</i>      | 96.12        | OP060628         |
| N32        | 950                | <i>Bacillus tequilensis</i>        | 99.58        | OP060629         |
| N33        | 1,209              | <i>Pseudomonas capeferrum</i>      | 98.76        | OP060630         |

Selected strains appear in bold.

TABLE 3 PGP properties and enzymatic activities showed by selected strains.

| PGP properties              | N4    | N8     | N10   | N12  |
|-----------------------------|-------|--------|-------|------|
| Phosphate solubilisation    | 11    | 12     | 15    | 14   |
| Siderophores production     | 73    | 44     | 13    | 10.2 |
| IAA production              | 1.562 | 17.939 | 1.266 | 1.00 |
| Biofilm formation           | +     | +      | +     | +    |
| N fixation                  | +     | +      | +     | +    |
| ACC deaminase activity      | 9.677 | 9.987  | —     | —    |
| <b>Enzymatic activities</b> |       |        |       |      |
| DNase                       | —     | —      | +     | +    |
| Amylase                     | —     | —      | —     | —    |
| Cellulase                   | —     | +      | +     | +    |
| Lipase                      | —     | —      | —     | —    |
| Pectinase                   | —     | —      | —     | —    |
| Protease                    | +     | +      | —     | —    |
| Chitinase                   | —     | —      | —     | —    |

N4: *Pseudomonas* sp. N4; N8: *Pseudomonas* sp. N8; N10: *Ensifer* sp. N10; N12: *Ensifer* sp. N12; +, presence of the activity; —, absence of the activity. Values of phosphate solubilisation and siderophores production express the diameter of the halo in mm. Values of IAA production are expressed in mg·L<sup>-1</sup>. Values of ACC deaminase activity are expressed in μmoles α-ketobutyrate·mg protein<sup>-1</sup>·h<sup>-1</sup>.

isolates (2 to 5) showed pectinase, lipase, chitinase or DNase activities (Supplementary Table 4).

Tolerance of the strains towards As, Cd, Cu, and Zn were determined and expressed as the maximum tolerable

concentration (Table 4; Supplementary Table 5). Endophytes showed good levels of metal/loids tolerance. They tolerated concentrations as high as up to 20 mM As, 2 mM Cd, 6 mM Cu and Zn.

Selection of endophytes

Among isolated endophytes, only N10 and N12 strains belonging to *Ensifer* genus were rhizobia able to nodulate *M. sativa*, so they were selected for assays *in planta*. N4 and N8 were selected as nodule enhancing bacteria (NEB) candidates based on their PGP properties and enzymatic activities, since they showed all the properties assayed and 2 enzymatic activities. They were also able to tolerate moderate levels of the assayed metal/loids (Table 4).

In vitro effect of endophytes in Medicago sativa germination and nodulation

The germination of *M. sativa* seeds was evaluated in the presence and absence of a mixture of metals/loids by inoculating them with the selected strains, performing individual inoculations (N4, N8, N10 and N12), co-inoculations combining each of the *Pseudomonas* and each of the rhizobia (N4+N10, N8+N10, N4+N12, and N8+N12) or inoculation with the four strains together (N4+N8+N10+N12). Inoculation improved seed germination and the consortium with the four strains reported the greatest increase, showing the highest percentage of germination both in absence and presence of metals

(Figures 1A,B). The increase in the germination rate in absence or presence of metals, followed this pattern: CSN>N8+N10>N4+N10>N8+N12>N4+N12>N8>N10>N12>N4>C-. In absence of As, differences in germination among seeds inoculated with the four strains and those co-inoculated con *Pseudomonas* and *Ensifer* were not statistically significant ( $p<0.001$ ), but these germination rates were significantly higher than those recorded in seeds inoculated with a single strain. Seeds inoculated with single strains did not show significant differences in germination rates among them. The same results could be observed in presence of As, with one single difference, since seeds inoculated with the consortium showed significantly higher germination rates than seeds co-inoculated with *Pseudomonas*

TABLE 4 Maximum tolerable concentration of metal/loid showed by selected strains.

| Strain | Cd (mM) | As (mM) | Cu (mM) | Zn (mM) |
|--------|---------|---------|---------|---------|
| N4     | 0.7     | 1       | 3       | 1.9     |
| N8     | 0.4     | 2.5     | 1.9     | 1.8     |
| N10    | 0.4     | 0.4     | 1.4     | 2.5     |
| N12    | 0.1     | 0       | 1.8     | 1.4     |

N4: *Pseudomonas* sp. N4; N8: *Pseudomonas* sp. N8; N10: *Ensifer* sp. N10; N12: *Ensifer* sp. N12.

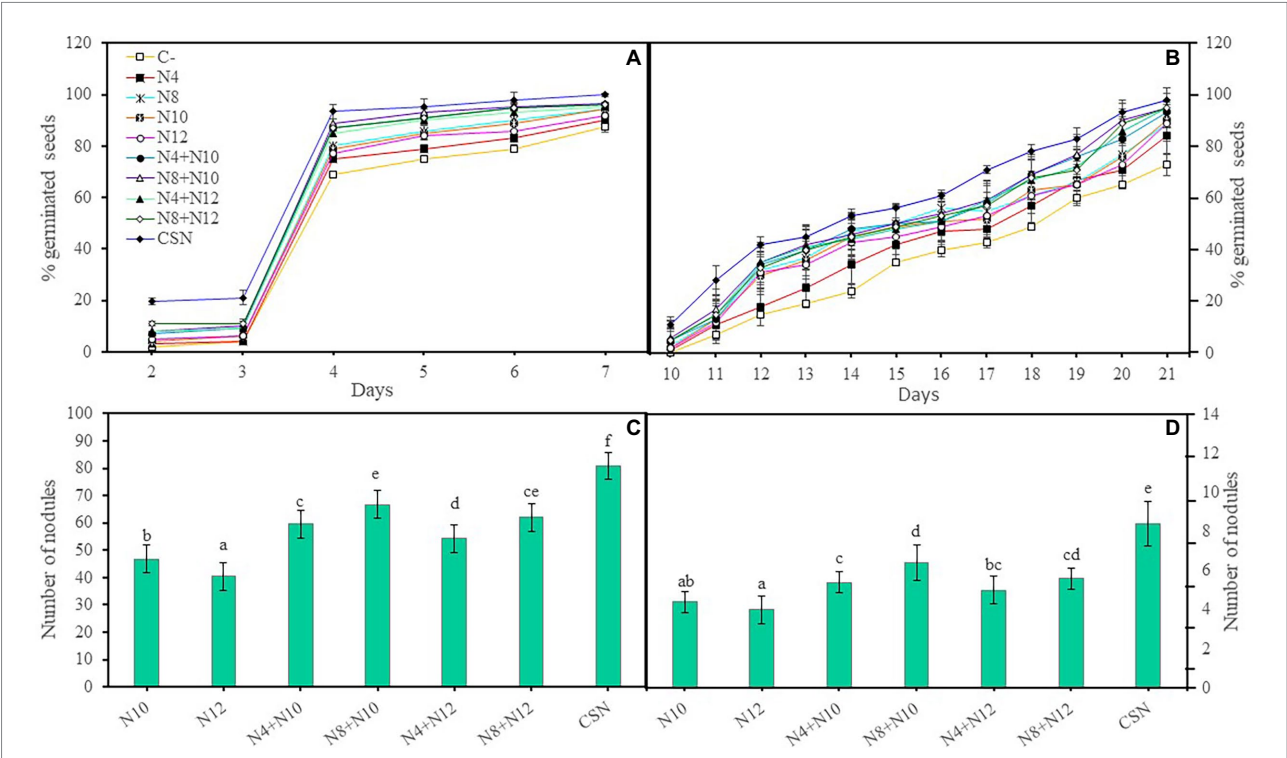


FIGURE 1 In vitro effects of inoculation of *M. sativa* with selected PGPNE. (A) Percentage of germinated seeds without metals and (B) with metals. Values are means±S.D. (n=50). (C) Number of nodules in plants without As and (D) with As. Values are means±S.D. (n=5). Different letters indicate statistical differences between means (One-way ANOVA, LSD test,  $p<0.0001$ ). C-: non inoculation; N4: inoculation with *Pseudomonas* sp. N4; N8: inoculation with *Pseudomonas* sp. N8; N10: inoculation with *Ensifer* sp. N10; N12: inoculation with *Ensifer* sp. N12; N4+N10: co-inoculation with *Pseudomonas* sp. N4 and *Ensifer* sp. N10; N8+N10: co-inoculation with *Pseudomonas* sp. N8 and *Ensifer* sp. N10; N4+N12: co-inoculation with *Pseudomonas* sp. N4 and *Ensifer* sp. N12; N8+N12: co-inoculation with *Pseudomonas* sp. N8 and *Ensifer* sp. N12; CSN: inoculation with *Pseudomonas* sp. N4, *Pseudomonas* sp. N8, *Ensifer* sp. N10 and *Ensifer* sp. N12.

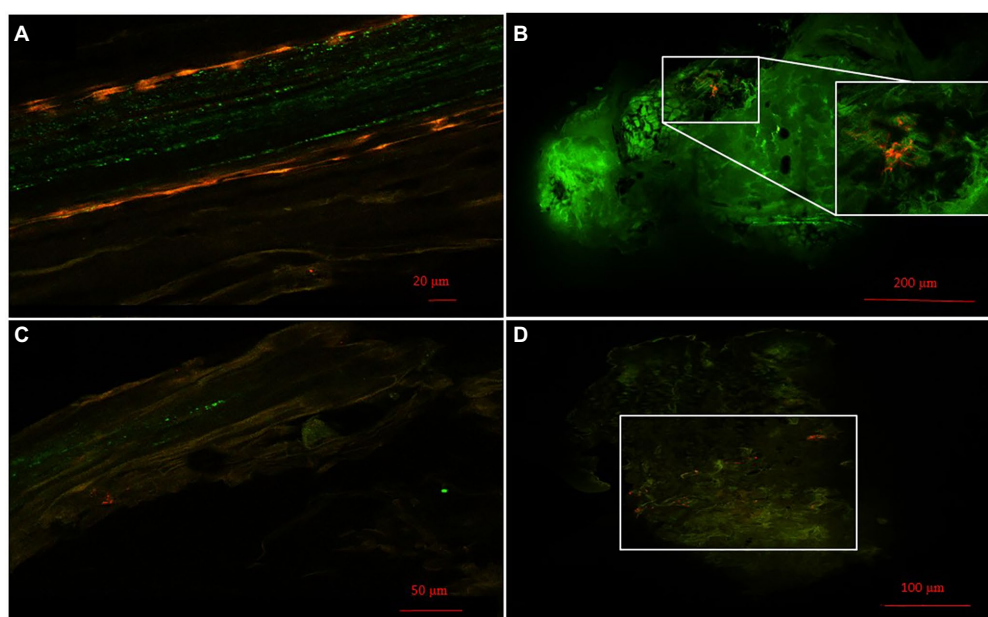


FIGURE 2

Bacterial colonization. (A) Images of roots and (B) nodules of colonized *M. sativa* 28 days after inoculation with *Pseudomonas* sp. N4 marked with mCherry and *Ensifer* sp. N10. (C) Images of roots and (D) nodules of colonized *M. sativa* 28 days after inoculation with *Pseudomonas* sp. N8 marked with mCherry and *Ensifer* sp. N10. The white square in (B,D) marks a group of *Pseudomonas* sp. N4 and *Pseudomonas* sp. N8, respectively, in the nitrogen fixation zone.

and *Ensifer* ( $p < 0.001$ ). Non-inoculated seeds showed the lowest rates of seed germination, with significant differences, both in absence and presence of As. These significant differences were recorded at the end of the experiment.

To evaluate the ability of the *Pseudomonas* strains to improve *M. sativa* nodulation induced by *Ensifer*, plant seedlings were inoculated or co-inoculated with combinations of *Pseudomonas* and *Ensifer* strains in square plates with or without As. Co-inoculation with either of the *Pseudomonas* and a *Ensifer* strain significantly increased the number of nodules, both in absence and presence of As, compared with the single inoculation with *Ensifer* (Figures 1D,E). The combination *Pseudomonas* sp. N8 and *Ensifer* sp. N10 induced more nodules than any other couple, although the plants inoculated with the combination of the four strains (CSN) showed the highest number of nodules in both conditions, with significant differences. *Ensifer* sp. N10 showed a better behavior in nodulation than N12 and *Pseudomonas* sp. N8 seemed to be better as nodule enhancing bacteria than N4.

### *Pseudomonas* behave as nodule endophytes in *Medicago sativa*

Localization of *Pseudomonas* strains was studied using confocal laser scanning microscopy (CLSM) and mCherry-labeled *Pseudomonas* sp. N4 and N8. Cells were visualized from 0.5 mm sections of roots and nodules of *M. sativa* co-inoculated with *Ensifer* sp. N10 and labelled N4 or N8. Examples of the results

obtained are presented in Figure 2. The presence of labelled bacteria with red fluorescence could be observed both in root (Figures 2A,C) and nodule cells (Figures 2B,D). Groups of bacteria were clearly seen in the nitrogen fixation zone of *M. sativa* nodules, marked with a white square in the figures (Figures 2B,D).

## Effect of inoculations under greenhouse conditions

### Inoculation increased plant biomass

*M. sativa* plants were grown and inoculated under greenhouse conditions using soil from the marshes of the Odiel River (Huelva). Plant inoculation with any of the strains increased biomass, both shoots and roots, compared with non-inoculated control plants (Figure 3A). Single inoculation with *Pseudomonas* sp. N8 reported higher plant shoot biomass than single inoculations with *Ensifer* or N4, that showed the lowest shoot and root biomasses among single inoculated plants. No significant differences in root biomass were found among plants inoculated with N8, N10 and N12. Co-inoculation with *Pseudomonas*-*Ensifer* couples produced higher values of root and shoot biomasses than any of the single inoculation treatments, except for plants inoculated with N4-N10 couple, that did not show significant differences in shoot biomass compared with plants inoculated with N8. N8 + N10 combination showed the highest value in plant shoot biomass among the *Pseudomonas*-*Ensifer* co-inoculation treatments, with significant differences (Figure 3A). Nevertheless,



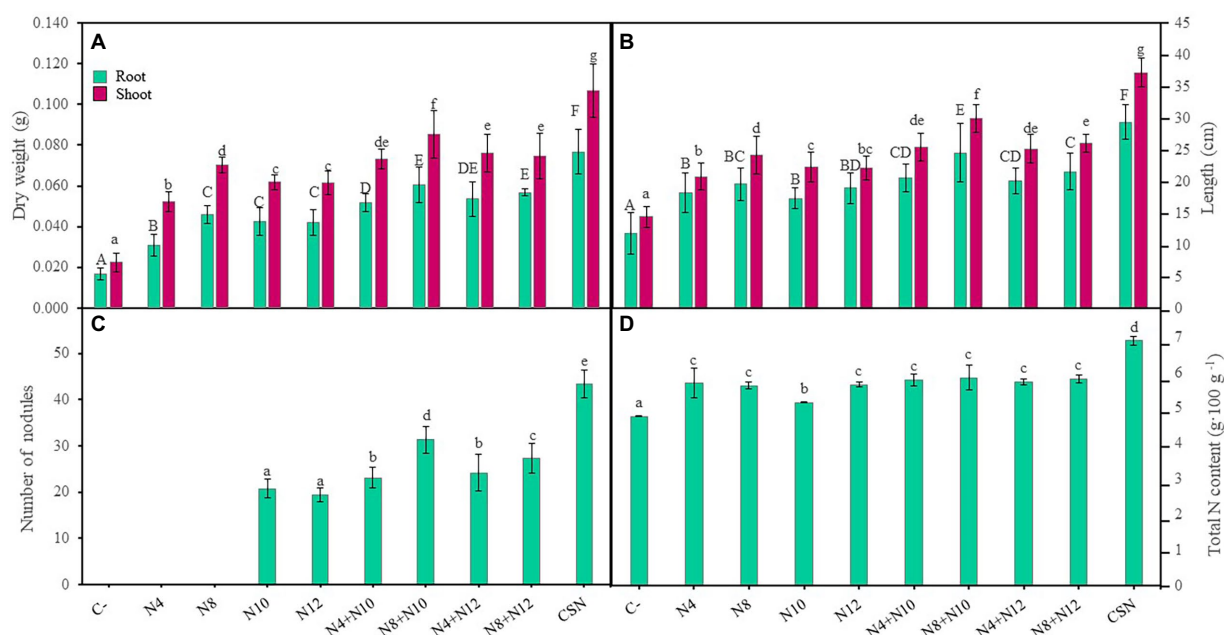


FIGURE 3

Effects of the inoculation of *M. sativa* plants with PGPNE. (A) Dry weight of shoot and roots, (B) length of shoot and roots, (C) number of nodules, and (D) nitrogen content after 60 days in pots containing soil from the high marshes of the Odiel River. Values are means  $\pm$  S.D. ( $n=16$ ). Different letters indicate statistical differences between means. Lowercase and uppercase letters are used to qualify different variables and are not comparable among them (One-way ANOVA, LSD test,  $p<0.001$ ). C-: non inoculation; N4: inoculation with *Pseudomonas* sp. N4; N8: inoculation with *Pseudomonas* sp. N8; N10: inoculation with *Ensifer* sp. N10; N12: inoculation with *Ensifer* sp. N12; N4+N10: co-inoculation with *Pseudomonas* sp. N4 and *Ensifer* sp. N10; N8+N10: co-inoculation with *Pseudomonas* sp. N8 and *Ensifer* sp. N10; N4+N12: co-inoculation with *Pseudomonas* sp. N4 and *Ensifer* sp. N12; N8+N12: co-inoculation with *Pseudomonas* sp. N8 and *Ensifer* sp. N12; CSN: inoculation with *Pseudomonas* sp. N4, *Pseudomonas* sp. N8, *Ensifer* sp. N10 and *Ensifer* sp. N12.

the highest values of root and shoot biomass were recorded in plants inoculated with the consortium of the four strains (CSN). Similarities could be observed using plant root and shoot lengths as parameters to compare inoculation treatments (Figure 3B). Plants co-inoculated with *Pseudomonas* sp. N8 and *Ensifer* reported longer shoots than those inoculated with a single strain, while the combination N8+N10 showed the longest roots and shoots among plants co-inoculated or inoculated with a single strain. Those inoculations including *Ensifer* and N4 showed no significant differences in root and shoot length compared with plants inoculated only with N8. The longest roots and shoots were observed in plants inoculated with the consortium (Figure 3B). These plants also presented the highest number of leaves with the widest diameter, with statistically significant differences compared to non-inoculated controls or any of the inoculation and co-inoculation treatments (Supplementary Figure 2).

### *Pseudomonas* enhanced plant nodulation

Regarding the number of nodules, *Pseudomonas* increased the number of nodules induced by *Ensifer*, showing co-inoculated plants more nodules than plants inoculated only with *Ensifer*, with significant differences (Figure 3C). Although this result was independent of the *Ensifer*-*Pseudomonas* combination used, plants co-inoculated with strains N8 and N10 showed higher number of nodules than any other couple. The highest number of nodules

was found again in plants inoculated with the consortium (Figure 3C), approximately 109 and 124% more nodules than plants inoculated with N10 and N12, respectively. Nitrogen content in stems and leaves of *M. sativa* plants was also evaluated (Figure 3D). Inoculation treatments increased the N content compared to non-inoculated plants, although no significant differences were found among single inoculation and co-inoculation treatments, except for single inoculation with N10, that reported lower values of N (Figure 3D). The highest content of N, with significant differences, was measured in plants inoculated with the consortium of the four strains.

### *Pseudomonas* ameliorated the physiological state of the plants

Several photosynthetic parameters were measured in order to determine the physiological state of the plants (Figure 4; Supplementary Figure 3). Inoculated plants showed higher values in all the parameters recorded compared to non-inoculated plants and the highest values were always measured in plants inoculated with the consortium, with significant differences. Values in the net photosynthetic rate ( $A_N$ ) could be described by the following pattern, with significant differences: CSN > N8+N10 > N8+N12 = N4+N10 = N4+N12 > N8=N4 > N12=N10 > C- (Figure 4A). With the exception of the inoculation with the consortium, no differences were found in the maximum quantum efficiency of the

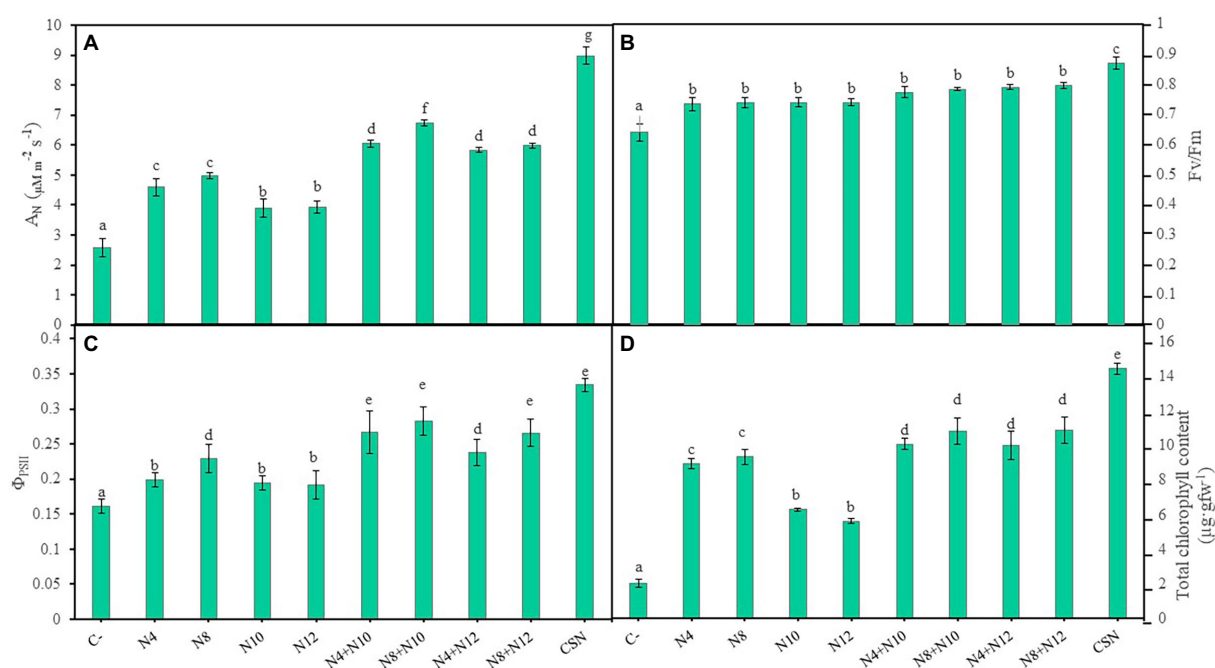


FIGURE 4

Photosynthetic parameters of *M. sativa* plants inoculated with PGPNE. (A) Net photosynthetic rate ( $A_N$ ), (B) maximum quantum efficiency of PSII photochemistry (Fv/Fm), (C) quantum yield of PSII photochemistry ( $\Phi_{PSII}$ ), and (D) total chlorophyll content after 60 days in pots containing soil from the high marshes of the Odiel River. Values are means  $\pm$  S.D. ( $n=16$ ). Different letters indicate statistical differences between means (One-way ANOVA, LSD test,  $p<0.0001$ ). C-: non inoculation; N4: inoculation with *Pseudomonas* sp. N4; N8: inoculation with *Pseudomonas* sp. N8; N10: inoculation with *Ensifer* sp. N10; N12: inoculation with *Ensifer* sp. N12; N4+N10: co-inoculation with *Pseudomonas* sp. N4 and *Ensifer* sp. N10; N8+N10: co-inoculation with *Pseudomonas* sp. N8 and *Ensifer* sp. N10; N4+N12: co-inoculation with *Pseudomonas* sp. N4 and *Ensifer* sp. N12; N8+N12: co-inoculation with *Pseudomonas* sp. N8 and *Ensifer* sp. N12; CSN: inoculation with *Pseudomonas* sp. N4, *Pseudomonas* sp. N8, *Ensifer* sp. N10 and *Ensifer* sp. N12.

PSII photochemistry (Fv/Fm) among inoculation conditions (Figure 4B). Concerning the quantum yield of the PSII photochemistry ( $\Phi_{PSII}$ ), results followed the pattern: CSN > N8 + N12 = N8 + N10 = N4 + N10 > N4 + N12 = N8 > N12 = N10 = N4 > C- (Figure 4C). In the same way, plants inoculated with the consortium showed the highest values in electron transport rate (ETR), followed by plants co-inoculated with N8 + N10 (Supplementary Figure 3). Finally, values of total chlorophyll content in plants could be described by a pattern similar to the one observed for Fv/Fm: CSN > N8 + N12 = N4 + N12 = N8 + N10 = N4 + N10 > N8 = N4 > N12 = N10 > C- (Figure 4D).

### *Pseudomonas* increased the activity of plant antioxidant enzymes

The influence of bacterial inoculations on plant response to stress was evaluated by determining the activity of different antioxidant enzymes in roots and leaves of *M. sativa* (Figure 5). All the enzymatic activities increased in response to inoculation, both in roots and shoots, compared to non-inoculated plants, with higher increases in roots than in shoots. The highest enzymatic activities were always recorded in plants inoculated with the consortium, with significant differences. Guaiacol peroxidase (Figure 5A) and ascorbate peroxidase (Figure 5D) activities presented similar results, showing plants inoculated with N8 + N10

the highest levels of activity in roots among plants co-inoculated or inoculated with single strains. Concerning catalase activity, plants co-inoculated with *Pseudomonas-Ensifer* couples had higher levels of activities in roots and shoots than those inoculated only with one strain, with the single exception of plants inoculated with N10, that showed the same level activity in shoots than co-inoculated plants (Figure 5C). Finally, plants inoculated with the combination N4 + N10 showed more superoxide dismutase activity in roots and shoots than any other inoculation condition, with the exception of plants inoculated with the consortium (Figure 5B).

### *Pseudomonas* increased metal accumulation in roots

Accumulation of As and the most abundant metals in the high marshes of the Odiel river was determined in *M. sativa* tissues at the end of the greenhouse experiment (Figure 6). The highest levels of metal/loids found in shoots were 1.5 ppm of As, 0.04 ppm of Cd, 27.76 ppm of Cu and 61.2 ppm of Zn, without significant differences among inoculation conditions (Supplementary Table 6). Different behavior was observed in roots. Single inoculations with rhizobia (N10 and N12) reduced As accumulation in roots compared to control plants (Figure 6A). Plants inoculated with rhizobia also showed the lowest values of Cu and Cd accumulated in roots

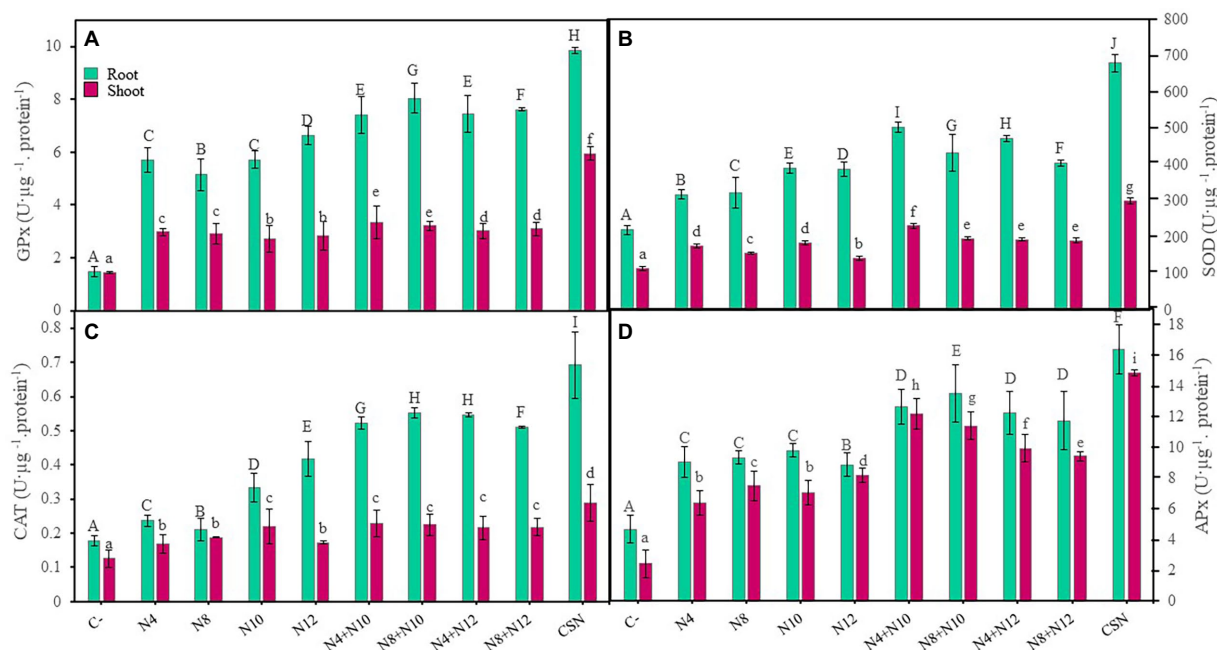


FIGURE 5

Antioxidant enzymes in *M. sativa* plants inoculated with PGPNE. (A) Guaiacol peroxidase, (B) superoxide dismutase, (C) catalase, and (D) ascorbate peroxidase activities after 60 days in pots containing soil from the high marshes of the Odiel River. Values are means  $\pm$  S.D. ( $n=16$ ). Different letters indicate statistical differences between means. Lowercase and uppercase letters are used to qualify different variables and are not comparable among them (One-way ANOVA; LSD test,  $p<0.001$ ). C-: non inoculation; N4: inoculation with *Pseudomonas* sp. N4; N8: inoculation with *Pseudomonas* sp. N8; N10: inoculation with *Ensifer* sp. N10; N12: inoculation with *Ensifer* sp. N12; N4+N10: co-inoculation with *Pseudomonas* sp. N4 and *Ensifer* sp. N10; N8+N10: co-inoculation with *Pseudomonas* sp. N8 and *Ensifer* sp. N10; N4+N12: co-inoculation with *Pseudomonas* sp. N4 and *Ensifer* sp. N12; N8+N12: co-inoculation with *Pseudomonas* sp. N8 and *Ensifer* sp. N12; CSN: inoculation with *Pseudomonas* sp. N4, *Pseudomonas* sp. N8, *Ensifer* sp. N10 and *Ensifer* sp. N12.

compared with the rest of inoculation conditions (Figures 6B,C). Concerning Zn, the lowest amounts were recorded in plants inoculated with N12 and the highest in plants inoculated with N8, while plants inoculated with the other strains (N4 and N10) accumulated the same amount of this metal (Figure 6D). On the contrary, the highest values of metal accumulation were found in roots of plants inoculated with the consortium of the four bacteria (Figure 6). In general, plants inoculated with *Pseudomonas-Ensifer* couples accumulated more As and metals in roots than those inoculated only with *Pseudomonas*, with the exceptions of Cu and Cd in plants inoculated with the couple N8-N10 (Figure 6).

## Discussion

Climate change and human activities are causing abiotic stress in many soils previously suitable for crops. Use of agrochemicals, heavy metals release, drought or salinity cause a great loss of nutrients and native microorganisms in the soil, altering plant adaptation and growth (García-Martí et al., 2019; Du et al., 2021). Environmentally friendly solutions to regenerate soils should include the use of leguminous plants, since they are high biomass producers, reduce the use of nitrogen-based fertilizers and can be used for fed or feeder in agriculture (Graham and Vance, 2003;

Ferreira et al., 2021). In addition, most legumes are metal phytostabilizers suitable for regeneration of metal contaminated soils (Jach et al., 2022). Legume adaptation and growth in nutrient-poor or degraded soils can be enhanced using adequate autochthonous rhizospheric or endophytic PGPB as inoculants (Monteoliva et al., 2022).

The objective pursued in this work was the isolation and characterization of endophytic bacteria from nodules of *Medicago* spp. plants growing in the estuary of the Odiel river (Huelva, Spain), capable of improving seed germination, nodulation and growth of *M. sativa* in soils with low nutrient content and moderate to high levels of heavy metals. 33 strains belonging to genera previously described as nodule endophytes, such as *Achromobacter*, *Bacillus*, *Enterobacter*, *Lelliottia*, *Pantoea*, *Priestia* or *Pseudomonas* (Aserse et al., 2013; Martínez-Hidalgo and Hirsch, 2017), were isolated. Among NRE, *Pseudomonas* was the most represented genus and only two isolated were nodule inducing rhizobia from *Ensifer* genus, the most common *Medicago* symbiont frequently isolated from wild legumes growing in arid soils (Mnasri et al., 2007; León-Barrios et al., 2009; Bessadok et al., 2020).

Characterization of the isolates revealed the presence of at least 4 out of 6 PGP properties studied, several enzymatic activities and moderate to high levels of As and metals tolerance in all of them. Strains *Pseudomonas* sp. N4 and *Pseudomonas* sp.

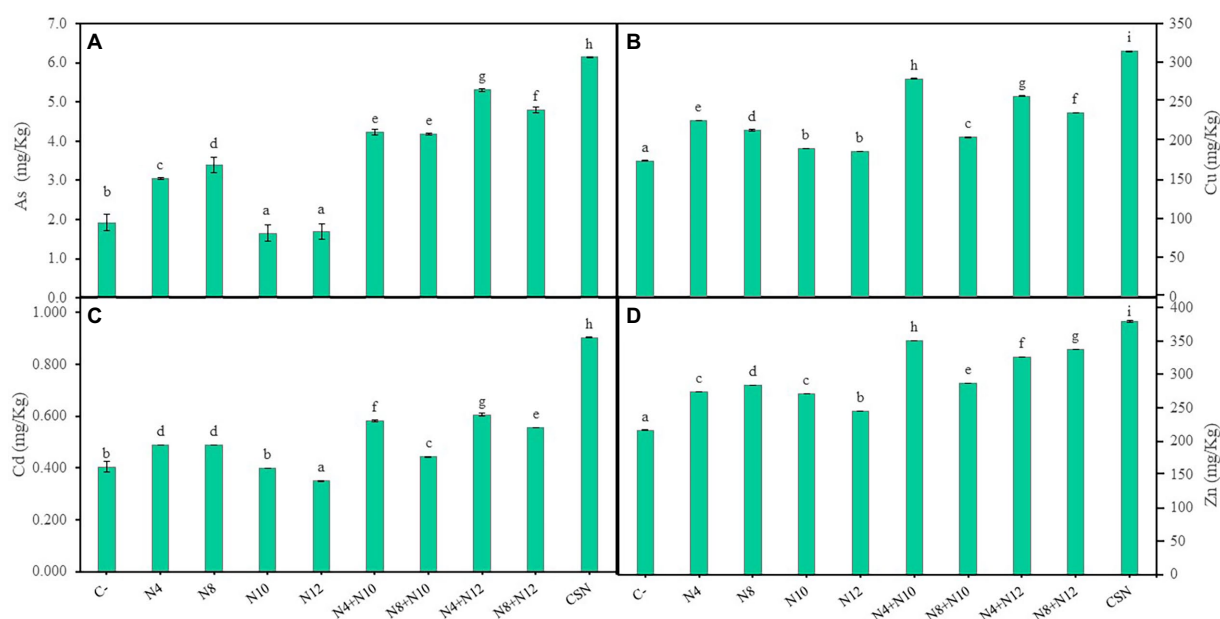


FIGURE 6

Accumulation of metal/loids in roots of *M. sativa*. (A) Accumulation of arsenic, (B) copper, (C) cadmium, and (D) zinc after 60 days in pots containing soil from the high marshes of the Odriel River. Values are means  $\pm$  S.D. ( $n=16$ ). Different letters indicate statistical differences between means (One-way ANOVA; LSD test,  $p<0.001$ ). C-: non inoculation; N4: inoculation with *Pseudomonas* sp. N4; N8: inoculation with *Pseudomonas* sp. N8; N10: inoculation with *Ensifer* sp. N10; N12: inoculation with *Ensifer* sp. N12; N4+N10: co-inoculation with *Pseudomonas* sp. N4 and *Ensifer* sp. N10; N8+N10: co-inoculation with *Pseudomonas* sp. N8 and *Ensifer* sp. N10; N4+N12: co-inoculation with *Pseudomonas* sp. N4 and *Ensifer* sp. N12; N8+N12: co-inoculation with *Pseudomonas* sp. N8 and *Ensifer* sp. N12; CSN: inoculation with *Pseudomonas* sp. N4, *Pseudomonas* sp. N8, *Ensifer* sp. N10 and *Ensifer* sp. N12.

N8, showing all the PGP properties assayed, were selected for *in planta* experiments to determine their potential as nodule enhancing endophytes (NEE) in co-inoculation with *Ensifer* sp. N10 and *Ensifer* sp. N12. In this work, strains N4 and N8 have proved to be nodule endophytes, since fluorescent m-Cherry labelled strains were observed inside *M. sativa* roots and nodules induced by *Ensifer*.

Inoculation with the selected endophytes improved *M. sativa* seeds germination both in presence and absence of As and metals. Several properties may have contributed to this effect: (i) ACC deaminase activity, observed in N4 and N8, that regulates stress level in plants through ethylene degradation (Penrose and Glick, 2003; Chandwani and Amaresan, 2022), (ii) IAA produced by the selected strains, a hormone involved in plant development (Khan et al., 2020; Hu et al., 2021), and (iii) cellulase activity presents in strains N8, N10 and N12, a lytic enzyme that could participate in plant cell wall degradation during seed germination (Flores-Duarte et al., 2022b). The combined effect of these and other properties would also explain why co-inoculation experiments showed better results than single inoculation with one strain and the highest percentage of germination was observed in seeds inoculated with the consortium of the four strains.

The ability of the selected NEE to promote *M. sativa* growth and nodulation in greenhouse conditions was evaluated in soils collected from Odriel river marshes, with low levels of nutrients and moderate to high amounts of As and metals. Inoculation with any of the strains

improved plant biomass, root and shoot length and number and diameter of the leaves. This improvement was generally higher in plants co-inoculated with *Pseudomonas-Ensifer* couples than in plants inoculated with one single strain. The highest plant weights and heights were recorded in plants inoculated with the four strains. The increase in the length of plant roots and shoots may be related to the production of IAA (Khan et al., 2020), that plays an essential role in the development and growth of plants, by increasing cell expansion and is an essential hormone in root development (Hu et al., 2021). Endophyte properties related with nutrient acquisition could also be involved in these results. P availability in the soil is a limiting factor for plant growth and development (Timofeeva et al., 2022). Endophytes could provide phosphorus through phosphate solubilization (Mei et al., 2021; Zhang et al., 2022). In legumes, P helps in the nodulation process, amino acid and proteins synthesis (Wang et al., 2020). Through siderophore production endophytes can provide essential metals such iron and Zn (Mahanty et al., 2017). Other related properties that influence legume growth could be biofilm formation, that is an important mechanism during bacterial attachment to the root, facilitating root colonization and endophyte entry and, at the same time, enhancing nutrient absorption (Das et al., 2012). Finally, the production of lytic enzymes by endophytes could benefit plant growth. These enzymes are essential in the symbiosis between plants and microorganisms, since they contribute to the degradation of organic matter, the colonization of bacteria, the acquisition of nutrients (Wang and Dai, 2010; Eid et al.,



2021), and the degradation of starch as an energy source in the germination stage (Walitang et al., 2017).

Concerning nitrogen, co-inoculation with *Ensifer* and *Pseudomonas* increased the number of nodules induced by *Ensifer* in single inoculations, both in presence and absence of metals, *in vitro* and in greenhouse conditions. Nevertheless, there were no significant differences in the amount of nitrogen accumulated in shoots among inoculation conditions, except in plants inoculated with the consortium that showed the highest levels of nitrogen with significant differences. ACC deaminase activity present in *Pseudomonas* could have facilitated the reduction of the stress levels in the plants by reducing ethylene (Singh et al., 2022), which in excess causes defoliation, senescence and inhibit cell elongation, among other effects (Fatma et al., 2022). In that way, ACC deaminase favors germination, nodulation, and the development of plants (Singh et al., 2022). ACC deaminase activity and IAA production also play an interesting role in the nodulation process by delaying the senescence of the nodule, creating an interaction with the bacteroid (Alemneh et al., 2020). Strains N4 and N8 grew in a nitrogen-free medium, suggesting that they could fix atmospheric nitrogen. In a work in progress, nitrogenase genes (*nifKDH*) have been amplified in these strains (data not shown). This could explain the high levels of nitrogen measured in plant inoculated with *Pseudomonas*.

The positive effects of *Pseudomonas-Ensifer* co-inoculation on plant development were also reflected in the physiological state of the plants, since co-inoculations improved most of the photosynthetic parameters analyzed:  $A_N$ ,  $\Phi_{PSII}$ , ETR and total chlorophyll, except for plants co-inoculated with N4 + N12 plants, that showed the same values of  $\Phi_{PSII}$  than plants inoculated with N8. In addition, plants inoculated with the consortium of the four strains showed the highest efficiency of photosystem II ( $\Phi_{PSII}$ ), the best balance of carbon and water assimilation, the greatest efficiency in the use of energy from the photochemical apparatus, and the biggest increase in total chlorophyll (Liu et al., 2020).

In this work, the levels of stress in *M. sativa* plants were measured by recording the activity of antioxidant defense enzymes, particularly catalase, guaiacol peroxidase, ascorbate peroxidase and superoxide dismutase, that act as protectors against reactive oxygen species (ROS). An excess of ROS production as well as a decrease in the antioxidant defense mechanism causes a breakdown of cell function, damaging the plant and reducing its development (Redondo-Gómez et al., 2011; Mesnoua et al., 2016). Our results showed higher enzymatic activities in plants co-inoculated with *Ensifer* and *Pseudomonas* than in single inoculated plants and the highest activities in plants inoculated with the consortium of the four bacteria. This pointed to the role of these bacteria in regulating stress mechanisms in plants. Induction of antioxidant enzymatic activities after inoculation with rhizospheric bacteria has been reported in plants of *M. sativa* under heavy metal stress (Raklami et al., 2019) and nutrient deficiency (Flores-Duarte et al., 2022b), and in crops such as maize, where inoculated plants showed an increase of catalase, peroxidase, and superoxide dismutase activities (Kukreti et al.,

2020; Chaudhary et al., 2021; Agri et al., 2022). Concerning endophytes, increased enzymatic activities have been reported recently in *M. sativa* plants growing under stress conditions and inoculated with a bacterial consortium containing *Variovorax* nodule endophytes (Flores-Duarte et al., 2022a).

The use of legumes and associated rhizobia is an interesting tool to fight against soil metal contamination, since legume interacting with rhizobia have the ability to accumulate high concentrations of metals particularly in roots, with low levels of translocation to shoots, without disturbing plant growth (Jach et al., 2022). In this work, the highest levels of As, Cd, Cu and Zn measured in shoots of *M. sativa* were much below those allowed for human or animal consumption (Junta de Andalucía and Consejería de Medio Ambiente, 1999), indicating that our strategy would not be dangerous for living beings in terms of metals mobilization. Regarding the accumulation of metals/loids in the roots, inoculation with *Pseudomonas* or *Pseudomonas-Ensifer* couples promoted metal accumulation and the highest levels of As, Cd, Cu and Zn were measured in *M. sativa* roots inoculated with the consortium of the four strains (CSN). In that way, inoculation with *Pseudomonas* strains enhanced the metal phytostabilization potential of *M. sativa* plants in soils with moderate to high levels of metals, without negative effects on plant growth.

Although combinations of *Pseudomonas* and *Ensifer* strains, and particularly those including N8, had a significant positive effect on *M. sativa* growth and nodulation, the best results were always recorded in plants inoculated with the consortium containing the four strains, demonstrating the advantages of using a consortium with several strains and the collaborative effects of their properties.

A consortium of three rhizospheric bacteria able to promote *M. sativa* growth and adaptation in estuarine soils with nutrients poverty has been recently reported (Flores-Duarte et al., 2022b). These PGPB inoculated as consortium in poor-nutrient soils increased plant shoot biomass (around 100%) and ameliorated *M. sativa* nodulation (around 50%) compared to plants inoculated only with rhizobia. Although we have to consider differences between soils to establish comparisons, particularly due to levels of metal contamination, in the current work our consortium of endophytes increased plant shoot biomass around 100% and also ameliorated *M. sativa* nodulation around 100% compared to plants inoculated only with the best performing rhizobia for each parameter. Despite these differences in nodulation improvement, both consortiums induced similar increases in plant N content (around 1 g/100g). Inoculation of *M. sativa* with the rhizospheric consortium also induced positive effects on plant photosynthetic status under nutrient deficiency (Flores-Duarte et al., 2022b). All the photosynthetic parameters recorded showed increased values in plants inoculated with the consortium compared to plants inoculated only with rhizobia, even though, parameters such as  $A_N$  or  $\Phi_{PSII}$  showed no significant differences (Flores-Duarte et al., 2022b). In this work, significant differences in the levels of all the photosynthetic parameters recorded, including  $A_N$  and  $\Phi_{PSII}$ , were observed between plants inoculated with the consortium and those inoculated with

rhizobia, suggesting that endophytes were more efficient in enhancing the photosynthetic status of the plant than rhizospheric bacteria.

The presence of moderate to high levels of metals in the soil, increasing *M. sativa* stress conditions, required the isolation and characterization of specific bacteria able to help the plant to deal with these particular environmental conditions. Our results suggest that inoculants based on non-rhizobial nodule endophytes could be useful and efficient tools to enhance legume adaptation and growth in metal contaminated and nutrient-poor soils. At least under stress conditions, endophytes could provide some advantages as PGPB compared to rhizospheric bacteria, in addition to their narrower relationship with the plant and the lack of competence with soil bacteria (Adeleke and Babalola, 2021; Dwibedi et al., 2022). In that way, it looks necessary to investigate microbiomes of a wide diversity of nitrogen-fixing nodules to find useful inoculants to be applied in different environmental conditions (Martínez-Hidalgo and Hirsch, 2017).

## Conclusion

Autochthonous *Pseudomonas* sp. N4 and *Pseudomonas* sp. N8 strains enhanced growth, nodulation and metal accumulation in roots of *M. sativa* plants inoculated with wild type *Ensifer* strains in soils with low nutrients content and moderate to high levels of metals, ameliorating the physiological state of the plants and helping to regulate plant stress mechanisms, thus facilitating plant adaptation to these abiotic stresses. Our results suggest that selected native PGPNE (plant growth promoting nodule endophytes) could be adequate biotools to promote legume adaptation, growth and phytostabilization potential in nutrient-poor and/or metal contaminated estuarine soils.

## Data availability statement

The datasets presented in this study can be found in online repositories. The names of the repository/repositories and accession number(s) can be found at: <https://www.ncbi.nlm.nih.gov/>, OP060607-OP0606030.

## Author contributions

IR-L and SN-T: conceptualization and writing—original draft preparation. NF-D and SC-D: methodology and investigation.

## References

- Abdu, N., Abdullahi, A. A., and Abdulkadir, A. (2017). Heavy metals and soil microbes. *Environ. Chem. Lett.* 15, 65–84. doi: 10.1007/s10311-016-0587-x
- Adeleke, B. S., and Babalola, O. O. (2021). The endosphere microbial communities, a great promise in agriculture. *Int. Microbiol.* 24, 1–17. doi: 10.1007/s10123-020-00140-2

SN-T: software. SN-T and NF-D: formal analysis. EM-N and SR-G: data curation. IR-L, EM-N, and EP: writing—review and editing and funding acquisition. IR-L and SR-G: supervision. EP: project administration. All authors contributed to the article and approved the submitted version.

## Funding

This research was funded by MCIN, project MCIN/AEI/10.13039/501100011033, UE “NextGenerationEU/PRTR (PDC2021-120951-I00) and Junta de Andalucía, I+D+I FEDER Andalucía project US-1262036 and PAIDI2020, project P20\_00682.

## Acknowledgments

We thank the personnel from the greenhouse and the microscopy service of the Central Services of the Universidad de Sevilla (CITIUS) for their help. NF-D also thanks Universidad de Sevilla for personal support through “Ayudas al estudio a refugiados” (Oficina de Cooperación al Desarrollo).

## Conflict of interest

The authors declare that the research was conducted in the absence of any commercial or financial relationships that could be construed as a potential conflict of interest.

## Publisher’s note

All claims expressed in this article are solely those of the authors and do not necessarily represent those of their affiliated organizations, or those of the publisher, the editors and the reviewers. Any product that may be evaluated in this article, or claim that may be made by its manufacturer, is not guaranteed or endorsed by the publisher.

## Supplementary material

The Supplementary material for this article can be found online at: <https://www.frontiersin.org/articles/10.3389/fmicb.2022.1005458/full#supplementary-material>

- Alemneh, A. A., Zhou, Y., Ryder, M. H., Denton, M. D., Denton, M., and Zhou, Y. (2020). Mechanisms in plant growth-promoting rhizobacteria that enhance legume-rhizobial symbioses. *J. Appl. Microbiol.* 129, 1133–1156. doi: 10.1111/jam.14754
- Aponte, H., Meli, P., Butler, B., Paolini, J., Matus, F., Merino, C., et al. (2020). Meta-analysis of heavy metal effects on soil enzyme activities. *Sci. Total Environ.* 737:139744. doi: 10.1016/j.scitotenv.2020.139744
- Arnon, D. I. (1949). Copper enzymes in isolated chloroplasts. polyphenoloxidase in beta vulgaris. *Plant Physiol.* 24, 1–15. doi: 10.1104/pp.24.1.1
- Aserse, A. A., Räsänen, L. A., Aseffa, F., Hailemariam, A., and Lindström, K. (2013). Diversity of sporadic symbionts and nonsymbiotic endophytic bacteria isolated from nodules of woody, shrub, and food legumes in Ethiopia. *Appl. Microbiol. Biotechnol.* 97, 10117–10134. doi: 10.1007/s00253-013-5248-4
- Bessadok, K., Navarro-Torre, S., Pajuelo, E., Mateos-Naranjo, E., Redondo-Gómez, S., Caviedes, M. A., et al. (2020). The ACC-deaminase producing bacterium *Variovorax* sp. CT7.15 as a tool for improving *Calicotome villosa* nodulation and growth in arid regions of Tunisia. *Microorganisms* 8:541. doi: 10.3390/microorganisms8040541
- Bouyoucos, G. J. (1936). Directions for making mechanical analyses of soils by the hydrometer method. *Soil Sci.* 42, 225–230. doi: 10.1097/00010694-193609000-00007
- Bradford, M. M. (1976). A rapid and sensitive method for the quantitation of microgram quantities of protein utilizing the principle of protein-dye binding. *Anal. Biochem.* 72, 248–254. doi: 10.1016/0003-2697(76)90527-3
- Caracciolo, A. B., and Terenzi, V. (2021). Rhizosphere microbial communities and heavy metals. *Microorganisms* 9:1462. doi: 10.3390/microorganisms9071462
- Carrasco, J. A., Armario, P., Pajuelo, E., Burgos, A., Caviedes, M. A., Lopez, J. A. C., et al. (2005). Isolation and characterisation of symbiotically effective *Rhizobium* resistant to arsenic and heavy metals after the toxic spill at the Aznalcollar pyrite mine. *Soil Biol. Biochem.* 37, 1131–1140. doi: 10.1016/j.soilbio.2004.11.015
- Chandwani, S., and Amaresan, N. (2022). Role of ACC deaminase producing bacteria for abiotic stress management and sustainable agriculture production. *Environ. Sci. Pollut. Res. Int.* 29, 22843–22859. doi: 10.1007/s11356-022-18745-7
- Chaudhary, P., Khatri, P., Gangola, S., Kumar, A., Kumar, R., and Sharma, A. (2021). Impact of nanochitosan and *Bacillus* spp. on health, productivity and defence response in *Zea mays* under field condition. *3 Biotech* 11:237. doi: 10.1007/s13205-021-02790-z
- Chaudhary, P., Singh, S., Chaudhary, A., Sharma, A., and Kumar, G. (2022). Overview of biofertilizers in crop production and stress management for sustainable agriculture. *Front. Plant Sci.* 13:930340. doi: 10.3389/fpls.2022.930340
- Chen, Y., Hu, W., Huang, B., Weindorf, D. C., Rajan, N., Liu, X., et al. (2013). Accumulation and health risk of heavy metals in vegetables from harmless and organic vegetable production systems of China. *Ecotoxicol. Environ. Saf.* 98, 324–330. doi: 10.1016/j.2013.09.037
- Das, N., Basak, L. V. G., Salam, J. A., and Abigail, E. A. (2012). Application of biofilms on remediation of pollutants- an overview. *J. Microbiol. Biotech. Res.* 2, 783–790.
- De Meyer, S. E., De Beuf, K., and Vekeman, B. A. (2015). Large diversity of non-rhizobial endophytes found in legume root nodules in Flanders (Belgium). *Soil Biol. Biochem.* 83, 1–11. doi: 10.1016/j.soilbio.2015.01.002
- del Castillo, I., Hernández, P., Lafuente, A., Rodríguez-Llorente, I., Caviedes, M., and Pajuelo, E. (2012). Self-bioremediation of cork-processing wastewaters by (chloro)phenol-degrading bacteria immobilised onto residual cork particles. *Water Res.* 46, 1723–1734. doi: 10.1016/j.watres.2011.12.038
- Döbereiner, J. (1995). “Isolation and identification of aerobic nitrogen-fixing bacteria from soil and plants,” in *Methods in applied soil microbiology and biochemistry*. eds. K. Alef and P. Nannipieri (London, UK: Academic Press), 134–141.
- Du, B., Chen, N., Song, L., Wang, D., Cai, H., Yao, L., et al. (2021). Alfalfa (*Medicago sativa* L.) MsCML46 gene encoding calmodulin-like protein confers tolerance to abiotic stress in tobacco. *Plant Cell Rep.* 40, 1907–1922. doi: 10.1007/s00299-021-02757-7
- Dwivedi, V., Rath, S. K., Joshi, M., Kaur, R., Kaur, G., Singh, D., et al. (2022). Microbial endophytes: application towards sustainable agriculture and food security. *Appl. Microbiol. Biotechnol.* 106, 5359–5384. doi: 10.1007/s00253-022-12078-8
- Ehrhardt, D. W., Atkinson, M. E., and Long, S. R. (1992). Depolarization of alfalfa root hair membrane potential by *Rhizobium meliloti* nod factors. *Science* 256, 998–1000. doi: 10.1126/10744524
- Eid, A. M., Fouda, A., Abdel-Rahman, M. A., Salem, S. S., Elsaied, A., Oelmüller, R., et al. (2021). Harnessing bacterial endophytes for promotion of plant growth and biotechnological applications: an overview. *Plan. Theory* 10:935. doi: 10.3390/plants10050935
- Elbeltagy, A., Nishioka, K., Suzuki, H., Sato, T., Sato, Y. I., Morisaki, H., et al. (2000). Isolation and characterization of endophytic bacteria from wild and traditionally cultivated rice varieties. *Soil Sci. Plant Nutr.* 46, 617–629. doi: 10.1080/00380768.2000.10409127
- Etesami, H., Jeong, B. R., and Glick, B. R. (2021). Contribution of arbuscular mycorrhizal fungi, phosphate-solubilizing bacteria, and silicon to P uptake by plant. *Front. Plant Sci.* 12:699618. doi: 10.3389/fpls.2021.699618
- FAO, ITPS. (2015) *Status of the World's soil resources (SWSR). - Main report*. Roma: FAO and Intergovernmental Technical Panel on Soils: Roma, Italy.
- Fasusi, O. A., Cruz, C., and Babalola, O. O. (2021). Agricultural sustainability: microbial biofertilizers in rhizosphere management. *Agriculture* 11:163. doi: 10.3390/agriculture11020163
- Fatma, M., Asgher, M., Iqbal, N., Rasheed, F., Sehar, Z., Sofo, A., et al. (2022). Ethylene signaling under stressful environments: analyzing collaborative knowledge. *Plants* 11:2211. doi: 10.3390/plants11172211
- Ferreira, H., Vasconcelos, M., Gil, A. M., and Pinto, E. (2021). Benefits of pulse consumption on metabolism and health: a systematic review of randomized controlled trials. *Crit. Rev. Food Sci. Nutr.* 61, 85–96. doi: 10.1080/10408398.2020.1716680
- Finan, T. M., Kunkel, B., De Vos, G. F., and Signer, E. R. (1986). Second symbiotic megaplasmid in *Rhizobium meliloti* carrying exopolysaccharide and thiamine synthesis genes. *J. Bacteriol.* 167, 66–72. doi: 10.1128/jb.167.1.66-72.1986
- Flores-Duarte, N. J., Mateos-Naranjo, E., Redondo-Gómez, S., Pajuelo, E., Rodríguez-Llorente, I. D., and Navarro-Torre, S. (2022b). Role of nodulation-enhancing rhizobacteria in the promotion of *Medicago sativa* development in nutrient-poor soils. *Plan. Theory* 11:1164. doi: 10.3390/plants11091164
- Flores-Duarte, N. J., Pérez-Pérez, J., Navarro-Torre, S., Mateos-Naranjo, E., Redondo-Gómez, S., Pajuelo, E., et al. (2022a). Improved *Medicago sativa* nodulation under stress assisted by *Variovorax* sp. endophytes. *Plan. Theory* 11:1091. doi: 10.3390/plants11081091
- García-Martí, M., Piñero, M. C., García-Sánchez, F., Mestre, T. C., López-Delacalle, M., Martínez, V., et al. (2019). Amelioration of the oxidative stress generated by simple or combined abiotic stress through the K<sup>+</sup> and Ca<sup>2+</sup> supplementation in tomato plants. *Antioxid.* 8:81. doi: 10.3390/8040081
- Genty, B., Briantais, J. M., and Baker, N. R. (1989). The relationship between the quantum yield of photosynthetic electron transport and quenching of chlorophyll fluorescence. *Biochim. Biophys. Acta Gen. Subj.* 990, 87–92. doi: 10.1016/S0304-4165(89)80016-9
- Gordon, S. A., and Weber, R. P. (1951). Colorimetric estimation of indole acetic acid. *Plant Physiol.* 26, 192–195. doi: 10.1104/pp.26.1.192
- Graham, P. H., and Vance, C. P. (2003). Legumes: importance and constraints to greater use. *Plant Physiol.* 131, 872–877. doi: 10.1104/pp.017004
- Herrera Marcano, T. (2011). Cadmium contamination in agricultural soils. *Venezuelas* 8, 42–47.
- Hiscox, J. D., and Israelstam, G. F. (1979). A method for the extraction of chlorophyll from leaf tissue without maceration. *Can. J. Bot.* 57, 1332–1334. doi: 10.1139/b79-163
- Hu, Q. Q., Shu, J. Q., Li, W. M., and Wang, G. Z. (2021). Role of auxin and nitrate signaling in the development of root system architecture. *Front. Plant Sci.* 12:690363. doi: 10.3389/fpls.2021.690363
- Hudson-Edwards, K. A., Schell, C., and y Macklin, M. G., (1999). Mineralogy y geochemistry of alluvium contaminated by metal mining in the Rio Tinto area, Southwest Spain. *Appl. Geochem.* 14, 1015–1030. doi: 10.1016/S0883-2927(99)00008-6
- Jach, M. E., Sajana, E., and Ziaja, M. (2022). Utilization of legume-nodule bacterial symbiosis in phytoremediation of heavy metal-contaminated soils. *Biology* 11:676. doi: 10.3390/biology11050676
- Junta de Andalucía, Consejería de Medio Ambiente. (1999). Los criterios y estándares para declarar un suelo contaminado en Andalucía y la metodología y técnicas de toma de muestra y análisis para su investigación. Available at: <https://www.ugr.es/~fjmartin/INFORMES/Criterios%20y%20estandares.pdf>. [Accessed July 2022].
- Kang, S.-M., Shahzad, R., Khan, M. A., Hasnain, Z., Lee, K.-E., Park, H.-S., et al. (2021). Ameliorative effect of indole-3-acetic acid- and siderophore-producing *Leclercia adecarboxylata* MO1 on cucumber plants under zinc stress. *J. Plant Interact.* 16, 30–41. doi: 10.1080/17429145.2020.1864039
- Khan, M. S., Gao, J., Chen, X., Zhang, M., Yang, F., Du, Y., et al. (2020). Isolation and characterization of plant growth-promoting endophytic bacteria *Paenibacillus polymyxa* SK1 from *Lilium lancifolium*. *Biomed. Res. Int.* 2020:8650957. doi: 10.1155/2020/8650957
- Krall, J. P., and Edwards, G. E. (1992). Relationship between photosystem II activity and CO<sub>2</sub> fixation in leaves. *Physiol. Plant.* 86, 180–187. doi: 10.1111/j.1399-3054.1992.tb01328.x
- Kukreti, B., Sharma, A., Chaudhary, P., Agri, U., and Maithani, D. (2020). Influence of nanosilicon dioxide along with bioinoculants on *Zea mays* and its rhizospheric soil. *3 Biotech* 10:345. doi: 10.1007/s13205-020-02329-8
- Legendijk, E. L., Validov, S., Lamers, G. E. M., de Weert, S., and Bloemberg, G. V. (2010). Genetic tools for tagging gram-negative bacteria with mCherry for



- visualization in vitro and in natural habitats, biofilm and pathogenicity studies. *FEMS Microbiol. Lett.* 305, 81–90. doi: 10.1111/j.1574-6968.2010.01916.x
- León-Barrios, M., Lorite, M. J., Donate-Correa, J., and Sanjuán, J. (2009). *Ensifer meliloti* bv. Lancerottense establishes nitrogen-fixing symbiosis with *Lotus* endemic to the Canary Islands and shows distinctive symbiotic genotypes and host range. *Syst. Appl. Microbiol.* 32, 413–420. doi: 10.1016/j.syapm.2009.04.003
- Liu, J., Liu, X., Zhang, Q., Li, S., Sun, Y., Lu, W., et al. (2020). Response of alfalfa growth to arbuscular mycorrhizal fungi and phosphate-solubilizing bacteria under different phosphorus application levels. *AMB Express* 10:200. doi: 10.1186/s13568-020-01137-w
- Lurthy, T., Cantat, C., Jeudy, C., Declerck, P., Gallardo, K., Barraud, C., et al. (2020). Impact of bacterial siderophores on iron status and ionome in pea. *Front. Plant Sci.* 11:730. doi: 10.3389/fpls.2020.00730
- Mahanty, T., Bhattacharjee, S., Goswami, M., Bhattacharyya, P., Das, B., Ghosh, A., et al. (2017). Biofertilizers: a potential approach for sustainable agriculture development. *Environ. Sci. Pollut. Res.* 24, 3315–3335. doi: 10.1007/s11356-016-8104-0
- Martínez-Hidalgo, P., and Hirsch, A. M. (2017). The nodule microbiome: N-2-fixing rhizobia do not live alone. *Phytobiomes J.* 1, 70–82. doi: 10.1094/PBIOMES-12-16-0019-RVW
- Mateos-Naranjo, E., Mesa, J., Pajuelo, E., Perez-Martin, A., Caviedes, M. A., and Rodríguez-Llorente, I. D. (2015). Deciphering the role of plant growth promoting rhizobacteria in the tolerance of the invasive cordgrass *Spartina densiflora* to physicochemical properties of marshes soils. *Plant Soil* 394, 45–55. doi: 10.1007/s11104-015-2504-7
- Mei, C., Chretien, R. L., Amaradasa, B. S., He, Y., Turner, A., and Lowman, S. (2021). Characterization of phosphate solubilizing bacterial endophytes and plant growth promotion in vitro and in greenhouse. *Microorganisms* 9:1935. doi: 10.3390/microorganisms9091935
- Mesa, J., Mateos-Naranjo, E., Caviedes, M. A., Redondo-Gómez, S., Pajuelo, E., and Rodríguez-Llorente, I. D. (2015b). Endophytic cultivable bacteria of the metal bioaccumulator *Spartina maritima* improve plant growth but not metal uptake in polluted marshes soils. *Front. Microbiol.* 6:1450. doi: 10.3389/fmicb.2015.01450
- Mesa, J., Naranjo, E. M., Caviedes, M., Redondo-Gómez, S., Pajuelo, E., and Rodríguez-Llorente, I. D. (2015a). Scouting contaminated estuaries: heavy metal resistant and plant growth promoting rhizobacteria in the native metal rhizoaccumulator *Spartina maritima*. *Mar. Pollut. Bull.* 90, 150–159. doi: 10.1016/j.marpolbul.2014.11.002
- Mesnau, M., Mateos-Naranjo, E., Barcia-Piedras, J. M., Perez-Romero, J. A., Lotmani, B., and Redondo-Gomez, S. (2016). Physiological and biochemical mechanisms preventing Cd-toxicity in the hyperaccumulator *Atriplex halimus* L. *Plant Physiol. Biochem.* 106, 30–38. doi: 10.1016/j.plaphy.2016.04.041
- Mnasri, B., Aouania, M. E., and Mhamdi, R. (2007). Nodulation and growth of common bean (*Phaseolus vulgaris*) under water deficiency. *Soil Biol. Biochem.* 39, 1744–1750. doi: 10.1016/j.soilbio.2007.01.030
- Monteoliva, M. I., Valetti, L., Taurian, T., Crociara, C. S., and Guzzo, M. C. (2022). “Synthetic communities of bacterial endophytes to improve the quality and yield of legume crops,” in *Legumes research*. eds. J. C. Jimenez-Lopez and A. Clemente, Vol. 1 [Working Title (London, UK: IntechOpen).
- Nautiyal, C. S. (1999). An efficient microbiological growth medium for screening phosphate solubilizing microorganisms. *FEMS Microbiol. Lett.* 170, 265–270. doi: 10.1111/j.1574-6968.1999.tb13383.x
- Navarro-Torre, S., Barcia-Piedras, J. M., Caviedes, M. A., Pajuelo, E., Redondo-Gómez, S., Rodríguez-Llorente, I. D., et al. (2017). Bioaugmentation with bacteria selected from the microbiome enhances *Arthrocnemum macrostachyum* metal accumulation and tolerance. *Mar. Pollut. Bull.* 117, 340–347. doi: 10.1016/j.marpolbul.2017.02.008
- Navarro-Torre, S., Bessadok, K., Flores-Duarte, N. J., Rodríguez-Llorente, I. D., Caviedes, M. A., and Pajuelo, E. (2020). “Helping legumes under stress situations: inoculation with beneficial microorganisms,” in *Legume crops*. ed. M. Hasanuzzaman (London, UK: Intech Open), 1–10. doi: 10.5772/intechopen.91857
- Navarro-Torre, S., Naranjo, E. M., Caviedes, M., Pajuelo, E., and Rodríguez-Llorente, I. (2016). Isolation of plant-growth-promoting and metal-resistant cultivable bacteria from *Arthrocnemum macrostachyum* in the Odiel marshes with potential use in phytoremediation. *Mar. Pollut. Bull.* 110, 133–142. doi: 10.1016/j.marpolbul.2016.06.070
- Navarro-Torre, S., Rodríguez-Llorente, I. D., Doukalli, B., Caviedes, M. A., and Pajuelo, E. (2019). Competition for alfalfa nodulation under metal stress by the metal-tolerant strain *Ochrobactrum cytisi* Azn6. *Ann. Appl. Biol.* 175, 184–192. doi: 10.1111/aab.12528
- Penrose, D. M., and Glick, B. R. (2003). Methods for isolating and characterizing ACC deaminase-containing plant growth-promoting rhizobacteria. *Physiol. Plant.* 118, 10–15. doi: 10.1034/j.1399-3054.2003.00086.x
- Poole, P., Ramachandran, V., and Terpolilli, V. (2018). Rhizobia: from saprophytes to endosymbionts. *Nat. Rev. Microbiol.* 16, 291–303. doi: 10.1038/nrmicro.2017.171
- Prescott, H. (2002). *Laboratory exercises in microbiology*, Vol. 466 (New York, USA: McGraw-Hill).
- Rajendran, G., Patel, M. H., and Joshi, S. J. (2012). Isolation and characterization of nodule-associated *Exiguobacterium* sp. from the root nodules of fenugreek (*Trigonella foenu-graecum*) and their possible role in plant growth promotion. *Int. J. Microbiol.* 2012:693982. doi: 10.1155/2012/693982
- Raklami, A., Oufdou, K., Tahiri, A. I., Mateos-Naranjo, E., Navarro-Torre, S., Rodríguez-Llorente, I. D., Meddich, A., Redondo-Gómez, S., and Pajuelo, E. (2019). Safe cultivation of *Medicago sativa* in metal-polluted soils from semi-arid regions assisted by heat- and metallo-resistant PGPR. *Microorganisms* 7:E212. doi:10.3390/microorganisms7070212
- Raza, A., Razzaq, A., Mehmood, S. S., Zou, X., Zhang, X., Lv, Y., et al. (2019). Impact of climate change on crops adaptation and strategies to tackle its outcome: a review. *Plan. Theory* 8:34. doi: 10.3390/plants8020034
- Redondo-Gómez, S., Andrades-Moreno, L., Mateos-Naranjo, E., Parra, R., Valera-Burgos, J., and Arco, R. (2011). Synergic effect of salinity and zinc stress on growth and photosynthetic responses of the cordgrass, *Spartina densiflora*. *J. Exp. Bot.* 62, 5521–5530. doi: 10.1093/jxb/err234
- Roy, S., Liu, W., Nandety, R. S., Crook, A., Mysore, K. S., Pislariu, C. I., et al. (2020). Celebrating 20 years of genetic discoveries in legume nodulation and symbiotic nitrogen fixation. *Plant Cell* 32, 15–41. doi: 10.1105/tpc.19.00279
- Schreiber, U., Schliwa, U., and Bilger, W. (1986). Continuous recording of photochemical and non-photochemical chlorophyll fluorescence quenching with a new type of modulation fluorometer. *Photosynth. Res.* 10, 51–62. doi: 10.1007/BF00024185
- Schwyn, B., and Neilands, J. B. (1987). Universal chemical assay for the detection and determination of siderophores. *Anal. Biochem.* 160, 47–56. doi: 10.1016/0003-2697(87)90612-9
- Shiraishi, A., Matsushita, N., and Hougetsu, T. (2010). Nodulation in black locust by the Gammaproteobacteria pseudomonas sp. and the Betaproteobacteria *Burkholderia* sp. *Syst. Appl. Microbiol.* 33, 269–274. doi: 10.1016/j.syapm.2010.04.005
- Singh, R. P., Ma, Y., and Shadan, A. (2022). Perspective of ACC-deaminase producing bacteria in stress agriculture. *J. Biotechnol.* 352, 36–46. doi: 10.1016/j.jbiotec.2022.05.002
- Singh, A., Sharma, R., Agrawal, M., and Marshall, F. (2010). Health risk assessment of heavy metals via dietary intake of foodstuffs from the wastewater irrigated site of a dry tropical area of India. *Food Chem. Toxicol.* 48, 611–619. doi: 10.1016/j.fct.2009.11.041
- Stagnari, F., Maggio, A., Galieni, A., and Pisante, M. (2017). Multiple benefits of legumes for agriculture sustainability: an overview. *Chem. Biol. Technol. Agric.* 4:2. doi: 10.1186/s40538-016-0085-1
- Timofeeva, A., Galyamova, M., and Sedykh, S. (2022). Prospects for using phosphate-solubilizing microorganisms as natural fertilizers in agriculture. *Plan. Theory* 11:2119. doi: 10.3390/plants11162119
- Velázquez, E., Martínez-Hidalgo, P., Carro, L., Alonso, P., Peix, A., Trujillo, M. E., et al. (2013). “Nodular endophytes: an untapped diversity,” in *Beneficial plant—Microbial interactions: Ecology and applications*. eds. B. R. M. González and J. González-López (Boca Raton, FL, USA: CRC Press), 214–236.
- Verma, S., and Kuila, A. (2019). Bioremediation of heavy metals by microbial process. *Environ. Technol. Innov.* 14:100369. doi: 10.1016/j.eti.2019.100369
- Vishwakarma, K., Kumar, N., Shandilya, C., Mohapatra, S., Bhayana, S., and Varma, A. (2020). Revisiting plant-microbe interactions and microbial consortia application for enhancing sustainable agriculture: a review. *Front. Microbiol.* 11:560406. doi: 10.3389/fmicb.2020.560406
- Walitang, D. I., Kim, K., Madhaiyan, M., Kim, Y. K., Kang, Y., and Sa, T. (2017). Characterizing endophytic competence and plant growth promotion of bacterial endophytes inhabiting the seed endosphere of rice. *BMC Microbiol.* 17:209. doi: 10.1186/s12866-017-1117-0
- Walkley, A., and Black, C. A. (1934). An examination of the Degtjareff method for determining soil organic matter and a proposed modification of the chromic acid titration method. *Soil Sci.* 37, 29–38. doi: 10.1097/00010694-193401000-00003
- Wang, Y., and Dai, C. C. (2010). Endophytes: a potential resource for biosynthesis, biotransformation and biodegradation. *Ann. Microbiol.* 61, 207–215. doi: 10.1007/s13213-010-0120-6
- Wang, Y., Yang, Z., Kong, Y., Li, X., Li, W., Du, H., et al. (2020). GmPAP12 is required for nodule development and nitrogen fixation under phosphorus starvation in soybean. *Front. Plant Sci.* 11:450. doi: 10.3389/fpls.2020.00450
- Yoon, S. H., Ha, S. M., Kwon, S., Lim, J., Kim, Y., Seo, H., et al. (2017). Introducing EzBioCloud: a taxonomically united database of 16S rRNA gene sequences and whole-genome assemblies. *Int. J. Syst. Evol. Microbiol.* 67, 1613–1617. doi: 10.1099/ijsem.0.001755
- Zhang, C., Cai, K., Li, M., Zheng, J., and Han, Y. (2022). Plant-growth-promoting potential of PGPE isolated from *Dactylois glomerata* L. *Microorganisms* 10:731. doi: 10.3390/microorganisms10040731





## OPEN ACCESS

## EDITED BY

Ravindra Soni,  
Indira Gandhi Krishi Vishva Vidyalyaya,  
India

## REVIEWED BY

Samy Selim,  
Al Jouf University,  
Saudi Arabia  
Regina Sharmila Dass,  
Pondicherry University,  
India  
Deep Chandra Suyal,  
Eternal University,  
India

## \*CORRESPONDENCE

Debdulal Banerjee  
✉ debu33@gmail.com;  
✉ db@mail.vidyasagar.ac.in

## SPECIALTY SECTION

This article was submitted to  
Microbiotechnology,  
a section of the journal  
Frontiers in Microbiology

RECEIVED 07 October 2022

ACCEPTED 29 December 2022

PUBLISHED 26 January 2023

## CITATION

Santra HK and Banerjee D (2023) Drought  
alleviation efficacy of a galactose rich  
polysaccharide isolated from endophytic  
*Mucor* sp. HELF2: A case study on rice plant.  
*Front. Microbiol.* 13:1064055.  
doi: 10.3389/fmicb.2022.1064055

## COPYRIGHT

© 2023 Santra and Banerjee. This is an open-  
access article distributed under the terms of  
the [Creative Commons Attribution License](https://creativecommons.org/licenses/by/4.0/)  
(CC BY). The use, distribution or reproduction  
in other forums is permitted, provided the  
original author(s) and the copyright owner(s)  
are credited and that the original publication  
in this journal is cited, in accordance with  
accepted academic practice. No use,  
distribution or reproduction is permitted  
which does not comply with these terms.

# Drought alleviation efficacy of a galactose rich polysaccharide isolated from endophytic *Mucor* sp. HELF2: A case study on rice plant

Hiran Kanti Santra and Debdulal Banerjee\*

Microbiology and Microbial Biotechnology Laboratory, Department of Botany and Forestry, Vidyasagar University, Midnapore, West Bengal, India

Endophytes play a vital role in plant growth under biotic and abiotic stress conditions. In the present investigation, a Galactose-Rich Heteropolysaccharide (GRH) with a molecular weight of  $2.98 \times 10^5$  Da was isolated from endophytic *Mucor* sp. HELF2, a symbiont of the East Indian screw tree *Helicteres isora*. OVAT (One Variable at A Time) experiment coupled with RSM (Response Surface Methodology) study exhibited 1.5-fold enhanced GRH production ( $20.10 \text{ g L}^{-1}$ ) in supplemented potato dextrose broth at a pH of 7.05 after 7.5 days of fermentation in  $26^\circ\text{C}$ . GRH has alleviated drought stress (polyethylene glycol induced) in rice seedlings (*Oryza sativa* ssp. indica MTU 7093 swarna) by improving its physicochemical parameters. It has been revealed that spray with a 50-ppm dosage of GRH exhibited an improvement of 1.58, 2.38, 3, and 4 times in relative water contents and fresh weight of the tissues, root length, and shoot length of the rice seedlings, respectively “in comparison to the control”. Moreover, the soluble sugars, prolines, and chlorophyll contents of the treated rice seedlings were increased up to 3.5 ( $0.7 \pm 0.05 \text{ mg/g}$  fresh weight), 3.89 ( $0.57 \pm 0.03 \text{ mg/g}$  fresh weight), and 2.32 ( $1,119 \pm 70.8 \mu\text{g/gm}$  of fresh weight) fold respectively, whereas malondialdehyde contents decreased up to 6 times. The enzymatic antioxidant parameters like peroxidase and superoxide dismutase and catalase activity of the 50ppm GRH treated seedlings were found to be elevated 1.8 ( $720 \pm 53 \text{ unit/gm/min}$  fresh weight), 1.34 ( $75.34 \pm 4.8 \text{ unit/gm/min}$  fresh weight), and up to 3 ( $100 \text{ ppm}$  treatment for catalase –  $54.78 \pm 2.91 \text{ unit/gm/min}$  fresh weight) fold, respectively. In this context, the present outcomes contribute to the development of novel strategies to ameliorate drought stress and could fortify the agro-economy of India.

## KEYWORDS

optimisation, drought stress alleviation, *Mucor* sp. HELF2, endophyte, hetero polysaccharide

## Introduction

The foundation of the global food economy is agriculture, and in a nation like India, Gross Domestic Production (GDP) is heavily reliant on the agrarian model. Crop loss due to biotic and abiotic stressors is a widespread issue that requires effective management techniques to keep the agroecosystem in good shape. Biotic stress-related issues can be addressed with a variety of chemical formulations, such as pesticides, herbicides, fungicides, and biological techniques, such as biological control agents (BCA) and plant growth promoters (PGPs), but abiotic stress management strategies have received scant attention. As a result, issues with salt and drought stress are severely impeding crop development and yield, with dryness being the most detrimental. Agriculture production is significantly declining globally (Chen et al., 2017). The problem is getting worse as a result of cases

of global warming and water scarcity. The agrarian economy is struggling with production-related problems as well as severe financial constraints (Vurukonda et al., 2016). According to reports, to fulfil this ambitious goal by 2050, food production must increase by up to 60 to 110 percent. Drought-related challenges must be immediately resolved (Naumann et al., 2018; Dey et al., 2019; Paglia and Parker, 2021). Therefore, it is urgent to discover a new, long-lasting solution to this global dilemma (Coleman-Derr and Tringe, 2014). One of the initial answers to that problem is to create stress-resistant varieties, but doing so takes time, is rigorous, species-specific, and is expensive (Santra and Banerjee, 2022a). One approach might be to cultivate crops on reclaimed drought-affected land while using foliar plant growth-promoting/stress-resisting chemicals. Rhizobacteria that promote plant growth have already been evaluated for this purpose, and less-studied endophyte or endophytic fungal or bacterial polysaccharides are currently showing promise in this field (Chen et al., 2017; Sun et al., 2020a,b).

Endophytes are ubiquitous in occurrence and are procured from nearly all plants and plant parts studied to date across the globe (Coleman-Derr and Tringe, 2014; Chatterjee et al., 2022). The symbionts of plant tissues known as endophytes help the plant grow and give tolerance in challenging conditions. Due to their horizontal gene transfer as a result of the co-evolution of the host and microorganisms, they share crucial genes of essential metabolomes (Santra et al., 2022; Santra and Banerjee, 2022b; Santra and Banerjee, 2022c). They have a reputation for being bioactive chemical mines that are simple to access using contemporary biotechnological methods. Plant growth-promoting endophytic bacteria and fungi reside on different internal plant tissues and organs, i.e., in stems, roots, flowers, leaves, fruits, and seeds. Endophytes have recently drawn attention because they are an effective tool for teaching plants to tolerate lethal abiotic stressors like drought, salt, and heavy metal toxicity (Cherif et al., 2015; Mesa et al., 2015; Pinedo et al., 2015; Constantin et al., 2019; Moghaddam et al., 2021) through adopting various mechanisms. The two most prevalent and important methods of building stress resistance are decreasing the levels of the key gaseous hormone ethylene through the activity of ACC (1-aminocyclopropane-1-carboxylate) deaminase and increasing the content of prolines in the tissues (Blaha et al., 2006; Gamalero and Bernard, 2012; Marasco et al., 2012). In addition to these, accumulation of siderophores and osmolytes, increased antioxidant and photosynthetic rates, synthesis of phytohormones and organic acids, and emission of volatile organic compounds are other important mechanisms used by endophytes to increase host plant abiotic stress tolerance (Tiwari et al., 2016; Vurukonda et al., 2016). Recent reports include that microbial symbionts or fungal endophytes are the co-evolution partners of green plants and promote habitat-specific stress tolerance in host plants (Rodriguez and Redman, 2008; Redman et al., 2011). A special type of long-chain polymeric secondary metabolite called exopolysaccharides (EPS) from endophytic sources holds immense agricultural utility especially in ameliorating drought and salt stress (Nadeem et al., 2014; Rolli et al., 2015).

In the current study, exopolysaccharide was extracted from the endophytic fungus *Mucor* sp. HELF2 (isolated from *Helicteres isora* flowers). The EPS was galactose-rich heteropolysaccharide (GRH) in composition. GRH was found to be effective in reducing drought stress conditions when applied to the foliar parts of the rice seedling *Oryza sativa* ssp. indica MTU 7093 swarna. GRH production by HELF2 was optimised by adopting statistical modelling using Minitab and the predicted model led to an enhancement of 1.5 times exopolysaccharide (GRH) production under optimised fermentation conditions. The application of 50 ppm GRH was discovered to be the

most efficient dosage, and the physical/biochemical traits of the treated plants were discovered to be higher than those of the untreated ones. Root and shoot length, fresh weight, enzymatic antioxidant profiles, and proline contents were improved remarkably after treatment. The membrane damage caused by lipid peroxidation was also minimised when GRH was applied *in vivo*. MDA content was reduced and SOD, CAT, and POD values were elevated. The current study illuminates the agricultural potential of endophytic exopolysaccharide, which has the potential to expand the field of sustainable development and improve the agro-economy of our nation's indigenous population.

## Materials and methods

### Isolation and identification of GRH-producing endophytic fungi

*Mucor* sp. HELF2 was isolated as an endophyte from the flower of an ethnomedicinally valuable plant *Helicteres isora* collected from forests in the East Singbhum district, Jharkhand, West Bengal, India, and stored, maintained on PDA slants and Petri plates at  $4 \pm 2^\circ\text{C}$  and  $25 \pm 2^\circ\text{C}$ , respectively. In brief, plant parts were thoroughly washed by running tap water for 5 min, sodium hypochlorite (2–10%) for 2 min, and hydrogen peroxide (2%) for 1 min, respectively, and explants were incubated on water agar plates at  $27^\circ\text{C}$  on biological oxygen demand incubator for endophyte isolation. Water agar plates were supplemented with antibiotics (streptomycin and tetracycline-  $50 \text{ mg L}^{-1}$ ) to avoid bacterial endophytes. The effectiveness of this sterilisation and isolation process was cross-checked by the explant imprintation technique described by Schulz et al. (1993). In brief, the aliquots used for explant sterilisation were spread on a water agar medium and incubated under the same conditions. After, 3–5 days of incubation, fungal hyphae emerged from the tissues and they were transferred to PDA plates for optimum growth (Schulz et al., 1993). Emerging fungal hyphal tips were transferred to PDA (Potato Dextrose Agar) medium and morphology (both macroscopic and microscopic) of the fungal isolate was recorded using light (Primo Star, Zeiss, Germany) and stereo microscope (Stemi 508, Zeiss, Germany).

The organism was identified by rDNA-based molecular technique as there was no reproductive structure produced by the endophytic fungi even in a medium with carnated leaves. In brief, genomic DNA of the fungal isolate was obtained (using DNeasy Plant Minikit-Qiagen, Germany) and a polymerase chain reaction was performed using the two universal primers named ITS1 (5'-TCCGTAGGTGAACC TTGCGG-3') and ITS4 (5'-TCCTCCGCTTATGATATGC-3'; Laich and Andrade, 2016; Landum et al., 2016). The PCR products were separated using 1% agarose gel in 1X TAE buffer (90 mM Tris-acetate and 2 mM EDTA, pH 8.0), stained with ethidium bromide ( $0.5 \mu\text{g mL}^{-1}$ ), and documented using BIO-RAD Gel Doc EZ imager version 5.1 (United States). PCR products were sent for direct bi-directional sequencing using ABI 3730xl Genetic Analyzer (Applied Biosystems, United States) to Bioserve Biotechnologies (India) Pvt. Ltd., A Repro Cell Company, Hyderabad, India. The obtained consensus sequence of 620 bp was used for further study. Sequences were submitted to GenBank and were compared to the GenBank database using BLAST. Fifteen sequences along with HELF2 were selected and aligned using the multiple alignment software program Clustal W and the phylogenetic tree was prepared using MEGA 11 (Tamura et al., 2021).

## Production of GRH and optimisation of culture conditions by OVAT technique

Endophytic fungi were grown in different 250 mL Erlenmeyer flasks with 50 mL potato dextrose broth in a shaker incubator at 120 rpm for 8 days. An initial medium pH of 6 and a medium temperature of 28°C were maintained.

To detect the optimum culture conditions for the maximum production of GRH, fungi were grown in varying fermentation times (4–10 days), then in different medium pH (5.5–7.9), and then at varying incubation temperatures (20–30°C) in separate Erlenmeyer flasks with separate PDB medium. To find out the requirement of additional nutrients for maximum GRH production and mycelial growth, various carbon sources (5g%, w/v of fructose, glucose, maltose, starch, rhamnose, raffinose, glycerol), various organic and inorganic nitrogen sources (0.4g% w/v of peptone, ammonium nitrate, urea, ammonium chloride, glycine and yeast extract) in different Erlenmeyer flasks were used with PDB as the basal medium. After the finalisation of the additional carbon and nitrogen sources, their optimum concentration was confirmed by using different concentrations of these products on a PDB medium and the respective biomass and GRH amounts were calculated. A variety of ionic salts (0.1 g%, w/v of  $\text{MgCl}_2$ ,  $\text{FeCl}_3$ , KCl, NaCl) and phosphate sources (0.1 g%, w/v including  $\text{NaH}_2\text{PO}_4$ ,  $\text{K}_2\text{HPO}_4$ ,  $\text{KH}_2\text{PO}_4$ ) were analysed separately to detect their role in fungal biomass and GRH production (Mahapatra and Banerjee, 2013, 2016).

To detect the  $\text{O}_2$  requirement, fungi were grown with different medium volumes in 250 mL Erlenmeyer flasks. Headspace volume, medium volume, total volume, and medium depth in flask culture were measured for the indirect measurement of the organism's  $\text{O}_2$  requirement (Wonglumsom et al., 2000).

## BBD based optimisation

Further optimisation was performed with the RSM (Response surface methodology). The investigational design was a Box–Behnken experimental setup with the four most important factors obtained from the OVAT system. The four independent factors had three different levels (−1, 0, and +1) each for the experiment. GRH production was set to a second-order polynomial equation by the means of multiple regression techniques. The model involving the most significant factors was derived. The system performance follows the subsequent second-order polynomial equation:  $Y = \beta_0 + \sum \beta_i X_i + \sum \beta_{ij} X_i X_j + \sum \beta_{ii} X_i^2$ , where  $Y$  is the predicted response or dependent variable,  $x_i$  and  $x_j$  are independent factors,  $\beta_0$  is the intercept of the regression equation,  $\beta_i$  is the linear coefficient,  $\beta_{ii}$  is the quadratic coefficient and  $\beta_{ij}$  is the interaction coefficient (Mahapatra and Banerjee, 2013, 2016).

## Estimation of GRH

Fungal biomass was separated from the culture extract by centrifugation at 10,000 rpm. Mycelial biomass was dried at 55°C for 24 h and weighed. The supernatant was concentrated in a rotary evaporator under low pressure at 40°C. Chilled absolute ethanol was added to the concentrated supernatant (5:1 v/v), mixed thoroughly, and kept for 24 h at freezing conditions finally, the recovery of viscous precipitate was done by centrifugation at 10,000 rpm for 10 min. The recovered polysaccharide was dialyzed in a cellulose membrane (MW

cut off 10,000) against distilled water for 24 h. It was tested for sugar and protein contents following the methods of Dubois et al. (1956) and Lowry (1951) with glucose and bovine serum albumin as the standard. Obtained EPS solution was concentrated in a rotary evaporator under low pressure at 40°C for characterisation.

## Characterisation of GRH

GRH was purified by gel chromatographic technique using a Sepharose-6B gel filtration column (65 × 2 cm) and average molecular weight was determined following the methods of Mahapatra and Banerjee (2013). The dried polysaccharide was subjected to characterisation using GC–MS with some pre-treatments (Proestos et al., 2006). Using a water bath at 70°C for 15 min, 100 mg of dried exopolysaccharide was combined with 1 mL MeOH, 20  $\mu\text{L}$  ribitol (which serves as an internal standard), and 20  $\mu\text{L}$  nor-leucine. The entire mixture was then centrifuged for 5 min at 10,000 rpm, and the supernatant was immediately dried and dissolved in 20  $\mu\text{L}$  of methoxyamine HCL for 120 min at 37°C. The final 1  $\mu\text{L}$  of the derivatized EPS sample was loaded onto the GC–MS for analysis of monosaccharide composition after 40  $\mu\text{L}$  of TMS (Trimethyl siloxane) had been added. The instrument was set up with a 30 m × 0.25 mm DB-5 Ultra Inert column. With a split ratio of 25:1, the inlet temperature was 230°C, and the MS transfer line temperature was 250°C. A constant flow mode was used for the column's flow, which was 1.3 mL min<sup>−1</sup> with an average linear starting velocity of 39 cm sec<sup>−1</sup>. Helium was used as the carrier gas, and ZB–1701 served as the guard column. The program was isothermal, holding at 70°C for 5 min, increasing by 10°C per minute to 180°C, holding for 2 min, increasing by 10°C per minute again to 220°C, holding for 1 min, and finally ramping up by 2.5°C per minute. Up to 265°C with a 1-min hold, then a ramp up to 285°C with a 1-min hold, and finally a climb of 1°C per min up to 290°C with a 0.6-min hold. The mass spectrum was obtained in scan mode from 40 to 650 amu with a detection threshold of 100 ion counts while the detector was in positive ion mode. Appropriate configurations (D-dextrorotatory and L-laevorotatory form) of the sugars were identified by matching them with the NIST library. To detect the sugar linkages, procedures of Ciucanu and Kerek (1984) and Das et al. (2009) were adopted using the GC–MS equipment.

## Exopolysaccharide (GRH)-mediated plant growth promotion under drought stress

Initially, healthy and disease-free rice seeds (*O. sativa* ssp. indica MTU-7093 Swarna) were surface sterilised with a series of surface disinfectants: sodium hypochlorite (2.5%) for 20 min, deionised double-distilled water (3–5 times thoroughly) and then soaked in water for germination followed by storing at 22°C for 72–96 h. Uniformly seeds were transferred to a hydroponics box supplemented with Hoagland solution and were replaced at an interval of 3–4 days (Chen et al., 2011). Seedlings reaching an age of 15–20 days were divided into four separate groups with the control group (un-inoculated water), 20 ppm, 50 ppm, and 100 ppm GRH application, respectively, at a frequency of 3 times a day (morning, noon, and afternoon) for 45 days. Simultaneously, 20% polyethylene glycol (PEG)-6,000 (for 7 days) was mixed with a hydroponic solution as a drought-inducing component, and all the biochemical tests were performed from drought-induced seedlings. The



fresh weight of rice seedlings was measured and leaves were stored at  $-20^{\circ}\text{C}$  for further biochemical estimations.

The relative water content (RWC) of the treated and control plants were calculated in percentage following the method of [Arndt et al. \(2015\)](#). Fresh leaves were plucked and fresh tissue weight (FW) was measured, then immersed in a 50 mL tube with distilled water, and placed in the dark at  $4^{\circ}\text{C}$  for 20 h. Further, the leaves were dried with filter paper and again weighed for turgid weight (TW) calculation. Lastly, the same leaves were incubated at  $80^{\circ}\text{C}$  for a period of 72 h and dry weight (DW) was measured immediately. Relative water content was calculated by the formula  $\text{RWC} (\%) = (\text{FW} - \text{DW}) / (\text{TW} - \text{DW})$ .

The chlorophyll content ( $\text{mg g}^{-1}$  of fresh weight) of the fresh leaves was measured according to the modified formula of [Lichtenthaler and Wellburn \(1983\)](#). Firstly, fresh leaves (0.5 g fresh weight) were split into small pieces and immediately dissolved in 50 mL methanol (80% v/v), covered with black paper, or kept in dark conditions for 24–36 h at  $28\text{--}30^{\circ}\text{C}$ . Centrifugation was performed and the supernatant was estimated (645 nm and 653 nm) for chlorophyll contents. Chlorophyll content ( $\text{mg L}^{-1}$  FW) =  $8.05 A_{653} + 20.29 A_{645}$ .

To calculate the proline contents of the seedling methods proposed by [Bates et al. \(1973\)](#) were adopted. Leaves (0.5 g fresh weight) were split into small pieces and put in a test tube. Further treatment was done by mixing with 5 mL of 3% sulfosalicylic acid, incubated in a water bath for 10 min and 2 mL of the supernatant was mixed thoroughly with 2 mL of acetic acid, and 3 mL of 2.5% ninhydrin. Finally, the mixture was incubated in the water bath for a time period of  $40 \text{ min}^{-1} \text{ h}$  and extracted using 4 mL methylbenzene, optical density was measured at 520 nm and compared with a proline standard curve.

Soluble sugar contents (in terms of  $\text{mg g}^{-1}$  fresh weight) were measured by the method of [Watanabe et al. \(2000\)](#). Fresh leaves (0.2 g fresh weight) were crushed in 80% v/v ethanol (10 mL) and centrifuged at  $8000 \text{ g}$  for 10 min at  $4^{\circ}\text{C}$ . We mixed 1 mL of supernatant thoroughly with 3 mL of anthrone reagent followed by heating at  $100^{\circ}\text{C}$  for 10–12 min, which was stopped by rapid cooling them on the ice. Finally, at 620 nm absorbance was estimated using glucose as a standard.

Malondialdehyde content ( $\text{nmol g}^{-1}$  fresh weight) was reported according to the method of [Del Buono et al. \(2011\)](#). 0.5 gm of fresh leaves were homogenised in 5% (w/v) trichloroacetic acid (TCA), centrifuged at  $12000 \text{ g}$  for a time period of approximately 15–20 min and then the supernatant was mixed with 5 mL of 0.5% thiobarbituric acid (TBA)-prepared with 20% TCA followed by incubation for 25 min and cooling at  $100^{\circ}\text{C}$  and room temperature, respectively. Finally, after centrifugation ( $7,500 \text{ g}$  for 5 min), the supernatant was measured for its absorbance at 450, 532, and 600 nm. The amount of MDA was calculated by the following formula  $\text{MDA content (nmol g}^{-1}) = 6.45 (A_{532} - A_{600}) - 0.56 A_{450}$ .

The methods of [Lei et al. \(2015\)](#) were followed for the measurement of peroxidase activity. The system contained multiple chemicals; 2.9 mL of 0.05 M phosphate buffer, 0.5 mL of 2%  $\text{H}_2\text{O}_2$ , 0.1 mL of 2% guaiacol, and also 0.1 mL of crude enzyme extract followed by the absorbance measurement at 470 nm. Lastly, POD activity was calculated as an amount of guaiacol oxidised per minute in nanomoles per minute per mg of protein. At the end of the reaction, the absorbance was measured at 470 nm. POD activity was defined as the amount of guaiacol oxidised per minute, and was expressed as nanomoles per minute per mg of protein.

Catalase activity was calculated following the protocols of [Lei et al. \(2015\)](#). 0.1 mL  $\text{H}_2\text{O}_2$  (2%) and 2 mL phosphate buffer (50 mM-pH 7.0) were mixed and the whole reaction was initiated by the addition of

0.1 mL of crude enzyme extract. Finally, the catalase activity was measured (at 240 nm) in terms of the decrease of values of  $\text{H}_2\text{O}_2$  per minute, as nanomoles/min/gm of protein.

Superoxide dismutase activity was assayed following the protocols of [Lei et al. \(2015\)](#). The whole system contained a series of valuable freshly prepared reagents; 1.5 mL of 0.05 M phosphate buffer, 0.3 mL of 130 mM methionine solution, 0.3 mL of 750  $\mu\text{M}$  nitroblue tetrazolium solution, 0.3 mL of 100  $\mu\text{M}$  EDTA  $-\text{Na}_2$  solution, 0.3 mL of 20  $\mu\text{M}$  lactochrome solution, 0.5 mL of distilled water and finally 0.1 mL of crude enzyme extract. The complete reaction was initiated at 4000 Lx of illumination for a constant 20 min with no interruption. The control set comprises the same set of reagents and illumination but with no crude enzyme extract, rather replaced with a phosphate buffer. The third setup of control contains only phosphate buffer followed by incubation in dark conditions for the same time period of 20 min. Finally, after the completion of the reaction, the absorbance was estimated at 560 nm of wavelength. One unit of SOD activity was defined as the amount of enzyme which inhibits NBT reduction by 50%, also the results were expressed as unit/mg protein.

## Statistical analysis

All experiments were performed in triplicate and the results are presented as means  $\pm$  standard errors (SE). Data were analysed by Prism GraphPad version 9.2.0 (332) software (San Diego, California, United States). BBD experiments were done in Minitab (version 20.2).

## Results

### Identification of the isolate

The organism had enormously intertwining hyphae and septate hyaline whitish mycelium, and it lacked any sexual or asexual reproductive structures ([Figures 1A–C](#)). rDNA sequence data of the isolate was deposited in GenBank (ON146358). A BLAST search of the earlier existing database indicates a close genetic connection with other species of *Mucor* and the evolutionary history of the endophytic fungal isolate HELF2 was included using the neighbour-joining method ([Saitou and Nei, 1987](#)). The most appropriate phylogenetic tree with a total branch length of 0.00649585 is represented in [Figure 1D](#). The tree was constructed to scale with branch lengths in similar units as those of the evolutionary distances used to infer the phylogenetic tree. The evolutionary distances between the species were analysed using the maximum composite likelihood method ([Tamura et al., 2021](#)) and were in the units of the number of base substitutions per site. Gaps and missing data were removed from the dataset. There was a total of 620 nucleotides in the final dataset.

### Optimisation of GRH production

*Mucor* sp. HELF2 was grown on a 250 mL Erlenmeyer flask in submerged condition for 10 days and the highest production of fungal GRH and biomass was detected after 8 days of fermentation ([Table 1](#)). A temperature of  $26^{\circ}\text{C}$  and a medium pH of 7.1 was found to be the most suitable one for GRH production. Glucose and peptone at a concentration of  $11 \text{ g L}^{-1}$  and  $5.5 \text{ g L}^{-1}$  were found to be the most



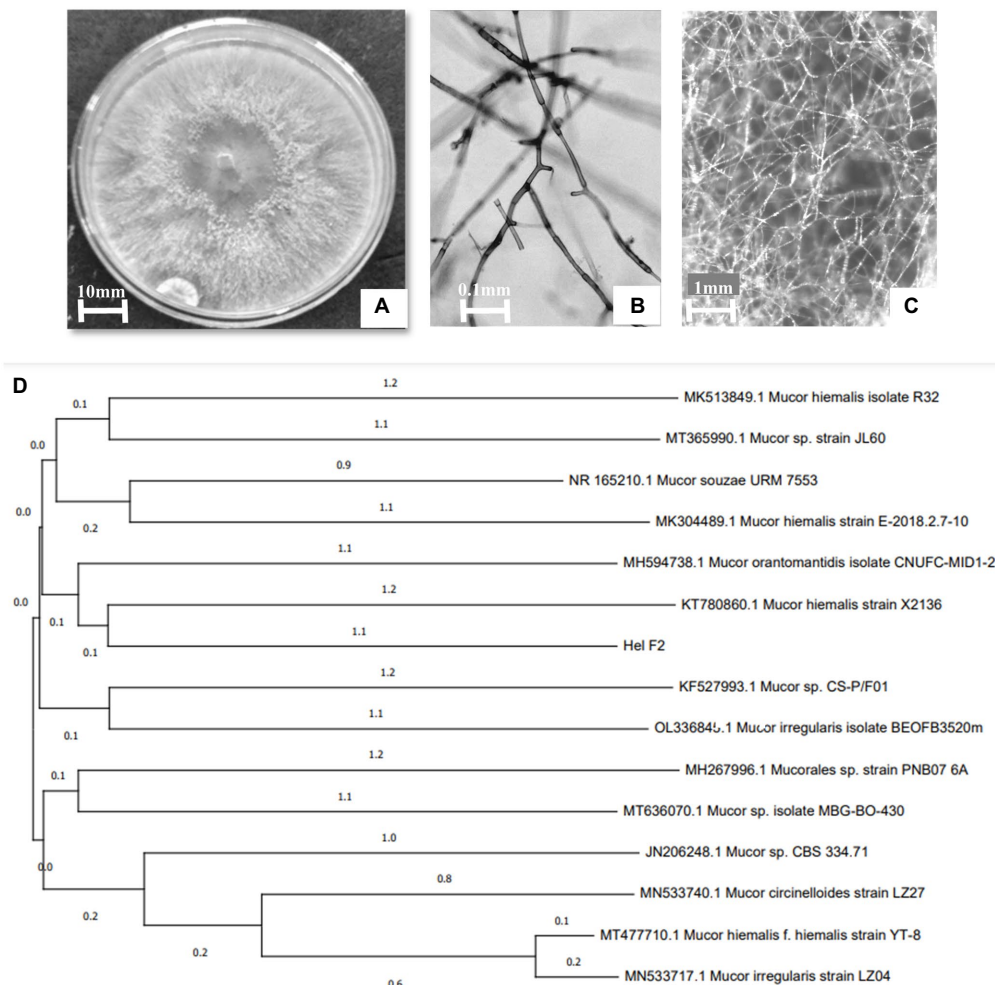


FIGURE 1

(A) 8-day old culture of HELF2 grown on PDA medium. Sterile hyphal aggregation without any sexual or asexual reproductive structures seen under a light (B) and stereo (C) microscope. (D) Phylogenetic tree shows the relationship of endophytic *Mucor* sp. HELF2 with other *Mucor* sp. strains.

appropriate ones for maximum GRH yield (Table 1). NaCl at a concentration of  $0.1 \text{ g L}^{-1}$  was the most effective salt (or source of metal ions) for GRH production. The detailed effect of different parameters on biomass and GRH production is summarised in Table 1.

The amount of dissolved oxygen in the fermentation medium affects EPS production. It depends on the medium volume, the headspace of the medium, and the medium depth. A medium volume of 75 mL in a 320 mL Erlenmeyer flask with 245 mL of headspace volume and 2.1 cm of medium depth and 2.53 cm of surface area was found to be the criteria for optimum GRH production (Table 2).

After OVAT optimisation RSM was adopted using a three-level Box Behnken Design. The most important four factors (glucose concentration, peptone concentration, medium pH, and fermentation time) with five replicates at the center points were established as a model for analysis of GRH production. The experimental design with variable predicted and measured values of GRH was presented in Table 3. Maximum GRH production was noted at the five replicated center points. The predicted response  $Y$  for GRH production by *Mucor* sp. HELF2 was described as coded factors in the following equation  $Y_{\text{GRH}} = 5.9810 - 0.168024x_1 - 0.39671x_2 - 0.09103x_3 - 0.37144x_4 - 0.25686x_1x_2 - 0.03737x_1x_3 + 0.09369x_1x_4 - 0.0367x_2x_3 + 0.32736x_2x_4 - 0.0337x_3x_4 - 0.65663x_1^2 - 0.6395x_2^2 - 0.50414$

$x_3^2 - 0.85426x_4^2$ . Here  $Y_{\text{GRH}}$  is the predicted GRH yield and  $x_1$ ,  $x_2$ ,  $x_3$ , and  $x_4$  are the four coded factors of glucose concentration, peptone concentration, medium pH, and fermentation time (day) respectively. A regression analysis with detailed statistical data related to the experiment is presented in Table 4. The F-test data of 1994.082 proved that the model was significant. The adjusted determinant coefficient ( $R^2 \text{ Adj}$ ) was found to be 0.9998 which represents that there is a high degree of correlation between the experimental and predicted values and there is more than 99% variation in response that could be predicted by second-order polynomial prediction equation. Adeq precision was reported to be 111.901 which indicates that the model is appropriate. The lack of fit  $F$ -value of 5.782 and  $p$ -value ( $p < 0.0001$ ) was not at all valuable to the pure error and the fitness of the model was perfect. The high degree of precision and uniformity of the investigational outcomes were proved by the  $p$  value of lack of fit- 0.2830 ( $> 0.05$ ) and a  $p$  value of probability ( $> F$  less than 0.05). The other linear and quadratic effects of glucose concentration, urea concentration, M-pH, and fermentation time were also significant ( $p < 0.0001$ ). Finally, three-dimensional response surface plots and contour plots were constructed by Minitab (20.2) for a clear understanding of the effects of the parameters on GRH production (Figure 2).

**TABLE 1** Effect of different fermentation influencing physical conditions and chemical supplements, on biomass and Galactose Rich Heteropolysaccharide production by endophytic fungi *Mucor* sp. HELF2 in submerged fermentation conditions.

| Parameters tested             | Effectors                                       | The concentration of the effectors (g L <sup>-1</sup> ) | Biomass (g L <sup>-1</sup> ) | GRH (g L <sup>-1</sup> ) |
|-------------------------------|---|---|------------------------------|--------------------------|
| Fermentation time (h)         | 4 days  | –   | 6.1 ± 0.04a                  | 13.42 ± 0.03a            |
|                               | 6 days  | –   | 5.99 ± 0.01a                 | 13.96 ± 0.04b            |
|                               | 8 days  | –   | 6.96 ± 0.8b                  | 14.44 ± 0.03c            |
|                               | 10 days   | –   | 5.76 ± 0.02c                 | 13.11 ± 0.05a            |
| Fermentation temperature (°C) | 22  | –   | 7.02 ± 0.03a                 | 14.48 ± 0.02a            |
|                               | 24  | –   | 7.18 ± 0.05a                 | 15.51 ± 0.07b            |
|                               | 26  | –   | 7.47 ± 0.01b                 | 16.51 ± 0.08c            |
|                               | 28  | –   | 6.96 ± 0.08a                 | 16.11 ± 0.09b            |
| Initial medium pH             | 6.9   | –   | 7.7 ± 0.07a                  | 17.51 ± 0.01a            |
|                               | 7.1   | –   | 7.81 ± 0.06b                 | 17.71 ± 0.04a            |
|                               | 7.3   | –   | 7.73 ± 0.01a                 | 17.41 ± 0.01a            |
|                               | 7.5   | –   | 7.6 ± 0.05c                  | 16.91 ± 0.04b            |
| Additional carbon sources     | Fructose  | –   | 7.88 ± 0.03a                 | 18.11 ± 0.01a            |
|                               | Glucose   | –   | 7.97 ± 0.05b                 | 19.12 ± 0.05b            |
|                               | Maltose   | –   | 7.9 ± 0.06a                  | 19.02 ± 0.03b            |
|                               | Starch  | –   | 7.82 ± 0.09c                 | 18.9 ± 0.03c             |
|                               | Rhamnose  | –   | 7.87 ± 0.01a                 | 18.93 ± 0.02c            |
|                               | Raffinose                                       | –   | 7.79 ± 0.02c                 | 18.82 ± 0.02c            |
|                               | Glycerol  | –   | 7.82 ± 0.06c                 | 18.51 ± 0.03d            |
| Additional nitrogen sources   | Peptone   | 0.4   | 8.71 ± 0.06a                 | 19.86 ± 0.03a            |
|                               | (NH <sub>4</sub> ) <sub>2</sub> SO <sub>4</sub> | 0.4   | 7.99 ± 0.02b                 | 19.28 ± 0.04b            |
|                               | NH <sub>4</sub> NO <sub>3</sub>                 | 0.4   | 8.1 ± 0.07b                  | 19.41 ± 0.04c            |
|                               | Urea  | 0.4   | 8.23 ± 0.04c                 | 19.52 ± 0.05c            |
|                               | NH <sub>4</sub> Cl                              | 0.4   | 8.16 ± 0.02b                 | 19.7 ± 0.06d             |
|                               | Glycine   | 0.4   | 8.2 ± 0.01c                  | 19.74 ± 0.05d            |
|                               | Yeast Extract                                   | 0.4   | 8.41 ± 0.09d                 | 19.12 ± 0.06b            |
| Glucose concentration         | Glucose   | 7   | 9.18 ± 0.05a                 | 19.9 ± 0.07a             |
|                               |   | 9   | 9.27 ± 0.06b                 | 20.18 ± 0.02b            |
|                               |   | 11  | 9.47 ± 0.05c                 | 20.23 ± 0.04b            |
|                               |   | 13  | 9.3 ± 0.06b                  | 20.12 ± 0.03b            |
| Peptone concentration         | Peptone   | 4.5   | 9.59 ± 0.07a                 | 20.24 ± 0.03a            |
|                               |   | 5   | 9.53 ± 0.08a                 | 20.32 ± 0.04a            |
|                               |   | 5.5   | 9.7 ± 0.01b                  | 20.5 ± 0.05b             |
|                               |   | 6   | 9.49 ± 0.06a                 | 20.42 ± 0.02b            |
| Different metal ions          | MgCl <sub>2</sub>                               | 0.1   | 9.3 ± 0.01a                  | 20.52 ± 0.06a            |
|                               | FeCl <sub>3</sub>                               | 0.1   | 9.39 ± 0.06b                 | 20.62 ± 0.03b            |
|                               | KCl   | 0.1   | 9.51 ± 0.07c                 | 20.81 ± 0.04c            |
|                               | NaCl  | 0.1   | 9.8 ± 0.04d                  | 20.92 ± 0.07d            |
|                               | NaH <sub>2</sub> PO <sub>4</sub>                | 0.1   | 9.48 ± 0.03c                 | 20.71 ± 0.08b            |
|                               | K <sub>2</sub> HPO <sub>4</sub>                 | 0.1   | 9.6 ± 0.07e                  | 20.51 ± 0.09a            |
|                               | KH <sub>2</sub> PO <sub>4</sub>                 | 0.1   | 9.57 ± 0.08e                 | 20.42 ± 0.10e            |

One-way ANOVA (Tukey's Multiple Comparison test) was performed to check the potential statistical differences in the case of the biomass (g L<sup>-1</sup>) and GRH production (g L<sup>-1</sup>) in different fermentation conditions (incubation time, temperature, the concentration of sugar and nitrogen sources, etc.). There were valid statistical differences in most of the cases ( $p < 0.05$ ), the different letters a, b, c, d, e, and f indicate a significant difference, and the same letter at two positions indicates no statistical differences.

**TABLE 2** Effect of medium volume, headspace volume, and medium depth on the dissolved oxygen level in the fermentation medium and their effect on GRH and biomass production.

| Medium volume (mL) | The total volume of the flask (mL) | Headspace volume (mL) | Medium depth (cm) | Surface area (cm) | Biomass (g L <sup>-1</sup> ) | GRH (g L <sup>-1</sup> )    |
|--------------------|------------------------------------|-----------------------|-------------------|-------------------|------------------------------|-----------------------------|
| 25                 | 320                                | 295                   | 1                 | 2.5               | 11.66 ± 0.18a                | 21.01 ± 0.021a <sub>1</sub> |
| 50                 | 320                                | 270                   | 1.5               | 2.58              | 11.8 ± 0.75a                 | 21.42 ± 0.049b <sub>1</sub> |
| 75                 | 320                                | 245                   | 2                 | 2.53              | 12.99 ± 0.43b                | 22.04 ± 0.089c <sub>1</sub> |
| 100                | 320                                | 220                   | 2.5               | 2.41              | 11.69 ± 0.64a                | 21.28 ± 0.071a <sub>1</sub> |

One-way ANOVA (Tukey's Multiple Comparison test) was performed to check the potential statistical differences between the data (column-wise) of biomass (g L<sup>-1</sup>), and GRH production (g L<sup>-1</sup>) in different medium volumes (mL). There was a valid statistical difference in most of the cases. Different letters (a, b for biomass and a<sub>1</sub>, b<sub>1</sub>, c<sub>1</sub> for GRH yield) indicates valid statistical differences ( $P < 0.05$ ).

**TABLE 3** Experimental design and outcomes of the Box–Behnken Design (BBD) for optimisation of the GRH production from *Mucor* sp. HELF2.

| Run | Independent variables |                      |                        |                      | Response [GRH yield (g L <sup>-1</sup> )] |                       |
|-----|-----------------------|----------------------|------------------------|----------------------|---|-----------------------|
|     | GC (x <sub>1</sub> )  | PC (x <sub>2</sub> ) | M-pH (x <sub>3</sub> ) | FT (x <sub>4</sub> ) | Measured                                  | Predicted             |
| 1   | -1(=10)               | -1(=5)               | 0(=7.1)                | 0(=8)                | 21.189a <sub>1</sub>                      | 21.602a <sub>1</sub>  |
| 2   | 1(=12)                | -1                   | 0                      | 0                    | 22.099a <sub>2</sub>                      | 22.177a <sub>2</sub>  |
| 3   | -1                    | 1(=6)                | 0                      | 0                    | 21.984a <sub>3</sub>                      | 22.067a <sub>3</sub>  |
| 4   | 1                     | 1                    | 0                      | 0                    | 21.684a <sub>4</sub>                      | 21.433a <sub>4</sub>  |
| 5   | 0(=11)                | 0(=5.5)              | -1(=6.9)               | -1(=7)               | 22.083a <sub>5</sub>                      | 22.162a <sub>5</sub>  |
| 6   | 0                     | 0                    | 1(=7.3)                | -1                   | 22.077a <sub>6</sub>                      | 22.123a <sub>6</sub>  |
| 7   | 0                     | 0                    | -1                     | 1(=9)                | 21.733a <sub>7</sub>                      | 21.848a <sub>7</sub>  |
| 8   | 0                     | 0                    | 1                      | 1                    | 21.779a <sub>8</sub>                      | 21.862a <sub>8</sub>  |
| 9   | -1                    | 0                    | 0                      | -1                   | 22.139a <sub>9</sub>                      | 22.032a <sub>9</sub>  |
| 10  | 1                     | 0                    | 0                      | -1                   | 21.873a <sub>10</sub>                     | 21.921a <sub>10</sub> |
| 11  | -1                    | 0                    | 0                      | 1                    | 21.789a <sub>11</sub>                     | 21.663a <sub>11</sub> |
| 12  | 1                     | 0                    | 0                      | 1                    | 21.686a <sub>12</sub>                     | 21.715a <sub>12</sub> |
| 13  | 0                     | -1                   | -1                     | 0                    | 22.206a <sub>13</sub>                     | 22.066a <sub>13</sub> |
| 14  | 0                     | 1                    | -1                     | 0                    | 21.876a <sub>14</sub>                     | 21.918a <sub>14</sub> |
| 15  | 0                     | -1                   | 1                      | 0                    | 22.164a <sub>15</sub>                     | 22.044a <sub>15</sub> |
| 16  | 0                     | 1                    | 1                      | 0                    | 21.853a <sub>16</sub>                     | 21.915a <sub>16</sub> |
| 17  | -1                    | 0                    | -1                     | 0                    | 22.114a <sub>17</sub>                     | 21.975a <sub>17</sub> |
| 18  | 1                     | 0                    | -1                     | 0                    | 21.899a <sub>18</sub>                     | 21.94a <sub>18</sub>  |
| 19  | -1                    | 0                    | 1                      | 0                    | 22.083a <sub>19</sub>                     | 21.957a <sub>19</sub> |
| 20  | 1                     | 0                    | 1                      | 0                    | 21.88a <sub>20</sub>                      | 21.933a <sub>20</sub> |
| 21  | 0                     | -1                   | 0                      | -1                   | 22.307a <sub>21</sub>                     | 22.199a <sub>21</sub> |
| 22  | 0                     | 1                    | 0                      | -1                   | 21.784a <sub>22</sub>                     | 21.824a <sub>22</sub> |
| 23  | 0                     | -1                   | 0                      | 1                    | 21.801a <sub>23</sub>                     | 21.675a <sub>23</sub> |
| 24  | 0                     | 1                    | 0                      | 1                    | 21.749a <sub>24</sub>                     | 21.772a <sub>24</sub> |
| 25  | 0                     | 0                    | 0                      | 0                    | 22.57a <sub>25</sub>                      | 22.583a <sub>25</sub> |
| 26  | 0                     | 0                    | 0                      | 0                    | 22.621a <sub>26</sub>                     | 22.583a <sub>26</sub> |
| 27  | 0                     | 0                    | 0                      | 0                    | 22.583a <sub>27</sub>                     | 22.583a <sub>27</sub> |
| 28  | 0                     | 0                    | 0                      | 0                    | 22.581a <sub>28</sub>                     | 22.583a <sub>28</sub> |
| 29  | 0                     | 0                    | 0                      | 0                    | 22.562a <sub>29</sub>                     | 22.583a <sub>29</sub> |

One-way ANOVA (Tukey's Multiple Comparison test) was performed to check the potential statistical differences ( $P < 0.05$ ) between the measured and predicted GRH production. There were no statistical differences between each data set (row-wise) and similar letters (a<sub>1</sub>-a<sub>29</sub>) in each row indicate the data are the same and lack statistical differences.

The model predicted a maximum response of 20.10 g L<sup>-1</sup> GRH yield when the necessary components are 5.2 g L<sup>-1</sup> of peptone, 10.5 g L<sup>-1</sup> of glucose, 7.05 MpH, and 180 (7.5 days) h of fermentation

time. These predictions were authenticated by performing laboratory experiments in flask culture by triplicate with an outcome of 19.951 ± 0.091 g L<sup>-1</sup> of GRH.

**TABLE 4** ANOVA for response surface quadratic regression model of Galactose Rich Heteropolysaccharide production by endophytic fungi *Mucor* sp. HELF2.

| Source              | DF | Sum of squares | Mean square | F-Value  | P-Value prob.>F |
|---------------------|----|----------------|-------------|----------|-----------------|
| Model               | 14 | 9.84399        | 0.19982     | 1994.082 | <0.001          |
| $x_1$ (GC)          | 1  | 0.38702        | 0.58191     | 1082.069 | <0.001          |
| $x_2$ (PC)          | 1  | 0.59729        | 0.81973     | 974.819  | <0.001          |
| $x_3$ (M pH)        | 1  | 0.49871        | 0.80132     | 908.019  | <0.001          |
| $x_4$ (FT)          | 1  | 0.29871        | 0.59713     | 801.011  | <0.001          |
| $x_1^2$ (GC*GC)     | 1  | 0.03152        | 0.57085     | 1109.039 | <0.001          |
| $x_2^2$ (PC*PC)     | 1  | 0.87199        | 0.87172     | 1339.760 | <0.001          |
| $x_3^2$ (M pH*M pH) | 1  | 0.37189        | 0.57831     | 1039.93  | <0.001          |
| $x_4^2$ (FT*FT)     | 1  | 0.81923        | 0.79849     | 916.14   | <0.001          |
| $x_1 x_2$ (GC*PC)   | 1  | 0.39905        | 0.71280     | 919.82   | <0.001          |
| $x_1 x_3$ (GC*M pH) | 1  | 0.41977        | 0.76862     | 808.015  | <0.001          |
| $x_1 x_4$ (GC*FT)   | 1  | 0.66890        | 0.92914     | 1139.19  | <0.001          |
| $x_2 x_3$ (PC*M pH) | 1  | 0.90972        | 0.98132     | 996.02   | <0.001          |
| $x_2 x_4$ (PC*FT)   | 1  | 0.56491        | 0.89032     | 1138.091 | <0.001          |
| $x_3 x_4$ (M pH*FT) | 1  | 0.69981        | 0.70237     | 767.091  | <0.001          |
| Residual            | 14 | 0.43781        | 0.20976     |          |                 |
| Lack-of-Fit         | 10 | 0.53500        | 0.90493     | 5.782    | 0.2830          |
| Pure Error          | 4  | 0.20778        | 0.96892     |          |                 |
| Cor total           | 28 | 8.16903        |             |          |                 |
| $R^2$               |    | 0.999209       |             |          |                 |
| Adj $R^2$           |    | 0.999800       |             |          |                 |
| Pred $R^2$          |    | 0.995062       |             |          |                 |
| Adeq precision      |    | 111.901        |             |          |                 |

## Characterisation of the exopolysaccharide

Exopolysaccharide produced by Endophytic *Mucor* sp. HELF2 was precipitated by applying chilled ethanol and crude EPS was then dialysed, and purified by gel filtration chromatography with a Sepharose-6B column. One major fraction obtained was eluted between 29 and 42 tubes (Figure 3C) and the colorimetric test confirms the absence of proteins in those fractions. The fraction was further investigated for monosaccharide analysis. The molecular weight of the homogeneous EPS was calculated from a calibration curve of standard dextran as  $\sim 2.98 \times 10^5$  Da (Figure 3D). Monosaccharide analysis of the derivatised EPS samples showed the occurrence of galactose, fucose, and glucose in a 13:2:1 ratio with D, L, and D configuration, respectively (Table 5). Each repeating unit of the fraction contained 13 galactose, two fucoses, and one glucose, which indicates that the studied EPS contained approximately 104 repeating units. We, therefore, considered that the Galactose Rich Heteropolysaccharide (GRH) could have been produced by endophytic *Mucor* sp. HELF2. FT-IR analysis of the EPS sample revealed the occurrence of strong absorption peaks at particular wavelengths of 3400.71, 2950.89, 1651.56, 1489.73 which represents C-H, O-H, C-O asymmetric stretching respectively, which indicates the basic characteristics and purity of the carbohydrate moiety. Figures 3A,B represent the FT-IR spectrum and GC-MS spectrum of the crude and derivatised EPS, respectively.

## Plant growth-promoting traits of the GRH

GRH-sprayed rice seedlings were found to be much healthier, and more vigorous in terms of their fresh weight and relative water contents in comparison to the control (only drought-inducing agent-PEG treated). The control plants were characterised by low growth, chlorosis, and wilting of leaves. The rice seedlings exhibited maximum growth promotion after continuous 14 days of GRH treatment. The relative water content and fresh weight of the 50ppm GRH treated plants were found to be higher than the plants of the control set, and plants treated with 20ppm and 100ppm GRH dosage. There was a 1.31, 2.38, and 1.74-time improvement in the fresh weight of seedlings in the 20, 50, and 100ppm GRH treated plants compared to the control. The relative water contents were also increased by 1.14, 1.58, and 1.26 times in 20, 50, and 100ppm GRH treated plants than the control one. There was a 3, and 4 times increase in root length and shoot length of the treated (50ppm GRH) plant, respectively, compared to the control. The fresh weight of the seedlings were found to be improved after the GRH treatment and the 50-ppm GRH application was also found to be the most effective in comparison to the control. Table 6 represents the improved physical characteristics of the treated seedlings. Figure 4 represents the treated (20, 50, and 100ppm) and control rice seedlings, showing their physical changes.

Not only physical but also biochemical characteristics were improved in the case of GRH-treated plants even after severe drought situations. The chlorophyll contents of the treated plants were found to be more elevated (2.32 times higher for 50ppm GRH treated one) than the untreated control



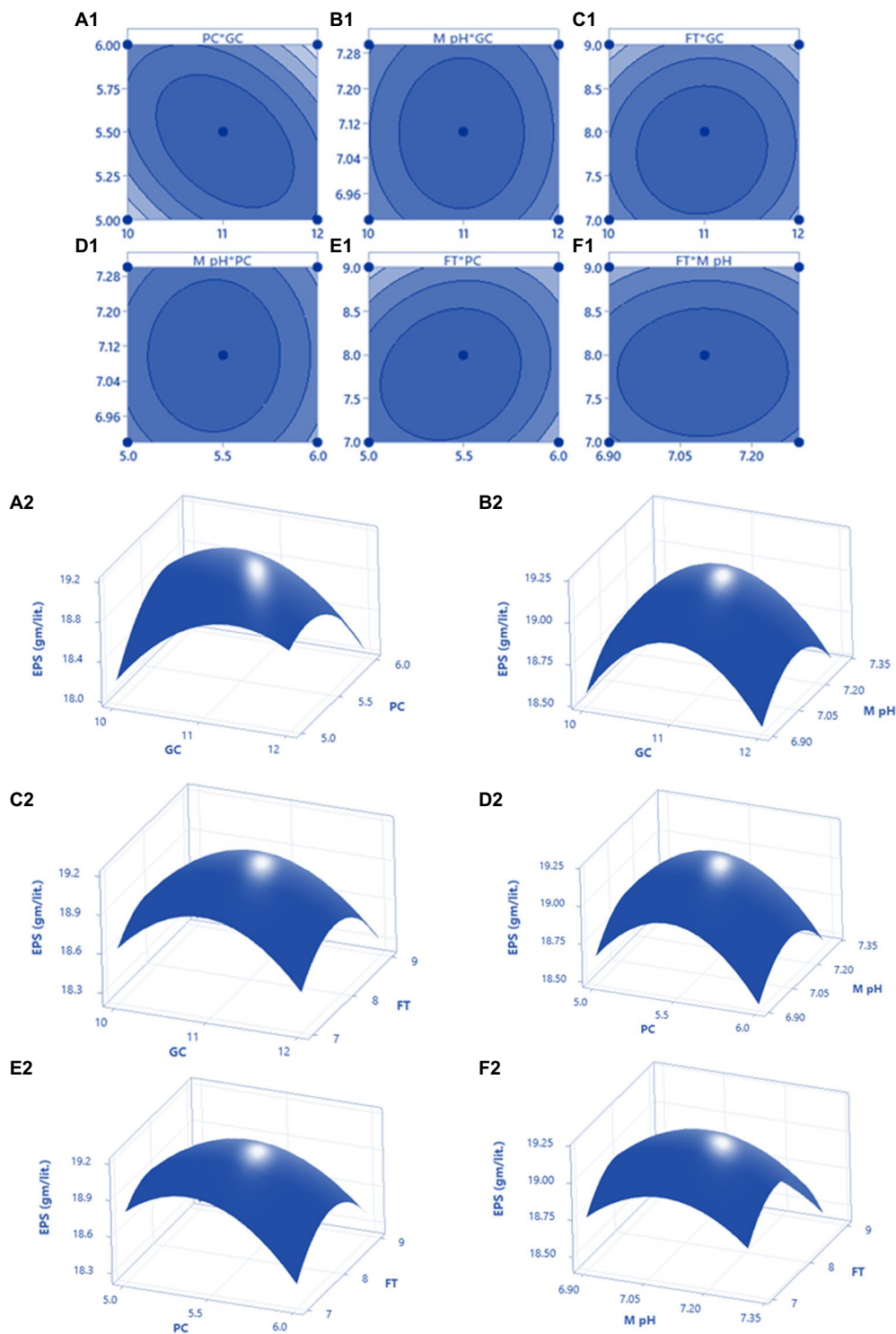


FIGURE 2

The 3D plot with 2D projection and contour plot showing the most important interactions of factors in RSM optimization of GRH production by HELF2. (A1,A2) between peptone concentration (PC) vs. glucose concentration (GC) at fermentation time (FT) 8days and medium pH 7.1 (M pH); (B1,B2) between M pH (7.1) and GC (11g/L<sup>-1</sup>) at FT (8days) and PC (5.5g/L<sup>-1</sup>); (C1,C2) between FT (8days) and GC (11g/L<sup>-1</sup>) at PC (5.5g/L<sup>-1</sup>) and M pH (7.1); (D1,D2) between M pH (7.1) and PC (5.5g/L<sup>-1</sup>) at FT (8days) and GC (11g/L<sup>-1</sup>); (E1,E2) between FT (8days) and PC (5.5g/L<sup>-1</sup>) at M pH (7.1) and GC (11g/L<sup>-1</sup>); (F1,F2) between FT (8days) and M pH (7.1) at GC (11g/L<sup>-1</sup>) and PC (5.5g/L<sup>-1</sup>).

(Figure 5A). The proline is a potent indicator of plant stress and higher proline contents indicate higher resistance towards stress and better adaptation to that stressful situation. Here the GRH-treated plant shows higher accumulations (approximately 3.89 times higher for 50 ppm GRH

treatment) of proline contents than the control ones (Figure 5B). The presence of increased soluble sugar content in the plant tissues also indicates the higher survival ability of plants in drought-stress situations. In this experiment, we found almost 3.5 times higher accumulation of

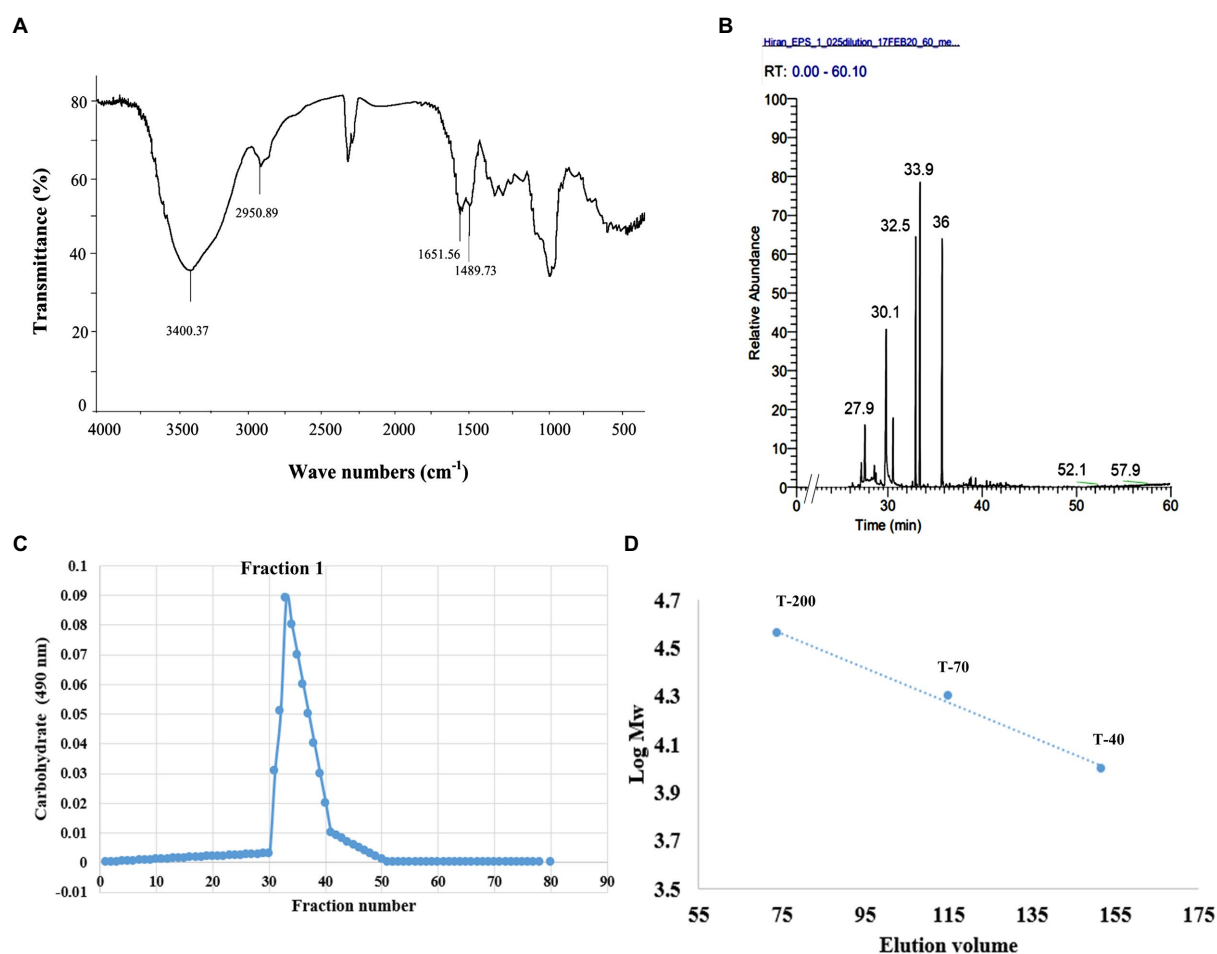


FIGURE 3

(A) FT-IR spectra of crude HELF2 GRH showing the necessary functional groups present in the sample. (B) GC-MS chromatogram of the derivatized fungal GRH showing the different peaks of monosaccharide compositions at different retention times. (C) Elution profile of the polysaccharide showing the occurrence of dominant fraction (F1) confirmed by carbohydrate test. (D) Standard curve of dextran needed for the detection of sugar concentration in the polysaccharide sample.

**TABLE 5** Monosaccharide units present in the Galactose Rich Heteropolysaccharide (synthesised by endophytic fungi *Mucor* sp. HELF2) are represented here with their respective sugar linkages and molar ratios.

| Methylated sugars           | Linkage types      | Molar ratio | Major fragments (m/z)  |
|-----------------------------|--------------------|-------------|--|
| 2,3,4-Me <sub>3</sub> -Gal- | 6)-Galp-(1-        | 5           | 40, 61, 72, 88, 103, 113, 131, 140, 159, 175, 191, 203, 219, 231 |
| 2,3-Me <sub>2</sub> -Galp   | -4,6)-β-D-Galp-(1- | 4           | 44,46,59,69,72,83,85,97,99, 119,127,129,141,157,161,187,200      |
| 3,4-Me <sub>2</sub> -Gal    | -2,6)-α-D-Galp-(1- | 4           | 44,72,89,100,131,157,173,189,233                                 |
| 2,3,4-Me <sub>3</sub> -Fuc  | α-L-Fucp-(1-       | 2           | 44,72,89,103,113,117, 131,161,175                                |
| 2,4-Me <sub>2</sub> -Glc    | -3,6)-D-Glcp-(1-   | 1           | 39,43,58,74,88,99,100, 119,130,144,160,174,191,209,215,234,246   |

**TABLE 6** Different physical parameters (fresh weight, root length, and shoot length) of GRH-treated and untreated drought-faced rice seedlings are represented here.

| Treatment group (concentration of EPS) | Fresh weight (mg) | Root length (cm)          | Shoot length (cm)          | Relative water contents (%)  |
|--|-------------------|---------------------------|----------------------------|------------------------------|
| Control                                | 97.81 ± 3.019a    | 2.01 ± 0.72a <sub>1</sub> | 9.6 ± 1.73a <sub>2</sub>   | 69.02 ± 1.890a <sub>3</sub>  |
| EPS 20 ppm                             | 128.93 ± 4.051b   | 3.13 ± 0.69b <sub>1</sub> | 13.36 ± 2.05b <sub>2</sub> | 79.11 ± 1.472b <sub>3</sub>  |
| EPS 50 ppm                             | 232.93 ± 3.610c   | 6.61 ± 1.32c <sub>1</sub> | 33.4 ± 3.28c <sub>2</sub>  | 109.31 ± 1.901c <sub>3</sub> |
| EPS 100 ppm                            | 171.11 ± 2.098d   | 4.53 ± 0.81d <sub>1</sub> | 23.41 ± 2.96d <sub>2</sub> | 87.39 ± 1.014d <sub>3</sub>  |

One-way ANOVA (Tukey's Multiple Comparison test) was performed to check the potential statistical differences and the treated (20, 50, and 100 ppm EPS foliar spray) plants showed statistically valid differences ( $P < 0.05$ , the four different letters for each of the four parameters (column-wise) indicates significance differences) from the control plant.

soluble sugar contents in 50 ppm GRH-treated plants in comparison to the only PEG-treated one (Figure 5C). On the other hand, the MDA (Malondialdehyde) content is found to be correlated with lipid peroxidation and membrane damage. Higher MDA content in the plant tissues indicates the detrimental situation induced by the stress factors. In the case of treated seedlings, there was a sharp six time decrease in MDA contents compared to the control (Figure 6A). Other enzymatic antioxidative parameters were found to be also elevated after GRH treatment even in extreme drought situations. SOD, CAT, and POD activities increased up to 1.44, 2.09, and 1.79 times, respectively, in the case of GRH-treated rice seedlings compared to those treated only with PEG (Figures 6B–D).

## Discussion

Agriculture is seen as the most important and crucial sector of the global economy, and it significantly affects our GDP (Gross Domestic

Production). The increased explosion in population in recent years has increased the demands for global agricultural output or food production by 60–100% by the end of 2050 to meet these growing needs, but the main obstacles are the lack of suitable fertile croplands and the rising instances of soil desertification due to insufficient precipitation, random evaporation, and a lack of freshwater resources, among other factors (Naumann et al., 2018; Dey et al., 2019; Paglia and Parker, 2021). Therefore, the primary requirement for a successful solution is the restoration of land or the development of salt or drought stress varieties. The development of drought-tolerant plants could temporarily meet the world's food demand and protect crop plants, but the situation becomes severe when drought conditions (like the 2011–17 California drought and the 1997–99 Melbourne Millennium drought) occur on large scales around the globe. The food supply chain is hampered, and even the forest environment is impacted (Allen et al., 2010). Therefore, it is strongly recommended that deep ecological techniques that use non-toxic, natural substances be developed to address these issues. Exopolysaccharides produced by microbes, especially endophytes could have a significant impact (Chen et al., 2017). Even in situations with salt and drought challenges, endophytic fungi and bacteria are well known for their ability to promote plant growth (Azad and Kaminskyj, 2016; Bibi et al., 2019; Ali et al., 2021; Gupta et al., 2021). There are many reports on how microorganisms (both endophytes and rhizospheric) can reduce abiotic stress (Hammami et al., 2016), and endophytes often play an osmoprotective role in maintaining good water chemistry (managing  $\text{Na}^+/\text{K}^+$  balance) within cells (Jha et al., 2011; Abdelaziz et al., 2017). Previous research has been undertaken, examining the role of endophytic fungi and bacteria in reducing the effects of salt stress in rice, maize, soybean, quinoa, barley, and barrel medic, as well as in the model plant *Arabidopsis thaliana* through endogenous hormone (abscisic acid) mediated morphological, biochemical (through ion balancing), and antioxidant defence-related pathways (Baltruschat et al., 2008; Bagheri et al., 2013; Jogawat et al., 2013; Li et al., 2017; Shahzad et al., 2017; Asaf et al., 2018; Fan et al., 2020; Ali et al., 2022; González-Teuber et al., 2022). Exo-polysaccharides and gamma-polyglutamic acid are also

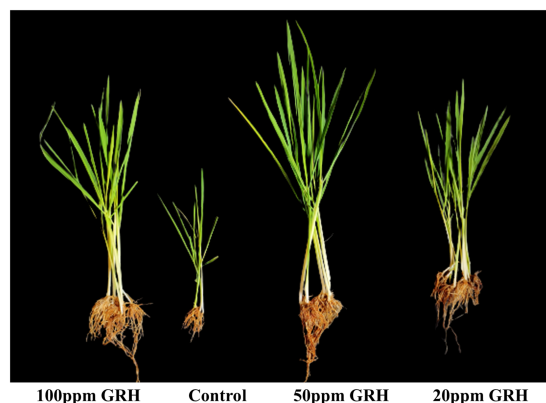


FIGURE 4  
Phenotypes of rice seedlings *Oryza sativa* ssp. indica MTU 7093 Swarna under drought stress (induced by PEG treatment) sprayed with 20, 50, and 100ppm EPS of *Mucor* sp. HELF2 endophyte.

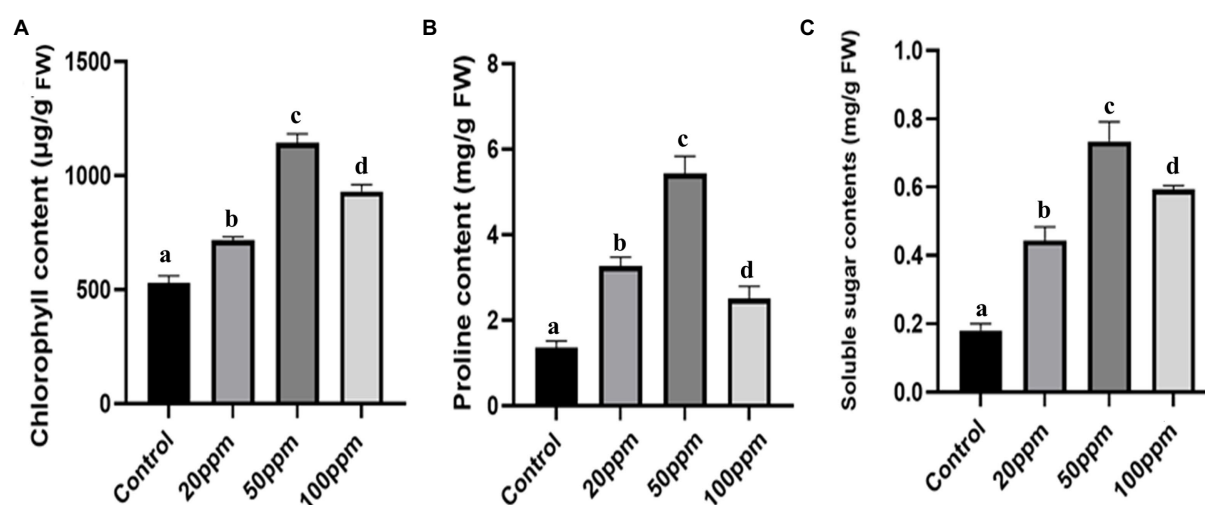


FIGURE 5  
The effect of GRH foliar spray (20, 50, and 100ppm) on chlorophyll content (A), soluble sugar content (B), proline content (C) of *O. sativa* ssp. indica MTU 7093 swarna in comparison to control. Values on the graphs are the means  $\pm$  Standard error (SE) of three replicates. Tukey's multiple comparison test was performed. The letters a, b, c, and d indicate significant differences compared to the control plant (At,  $p < 0.05$ ).

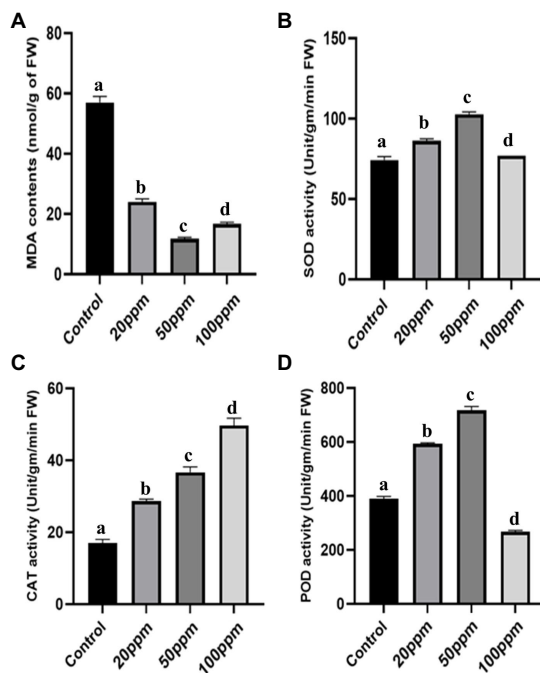


FIGURE 6

The effect of GRH foliar spray (20, 50, and 100ppm) on malondialdehyde (MDA) contents (A), peroxidase (POD) activity (B), catalase (CAT) activity (C), superoxide dismutase (SOD) activity (D) of *O. sativa* ssp. indica MTU 7093 swarna in comparison to control. Values on the graphs are the means  $\pm$  Standard error (SE) of three replicates. Tukey's multiple comparison test was performed. The letters a, b, c, and d indicate significant differences compared to the control plant (At,  $p < 0.05$ ).

discovered to be the most useful compounds released by plant growth-promoting microbes and have exceptional biotic and abiotic stress tolerance (Livingston et al., 2009; Lei et al., 2017). Here, drought stress ameliorating properties of GRH was evaluated on rice plants. Due to their widespread popularity around the world, rice seedlings (*Oryza sativa* ssp. indica MTU 7093 Swarna- Indian subcontinental cultivar) were taken into consideration for their studies on drought relief. It is a very demanding staple food, especially in China, India, and Japan (Uga et al., 2013; Zhu, 2016), and has greater irrigation water needs (Bouman et al., 2005, 2007). According to recent studies, around forty-two million hectares of rice farming face significant challenges because of a lack of water. To formulate an appropriate response, we reported on how Galactose Rich Heteropolysaccharide reduces the effects of drought stress on rice plants. Chen et al. (2017) and Santra and Banerjee (2022a) both found that the application of direct endophyte and EPS produced from endophyte alleviated salt and drought stress in wheat and rice plants, respectively. Due to their high polymeric configurations, effective water-holding capacities, and strong affinity to create bio-films or similar sorts of aggregations, polysaccharides are thought to have significant crop resistance (against both biotic and abiotic) enhancers and plant growth promoters (Muley et al., 2019). Chitosan,  $\beta$ -D-glucan, and other microbial polysaccharides have been found to have growth-stimulating and systemic disease resistance-inducing characteristics on cash crops such as *Solanum lycopersicum*, *Hordeum vulgare*, *Solanum tuberosum*, *Saccharum officinarum*, *Gossypium herbaceum*, and *Glycine max* (Uyen, 2014; Gandra et al., 2016; Blainski et al., 2018; Zhang et al., 2020).

The physical and biochemical traits of seedlings treated with GRH significantly improved. Proline levels and soluble sugar characteristics were also found to be altered, improving the stress-tolerating enzyme profile and enabling the plant to adapt to dry circumstances more successfully. The lower levels of MDA suggest that lipid peroxidation has significantly decreased and that membrane damage has become less frequent. The best concentration of EPS (i.e., Galactose rich heteropolysaccharide- GRH) for controlling the stressful condition was 50 ppm. Lower treatment doses are not sufficient to cause a noticeable change in the plantlets, whereas greater concentrations of GRH are likely to have a negative effect on the health of the plant. The findings of Sun et al. (2020b) are consistent with our findings because the 50 ppm EPS application was also determined to be the best-fitting one in that instance. Through a rise in endogenous ABA levels, polysaccharide treatments affect the stomatal physiology of the test plants' leaves and cause partial stomatal closure, which minimises water evaporation. To improve the internal water levels of the tissues, which are essential for the plant's proper growth and metabolism, these bioactive compounds function as anti-transpirant agents (Vishwakarma et al., 2017). Treatments with GRH increase the relative water contents of the tissues in this instance as well. The uniform build-up of rigid and highly water-soluble osmolytes (such as sugars, amino acids, and prolines) throughout the plant tissues, which provides subcellular stability and integrity, is another mechanism by which exopolysaccharide-mediated drought stress relief works (Hare et al., 1998; Krishnan et al., 2008). Increased levels of osmolyte aggregation raise osmotic pressure, which in turn induces higher water intake and insignificant water outflow. This keeps the cells' critical osmotic pressure constant needed for optimum cell growth and division (Kaur and Asthir, 2015). The proline and soluble sugar levels (osmolytes) are increased by 50 ppm of GRH treatment in the current study as well, balancing the ideal subcellular environment for a healthy water weight required for cell growth. Proline is found to be an important osmo-regulator, and its exogenous administration increases hosts' resistance to abiotic stress (Yoshida et al., 1997; Ben Ahmed et al., 2010). For abiotically challenged plants, exogenous administration of water-soluble polysaccharides also demonstrates a similar response and causes a significant rise in proline levels (Yu et al., 2017; Zou et al., 2018). Thus, in this instance, GRH functions as a biological elicitor or priming agent that activates the cascades of biochemical processes required for water balance and antioxidant defence—ROS scavenging. Thus, as seen in the cases of rice, parsley, and tobacco, polysaccharides generate faster activation of transcription factors leading to the expression of defence-related genes, increasing the alleviation of drought stress (Conrath et al., 2002; Ortmann et al., 2006; Bozsoki et al., 2017). In drought-stricken areas, microbial exopolysaccharide enhances plant development by up- and down-regulating the expression of proline synthase and proline dehydrogenase, respectively (Sun et al., 2020a). By increasing SOD, POD, and CAT levels and fostering the effective operation of cellular biochemical machinery, which is essential for the survival of the plant, osmolytes also effectively eliminate harmful free radicals (reactive oxygen species) under drought stress (Sun et al., 2020b). The three key members of the antioxidant system SOD, CAT, and POD act in an integrated approach, where SOD acts as the first line of defence and converts superoxide free radicals to  $H_2O_2$ , which is further catalysed into water and oxygen by CAT and POD (Das and Roychoudhury, 2014). Last but not least, the MDA concentrations decrease, reducing the peroxidation of membrane proteins and lipids (Fu et al., 2010; Miller et al., 2010). Spraying potato and wheat with chitosan, polysaccharides from *Ganoderma lucidum*,



*Lactobacillus plantarum*, and *Pantoea agglomerans*, respectively, activates the antioxidant defence cascades (Ortmann et al., 2006; Blainski et al., 2018; Muley et al., 2019; Zhang et al., 2020). Here, foliar GRH spray applied at a dosage of 50 ppm enhanced the SOD, POD, and CAT levels while concurrently lowering the MDA contents.

The bio-active GRH produced by *Mucor* sp. HELF2 was a polymer of D-galactose, L-fucose, and D-glucose (molar ratio—13:2:1) with a molecular weight of  $2.98 \times 10^5$  Da. Galacto-rhamnan and beta-glucan exopolysaccharides with molecular weights of  $1.87 \times 10^5$  and  $2 \times 10^5$  Da were found in endophytic *Fusarium* sp. SD5 and *Pestalotiopsis* sp. BC55, respectively, according to Mahapatra and Banerjee's reports from 2013 and 2016. Polysaccharides from edible mushroom *Termitomyces heimii*, and *Meripilus giganteus* also represents a similar type of monosaccharide compositions of L-fucose, D-galactose, and D-glucose, etc. (Maity et al., 2017, 2020). The EPS manufacturing process was optimised for carbon, nitrogen sources, a medium pH, and fermentation temperature to produce the greatest quantity of polysaccharides. The appropriate oxygen demand was also considered. The optimisation data makes it possible to quickly and affordably obtain the polysaccharides in large quantities. The results of the current inquiry on the optimization of GRH production broadly concur with those of Mahapatra and Banerjee (2013, 2016).

The present study examined endophytic exopolysaccharides (GRH) from an ecologically valuable plant and checked the drought tolerance action of the GRH on rice plants. Finally, varying concentrations of fungal EPS were used to reduce the effects of drought stress. Our research clarifies the idea of creating rice types resistant to drought through the external application of EPS, which supports environmentally friendly farming methods. This study provides the first evidence of the use of endophytic *Mucor* sp. HELF2 produced D-galactose-rich heteropolysaccharide to reduce drought stress in rice seedlings.

## Conclusion

In the present study, rice seedling dehydration stress was lessened by a galactose-rich heteropolysaccharide derived from endophytic *Mucor* sp. HELF2. The outcome illustrated that treated plants had higher fresh weights, relative water contents, and chlorophyll levels. While the MDA concentration reduced, osmolytes such as soluble sugars, proline, as well as the antioxidant defence enzymes SOD, CAT, and POD, increased. The results support the conclusion that foliar spray of

Galactose Rich Heteropolysaccharide efficiently promotes drought resistance in rice plants. GRH production was also optimised by adopting OVAT and RSM techniques and there was a 1.5-fold ( $20.10 \text{ g L}^{-1}$ ) enhancement in GRH production in optimised fermentation conditions. The ability of GRH to alleviate the effects of drought stress on rice plants and the high yield of GRH makes it suitable for commercial exploitation. The current investigation's findings may encourage sustainable farming methods and have an impact on the cultivation of crops in drought-prone areas.

## Data availability statement

The datasets presented in this study can be found in online repositories. The names of the repository/repositories and accession number(s) can be found at: <https://www.ncbi.nlm.nih.gov/genbank/>, ON146358.

## Author contributions

HS designed and performed the experiments, and prepared the draft of the manuscript. DB designed the experiment and finalised the manuscript. All authors contributed to the article and approved the submitted version.

## Conflict of interest

The authors declare that the research was conducted in the absence of any commercial or financial relationships that could be construed as a potential conflict of interest.

## Publisher's note

All claims expressed in this article are solely those of the authors and do not necessarily represent those of their affiliated organizations, or those of the publisher, the editors and the reviewers. Any product that may be evaluated in this article, or claim that may be made by its manufacturer, is not guaranteed or endorsed by the publisher.

## References

- Abdelaziz, M. E., Kim, D., Ali, S., Fedoroff, N. V., and Al-Babili, S. (2017). The endophytic fungus *Piriformospora indica* enhances *Arabidopsis thaliana* growth and modulates Na<sup>+</sup>/K<sup>+</sup> homeostasis under salt stress conditions. *Plant Sci.* 263, 107–115. doi: 10.1016/j.plantsci.2017.07.006
- Ali, R., Gul, H., Hamayun, M., Rauf, M., Iqbal, A., Shah, M., et al. (2021). *Aspergillus awamori* ameliorates the physicochemical characteristics and mineral profile of mung bean under salt stress. *Chemical and Biological Technologies in Agriculture* 8, 1–13. doi: 10.1186/s40538-021-00208-9
- Ali, R., Gul, H., Rauf, M., Arif, M., Hamayun, M., Husna, , et al. (2022). growth-promoting endophytic fungus (*Stemphylium lycopersici*) ameliorates salt stress tolerance in maize by balancing ionic and metabolic status. *Front. Plant Sci.* 13:565. doi: 10.3389/fpls.2022.890565
- Allen, C. D., Macalady, A. K., Chenchouni, H., Bachelet, D., McDowell, N., Vennetier, M., et al. (2010). A global overview of drought and heat-induced tree mortality reveals emerging climate change risks for forests. *For. Ecol. Manag.* 259, 660–684. doi: 10.1016/j.foreco.2009.09.001
- Arndt, S. K., Irawan, A., and Sanders, G. J. (2015). Apoplastic water fraction and rehydration techniques introduce significant errors in measurements of relative water content and osmotic potential in plant leaves. *Physiol. Plant.* 155, 355–368. doi: 10.1111/pp.12380
- Asaf, L., Sajjad, M. H., Khan, A. L., Waqas, M., Khan, M. A., Jan, R., et al. (2018). Salt tolerance of *Glycine max*. L induced by endophytic fungus *aspergillus flavus* CSH1, via regulating its endogenous hormones and antioxidative system. *Plant Physiol. Biochem.* 128, 13–23. doi: 10.1016/j.plaphy.2018.05.007
- Azad, K., and Kaminskyj, S. (2016). A fungal endophyte strategy for mitigating the effect of salt and drought stress on plant growth. *Symbiosis* 68, 73–78. doi: 10.1007/s13199-015-0370-y
- Bagheri, A. A., Saadatmand, S., Niknam, V., Nejadatari, T., and Babaeizad, V. (2013). Effect of endophytic fungus, *Piriformospora indica*, on growth and activity of antioxidant enzymes of rice (*Oryza sativa* L.) under salinity stress. *Int. J. Adv. Biol. Biomed. Res.* 1, 1337–1350.
- Baltruschat, H., Fodor, J., Harrach, B. D., Niemczyk, E., Barna, B., Gullner, G., et al. (2008). Salt tolerance of barley induced by the root endophyte *Piriformospora indica* is associated with a strong increase in antioxidants. *New Phytol.* 180, 501–510. doi: 10.1111/j.1469-8137.2008.02583.x
- Bates, L. S., Waldren, R. P., and Teare, I. D. (1973). Rapid determination of free proline for water-stress studies. *Plant Soil* 39, 205–207. doi: 10.1007/BF00018060
- Ben Ahmed, C., Ben Rouina, B., Sensoy, S., Boukhriess, M., and Ben Abdullah, F. (2010). Exogenous proline effects on photosynthetic performance and antioxidant defense system of young olive tree. *J. Agric. Food Chem.* 58, 4216–4222. doi: 10.1021/jf9041479

- Bibi, N., Jan, G., Jan, F. G., Hamayun, M., Iqbal, A., Hussain, A., et al. (2019). *Cochliobolus* sp. acts as a biochemical modulator to alleviate salinity stress in okra plants. *Plant Physiol. Biochem.* 139, 459–469. doi: 10.1016/j.plaphy.2019.04.019
- Blaha, D., Prigent-Combaret, C., Mirza, M. S., and Moënné-Loccoz, Y. (2006). Phylogeny of the 1-aminocyclopropane-1-carboxylic acid deaminase-encoding gene *acdS* in phytochemical and pathogenic Proteobacteria and relation with strain biogeography. *FEMS Microbiol. Ecol.* 56, 455–470. doi: 10.1111/j.1574-6941.2006.00082.x
- Blainski, J., da Rocha Neto, A. C., Schmidt, E. C., Voltolini, J. A., Rossi, M. J., di Piero, R. M., et al. (2018). Exopolysaccharides from *Lactobacillus plantarum* induce biochemical and physiological alterations in tomato plant against bacterial spot. *Appl. Microbiol. Biotechnol.* 102, 4741–4753. doi: 10.1007/s00253-018-8946-0
- Bouman, B. A., Humphreys, E., Tuong, T. P., and Barker, R. (2007). Rice and water. *Adv. Agron.* 92, 187–237. doi: 10.1016/S0065-2113(04)92004-4
- Bouman, B. A. M., Peng, S., Castaneda, A. R., and Visperas, R. M. (2005). Yield and water use of irrigated tropical aerobic rice systems. *Agric. Water Manag.* 74, 87–105. doi: 10.1016/j.agwat.2004.11.007
- Bozsoki, Zoltan, Cheng, Jeryl, Feng, Feng, Gysel, Kira, Vinther, Maria, Andersen, Kasper R., et al. "Receptor-mediated chitin perception in legume roots is functionally separable from nod factor perception." *Proceedings of the National Academy of Sciences*, 114. (2017). E8118-E 8127.
- Chatterjee, S., Ghosh, S., and Mandal, N. C. (2022). Potential of an endophytic fungus *Alternaria tenuissima* PE2 isolated from *Psidium guajava* L. for the production of bioactive compounds. *S. Afr. J. Bot.* 150, 658–670. doi: 10.1016/j.sajb.2022.08.016
- Chen, Y., Mao, W., Tao, H., Zhu, W., Qi, X., Chen, Y., et al. (2011). Structural characterization and antioxidant properties of an exopolysaccharide produced by the mangrove endophytic fungus *Aspergillus* sp. Y16. *Bioresour. Technol.* 102, 8179–8184. doi: 10.1016/j.biortech.2011.06.048
- Chen, C., Xin, K., Liu, H., Cheng, J., Shen, X., Wang, Y., et al. (2017). *Pantoea alhagi*, a novel endophytic bacterium with ability to improve growth and drought tolerance in wheat. *Sci. Rep.* 7, 1–14. doi: 10.1038/srep41564
- Cherif, H., Marasco, R., Rolli, E., Ferjani, R., Fusi, M., Soussi, A., et al. (2015). Oasis desert farming selects environment-specific date palm root endophytic communities and cultivable bacteria that promote resistance to drought. *Environ. Microbiol. Rep.* 7, 668–678. doi: 10.1111/1758-2229.12304
- Ciucanu, I., and Kerek, F. (1984). A simple and rapid method for the permethylation of carbohydrates. *Carbohydr. Res.* 131, 209–217. doi: 10.1016/0008-6215(84)85242-8
- Coleman-Derr, D., and Tringe, S. G. (2014). Building the crops of tomorrow: advantages of symbiont-based approaches to improving abiotic stress tolerance. *Front. Microbiol.* 5:283. doi: 10.3389/fmicb.2014.00283
- Conrath, U., Pieterse, C. M. J., and Brigitte, M.-M. (2002). Priming in plant–pathogen interactions. *Trends Plant Sci.* 7, 210–216.
- Constantin, M. E., Francisco, J. D. L., Babette, V. V., Martijn, R., and Frank, L. W. T. (2019). Endophyte-mediated resistance in tomato to *Fusarium oxysporum* is independent of ET, JA, and SA. *Front. Plant Sci.* 10:979.
- Das, D., Mondal, S., Maiti, D., Roy, S. K., and Islam, S. S. (2009). Structural characterization of dietary fiber of green chalcumra (*Benincasa hispida*) fruit by NMR spectroscopic analysis. *Nat. Prod. Commun.* 4:1934578X0900400. doi: 10.1177/1934578X0900400421
- Das, K., and Roychoudhury, A. (2014). Reactive oxygen species (ROS) and response of antioxidants as ROS-scavengers during environmental stress in plants. *Front. Environ. Sci.* 2:53. doi: 10.3389/fenvs.2014.00053
- Del Buono, D., Ioli, G., Nasini, L., and Proietti, P. (2011). A comparative study on the interference of two herbicides in wheat and Italian ryegrass and on their antioxidant activities and detoxification rates. *J. Agric. Food Chem.* 59, 12109–12115. doi: 10.1021/jf2026555
- Dey, R., Lewis, S. C., Arblaster, J. M., and Abram, N. J. (2019). A review of past and projected changes in Australia's rainfall. *Wiley Interdiscip. Rev.: Climate Change* 10:e577. doi: 10.1002/wcc.577
- Dubois, M., Gilles, K. A., Hamilton, J. K., Rebers, P. T., and Smith, F. (1956). Colorimetric method for determination of sugars and related substances. *Anal. Chem.* 28, 350–356. doi: 10.1021/ac60111a017
- Fan, D., Subramanian, S., and Smith, D. L. (2020). Plant endophytes promote growth and alleviate salt stress in *Arabidopsis thaliana*. *Sci. Rep.* 10, 1–18. doi: 10.1038/s41598-020-69713-5
- Fu, Q., Liu, C., Ding, N., Lin, Y., and Guo, B. (2010). Ameliorative effects of inoculation with the plant growth-promoting rhizobacterium *Pseudomonas* sp. DW1 on growth of eggplant (*Solanum melongena* L.) seedlings under salt stress. *Agric. Water Manag.* 97, 1994–2000. doi: 10.1016/j.agwat.2010.02.003
- Gamalerio, G.-G. E., and Bernard, R. G. (2012). "Ethylene and abiotic stress tolerance in plants." in *Environmental adaptations and stress tolerance of plants in the era of climate change*. (New York, NY: Springer), 395–412.
- Gandra, J. R., Oliveira, E. R., Takiya, C. S., Goes, R. H. T. B., Paiva, P. G., Oliveira, K. M. P., et al. (2016). Chitosan improves the chemical composition, microbiological quality, and aerobic stability of sugarcane silage. *Anim. Feed Sci. Technol.* 214, 44–52. doi: 10.1016/j.anifeeds.2016.02.020
- González-Teuber, M., Contreras, R. A., Zúñiga, G. E., Barrera, D., and Bascuñán-Godoy, L. (2022). Synergistic association with root endophytic fungi improves morpho-physiological and biochemical responses of *Chenopodium quinoa* to salt stress. *Front. Ecol. Evol.* 9:787318. doi: 10.3389/feco.2021.787318
- Gupta, S., Schillaci, M., Walker, R., Smith, P., Watt, M., and Roessner, U. (2021). Alleviation of salinity stress in plants by endophytic plant-fungal symbiosis: current knowledge, perspectives and future directions. *Plant Soil* 461, 219–244. doi: 10.1007/s11274-020-04618-w
- Hammami, H., Baptista, P., Martins, F., Gomes, T., Abdely, C., and Mahmoud, O. M.-B. (2016). Impact of a natural soil salinity gradient on fungal endophytes in wild barley (*Hordeum maritimum* with.). *World J. Microbiol. Biotechnol.* 32, 1–11. doi: 10.1007/s11274-016-2142-0
- Hare, P. D., Cress, W. A., and Van Staden, J. (1998). Dissecting the roles of osmolyte accumulation during stress. *Plant Cell Environ.* 21, 535–553. doi: 10.1046/j.1365-3040.1998.00309.x
- Jha, Y., Subramanian, R. B., and Patel, S. (2011). Combination of endophytic and rhizospheric plant growth promoting rhizobacteria in *Oryza sativa* shows higher accumulation of osmoprotectant against saline stress. *Acta Physiol. Plant.* 33, 797–802. doi: 10.1007/s11738-010-0604-9
- Jogawat, A., Saha, S., Bakshi, M., Dayaman, V., Kumar, M., Dua, M., et al. (2013). *Piriformospora indica* rescues growth diminution of rice seedlings during high salt stress. *Plant Signal. Behav.* 8:e26891. doi: 10.4161/psb.26891
- Kaur, G., and Asthir, B. J. B. P. (2015). Proline: a key player in plant abiotic stress tolerance. *Biol. Plant.* 59, 609–619. doi: 10.1007/s10535-015-0549-3
- Krishnan, N., Dickman, M. B., and Becker, D. F. (2008). Proline modulates the intracellular redox environment and protects mammalian cells against oxidative stress. *Free Radic. Biol. Med.* 44, 671–681. doi: 10.1016/j.freeradbiomed.2007.10.054
- Laich, F., and Andrade, J. (2016). *Penicillium pedernalense* sp. nov., isolated from whiteleg shrimp heads waste compost. *Int. J. Syst. Evol.* 66, 4382–4388. doi: 10.1099/ijsem.0.001360
- Landum, M. C., Félix, M. R., Alho, J., Garcia, R., Cabrita, M. J., Rei, F., et al. (2016). Antagonistic activity of fungi of *Olea europaea* L. against *Colletotrichum acutatum*. *Microbiol. Res.* 183, 100–108. doi: 10.1016/j.micres.2015.12.001
- Lei, P., Pang, X., Feng, X., Li, S., Chi, B., Wang, R., et al. (2017). The microbe-secreted isopeptide poly- $\gamma$ -glutamic acid induces stress tolerance in *Brassica napus* L. seedlings by activating crosstalk between H<sub>2</sub>O<sub>2</sub> and Ca<sup>2+</sup>. *Sci. Rep.* 7, 1–15. doi: 10.1038/srep41618
- Lei, P., Xu, Z., Ding, Y., Tang, B., Zhang, Y., Li, H., et al. (2015). Effect of poly ( $\gamma$ -glutamic acid) on the physiological responses and calcium signaling of rape seedlings (*Brassica napus* L.) under cold stress. *J. Agric. Food Chem.* 63, 10399–10406. doi: 10.1021/acs.jafc.5b04523
- Li, L., Li, L., Wang, X., Zhu, P., Hongqing, W., and Qi, S. (2017). Plant growth-promoting endophyte *Piriformospora indica* alleviates salinity stress in *Medicago truncatula*. *Plant Physiol. Biochem.* 119, 211–223. doi: 10.1016/j.plaphy.2017.08.029
- Lichtenthaler, H. K., and Wellburn, A. R. (1983). Determinations of total carotenoids and chlorophylls *a* and *b* of leaf extracts in different solvents, vol. 11, 591–592.
- Livingston, D. P., Hinch, D. K., and Heyer, A. G. (2009). Fructan and its relationship to abiotic stress tolerance in plants. *Cell. Mol. Life Sci.* 66, 2007–2023. doi: 10.1007/s00118-009-0002-x
- Lowry, O. H. (1951). Protein measurement with the Folin phenol reagent. *J. Biol. Chem.* 193, 265–275. doi: 10.1016/S0021-9258(19)52451-6
- Mahapatra, S., and Banerjee, D. (2013). Optimization of a bioactive exopolysaccharide production from endophytic *fusarium solani* SD5. *Carbohydr. Polym.* 97, 627–634. doi: 10.1016/j.carbpol.2013.05.039
- Mahapatra, S., and Banerjee, D. (2016). Production and structural elucidation of exopolysaccharide from endophytic *Pestalotiopsis* sp. BC55. *Int. J. Macromol.* 82, 182–191. doi: 10.1016/j.jbiomac.2015.11.035
- Maity, P., Nandi, A. K., Manna, D. K., Pattanayak, M., Sen, I. K., Bhanja, S. K., et al. (2017). Structural characterization and antioxidant activity of a glucan from *Meripilus giganteus*. *Carbohydr. Polym.* 157, 1237–1245. doi: 10.1016/j.carbpol.2016.11.006
- Maity, P., Nandi, A. K., Pattanayak, M., Manna, D. K., Sen, I. K., Chakraborty, I., et al. (2020). Structural characterization of a heteroglycan from an edible mushroom *Termitomyces heimii*. *Int. J. Biol. Macromol.* 151, 305–311. doi: 10.1016/j.jbiomac.2020.02.120
- Marasco, R., Rolli, E., Ettoumi, B., Vigani, G., Mapelli, F., Borin, S., et al. (2012). A drought resistance-promoting microbiome is selected by root system under desert farming. *PLoS one* 7:e48479. doi: 10.1371/journal.pone.0048479
- Mesa, J., Mateos-Naranjo, E., Cavedes, M. A., Redondo-Gómez, S., Pajuelo, E., and Rodríguez-Llorente, I. D. (2015). Endophytic cultivable bacteria of the metal bio-accumulator *Spartina maritima* improve plant growth but not metal uptake in polluted marshes soils. *Front. Microbiol.* 6:1450. doi: 10.3389/fmicb.2015.01450
- Miller, G. A. D., Suzuki, N., Ciftci-Yilmaz, S. U. L. T. A. N., and Mittler, R. O. N. (2010). Reactive oxygen species homeostasis and signalling during drought and salinity stresses. *Plant Cell Environ.* 33, 453–467. doi: 10.1111/j.1365-3040.2009.02041.x
- Moghaddam, M. S. H., Naser, S., Jalal, S., and Niloufar, H.-D. (2021). Desert-adapted fungal endophytes induce salinity and drought stress resistance in model crops. *Plant Physiol. Biochem.* 160, 225–238.
- Muley, A. B., Shingote, P. R., Patil, A. P., Dalvi, S. G., and Suprasanna, P. (2019). Gamma radiation degradation of chitosan for application in growth promotion and induction of stress tolerance in potato (*Solanum tuberosum* L.). *Carbohydr. Polym.* 210, 289–301. doi: 10.1016/j.carbpol.2019.01.056

- Nadeem, S. M., Ahmad, M., Zahir, Z. A., Javaid, A., and Ashraf, M. (2014). The role of mycorrhizae and plant growth promoting rhizobacteria (PGPR) in improving crop productivity under stressful environments. *Biotechnol. Adv.* 32, 429–448. doi: 10.1016/j.biotechadv.2013.12.005
- Naumann, G., Alfieri, L., Wyser, K., Mentaschi, L., Betts, R. A., Carrao, H., et al. (2018). Global changes in drought conditions under different levels of warming. *Geophys. Res. Lett.* 45, 3285–3296. doi: 10.1002/2017GL076521
- Ortmann, I., Conrath, U., and Moerschbacher, B. M. (2006). Exopolysaccharides of *Pantoea agglomerans* have different priming and eliciting activities in suspension-cultured cells of monocots and dicots. *FEBS Lett.* 580, 4491–4494. doi: 10.1016/j.febslet.2006.07.025
- Paglia, E., and Parker, C. (2021). “The intergovernmental panel on climate change: guardian of climate science” in *Guardians of public value*. ed. A. Boin (Cham: Palgrave Macmillan), 295–321.
- Pinedo, I., Ledger, T., Greve, M., and Poupin, M. J. (2015). *Burkholderia phytofirmans* PsJN induces long-term metabolic and transcriptional changes involved in *Arabidopsis thaliana* salt tolerance. *Front. Plant Sci.* 6:466. doi: 10.3389/fpls.2015.00466
- Proestos, C., Bozaris, I. S., Nychas, G. J., and Komaitis, M. (2006). Analysis of flavonoids and phenolic acids in Greek aromatic plants: investigation of their antioxidant capacity and antimicrobial activity. *Food Chem.* 95, 664–671. doi: 10.1016/j.foodchem.2005.01.049
- Redman, R. S., Kim, Y. O., Woodward, C. J. D. A., Greer, C., Espino, L., Doty, S. L., et al. (2011). Increased fitness of rice plants to abiotic stress via habitat adapted symbiosis: a strategy for mitigating impacts of climate change. *PLoS One* 6:e14823. doi: 10.1371/journal.pone.0014823
- Rodriguez, R., and Redman, R. (2008). More than 400 million years of evolution and some plants still can't make it on their own: plant stress tolerance via fungal symbiosis. *J. Exp. Bot.* 59, 1109–1114. doi: 10.1093/jxb/erm342
- Rolli, E., Marasco, R., Vigani, G., Ettoumi, B., Mapelli, F., Deangelis, M. L., et al. (2015). Improved plant resistance to drought is promoted by the root-associated microbiome as a water stress-dependent trait. *Environ. Microbiol.* 17, 316–331. doi: 10.1111/1462-2920.12439
- Saitou, N., and Nei, M. (1987). The neighbor-joining method: a new method for reconstructing phylogenetic trees. *Mol. Biol. Evol.* 4, 406–425. PMID: 3447015
- Santra, H. K., and Banerjee, D. (2022a). Production, optimization, characterization and drought stress resistance by  $\beta$ -glucan rich heteropolysaccharide from an endophytic fungi *Colletotrichum alatae* LCS1 isolated from clubmoss (*Lycopodium clavatum*). *Front. Fungal Biol.* 2:65. doi: 10.3389/fpubb.2021.796010
- Santra, H. K., and Banerjee, D. (2022b). Bioactivity study and metabolic profiling of *Colletotrichum alatae* LCS1, an endophyte of club moss *Lycopodium clavatum* L. *PLoS one* 17:e0267302. doi: 10.1371/journal.pone.0267302
- Santra, H. K., and Banerjee, D. (2022c). Broad-Spectrum antimicrobial action of cell-free culture extracts and volatile organic compounds produced by endophytic fungi *Curvularia Eragrostidis*. *Front. Microbiol.* 13:561. doi: 10.3389/fmicb.2022.920561
- Santra, H. K., Maity, S., and Banerjee, D. (2022). Production of bioactive compounds with broad spectrum bactericidal action, bio-film inhibition and antilarval potential by the secondary metabolites of the endophytic fungus *Cochliobolus* sp. APS1 isolated from the Indian medicinal herb *Andrographis paniculata*. *Molecules* 27:1459. doi: 10.3390/molecules27051459
- Schulz, B., Wanke, U., Draeger, S., and Aust, H.-J. (1993). Endophytes from herbaceous plants and shrubs: effectiveness of surface sterilization methods. *Mycol. Res.* 97, 1447–1450.
- Shahzad, R., Khan, A. L., Bilal, S., Waqas, M., Kang, S.-M., and Lee, I.-J. (2017). Inoculation of abscisic acid-producing endophytic bacteria enhances salinity stress tolerance in *Oryza sativa*. *Environ. Exp. Bot.* 136, 68–77. doi: 10.1016/j.envexpbot.2017.01.010
- Sun, L., Lei, P., Wang, Q., Ma, J., Zhan, Y., Jiang, K., et al. (2020a). The endophyte *Pantoea alhagi* NX-11 alleviates salt stress damage to rice seedlings by secreting exopolysaccharides. *Front. Microbiol.* 10:3112. doi: 10.3389/fmicb.2019.03112
- Sun, L., Yang, Y., Wang, R., Li, S., Qiu, Y., Lei, P., et al. (2020b). Effects of exopolysaccharide derived from *Pantoea alhagi* NX-11 on drought resistance of rice and its efficient fermentation preparation. *Int. J. Biol. Macromol.* 162, 946–955. doi: 10.1016/j.ijbiomac.2020.06.199
- Tamura, K., Stecher, G., and Kumar, S. (2021). MEGA11: molecular evolutionary genetics analysis version 11. *Mol. Biol. Evol.* 38, 3022–3027. doi: 10.1093/molbev/msab120
- Tiwari, S., Lata, C., Chauhan, P. S., and Nautiyal, C. S. (2016). *Pseudomonas putida* attunes morphophysiological, biochemical and molecular responses in *Cicer arietinum* L. during drought stress and recovery. *Plant Physiol. Biochem.* 99, 108–117. doi: 10.1016/j.plaphy.2015.11.001
- Uga, Y., Sugimoto, K., Ogawa, S., Rane, J., Ishitani, M., Hara, N., et al. (2013). Control of root system architecture by DEEPER ROOTING 1 increases rice yield under drought conditions. *Nat. Genet.* 45, 1097–1102. doi: 10.1038/ng.2725
- Uyen, N. H. P. (2014). Radiation degradation of (1 $\rightarrow$ 3)- $\beta$ -D-glucan from yeast with a potential application as a plant growth promoter. *Int. J. Biol. Macromol.* 69, 165–170. doi: 10.1016/j.ijbiomac.2014.05.041
- Vishwakarma, K., Upadhyay, N., Kumar, N., Yadav, G., Singh, J., Mishra, R. K., et al. (2017). Absciscic acid signaling and abiotic stress tolerance in plants: a review on current knowledge and future prospects. *Front. Plant Sci.* 8:161. doi: 10.3389/fpls.2017.00161
- Vurukonda, S. S. K. P., Vardharajula, S., Shrivastava, M., and SkZ, A. (2016). Enhancement of drought stress tolerance in crops by plant growth promoting rhizobacteria. *Microbiol. Res.* 184, 13–24. doi: 10.1016/j.micres.2015.12.003
- Watanabe, S., Kojima, K., Ide, Y., and Sasaki, S. (2000). Effects of saline and osmotic stress on proline and sugar accumulation in *Populus euphratica* in vitro. *Plant Cell Tissue Organ Cult.* 63, 199–206. doi: 10.1023/A:1010619503680
- Wonglumsom, W., Vishnubhatla, A., and Fung, D. Y. C. (2000). Effect of volume of liquid enrichment medium containing oxyrase<sup>®</sup> on growth of *campylobacter jejuni* 1. *J RAPID METH AUT MIC* 8, 111–139. doi: 10.1111/j.1745-4581.2000.tb00354.x
- Yoshida, Y., Kiyosue, T., Nakashima, K., Yamaguchi-Shinozaki, K., and Shinozaki, K. (1997). Regulation of levels of proline as an osmolyte in plants under water stress. *Plant Cell Physiol.* 38, 1095–1102. doi: 10.1093/oxfordjournals.pcp.a029093
- Yu, Z., He, C., Jaime, A., da Silva, T., Zhang, G., Dong, W., et al. (2017). Molecular cloning and functional analysis of DoUGE related to water-soluble polysaccharides from *Dendrobium officinale* with enhanced abiotic stress tolerance. *Plant Cell, Tissue and Organ Culture (PCTOC)* 131, 579–599. doi: 10.1007/s11240-017-1308-2
- Zhang, X., Aweya, J. J., Huang, Z. X., Kang, Z. Y., Bai, Z. H., Li, K. H., et al. (2020). In vitro fermentation of *Gracilaria lemaneiformis* sulfated polysaccharides and its Agaro-oligosaccharides by human fecal inocula and its impact on microbiota, Cheong. *Carbohydr. Polym.* 234:115894. doi: 10.1016/j.carbpol.2020.115894
- Zhu, J. K. (2016). Abiotic stress signaling and responses in plants. *Cells* 167, 313–324. doi: 10.1016/j.cell.2016.08.029
- Zou, P., Xueli, L., Jing, C., Yuan, Y., Yi, L., Zhang, C., et al. (2018). Low-molecular-weight polysaccharides from *Pyropia yezoensis* enhance tolerance of wheat seedlings (*Triticum aestivum* L.) to salt stress. *Front. Plant Sci.* 9:427. doi: 10.3389/fpls.2018.00427





## OPEN ACCESS

## EDITED BY

George Newcombe,  
University of Idaho,  
United States

## REVIEWED BY

Debdulal Banerjee,  
Vidyasagar University,  
India  
Shaikhul Islam,  
Bangladesh Agricultural Research Council,  
Bangladesh

## \*CORRESPONDENCE

Omar A. Hewedy  
✉ hewedy.omar@gmail.com

## SPECIALTY SECTION

This article was submitted to  
Microbiotechnology,  
a section of the journal  
Frontiers in Microbiology

RECEIVED 09 January 2023

ACCEPTED 21 February 2023

PUBLISHED 14 March 2023

## CITATION

Sehim AE, Hewedy OA, Altammar KA,  
Alhumaidi MS and Abd Elghaffar RY (2023)  
*Trichoderma asperellum* empowers tomato  
plants and suppresses *Fusarium oxysporum*  
through priming responses.  
*Front. Microbiol.* 14:1140378.  
doi: 10.3389/fmicb.2023.1140378

## COPYRIGHT

© 2023 Sehim, Hewedy, Altammar, Alhumaidi  
and Abd Elghaffar. This is an open-access  
article distributed under the terms of the  
[Creative Commons Attribution License \(CC BY\)](https://creativecommons.org/licenses/by/4.0/).  
The use, distribution or reproduction in other  
forums is permitted, provided the original  
author(s) and the copyright owner(s) are  
credited and that the original publication in this  
journal is cited, in accordance with accepted  
academic practice. No use, distribution or  
reproduction is permitted which does not  
comply with these terms.

# *Trichoderma asperellum* empowers tomato plants and suppresses *Fusarium oxysporum* through priming responses

Amira E. Sehim<sup>1</sup>, Omar A. Hewedy<sup>2,3\*</sup>, Khadijah A. Altammar<sup>4</sup>,  
Maryam S. Alhumaidi<sup>4</sup> and Rasha Y. Abd Elghaffar<sup>1</sup>

<sup>1</sup>Botany and Microbiology Department, Faculty of Science, Benha University, Benha, Egypt,

<sup>2</sup>Department of Plant Agriculture, University of Guelph, Guelph, ON, Canada, <sup>3</sup>Department of Genetics,  
Faculty of Agriculture, Menoufia University, Shebeen El-Kom, Egypt, <sup>4</sup>Department of Biology, College of  
Science, University of Hafr Al Batin, Hafar Al Batin, Saudi Arabia

Plant-associated microbes play crucial roles in plant health and promote growth under stress. Tomato (*Solanum lycopersicum*) is one of the strategic crops grown throughout Egypt and is a widely grown vegetable worldwide. However, plant disease severely affects tomato production. The post-harvest disease (*Fusarium* wilt disease) affects food security globally, especially in the tomato fields. Thus, an alternative effective and economical biological treatment to the disease was recently established using *Trichoderma asperellum*. However, the role of rhizosphere microbiota in the resistance of tomato plants against soil-borne *Fusarium* wilt disease (FWD) remains unclear. In the current study, a dual culture assay of *T. asperellum* against various phytopathogens (e.g., *Fusarium oxysporum*, *F. solani*, *Alternaria alternata*, *Rhizoctonia solani*, and *F. graminearum*) was performed *in vitro*. Interestingly, *T. asperellum* exhibited the highest mycelial inhibition rate (53.24%) against *F. oxysporum*. In addition, 30% free cell filtrate of *T. asperellum* inhibited *F. oxysporum* by 59.39%. Various underlying mechanisms were studied to explore the antifungal activity against *F. oxysporum*, such as chitinase activity, analysis of bioactive compounds by gas chromatography–mass spectrometry (GC–MS), and assessment of fungal secondary metabolites against *F. oxysporum* mycotoxins in tomato fruits. Additionally, the plant growth-promoting traits of *T. asperellum* were studied (e.g., IAA production, Phosphate solubilization), and the impact on tomato seeds germination. Scanning electron microscopy, plant root sections, and confocal microscopy were used to show the mobility of the fungal endophyte activity to promote tomato root growth compared with untreated tomato root. *T. asperellum* enhanced the growth of tomato seeds and controlled the wilt disease caused by the phytopathogen *F. oxysporum* by enhancing the number of leaves as well as shoot and root length (cm) and fresh and dry weights (g). Furthermore, *Trichoderma* extract protects tomato fruits from post-harvest infection by *F. oxysporum*. Taking together, *T. asperellum* represents a safe and effective controlling agent against *Fusarium* infection of tomato plants.

## KEYWORDS

*Trichoderma asperellum*, tomato, *Fusarium oxysporum*, IAA, biological control, root anatomy, confocal microscopy



## Introduction

Tomato (*Solanum lycopersicon* L.) is one of the most essential and widespread horticultural crops worldwide (Pritesh and Subramanian, 2011; Bawa, 2016), and it is a rich source of vitamins A and C (Pramanik and Mohapatra, 2017; Boccia et al., 2019). Egypt is a top-five tomato producer, accounting for 7.2 to 8.6 million tons annually (Nakai, 2018). However, there is a significant concern regarding food security, as demographic projections indicate that the global population will rise to 9.5 billion by 2050 (Attia et al., 2022). Food security and safety are increasingly threatened as the human population continues to expand due to soil-borne fungal pathogens emerging worldwide. In addition, such pathogens can reduce crop productivity in greenhouse and field conditions (e.g., vegetable crops), consequently causing severe losses to global food security (Almeida et al., 2019). Fungal diseases cause over 1.6 million deaths annually, and over one billion people suffer from severe fungal infections. Moreover, fungal pathogens are considered the highest threat to plant-host species, representing the main reason for reducing plant growth (approximately 65%) (Zhang and Ma, 2017; Almeida et al., 2019; Hewedy et al., 2020a,b). In addition, toxigenic fungi are the most important plant pathogens, causing diseases such as *Fusarium oxysporum* species complex (FOSC) (Zhang and Ma, 2017; Hewedy et al., 2020a,b), *Rhizoctonia solani* (Ghazala et al., 2022), *Fusarium solani* (Saengchan et al., 2022), and *Fusarium graminearum* (de Chaves et al., 2022). The plant root is the key site for interacting with the host plant, microbial pathogens, and the rhizosphere microbiome (Zhalnina et al., 2018). Furthermore, plants have become more susceptible to disease due to continuous exposure to stress and climatic changes worldwide (Attia et al., 2022). Tomato plants are affected by numerous infections caused by many different agents, including fungus, bacteria, viruses, and physiological disorders, responsible for symptoms including fruit spots, rots, wilts, and leaf spots/blights (Jones et al., 2014; Elshafie et al., 2017). *F. oxysporum* f. sp. *lycopersici* (Fol) is a potent fungal pathogen infects tomato crops by penetrating the roots. This pathogen causes yellowing of lower leaves, browning of vascular tissues, and wilting symptoms in tomato seedlings above the soil line with substantial yield losses (Borrero et al., 2012; Li et al., 2018). Moreover, infection of tomato plants is achieved by spore germination or mycelium, leading to higher plant transpiration and lower nutrient translocation, causing wilting crown and root rot and, eventually, death of the plant (Akbar et al., 2018; Manikandan et al., 2018). *Fusarium oxysporum* is a widely distributed and phylogenetically diverse species known as a mycotoxin producer (Irzykowska et al., 2012) and is ranked fifth out of the 10 most lethal (death-causing) plant pathogens. Two main formae speciales are *F. oxysporum* f. sp. *lycopersici* (FOL) and *F. oxysporum* f. sp. *radicis-lycopersici* (FORL) (Ribeiro et al., 2022). FOL is responsible for *Fusarium* wilt, and FORL causes *Fusarium* crown and root rot, among the most studied plant diseases. In Egypt, the damage to tomato crop production due to *F. oxysporum* wilt occurred in 67% of the total planted area (Selim and El-Gammal, 2015). In addition, some fungal species produce mycotoxins (e.g., aflatoxin) on plants which negatively affects the post-harvest treatments and helps to spread the causal agent between the next generation of seeds (Marshall et al., 2020). Thus, various methods, such as chemicals and pesticides, are employed to

control and alleviate plant diseases (Ristaino et al., 2021). However, using fungicides to control *Fusarium* wilt is ineffective because fungal conidia stay viable for a long time, and pesticide residues are harmful to human health (Attia et al., 2022). Therefore, new control strategies must be developed with the aim of economic and environmental sustainability in plant and crop protection (Hernández-Aparicio et al., 2021). Biological control is a desirable alternative method to control the *Fusarium* wilt infection by using antagonistic nonpathogenic microorganisms to minimize the harmful effects in numerous crops (Glick, 2012). Chemical fungicides and soil fumigation have been widely used for controlling FWD disease. *Trichoderma* strains are vital anti-pathogen biocontrol agents (Pal and Gardener, 2006; Contreras-Cornejo et al., 2016; Zhang et al., 2022). This genus is a ubiquitous filamentous fungi that grow in the rhizosphere and colonizes plant roots as an opportunistic, avirulent plant symbiont (Harman, 2006). As *Trichoderma* species is a known aggressive wide range of soil fungal pathogens worldwide to suppress soil fungal diseases and plant pathogen invasion. They are frequently applied as biofungicides against pathogens such as *Botrytis cinerea*, *Fusarium* spp., *Pythium* spp., *Rhizoctonia solani*, and *Sclerotium rolfsii* on crops of economic importance (Mohiddin et al., 2010; Olowe et al., 2022; Sharma et al., 2022). *Trichoderma* fungi indirectly exert their biological control machinery toward fungal pathogens by competition for nutrients and space, antibiosis, production of growth-promoting substances (e.g., IAA, nutrient uptake) (Lei and Zhang, 2015; França et al., 2017) or by secretion of bioactive metabolites, some cell wall-degrading enzymes (CWDEs), such as chitinases and  $\beta$ -1,3-glucanases and mycoparasitism (Elshahawy and El-Mohamedy, 2019; Sallam et al., 2019). Mycoparasitism is the most efficient antifungal mechanism of *Trichoderma* spp. (e.g., *T. virens*, *T. harzianum*) via recognizing the pathogen and growing alongside the pathogen hyphae, then dissolution and death of the pathogen (Benítez et al., 2004; Sharon et al., 2007; Hewedy et al., 2020a,b; Contreras-Cornejo et al., 2021; Taylor et al., 2021; Mukherjee et al., 2022). Various factors such as native environmental habitats, strains, pathogen species, and laboratory findings for testing their antifungal activities affect the *Trichoderma* biocontrol machinery. *Trichoderma asperellum* is a promising strain based on *in vitro* assays against plant fungal phytopathogens. For example, *T. asperellum* GDFS1009 has been shown to suppress *F. oxysporum* f. sp. *cucumerinum* (*Fusarium* wilt of cucumber) and *Fusarium graminearum* infections (Wu et al., 2017; Ketta and Hewedy, 2021), with 98 and 91% inhibition of colony radial growth, respectively, to cope with biotic stresses (Kamaruzzaman et al., 2021). In this context, the discovery of a sustainable solution is the main aim of this study to select and test a potent fungal strain to reduce the negative influence of fungal pathogenicity with the aim of controlling plant disease as well as improving plant growth and plant health to sustain food production. Thus, in this study, we sought to isolate *T. asperellum* from the rhizosphere of garlic (*Allium sativum*), identified using the ITS gene, test the antifungal activities against different fungal pathogens, and focus on the causal agent that causes FWD. Moreover, exploring the antagonistic mechanisms such as chitinase activity and bioactive secondary metabolites, as well as the role of *T. asperellum* for tomato growth promotion (e.g., IAA, P solubilization). Moreover, we present a new trend regarding post-harvest applications using fungal secondary

metabolites against *F. oxysporum* mycotoxins to achieve sustainable food production in an eco-friendly environment. Finally, we used confocal microscopy as a throughput technique to explore the mobility of *Trichoderma* in the tomato roots.

## Materials and methods

### Phytopathogens and antagonistic strain

Five phytopathogenic fungi (*F. oxysporum*, *F. solani*, *F. graminearum*, *Alternaria alternata*, and *Rhizoctonia solani*) were obtained from Agriculture Research Center, Giza, Egypt. *Trichoderma* isolate (Biocontrol agent) was isolated from the garlic (*Allium sativum*) rhizosphere soil by serial dilution method. Briefly, the rhizospheric soil sample (10 g) was suspended in 90 mL of sterile distilled water, and the mixture was shaken at (200 rpm) for 30 min. Next, the soil suspension was serially diluted up to ( $10^{-3}$ ) dilution, then 100  $\mu$ L was spread on Potato Dextrose Agar (PDA) plates supplemented with chloramphenicol (50 mg/L) and streptomycin (15 mg/L) to suppress bacterial growth (Woldeamanuale, 2017). Subsequently, the inoculated plates were incubated at 28°C for 5–7 days. At the end of the incubation period, the fungal isolate was purified, kept on slants at 4°C, and subcultured every 4 weeks (López Errasquín and Vázquez, 2003). The pure culture of the fungal isolate was characterized using morphological and microscopical characteristics (Harman and Kubicek, 2002) and confirmed by molecular identification.

### Molecular identification

Genomic DNA was extracted with the QIAamp DNeasy Plant Mini kit according to the manufacturer's instructions. Amplification of the fungal ITS region was carried out with forward ITS1 (5' TCC-GTA-GGT-GAA-CCT-GCG-G 3') and reverse ITS4 (5' TCC-TCC-GCT-TAT-TGA-TAT-GC 3') primers (White et al., 1990). The polymerase chain reaction program was performed as previously described (Hewedy et al., 2020c). The homology of the ITS rDNA sequence of the isolate was analyzed using the BLAST program from the GenBank database.<sup>1</sup>

### *In vitro* antagonistic activity of *Trichoderma asperellum* against phytopathogenic fungi

The antagonistic activity of *T. asperellum* against fungal pathogens was evaluated by dual culture assay (Awad et al., 2018). One mycelial disk of the pathogen (6 mm diameter) was deposited on one side of the Petri plate, and another disk of (antagonist) was deposited equidistantly on the other side. PDA plates containing only disks from the pathogen mycelium were used as controls. All the experiments were conducted in triplicates. After 7 days of incubation at 28°C, the radial growth of the phytopathogens in the control and treatment

plates was measured, and the percentage of inhibition of radial mycelial growth (PIRG) was calculated using the following equation:

$$\%PIRG = R1 - R2 / R1 \times 100$$

where R1 = radial growth of the phytopathogen in the control plate; R2 = radial growth in the presence of an antagonist (Fishal et al., 2022).

### Effect of *Trichoderma asperellum* culture filtrates on *Fusarium oxysporum*

Based on the dual culture assay results, the maximum growth inhibition was recorded against *F. oxysporum*. Thus, different concentrations of the culture of *T. asperellum* filtrate were tested against *F. oxysporum*. *T. asperellum* was inoculated in 50 mL of potato dextrose broth and incubated at 28°C for 14 days on a rotary shaker at 150 rpm. Cell-free supernatant was obtained by filtration through Whatman filter paper No. 1. The filtrate was sterilized using a 0.2  $\mu$ m pore biological membrane filter (Jangir et al., 2019). Each sterilized filtrate was mixed into a PDA medium to obtain 5, 15, and 30% (v/v). Finally, 20 mL of the medium was amended with different filtrate concentrations and poured into 90 mm Petri plates. The secondary metabolites in the filtrate were tested for their efficacy against the test pathogens. The test pathogen was centrally inoculated with an individual equal disk (5 mm) of seven-day-old culture. PDA plates inoculated with pathogens without culture filtrates served as a control. Three replicates were maintained for each treatment and incubated at 28°C. The percentage inhibition of mycelial growth was calculated as mentioned above.

### Scanning electron microscopy

The confrontation of hyphal interaction between *F. oxysporum* and *T. asperellum* was also examined by SEM. Briefly, a mycelial disk (5 mm) of both microbes was cultured on PDA for 4–5 days of incubation. The plate cultures were examined under a light microscope to check the early touch stage. The contact interactions were labeled, and 1 cm agar blocks were removed for SEM preparation, fixed with osmium tetroxide, and then dehydrated using a serial dilution of the ethyl alcohol and acetone. A critical point drier (Tousimis Autosamdri-815 Coater) was then used to dry the processed samples with gold using a sputter coater. Then, the mycoparasitism and the hyphae interactions were examined by SEM (JEOL JSM 6510 Iv). The microscope was operated at 30 KV at EM Unit, Mansoura University, Egypt. Three replicates were included for each sample (Su et al., 2010).

### Assessment of plant growth-promoting and antifungal properties of *Trichoderma asperellum*

#### Indole-3- acetic acid

*Trichoderma asperellum* was grown on potato dextrose broth (PDB) supplemented with L-Tryptophan (0.1 g/L) for 4–5 days at

<sup>1</sup> <http://www.ncbi.nlm.gov/BLAST/>

$28 \pm 2^\circ\text{C}$  on a rotary shaker at 150 rpm (Nandini et al., 2021). Next, both mycelium and debris were separated by filtration and centrifugation, respectively. Briefly, 1 mL of the culture filtrate and 4 mL of Salkowski reagent (1 mL of 0.5 M ferric chloride in 50 mL of 35% perchloric acid) were mixed and kept for 30 min in the dark for color change. The generation of pink indicated the production of IAA. The optical density was detected and measured at 530 nm using a spectrophotometer (JENWAY 6315). A standard curve of IAA concentrations was designed to evaluate the corresponding concentration of IAA-released *T. asperellum* in the bioassay media.

### Phosphate solubilization efficacy of *Trichoderma asperellum*

A plug of *T. asperellum* (5 mm) was grown on a modified NBRIP medium (Nautiyal, 1999) supplemented by Bromophenol blue as an indicator for 7 days at  $28^\circ\text{C}$ . The medium contained the following composition ( $\text{g L}^{-1}$ : 10.0 glucose),  $0.5\text{MgCl}_2 \cdot 6\text{H}_2\text{O}$ ,  $0.25\text{MgSO}_4 \cdot 7\text{H}_2\text{O}$ ,  $0.2\text{KCl}$ ,  $0.1(\text{NH}_4)_2\text{SO}_4$  and 15.0 agar, with the addition of 50 mL of  $\text{K}_2\text{HPO}_4$  (10% w/v) and 100 mL of  $\text{CaCl}_2$  (10% w/v) to precipitate insoluble calcium phosphate ( $\text{CaHPO}_4$ ). The pH of the medium was adjusted to 7.0. After incubation, a yellow halo zone around the fungal colony indicated phosphate solubilizing ability. The solubilization zone and colony diameters were measured and calculated using the equation below to indicate the solubilization efficiency (Pande et al., 2017; Aloisio et al., 2019).

$$\text{SE} = (\text{Solubilization diameter}) / (\text{Growth diameter}) \times 100.$$

### Chitinase activity of *Trichoderma asperellum*

Chitinase detection medium with ingredients/per liter: 0.3 g of  $\text{MgSO}_4 \cdot 7\text{H}_2\text{O}$ , 3.0 g  $(\text{NH}_4)_2\text{SO}_4$ , 2.0 g of  $\text{KH}_2\text{PO}_4$ , 1.0 g of citric acid monohydrate, 15 g of agar, 200  $\mu\text{L}$  of Tween-80, 4.5 g of colloidal chitin and 0.15 g of bromocresol purple pH (4.7), was prepared and autoclaved at  $121^\circ\text{C}$  for 15 min. Then, the plates were inoculated with a fresh culture plug of *T. asperellum*, incubated at  $25 \pm 2^\circ\text{C}$  for 7 days, and were observed for colored zone formation (Agrawal and Kotasthane, 2012).

## *Trichoderma asperellum* promotes tomato plant growth

### Inoculum preparation

Seven-day-old pure culture of *T. asperellum* was used. After cultivation on PDA slants and incubation at  $28^\circ\text{C}$ , sterile water was poured into the slants, and the spores were scraped with a sterile glass rod. The spore suspension was filtered and put into tubes, and the spore concentration of *T. asperellum* was adjusted at  $1 \times 10^6$  spore/mL (Scudeletti et al., 2021; Natsopoulos et al., 2022).

### Effect of *Trichoderma asperellum* on tomato seeds germination and growth promotion

Tomato seeds of (Hybrid Madera F1) were used in all experiments. The tomato seeds were surface sterilized with 2.5% (v/v) sodium hypochlorite for 10 min and rinsed three times with distilled water before seed inoculation. Afterward, the seeds were immersed for 24 h in fungal suspensions prepared at  $1.0 \times 10^6$  spore  $\text{mL}^{-1}$ . The control treatment consisted of seeds immersed only in sterile distilled

water for the same period. The seeds were deposited in Petri dishes containing autoclaved tissue papers moistened with sterile water (16 seeds per dish) that were sealed with parafilm to prevent evaporation and then incubated at  $28^\circ\text{C}$  for 7 days (Kipngeno et al., 2015; Barroso et al., 2019). Each treatment was replicated three times. The germination rate (%) was estimated by counting the number of seeds germinating after one week of cultivation.

Three sterilized tomato seeds were transferred to one side of the plate prepared with water agar containing 0.2% (w/v) glucose (Yoo et al., 2018). The other side contained a *T. asperellum* disk (5 mm) grown on PDA. Plates without inoculum were considered a control, and the plates were incubated for 3–4 days in darkness at  $28^\circ\text{C}$ . After the incubation period, the germination percentage (GP) was evaluated according to the following equation:

$$\text{GP} (\%) = n / N \times 100$$

where:  $n$  = number of germinated seeds;  $N$  = total number of seeds.

Next, treated and untreated (control) seeds were sown in pots (8 cm) in diameter containing a mixture of sterilized peat moss and soil (1:2 w/w) at 28 g/pot, with a density of five seeds per pot. Pots were maintained under controlled conditions in the growth chamber ( $22 \pm 3^\circ\text{C}$ ). Experiments were performed using a completely randomized design (CRD) with two treatments and three replicates. The pots were rotated three times a week to ensure uniform growth conditions in the growth chamber. After 21 days, plant samples were taken to measure the shoot height (cm), the root length (cm), and plant biomass. The seedling vigor index (VI) was calculated as described by Buriro et al. (2011).

$$\text{Seedling vigor index} = [\text{seedling length (cm)} \times \text{GP} (\%)]$$

### Confocal microscopic assay

The interaction between *T. asperellum* strain and the tomato-root system during the early stages of root colonization was examined by confocal microscopy. SYTOX Green (Thermo Fisher Scientific-United States) was used for *Trichoderma* staining. Briefly, tomato roots were carefully removed from the sterilized soil and gently swirled 4–5 times in autoclaved water to wash the clay particles. Then, the primary root was stained using  $10 \mu\text{M}$  propidium iodide (PI) for 10 min to label the plant cell wall and washed by  $\text{ddH}_2\text{O}$  4–5 times. Subsequently, the root was placed on a glass slide to facilitate the visualization of the localization of *T. asperellum* (green) in the tomato root (red) surface as a plant growth promoter (Chacón et al., 2007).

### Estimation of the biocontrol efficiency of *Trichoderma asperellum* against *Fusarium* wilt disease

Sterilized tomato seeds were sown in pots (8 cm) in diameter containing 28 g of sterilized peat moss and soil (1:2, w/w). Each pot contains five seeds, and the experiment included four treatments as follows:

1. Control (distilled water) only.
2. Pathogen (*F. oxysporum*) only.



3. Bioagent (*T. asperellum*) only.
4. *Trichoderma* + *Fusarium*.

Tomato plants were inoculated and kept at 25°C for 21 days, and the parameters of plant phenotype were measured, including the root length, shoot, and fresh weight. The shoots and the roots were dried in an oven at 70°C until constant weight (Mwangi et al., 2011).

### Tomato root anatomy under biotic stress

The roots of tomato plants were sectioned and studied anatomically. The wax method was used in this experiment (Johansen, 1940). Briefly, plant roots were fixed for 72 h using FAA (formalin: acetic acid: alcohol 90:5:5) fixative. Then, roots were washed several times using distilled water and dehydrated using serial concentrations of alcohol 50, 70, 90, 95, and 100% (v/v), respectively. For clearing, they were transferred every 3 h from a mixture of 1:1 cedarwood oil: and absolute alcohol into pure cedarwood oil, followed by a mixture of cedarwood oil and xylene, and left overnight in pure xylene. Wax embedding was carried out in an oven adjusted at 60°C, embedded in clear wax, and sectioned using a rotatory microtome. Staining was done using safranin and fast green stains. Sections were mounted in a drop of Canada balsam, covered, and left to dry. The prepared slides of each root treatment were repeatedly examined under the light microscope (LEICA DM750) at the Microscopy Department, Faculty of Agriculture, Cairo University.

## *Trichoderma asperellum* protects tomato fruits against FWD

### Preparation of *Trichoderma asperellum* crude extract

Bioactive secondary metabolites of *T. asperellum* were extracted using ethyl acetate solvent, as previously described by Chen et al. (2018). *Trichoderma* was grown in a PDB medium and incubated on a rotary shaker (150 rpm) for 21 days at 28°C. After the incubation period, the fermented broth was filtered through Whatman filter paper No. 1, and the metabolites produced by the fungus were extracted from an equal volume of ethyl acetate. An equal volume of ethyl acetate was added to the filtrate and vigorously shaken for 5 min at room temperature. The mixtures were transferred to separating funnels, and the organic layers of ethyl acetate were allowed to separate from the aqueous layers. Then, the ethyl acetate layer was allowed to dry at room temperature, and the dried extracts were stored at 4°C for further use.

### Assessment of extracted secondary metabolites against mycotoxigenic *Fusarium oxysporum* in tomato fruits

The antifungal activity of the *T. asperellum* extract was evaluated against *Fusarium* on tomato fruits, which were obtained from the supermarket, were initially washed under running water, sterilized for 2 min in 2% (v/v) sodium hypochlorite, and then rinsed with sterile water. Watery fruits were placed in plastic trays (sterilized with 70% (v/v) ethanol and under UV) and dried for 2 h under a laminar flow cabinet. The fruits were wounded with a

sterile needle, and 20 µl of the pathogen spore suspension at 10<sup>4</sup> spores/mL was inoculated onto the wound. Subsequently, the drop was dried for 1 h. Finally, tomato fruits were treated with 20 µl of *Trichoderma* crude extract in the same wound where the pathogen inoculum had been applied. The treated tomato fruits were dried under a laminar flow cabinet until the droplet was completely dry, and the closed trays were incubated at room temperature (Stracquadanio et al., 2021; Maliehe et al., 2022). The untreated positive control was inoculated with the spore suspension of the pathogen, and the negative control was inoculated with *Trichoderma* extract. Fruits were monitored daily, and results were evaluated on the 11th day of incubation. The diameter of the lesions was also observed.

### Mycotoxin analysis

Two grams of ground tomato fruits were mixed with 8 mL (80 acetonitrile (ACN): 20 H<sub>2</sub>O) and shaken for 20 min. Then, the mixture was centrifuged at 3500 rpm for 10 min and filtered through a 0.45 µm nylon filter. After filtration, the extract was diluted (1:4) with water containing 5 mM ammonium acetate. Analysis of mycotoxins (FB1, FB2, DON, and ZEN) was performed using liquid chromatography-electrospray ionization-tandem mass spectrometry (LC-ESI-MS/MS) with an ExionLC AC system for separation and SCIEX Triple Quad 5,500+ MS/MS system equipped with electrospray ionization (ESI) for detection. The instrument data were collected and processed using the SCIEX OS 1.6.10.40973 software. The targeted analytes were separated with an Agilent Zorbax Eclipse Plus C18 Column (4.6 × 100 mm, 1.8 µm) (Waskiewicz et al., 2010). The mobile phases consisted of two eluents containing 10 mM ammonium formate, eluent A was 0.1% (v/v) formic acid in the water, and eluent B was 0.1% (v/v) formic acid in methanol (LC grade). The mobile phase gradient was programmed as follows: 10% B at 0 min, 10–30% B from 0.0–2.0 min, 30–100% B from 2.0–11.0 min, 100% B from 11.0–11.5 min, 100–10% B from 11.5–12.0 min, 10% B from 12.0 to 15.0 min. The flow rate was 0.6 mL/min, and the injection volume was 10 µl. For MS/MS analysis, positive ionization mode (+MRM) was applied with the following parameters: curtain gas: 20 psi; collision gas: 9 psi; nebulizer current: 3; source temperature: 600°C; ion source gas 1 (nebulizer gas): 60 psi.

### GC–MS analysis

The chemical composition of *T. asperellum* crude extract was assessed to detect the active constituents exhibiting antifungal activity. GC–MS was performed using a Trace GC1310-ISQ mass spectrometer (Thermo Scientific, Austin, TX, United States) with a direct capillary column TG–5MS (30 m × 0.25 mm × 0.25 µm film thickness). The column oven temperature was initially held at 50°C and then increased by 5°C/min to 230°C for 2 min, then increased to the final temperature of 290°C by 30°C/min and held for 2 min. The injector and MS, transfer line temperatures, were kept at 250°C and 260°C; Helium was used as a carrier gas at a 1 mL/min constant flow rate. The solvent delay was 3 min, and diluted samples of 1 µl were injected automatically using Autosampler AS1300 coupled with GC in the split mode. In full scan mode, EI/MS were collected at 70 eV ionization voltages over m/z 40–1,000. The ion source temperature was set at 200°C, and the components were identified by comparing their retention times and mass spectra with those of



the WILEY 09 and NIST 11 mass spectral databases (Mulatu et al., 2022).

### Statistical analysis

Analysis of variance (ANOVA) was assessed using IBM SPSS Statistics Version 28. The experiments were conducted using a completely randomized design with three replicates. The growth of the fungal strains was compared by t-test, and their biocontrol activities were evaluated by Fisher's least significant difference (LSD) test at the 5% significance level.

## Results

### Isolation, morphological and molecular identification

*Trichoderma asperellum* was isolated from garlic rhizosphere soil by plate dilution, and the pure culture was maintained on a Potato dextrose agar (PDA) medium. Macroscopic morphology of *T. asperellum* revealed the rapid growth of the colony (3–4) days with 1–2 concentric rings. The mycelium, initially of a white color, acquired green and yellow shades or remained white due to the abundant production of conidia (Figure 1A). Regarding microscopic observations, *T. asperellum* showed globous, subglobous, or ovoid conidia, ampuliform phialides, and branched conidiophores, as shown in Figures 1B,C. The identification of the fungal isolate was further confirmed by analysis of the ITS sequence. One band of 531 bp was amplified using ITS primers, and the sequence alignments were performed using the Basic Local Alignment Search Tool (BLAST) to determine the phylogenetic positions of our strain with other *Trichoderma* strains on the GenBank. The fungal strain had (100%) matched identify with *T. asperellum* (Figure 1D). Moreover, the ITS sequence of *T. asperellum* was submitted to GenBank under the accession number (OQ130157).

### Evaluation of the antagonistic activity of *Trichoderma asperellum* against phytopathogens

*Trichoderma asperellum* was tested against several plant pathogenic fungi (*F. oxysporum*, *F. solani*, *F. graminearum*, *A. alternata*, and *R. solani*) to assess the antifungal activity using dual culture assay. Results showed that *T. asperellum* could inhibit the radial mycelial growth of all tested pathogens. The maximum growth rate inhibition (53.23%) was recorded against *F. oxysporum* followed by *F. graminearum* (45%), *F. solani* (43.19%), and *R. solani* (30.89%). In contrast, the lowest inhibitory activity percentage was exhibited against *A. alternata* (20.67%) (Table 1; Figure 2A). Based on the dual culture assay results, the highest growth rate inhibition was displayed against *F. oxysporum*. Therefore, different concentrations of sterilized culture filtrate of *T. asperellum* were tested against *F. oxysporum* to evaluate the optimum inhibiting concentration. Results showed that the inhibitory activity increased by increasing the sterilized culture filtrate concentration, and the maximum inhibitory activity

percentage (59.38%) was observed at a concentration of 30% (Table 2; Figure 2B).

### Scanning electron microscopy

The mycoparasitic nature of *T. asperellum* on *F. oxysporum* as a dual culture was examined by SEM (Figure 3). Interestingly, *T. asperellum* hyphae grew over the hyphae of *F. oxysporum*, followed by quick and excessive coiling. Finally, *F. oxysporum* lysis was eventually observed (Figures 3D–F).

### Plant growth-promoting and antifungal properties of *Trichoderma asperellum*

To assess the growth-promoting effects of *T. asperellum* on plant development, the plant growth hormone IAA was measured using a colorimetric assay. Results showed that the amount of IAA produced by *T. asperellum* was ( $12.5 \pm 0.5742 \mu\text{g mL}^{-1}$ ). Moreover, *T. asperellum* could solubilize phosphate, exhibiting phosphorus solubilization indices of 100% (Figures 4E,F). Additionally, *T. asperellum* showed high chitinase activity in a colloidal chitin medium supplemented with bromocresol purple (with final acidic pH of 4.7). *Trichoderma*, breakdown chitin to N- acetyl glucosamine shifting pH toward the alkalinity, which changes the medium color to purple (Figures 4B,C).

### Effect of *Trichoderma asperellum* on tomato seeds germination and growth promotion

Data illustrated in Figure 5; Supplementary Figure S1 indicated that *T. asperellum* treatment enhanced seed germination, root and shoot length, and vigor index in tomato seedlings. After 7 days, seeds treated with spore suspension of *T. asperellum* ( $10^6$  spore mL<sup>-1</sup>) resulted in the highest seed germination rates (100%), as compared to the control (81.25%). Also, it can be seen that in the presence of *T. asperellum* grown on PDA in split interaction, the germination rate of seeds was enhanced (100%) as compared to an un-inoculated plate (66.6%) as presented in Figures 5C,D. In addition, *T. asperellum* inoculation promoted tomato growth parameters (Figures 5E,F). We observed that the Average shoot length of plants inoculated with *T. asperellum* simultaneously was 14.5% longer than the control. The average root length was also 17.6% longer than the control treatment (Figures 5G,H).

### Confocal microscopy

The capacity of the fungus *T. asperellum* to colonize tomato roots and stimulate plant growth was observed using a confocal imaging assay. Sterilized tomato seeds were inoculated with *Trichoderma* spores before germination on Petri dishes (150 mm) and kept in the dark for 3 days to study the early stages of the fungal root colonization. Interestingly, the root elongation of tomato seedlings and intercellular hyphal growth were observed compared with the uninoculated treatment (control) (Figures 5I,J). To obtain more insight, an *in vitro*

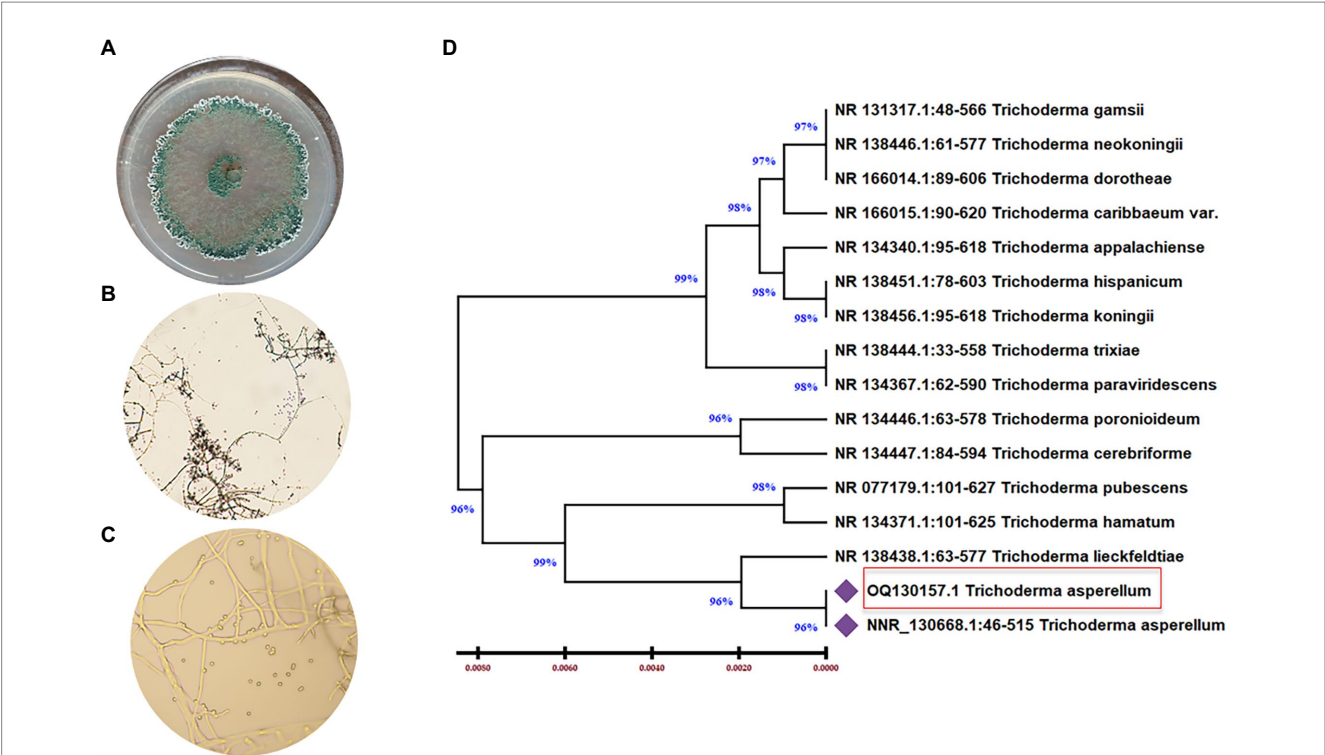


**FIGURE 1** Morphological and molecular identification of *T. asperellum*. **(A)** The cultural view of *T. asperellum* grown on synthetic nutrient agar (SNA) media at 28°C for five days, which shows a ring around the original inoculum, **(B,C)** Microscopic view of conidia and conidiophores. **(D)** Molecular phylogenetic based on rDNA internal transcribed spacers (ITS) analyzes of *T. asperellum* by maximum Likelihood Model of MEGA11.0. The evolutionary distances were computed using the Maximum Composite Likelihood method and are in the units of the number of base substitutions per site. The proportion of sites where at least 1 unambiguous base is present in at least 1 sequence for each descendent clade is shown next to each internal node in the tree. This analysis involved 16 nucleotide sequences. All ambiguous positions were removed for each sequence pair (pairwise deletion option). The percentage of replicate trees in which the associated taxa clustered together in the bootstrap test (500 replicates) are shown next to the branches. The tree is drawn to scale, with branch lengths in the same units as those of the evolutionary distances used to infer the phylogenetic tree.

**TABLE 1** Antagonistic activity of *T. asperellum* against some phytopathogenic fungi.

| Bioagent             | Phytopathogenic fungi |          |                  |          |                       |          |                     |          |                  |          |
|----------------------|-----------------------|----------|------------------|----------|-----------------------|----------|---------------------|----------|------------------|----------|
|                      | <i>F. oxysporum</i>   |          | <i>F. solani</i> |          | <i>F. graminearum</i> |          | <i>A. alternata</i> |          | <i>R. solani</i> |          |
|                      | RMG (cm)              | PIRG (%) | RMG (cm)         | PIRG (%) | RMG (cm)              | PIRG (%) | RMG (cm)            | PIRG (%) | RMG (cm)         | PIRG (%) |
| Control              | 6.43 ± 0.03           | 0.00     | 5.63 ± 0.15      | 0.00     | 6.00 ± 0.05           | 0.00     | 4.16 ± 0.03         | 0.00     | 7.18 ± 0.11      | 0.00     |
| <i>T. asperellum</i> | 3.01 ± 0.04           | 53.23    | 3.20 ± 0.17      | 43.19    | 3.30 ± 0.11           | 45       | 3.30 ± 0.05         | 20.67    | 4.96 ± 0.12      | 30.89    |

RMG, Radial Mycelial growth; PIRG, Percent inhibition of Radial Mycelial growth; ± SE.

experiment was carried out to study the effect of a biocontrol agent at the initial stage of root colonization by *T. asperellum* to understand its influence on tomato growth promotion. After inoculation, tomato roots were covered with conidia. Initial contact between conidia and the root was primarily at the region of root hairs.

Effect of *Trichoderma asperellum* on the growth of tomato plants under biotic stress of *Fusarium oxysporum*

There was a notable variation between the tomato plants inoculated with *Trichoderma* and *Fusarium* individually, as shown in Figure 6A. Data presented in Figures 5K,L showed that *T. asperellum*

improved the growth of tomato plants under *Fusarium* infection. In addition, Figures 6B–D showed a significant increase in the root length and the fresh weights of shoots between the control (untreated) and the inoculated tomato plants with *Trichoderma* under biotic stress. The inhibitory effects of *Trichoderma* inoculation against *Fusarium* invasion were demonstrated in Figure 6A. *Fusarium* pathogen invaded the root system and significantly decreased roots and shoot dry weights, the number of leaves, and root length. In addition, there was a marked increase in the root length and shoot fresh weight during the *Trichoderma*-*Fusarium* interactions (Figures 6C–D). *T. asperellum* controlled the FWD caused by *F. oxysporum* by enhancing the plant phenotypes, including shoot and root length (cm), shoot and fresh root weight (g), shoot and root dry weight (g), as well as the number of leaves. It can be seen that number

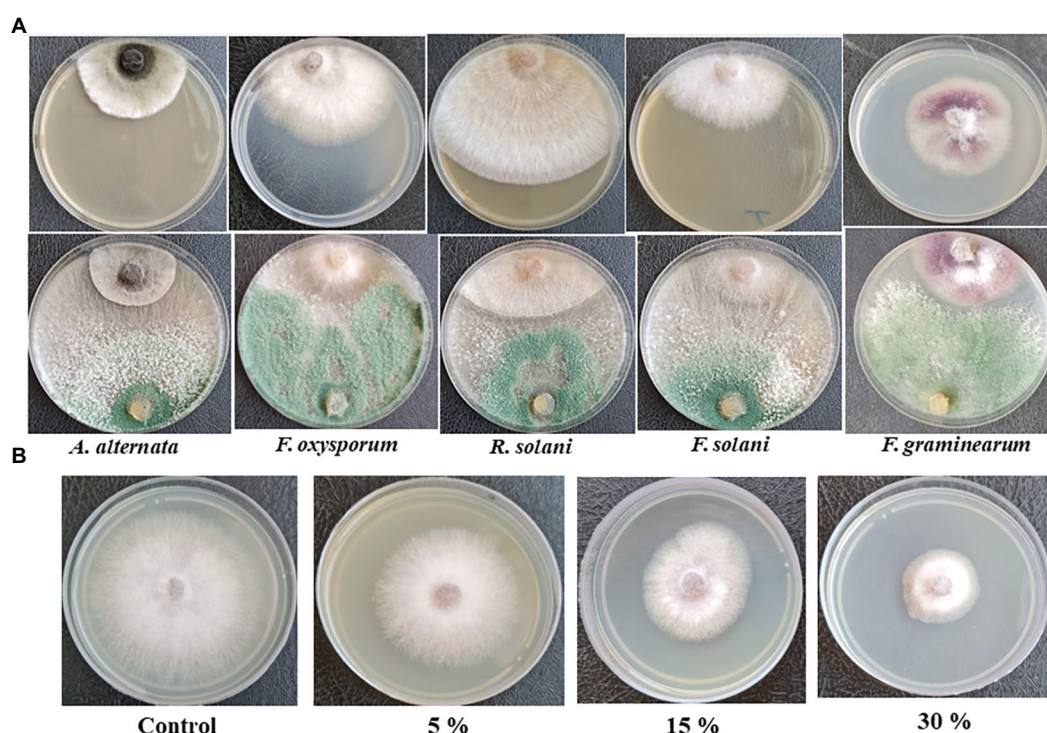


FIGURE 2

(A) Antagonistic activity of *T. asperellum* against plant pathogenic fungi in dual culture assay, (B) Effect of different concentrations of *T. asperellum* filtrate on *F. oxysporum* growth.

TABLE 2 Effect of different concentrations of *T. asperellum* culture filtrate against *F. oxysporum*.

| Culture filtrate concentrations (%) | <i>F. oxysporum</i> (RMG) (cm) | PIRG (%) |
|-------------------------------------|--------------------------------|----------|
| Control                             | 7.63 ± 0.03                    | 0.0      |
| 5                                   | 5.34 ± 0.08                    | 30       |
| 15                                  | 4.65 ± 0.02                    | 39.03    |
| 30                                  | 3.10 ± 0.05                    | 59.38    |

RMG, Radial Mycelial growth; PIRG, Percent inhibition of Radial Mycelial growth; ± SE.

of leaves in plants inoculated with *Trichoderma* was (45%) higher than the number of leaves in the treated plants with *Fusarium* alone.

## Root anatomy

Transverse sections of tomato roots treated with *T. asperellum* and the interactions between bioagent and the fungal pathogen were studied to evaluate their impact on root health. Interestingly, the inoculation of tomato roots with *Trichoderma* increased whole root thickness and the number of xylem vessels compared to the control (Figures 7A,D,G). The highest degradation area of the root cortex was observed in plants infested with *F. oxysporum*. Lateral root (LR) development was also detected in the treated tomato roots with *T. asperellum* (Figure 7F). However, the combination of *T. asperellum* and *F. oxysporum* enhanced the root thickness in the cortex of the tomato tap root (Figure 7I). Light microscope sections showed that *Trichoderma* enhanced the cortex and xylem diameters. It was also

noted that the xylem and the endodermis diameters were thinner in control roots than in other treatments; this trend was the same in both hybrids (Figures 7C,E,I).

## Biocontrol efficiency on tomato fruits against FWD

The disease control efficacy of *T. asperellum* against *F. oxysporum* is shown in Figures 8A–C. After 11 days of storage, tomato fruits inoculated with *F. oxysporum* and treated with *T. asperellum* extract showed an increase in shelf-life compared with the untreated control (*Fusarium* only). Moreover, tomato fruits inoculated with *Trichoderma* metabolites showed a significant reduction in lesion diameter compared to the pathogen-treated fruits (Figure 8). Results indicated that *T. asperellum* exhibited a significant inhibitory effect against *F. oxysporum*. In addition, the mycotoxins typically produced by *Fusarium* species (FB1, FB2, ZEN, and DON) were not detected by LC–MS/MS analysis, even in the untreated controls.

## GC–MS analysis

The GC–MS analysis of the ethyl acetate extract of *T. asperellum* revealed the presence of different bioactive compounds (Figure 8D). The compound name, molecular formula (MF), molecular weight (MW), concentration (peak area %), and retention time (RT) are present in Table 3. Interestingly, the most predominant compounds were 1,2-Benzenedicarboxylic acids (32.15%), Palmitic Acid, TMS



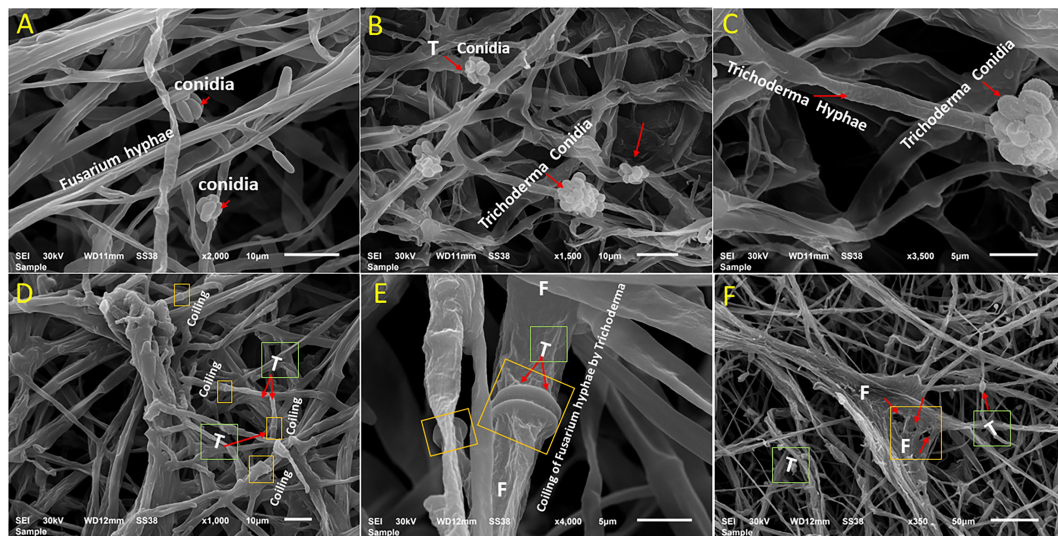


FIGURE 3

Scanning electron microscopy interpretations of the mycoparasitic of *T. asperellum* on *F. oxysporum*. (A) *Fusarium* pathogen alone, (B,C) *T. asperellum* alone (endophytic hyphae and conidia), (D) Mycelium of both fungi in contact via growing of *Trichoderma* hyphae (T) over *Fusarium* hyphae, (E) Coiling of *Fusarium* hyphae (F) by *Trichoderma* (T) as one of the antagonistic mechanisms (arrows), (F) Deformation of *F. oxysporum* by *T. asperellum*.

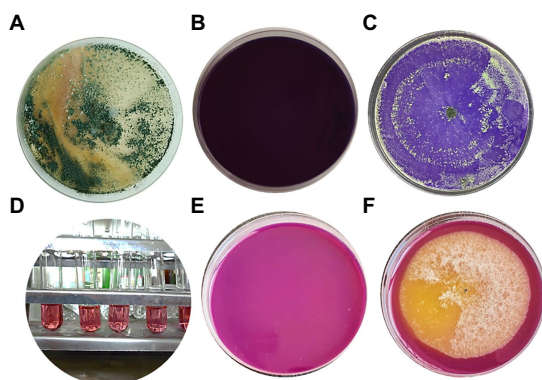


FIGURE 4

(A) *Trichoderma asperellum* strain grown on PDA at 28°C for seven days. (B,C) Screening of *T. asperellum* for chitinase activity on medium supplemented with colloidal chitin and control without inoculum. (D) IAA production by *T. asperellum* (5 replicates). (E,F) Phosphate solubilization of *T. asperellum* on NBRIP media supplemented with bromophenol blue as an indicator. (E) Uninoculated (control), (F) inoculated with *T. asperellum*.

derivative (17.05%), D-Glucopyranose, 5TMS derivative(7.04%), Myo-Inositol, 6TMS derivative(4.55%), Oleic Acid, (Z)-, TMS derivative (2.82%), 9,12,15-OCTADECATRIENOIC ACID, 2-[(TRIMETHYLSILYL) OXY]-1-[[[(TRIMETHYLSILYL) OXY] MET HYL]ETHYL ESTER, (Z, Z, Z)-(1.35%), 4H-1-Benzopyran-4-one,2-(3,4-Dihydroxyphenyl)-6,8-DI- $\alpha$ -D-Glucopyranosyl-5, 7-Dihydroxy (1.35%) and Stearic acid, TMS derivative (0.82%).

## Discussion

Various antagonistic activities were studied against different fungal pathogens using *T. asperellum*, as shown in Figure 3. This was sufficient

evidence to conclude that the *Trichoderma* strain could be a bio-control agent and stimulate plant health via secondary metabolites and hormone production. In addition, this strain has the capability to sustain beneficial interaction with the host plant under stressful biotic conditions. Several *Trichoderma* isolates have been reported to suppress FWD (Srivastava et al., 2010; Marzano et al., 2013). *Trichoderma* species also have the potential of antagonistic interactions with different plant pathogens, which determines the biocontrol efficiency of the fungal pathogens. Mycoparasitism, antibiosis, competition for nutrients, and induced systemic resistance in plants are diverse antifungal activities of *Trichoderma* spp. (Druzhinina et al., 2011; Modrzewska et al., 2022). Therefore, these studies showed the successful application of *Trichoderma* in the field, which could impair plant health and productivity and suppress the *Fusarium* wilt disease. Additionally, this study investigated the contribution of *T. asperellum* to P solubilization and IAA production. Experiments were conducted in duplicate to investigate the ability of *Trichoderma* to promote plant growth. *Trichoderma* produced a clear halo around its colonies, which solubilized soluble P in vitro. Interestingly, *T. asperellum* released an auxin-like phytohormone that significantly increased the total root length of tomato plants. Since the tomato is one of the most produced crop plants growing in fields and greenhouses worldwide, this study evaluated the mechanism by which *Trichoderma* assisted tomato roots in response to *Fusarium* infection during plant growth. Plant roots exploit morphological plasticity to adapt and respond to different soil environments (Alaguero-Cordovilla et al., 2018). However, most of the investigated *Trichoderma* species colonize the root surface or inhabit inside root tissues as endophytes (Bailey et al., 2006). *Trichoderma* application with tomato seedlings shows adequate protection against *F. oxysporum*. Interestingly, the *T. asperellum* also benefitted plant growth promotion via root elongation during the pathogen attacks (Figure 5G). This is consistent with the dual cultural assay data between the biological agents and the pathogen infection, which decreased the hyphal growth. The results showed that the highest growth rate inhibition was displayed against *F. oxysporum*, causing FWD.



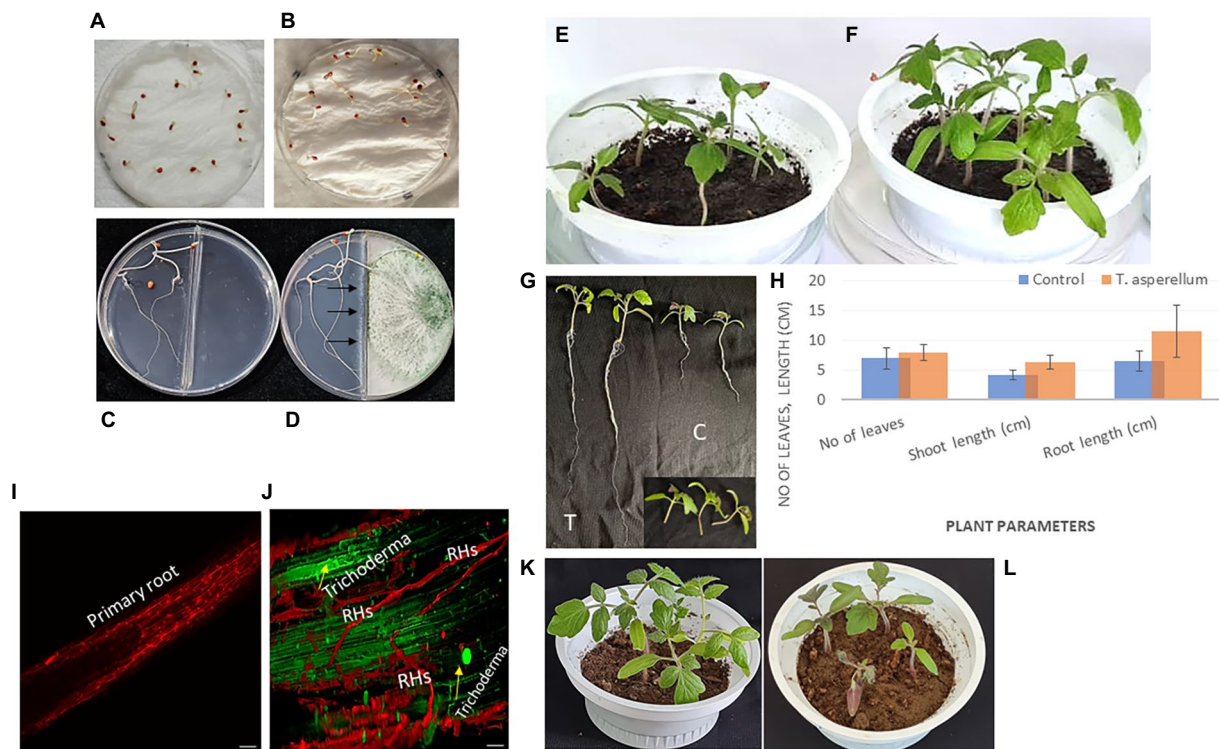


FIGURE 5

*Trichoderma asperellum* colonizes a tomato plant's root system and promotes root elongation. (A) Seeds treated with distilled water. (B) Seeds treated with a spore suspension of *T. asperellum*. (C) Split interaction of seeds growing on water agar medium without *Trichoderma* treatment (control). (D) Split interaction with *Trichoderma* treatment. (E,F) Tomato plants are grown in the presence of *Trichoderma* after seed coating (pot at right) and without microbial inoculation (control only) (pot at left). (G) Promotion of root and shoot length via *Trichoderma* inoculation (T) compared to untreated plants (C). (H) Plant parameters include the number of leaves, shoot length, and root length with *Trichoderma* inoculation and control treatment. *In vivo* tests indicated the growth-promoting potential of this fungal endophyte. *Trichoderma* could boost plant growth by activating either an individual or numerous mechanisms. (I,J) Representative confocal laser scanning microscopical analysis illustrating the early and robust colonization of tomato roots/root hairs (RHs) by *T. asperellum* compared with the control (without microbial inoculation) using CLSM with a Leica TCS SP2. (K,L) Tomato plants are grown in the presence of *T. asperellum* after three weeks from seed coating (pot at left) and plants infected with *Fusarium* (pot at right).

A precise *in vitro* experimental design was established to explore the impact of *Trichoderma* inoculation on the tomato root system during early growth (Figure 5D). Our results revealed that the biocontrol agent led to observed differences during early growth. The treatments were categorized into tomato roots with no microbial inoculation (control) and root inoculation with *Trichoderma*. The effect of *Trichoderma* strain on plant growth under abiotic stress was initially evaluated by measuring the root and shoot length and the number of leaves. In addition, the fungal inoculation significantly increased the plant parameters compared to untreated plants (control), as shown in Figure 5H. In that context, some studies have revealed that the inoculation of *T. harzianum* SQR-T037 improved the growth of tomato plants under greenhouse and field conditions (Cai et al., 2013, 2015).

The root system is essential for plant growth because of its basic functions in the selective absorption of water and nutrients (Karthika et al., 2018; Das et al., 2022), storage organ, and a selective barrier against pathogens (Wiedemeier et al., 2002; Atkinson et al., 2014). Characterization of root morphology and cellular development of two tomato species, *S. pennellii* and *S. lycopersicum* 'M82' during early growth were studied by Ron et al. (2013). This study provided significant differences in an extensive range of root traits with

developmental significance. In addition, the newly emerged lateral roots (LRs) were significantly correlated with *Trichoderma* inoculation in tomato plants (Figure 7F). In addition, *Trichoderma* (green) colonized tomato roots (red), which visualized its mobility by the confocal imaging microscope (Figure 5J). It is well known that *Trichoderma* strains are able to colonize plant roots and stimulate the growth via the production of phytohormones, thus playing a crucial role in regulating the plant root system (Benítez et al., 2004; Harman et al., 2004; Cai et al., 2013). These findings agreed with our observations which suggested that improving plant growth occurs through a direct effect of *Trichoderma* species on root development.

Furthermore, *Trichoderma* can regulate plant growth through other mechanisms, such as mineral solubilization, to sustain plant health. These findings were consistent with the results found in this study when inoculating tomato seeds with *T. asperellum* in healthy conditions or under pathogenic stress. Tomato root colonization and *Trichoderma* mobility were visualized using confocal laser imaging (Figure 5J) in the rhizosphere to discover the tomato root-*Trichoderma* interactions. Tomato seeds were sterilized, germinated, and inoculated, and seedlings were grown under the conditions described (Simons et al., 1996). *Trichoderma* and *Fusarium* were labeled with autofluorescent protein (AFP) markers to visualize their interactions

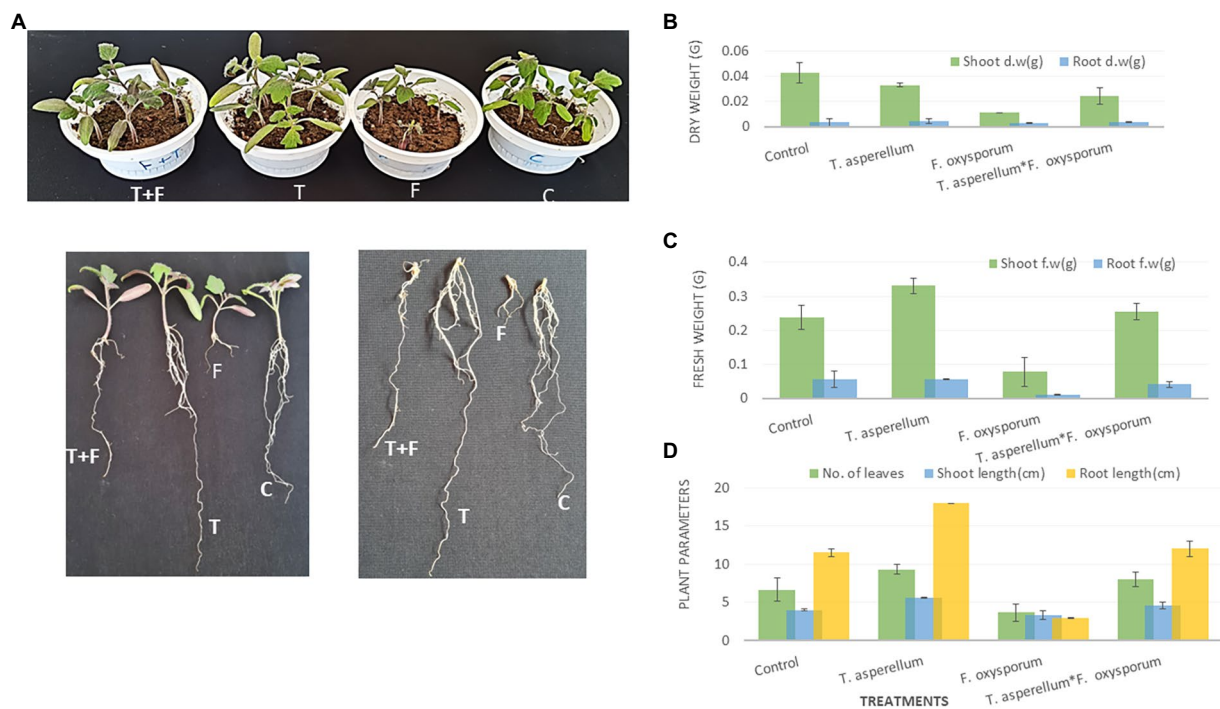


**FIGURE 6** The Effect of *T. asperellum* on the growth of tomato plants under biotic stress of *F. oxysporum* including (A); T-*Trichoderma* enhances both root and shoot of tomato seedlings, F-*Fusarium* can penetrate tomato roots and cause wilting or root rotting diseases, T+F-the interaction between the fungal endophyte and the pathogen, C-tomato plants without microbial treatment. Shoot and root dry weight (B). Shoot and root fresh weight and (C). The number of leaves, shoot, and root length (cm) (D).

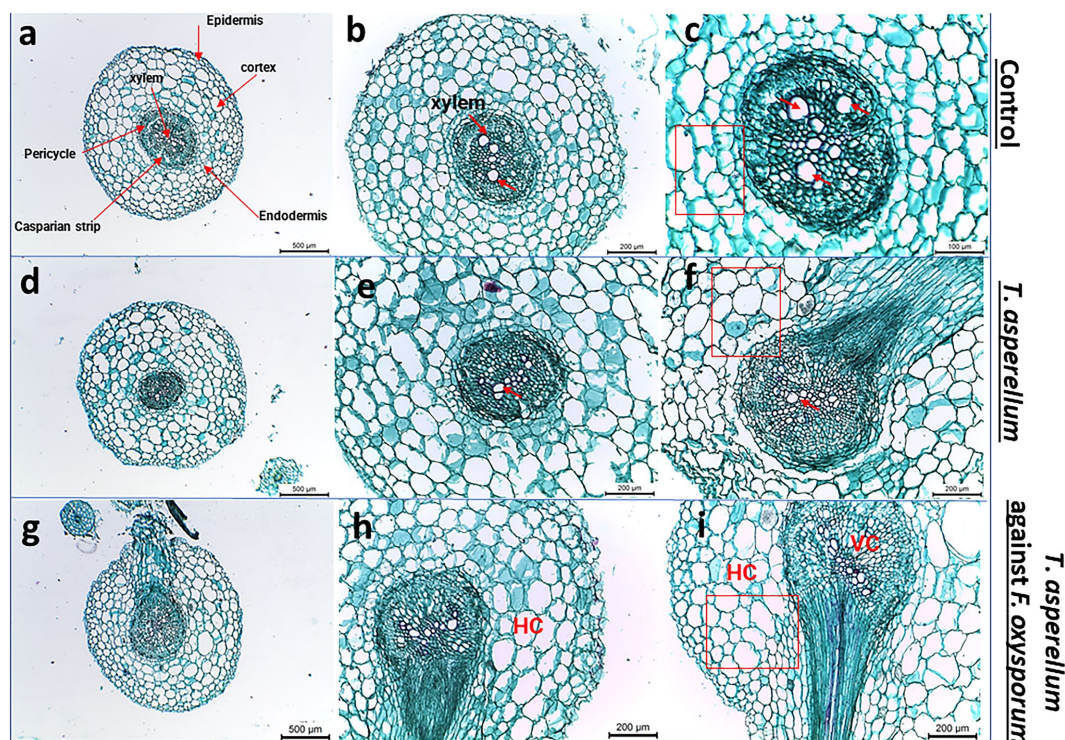


**FIGURE 7** Light microscope images of tomato root cross sections near the root tip taken from plants grown under biotic stress. (A–C) Healthy tomato root, (D–F) Transverse sections of tomato roots plant treated with *Trichoderma*, (G–I) shows the root cross-sections after applying *Trichoderma* against *Fusarium* pathogen. Red arrows indicate the xylem vessels.



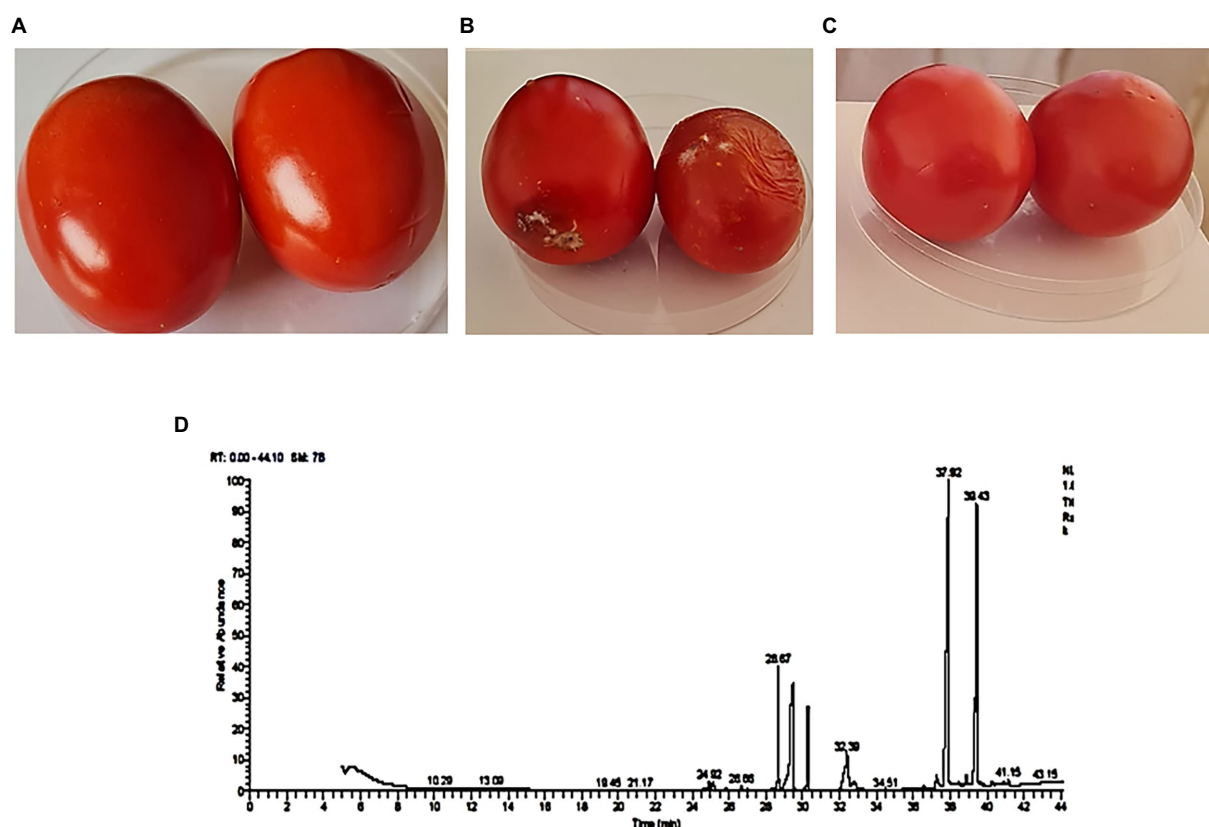


FIGURE 8

Biocontrol efficacy of *T. asperellum* crude extract against *F. oxysporum*. (A) Tomato fruit inoculated with *T. asperellum* extract. (B) Tomato fruit inoculated with a spore suspension of *F. oxysporum* only. (C) Tomato fruit inoculated with *T. asperellum* extract and *F. oxysporum*. (D) The fraction of bioactive secondary metabolites were detected using a GC–MS chromatogram obtained from *T. asperellum*.

using confocal laser scanning microscopy (CLSM). This study better understood the biocontrol interaction and mycoparasitic activity (Bloembergen, 2007).

Similarly, our study showed the fungal mobility in the tomato rhizosphere, which stimulates root growth promotion (Bolwerk and Lugtenberg, 2005), as shown in Figures 5I,J, which illustrates the early and robust stage of tomato root colonization. In addition to direct parasitism of plant pathogens, interactions with *Trichoderma* enhance plant fitness in response to biotic and abiotic stresses (Bolwerk et al., 2005; Hermosa et al., 2012). All microbes generally hunt for food, of which the root supplies a substantial amount of exudate. Visualization of plant-microbe and microbe-microbe interactions during the plant developmental stages is essential to understanding the underlying mechanisms behind the root exudates/signaling and microbial colonization *via* tracking microbial mobility. In addition, it explores the various mechanisms of biological control by increasing tolerance to abiotic stress and stimulating defense strategies against fungal pathogens (Hermosa et al., 2012). Tomato seedlings inoculated with *Burkholderia tropica* strain MT0-293 exhibited some activities in plant growth promotion and biological control under greenhouse conditions (Bernabeu et al., 2015). They studied the performance of the microbial colonization of different vegetal tissues. A later confocal microscopy study also revealed that *T. harzianum* could colonize the epidermis and cortex of tomato roots (Chacón et al., 2007). In a recent study, *T. harzianum* T-78 enhanced the resistance of tomato plants against the root-knot nematode *Meloidogyne incognita* through

priming for salicylic acid (SA)- and jasmonic acid (JA)-regulated defenses (Martínez-Medina et al., 2017). Root colonization by *Trichoderma* requires a complex molecular dialog between the fungus and plant. This colonization is limited to the outermost layers of the root and does not penetrate the plant vascular bundle, which increases the resilience of abiotic stresses (i.e., salinity and drought). In addition, improving the capacity to absorb nutrients and actively stimulates plant growth (Contreras-Cornejo et al., 2021). *T. atroviride* AN35 and *T. cremeum* AN392 colonized the roots of wheat plants. The microscopic imaging showed that the hyphae of the *Trichoderma* grew on the root surface of wheat and corn (*Zea mays*) seedlings (Contreras-Cornejo et al., 2018). This behavior was also observed in *T. atroviride* during the colonization of *Arabidopsis* roots (Salas-Marina et al., 2011). A study by Ruano-Rosa et al. (2016) showed the root colonization process between *T. harzianum* and olive crops.

*Trichoderma* species are known to produce a wide range of bioactive secondary metabolites that are known to have antifungal, antibacterial, and toxic properties to control a wide range of phytopathogens, such as *Fusarium* species, *Botrytis cinerea*, *Pythium* species, *Rhizoctonia solani*, *Sclerotinia sclerotiorum*, and *Ustilago maydis* (Hermosa et al., 2014; Khan et al., 2020). Analysis by GC–MS is essential for the identification of natural compounds of the microbe to explore the underlying mechanisms of the antifungal activity (Siddiquee et al., 2012; Qualhato et al., 2013; Meena et al., 2017). Usually, volatile compounds are identified, such as aromatic compounds, fatty acids, general hydrocarbons, and hydroxy or amino

TABLE 3 Bioactive compounds identified in *T. asperellum* crude extract using GC–MS analysis.

| T No. | R.T.  | Area % | Name of the compound  | Formula  | Molecular weight |
|-------|-------|--------|---|--|------------------|
| 1     | 5.46  | 1.03   | Methanol, TBDMS derivative  | C <sub>7</sub> H <sub>18</sub> OSi                             | 146              |
| 2     | 24.92 | 0.51   | D-(–)-Fructofuranose, pentakis(trimethylsilyl) ether (isomer 2)   | C <sub>21</sub> H <sub>52</sub> O <sub>6</sub> Si <sub>5</sub> | 540              |
| 3     | 25.18 | 0.31   | D-(–)-Ribofuranose, tetrakis(trimethylsilyl) ether (isomer 1)   | C <sub>17</sub> H <sub>42</sub> O <sub>5</sub> Si <sub>4</sub> | 438              |
| 4     | 26.66 | 0.23   | D-(+)-Galactopyranose, 5TMS derivative (isomer 2)   | C <sub>21</sub> H <sub>52</sub> O <sub>6</sub> Si <sub>5</sub> | 540              |
| 5     | 28.67 | 7.04   | D-Glucopyranose, 5TMS derivative  | C <sub>21</sub> H <sub>52</sub> O <sub>6</sub> Si <sub>5</sub> | 540              |
| 6     | 29.46 | 17.05  | Palmitic Acid, TMS derivative   | C <sub>19</sub> H <sub>40</sub> O <sub>2</sub> Si              | 328              |
| 7     | 30.28 | 4.55   | Myo-Inositol, 6TMS derivative   | C <sub>24</sub> H <sub>60</sub> O <sub>6</sub> Si <sub>6</sub> | 612              |
| 8     | 32.40 | 2.82   | 9-Octadecenoic acid, (E)-, TMS derivative   | C <sub>21</sub> H <sub>42</sub> O <sub>2</sub> Si              | 354              |
| 9     | 32.40 | 2.82   | 11-cis-octadecenoic acid 1TMS   | C <sub>21</sub> H <sub>42</sub> O <sub>2</sub> Si              | 354              |
| 10    | 32.40 | 2.82   | 13-Octadecenoic acid, (E)-, TMS derivative  | C <sub>21</sub> H <sub>42</sub> O <sub>2</sub> Si              | 354              |
| 11    | 32.40 | 2.82   | Oleic Acid, (Z)-, TMS derivative  | C <sub>21</sub> H <sub>42</sub> O <sub>2</sub> Si              | 354              |
| 12    | 32.83 | 0.82   | Octadecanoic acid, trimethylsilyl ester   | C <sub>21</sub> H <sub>44</sub> O <sub>2</sub> Si              | 356              |
| 13    | 32.83 | 0.82   | 10,12-Docosadiynedioic acid, 2TMS derivative  | C <sub>28</sub> H <sub>50</sub> O <sub>4</sub> Si <sub>2</sub> | 506              |
| 14    | 32.83 | 0.82   | Stearic acid, TMS derivative  | C <sub>21</sub> H <sub>44</sub> O <sub>2</sub> Si              | 356              |
| 15    | 32.83 | 0.82   | 5,8,11-Eicosatriynoic acid, tert-butyltrimethylsilyl ester  | C <sub>26</sub> H <sub>42</sub> O <sub>2</sub> Si              | 414              |
| 16    | 37.28 | 1.35   | 4H-1-Benzopyran-4-one,2-(3,4-Dihydroxyphenyl)-6,8-DI- <i>α</i> -D-Glucopyranosyl-5, 7-Dihydroxy               | C <sub>27</sub> H <sub>30</sub> O <sub>16</sub>                | 610              |
| 17    | 37.28 | 1.35   | 9,12,15-Octadecatrienoic acid, 2-[(trimethylsilyl)oxy]-1-[[[(trimethylsilyl)oxy] methyl]ethyl ester, (Z,Z,Z)- | C <sub>27</sub> H <sub>52</sub> O <sub>4</sub> Si <sub>2</sub> | 496              |
| 18    | 37.91 | 32.15  | 1,2-Benzenedicarboxylic acid  | C <sub>24</sub> H <sub>38</sub> O <sub>4</sub>                 | 390              |

R.T, Retention time.

compound metabolites (Siddiquee et al., 2012). In the present study, 18 bioactive compounds were detected in the crude extract of *T. asperellum* by GC–MS analysis. The most commonly identified compounds were fatty acids and their derivatives, esters such as 1,2-Benzenedicarboxylic acid, Palmitic acids, Oleic acid, 9-Octadecenoic acid (E), methyl ester, and 9,12,15-Octadecatrienoic acid, methyl ester, (Z, Z, Z), sugars (D-Glucopyranose) and sugar alcohol (Myo-Inositol). It was investigated that sugars are essential to fuel the energy required for defenses and serve as signals for regulating defense genes in plant-microbe interactions (Roitsch et al., 2003; Bolton, 2009). Myo-inositol plays essential roles in stress responses, development, and many other processes (Michell, 2008; Valluru and Van den Ende, 2011). Moreover, the volatile metabolites play essential roles in mycoparasitic interactions between *Trichoderma* and plants (Altieri et al., 2009). 1,2 Benzenedicarboxylic acid has antifungal activity (Chen et al., 2020). Liu et al. (2008) emphasized the antifungal activity of palmitic acid against four economically important phytopathogenic fungi (*Alternaria solani*, *Colletotrichum lagenarium*, *Fusarium oxysporum* f. sp. *cucumerinum*, and *F. oxysporum* f. sp. *lycopersici*). Walters et al. (2004) examined the antifungal ability of oleic acid against plant pathogenic fungi. They verified that a 1,000  $\mu$ M could reduce the mycelial growth of all tested fungi (*Rhizoctonia solani*, *Pythium ultimum*, *Pyrenophora avenae*, and *C. perniciosa*). The primary mechanism of the antifungal action of fatty acids states that fatty acids insert themselves into the lipid bilayers of fungal membranes compromising membrane integrity, resulting in an uncontrolled release of intracellular electrolytes and proteins, eventually leading to cytoplasmic disintegration of fungal cells (Avis and Bélanger, 2001). Thus, these fatty acids play a vital role in

the extract of *T. asperellum* by controlling the growth of *F. oxysporum*. Therefore, it protects tomato plants from *Fusarium* diseases.

Surprisingly, the mycotoxins naturally produced by *Fusarium* species (FB1, FB2, ZEN, and DON) were not detected by LC–MS analysis, even in the untreated controls. Our results agree with Stracquadanio et al. (2021), who showed that *F. graminearum* had no mycotoxin production in tomato fruits. Likewise, in the studies by Lori et al. (2003) and Haidukowski et al. (2005) on the same strain, *F. graminearum* ITEM 126 showed mycotoxin production in contaminated wheat kernels. This could be because this strain does not produce mycotoxins when infecting tomatoes but only in small grain cereals and maize (Munkvold, 2017).

## Conclusion

Tomato is a global economically essential vegetable crop. However, FOL is the causal agent of the FWD of tomato crops. Biological control offers a promising eco-friendly method to manage this disease. The *Trichoderma* strain is successfully used as a bio-control agent because it stimulates the plant immune system against pathogen attacks. Its growth-promoting ability in soil provides an additional benefit in the agricultural application of fertilizers and antifungal activity. Furthermore, a combination of the *in vitro* and *planta* experiments will improve the role of this fungus on plant performance. In addition, the fungus successfully promotes plant growth in controlled conditions. The plant growth-promoting traits and biocontrol efficiency of the *Trichoderma* strain were also evaluated based on the recurring role of *T. asperellum* as a biocontrol



agent against various fungal pathogens. *T. asperellum* displayed the highest antagonistic activity against *F. oxysporum* at 53.24%, and 30% free cell filtrate inhibited *F. oxysporum* at 59.39% as well. This study provides vital insights into the plant-microbe interaction and the microbe-microbe interactions, including diverse antagonistic mechanisms. For instance, chitinase activity, IAA, and P solubility were observed *in vitro* assays, indicating *Trichoderma*'s capability to control the fungal pathogen and enhance plant growth. Additionally, using confocal microscopy, tomato root colonization was visualized to understand the mobility of the *Trichoderma* strain in the host plant. These data suggest microbial application in seed coating or foliar spraying, which may improve food safety by applying beneficial microbes. In sum, improving the efficacy and development of biocontrol agents to help small farmers will increase their crop productivity in an accessible and economical way. Thereby positively impacting farmers' profits and sustaining the food safety approaches. In addition, developing sustainable crops that could be grown with little to no pesticides and/or chemical fertilizers reduces costs for farmers in developing areas. Moreover, developing novel and environmentally friendly approaches is essential to reduce the FWD incidence and yield loss in tomato crops. Therefore, more field applications with this *Trichoderma* strain are required. In addition, the transcriptome profiles of the root system following microbial treatment and the influence of endophytic fungi on tomato metabolism.

## Data availability statement

The datasets presented in this study can be found in online repositories. The names of the repository/repositories and accession number(s) can be found in the article/Supplementary material.

## References

- Agrawal, T., and Kotasthane, A. S. (2012). Chitinolytic assay of indigenous *Trichoderma* isolates collected from different geographical locations of Chhattisgarh in Central India. *Springerplus* 1, 1–10. doi: 10.1186/2193-1801-1-73
- Akbar, A., Hussain, S., and Ali, G. S. (2018). Germplasm evaluation of tomato for resistance to the emerging wilt pathogen *Fusarium equiseti*. *J. Agric. Stud* 5:174. doi: 10.5296/jas.v6i3.13433
- Alaguero-Cordovilla, A., Gran-Gómez, F. J., Tormos-Moltó, S., and Pérez-Pérez, J. M. (2018). Morphological characterization of root system architecture in diverse tomato genotypes during early growth. *Int. J. Mol. Sci.* 19:3888. doi: 10.3390/ijms19123888
- Almeida, F., Rodrigues, M. L., and Coelho, C. (2019). The still underestimated problem of fungal diseases worldwide. *Front. Microbiol.* 10:214. doi: 10.3389/fmicb.2019.00214
- Aloisio, F. C., Junior, F. B., Lillian, C., Luciane, D. O. M., and De Oliveira, J. O. (2019). Efficiency of *Trichoderma asperellum* UFT 201 as plant growth promoter in soybean. *Afr. J. Agric. Res.* 14, 263–271. doi: 10.5897/AJAR2018.13556
- Altieri, C., Bevilacqua, A., Cardillo, D., and Sinigaglia, M. (2009). Antifungal activity of fatty acids and their monoglycerides against *Fusarium* spp. in a laboratory medium. *Int. J. Food Sci. Technol.* 44, 242–245. doi: 10.1111/j.1365-2621.2007.01639.x
- Atkinson, J. A., Rasmussen, A., Traini, R., Voß, U., Sturrock, C., Mooney, S. J., et al. (2014). Branching out in roots: uncovering form, function, and regulation. *Plant Physiol.* 166, 538–550. doi: 10.1104/pp.114.245423
- Attia, M. S., Abdelaziz, A. M., Al-Askar, A. A., Arishi, A. A., Abdelhakim, A. M., and Hashem, A. H. (2022). Plant growth-promoting fungi as biocontrol tool against *Fusarium* wilt disease of tomato plant. *J. Fungi* 8:775. doi: 10.3390/jof8080775
- Avis, T. J., and Bélanger, R. R. (2001). Specificity and mode of action of the antifungal fatty acid cis-9-heptadecenoic acid produced by *Pseudozyma flocculosa*. *Appl. Environ. Microbiol.* 67, 956–960. doi: 10.1128/AEM.67.2.956-960.2001
- Awad, N. E., Kassem, H. A., Hamed, M. A., El-Feky, A. M., El-naggar, M. A. A., Mahmoud, K., et al. (2018). Isolation and characterization of the bioactive metabolites from the soil derived fungus *Trichoderma viride*. *Mycology* 9, 70–80. doi: 10.1080/21501203.2017.1423126
- Bailey, B. A., Hanhong Bae, M. D., Strem, D. P. R., Thomas, S. E., Crozier, J., Samuels, G. J., et al. (2006). Fungal and plant gene expression during the colonization of cacao seedlings by endophytic isolates of four *Trichoderma* species. *Planta* 224, 1449–1464. doi: 10.1007/s00425-006-0314-0
- Barroso, F. M., Muniz, P. H. P. C., Milan, M. D., Silva, W., dos Santos, N., de Faria, C., et al. (2019). Growth promotion of parsley (*Petroselinum crispum* L.) using commercial strains of *Trichoderma* spp. *J. Agric. Sci.* 11, 493–499. doi: 10.5539/jas.v11n4p493
- Bawa, I. (2016). Management strategies of *Fusarium* wilt disease of tomato incited by *Fusarium oxysporum* f. sp. *lycopersici* (Sacc.) a review. *Int. J. Adv. Acad. Res.* 2, 1–16.
- Benítez, T., Rincón, A. M., Carmen Limón, M., and Codon, A. C. (2004). Biocontrol mechanisms of *Trichoderma* strains. *Int. Microbiol.* 7, 249–260.
- Bernabeu, P. R., Pistorio, M., Torres-Tejerizo, G., Estrada-De, P., Santos, L., Galar, M. L., et al. (2015). Colonization and plant growth-promotion of tomato by *Burkholderia tropica*. *Sci. Hortic.* 191, 113–120. doi: 10.1016/j.scienta.2015.05.014
- Bloemberg, G. V. (2007). Microscopic analysis of plant-bacterium interactions using auto fluorescent proteins. *Eur. J. Plant Pathol.* 119, 301–309. doi: 10.1007/978-1-4020-6776-1\_6
- Boccia, F., Di Donato, P., Covino, D., and Poli, A. (2019). Food waste and bioeconomy: a scenario for the Italian tomato market. *J. Clean. Prod.* 227, 424–433. doi: 10.1016/j.jclepro.2019.04.180
- Bolton, M. D. (2009). Primary metabolism and plant defense—fuel for the fire. *Mol. Plant-Microbe Interact.* 22, 487–497. doi: 10.1094/MPMI-22-5-0487
- Bolwerk, A., Lagopodi, A. L., Lugtenberg, B. J. J., and Bloemberg, G. V. (2005). Visualization of interactions between a pathogenic and a beneficial *Fusarium* strain during biocontrol of tomato foot and root rot. *Mol. Plant-Microbe Interact.* 18, 710–721. doi: 10.1094/MPMI-18-0710
- Bolwerk, A., and Lugtenberg, B. J. J. (2005). "Visualization of interactions of microbial biocontrol agents and phytopathogenic fungus *Fusarium oxysporum* f. sp. *radicis-lycopersici* on tomato roots," in *PGPR: Biocontrol and Biofertilization*. ed. Z. A. Siddiqui (Dordrecht: Springer), 217–231.

## Author contributions

AS, RA, KA, and OH designed the study. AS, RA, and OH wrote the original manuscript. AS and RA conducted all the *in vitro* experiments, confocal work, and collected the data. AS, RA, and OH conducted the *in planta* assays. OH performed the ITS sequencing to confirm fungal genus taxonomy. OH, KA, and MA performed the statistical analysis and edited the manuscript. All authors contributed to the article and approved the submitted version.

## Conflict of interest

The authors declare that the research was conducted in the absence of any commercial or financial relationships that could be construed as a potential conflict of interest.

## Publisher's note

All claims expressed in this article are solely those of the authors and do not necessarily represent those of their affiliated organizations, or those of the publisher, the editors and the reviewers. Any product that may be evaluated in this article, or claim that may be made by its manufacturer, is not guaranteed or endorsed by the publisher.

## Supplementary material

The Supplementary material for this article can be found online at: <https://www.frontiersin.org/articles/10.3389/fmicb.2023.1140378/full#supplementary-material>

- Borrero, C., Trillas, M. I., Delgado, A., and Avilés, M. (2012). Effect of ammonium/nitrate ratio in nutrient solution on control of *Fusarium* wilt of tomato by *Trichoderma asperellum* T34. *Plant Pathol.* 61, 132–139. doi: 10.1111/j.1365-3059.2011.02490.x
- Buriro, M., Oad, F. C., Keerio, M. I., Tunio, S., Gandahi, A. W., Hassan, S. W. U., et al. (2011). Wheat seed germination under the influence of temperature regimes. *Sarhad J. Agric.* 27, 539–543.
- Cai, F., Chen, W., Wei, Z., Pang, G., Li, R., Ran, W., et al. (2015). Colonization of *Trichoderma harzianum* strain SQR-T037 on tomato roots and its relationship to plant growth, nutrient availability and soil microflora. *Plant Soil* 388, 337–350. doi: 10.1007/s11104-014-2326-z
- Cai, F., Guanghui, Y., Wang, P., Wei, Z., Lin, F., Shen, Q., et al. (2013). Harzianolide, a novel plant growth regulator and systemic resistance elicitor from *Trichoderma harzianum*. *Plant Physiol. Biochem.* 73, 106–113. doi: 10.1016/j.plaphy.2013.08.011
- Chacón, M. R., Rodríguez-Galán, O., Benítez, T., Sousa, S., Rey, M., Llobell, A., et al. (2007). Microscopic and transcriptome analyses of early colonization of tomato roots by *Trichoderma harzianum*. *Int. Microbiol.* 10, 19. doi: 10.2436/20.1501.01.4
- Chen, X., Huang, Y., and Huang, Z. (2018). Combination of ethyl acetate extract of *Trichoderma hamatum* fermentation broth and fungicide carbendazim enhances inhibition against *Sclerotinia sclerotiorum* under laboratory conditions Pakistan. *J. Zool.* 50, 2239–2247. doi: 10.17582/journal.pjz.2018.50.6.2239.2247
- Chen, J. H., Xiang, W., Cao, K. X., Lu, X., Yao, S. C., Hung, D., et al. (2020). Characterization of volatile organic compounds emitted from endophytic *Burkholderia cenocepacia* ETR-B22 by SPME-GC-MS and their inhibitory activity against various plant fungal pathogens. *Molecules* 25:3765. doi: 10.3390/molecules25173765
- Contreras-Cornejo, H. A., Macías-Rodríguez, L., Del-Val, E., and Larsen, J. (2016). Ecological functions of *Trichoderma* spp. and their secondary metabolites in the rhizosphere: interactions with plants. *FEMS Microbiol. Ecol.* 92:fw036. doi: 10.1093/femsec/fw036
- Contreras-Cornejo, H. A., Macías-Rodríguez, L., Del-Val, E., and Larsen, J. (2018). The root endophytic fungus *Trichoderma atroviride* induces foliar herbivory resistance in maize plants. *Appl. Soil Ecol.* 124, 45–53. doi: 10.1016/j.apsoil.2017.10.004
- Contreras-Cornejo, H. A., Viveros-Bremaunt, F., Del-Val, E., Macías-Rodríguez, L., López-Carmona, D. A., Alarcón, A., et al. (2021). Alterations of foliar arthropod communities in a maize agroecosystem induced by the root-associated fungus *Trichoderma harzianum*. *J. Pest. Sci.* 94, 363–374. doi: 10.1007/s10340-020-01261-3
- Das, P. P., Singh, K. R. B., Nagpure, G., Mansoori, A., Singh, R. P., Ghazi, I. A., et al. (2022). Plant-soil-microbes: a tripartite interaction for nutrient acquisition and better plant growth for sustainable agricultural practices. *Environ. Res.* 214:113821. doi: 10.1016/j.envres.2022.113821
- de Chaves, M., Antunes, P. R., Souza, B., da Costa, R., de Paschoal, I., Teixeira, M. L., et al. (2022). Fungicide resistance in *Fusarium graminearum* species complex. *Curr. Microbiol.* 79, 1–9. doi: 10.1007/s00284-021-02759-4
- Druzhinina, I. S., Seidl-Seiboth, V., Herrera-Estrella, A., Horwitz, B. A., Kenerley, C. M., Monte, E., et al. (2011). *Trichoderma*: the genomics of opportunistic success. *Nat. Rev. Microbiol.* 9, 749–759. doi: 10.1038/nrmicro2637
- Elshafie, H. S., Sakr, S., Bufo, S. A., and Camele, I. (2017). An attempt of biocontrol the tomato-wilt disease caused by *Verticillium dahliae* using *Burkholderia gladioli* pv. *agaricola* and its bioactive secondary metabolites. *Int. J. Plant Biol.* 8:7263. doi: 10.4081/pb.2017.7263
- Elshahawy, I. E., and El-Mohamedy, R. S. (2019). Biological control of Pythium damping-off and root-rot diseases of tomato using *Trichoderma* isolates employed alone or in combination. *J. Plant Pathol.* 101, 597–608. doi: 10.1007/s42161-019-00248-z
- Fishal, E. M., Mohd, I. B., Razak, A., Bohari, N. H., and Nasir, M. A. M. (2022). In vitro screening of endophytic *Trichoderma* sp. isolated from oil palm in FGV plantation against *Ganoderma boninense*. *Adv. Microbiol.* 12, 443–457. doi: 10.4236/aim.2022.127031
- França, D. V., Cardozo, K. C., Kupper, M. M., Magri, R., Gomes, T. M., and Rossi, F. (2017). *Trichoderma* spp. isolates with potential of phosphate solubilization and growth promotion in cherry tomato. *Pesqui. Agropec. Trop.* 47, 360–368. doi: 10.1590/1983-40632017v4746447
- Ghazala, I., Charfeddine, M., Charfeddine, S., Haddar, A., Ellouz-Chaabouni, S., and Gargouri-Bouzd, R. (2022). Lipopeptides from *Bacillus mojavensis* I4 confer induced tolerance toward *Rhizoctonia solani* in potato (*Solanum tuberosum*). *Physiol. Mol. Plant Pathol.* 121:101895. doi: 10.1016/j.pmpp.2022.101895
- Glick, B. R. (2012). Plant growth-promoting bacteria: mechanisms and applications. *Scientifica* 2012:963401:15. doi: 10.6064/2012/963401
- Haidukowski, M., Pascale, M., Perrone, G., Pancaldi, D., Campagna, C., and Visconti, A. (2005). Effect of fungicides on the development of *Fusarium* head blight, yield and deoxynivalenol accumulation in wheat inoculated under field conditions with *Fusarium graminearum* and *Fusarium culmorum*. *J. Sci. Food Agric.* 85, 191–198. doi: 10.1002/jsfa.1965
- Harman, G. E. (2006). Overview of mechanisms and uses of *Trichoderma* spp. *Phytopathology* 96, 190–194. doi: 10.1094/PHYTO-96-0190
- Harman, G. E., and Christian, P. K. (2002). *Trichoderma and Gliocladium. Volume 1: Basic biology, taxonomy and genetics*. CRC Press.
- Harman, G. E., Howell, C. R., Viterbo, A., Chet, I., and Lorito, M. (2004). *Trichoderma* species—opportunistic, avirulent plant symbionts. *Nat. Rev. Microbiol.* 2, 43–56. doi: 10.1038/nrmicro797
- Hermosa, R., Cardoza, R. E., Rubio, M. B., Gutiérrez, S., and Monte, E. (2014). “Secondary metabolism and antimicrobial metabolites of *Trichoderma*” in *Biotechnology and Biology of Trichoderma*. eds. I. Druzhinina and M. Tuohy (Amsterdam, Netherlands: Elsevier), 125–137.
- Hermosa, R., Viterbo, A., Chet, I., and Monte, E. (2012). Plant-beneficial effects of *Trichoderma* and of its genes. *Microbiology* 158, 17–25. doi: 10.1099/mic.0.052274-0
- Hernández-Aparicio, F., Lisón, P., Rodrigo, I., Bellés, J. M., and López-Gresa, M. P. (2021). Signaling in the tomato immunity against *Fusarium oxysporum*. *Molecules* 26:1818. doi: 10.3390/molecules26071818
- Hewedy, O. A., Abdel, K. S., Lateif, M. F., Seleiman, A. S., Albarakaty, F. M., and El-Meihy, R. M. (2020b). Phylogenetic diversity of *Trichoderma* strains and their antagonistic potential against soil-borne pathogens under stress conditions. *Biology* 9:189. doi: 10.3390/biology9080189
- Hewedy, O. A., Abdel-Lateif, K. S., and Bakr, R. A. (2020a). Genetic diversity and biocontrol efficacy of indigenous *Trichoderma* isolates against *Fusarium* wilt of pepper. *J. Basic Microbiol.* 60, 126–135. doi: 10.1002/jobm.201900493
- Hewedy, O. A., El-Zanaty, A. M., and Fahmi, A. I. (2020c). “Screening and identification of novel cellulolytic *Trichoderma* species from Egyptian habitats.” *BioTechnology. Journal of Biotechnology Computational Biology and Bionanotechnology* 101.
- Izykowska, L., Bocianowski, J., Waśkiewicz, A., Weber, Z., Karolewski, Z., Goliński, P., et al. (2012). Genetic variation of *Fusarium oxysporum* isolates forming fumonisin B1 and moniliformin. *J. Appl. Genet.* 53, 237–247. doi: 10.1007/s13353-012-0087-z
- Jangir, M., Sharma, S., and Sharma, S. (2019). Target and non-target effects of dual inoculation of biocontrol agents against *Fusarium* wilt in *Solanum lycopersicum*. *Biol. Control* 138:104069. doi: 10.1016/j.biocontrol.2019.104069
- Johansen, D. A. (1940). *Plant Microtechnique*. McGraw Hill Book Company Inc., London, UK.
- Jones, J. B., Zitter, T. A., Momol, T. M., and Miller, S. A. (2014). *Compendium of Tomato Diseases and Pests*. United States: APS Press.
- Kamaruzzaman, M., Islam, M. S., Mahmud, S., Polash, S. A., Razia Sultana, M., Hasan, A., et al. (2021). *In vitro* and *in silico* approach of fungal growth inhibition by *Trichoderma asperellum* HbGT6-07 derived volatile organic compounds. *Arab. J. Chem.* 14:103290. doi: 10.1016/j.arabjc.2021.103290
- Karthika, K. S., Rashmi, I., and Parvathi, M. S. (2018). “Biological functions, uptake and transport of essential nutrients in relation to plant growth,” in *Plant Nutrients and Abiotic Stress Tolerance*. eds. M. Hasanuzzaman, M. Fujita, H. Oku, K. Nahar and B. Hawrylak-Nowak (Singapore: Springer), 1–49.
- Ketta, H. A., and Hewedy, O. A. E.-R. (2021). Biological control of *Phaseolus vulgaris* and *Pisum sativum* root rot disease using *Trichoderma* species. *Egypt. J. Biol. Pest Control* 31, 1–9. doi: 10.1186/s41938-021-00441-2
- Khan, R. A. A., Najeeb, S., Mao, Z., Ling, J., Yang, Y., Li, Y., et al. (2020). Bioactive secondary metabolites from *Trichoderma* spp. against phytopathogenic bacteria and root-knot nematode. *Microorganisms* 8, 401–402. doi: 10.3390/microorganisms8030401
- Kipngeno, P., Losenge, T., Maina, N., Kahangi, E., and Juma, P. (2015). Efficacy of *Bacillus subtilis* and *Trichoderma asperellum* against *Pythium aphanidermatum* in tomatoes. *Biol. Control* 90, 92–95. doi: 10.1016/j.biocontrol.2015.05.017
- Lei, Z. H. A. O., and Zhang, Y.-q. (2015). Effects of phosphate solubilization and phytohormone production of *Trichoderma asperellum* Q1 on promoting cucumber growth under salt stress. *J. Integr. Agric.* 14, 1588–1597. doi: 10.1016/S2095-3119(14)60966-7
- Li, Y.-T., Hwang, S.-G., Huang, Y.-M., and Huang, C.-H. (2018). Effects of *Trichoderma asperellum* on nutrient uptake and *Fusarium* wilt of tomato. *Crop Prot.* 110, 275–282. doi: 10.1016/j.cropro.2017.03.021
- Liu, S., Ruan, W., Li, J., Xu, H., Wang, J., Gao, Y., et al. (2008). Biological control of phytopathogenic fungi by fatty acids. *Mycopathologia* 166, 93–102. doi: 10.1007/s11046-008-9124-1
- López Errasquín, E., and Vázquez, C. (2003). Tolerance and uptake of heavy metals by *Trichoderma atroviride* isolated from sludge. *Chemosphere* 50, 137–143. doi: 10.1016/S0045-6535(02)00485-X
- Lori, G., Sisterna, M., Haidukowski, M., and Rizzo, I. (2003). *Fusarium graminearum* and deoxynivalenol contamination in the durum wheat area of Argentina. *Microbiol. Res.* 158, 29–35. doi: 10.1078/0944-5013-00173
- Maliche, T. S., Mbambo, M., Nqotheni, M. I., Senzo, N. S., and Shandu, J. S. E. (2022). Antibacterial effect and mode of action of secondary metabolites from fungal endophyte associated with *Aloe ferox* Mill. *Microbiol. Res.* 13, 90–101. doi: 10.3390/microbiolres13010007
- Manikandan, R., Harish, S., Karthikeyan, G., and Raguchander, T. (2018). Comparative proteomic analysis of different isolates of *Fusarium oxysporum* f. sp. *lycopersici* to exploit the differentially expressed proteins responsible for virulence on tomato plants. *Front. Microbiol.* 9:420. doi: 10.3389/fmicb.2018.00420
- Marshall, H., Meneely, J. P., Quinn, B., Zhao, Y., Bourke, P., Gilmore, B. F., et al. (2020). Novel decontamination approaches and their potential application for post-harvest aflatoxin control. *Trends Food Sci. Technol.* 106, 489–496. doi: 10.1016/j.tifs.2020.11.001

- Martínez-Medina, A., Appels, F. V. W., and van Wees, S. C. M. (2017). Impact of salicylic acid-and jasmonic acid-regulated defences on root colonization by *Trichoderma harzianum* T-78. *Plant Signal. Behav.* 12:e1345404. doi: 10.1080/15592324.2017.1345404
- Marzano, M., Gallo, A., and Altomare, C. (2013). Improvement of biocontrol efficacy of *Trichoderma harzianum* vs. *Fusarium oxysporum* f. sp. *lycopersici* through UV-induced tolerance to fusaric acid. *Biol. Control* 67, 397–408. doi: 10.1016/j.biocontrol.2013.09.008
- Meena, M., Swapnil, P., Zehra, A., Dubey, M. K., and Upadhyay, R. S. (2017). Antagonistic assessment of *Trichoderma* spp. by producing volatile and non-volatile compounds against different fungal pathogens. *Arch. Phytopathol. Plant Protect.* 50, 629–648. doi: 10.1080/03235408.2017.1357360
- Michell, R. H. (2008). Inositol derivatives: evolution and functions. *Nat. Rev. Mol. Cell Biol.* 9, 151–161. doi: 10.1038/nrm2334
- Modrzejewska, M., Bryła, M., Kanabus, J., and Pierzgałski, A. (2022). *Trichoderma* as a biostimulator and biocontrol agent against *Fusarium* in the production of cereal crops: opportunities and possibilities. *Plant Pathol.* 71, 1471–1485. doi: 10.1111/ppa.13578
- Mohiddin, F. A., Khan, M. R., Khan, S. M., and Bhat, B. H. (2010). Why *Trichoderma* is considered super hero (super fungus) against the evil parasites? *Plant Pathol. J.* 9, 92–102. doi: 10.3923/ppj.2010.92.102
- Mukherjee, P. K., Mendoza-Mendoza, A., Zeilinger, S., and Horwitz, B. A. (2022). Mycoparasitism as a mechanism of *Trichoderma*-mediated suppression of plant diseases. *Fungal Biol. Rev.* 39, 15–33. doi: 10.1016/j.fbr.2021.11.004
- Mulatu, A., Megersa, N., Tolcha, T., Alemu, T., and Vetukuri, R. R. (2022). Bioassay evaluation, GC-MS analysis and acute toxicity assessment of Methanolic extracts of *Trichoderma* species in an animal model. *bioRxiv* 2022:480498. doi: 10.1101/2022.02.15.480498
- Munkvold, G. P. (2017). *Fusarium* species and their associated mycotoxins. *Methods Mol. Biol.* 154, 51–106. doi: 10.1007/978-1-4939-6707-0\_4
- Mwangi, M. W., Monda, E. O., Okoth, S. A., and Jefwa, J. M. (2011). Inoculation of tomato seedlings with *Trichoderma harzianum* and *Arbuscular mycorrhizal* fungi and their effect on growth and control of wilt in tomato seedlings. *Braz. J. Microbiol.* 42, 508–513. doi: 10.1590/S1517-83822011000200015
- Nakai, J. (2018). *Food and Agriculture Organization of the United Nations and the Sustainable Development Goals*. Sustainable Development, No. 22.
- Nandini, B., Puttaswamy, H., Saini, R. K., Prakash, H. S., and Geetha, N. (2021). Trichovariability in rhizosphere soil samples and their biocontrol potential against downy mildew pathogen in pearl millet. *Sci. Rep.* 11, 1–15. doi: 10.1038/s41598-021-89061-2
- Natsopoulos, D., Tziolias, A., Lagogiannis, I., Mantzoukas, S., and Eliopoulos, P. A. (2022). Growth-promoting and protective effect of *Trichoderma atroviride* and *T. simmonsii* on tomato against soil-borne fungal pathogens. *Crops* 2, 202–217. doi: 10.3390/crops2030015
- Nautiyal, C. S. (1999). An efficient microbiological growth medium for screening phosphate solubilizing microorganisms. *FEMS Microbiol. Lett.* 170, 265–270. doi: 10.1111/j.1574-6968.1999.tb13383.x
- Olowe, O. M., Nicola, L., Asemoloye, M. D., Akanmu, A. O., and Babalola, O. O. (2022). *Trichoderma*: potential bio-resource for the management of tomato root diseases in Africa. *Microbiol. Res.* 257:126978. doi: 10.1016/j.micres.2022.126978
- Pal, K. K., and Gardener, B. M. (2006). *Biological Control of Plant Pathogens*. St. Paul, MN: American Psychopathological Society.
- Pande, A., Pandey, P., Mehra, S., Singh, M., and Kaushik, S. (2017). Phenotypic and genotypic characterization of phosphate solubilizing bacteria and their efficiency on the growth of maize. *J. Genet. Eng. Biotechnol.* 15, 379–391. doi: 10.1016/j.jgeb.2017.06.005
- Pramanik, K., and Mohapatra, P. P. (2017). Role of auxin on growth, yield and quality of tomato-a review. *Int. J. Curr. Microbiol. Appl. Sci.* 6, 1624–1636. doi: 10.20546/ijcmas.2017.611.195
- Prites, P., and Subramanian, R. B. (2011). PCR based method for testing *Fusarium* wilt resistance of tomato. *Afr. J. Basic Appl. Sci.* 3:222.
- Qualhato, T. F., Lopes, F. A. C., Steindorff, A. S., Brandão, R. S., Jesuino, R. S. A., and Ulhoa, C. J. (2013). Mycoparasitism studies of *Trichoderma* species against three phytopathogenic fungi: evaluation of antagonism and hydrolytic enzyme production. *Biotechnol. Lett.* 35, 1461–1468. doi: 10.1007/s10529-013-1225-3
- Ribeiro, J. A., Albuquerque, A., Materatski, P., Patanita, M., Varanda, C. M. R., Félix, M. D. R., et al. (2022). Tomato response to *Fusarium* spp. infection under field conditions: study of potential genes involved. *Horticultrae* 8:433. doi: 10.3390/horticultrae8050433
- Ristaino, J. B., Anderson, P. K., Bebb, D. P., Brauman, K. A., Cunliffe, N. J., Fedoroff, N. V., et al. (2021). The persistent threat of emerging plant disease pandemics to global food security. *Proc. Natl. Acad. Sci.* 118:e2022239118. doi: 10.1073/pnas.2022239118
- Roitsch, T., Talibrea, M. E., Hofmann, M., Proels, R., and Sinha, A. K. (2003). Extracellular invertase: key metabolic enzyme and PR protein. *J. Exp. Bot.* 54, 513–524. doi: 10.1093/jxb/erg050
- Ron, M., Dorrity, M. W., de Lucas, M., Ted Toal, R., Hernandez, I., Little, S. A., et al. (2013). Identification of novel loci regulating interspecific variation in root morphology and cellular development in tomato. *Plant Physiol.* 162, 755–768. doi: 10.1104/pp.113.217802
- Ruano-Rosa, D., Prieto, P., Rincón, A. M., Gómez-Rodríguez, M. V., Valderrama, R., Barroso, J. B., et al. (2016). Fate of *Trichoderma harzianum* in the olive rhizosphere: time course of the root colonization process and interaction with the fungal pathogen *Verticillium dahliae*. *BioControl* 61, 269–282. doi: 10.1007/s10526-015-9706-z
- Saengchan, C., Sangpueak, R., Le Thanh, T., Phansak, P., and Buensanteai, N. (2022). Induced resistance against *Fusarium solani* root rot disease in cassava plant (*Manihot esculenta* Crantz) promoted by salicylic acid and *Bacillus subtilis*. *Acta Agric. Scand. B Soil Plant Sci.* 72:526. doi: 10.1080/09064710.2021.2018033
- Salas-Marina, M. A., Silva-Flores, M. A., Uresti-Rivera, E. E., Castro-Longoria, E., Herrera-Estrella, A., and Casas-Flores, S. (2011). Colonization of Arabidopsis roots by *Trichoderma atroviride* promotes growth and enhances systemic disease resistance through jasmonic acid/ethylene and salicylic acid pathways. *Eur. J. Plant Pathol.* 131, 15–26. doi: 10.1007/s10658-011-9782-6
- Sallam, N., Eraky, A. M. I., and Sallam, A. (2019). Effect of *Trichoderma* spp. on *Fusarium* wilt disease of tomato. *Mol. Biol. Rep.* 46, 4463–4470. doi: 10.1007/s11033-019-04901-9
- Scudelletti, D., Crucioli, C. A. C., Bossolani, J. W., Moretti, L. G., Momesso, L., Tubana, B. S., et al. (2021). *Trichoderma asperellum* inoculation as a tool for attenuating drought stress in sugarcane. *Front. Plant Sci.* 12:645542. doi: 10.3389/fpls.2021.645542
- Selim, M. E., and El-Gammal, N. A. (2015). Role of fusaric acid mycotoxin in pathogenesis process of tomato wilt disease caused by *Fusarium oxysporum*. *J. Bioproc. Biotech.* 5:1. doi: 10.4172/2155-9821.1000255
- Sharma, A., Salwan, R., Kaur, R., Sharma, R., and Sharma, V. (2022). Characterization and evaluation of bioformulation from antagonistic and flower inducing *Trichoderma asperellum* isolate UCRD5. *Biocatal. Agric. Biotechnol.* 43:102437. doi: 10.1016/j.bcab.2022.102437
- Sharon, E., Chet, I., Viterbo, A., Bar-Eyal, M., Nagan, H., Samuels, G. J., et al. (2007). Parasitism of *Trichoderma* on *Meloidogyne javanica* and role of the gelatinous matrix. *Eur. J. Plant Pathol.* 118, 247–258. doi: 10.1007/s10658-007-9140-x
- Siddiquee, S., Cheong, B. E., Taslima, K., Kausar, H., and Hasan, M. M. (2012). Separation and identification of volatile compounds from liquid cultures of *Trichoderma harzianum* by GC-MS using three different capillary columns. *J. Chromatogr. Sci.* 50, 358–367. doi: 10.1093/chromsci/bms012
- Simons, M., Van Der Bij, A. J., Brand, I., De Weger, L. A., Wijffelman, C. A., and Lugtenberg, B. J. (1996). Gnotobiotic system for studying rhizosphere colonization by plant growth-promoting pseudomonas bacteria. *Mol. Plant Microbe Interact.* 9, 600–607. doi: 10.1094/MPMI-9-0600
- Srivastava, R., Khalid, A., Singh, U. S., and Sharma, A. K. (2010). Evaluation of arbuscular mycorrhizal fungus, fluorescent pseudomonas and *Trichoderma harzianum* formulation against *Fusarium oxysporum* f. sp. *lycopersici* for the management of tomato wilt. *Biol. Control* 53, 24–31. doi: 10.1016/j.biocontrol.2009.11.012
- Stracquadanio, C., Luz, C., La Spada, F., Meca, G., and Cacciola, S. O. (2021). Inhibition of Mycotoxigenic fungi in different vegetable matrices by extracts of *Trichoderma* species. *J. Fungi (Basel)* 7:445. doi: 10.3390/jof7060445
- Su, S., Zeng, X., Bai, L., Jiang, X., and Li, L. (2010). Bioaccumulation and biovolatilisation of pentavalent arsenic by Penicillin janthinellum, *Fusarium oxysporum* and *Trichoderma asperellum* under laboratory conditions. *Curr. Microbiol.* 61, 261–266. doi: 10.1007/s00284-010-9605-6
- Taylor, J. T., Krieger, I., Crutcher, F. K., Jamieson, P., Horwitz, B. A., Kolomiets, M. V., et al. (2021). A class I hydrophobin in *Trichoderma virens* influences plant-microbe interactions through enhancement of enzyme activity and MAMP recognition. *bioRxiv* 2021:425738. doi: 10.1101/2021.01.07.425738
- Valluru, R., and Van den Ende, W. (2011). Myo-inositol and beyond-emerging networks under stress. *Plant Sci.* 181, 387–400. doi: 10.1016/j.plantsci.2011.07.009
- Walters, D., Raynor, L., Mitchell, A., Walker, R., and Walker, K. (2004). Antifungal activities of four fatty acids against plant pathogenic fungi. *Mycopathologia* 157, 87–90. doi: 10.1023/B:MYCO.0000012222.68156.2c
- Waskiewicz, A., Golinski, P., Karolewski, Z., Irzykowska, L., Bocianowski, J., Kostecki, M., et al. (2010). Formation of fumonisins and other secondary metabolites by *Fusarium oxysporum* and *F. proliferatum*: a comparative study. *Food Addit. Contam.* 27, 608–615. doi: 10.1080/19440040903551947
- White, T. J., Bruns, T. D., Lee, S. B., and Taylor, J. W. (1990). Amplification and direct sequencing of fungal ribosomal RNA genes for phylogenetics. *PCR Protoc.* 18, 315–322. doi: 10.1016/B978-0-12-372180-8.50042-1
- Wiedemeier, A. M. D., Judy-March, J. E., Hocart, C. H., Wasteneys, G. O., Williamson, R. E., and Baskin, T. I. (2002). Mutant alleles of Arabidopsis RADIALLY SWOLLEN 4 and 7 reduce growth anisotropy without altering the transverse orientation of cortical microtubules or cellulose microfibrils. *Development* 129, 4821–4830. doi: 10.1242/dev.129.20.4821
- Woldeamanuale, T. (2017). Isolation, screening and identification of cadmium tolerant fungi and their removal potential. *J. Forensic Sci. Crim. Investig.* 5:555656. doi: 10.19080/JFSCI.2017.05.555656
- Wu, Q., Sun, R., Ni, M., Jia, Y., Li, Y., Chuanjin, Y., et al. (2017). Identification of a novel fungus, *Trichoderma asperellum* GDFS1009, and comprehensive evaluation of its biocontrol efficacy. *PLoS One* 12:e0179957. doi: 10.1371/journal.pone.0179957

Yoo, S.-J., Shin, D. J., Won, H. Y., Song, J., and Sang, M. K. (2018). *Aspergillus terreus* JF27 promotes the growth of tomato plants and induces resistance against *Pseudomonas syringae* pv. Tomato. *Mycobiology* 46, 147–153. doi: 10.1080/12298093.2018.1475370

Zhalnina, K., Louie, K. B., Hao, Z., Mansoori, N., Nunes, U., da Rocha, S., et al. (2018). Dynamic root exudate chemistry and microbial substrate preferences drive patterns in rhizosphere microbial community assembly. *Nat. Microbiol.* 3, 470–480. doi: 10.1038/s41564-018-0129-3

Zhang, Y., and Ma, L.-J. (2017). Deciphering pathogenicity of *Fusarium oxysporum* from a phylogenomics perspective. *Adv. Genet.* 100, 179–209. doi: 10.1016/bs.adgen.2017.09.010

Zhang, Y., Xiao, J., Yang, K., Wang, Y., Tian, Y., and Liang, Z. (2022). Transcriptomic and metabonomic insights into the biocontrol mechanism of *Trichoderma asperellum* M45a against watermelon *Fusarium* wilt. *PLoS One* 17:e0272702. doi: 10.1371/journal.pone.0272702





## OPEN ACCESS

## EDITED BY

Eric Altermann,  
Massey University, New Zealand

## REVIEWED BY

Parul Chaudhary,  
Graphic Era Hill University, India  
Rubea Devi,  
Eternal University, India  
Sudhir K. Upadhyay,  
Veer Bahadur Singh Purvanchal University, India

## \*CORRESPONDENCE

Mohsin Tariq  
✉ mhsintariq@gcu.edu.pk;  
✉ mruaf@hotmail.com  
Muhammad Shafiq Shahid  
✉ mshahid@squ.edu.om

RECEIVED 20 January 2023

ACCEPTED 15 November 2023

PUBLISHED 04 December 2023

## CITATION

Zahra ST, Tariq M, Abdullah M, Zafar M,  
Yasmeen T, Shahid MS, Zaki HEM and  
Ali A (2023) Probing the potential of salinity-  
tolerant endophytic bacteria to improve the  
growth of mungbean [*Vigna radiata* (L.)  
Wilczek].  
*Front. Microbiol.* 14:1149004.  
doi: 10.3389/fmicb.2023.1149004

## COPYRIGHT

© 2023 Zahra, Tariq, Abdullah, Zafar, Yasmeen,  
Shahid, Zaki and Ali. This is an open-access  
article distributed under the terms of the  
[Creative Commons Attribution License \(CC BY\)](https://creativecommons.org/licenses/by/4.0/).  
The use, distribution or reproduction in other  
forums is permitted, provided the original  
author(s) and the copyright owner(s) are  
credited and that the original publication in this  
journal is cited, in accordance with accepted  
academic practice. No use, distribution or  
reproduction is permitted which does not  
comply with these terms.

# Probing the potential of salinity-tolerant endophytic bacteria to improve the growth of mungbean [*Vigna radiata* (L.) Wilczek]

Syeda Tahseen Zahra<sup>1</sup>, Mohsin Tariq <sup>1\*</sup>, Muhammad Abdullah<sup>1</sup>,  
Marriam Zafar<sup>1</sup>, Tahira Yasmeen<sup>2</sup>, Muhammad Shafiq Shahid <sup>3\*</sup>,  
Haitham E. M. Zaki<sup>4,5</sup> and Amanat Ali<sup>6</sup>

<sup>1</sup>Department of Bioinformatics and Biotechnology, Government College University Faisalabad, Faisalabad, Punjab, Pakistan, <sup>2</sup>Department of Environmental Sciences, Government College University Faisalabad, Faisalabad, Punjab, Pakistan, <sup>3</sup>Department of Plant Sciences, College of Agricultural and Marine Sciences, Sultan Qaboos University, Muscat, Oman, <sup>4</sup>Horticulture Department, Faculty of Agriculture, Minia University, El-Minia, Egypt, <sup>5</sup>Applied Biotechnology Department, University of Technology and Applied Sciences-Sur, Sur, Oman, <sup>6</sup>Nuclear Institute of Agriculture (NIA), Tandojam, Pakistan

Soil salinity is one of the major limiting factors in plant growth regulation. Salinity-tolerant endophytic bacteria (STEB) can be used to alleviate the negative effects of salinity and promote plant growth. In this study, thirteen endophytic bacteria were isolated from mungbean roots and tested for NaCl salt-tolerance up to 4%. Six bacterial isolates, TMB2, TMB3, TMB5, TMB6, TMB7 and TMB9, demonstrated the ability to tolerate salt. Plant growth-promoting properties such as phosphate solubilization, indole-3-acetic acid (IAA) production, nitrogen fixation, zinc solubilization, biofilm formation and hydrolytic enzyme production were tested *in vitro* under saline conditions. Eight bacterial isolates indicated phosphate solubilization potential ranging from 5.8–17.7  $\mu\text{g mL}^{-1}$ , wherein TMB6 was found most efficient. Ten bacterial isolates exhibited IAA production ranging from 0.3–2.1  $\mu\text{g mL}^{-1}$ , where TMB7 indicated the highest potential. All the bacterial isolates except TMB13 exhibited nitrogenase activity. Three isolates, TMB6, TMB7 and TMB9, were able to solubilize zinc on tris-minimal media. All isolates were capable of forming biofilm except TMB12 and TMB13. Only TMB2, TMB6 and TMB7 exhibited cellulase activity, while TMB2 and TMB7 exhibited pectinase production. Based on *in vitro* testing, six efficient STEB were selected and subjected to the further studies. 16S rRNA gene sequencing of efficient STEB revealed the maximum similarity between TMB2 and *Rhizobium pusense*, TMB3 and *Agrobacterium leguminum*, TMB5 and *Achromobacter denitrificans*, TMB6 and *Pseudomonas extremorientalis*, TMB7 and *Bradyrhizobium japonicum* and TMB9 and *Serratia quinivorans*. This is the first international report on the existence of *A. leguminum*, *A. denitrificans*, *P. extremorientalis* and *S. quinivorans* inside the roots of mungbean. Under controlled-conditions, inoculation of *P. extremorientalis* TMB6, *B. japonicum* TMB7 and *S. quinivorans* TMB9 exhibited maximum potential to increase plant growth parameters; specifically plant dry weight was increased by up to 52%, 61% and 45%, respectively. Inoculation of *B. japonicum* TMB7 displayed the highest potential to increase plant proline, glycine betaine and total soluble proteins contents by 77%, 78% and 64%, respectively, compared to control under saline conditions. It is suggested that the efficient STEB could be used as biofertilizers for mungbean crop productivity under saline conditions after field-testing.

## KEYWORDS

mungbean, biofertilizer, salt-tolerance, endophytic bacteria, *Bradyrhizobium japonicum*

## Introduction

Mungbean [*Vigna radiata* (L.) Wilczek] is a highly nutritious food and considered as the most important pulse crop worldwide. It is preferred in our daily diet due to the presence of sulfur comprising amino acids and high phosphorus content. The global mungbean cultivated area is approximately 7.3 million hectares with an average yield of 721 kg ha<sup>-1</sup> (Nair and Schreinemachers, 2020). This crop has a strategic position in Asian countries for its nutritional security, being rich in carbohydrates, proteins, vitamins and minerals. In Pakistan, the total area under cultivation of mungbean is approximately 302,000 hectare with a production of 264,000 tonne (Javed et al., 2021; Economic Survey of Pakistan, 2021–2022). Mungbean seeds are highly nutritious, containing 59–65% carbohydrates, 24–28% proteins, 3.5–4.5% fibers, 1–1.5% fats and 334–344 kcal energy (Sehrawat et al., 2021). Mungbean is used as a staple food in different Asian countries including Pakistan, Thailand, India and the Philippines (Delic et al., 2009).

The production of legume grains retards due to numerous abiotic stresses, particularly salt stress, which impairs the activity of symbiotic bacteria and reduces the plant growth (Pataczek et al., 2018; Kartik et al., 2021). Salinity negatively impacts plant physiological activities by plant dehydration, disrupting ionic and osmotic balance, which ultimately causes plant death (Shahzad et al., 2017; Majeed and Muhammad, 2019). Mungbean is highly sensitive towards salinity with a threshold level of electrical conductivity (EC) of 1.8 dS m<sup>-1</sup> (Pataczek et al., 2018). Plants adopt different strategies such as antioxidant synthesis, osmosensing and maintaining the ionic-homeostasis to cope with salt stress (Chauhan et al., 2022). Ecofriendly salt-tolerant plant growth-promoting bacteria (PGPB) are promiscuous to improve these mechanisms of plants to tolerate salinity.

The agriculture sector largely relies on the synthetic fertilizers, specifically urea and diammonium phosphate (Economic Survey of Pakistan, 2021–2022). Chemical fertilizers are made up of salts of nitrate, ammonium, phosphorus, and potassium, as well as a variety of heavy metals and regular nucleosides (Sabry, 2015). Chemical fertilizer use has increased dramatically in recent years. Careless use of chemical fertilizer results in the accumulation of heavy metals in plant structures, which then infiltrate our food chain (Savci, 2012; Alsafran et al., 2022). It can pollute our environment by contaminating water, soil and air, which entails huge environmental costs and pose serious threats to human health. Extensive use of chemical fertilizers has distorted the nitrogen cycle and other biological processes; prompting global concerns about increased emission of nitrogen oxides, soil acidification and water eutrophication (Fox et al., 2007; Conway and Pretty, 2013; Singh et al., 2019). Widespread application of fertilizers, urbanization, large scale farming and improper farming practices are some of the major causes of soil salinity. The soil salinization is increasing day by day and contaminates agricultural land (Upadhyay and Chauhan, 2022). Alternative methods are required to meet the food demand in a sustainable manner.

Biofertilizers are environment-friendly alternatives to chemical fertilizers. Biofertilizers contain PGPB, which can be applied to the soil or seed surfaces to promote plant growth by improving nutrient availability to plants and controlling phytopathogens (Agri et al., 2022; Valle-Romero et al., 2023). Biofertilizers are host specific, so the nutrients provided by them are less prone to leaching and volatilization, making them ideal for sustainable agriculture (Bhardwaj et al., 2014; Simarmata et al., 2016; Imran et al., 2021). PGPB improve plant growth directly by a variety of mechanisms, primarily including nitrogen fixation, phosphate solubilization and phytohormone production; and indirectly by bioantagonism and inducing systemic resistance (Upadhyay et al., 2022). These beneficial bacteria are mostly present in the plant rhizosphere, root interior and inside nodules. Efficiency of biofertilizers reduces due to the salt stress, as salinity impairs the bacterial cell metabolism and reduces the production of plant growth-promoting substances (Deshwal and Kumar, 2013). The high salt concentration adversely affects the important processes such as decomposition, nitrification, denitrification, soil biodiversity and microbial activity (Kumawat et al., 2022). Salt-tolerant PGPB produce phytostimulants, plant defense-related enzymes including catalases, superoxide dismutases, peroxidases and glucanases, upregulate the expression of Na<sup>+</sup>/K<sup>+</sup> ion channel proteins, which helps to maintain ionic homeostasis and increase plant growth (Chauhan and Upadhyay, 2023; Singh et al., 2023).

Endophytic bacteria have magnanimous potential to promote plant growth, since they live in the closer proximity or inside the plant (Chanway et al., 2000; Dalal and Kulkarni, 2013; Afzal et al., 2019). They are better protected from the challenging environment as they invade plant roots and reside in the root cortical region (Compant et al., 2005; Ryan et al., 2008; Zhang et al., 2020). Endophytic bacteria have a better ability to symbiotically associate with their host plants compared to rhizospheric bacteria (Bacilio-Jiménez et al., 2003). Endophytes regulate plant defense mechanisms by producing antioxidants and to mitigate the oxidative damage caused by salt stress and help plants to tolerate the stress (Jhuma et al., 2021; Chaudhary et al., 2022; Kamran et al., 2022). Moreover, they upregulate the expression of SOS1 Na<sup>+</sup>/K<sup>+</sup> antiporter which control the Na<sup>+</sup> and K<sup>+</sup> efflux to maintain ionic-homeostasis inside the plant cell (Tyagi et al., 2022). Several endophytic bacteria well-known for improving plant growth are *Burkholderia*, *Herbaspirillum*, *Pantoea*, *Gluconobacter*, *Klebsiella*, *Rahnella*, *Pseudomonas*, *Bacillus*, *Xanthomonas*, *Stenotrophomonas*, *Variovorax* (Riggs et al., 2001; Rosenblueth and Martínez-Romero, 2006; Doty et al., 2009; Rat et al., 2021).

In this study, salinity-tolerant endophytic bacteria (STEB) were isolated from the mungbean root and characterized *in vitro* for the plant growth-promoting properties under saline conditions. Potential bacteria from the *in vitro* testing were phylogenetically identified by 16S rRNA gene sequence analysis and evaluated under controlled-conditions for plant growth-promoting properties under saline conditions.

## Materials and methods

### Sample collection and isolation of endophytic bacteria

A 8-week-old Mungbean [*Vigna radiata* (L.) Wilczek] plants were collected from the cultivation site of Government College University Faisalabad, Pakistan (GPS coordinates at 31°23'42.5" N and 73°01'45.5" E). Intact roots were washed with water, and surface sterilized by dipping in 5% bleach for 2 min and 70% ethanol for 30 s. Roots were washed with sterilized water to remove the effect of chemicals. One-gram roots were separated from the plants using sterilized forceps and crushed in a sterilized mortar pestle within 3 mL saline solution (0.85% NaCl). Each root suspension was serially diluted up to  $10^{-5}$  dilution. An aliquot of 100  $\mu$ L from each dilution was spread on yeast extract mannitol (YEM) plates and incubated at  $28 \pm 2^\circ\text{C}$  for 48 h (Shahid et al., 2015; Tsegaye et al., 2019). Bacterial colonies showing different morphology were selected and purified by sub-culturing (Adamu-Governor et al., 2018). Size and shape of bacterial cells were observed under light microscope. Gram's reaction was also performed according to Wang et al. (2017).

### Screening of salt-tolerant endophytic bacteria

Salt-tolerance ability of isolated bacteria was evaluated according to Verma et al. (2020), at varying levels of NaCl concentrations. YEM broth (20 mL) in a 50 mL flask was prepared containing different concentrations of NaCl, i.e., 0.5, 0.1, 1.5, 2, 3 and 4% (w/v). Bacterial culture (0.1 mL) was inoculated in each flask and incubated at  $28 \pm 2^\circ\text{C}$  for 42 h. Bacterial culture without salt was used as control. Optical density (OD) of bacterial growth was recorded after every 6 h at 600 nm using spectrophotometer (Patil et al., 2014).

### Phosphate solubilization

Screening of phosphate solubilizing bacteria was performed according to Oo et al. (2020) with some modifications. A single colony of bacterial isolate was spotted on Pikovskaya's agar plate supplemented with 2% NaCl (w/v) and incubated at  $28 \pm 2^\circ\text{C}$  for 7 days. Halo zone formation was observed around colonies to identify phosphate solubilization potential (Linu et al., 2019; Nacoon et al., 2020). Phosphate solubilization was quantified by the Phospho-molybdate blue color method according to Khan et al. (2022). Bacterial cultures were grown in Pikovskaya's broth supplemented with 2% NaCl (w/v) and incubated at  $28 \pm 2^\circ\text{C}$  for 7 days. After incubation, bacterial cultures were centrifuged for 10 min at 13,000 rpm and 1 mL of supernatant was mixed with 0.2 mL Phospho-molybdate reagent, blue color production was observed, and absorbance was recorded at 882 nm using spectrophotometer. A phosphate standards curve was prepared to quantify phosphate concentration of samples (Behera et al., 2017).

### Indole-3-acetic acid production

Indole-3-acetic acid (IAA) production of bacterial isolates was determined by Salkowski's calorimetric assay. Bacterial cultures

were grown in YEM broth, supplemented with L-tryptophan ( $100 \mu\text{g mL}^{-1}$ ) and 2% NaCl (w/v), incubated at  $28 \pm 2^\circ\text{C}$  for 48 h and centrifuged at 12,000 rpm for 10 min. Salkowski's reagent (4 mL) was mixed with 1 mL of supernatant, gently mixed and incubated for 30 min at room temperature (Bhattacharyya et al., 2020). Pink coloration was taken as indication of IAA production and its absorbance was measured at 530 nm using spectrophotometer. An IAA standards curve was prepared to quantify IAA concentration of samples (Myo et al., 2019; Hyder et al., 2020).

### Nitrogen fixation

The ability of bacterial isolates to fix nitrogen was tested by inoculating a single colony on solid nitrogen free media [containing ( $\text{g L}^{-1}$ ) mannitol 20 g,  $\text{K}_2\text{HPO}_4$  0.2 g, NaCl 0.2 g,  $\text{MgSO}_4$  0.2 g,  $\text{K}_2\text{SO}_4$  0.1 g,  $\text{CaCO}_3$  5.0 g, agar 20 g] supplemented with 2% NaCl (w/v) and incubated at  $28 \pm 2^\circ\text{C}$  for 48 h. After incubation, nitrogen fixation was determined based on the bacterial growth and recorded as arbitrary values weak (+), moderate (++), strong (+++) or negative (−) (Hardarson and Danso, 1993; Mirza and Rodrigues, 2012).

### Zinc mobilization

*In vitro* qualitative screening of zinc solubilizing bacterial isolates was measured by adopting the protocol of Ramesh et al. (2014), with some modifications. Tris-minimal agar (TMA) medium supplemented with 2% NaCl (w/v), containing insoluble 0.1% zinc source, i.e., ZnO and  $\text{ZnCO}_3$ , separately. Supplemented TMA plates were spot inoculated with freshly grown bacterial cultures and incubated in the dark at  $28 \pm 2^\circ\text{C}$  for 7 days. Halo zone formation around the bacterial colony was observed and zinc solubilization efficiency (ZSE) was calculated according to the formula (Rezaeiniko et al., 2022; Upadhyay et al., 2022).

$$\text{ZSE} = \left( \frac{\text{diameter of solubilization halo}}{\text{diameter of the colony}} \right) \times 100.$$

### Cellulase and pectinase activity assay

Cellulolytic activity of bacterial isolates was assessed by spot inoculating individual colonies onto carboxymethyl cellulose ( $10 \text{ g L}^{-1}$ ) agar plates supplemented with 2% NaCl (w/v) and incubated at  $28 \pm 2^\circ\text{C}$  for 3 days (Islam and Roy, 2018). Plates were stained with 0.2% Congo red dye for 15 min and washed with distilled water. The appearance of a halo zone around the colony indicates cellulase activity of bacteria (Suárez-Moreno et al., 2019).

Pectinase production was determined by inoculating bacterial colonies onto pectin ( $10 \text{ g L}^{-1}$ ) agar plates, supplemented with 2% NaCl (w/v) and incubated at  $28 \pm 2^\circ\text{C}$  for 7 days (Devi et al., 2022). Plates were stained with 1% iodine solution for 15 min and washed with distilled water. The formation of a halo zone around the colony indicated pectinase activity of bacterial cultures (Tsegaye et al., 2019).

## Biofilm formation assay

Biofilm formation by bacterial isolates was tested according to Zahra et al. (2023), by using a microtiter plate. Bacterial isolates were grown up to an optical density ( $OD_{600\text{ nm}}$ ) of 2 in YEM broth medium, supplemented with 2% NaCl (w/v). Bacterial cultures were centrifuged at 6,000 rpm for 2 min. The supernatant was discarded and the pellet was washed with sterile water. The bacterial cells were resuspended in fresh YEM broth and diluted to an  $OD_{600\text{ nm}}$  of 0.2. An aliquot (150  $\mu\text{L}$ ) of each bacterial cell suspension was added to 96-well polyvinyl chloride (PVC) plate in six replicates and incubated at 28°C for 48 h. After incubation, each bacterial culture was removed from wells and gently washed with sterilized water. Wells were stained with 150  $\mu\text{L}$  of crystal violet (0.001%) for 15 min. After staining, crystal violet was removed, and wells were washed with sterilized water and air dried. Crystal violet dye absorbed by the wells was solubilized by adding 150  $\mu\text{L}$  of 95% ethanol. Biofilm formation was quantified by measuring the amount of absorbed dye at  $OD_{570\text{ nm}}$  in a microtiter plate reader (Sampedro et al., 2020; Jhuma et al., 2021).

## Microbial compatibility assay

Microbial compatibility tests of bacterial isolates were assessed according to Tariq et al. (2014) by pour plate technique to determine the compatibility of isolates with each other. In this assay, a pairs of bacterial isolates was designated as A and B, and checked for compatibility. Log phase grown culture of isolate A was diluted to  $10^4\text{ cfu mL}^{-1}$  and 3 mL of the culture was mixed in 25 mL hand-cool molten nutrient agar medium. It was poured into Petri plates and incubated at  $28 \pm 2^\circ\text{C}$  for 24 h. Concentrated culture (3  $\mu\text{L}$ ) of isolate B was inoculated in the center of the plate and incubated at  $28 \pm 2^\circ\text{C}$  for 48 h. The zone of inhibition that developed around bacterial isolate B was recorded. The appearance of a zone of inhibition represented that the bacterial pair was not compatible with each other, represented by a red box. If no zone of inhibition appeared, the bacterial pair was considered compatible and represented by a green box. Each isolate pair was tested in this manner, and compatibility and non-compatibility was presented as green and red box, respectively (Zul et al., 2022).

## Molecular identification and phylogenetic analysis of efficient endophytic bacteria

Six efficient STEB were identified phylogenetically by sequencing the 16S rRNA gene, according to La Pierre et al. (2017). The 16S rRNA gene was amplified using universal primers fD1 (5'-AGAGTTTGATCCTGGCTCAG-3') and rD1 (5'-AAGGAGGTGATCCAGCC-3') (Weisburg et al., 1991). A 25  $\mu\text{L}$  reaction mixture was prepared for 16S rRNA gene amplification by using the PCR recipe [10X Taq polymerase buffer 2.5  $\mu\text{L}$ , 2 mM dNTPs 2.5  $\mu\text{L}$ , (10 pmoles  $100\text{ }\mu\text{L}^{-1}$ ) primers fD1 & rD1 2  $\mu\text{L}$ , 25 mM MgCl 2  $\mu\text{L}$ , (5 U  $\mu\text{L}$ ) Taq polymerase enzyme 0.3  $\mu\text{L}$ , H<sub>2</sub>O 11.7  $\mu\text{L}$ , (20 ng  $\mu\text{L}^{-1}$ ) template DNA 2  $\mu\text{L}$ ]. The reaction mixture was placed in a thermocycler for amplification and adjusted initial denaturation to 5 min at 94°C, followed by 30 cycles of denaturation at 94°C for 60 s, primer annealing at 55°C for 50 s, primer extension at 72°C for

1 min 40 s and final extension at 72°C for 5 min. After amplification, the amplicons were examined in a gel documentation system on 1% agarose gel. The amplified products were purified through ThermoScientific GeneJET PCR Purification Kit and Sanger sequenced using the commercial service of Macrogen, Korea. Forward and reverse sequences were assembled manually and compared with database sequences by using NCBI BLAST tool (Altschul, 1990). Closely related authentic sequences were retrieved from databases, and pairwise sequence comparisons were performed using Sequence Demarcation Tool (SDT) v.1.2 (Zhang et al., 2000; Muhire et al., 2014). A phylogenetic tree was constructed using the maximum likelihood method as implemented by MEGA 11 with 1,000 bootstrap values (Kumar et al., 2016; Noori et al., 2021).

## Controlled-conditions experiment and biochemical analysis

The controlled-condition experiment was conducted on mungbean cultivar NM-2021 with eight treatments (TMB2, TMB3, TMB5, TMB6, TMB7, TMB9, consortia and water as control) in completely randomized design (CRD) with four replicates. Freshly grown bacterial culture was centrifuged (6,000 rpm) and bacterial pellet was resuspended in sterilized water adjust OD 0.5 (Mishra et al., 2009). Seeds were surface sterilized with 5% bleach for 2 min and washed with sterilized water. Surface-sterilized seeds were placed on Petri plates containing moist filter paper and incubated at  $25 \pm 2^\circ\text{C}$  in a dark room for 2 days. Uniformly sized seedlings were transferred into pots containing sterilized soil, supplemented with 1% NaCl. Plants were placed in a growth chamber at  $35 \pm 2^\circ\text{C}$  during the day and  $25 \pm 2^\circ\text{C}$  at night. Bacterial culture (100  $\mu\text{L}$ ) of each treatment was applied to the roots of each plant. Plants were watered with 10 mL of quarter-strength nitrogen-free Hoagland's solution and sterilized water on alternating days. Plants were harvested after 6 weeks of germination and agronomical parameters including root length, shoot length, plant fresh weight, plant dry weight and number of nodules per plant were recorded (Tounsi-Hammami et al., 2022). The agronomical data was statistically analyzed using CoStat window version software (Cardinali and Nason, 2013).

## Proline contents

Proline contents were determined according to Bates et al. (1973) with some modifications. Leaf samples (0.5 g) were ground in liquid nitrogen and 10 mL chilled K-P buffer was added. The mixture was centrifuged at 13,000 rpm for 5 min. Supernatant (0.5 mL) was transferred in a test tube containing 1 mL of 3% sulphosalicylic acid and incubated at 95°C for 5 min in a water bath. After incubation, the mixture was cooled down at room temperature and 1 mL of glacial acetic acid and ninhydrin was gently added, mixed and incubated at 95°C for 20 min in a water bath. The mixture was immediately cooled down on ice. Toluene (2 mL) was added in the mixture, vortexed and incubated at room temperature for 20 min. After incubation, two layers were developed. The upper layer was carefully collected and absorbance was recorded at 520 nm using spectrophotometer. The proline contents were measured by comparing the absorbance with standard curve (Sapre et al., 2022).



TABLE 1 Colony and cell morphology of mungbean root endophytic bacteria.

| Isolate | Colony morphology                                   | Cell morphology | Gum production | Gram staining |
|---------|---|-----------------|----------------|---------------|
| TMB1    | Medium, double ringed, light pink, smooth, flat     | Small rod       | +              | +             |
| TMB2    | Large, circular, milky white, smooth, flat          | Rod             | +              | –             |
| TMB3    | Very small, circular, white, smooth, flat           | Rod             | +              | –             |
| TMB4    | Very small, circular, pink, wavy, flat              | Circular        | –              | +             |
| TMB5    | Small, circular, light yellowish, smooth, flat      | Small rod       | +              | –             |
| TMB6    | Large, irregular, yellowish, wavy, flat             | Rod             | +              | –             |
| TMB7    | Small, circular, light pink, smooth, flat           | Small rod       | +              | –             |
| TMB8    | Medium, circular, milky white, wavy, flat           | Circular        | +              | +             |
| TMB9    | Small, circular, pink, wavy, flat                   | Rod             | –              | –             |
| TMB10   | Small, irregular, white, wavy, flat                 | Circular        | +              | –             |
| TMB11   | Small, circular, milky white, smooth, flat          | Rod             | –              | –             |
| TMB12   | Very small, circular, white, smooth, flat           | Small rod       | –              | +             |
| TMB13   | Very small, circular, yellowish white, smooth, flat | Rod             | +              | –             |

## Total soluble proteins

Total soluble proteins were quantified according to Bradford (1976) modified method. Leaf samples (0.5 g) were ground in chilled K-P buffer. After grinding, the mixture was centrifuged at 13,000 rpm for 5 min. Supernatant (0.1 mL) was collected, Bradford reagent (1 mL) was added and incubated at room temperature for 30 min in dark. After incubation, absorbance was recorded at 595 nm using spectrophotometer. Total soluble proteins were measured by comparing the absorbance with standard curve.

## Glycine betaine

Glycine betaine in leaf tissues was estimated by following the modified protocol of Nawaz and Wang (2020). Fresh leaf samples (0.5 g) were ground in 10 mL chilled K-P buffer, vortexed and centrifuged at 13,000 rpm for 5 min. Supernatant (0.5 mL) was collected in a separate test tube and 1 mL of H<sub>2</sub>SO<sub>4</sub> was added. KI<sub>3</sub> (0.2 mL) was added into the reaction mixture and incubated at –4°C for 90 min. After incubation, 2.8 mL chilled dH<sub>2</sub>O and 6 mL of 1–2 dichloroethane was added into the mixture and incubated at room temperature for 30 min. Two layers were formed. The lower layer of red color was collected carefully, and absorbance was measured at 365 nm using a spectrophotometer. Quantify of glycine betaine contents was measured by comparing the absorbance with the standard curve.

## Results and discussion

### Isolation of endophytic bacteria

Bacterial colonies were observed on the plates after incubation. Based on colony size, shape, color, edges, surface and gum production, thirteen bacterial morphotypes were selected. Cell morphology of all bacterial isolates was rod shaped, except TMB4, TMB8 and TMB10, which showed circular cell shape. Only four bacterial isolates, TMB1, TMB4, TMB8 and TMB12, were Gram's positive, while the rest of the bacteria were Gram's negative (Table 1). Legume roots contain a large array of endophytic bacteria, which may play an important role in

plant growth promotion directly and indirectly (Bhutani et al., 2018a). Our results are in agreement with several studies that confirmed the occurrence of bacteria in the legume root samples. Chaudhary et al. (2021) isolated *Rhizobium pusense* from the roots of mungbean and evaluated its plant growth-promoting properties. Bhutani et al. (2021) also isolated endophytic bacteria from surface sterilized roots of mungbean that demonstrated high potential to improve plant growth. Abedinzadeh et al. (2019) also isolated endophytic bacteria from roots of maize and reported that these bacteria have the ability to tolerate salinity and increase plant growth. Similarly, Hung and Annapurna (2004) also isolated 65 endophytic bacteria from soybean root and nodules.

### Screening of salt-tolerant endophytic bacteria

Salinity tolerance was examined in mungbean isolates at different NaCl concentrations ranging from 0.5–4%. There was significant inhibition in bacterial growth at 3 and 4% NaCl concentration. Six bacterial isolates, TMB2, TMB3, TMB5, TMB6, TMB7 and TMB9, were able to tolerate salinity level up to 2% NaCl concentration (Figure 1), whereas three isolates, TMB1, TMB8 and TMB10, showed minor growth inhibition at 2% NaCl. The remaining four isolates, TMB4, TMB11, TMB12 and TMB13, showed significant growth inhibition at 2% NaCl salinity concentration (Supplementary Table S1). Salinity is one of the major problems for crop productivity in Pakistan due to the presence of salt contents in the soil and water (Vaishnav et al., 2019; Kartik et al., 2021). Adaptability of the bacterial inoculants to the stressed environment of any cultivation region is considered as a promiscuous feature for its use as biofertilizers (Pérez-Rodríguez et al., 2020). Recently, Kumar et al. (2021) screened salt tolerant bacteria at different concentrations of NaCl and further characterized them for plant growth promotion. Khan et al. (2015) also isolated rhizospheric and endophytic bacteria, and reported that these bacterial isolates tolerate higher concentrations of NaCl. Salinity affected soil is defined as a soil that has electrical conductivity (EC) value greater than 4 dS m<sup>–1</sup> (Munns and James, 2003). EC value of 4

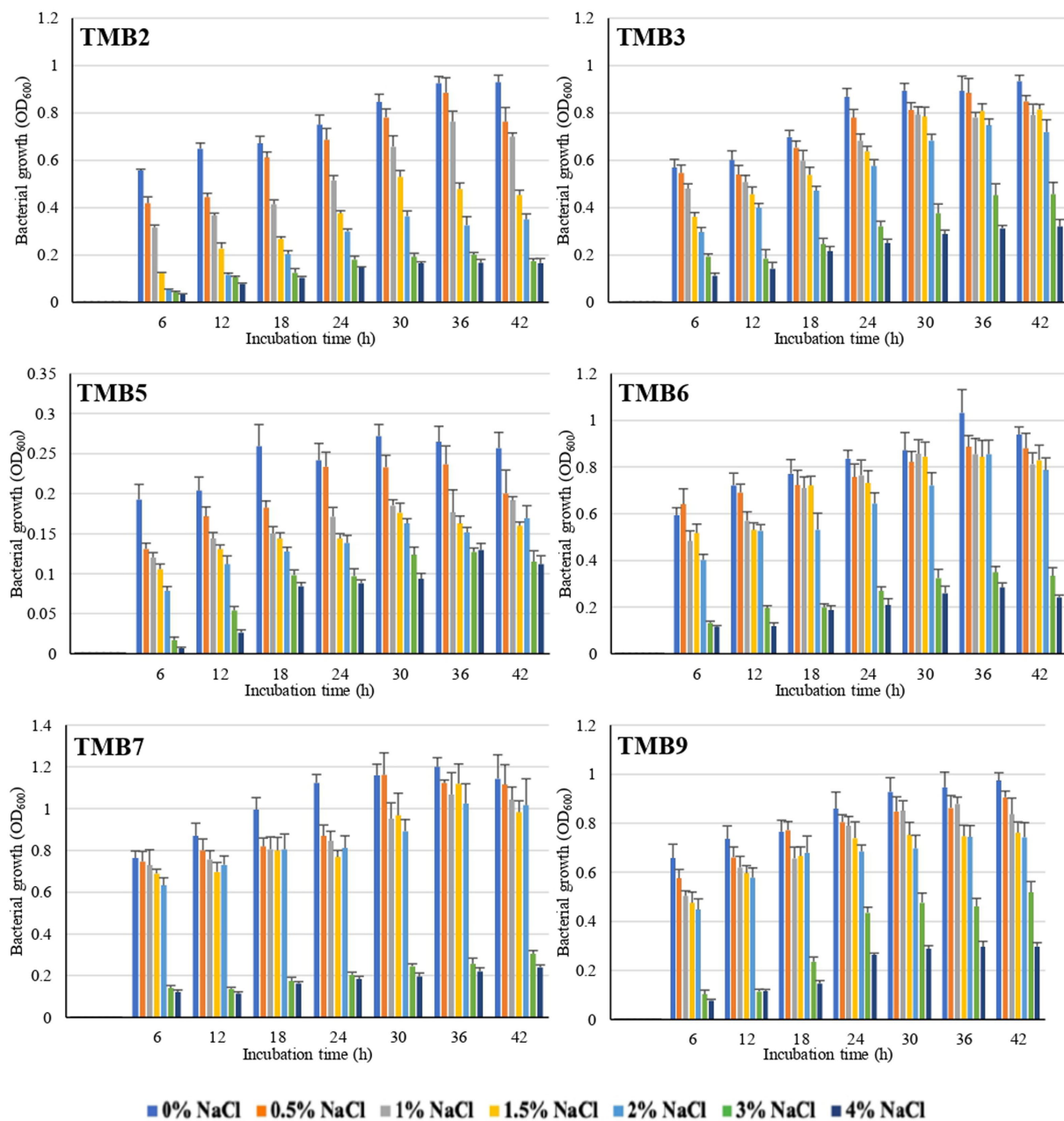


FIGURE 1

Graphical representation of mungbean root endophytic bacteria to tolerate salinity at different salt concentrations. Six bacterial isolates, TMB2, TMB3, TMB5, TMB6, TMB7 and TMB9, displayed salt-tolerance and grew well upto 2% NaCl. Growth readings of all bacterial isolates under saline conditions are mentioned in the [Supplementary material](#).

$\text{dS m}^{-1}$  is equal to 0.22% NaCl concentration and EC value of  $25.8 \text{ dS m}^{-1}$  is equal to 2% NaCl concentration (observation during lab general experiments). Therefore, the potential endophytic bacteria exhibited salt tolerance ability up to 2% NaCl concentration were considered potential candidates for their use as biofertilizers at salinity affected soils. 2% NaCl is the highest realistic-concentration of salt to test microbes for salinity-tolerance, as it is the maximum concentration reported at most of the salinized land worldwide. The world's well-known saline sites including Solonchaks (Russia), Halosols (China) and Salida (United States) have an EC ranging  $8\text{--}15 \text{ dS m}^{-1}$  (Egamberdieva et al., 2019). Soil and irrigation water in Pakistan

generally have high soluble salt contents, which is a major limiting factor for plant growth. The value of EC in heavily salt affected soil of Pakistan at Uchhali Lake in the Salt Range region is  $15.42 \text{ dS m}^{-1}$ , which is equal to 1.2% NaCl (Hameed et al., 2009). A concentration higher than 2% salinity is very stringent to test bacterial salt-tolerance and might result in losing too many potential bacteria. Cortés-Lorenzo et al. (2015) demonstrated that higher levels of salinity inhibited the nitrification process of nitrite-oxidizing bacteria. Hong et al. (2013) also reported that higher salinity can reduce the metabolic activity of microorganisms, results in bacterial growth inhibition and cell death. As the tested bacteria of the current study demonstrated

TABLE 2 *In vitro* testing of plant growth-promoting attributes of mungbean root endophytic bacteria.

| Isolates | Phosphate Solubilization ( $\mu\text{g mL}^{-1}$ ) | IAA Production ( $\mu\text{g mL}^{-1}$ ) | Nitrogen fixation | Zinc solubilization efficiency (ZnO) | Zinc solubilization efficiency ( $\text{ZnCO}_3$ ) | Cellulase activity index | Pectinase activity index | Biofilm formation ( $\text{OD}_{570\text{nm}}$ ) |
|----------|--|--|-------------------|--------------------------------------|--|--------------------------|--------------------------|--|
| TMB1     | 0  | $6.8 \pm 0.4$                            | +                 | 0                                    | 0  | 0                        | 0                        | $0.11 \pm 0.012$                                 |
| TMB2     | $8.1 \pm 0.44$                                     | $1.1 \pm 0.18$                           | +++               | 0                                    | 0  | 1.66                     | 1.2                      | $0.53 \pm 0.049$                                 |
| TMB3     | $5.8 \pm 0.32$                                     | $3.3 \pm 0.28$                           | ++                | 0                                    | 0  | 0                        | 0                        | $1.59 \pm 0.043$                                 |
| TMB4     | 0  | 0  | +                 | 0                                    | 0  | 0                        | 0                        | $0.63 \pm 0.039$                                 |
| TMB5     | $7.9 \pm 0.46$                                     | $1 \pm 0.19$                             | ++                | 0                                    | 0  | 0                        | 0                        | $0.91 \pm 0.021$                                 |
| TMB6     | $17.7 \pm 0.62$                                    | $1.4 \pm 0.33$                           | ++                | 260%                                 | 200%   | 1.75                     | 0                        | $2.59 \pm 0.041$                                 |
| TMB7     | $17.23 \pm 0.22$                                   | $12.1 \pm 0.51$                          | +++               | 237%                                 | 177%   | 1.5                      | 1.4                      | $1.83 \pm 0.041$                                 |
| TMB8     | $16.9 \pm 0.33$                                    | $3 \pm 0.18$                             | +                 | 0                                    | 0  | 0                        | 0                        | $1.55 \pm 0.032$                                 |
| TMB9     | $13.8 \pm 0.68$                                    | $4.6 \pm 0.27$                           | +++               | 233%                                 | 140%   | 0                        | 0                        | $1.41 \pm 0.052$                                 |
| TMB10    | $11.2 \pm 0.6$                                     | $0.3 \pm 0.33$                           | ++                | 0                                    | 0  | 0                        | 0                        | $0.96 \pm 0.02$                                  |
| TMB11    | 0  | 0  | +                 | 0                                    | 0  | 0                        | 0                        | $0.51 \pm 0.029$                                 |
| TMB12    | 0  | 0  | +                 | 0                                    | 0  | 0                        | 0                        | 0  |
| TMB13    | 0  | $2.8 \pm 0.12$                           | 0                 | 0                                    | 0  | 0                        | 0                        | 0  |

salinity-tolerance upto 2% NaCl concentration, the beneficial characteristics of these bacteria may remain unaffected even in the saline environment. Such bacteria are promising to be used as biofertilizers for crop production at salinity affected soil and the farmland irrigated with saline-water. It is strongly suggested that biofertilizer bacteria should be tested for salt stress tolerances before application, as most of the irrigation water and soils are affected with high concentration of salts.

## Characterization of STEB for plant growth-promoting properties

Phosphate solubilization was examined in mungbean isolates under saline conditions. Out of 13 mungbean isolates, TMB2, TMB3, TMB5, TMB6, TMB7, TMB8, TMB9 and TMB10, showed phosphate solubilization ranging from  $5.8$ – $17.7 \mu\text{g mL}^{-1}$ . TMB6 exhibited the highest phosphate solubilization ability, whereas TMB3 exhibited the lowest phosphate solubilization ability (Table 2). Phosphate is one of the most crucial nutrients for balanced plant growth. Deficiency of phosphate in plants usually results in stunted growth of plants (Lun et al., 2018). Previously, Hakim et al. (2020) isolated endophytic bacteria from mungbean and explained the phosphate solubilizing potential of these bacteria upto  $195 \mu\text{g mL}^{-1}$ . Recently, Belkebla et al. (2022) demonstrated that halotolerant PGPB isolated from south of Algeria exhibit phosphate solubilizing potential and improve wheat growth. Mahdi et al. (2021) also reported that halotolerant endophytic bacteria have the ability to solubilize phosphate and promote seed germination. Likewise, Mei et al. (2021) also demonstrated that endophytic bacteria have the potential to solubilize phosphate and their application resulted in increased pepper and tomato growth.

IAA was quantified by spectrophotometric pink coloration estimation method. Ten isolates, TMB1, TMB2, TMB3, TMB5, TMB6, TMB7, TMB8, TMB9, TMB10 and TMB13, showed IAA production ranging from  $0.3$ – $12.1 \mu\text{g mL}^{-1}$  at 2% NaCl supplementation. TMB7

showed the highest production of IAA, whereas TMB10 showed the lowest production of IAA (Table 2). IAA is a phytohormone also produced by many bacteria, which is involved in cell division, cell enlargement and root elongation (Bhutani et al., 2018b). Our results are in agreement with Widowati and Sukiman (2019), who reported IAA production up to  $12.28 \mu\text{g mL}^{-1}$  in the endophytic bacteria of mungbean. Saleem et al. (2021) also demonstrated the mitigating efficiency of IAA production from salt tolerant bacteria isolated from cotton. Jabborova et al. (2020) also reported that endophytic bacteria have ability to produce IAA. Recently, Desai et al. (2023) explained the ability of salt-tolerant PGPB isolated from mungbean to produce IAA under salt stress. IAA production is one of the very important features for the screening of plant beneficial bacteria.

Nitrogen fixation ability of mungbean root endophytic bacteria was tested by growing bacteria on NFM agar plates. All isolates showed nitrogen fixation ability except TMB13 under saline conditions. TMB2, TMB7 and TMB9 showed highest ability (Table 2). Nitrogen is the most important element for plant growth and development. Bacteria produce nitrogenase enzyme to fix the atmospheric nitrogen (Gu et al., 2018). Favero et al. (2021a) isolated the nodule endophytic bacteria from the mungbean, which showed nodule formation and nitrogen fixation capability. *Bradyrhizobium* sp. exhibited the maximum potential for nodulation and nitrogen fixation. Tang et al. (2020) also reported that endophytic bacteria have the potential to fix biological nitrogen in tropical forest soil. Zhang et al. (2022) also identified that endophytic bacteria isolated from cassava roots exhibit nitrogen fixation ability. Potential root-associated bacteria can fix atmospheric nitrogen and alleviate nutrient stress in plants.

Zinc is an essential micronutrient involved in several cellular processes including metabolism, mitochondrial activity mitosis and cell development. It mainly participates in the redox reactions and works as a catalyst for enzymes (Ditta et al., 2022). Out of 13 root endophytic bacteria of mungbean, only three isolates, TMB6, TMB7 and TMB9, were able to solubilize zinc on tris minimal media

supplemented with zinc oxide and zinc carbonate under saline conditions. TMB6 showed higher solubilization efficiency of 260% in zinc oxide and 200% in zinc carbonate media (Table 2). Previously, Singh et al. (2020) explained the zinc solubilizing ability of *Burkholderia arboris* and demonstrated the positive role of its inoculation in mungbean cultivation. Zinc solubilizing potential of bacteria was reported by several studies, which play crucial roles in soil fertility (Rani et al., 2022; Verma et al., 2022). Similarly, Ali et al. (2022) also demonstrated that endophytic bacteria have the potential to solubilize zinc and their combination with synthetic fertilizer significantly increased the plant growth compared to the sole application of chemical fertilizer.

Cellulase and pectinase activity of mungbean rhizobacteria was observed on NaCl supplemented plates. Out of 13 isolates, only TMB2, TMB6 and TMB7 showed cellulase activity, where TMB6 showed highest activity with 1.75 index. Only two isolates, TMB2 and TMB7, exhibited pectinase activity (Table 2). Cellulase and pectinase belongs to the family of hydrolytic enzymes. Hydrolytic enzymes play a pivotal role in the decomposition of dead organic matter present in the soil and provide nutrients to plants (Reetha et al., 2014). Recently, Reddy et al. (2022) reported PGPR have the ability to produce hydrolytic enzymes. Bhutani et al. (2021) also isolated cellulase and pectinase producing bacteria from the mungbean endosphere, which showed plant growth-promoting (PGP) potential. Dogan and Taskin (2021) also demonstrated that endophytic bacteria isolated from *Poaceae* plant displayed cellulase and pectinase production ability. Borah et al. (2019) also reported that endophytic bacteria from tea plant exhibit cellulase and pectinase activity. Cellulase and pectinase might enable bacteria to invade the roots and nodules of host plant. Futuristic comprehensive studies should be designed to explore the role of hydrolytic enzymes in root/nodule invasion and plant growth promotion by developing cellulase and pectinase negative mutants or using other cutting-edge techniques.

Biofilm formation activity was examined in microtiter plate assay. All bacterial isolates except TMB12 and TMB13 showed biofilm formation ranging 0.11–2.59 at OD<sub>570nm</sub>. TMB6 showed the highest efficiency of biofilm formation, while TMB1 showed the lowest efficiency of biofilm formation (Table 2). Several PGPR can effectively interact with the plants root zone and form biofilm on its surface, which protects plants against environmental stresses (Ansari and Ahmad, 2018). Previously, Yasmeen et al. (2020) isolated halotolerant bacteria from saline soil and demonstrated their biofilm formation ability under salt stress. Alaa (2018) also reported that *Pseudomonas anguilliseptica* have biofilm formation potential under different levels of salts. Generally, efficient biofilm forming bacteria perform their inherent functions effectively, even in the challenging environment (Tariq et al., 2014).

Antibiosis activity of isolates was checked by growing pair of bacteria together in an overlay plate assay. Bacterial isolates, TMB1, TMB2, TMB3, TMB5, TMB6, TMB7, TMB8 and TMB9, displayed maximum compatibility to grow together. TMB7 demonstrated the highest compatibility with all isolates except TMB13 (Figure 2). Kumawat et al. (2021) demonstrated that *Rhizobium* sp. and *Enterococcus mundtii* have growth compatibility. When these bacteria applied in consortia on mungbean the growth parameters of mungbean were increased as compared to single inoculation. Latha et al. (2009) also isolated *P. fluorescens* (Pf1 and Py15) and *B. subtilis* (Bs16) from tomato

and demonstrated that all of three bacterial strains are compatible to grow together. Similarly, Ashraf et al. (2019) isolated four plant growth-promoting rhizobacteria (PGPR) isolates from wheat rhizosphere and checked their antimicrobial activity against three bacterial strains *Vibrio cholera*, *Enterobacter aerogenes*, and *Klebsiella pneumoniae*. Only one isolate showed antimicrobial activity against *K. pneumoniae* while others were compatible to each other. Compatible bacteria do not inhibit the growth of each other and perform effectively in consortium to promote plant growth.

## Phylogenetic identification of efficient STEB

Amplification of 16S rRNA gene using fD1 and rD1 primers produced approximately 1,500 bp DNA band as shown in Figure 3. After sequencing and assembling, DNA sequence contigs of more than 1,400 nt were generated. Sequences of 16S rRNA showed maximum similarity of more than 98% with the different sequences available in nucleotide databases and identified TMB2 as *Rhizobium pusense*, TMB3 as *Agrobacterium leguminum*, TMB5 as *Achromobacter denitrificans*, TMB6 as *Pseudomonas extremorientalis*, TMB7 as *Bradyrhizobium japonicum* and TMB9 as *Serratia quinivorans*. Sequences were deposited in NCBI GenBank under the accession numbers OP935921–OP935926 (Table 3). Phylogenetic tree of these sequences was constructed with 42 authentic sequences belonging to 6 identified genera using maximum likelihood method with 1,000 bootstrap value and *Methanoregula boonei* was used as outgroup. All the sequences were grouped into 3 clades belonging to common ancestor. TMB7 was placed in clade 1, TMB6, TMB5

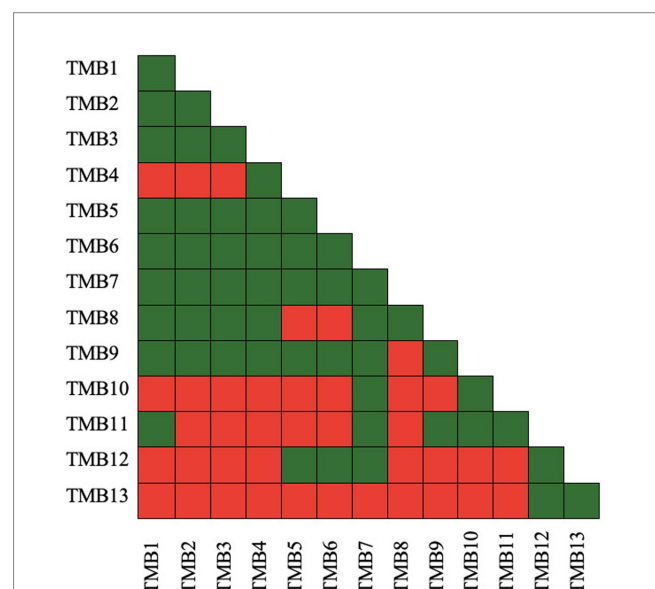
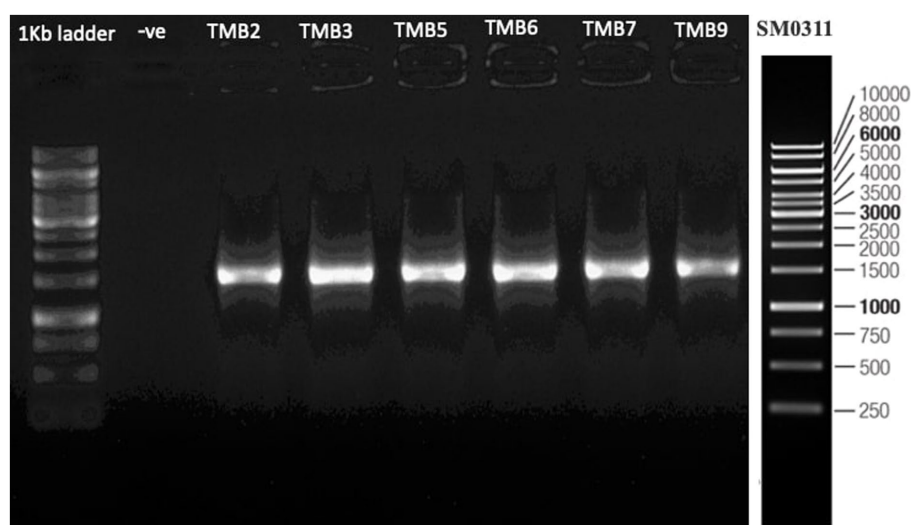


FIGURE 2

Antibiosis activity of mungbean root endophytic bacteria. Green color presents bacterial compatibility to grow together, while red color presents inhibitory interaction between bacteria. TMB7 demonstrated growth compatibility with most of the bacterial isolates, while TMB13 demonstrated growth inhibitory interaction with most of the bacterial isolates.





**FIGURE 3**  
16S rRNA gene amplification of potential bacterial isolates. Amplification of DNA bands of 1,500 bp were produced, which were confirmed by comparing with 1 kb DNA ladder.

**TABLE 3** Taxonomic identification of potential salinity-tolerant endophytic bacteria.

| Bacterial isolates | Taxonomic identification            | Percentage identity | Accession numbers |
|--------------------|-------------------------------------|---------------------|-------------------|
| TMB2               | <i>Rhizobium pusense</i>            | 98.81%              | OP935921          |
| TMB3               | <i>Agrobacterium leguminum</i>      | 99.79%              | OP935922          |
| TMB5               | <i>Achromobacter denitrificans</i>  | 99.17%              | OP935923          |
| TMB6               | <i>Pseudomonas extremorientalis</i> | 98.93%              | OP935924          |
| TMB7               | <i>Bradyrhizobium japonicum</i>     | 100%                | OP935925          |
| TMB9               | <i>Serratia quinivorans</i>         | 98.30%              | OP935926          |

and TMB9 in clade 2 and TMB2 and TMB3 in clade 3 shown in Figure 4. A color coded pairwise identity matrix was also created, in which each colored cell represents the percentage identity of two sequences. The identity percentages between the selected sequences were ranging 80–100 (Figure 5).

Existence of *Rhizobium pusense* and *Bradyrhizobium japonicum* in mungbean root has been reported in the literature. *Rhizobium pusense* colonize mungbean roots and improve plant growth by producing phytohormones (Chaudhary et al., 2021). Similarly, Nguyen et al. (2022) demonstrated the occurrence of *Rhizobium pusense* in rice and increased its growth and yield upon inoculation. Members of genus *Bradyrhizobium* dominantly exist in the roots and nodules of mungbean and soybean. Favero et al. (2021b) isolated *Bradyrhizobium japonicum* from mungbean nodules and demonstrated the positive effect on yield and growth of mungbean plant. Yasmeen et al. (2012) also explained that occurrence of *Bradyrhizobium japonicum* in mungbean. Similarly, Chhetri et al. (2019) isolated *Bradyrhizobium japonicum* from root nodules of soybean. Generally, bacteria belonging to *Rhizobia* are well-known for nitrogen fixation, which ultimately increases crop yield (Anjum et al., 2006).

In this study, we reported the occurrence of *Agrobacterium leguminum*, *Achromobacter denitrificans*, *Pseudomonas*

*extremorientalis* and *Serratia quinivorans* in the roots of mungbean for the first time. Recently, Castellano-Hinojosa et al. (2021) isolated *A. leguminum* from the *Phaseolus vulgaris* nodules and claimed it as a novel species based on the data obtained from colony morphology, sequence analysis, phylogenetic analysis and taxonomic characterization. Previously, Sultana et al. (2020) isolated *A. denitrificans* from the rice plant, which showed PGP properties under salt stress. Wang et al. (2019) isolated *P. extremorientalis* from the rhizosphere of pear plant. Kaur et al. (2022) reported the existence of *P. extremorientalis* in the endophytic region of wheat. *P. extremorientalis* improved plant growth under salt stress by reducing harmful effects of salt (Egamberdieva et al., 2016). Recently, researchers have revealed the existence of *S. quinivorans* in the oak, *Petroselinum crispum* and *Picrorhiza kurroa* (Kumar et al., 2021; Reis et al., 2021; Chlebek et al., 2022). Novel plant-bacterial associations might be due to the changes in environmental conditions.

## Biofertilizers potential of STEB under controlled-conditions

Potential isolates including TMB2, TMB3, TMB5, TMB6, TMB7, TMB9 and consortia were tested for PGP properties under

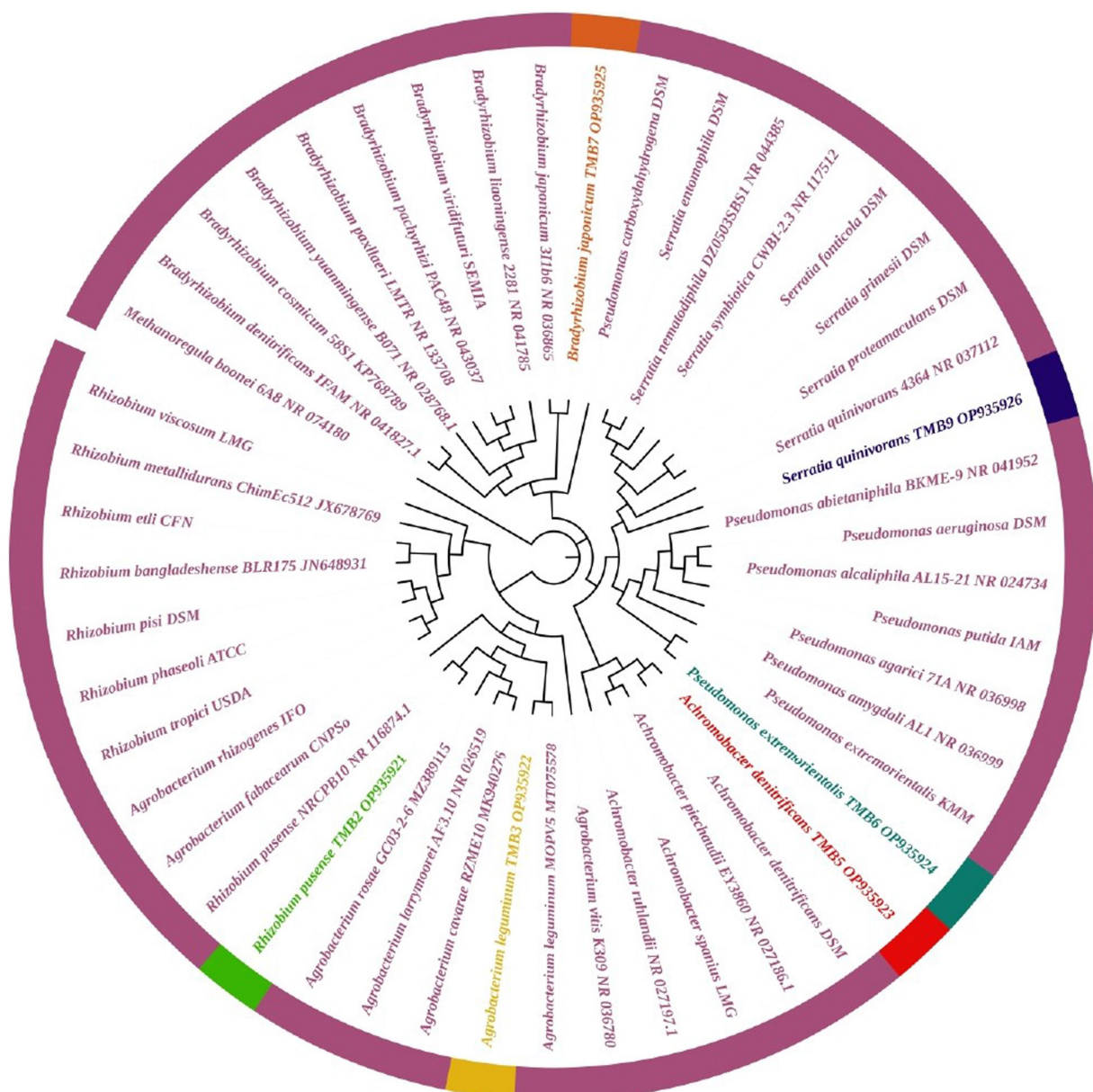


FIGURE 4

Phylogenetic tree of mungbean root endophytic bacteria. All the sequences were grouped into 3 clades. TMB2 positioned in the neighborhood of *Rhizobium pusense*, TMB3 in *Agrobacterium leguminum*, TMB5 in *Achromobacter denitrificans*, TMB6 in *Pseudomonas extremorientalis*, TMB7 in *Bradyrhizobium japonicum* and TMB9 in *Serratia quinivorans*.

controlled-conditions experiment (Supplementary Figure S1). After 6 weeks of inoculation, agronomical parameters were calculated and statistically analyzed (Table 4). Inoculation of bacterial isolates, *P. extremorientalis* TMB6, *B. japonicum* TMB7 and *S. quinivorans* TMB9, showed maximum potential in improving plant growth parameters. TMB2, TMB6 and TMB7 showed a significant increase in root length compared to control. All isolates exhibited a significant increase in shoot length compared to control except consortia. TMB6 and TMB7 showed a significant increase in plant fresh weight. *P. extremorientalis* TMB6, *B. japonicum* TMB7 and *S. quinivorans* TMB9 were most efficient and showed a significant increase in plant dry weight by 52, 61 and 45%, respectively, compared to control. Nodulation was observed by the inoculation of TMB2, TMB7 and consortia. Inoculation of *B. japonicum* TMB7 showed maximum

potential to increase plant growth parameters, i.e., root length (59%), shoot length (45%), fresh weight (67%) and dry weight (61%) among all isolates. Consortia did not show any positive effect on plant growth. Biochemical attributes, i.e., proline content, glycine betaine and total soluble proteins were increased by all treatments of root endophytic bacteria under salt stress as shown in Figure 6. Inoculation of TMB7 showed significant potential to increase proline contents by 77%, glycine betaine by 78% and total soluble proteins by 64% compared to control.

PGPB have the ability to enhance plant biochemical attributes such as proline, glycine betaine and total soluble proteins under salt stress to overcome the effects of salinity on plant growth. Proline and glycine betaine play an important role as osmoprotectants and osmoregulatory elements to reduce the harmful effects of salinity by

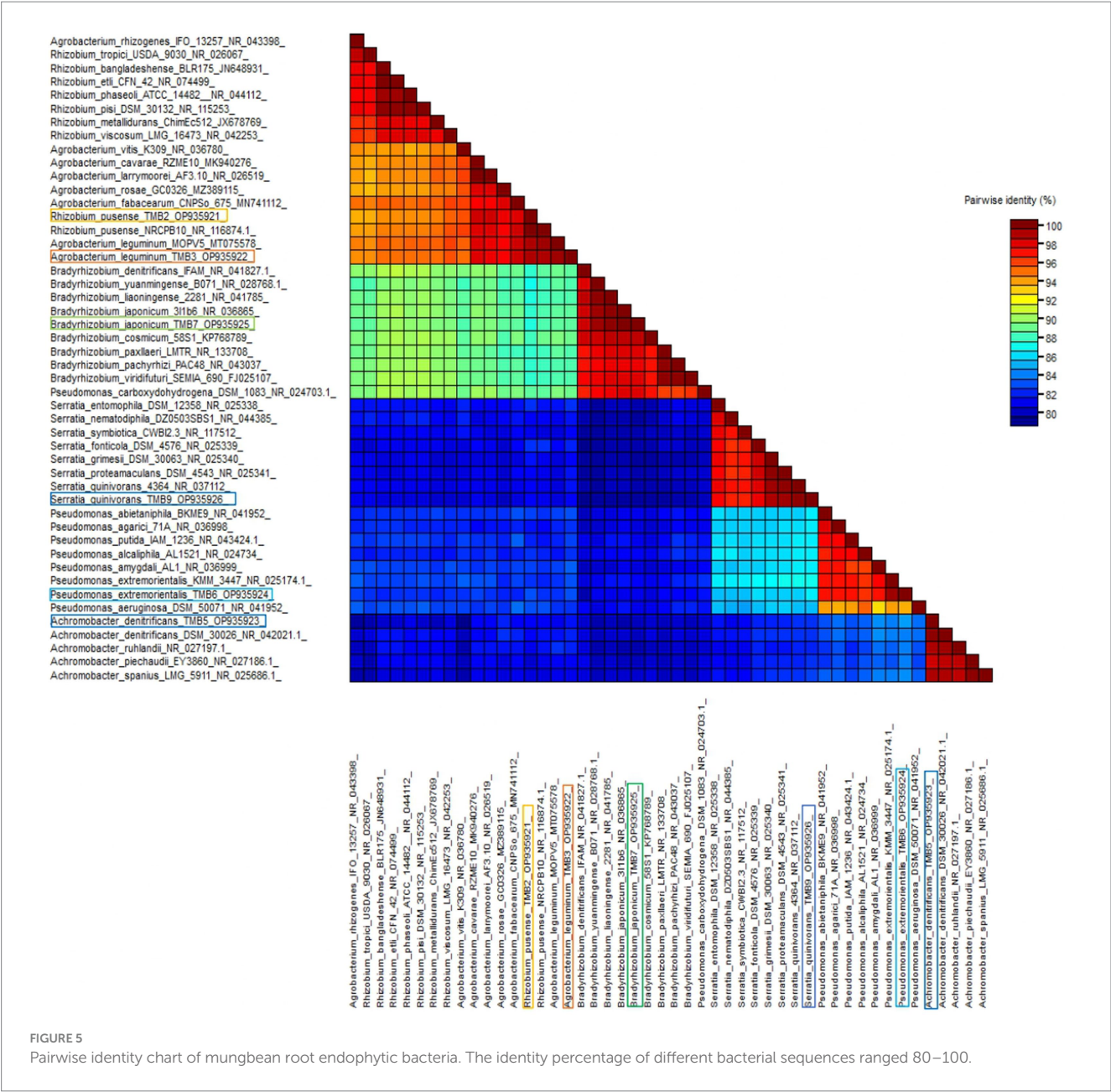


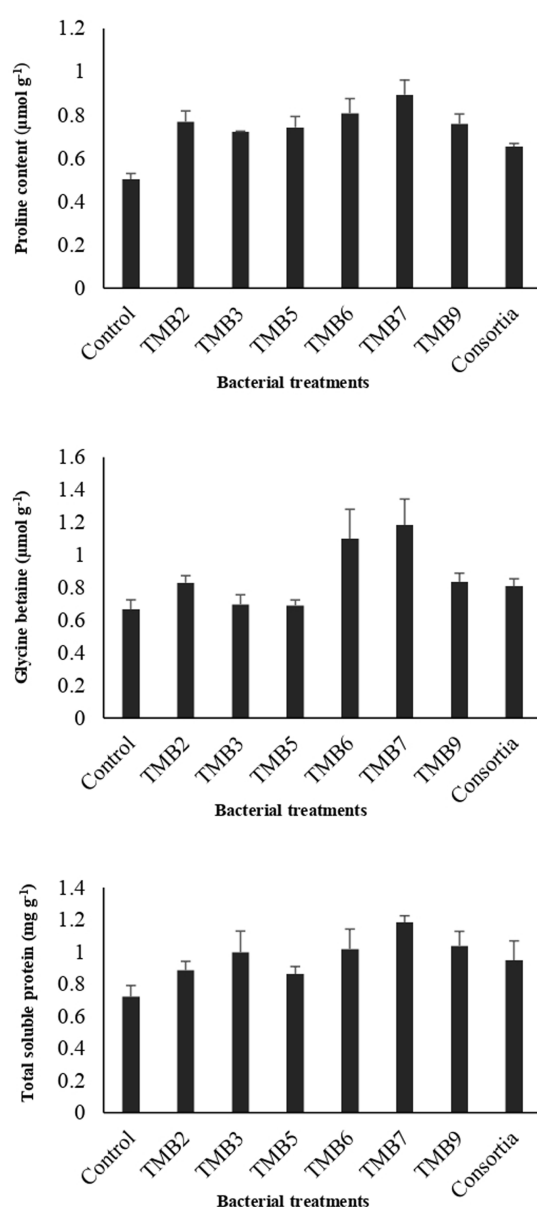
FIGURE 5  
Pairwise identity chart of mungbean root endophytic bacteria. The identity percentage of different bacterial sequences ranged 80–100.

TABLE 4 Effect of potential salinity-tolerant endophytic bacteria on mungbean growth under controlled-conditions.

| Treatment  | Root length (cm)         | Shoot length (cm)       | Plant fresh weight (mg)  | Plant dry weight (mg)    | Number of nodules per plant |
|------------|--------------------------|-------------------------|--------------------------|--------------------------|-----------------------------|
| Control    | 21 ± 1.7 <sup>cd</sup>   | 30.8 ± 1.3 <sup>b</sup> | 737 ± 10 <sup>c</sup>    | 82.5 ± 8 <sup>cd</sup>   | 0                           |
| TMB2       | 29.5 ± 1.32 <sup>a</sup> | 42.8 ± 1.6 <sup>a</sup> | 950 ± 30 <sup>d</sup>    | 110 ± 20 <sup>abc</sup>  | 26 ± 0.8 <sup>b</sup>       |
| TMB3       | 29.3 ± 1.4 <sup>ab</sup> | 42 ± 2.0 <sup>a</sup>   | 920 ± 60 <sup>d</sup>    | 90 ± 8 <sup>bcd</sup>    | 0                           |
| TMB5       | 22 ± 1.5 <sup>cd</sup>   | 41.5 ± 1.7 <sup>a</sup> | 970 ± 50 <sup>d</sup>    | 105 ± 20 <sup>abcd</sup> | 0                           |
| TMB6       | 31.5 ± 1.3 <sup>a</sup>  | 43 ± 1.1 <sup>a</sup>   | 1,160 ± 40 <sup>ab</sup> | 125 ± 6 <sup>ab</sup>    | 0                           |
| TMB7       | 33.3 ± 1.8 <sup>a</sup>  | 44.8 ± 0.9 <sup>a</sup> | 1,230 ± 20 <sup>a</sup>  | 132.5 ± 8 <sup>a</sup>   | 31.3 ± 0.5 <sup>a</sup>     |
| TMB9       | 24.8 ± 1.1 <sup>bc</sup> | 42.5 ± 0.6 <sup>a</sup> | 1,080 ± 40 <sup>bc</sup> | 120 ± 12 <sup>ab</sup>   | 0                           |
| Consortia  | 19 ± 2.1 <sup>d</sup>    | 32.3 ± 0.9 <sup>b</sup> | 640 ± 20 <sup>c</sup>    | 72.5 ± 6 <sup>c</sup>    | 19.5 ± 1 <sup>c</sup>       |
| LSD (0.05) | 4.53                     | 3.9                     | 117                      | 37                       | 1.4                         |
| ANOVA      | ***                      | ***                     | ***                      | *                        | ***                         |

Each value represents mean ( $n = 4$ ) ± standard error. Values followed by the different letters in same column indicate significant difference and followed by same letters are not significantly different. \*Represents significance and \*\*\* represents high significance. LSD, least significant difference.





**FIGURE 6**  
Effect of potential salt-tolerant endophytic bacteria (STEB) on biochemical contents of mungbean under salt stress. Concentrations of proline, glycine betaine and total soluble proteins were determined. Inoculation of TMB7 showed significant potential to increase proline contents by 77%, glycine betaine by 78% and total soluble proteins by 64% compared to control.

boosting the defense mechanism against oxidative damage under salt stress conditions (Diagne et al., 2020). Our results are in agreement with the previous studies which reported that the inoculations of bacteria enhanced legumes plant biochemical properties such as proline and glycine betaine content under salt stress (Ashraf and Bashir, 2003). Irshad et al. (2021) demonstrated that inoculation of *Rhizobium* sp. enhanced salt tolerance in *medicago truncatula* by increasing glycine betaine, proline, total soluble proteins and solutes contents. Mushtaq et al. (2021) also revealed that inoculation of *Rhizobium* enhanced total soluble proteins and proline contents in *Cicer arietinum* to alleviate salt stress.

Kaur et al. (2022) described that the inoculation of *P. extremorientalis* on pearl millet increased plant growth parameters which are in agreement with our results. Devi et al. (2022) also demonstrated that inoculation of *P. extremorientalis* increased the plant growth parameters such as fresh weight, dry weight, shoot length and root length of chili. Similarly, Kiruthika and Arunkumar (2021) also demonstrated that inoculation of *B. japonicum* increased fresh and dry weight of mungbean. Miljaković et al. (2022) also reported that inoculation of *B. japonicum* improved growth parameters of soybean. Similarly, Zveushe et al. (2023) demonstrated that *Bradyrhizobium japonicum* enhanced plant growth parameters of soybean under salt stress. Our results are in agreement with Kumar et al. (2021), who demonstrated the potential role of *S. quinivorans* inoculation to increase the growth of *Picrorhiza kurroa* under control condition experiments. In this study, consortia did not perform well for plant growth promotion. Our results are in disagreement with Mogal et al. (2022) who reported that consortia of rhizobial bacteria have positive effects on plant growth parameters of mungbean. Previously, Consentino et al. (2022) described that inoculation of consortia did not improve growth parameters of lettuce, compared to the inoculation of pure bacterial culture. Poor performance of bacterial consortia can be attributed to the antagonism which may exist among the different bacteria of consortia. Single inoculations performed better for mungbean growth promotion and the extent of growth improvement corresponds to the bacterial ability to produce plant growth-promoting substances.

## Conclusion

Out of thirteen root endophytic bacteria, six isolates, TMB2, TMB3, TMB5, TMB6, TMB7 and TMB9, were able to tolerate salinity up to 2% NaCl and have the *in vitro* potential to produce plant growth-promoting substances under salt stress conditions. Phylogenetic analysis revealed the novel association of *Agrobacterium leguminum*, *Achromobacter denitrificans*, *Pseudomonas extremorientalis* and *Serratia quinivorans* with roots of mungbean. Inoculation of bacterial isolates, *Pseudomonas extremorientalis* TMB6, *Bradyrhizobium japonicum* TMB7 and *Serratia quinivorans* TMB9, showed maximum potential in improving plant growth and development under salt stress conditions. These potential salt-tolerant endophytic bacteria can be used as biofertilizer after field-testing for better production of mungbean crop at salt-affected lands.

## Data availability statement

The datasets presented in this study can be found in online repositories. The names of the repository/repositories and accession number(s) can be found in the article/Supplementary material.

## Author contributions

MT and SZ conceived the project and designed the study. SZ, MT, AA, and MA collected the samples and performed the experiments. SZ, MT, MA, MZ, and MS performed data analysis. SZ, MT, MA, MZ, and TY wrote the manuscript. SZ, MT, TY, HZ, and MA applied statistics and critically reviewed manuscript. All authors contributed to the article and approved the submitted version.



## Funding

The current work was funded by Higher Education Commission (HEC) Pakistan under the NRP research project no. 8278/Punjab/NRP/R&D/HEC/2017 awarded to MT.

## Acknowledgments

Authors are highly thankful to Satya Kirri, Graduate Student, Department of Biological Chemistry, University of California, Irvine, USA, for proofreading and improving the write-up of manuscript.

## Conflict of interest

The authors declare that the research was conducted in the absence of any commercial or financial relationships that could be construed as a potential conflict of interest.

## References

- Abedinzadeh, M., Etesami, H., and Alikhani, H. A. (2019). Characterization of rhizosphere and endophytic bacteria from roots of maize (*Zea mays* L.) plant irrigated with wastewater with biotechnological potential in agriculture. *Biotechnol. Rep.* 21:e00305. doi: 10.1016/j.btre.2019.e00305
- Adamu-Governor, O. L., Shittu, T. A., Afolabi, O. R., and Uzochukwu, S. V. A. (2018). Screening for gum-producing lactic acid bacteria in oil palm (*Elaeis guineensis*) and Raphia palm (*Raphia regalis*) sap from South-West Nigeria. *Food Sci. Nutr.* 6, 2047–2055. doi: 10.1002/fsn3.750
- Afzal, I., Shinwari, Z. K., Sikandar, S., and Shahzad, S. (2019). Plant beneficial endophytic bacteria: mechanisms, diversity, host range and genetic determinants. *Microbiol. Res.* 221, 36–49. doi: 10.1016/j.micres.2019.02.001
- Agri, U., Chaudhary, P., Sharma, A., and Kukreti, B. (2022). Physiological response of maize plants and its rhizospheric microbiome under the influence of potential bioinoculants and nanochitosan. *Plant Soil* 474, 451–468. doi: 10.1007/s11104-022-05351-2
- Alaa, F. M. (2018). Effectiveness of exopolysaccharides and biofilm forming plant growth promoting rhizobacteria on salinity tolerance of faba bean (*Vicia faba* L.). *Afr. J. Microbiol. Res.* 12, 399–404. doi: 10.5897/AJMR2018.8822
- Ali, M., Sharif, M., Ahmad, W., and Ahmed, I. (2022). Assessing potent zinc solubilizing bacteria to augment wheat yield and zinc biofortification. *Gesunde Pflanzen* 75, 1061–1073. doi: 10.1007/s10343-022-00757-5
- Alsafran, M., Saleem, M. H., Al Jabri, H., Rizwan, M., and Usman, K. (2022). Principles and applicability of integrated remediation strategies for heavy metal removal/recovery from contaminated environments. *J. Plant Growth Regul.* 42, 3419–3440. doi: 10.1007/s00344-022-10803-1
- Altschul, S. (1990). Basic local alignment search tool. *J. Mol. Biol.* 215, 403–410. doi: 10.1016/S0022-2836(05)80360-2
- Anjum, M. S., Ahmed, Z. I., and Rauf, C. A. (2006). Effect of *Rhizobium* inoculation and nitrogen fertilizer on yield and yield components of mungbean. *Int. J. Agric. Biol.* 8, 238–240. doi: 10.4236/ajps.2013.412282
- Ansari, F. A., and Ahmad, I. (2018). Biofilm development, plant growth promoting traits and rhizosphere colonization by *Pseudomonas entomophila* FAP1: a promising PGPR. *Adv. Microbiol.* 8, 235–251. doi: 10.4236/aim.2018.83016
- Ashraf, A., Bano, A., and Ali, S. A. (2019). Characterization of plant growth-promoting rhizobacteria from rhizosphere soil of heat-stressed and unstressed wheat and their use as bio-inoculant. *Plant Biol.* 21, 762–769. doi: 10.1111/plb.12972
- Ashraf, M., and Bashir, A. (2003). Salt stress induced changes in some organic metabolites and ionic relations in nodules and other plant parts of two crop legumes differing in salt tolerance. *Flora Morphol. Distrib. Funct. Ecol. Plants* 198, 486–498. doi: 10.1078/0367-2530-00121
- Bacilio-Jiménez, M., Aguilar-Flores, S., Ventura-Zapata, E., Pérez-Campos, E., Bouqulet, S., and Zenteno, E. (2003). Chemical characterization of root exudates from rice (*Oryza sativa*) and their effects on the chemotactic response of endophytic bacteria. *Plant Soil* 249, 271–277. doi: 10.1023/A:1022888900465
- Bates, L. S., Waldren, R. A., and Teare, I. D. (1973). Rapid determination of free proline for water-stress studies. *Plant Soil* 39, 205–207. doi: 10.1007/BF00018060
- Behera, B. C., Yadav, H., Singh, S. K., Mishra, R. R., Sethi, B. K., Dutta, S. K., et al. (2017). Phosphate solubilization and acid phosphatase activity of *Serratia* sp. isolated from mangrove soil of Mahanadi river delta, Odisha, India. *J. Genet. Eng. Biotechnol.* 15, 169–178. doi: 10.1016/j.jgeb.2017.01.003
- Belkebla, N., Bessai, S. A., Melo, J., Caeiro, M. F., Cruz, C., and Nabti, E. H. (2022). Restoration of *Triticum aestivum* growth under salt stress by phosphate-solubilizing bacterium isolated from southern Algeria. *Agronomy* 12:2050. doi: 10.3390/agronomy12092050
- Bhardwaj, D., Ansari, M. W., Sahoo, R. K., and Tuteja, N. (2014). Biofertilizers function as key player in sustainable agriculture by improving soil fertility, plant tolerance and crop productivity. *Microb. Cell Factories* 13:66. doi: 10.1186/1475-2859-13-66
- Bhattacharyya, C., Banerjee, S., Acharya, U., Mitra, A., Mallick, I., Halder, A., et al. (2020). Evaluation of plant growth promotion properties and induction of antioxidative defense mechanism by tea rhizobacteria of Darjeeling, India. *Sci. Rep.* 10, 1–19. doi: 10.1038/s41598-020-72439-z
- Bhutani, N., Maheshwari, R., Kumar, P., Dahiya, R., and Suneja, P. (2021). Bioprospecting for extracellular enzymes from endophytic bacteria isolated from *Vigna radiata* and *Cajanus cajan*. *J. Appl. Biol. Biotechnol.* 9, 26–34. doi: 10.7324/JABB.2021.9304
- Bhutani, N., Maheshwari, R., Negi, M., and Suneja, P. (2018b). Optimization of IAA production by endophytic *Bacillus* spp. from *Vigna radiata* for their potential use as plant growth promoters. *Israel J. Plant Sci.* 65, 83–96. doi: 10.1163/22238980-00001025
- Bhutani, N., Maheshwari, R., and Suneja, P. (2018a). Isolation and characterization of plant growth promoting endophytic bacteria isolated from *Vigna radiata*. *Indian J. Agric. Res.* 52, 596–603. doi: 10.18805/IJAR.A-5047
- Borah, A., Das, R., Mazumdar, R., and Thakur, D. (2019). Culturable endophytic bacteria of *Camellia* species endowed with plant growth promoting characteristics. *J. Appl. Microbiol.* 127, 825–844. doi: 10.1111/jam.14356
- Bradford, M. M. (1976). A rapid and sensitive method for the quantitation of microgram quantities of protein utilizing the principle of protein-dye binding. *Anal. Biochem.* 72, 248–254. doi: 10.1016/0003-2697(76)90527-3
- Cardinali, A., and Nason, G. P. (2013). Costationarity of locally stationary time series using costat. *J. Stat. Softw.* 55, 1–22. doi: 10.18637/jss.v055.i01
- Castellano-Hinojosa, A., Correa-Galeote, D., Ramírez-Bahena, M. H., Tortosa, G., González-López, J., Bedmar, E. J., et al. (2021). *Agrobacterium leguminum* sp. nov., isolated from nodules of *Phaseolus vulgaris* in Spain. *Int. J. Syst. Evol. Microbiol.* 71:005120. doi: 10.1099/ijsem.0.005120
- Chanway, C., Shishido, M., Nairn, J., Jungwirth, S., Markham, J., Xiao, G., et al. (2000). Endophytic colonization and field responses of hybrid spruce seedlings after inoculation with plant growth-promoting rhizobacteria. *For. Ecol. Manag.* 133, 81–88. doi: 10.1016/S0378-1127(99)00300-X

## Publisher's note

All claims expressed in this article are solely those of the authors and do not necessarily represent those of their affiliated organizations, or those of the publisher, the editors and the reviewers. Any product that may be evaluated in this article, or claim that may be made by its manufacturer, is not guaranteed or endorsed by the publisher.

## Supplementary material

The Supplementary material for this article can be found online at: <https://www.frontiersin.org/articles/10.3389/fmicb.2023.1149004/full#supplementary-material>

### SUPPLEMENTARY FIGURE

Effect of inoculation of potential salt-tolerant endophytic bacteria (STEB) on mungbean growth under controlled-conditions. Inoculation of bacterial isolates, *P. extremorientalis* TMB6, *B. japonicum* TMB7 and *S. quinivorans* TMB9, showed maximum potential in improving plant growth parameters. Photographed at 4-week stage.

- Chaudhary, P., Agri, U., Chaudhary, A., Kumar, A., and Kumar, G. (2022). Endophytes and their potential in biotic stress management and crop production. *Front. Microbiol.* 13:933017. doi: 10.3389/fmicb.2022.933017
- Chaudhary, T., Gera, R., and Shukla, P. (2021). Deciphering the potential of *Rhizobium pusense* MB-17a, a plant growth-promoting root endophyte, and functional annotation of the genes involved in the metabolic pathway. *Front. Bioeng. Biotechnol.* 8:617034. doi: 10.3389/fbioe.2020.617034
- Chauhan, P. K., and Upadhyay, S. K. (2023). Exo-polysaccharide producing bacteria can induce maize plant growth and soil health under saline conditions. *Biotechnol. Genet. Eng. Rev.* 1–20. doi: 10.1080/02648725.2022.2163812
- Chauhan, P. K., Upadhyay, S. K., Tripathi, M., Singh, R., Krishna, D., Singh, S. K., et al. (2022). Understanding the salinity stress on plant and developing sustainable management strategies mediated salt-tolerant plant growth-promoting rhizobacteria and CRISPR/Cas9. *Biotechnol. Genet. Eng. Rev.* 1–37. doi: 10.1080/02648725.2022.2131958
- Chhetri, T. K., Subedee, B. R., and Pant, B. (2019). Isolation, identification and production of encapsulated *Bradyrhizobium japonicum* and study on their viability. *Nepal J. Biotechnol.* 7, 39–49. doi: 10.3126/njb.v7i1.26950
- Chlebek, D., Grebtsova, V., Piński, A., Żur-Pińska, J., and Hupert-Kocurek, K. (2022). Genetic determinants of antagonistic interactions and the response of new endophytic strain *Serratia quinivorans* KP32 to fungal phytopathogens. *Int. J. Mol. Sci.* 23:15561. doi: 10.3390/ijms232415561
- Compant, S., Reiter, B., Sessitsch, A., Nowak, J., Clément, C., and Ait Barka, E. (2005). Endophytic colonization of *Vitis vinifera* L. by plant growth-promoting bacterium *Burkholderia* sp. strain PsJN. *Appl. Environ. Microbiol.* 71, 1685–1693. doi: 10.1128/AEM.71.4.1685-1693.2005
- Consentino, B. B., Aprile, S., Roupheal, Y., Ntatsi, G., De Pasquale, C., Iapichino, G., et al. (2022). Application of PGPB combined with variable N doses affects growth, yield-related traits, N-fertilizer efficiency and nutritional status of lettuce grown under controlled condition. *Agronomy* 12:236. doi: 10.3390/agronomy12020236
- Conway, G. R., and Pretty, J. N. (2013). *Unwelcome Harvest: Agriculture and Pollution*. United Kingdom: Routledge.
- Cortés-Lorenzo, C., Rodríguez-Díaz, M., Sipkema, D., Juárez-Jiménez, B., Rodelas, B., Smidt, H., et al. (2015). Effect of salinity on nitrification efficiency and structure of ammonia-oxidizing bacterial communities in a submerged fixed bed bioreactor. *Chem. Eng. J.* 266, 233–240. doi: 10.1016/j.cej.2014.12.083
- Dalal, J., and Kulkarni, N. (2013). Population dynamics and diversity of endophytic bacteria associated with soybean (*Glycine max* (L.) Merrill). *Br. Microbiol. Res. J.* 3, 96–105. doi: 10.9734/BMRJ/2013/2302
- Delic, D., Stajkovic, O., Kyzmanovic, D., Rasulic, N., Knezevic, S., and Milicic, B. (2009). The effects of rhizobial inoculation on growth and yield of *Vigna mungo* L. in Serbian soils. *Biotechnol. Anim. Husb.* 25, 1197–1202.
- Desai, S., Mistry, J., Shah, F., Chandwani, S., Amareesan, N., and Supriya, N. R. (2023). Salt-tolerant bacteria enhance the growth of mung bean (*Vigna radiata* L.) and uptake of nutrients, and mobilize sodium ions under salt stress condition. *Int. J. Phytoremediation* 25, 66–73. doi: 10.1080/15226514.2022.2057419
- Deshwal, V. K., and Kumar, P. (2013). Effect of salinity on growth and PGPR activity of *Pseudomonads*. *J. Acad. Ind. Res.* 2, 353–356.
- Devi, N. O., Tombisana Devi, R. K., Debbarma, M., Hajong, M., and Thokchom, S. (2022). Effect of endophytic *Bacillus* and arbuscular mycorrhiza fungi (AMF) against *Fusarium* wilt of tomato caused by *Fusarium oxysporum* f. sp. lycopersici. *Egyptian J. Biol. Pest Control* 32, 1–14. doi: 10.1186/s41938-021-00499-y
- Diagne, N., Ndour, M., Djighaly, P. I., Ngom, D., Ngom, M. C. N., Ndong, G., et al. (2020). Effect of plant growth promoting rhizobacteria (PGPR) and arbuscular mycorrhizal fungi (AMF) on salt stress tolerance of *Casuarina obesa* (Miq.). *Front. Sustain. Food Syst.* 4:601004. doi: 10.3389/fsufs.2020.601004
- Ditta, A., Ullah, N., Imtiaz, M., Li, X., Jan, A. U., Mehmood, S., et al. (2022). “Zn biofortification in crops through Zn-solubilizing plant growth-promoting Rhizobacteria” in *Sustainable Plant Nutrition under Contaminated Environments*. ed. M. Qaisar (Cham: Springer International Publishing), 115–133.
- Dogan, G., and Taskin, B. (2021). Hydrolytic enzymes producing bacterial endophytes of some *Poaceae* plants. *Pol. J. Microbiol.* 70, 297–304. doi: 10.33073/pjm-2021-026
- Doty, S. L., Oakley, B., Xin, G., Kang, J. W., Singleton, G., Khan, Z., et al. (2009). Diazotrophic endophytes of native black cottonwood and willow. *Symbiosis* 47, 23–33. doi: 10.1007/BF03179967
- Economic Survey of Pakistan, (2021–2022). Available at: [https://www.finance.gov.pk/survey/chapter\\_22/PES02-AGRICULTURE.pdf](https://www.finance.gov.pk/survey/chapter_22/PES02-AGRICULTURE.pdf)
- Egamberdieva, D., Li, L., Lindström, K., and Räsänen, L. A. (2016). A synergistic interaction between salt-tolerant *Pseudomonas* and *Mesorhizobium* strains improves growth and symbiotic performance of liquorice (*Glycyrrhiza uralensis* fish.) under salt stress. *Appl. Microbiol. Biotechnol.* 100, 2829–2841. doi: 10.1007/s00253-015-7147-3
- Egamberdieva, D., Wirth, S., Bellingrath-Kimura, S. D., Mishra, J., and Arora, N. K. (2019). Salt-tolerant plant growth promoting rhizobacteria for enhancing crop productivity of saline soils. *Front. Microbiol.* 10:2791. doi: 10.3389/fmicb.2019.02791
- Favero, V. O., Carvalho, R. H., Motta, V. M., Leite, A. B. C., Coelho, M. R. R., Xavier, G. R., et al. (2021b). *Bradyrhizobium* as the only rhizobial inhabitant of mung bean (*Vigna radiata*) nodules in tropical soils: a strategy based on microbiome for improving biological nitrogen fixation using bio-products. *Front. Plant Sci.* 11:602645. doi: 10.3389/fpls.2020.602645
- Favero, V. O., de Carvalho, R. H., Leite, A. B. C., de Freitas, K. M., Zilli, J. E., Xavier, G. R., et al. (2021a). Characterization and nodulation capacity of native bacteria isolated from mung bean nodules used as a trap plant in Brazilian tropical soils. *Appl. Soil Ecol.* 167:104041. doi: 10.1016/j.apsoil.2021.104041
- Fox, J. E., Gullledge, J., Engelhaupt, E., Burrow, M. E., and McLachlan, J. A. (2007). Pesticides reduce symbiotic efficiency of nitrogen-fixing rhizobia and host plants. *Proc. Natl. Acad. Sci.* 104, 10282–10287. doi: 10.1073/pnas.0611710104
- Gu, J., Li, Z., Mao, Y., Struik, P. C., Zhang, H., Liu, L., et al. (2018). Roles of nitrogen and cytokinin signals in root and shoot communications in maximizing of plant productivity and their agronomic applications. *Plant Sci.* 274, 320–331. doi: 10.1016/j.plantsci.2018.06.010
- Hakim, S., Mirza, B. S., Imran, A., Zaheer, A., Yasmin, S., Mubeen, F., et al. (2020). Illumina sequencing of 16S rRNA tag shows disparity in rhizobial and non-rhizobial diversity associated with root nodules of mung bean (*Vigna radiata* L.) growing in different habitats in Pakistan. *Microbiol. Res.* 231:126356. doi: 10.1016/j.micres.2019.126356
- Hameed, M., Ashraf, M., and Naz, N. (2009). Anatomical adaptations to salinity in cogan grass [*Imperata cylindrica* (L.) Raeuschel] from the salt range, Pakistan. *Plant Soil* 322, 229–238. doi: 10.1007/s1104-009-9911-6
- Hardarson, G., and Danso, S. K. A. (1993). Methods for measuring biological nitrogen fixation in grain legumes. *Plant Soil* 152, 19–23. doi: 10.1007/BF00016330
- Hong, J., Li, W., Lin, B., Zhan, M., Liu, C., and Chen, B. Y. (2013). Deciphering the effect of salinity on the performance of submerged membrane bioreactor for aquaculture of bacterial community. *Desalination* 316, 23–30. doi: 10.1016/j.desal.2013.01.015
- Hung, P. Q., and Annapurna, K. (2004). Isolation and characterization of endophytic bacteria in soybean (*Glycine* sp.). *Omonrice* 12, 92–101.
- Hyder, S., Gondal, A. S., Rizvi, Z. F., Ahmad, R., Alam, M. M., Hannan, A., et al. (2020). Characterization of native plant growth promoting rhizobacteria and their anti-oomycete potential against *Phytophthora capsici* affecting chilli pepper (*Capsicum annum* L.). *Sci. Rep.* 10, 1–15. doi: 10.1038/s41598-020-69410-3
- Imran, A., Hakim, S., Tariq, M., Nawaz, M. S., Larai, I., Gulzar, U., et al. (2021). Diazotrophs for lowering nitrogen pollution crises: looking deep into the roots. *Front. Microbiol.* 12:861. doi: 10.3389/fmicb.2021.637815
- Irshad, A., Rehman, R. N. U., Abrar, M. M., Saeed, Q., Sharif, R., and Hu, T. (2021). Contribution of rhizobium-legume symbiosis in salt stress tolerance in *medicago truncatula* evaluated through photosynthesis, antioxidant enzymes, and compatible solutes accumulation. *Sustainability* 13:3369. doi: 10.3390/su13063369
- Islam, F., and Roy, N. (2018). Screening, purification and characterization of cellulase from cellulase producing bacteria in molasses. *BMC. Res. Notes* 11, 1–6. doi: 10.1186/s13104-018-3558-4
- Jabborova, D., Annapurna, K., Fayzullaeva, M., Sulaymonov, K., Kadirova, D., Jabbarov, Z., et al. (2020). Isolation and characterization of endophytic bacteria from ginger (*Zingiber officinale* Rosc.). *Ann. Phytomed.* 9, 116–121. doi: 10.21276/ap.2020.9.1.14
- Javed, S., Javid, A., Hanif, U., Bahadur, S., Sultana, S., Shuaib, M., et al. (2021). Effect of necrotrophic fungus and PGPR on the comparative histochemistry of *Vigna radiata* by using multiple microscopic techniques. *Microsc. Res. Tech.* 84, 2737–2748. doi: 10.1002/jemt.23836
- Jhuma, T. A., Rafeya, J., Sultana, S., Rahman, M. T., and Karim, M. M. (2021). Isolation of endophytic salt-tolerant plant growth-promoting Rhizobacteria from *Oryza sativa* and evaluation of their plant growth-promoting traits under salinity stress condition. *Front. Sustain. Food Syst.* 5:687531. doi: 10.3389/fsufs.2021.687531
- Kamran, M., Imran, Q. M., Ahmed, M. B., Falak, N., Khatoon, A., and Yun, B. W. (2022). Endophyte-mediated stress tolerance in plants: a sustainable strategy to enhance resilience and assist crop improvement. *Cells* 11:3292. doi: 10.3390/cells11203292
- Kartik, V. P., Jinal, H. N., and Amareesan, N. (2021). Inoculation of cucumber (*Cucumis sativus* L.) seedlings with salt-tolerant plant growth promoting bacteria improves nutrient uptake, plant attributes and physiological profiles. *J. Plant Growth Regul.* 40, 1728–1740. doi: 10.1007/s00344-020-10226-w
- Kaur, T., Devi, R., Kumar, S., Kour, D., and Yadav, A. N. (2022). Plant growth promotion of pearl millet (*Pennisetum glaucum* L.) by novel bacterial consortium with multifunctional attributes. *Biologia* 78, 621–631. doi: 10.1007/s11756-022-01291-5
- Khan, M. U., Sessitsch, A., Harris, M., Fatima, K., Imran, A., Arslan, M., et al. (2015). Cr-resistant rhizo- and endophytic bacteria associated with *Prosopis juliflora* and their potential as phytoremediation enhancing agents in metal-degraded soils. *Front. Plant Sci.* 5:755. doi: 10.3389/fpls.2014.00755
- Khan, I., Zada, S., Rafiq, M., Sajjad, W., Zaman, S., and Hasan, F. (2022). Phosphate solubilizing epilithic and endolithic bacteria isolated from clastic sedimentary rocks, Murree lower Himalaya, Pakistan. *Arch. Microbiol.* 204, 1–11. doi: 10.1007/s00203-022-02946-2
- Kiruthika, S., and Arunkumar, M. (2021). A comprehensive study on IAA production by *Bradyrhizobium japonicum* and *Bacillus subtilis* and its effect on *Vigna radiata* plant growth. *Indian J. Agric. Res.* 55, 570–576. doi: 10.18805/IJARE.A-5521

- Kumar, A., Singh, S., Mukherjee, A., Rastogi, R. P., and Verma, J. P. (2021). Salt-tolerant plant growth-promoting *Bacillus pumilus* strain JPV511 to enhance plant growth attributes of rice and improve soil health under salinity stress. *Microbiol. Res.* 242:126616. doi: 10.1016/j.micres.2020.126616
- Kumar, S., Stecher, G., and Tamura, K. (2016). MEGA7: molecular evolutionary genetics analysis version 7.0 for bigger datasets. *Mol. Biol. Evol.* 33, 1870–1874. doi: 10.1093/molbev/msw054
- Kumawat, C., Kumar, A., Parshad, J., Sharma, S. S., Patra, A., Dogra, P., et al. (2022). Microbial diversity and adaptation under salt-affected soils: a review. *Sustainability* 14:9280. doi: 10.3390/su14159280
- Kumawat, K. C., Sharma, P., Nagpal, S., Gupta, R. K., Sirari, A., Nair, R. M., et al. (2021). Dual microbial inoculation, a game changer?—bacterial biostimulants with multifunctional growth promoting traits to mitigate salinity stress in spring Mungbean. *Front. Microbiol.* 11:600576. doi: 10.3389/fmicb.2020.600576
- La Pierre, K. J., Simms, E. L., Tariq, M., Zafar, M., and Porter, S. S. (2017). Invasive legumes can associate with many mutualists of native legumes, but usually do not. *Ecol. Evol.* 7, 8599–8611. doi: 10.1002/ece3.3310
- Latha, P., Anand, T., Ragupathi, N., Prakasam, V., and Samiyappan, R. (2009). Antimicrobial activity of plant extracts and induction of systemic resistance in tomato plants by mixtures of PGPR strains and Zimmu leaf extract against *Alternaria solani*. *Biol. Control* 50, 85–93. doi: 10.1016/j.biocontrol.2009.03.002
- Linu, M. S., Asok, A. K., Thampi, M., Sreekumar, J., and Jisha, M. S. (2019). Plant growth promoting traits of indigenous phosphate solubilizing *Pseudomonas aeruginosa* isolates from Chilli (*Capsicum annuum* L.) rhizosphere. *Commun. Soil Sci. Plant Anal.* 50, 444–457. doi: 10.1080/00103624.2019.1566469
- Lun, F., Liu, J., Ciais, P., Nesme, T., Chang, J., Wang, R., et al. (2018). Global and regional phosphorus budgets in agricultural systems and their implications for phosphorus-use efficiency. *Earth Syst. Sci. Data* 10, 1–18. doi: 10.5194/essd-10-1-2018
- Mahdi, I., Hafidi, M., Allaoui, A., and Biskri, L. (2021). Halotolerant endophytic bacterium *Serratia rubideae* ED1 enhances phosphate solubilization and promotes seed germination. *Agriculture* 11:224. doi: 10.3390/agriculture11030224
- Majeed, A., and Muhammad, Z. (2019). “Salinity: a major agricultural problem—causes, impacts on crop productivity and management strategies” in *Plant Abiotic Stress Tolerance: Agronomic, Molecular and Biotechnological Approaches*. eds. H. Mirza, R. H. Rehman, N. Kamrun and F. A. Hesham (Springer, Cham) 83–99.
- Mei, C., Chretien, R. L., Amaradasa, B. S., He, Y., Turner, A., and Lowman, S. (2021). Characterization of phosphate solubilizing bacterial endophytes and plant growth promotion *in vitro* and in greenhouse. *Microorganisms* 9:1935. doi: 10.3390/microorganisms9091935
- Miljaković, D., Marinković, J., Tamindžić, G., Đorđević, V., Tintor, B., Milošević, D., et al. (2022). Bio-priming of soybean with *Bradyrhizobium japonicum* and *Bacillus megaterium*: strategy to improve seed germination and the initial seedling growth. *Plan. Theory* 11:1927. doi: 10.3390/plants11151927
- Mirza, B. S., and Rodrigues, J. L. (2012). Development of a direct isolation procedure for free-living diazotrophs under controlled hypoxic conditions. *Appl. Environ. Microbiol.* 78, 5542–5549. doi: 10.1128/AEM.00714-12
- Mishra, P. K., Mishra, S., Bisht, S. C., Selvakumar, G., Kundu, S., Bisht, J. K., et al. (2009). Isolation, molecular characterization and growth-promotion activities of a cold tolerant bacterium *Pseudomonas* sp. NARs9 (MTCC9002) from the Indian Himalayas. *Biol. Res.* 42, 305–313. doi: 10.4067/S0716-97602009000300005
- Mogal, C. S., Solanki, V. H., Kansara, R. V., Jha, S., Singh, S., Parekh, V. B., et al. (2022). UHPLC-MS/MS and QRT-PCR profiling of PGP agents and *Rhizobium* spp. of induced phytohormones for growth promotion in mungbean (var. Co4). *Heliyon* 8:e09532. doi: 10.1016/j.heliyon.2022.e09532
- Muhire, B. M., Varsani, A., and Martin, D. P. (2014). SDT: a virus classification tool based on pairwise sequence alignment and identity calculation. *PLoS One* 9:e108277. doi: 10.1371/journal.pone.0108277
- Munns, R., and James, R. A. (2003). Screening methods for salinity tolerance: a case study with tetraploid wheat. *Plant Soil* 253, 201–218. doi: 10.1023/A:1024553303144
- Mushtaq, Z., Faizan, S., Gulzar, B., and Hakeem, K. R. (2021). Inoculation of *Rhizobium* alleviates salinity stress through modulation of growth characteristics, physiological and biochemical attributes, stomatal activities and antioxidant defence in *Cicer arietinum* L. *J. Plant Growth Regul.* 40, 2148–2163. doi: 10.1007/s00344-020-10267-1
- Myo, E. M., Ge, B., Ma, J., Cui, H., Liu, B., Shi, L., et al. (2019). Indole-3-acetic acid production by *Streptomyces fradiae* NKZ-259 and its formulation to enhance plant growth. *BMC Microbiol.* 19, 1–14. doi: 10.1186/s12866-019-1528-1
- Nacoon, S., Jogloy, S., Riddech, N., Mongkolthanaruk, W., Kuyper, T. W., and Boonlue, S. (2020). Interaction between phosphate solubilizing bacteria and arbuscular mycorrhizal fungi on growth promotion and tuber inulin content of *Helianthus tuberosus* L. *Sci. Rep.* 10, 1–10. doi: 10.1038/s41598-020-61846-x
- Nair, R., and Schreinemachers, P. (2020). “Global status and economic importance of mungbean” in *The Mungbean Genome*. eds. M. N. Ramakrishnan, S. Roland and L. Suk-Ha (Cham: Springer International Publishing), 1–8.
- Nawaz, M., and Wang, Z. (2020). Absciscic acid and glycine betaine mediated tolerance mechanisms under drought stress and recovery in *Axonopus compressus*: a new insight. *Sci. Rep.* 10:6942. doi: 10.1038/s41598-020-63447-0
- Nguyen, P. M., Nguyen, H. T., Le, H. T. T., Nguyen, L. B., Tran, P. H., Dinh, Y. B., et al. (2022). The effects of *Rhizobium* inoculation on the growth of Rice (*Oryza sativa* L.) and white radish (*Raphanus sativus* L.). *IOP Conf. Ser. Earth Environ. Sci.* 995:012053. doi: 10.1088/1755-1315/995/1/012053
- Noori, F., Etesami, H., Noori, S., Forouzan, E., Jouzani, G. S., and Malboobi, M. A. (2021). Whole genome sequence of *Pantoea agglomerans* ANP8, a salinity and drought stress-resistant bacterium isolated from alfalfa (*Medicago sativa* L.) root nodules. *Biotechnol. Rep.* 29:e00600. doi: 10.1016/j.btre.2021.e00600
- Oo, K. T., Win, T. T., Khai, A. A., and Fu, P. (2020). Isolation, screening and molecular characterization of multifunctional plant growth promoting rhizobacteria for a sustainable agriculture. *Am. J. Plant Sci.* 11, 773–792. doi: 10.4236/ajps.2020.116055
- Pataczek, L., Zahir, Z. A., Ahmad, M., Rani, S., Nair, R., Schafleitner, R., et al. (2018). Beans with benefits—the role of Mungbean (*Vigna radiata*) in a changing environment. *Am. J. Plant Sci.* 9, 1577–1600. doi: 10.4236/ajps.2018.97115
- Patil, S. M., Patil, D. B., Patil, M. S., Gaikwad, P. V., Bhamburdekar, S. B., and Patil, P. J. (2014). Isolation, characterization and salt tolerance activity of *Rhizobium* sp. from root nodules of some legumes. *Int. J. Curr. Microbiol. App. Sci.* 3:1005.
- Pérez-Rodríguez, M. M., Piccoli, P., Anzuay, M. S., Baraldi, R., Neri, L., Taurian, T., et al. (2020). Native bacteria isolated from roots and rhizosphere of *Solanum lycopersicum* L. increase tomato seedling growth under a reduced fertilization regime. *Sci. Rep.* 10, 1–14. doi: 10.1038/s41598-020-72507-4
- Ramesh, A., Sharma, S. K., Sharma, M. P., Yadav, N., and Joshi, O. P. (2014). Inoculation of zinc solubilizing *Bacillus aryabhattai* strains for improved growth, mobilization and biofortification of zinc in soybean and wheat cultivated in Vertisols of Central India. *Appl. Soil Ecol.* 73, 87–96. doi: 10.1016/j.apsoil.2013.08.009
- Rani, N., Kaur, G., Kaur, S., Mutreja, V., Upadhyay, S. K., and Tripathi, M. (2022). Comparison of diversity and zinc solubilizing efficiency of rhizobacteria obtained from solanaceous crops under polyhouse and open field conditions. *Biotechnol. Genet. Eng. Rev.* 1–22. doi: 10.1080/02648725.2022.2157949
- Rat, A., Naranjo, H. D., Krigas, N., Grigoriadou, K., Maloupa, E., Alonso, A. V., et al. (2021). Endophytic bacteria from the roots of the medicinal plant *Alkanna tinctoria* Tausch (*Boraginaceae*): exploration of plant growth promoting properties and potential role in the production of plant secondary metabolites. *Front. Microbiol.* 12:633488. doi: 10.3389/fmicb.2021.633488
- Reddy, E. C., Reddy, G. S., Goudar, V., Sriramula, A., Swarnalatha, G. V., Al Tawaha, A. R. M., et al. (2022). “Hydrolytic enzyme producing plant growth-promoting Rhizobacteria (PGPR) in plant growth promotion and biocontrol” in *Secondary Metabolites and Volatiles of PGPR in Plant-Growth Promotion*. eds. R. Z. Sayyed and G. U. Virgilio (Cham: Springer International Publishing), 303–312.
- Reetha, S., Selvakumar, G., Bhuvaneswari, G., Thamizhiniyan, P., and Ravimycin, T. (2014). Screening of cellulase and pectinase by using *Pseudomonas fluorescens* and *Bacillus subtilis*. *Int. Lett. Nat. Sci.* 13, 75–80. doi: 10.56431/p-ao2yow
- Reis, F., Pereira, A. J., Tavares, R. M., Baptista, P., and Lino-Neto, T. (2021). Cork oak forests soil bacteria: potential for sustainable agroforest production. *Microorganisms* 9:1973. doi: 10.3390/microorganisms9091973
- Rezaeiniko, B., Enayatzamir, N., and Norouzi Masir, M. (2022). Changes in soil zinc chemical fractions and improvements in wheat grain quality in response to zinc solubilizing bacteria. *Commun. Soil Sci. Plant Anal.* 53, 622–635. doi: 10.1080/00103624.2021.2017962
- Riggs, P. J., Chelius, M. K., Iniguez, A. L., Kaeppler, S. M., and Triplett, E. W. (2001). Enhanced maize productivity by inoculation with diazotrophic bacteria. *Funct. Plant Biol.* 28, 829–836. doi: 10.1071/PP01045
- Rosenblueth, M., and Martínez-Romero, E. (2006). Bacterial endophytes and their interactions with hosts. *Mol. Plant-Microbe Interact.* 19, 827–837. doi: 10.1094/MPMI-19-0827
- Ryan, R. P., Germaine, K., Franks, A., Ryan, D. J., and Dowling, D. N. (2008). Bacterial endophytes: recent developments and applications. *FEMS Microbiol. Lett.* 278, 1–9. doi: 10.1111/j.1574-6968.2007.00918.x
- Sabry, A. (2015). Synthetic fertilizers; role and hazards. *Fertil. Technol.* 1, 110–133. doi: 10.13140/RG.2.1.2395.3366
- Saleem, S., Iqbal, A., Ahmed, F., and Ahmad, M. (2021). Phytobeneficial and salt stress mitigating efficacy of IAA producing salt tolerant strains in *Gossypium hirsutum*. *Saudi J. Biol. Sci.* 28, 5317–5324. doi: 10.1016/j.sjbs.2021.05.056
- Sampedro, I., Pérez-Mendoza, D., Toral, L., Palacios, E., Arriagada, C., and Llamas, I. (2020). Effects of halophyte root exudates and their components on chemotaxis, biofilm formation and colonization of the halophilic bacterium *Halomonas anticariensis* FP35T. *Microorganisms* 8:575. doi: 10.3390/microorganisms8040575
- Sapre, S., Gontia-Mishra, I., and Tiwari, S. (2022). Plant growth-promoting rhizobacteria ameliorates salinity stress in pea (*Pisum sativum*). *J. Plant Growth Regul.* 41, 647–656. doi: 10.1007/s00344-021-10329-y



- Savci, S. (2012). An agricultural pollutant: chemical fertilizer. *Int. J. Environ. Sci. Dev.* 3, 73–80. doi: 10.7763/IJESD.2012.V3.191
- Sehrawat, N., Yadav, M., Sharma, A. K., Kumar, S., Singh, M., Kumar, V., et al. (2021). Mungbean (*Vigna radiata* L. Wilczek) as functional food, agronomic importance and breeding approach for development of climate resilience: current status and future perspectives. *Asian J. Biol. Life Sci.* 10, 87–92. doi: 10.5530/ajbls.2021.10.14
- Shahid, M., Hameed, S., Tariq, M., Zafar, M., Ali, A., and Ahmad, N. (2015). Characterization of mineral phosphate-solubilizing bacteria for enhanced sunflower growth and yield-attributing traits. *Ann. Microbiol.* 65, 1525–1536. doi: 10.1007/s13213-014-0991-z
- Shahzad, R., Khan, A. L., Bilal, S., Waqas, M., Kang, S. M., and Lee, I. J. (2017). Inoculation of abscisic acid-producing endophytic bacteria enhances salinity stress tolerance in *Oryza sativa*. *Environ. Exp. Bot.* 136, 68–77. doi: 10.1016/j.envexpbot.2017.01.010
- Simarmata, T., Turmuktini, T., Fitriatin, B. N., and Setiawati, M. R. (2016). Application of bioameliorent and biofertilizers to increase the soil health and rice productivity. *HAYATI J. Biosci.* 23, 181–184. doi: 10.1016/j.hjb.2017.01.001
- Singh, T. B., Sahai, V., Goyal, D., Prasad, M., Yadav, A., Shrivastav, P., et al. (2020). Identification, characterization and evaluation of multifaceted traits of plant growth promoting rhizobacteria from soil for sustainable approach to agriculture. *Curr. Microbiol.* 77, 3633–3642. doi: 10.1007/s00284-020-02165-2
- Singh, M., Singh, D., Gupta, A., Pandey, K. D., Singh, P. K., and Kumar, A. (2019). “Plant growth promoting rhizobacteria: application in biofertilizers and biocontrol of phytopathogens” in *PGPR Amelioration in Sustainable Agriculture*. eds. K. S. Amit, K. Ajay and K. S. Pawan (Sawston, Cambridge: Woodhead Publishing), 41–66.
- Singh, P., Singh, R. K., Li, H. B., Guo, D. J., Sharma, A., Verma, K. K., et al. (2023). Nitrogen fixation and phytohormone stimulation of sugarcane plant through plant growth promoting diazotrophic *Pseudomonas*. *Biotechnol. Genet. Eng. Rev.* 1–21. doi: 10.1080/02648725.2023.2177814
- Suárez-Moreno, Z. R., Vinchira-Villarraga, D. M., Vergara-Morales, D. I., Castellanos, L., Ramos, F. A., Guarnaccia, C., et al. (2019). Plant-growth promotion and biocontrol properties of three *Streptomyces* spp. isolates to control bacterial rice pathogens. *Front. Microbiol.* 10:290. doi: 10.3389/fmicb.2019.00290
- Sultana, S., Paul, S. C., Parveen, S., Alam, S., Rahman, N., Jannat, B., et al. (2020). Isolation and identification of salt-tolerant plant-growth-promoting rhizobacteria and their application for rice cultivation under salt stress. *Can. J. Microbiol.* 66, 144–160. doi: 10.1139/cjm-2019-0323
- Tang, A., Haruna, A. O., Majid, N. M. A., and Jalloh, M. B. (2020). Potential PGPR properties of cellulolytic, nitrogen-fixing, phosphate-solubilizing bacteria in rehabilitated tropical forest soil. *Microorganisms* 8:442. doi: 10.3390/microorganisms8030442
- Tariq, M., Hameed, S., Yasmeen, T., Zahid, M., and Zafar, M. (2014). Molecular characterization and identification of plant growth promoting endophytic bacteria isolated from the root nodules of pea (*Pisum sativum* L.). *World J. Microbiol. Biotechnol.* 30, 719–725. doi: 10.1007/s11274-013-1488-9
- Tounsi-Hammami, S., Hammami, Z., Dhane-Fitouri, S., Le Roux, C., and Jeddi, F. B. (2022). A mix of agrobacterium strains reduces nitrogen fertilization while enhancing economic returns in field trials with durum wheat in contrasting agroclimatic regions. *J. Soil Sci. Plant Nutr.* 22, 4816–4833. doi: 10.1007/s42729-022-00962-1
- Tsegaye, Z., Yimam, M., Bekele, D., Chaniyalew, S., and Assefa, F. (2019). Characterization and identification of native plant growth-promoting bacteria colonizing tef (*Eragrostis Tef*) rhizosphere during the flowering stage for a production of bio inoculants. *Biomed. J. Sci. Tech. Res.* 22, 16444–16456. doi: 10.26717/BJSTR.2019.22.003710
- Tyagi, J., Chaudhary, P., Mishra, A., Khatwani, M., Dey, S., and Varma, A. (2022). Role of endophytes in abiotic stress tolerance: with special emphasis on *Serendipita indica*. *Int. J. Environ. Res.* 16:62. doi: 10.1007/s41742-022-00439-0
- Upadhyay, V. K., Singh, A. V., Khan, A., Singh, J., Pareek, N., and Raghav, A. (2022). FE-SEM/EDX based zinc mobilization analysis of *Burkholderia cepacia* and *Pantoea rodasi* and their functional annotation in crop productivity, soil quality, and zinc biofortification of Paddy. *Front. Microbiol.* 13:852192. doi: 10.3389/fmicb.2022.852192
- Upadhyay, S. K., and Chauhan, P. K. (2022). Optimization of eco-friendly amendments as sustainable asset for salt-tolerant plant growth-promoting bacteria mediated maize (*Zea Mays* L.) plant growth, Na uptake reduction and saline soil restoration. *Environ. Res.* 211:113081. doi: 10.1016/j.envres.2022.113081
- Upadhyay, S. K., Rajput, V. D., Kumari, A., Espinosa-Saiz, D., Menendez, E., Minkina, T., et al. (2022). Plant growth-promoting rhizobacteria: a potential bio-asset for restoration of degraded soil and crop productivity with sustainable emerging techniques. *Environ. Geochem. Health*, 1–24. doi: 10.1007/s10653-022-01433-3
- Vaishnav, A., Shukla, A. K., Sharma, A., Kumar, R., and Choudhary, D. K. (2019). Endophytic bacteria in plant salt stress tolerance: current and future prospects. *J. Plant Growth Regul.* 38, 650–668. doi: 10.1007/s00344-018-9880-1
- Valle-Romero, P., García-López, J. V., Redondo-Gómez, S., Flores-Duarte, N. J., Rodríguez-Llorente, I. D., Idaszkin, Y. L., et al. (2023). Biofertilization with PGP Bacteria improve strawberry plant performance under sub-optimum phosphorus fertilization. *Agronomy* 13:335. doi: 10.3390/agronomy13020335
- Verma, D., Meena, R. H., Sukhwai, A., Jat, G., Meena, S. C., Upadhyay, S. K., et al. (2022). Effect of ZSB with graded levels of zinc fertilizer on yield and zinc uptake under maize cultivation. *Proc. Natl. Acad. Sci. India Sec. B Biol. Sci.* 93, 379–385. doi: 10.1007/s40011-022-01433-4
- Verma, M., Singh, A., Dwivedi, D. H., and Arora, N. K. (2020). Zinc and phosphate solubilizing *Rhizobium radiobacter* (LB2) for enhancing quality and yield of loose leaf lettuce in saline soil. *Environ. Sustain.* 3, 209–218. doi: 10.1007/s42398-020-00110-4
- Wang, Y., Wang, C., Wang, L., Liu, Q., Dong, T., Hou, P., et al. (2019). Identification, optimization of fermentation conditions of antagonistic bacterium *Pseudomonas extremorientalis* against *Botrytis cinerea* on pear and evaluation of its biocontrol efficacy. *Chinese J. Biol. Control* 35, 437–448. doi: 10.16409/j.cnki.2095-039x.2019.03.007
- Wang, W., Zhu, Y., and Chen, X. (2017). Selective imaging of gram-negative and gram-positive microbiotas in the mouse gut. *Biochemistry* 56, 3889–3893. doi: 10.1021/acs.biochem.7b00539
- Weisburg, W. G., Barns, S. M., Pelletier, D. A., and Lane, D. J. (1991). 16S ribosomal DNA amplification for phylogenetic study. *J. Bacteriol.* 173, 697–703. doi: 10.1128/jb.173.2.697-703.1991
- Widowati, T., and Sukiman, H. (2019). Production of indole acetic acid by *Enterobacter cloacae* H3 isolated from Mungbean (*Vigna radiata*) and its potential supporting the growth of soybean seedling. *IOP Conf. Ser. Earth Environ. Sci.* 308:012040. doi: 10.1088/1755-1315/308/1/012040
- Yasmeen, T., Ahmad, A., Arif, M. S., Mubin, M., Rehman, K., Shahzad, S. M., et al. (2020). Biofilm forming rhizobacteria enhance growth and salt tolerance in sunflower plants by stimulating antioxidant enzymes activity. *Plant Physiol. Biochem.* 156, 242–256. doi: 10.1016/j.plaphy.2020.09.016
- Yasmeen, T., Hameed, S., Tariq, M., and Ali, S. (2012). Significance of arbuscular mycorrhizal and bacterial symbionts in a tripartite association with *Vigna radiata*. *Acta Physiol. Plant.* 34, 1519–1528. doi: 10.1007/s11738-012-0950-x
- Zahra, S. T., Tariq, M., Abdullah, M., Azeem, F., and Ashraf, M. A. (2023). Dominance of *Bacillus* species in the wheat (*Triticum aestivum* L.) rhizosphere and their plant growth promoting potential under salt stress conditions. *PeerJ* 11:e14621. doi: 10.7717/peerj.14621
- Zhang, Z., Schwartz, S., Wagner, L., and Miller, W. (2000). A greedy algorithm for aligning DNA sequences. *J. Comput. Biol.* 7, 203–214. doi: 10.1089/10665270050081478
- Zhang, X., Tong, J., Dong, M., Akhtar, K., and He, B. (2022). Isolation, identification and characterization of nitrogen fixing endophytic bacteria and their effects on *cassava* production. *PeerJ* 10:e12677. doi: 10.7717/peerj.12677
- Zhang, L., Zhang, W., Li, Q., Cui, R., Wang, Z., Wang, Y., et al. (2020). Deciphering the root endosphere microbiome of the desert plant *Alhagi sparsifolia* for drought resistance-promoting bacteria. *Appl. Environ. Microbiol.* 86, e02863–e02819. doi: 10.1128/AEM.02863-19
- Zul, D., Elviana, M., Ismi, K. R. N., Tassiyah, K. R., Siregar, B. A., Gafur, A., et al. (2022). Potential of PGPR isolated from rhizosphere of pulpwood trees in stimulating the growth of *Eucalyptus pellita* F. Muell. *Int. J. Agric. Technol.* 18, 401–420.
- Zveushe, O. K., de Dios, V. R., Zhang, H., Zeng, F., Liu, S., Shen, S., et al. (2023). Effects of co-inoculating *Saccharomyces* spp. with *Bradyrhizobium japonicum* on atmospheric nitrogen fixation in soybeans (*Glycine max* (L.)). *Plan. Theory* 12:681. doi: 10.3390/plants12030681



# Frontiers in Microbiology

Explores the habitable world and the potential of microbial life

The largest and most cited microbiology journal which advances our understanding of the role microbes play in addressing global challenges such as healthcare, food security, and climate change.

## Discover the latest Research Topics

[See more →](#)

### Frontiers

Avenue du Tribunal-Fédéral 34  
1005 Lausanne, Switzerland  
[frontiersin.org](https://frontiersin.org)

### Contact us

+41 (0)21 510 17 00  
[frontiersin.org/about/contact](https://frontiersin.org/about/contact)

